MM 2010-01

SYNTHESIS OF THE NORTHEASTERN SUPERIOR PROVINCE

Documents complémentaires

Additional Files

Licence

License

Cette première page a été ajoutée au document et ne fait pas partie du rapport tel que soumis par les auteurs.

Énergie et Ressources naturelles
Québec

SYNTHESIS OF THE NORTHEASTERN SUPERIOR PROVINCE

MM 2010-01

Martin Simard
Coordinator

Québec

Synthesis of the Northeastern Superior Province

Martin Simard
Coordinator

MM 2010-01

ABSTRACT

The Far North Program was an ambitious geological mapping initiative that took place in northern Québec from 1997 to 2003. During this time, 21 new geological surveys were conducted north of the 55th parallel at a scale of 1/250,000, covering more than 350,000 km^2. Ore deposit studies, metallogeny, geochronology, and geochemistry work, as well as many research projects were carried out in conjunction with the geological surveys. All of this work resulted in the acquisition of a significant amount of new geoscience data for this extensive yet little-known territory.

Work conducted under the Far North Program primarily focused on the Archean rocks of the northeastern Superior Province (NESP). This area comprises the bulk of the Minto Subprovince, the north part of the La Grande Subprovince, and the northwest corner of the Ashuanipi Subprovince.

This document is divided into seven chapters: 1) *Background*, in which the broad outlines of the project and the document are described; 2) *Regional geological setting*, where the main lithotectonic subdivisions of the NESP are described; 3) *Stratigraphy and geochronology*, which provides a description of stratigraphic units in the NESP and proposes regional and time correlations for these units; 4) *Geochemistry and neodymium isotope data*, in which rocks from the various units are compared on a geochemical basis and the existence of proto-cratons is interpreted based on Nd model ages; 5) *Geological evolution*, which describes the major phases of evolution and construction of the Archean crust in the NESP; 6) *Proterozoic mafic dyke swarms* are discussed in terms of orientation and age; and 7) *Mineral occurrences and metallogeny* presents a classification of mineral occurrences in the NESP, their importance and economic potential.

Seven thematic maps at a scale of 1/750,000 and one stratigraphic legend are provided, namely: a lithological map, a stratigraphic map and its legend, a map of isotopic age determinations, a map of neodymium isotopes, a map of mafic dykes and swarms, a mineral occurrence map, and a map of metamorphic assemblages.

DOCUMENT PUBLISHED BY THE DIRECTION GÉNÉRALE DE GÉOLOGIE QUÉBEC

Direction générale

Robert Marquis

Bureau de l'exploration géologique du Québec

Sylvain Lacroix

Direction de l'information géologique

Luc Charbonneau

Critical Review

Louis Madore

Charles Maurice

Coordinator

Martin Simard

Authors

Martin Simard, Jean-Yves Labbé, Charles Maurice, and Pierre Lacoste

Alain Leclair (GSC Northern Canada)

Michel Boily (GÉON)

Editing

Marie Racine (Consultant)

Charles Gosselin

Graphic Design

Charlotte Grenier

André Tremblay

Technical Supervision

Charlotte Grenier

Manuscript accepted for publication June 30, 2008

Dépôt légal – Bibliothèque et Archives nationales du Québec
ISBN : 978-2-550-60333-7

TABLE OF CONTENTS

MAPS (INSERTS)

C001 - Lithological Map of the Northeastern Superior Province
C002 - Stratigraphic Map of the Northeastern Superior Province
C003 - Legend of the Stratigraphic Map of the Northeastern Superior Province
C004 - Isotopic Age Determinations in the Northeastern Superior Province
C005 - Neodymium Isotopes in the Northeastern Superior Province
C006 - Mafic Dykes and Swarms in the Northeastern Superior Province
C007 - Mineral Occurrences in the Northeastern Superior Province
C008 - Map of Metamorphic Assemblages and Textures in the Northeastern Superior Province

CHAPTER 1
BACKGROUND

Martin Simard and Alain Leclair

The Far North Program was one of the most ambitious geological mapping initiatives ever conducted in Québec. With this program, the government of Québec wanted to open new territories to mineral exploration through the acquisition of new geoscience data in a poorly known region covering a surface area of about 350,000 km^2 in Nunavik, north of the 55th parallel (Figure 1.1). The program was launched in 1997, with an extensive lake-bottom sediment geochemistry survey jointly funded by the Ministère des Ressources naturelles and five mining companies (Cambior, Falconbridge, Noranda, SOQUEM, and Virginia Mines). The 26,220 samples collected at a 12-km^2 spacing were used to generate targets that prompted a few mining companies to launch exploration programs.

The Far North Program then continued with an extensive geological mapping campaign that took place from 1998 to 2003. During this time, 21 new geological surveys at a scale of 1/250,000 were conducted (Figure 1.1). Surveying this huge landmass devoid of road access required complex and costly logistics as well as the participation of numerous geologists, geological assistants and technicians, whether for fieldwork, data entry, and production of geological maps. The involvement of multidisciplinary teams during the entire length of the program made it possible to collect geoscience data related to several different fields of study. Ore deposit studies, metallogeny, geochronology, and geochemistry work, as well as several research projects conducted in partnership with universities, were carried out concurrently with mapping surveys. All of this work led to the publication of numerous geological reports and maps, study reports, promotional documents, scientific articles, not to mention the significant contribution to Québec's Geomining Information System (SIGÉOM).

The bedrock in Québec's Far North is predominantly composed of Archean assemblages belonging to the northeastern Superior Province (NESP). The stratigraphic approach adopted during geological mapping led to the recognition of regional units that bear the footprint of geological events that affected the latter at different times during the Archean. The spatial distribution of these units and related geochronology and isotopic data attest to a complex evolution spanning more than 1.2 Ga (billion years). This geological evolution calls into play periods of growth and reworking of the Archean crust, from 3.82 to 2.62 Ga. Newly acquired geoscience data also made it possible to distinguish two major terranes that evolved differently through time and that played an important role in the distribution of stratigraphic units. Interpretation of these new data led us to reconsider the role and significance of the main lithotectonic assemblages proposed for the NESP by the Geological Survey of Canada (Chapter 2). These assemblages, initially interpreted as the products of accretion of various terrains, appear instead to reflect the distribution of certain stratigraphic units with contrasting geophysical signatures. Field visits of several mineral occurrences as well as a compilation of all available data on mineral deposits were used to draw a clearer portrait of the mineral potential of the NESP, particularly within metamorphosed volcano-sedimentary belts. More than 21 types of mineral occurrences were recognized, attesting to the diverse economic potential of this region.

MAIN CONSTITUENTS OF THIS DOCUMENT

This synthesis is based on data presented in all of the geological maps and reports, thematic studies, and promotional documents published by the government of Québec. It also takes into account previous work by the Geological Survey of Canada, as well as research publications in the form of geoscientific papers and university monographs. This volume and the related georeferenced database represent a valuable source of geological knowledge for stakeholders in the mining industry and the entire geoscience community at work in Québec's Far North.

Compilation work, interpretation, writing and editing work that led to the publication of this report was carried out by several authors who also took part, along with many other geologists, in geological mapping surveys, thematic studies, geological reports, as well as data entry in Québec's Geomining Information System (SIGÉOM) and data processing using the Système de production de cartes à petites échelles (SPCPE - small-scale map production system). In addition, work related to the synthesis of geochemical and isotopic data was conducted by Michel Boily, an expert from GÉON.

This document comprises seven main themes: *a) background; b) regional geological setting; c) stratigraphy and geochronology; d) geochemistry and Nd isotope data; e) geological evolution; f) Proterozoic mafic dyke swarms; g) mineral occurrences and metallogeny*. It comes with seven thematic maps and one stratigraphic legend (inserts), namely: a lithological map, a stratigraphic map with its

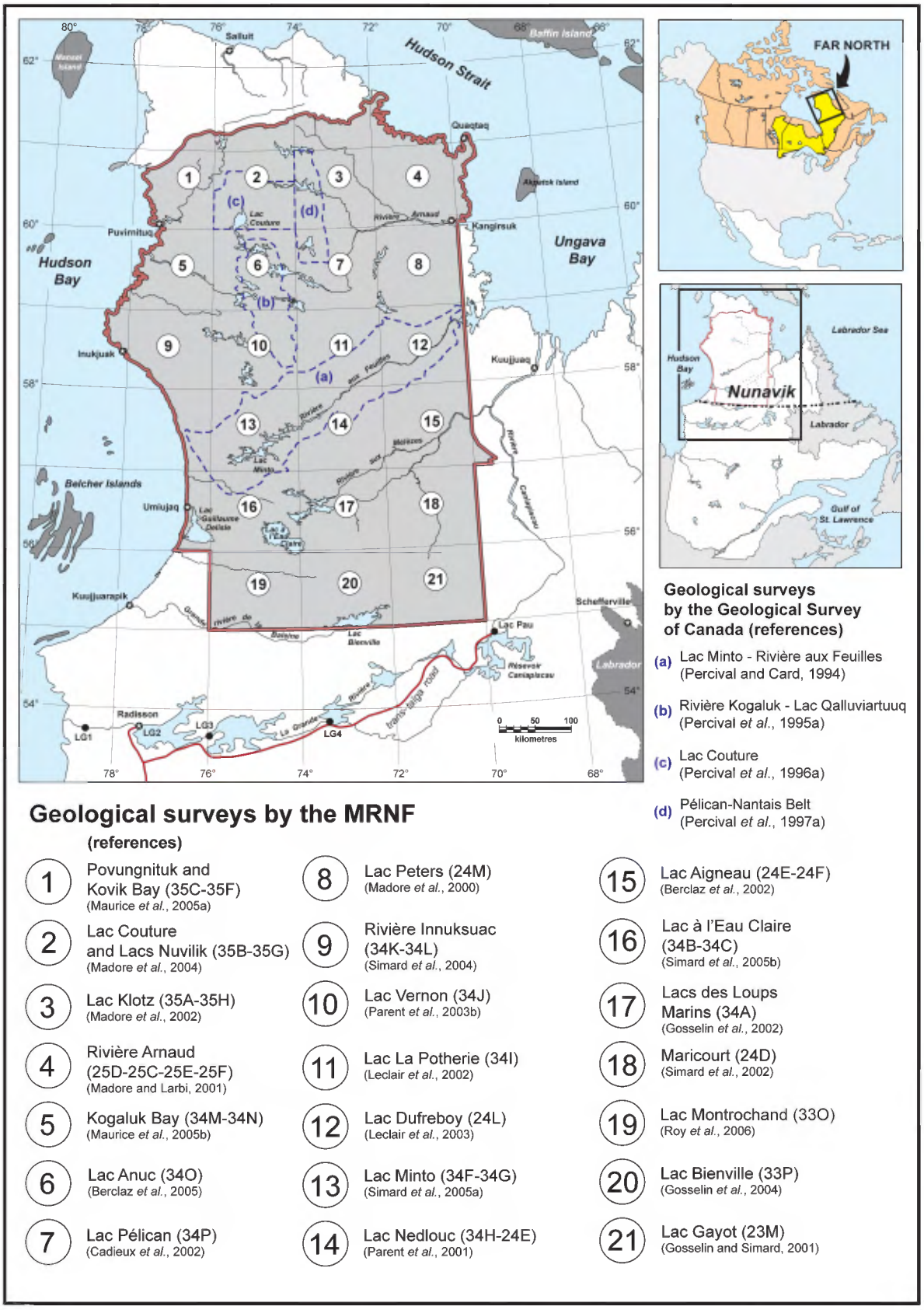

FIGURE 1.1 – Area covered by the Far North Program and location of the main mapping surveys conducted by the MRNF and the GSC.

legend, a map of isotopic age determinations, a map of neodymium isotopes, a map of mafic dykes and swarms, a mineral occurrence map, and a map of metamorphic assemblages and textures. These maps are also available in digital format (ArcGIS) via E-Sigeom (Examine), at: http://www.mrnfp.gouv.qc.ca/english/products-services/mines.jsp.

The chapter on *regional geological setting* positions the study area within the Superior Province. It also describes the main characteristics of the NESP, its two terranes as well as its various geological domains and proposed modifications to their respective boundaries.

The chapter on *stratigraphy and geochronology* provides a description of stratigraphic units. It also discusses geochronology data derived either from age determinations made by the MRNF during the Far North Program or those made by the GSC and published or mentioned in scientific papers and geological maps. This dataset was used to interpret the age of the various stratigraphic units and to build an evolution model integrating the latter. Two maps accompany this chapter. The stratigraphic map shows the regional distribution of stratigraphic units. The accompanying legend provides a brief description of each unit and shows two diagrams illustrating the time distribution of stratigraphic units. The second map shows the regional distribution of crystallization ages and inherited zircon ages based on MRNF and GSC data.

The chapter on *geochemistry and neodymium isotope data* draws parallels based on the chemical composition of Archean units that display comparable geological characteristics. This comparative analysis is used to emphasize geochemical distinctions between units as a function of spatial distribution and age. This chapter also discusses Nd isotope geochemistry and describes the regional distribution of mantle extraction model ages. Based on these data, two terranes with distinct evolution patterns are recognized. The map that accompanies this chapter shows the regional distribution of model ages interpreted from Nd isotope data.

The chapter on *geological evolution* describes the main phases of evolution and construction of the Archean crust based on stratigraphic, geochronological, isotopic, and geochemical data presented in the previous chapters.

The chapter on *mafic dyke swarms* provides a compilation and description of Proterozoic mafic dyke swarms based on orientation and age. The map accompanying this chapter shows the regional distribution of the various swarms, their relative importance, and the preferential orientation of dykes in each swarm.

The chapter on *mineral occurrences and metallogeny* presents a classification of mineral occurrences in the NESP, based on the mode of occurrence, structural setting, composition of host rock, and age of mineralization. For many categories, a description of known world-class deposits of the same type highlights the economic significance of this type of deposit and a discussion outlines the potential for discovery in the Far North. The mineral occurrence map shows the distribution of showings and deposits as well as their association with the different types of mineral occurrences recognized in the Far North.

As a complement, the regional map of *metamorphic assemblages and textures* presents the interpreted distribution of metamorphic facies based on thin section observations of mineral parageneses. It comes with an explanatory note.

Given its content, this document does not replace previous documents, but rather provides a global overview of the geology of the northeastern Superior Province by emphasizing the most significant results of studies conducted in this region. Readers seeking more detailed information should consult the geological maps and reports for each map area (see references and Figure 1.1), the regional geological compilation by Leclair (2005), the stratigraphic lexicon of Archean units (Simard, 2008), as well as the report discussing a sub-set of the geochronology dataset. (David *et al.,* 2008*)*.

ACKNOWLEDGEMENTS

The successful completion of the Far North Program is the result of a collaborative effort involving many individuals who, through their commitment and dedication, made a significant contribution to this project. Geological surveys sponsored by the Ministère des Ressources naturelles et de la Faune du Québec were conducted by multidisciplinary teams bringing together the authors of this report, their colleagues at Géologie Québec, as well as many university students, external experts and specialists. We would particularly like to acknowledge the following geologists, with whom we shared the responsibility of mapping projects: Daniel Bandyayera, Jean Bédard, Alain Berclaz, Pierre Brouillette, Anne-Marie Cadieux, Serge Chevé, Jean David, Charles Gosselin, Youcef Larbi, Louis Madore, Martin Parent, Patrice Roy, Robert Thériault, and Sophie Turcotte. We would also like to acknowledge the significant contributions of the following: Mona Baker, Marc Beaumier, Yan Bourassa, Jean Choinière, Denis-Jacques Dion, Philippe Ferron, Don Francis, Laurent Godin, Normand Goulet, Michel Hocq, Isabelle Lafrance, François Leclerc, Michel Leduc, Denis Lefebvre, Gabrièle Lemieux, Pierre Nadeau, Michel Parent, Olivier Rabeau, Ross Stevenson, Peter Thompson, and Pierre Verpaelst. Certain interpretations presented in this document are specifically based on publications from the latter geologists. Finally, we extend our sincere gratitude to the numerous geologists, geological assistants, cooks, camp managers, helicopter pilots and mechanics, as well as the entire administrative and support staff at Géologie Québec who was involved, directly or indirectly, in the completion of the Far North Program over the years.

This document benefited from a judicious and constructive critical review by Louis Madore (Bureau de la géoinformation) and Charles Maurice (Bureau d'exploration géologique du Québec). Editing of this document was performed by Marie Racine. The authors specifically wish to thank Frédéric St-Pierre, Patrick Olivier, and Nelson Leblond

(Bureau de la géoinformation), who skilfully used the SPCPE and ArcGIS to generate digital thematic maps. We also wish to thank Charlotte Grenier, Carole Roy, and André Tremblay, who participated in the preparation of various figures, as well as a number of geomatics and mineral resource technicians from the Bureau de la géoinformation, who digitized data and updated geological maps in SIGÉOM.

CHAPTER 2
REGIONAL GEOLOGICAL SETTING OF THE NORTHEASTERN SUPERIOR PROVINCE

Alain Leclair

SUPERIOR PROVINCE

The Superior Province forms the core of the Canadian Shield and the North American continent. It corresponds to an extensive Archean craton (1.6 million km^2), nearly half of which is located in Québec (Hocq, 1994; Card and Poulsen, 1998). The Superior Province is largely composed of Neoarchean rocks (2.8 to 2.5 Ga). However, recent isotopic studies (U/Pb geochronology data from inherited zircons and whole-rock Sm/Nd data) have successfully traced early magmatic events and identified important Mesoarchean and Paleoarchean domains (3.6 to 2.8 Ga) (Tomlinson *et al.*, 2004; Boily *et al.*, 2006a and 2006b; Percival *et al.*, submitted). A few rare earlier (>3.6 Ga) units are also recognized, representing the remains of an Eoarchean crust (Böhm *et al.*, 2003; David *et al.*, 2004). The cratonization of these Archean rocks took place between 2.6 and 2.5 Ga. During the Proterozoic, the Superior Province craton was affected, along its west, north, and east margins by the Trans-Hudsonian orogeny and along its southern edge by the Grenvillian orogeny (Hoffman, 1988 and 1989; Card and Poulsen, 1998). Fracturing led to the emplacement of several mafic dyke swarms (Buchan and Ernst, 2004; Maurice, Chapter 6) and supracrustal sequences were deposited unconformably atop the Archean basement.

The Superior Province is traditionally subdivided into several subprovinces (Stockwell, 1982; Card and Ciesielski, 1986; Card, 1990; Card and Poulsen, 1998) on the basis of lithological, structural, metamorphic, geochronological, and geophysical criteria (Figure 2.1). Four main types of subprovinces are recognized, in which many terranes, domains, complexes, and greenstone belts have been defined (Stott, 1997; Card and Poulsen, 1998; Percival *et al.*, 1992, 2001, and submitted; Tomlinson *et al.*, 2004; Leclair, 2005; Boily *et al.*, 2009; Chapter 4). In general, metasedimentary subprovinces and volcano-plutonic subprovinces show relatively weak magnetic signatures with regular or sinuous patterns, whereas plutonic subprovinces and gneissic subprovinces are characterized by positive magnetic anomalies.

In Québec, the Superior Province may be divided into two main areas. The southern part, primarily composed of sedimentary, volcanic, and plutonic rocks, is characterized by alternating linear subprovinces with an E-W-trending regional structural pattern (Figure 2.1). The northern part, almost entirely plutonic, corresponds to the Minto Subprovince and is divided into a number of different geological domains, trending NNW-SSE. These domains contain extensive charnockitic units and display a strong magnetic relief (figures 2.2 and 2.3). The origin of this shift in structural orientation between the two parts of the Superior remains unclear. Percival *et al.* (2006) mentioned that the bend in the regional structural pattern may reflect an oroclinal flexure produced by trans-rotational tectonics, a change in tectonic regime from north to south, or a "corner effect" around a protocraton during Neoarchean-aged magmatism and deformation.

NORTHEASTERN SUPERIOR PROVINCE

The northeastern Superior Province (NESP) is mainly composed of Archean plutonic rocks (attached lithological map; Leclair, 2005). These felsic to ultramafic igneous rocks are variably foliated and have preserved, to varying degrees, their primary textures. Felsic plutonic rocks are the most common and the most widespread. They are composed of tonalite (40%), granite (20%), granodiorite (15%), charnockitic rocks (15%) and more rarely, monzonite and syenite (<1%). They generally occur as elongated sheets that define the dominant structural style in the region. Small isolated plutons of diorite, gabbro, and ultramafic rocks represent less than 2% of the bedrock. Metavolcanic and metasedimentary rocks account for less than 10% of all Archean rocks (attached lithological map; Leclair, 2005). They form isolated lens-shaped units or dismembered, discontinuous belts enclosed within intrusive bodies. The better-preserved belts may reach up to 10 km in width by 120 km in length.

The NESP is bordered by Paleoproterozoic sedimentary and volcanic rocks. To the east, we find rocks of the Labrador Trough related to the New Québec Orogen (Wardle *et al.*, 2002; Clark and Wares, 2006), to the north, rocks of the Ungava Trough associated with the Ungava Orogen (Taylor, 1982; St-Onge and Lucas, 1990; Lamothe, 1994), and to the west, rocks of the Richmond Gulf Graben (Dimroth *et al.*, 1970; Chandler, 1988) (Figure 2.2). Paleoproterozoic sedimentary rocks also occur unconformably overlying the NESP, forming small isolated outliers scattered along a broadly E-W-trending axis near the 56th parallel (Eade, 1966; Clark, 1984). Finally, at least a dozen Proterozoic dyke swarms crosscut the Archean bedrock (Buchan and Ernst, 2004; Maurice *et al.*, 2005b; Chapter 6).

Pennsylvanian impactites (Bostock, 1969; Rondot *et al.*, 1993) contain enclaves of Ordovician limestone, outcropping on a ring of islands in the centre of Lac à l'Eau Claire. Silurian impactites (Bottomley *et al.*, 1990) were also observed in Quaternary unconsolidated deposits bordering the Lac Couture astrobleme (Madore *et al.*, 2004). Finally, the Pingualuit Crater, formerly referred to as the New Québec Crater, is the result of a younger impact; some of its clasts were dated at 1.3 Ma (Grieve *et al.*, 1989).

Work conducted under the Far North Program made it possible to assign Archean lithological assemblages to various stratigraphic units, establish their ages, determine their geochemical characteristics, and assess their economic potential. This new knowledge, combined with the results of previous work, is used to establish a new geological interpretation of the northeastern Superior Province.

Overview of previous work

The first geological observations of the northeastern Superior Province were made by geologists from the Geological Survey of Canada, namely Bell (1877 and 1885) and Low (1889, 1898, and 1902) during a series of expeditions along the coastal regions of the Ungava Peninsula and further inland, along rivers and tributaries. The regional geology was also briefly described following traverses across the peninsula, via its lakes and rivers (Flaherty, 1918; Aubert de la Rue, 1948). Further geological observations were published by Kranck (1951) along the east coast of Hudson Bay and by Kretz (1960), who published a map of the north part of the Ungava Peninsula at a scale of 1/1,013,760. But it wasn't until the 1950's and 1960's that the Geological Survey of Canada began systematically

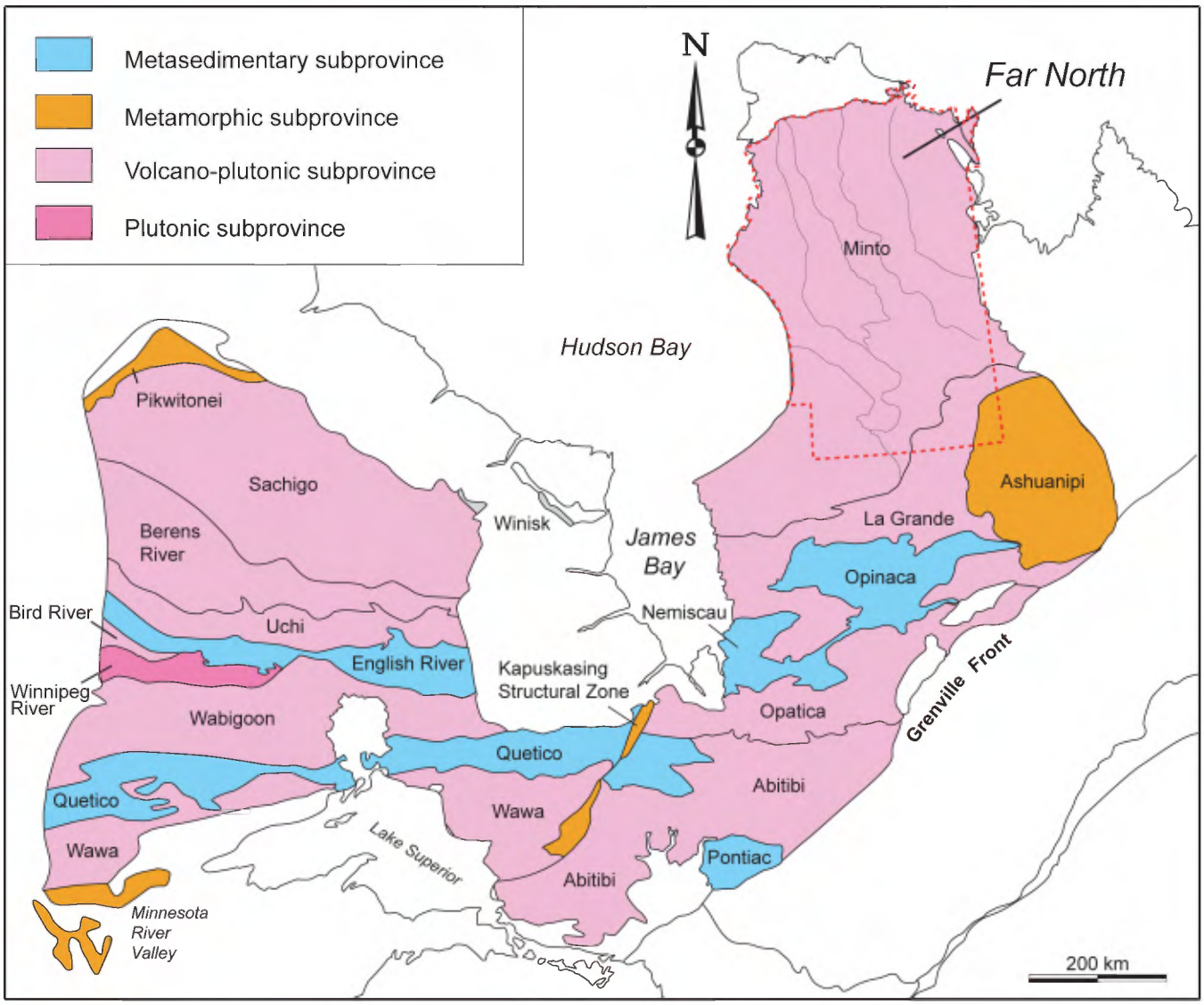

FIGURE 2.1 – Subdivisions of the Superior Province.

mapping the northeastern Superior Province as a whole. Helicopter-based reconnaissance geological surveys were conducted by Eade (1966) and Stevenson (1968) between parallels 52° and 61° North. Two geological maps at a scale of 1/1,000,000 were published, and later integrated to the geological map of Québec (Avramtchev, 1985). These maps are based on observations collected along predetermined flight lines, with observation sites spaced about 10 km apart. During this time, Lee (1965) also mapped the Archean and Proterozoic rocks (including the Nuvvuagittuq Belt; Chapter 3) located along the coast, south of Inukjuak, at a scale of 1 mile to 1 inch. Reconnaissance mapping of the remainder of the Ungava Peninsula was completed by Taylor (1982), who produced a map of the area located north of the 61st parallel, at a scale of 1/250,000. Note that Pennsylvanian-age rocks related to a meteorite impact on the islands in Lac à l'Eau Claire were mapped by Kranck and Sinclair (1963), Bostock (1969), and Rondot *et al.* (1993).

In the 1980's and 1990's, the Geological Survey of Canada continued its work in the northeastern Superior Province. Card and Ciesielski (1986) were the first to subdivide the area into four main subprovinces: 1) the volcano-plutonic La Grande Subprovince to the south; 2) the plutonic Bienville Subprovince in the centre; 3) the plutonic and high-grade metamorphic Ashuanipi Subprovince to the east; and 4) the plutonic-gneissic Minto Subprovince to the north. Subsequently, the GSC conducted a geological survey at 1/500,000 scale along the Rivière aux Feuilles (Percival and Card, 1994), then three other surveys at 1/250,000 scale in other areas to the north (Percival *et al.*, 1995a, 1996a, and 1997a). Based on this work, the boundaries between the four subprovinces were modified and the Minto Subprovince was subdivided into various domains, based on geological and geophysical criteria. Through this work, various volcano-sedimentary belts were also documented, namely the Vizien (Percival and Card, 1992; Percival *et al.*, 1993; Skulski and Percival, 1996), Kogaluc and Qalluviartuuq (Percival *et al.*, 1995b), Duquet (Percival *et al.*, 1996b), and Pélican-Nantais (Percival *et al.*, 1997b) belts. Following work conducted in the Kuujjuarapik, Lac à l'Eau Claire, and Lac Bienville areas, Ciesielski (1998 and 2000) repositioned the Bienville Subprovince boundary slightly further south relative to the location proposed by Card and Ciesielski (1986).

A few geological surveys of limited extent were also conducted in the NESP from the late 1980's until the start of the Far North Program. Lamothe (1997) mapped the Lac Dupire volcano-sedimentary belt at a scale of 1/50,000. Some surveys carried out in bordering regions, namely in the Paleoproterozoic Ungava Orogen (Lamothe *et al.*, 1984; Moorhead, 1988, 1989, and 1996; Roy, 1989; Togola, 1992; St-Onge and Lucas, 1993 and 1997) and New Québec Orogen (Dimroth, 1978; Dressler, 1979; Clark and Wares, 2006) also covered adjacent Archean rocks of the Superior Province. In the Lac Guillaume-Delisle area, Paleoproterozoic sequences in the Richmond Gulf Graben were mapped at a scale of 1/100,000 by Chandler (1988).

The Far North Program was launched in 1997 with an extensive lake-bottom sediment survey and continued with a vast geological mapping campaign that took place from 1998 to 2003 (Chapter 1).

The Geological Survey of Canada produced Quaternary geology maps, kimberlite indicator mineral reconnaissance survey maps, and glacial flow indicator maps for several areas in the Far North (Paradis and Parent, 2005; Parent *et al.*, 2002, 2003a, and 2004). Geochemistry studies to establish the distribution of elements in the secondary environment and the diamond potential of the Far North region were also conducted (Beaumier, 2001; Beaumier *et al.*, 2002a and 2002b).

Prospecting and mineral exploration began in the northeastern Superior Province in the late 1940's and has continued intermittently to this day, influenced both by worldwide demand for various base and precious metals and by the results of surveys and studies conducted under the Far North Program. A detailed overview of previous work carried out by various mining companies, independently or in consortiums, is presented in Chapter 7.

Subdivisions of the northeastern Superior Province

The subdivision of the NESP into subprovinces and geologically and geophysically distinctive domains served as a basis for the development of a tectonomagmatic model for the region (Percival and Skulski, 2000; Percival *et al.*, 2001). The latter authors suggested that the various domains in the Minto Subprovince correspond to "lithotectonic terrains" juxtaposed by lateral accretion. However, certain recent studies suggest instead a model based on vertical tectonics (Bédard *et al.*, 2003; Bédard, 2006). The results of mapping surveys conducted under the Far North Program led to a few modifications to the NESP subdivision and called into question the importance of domains in the craton's evolution. This work also revealed the existence of two major terranes, the Rivière Arnaud Terrane to the north and the Hudson Bay Terrane to the south and west, that evolved differently through time (Figure 2.2).

Subdivisions of the NESP involve four types of geological, geophysical, or tectonic features:

1. Subprovinces represent regions with similar lithological, structural, metamorphic, geochronological, and geophysical characteristics, but may contain many domains;
2. Domains are distinguished from one another by their lithological and stratigraphic characteristics and by their aeromagnetic signature, but also by their geochronological, isotopic, and structural characteristics;
3. A structural complex composed of Archean rocks strongly affected by Proterozoic ductile deformation;
4. Terranes are defined based on geochronology and isotope data as well as the broad stratigraphic assemblages they comprise. Terranes may encompass several domains or subprovinces.

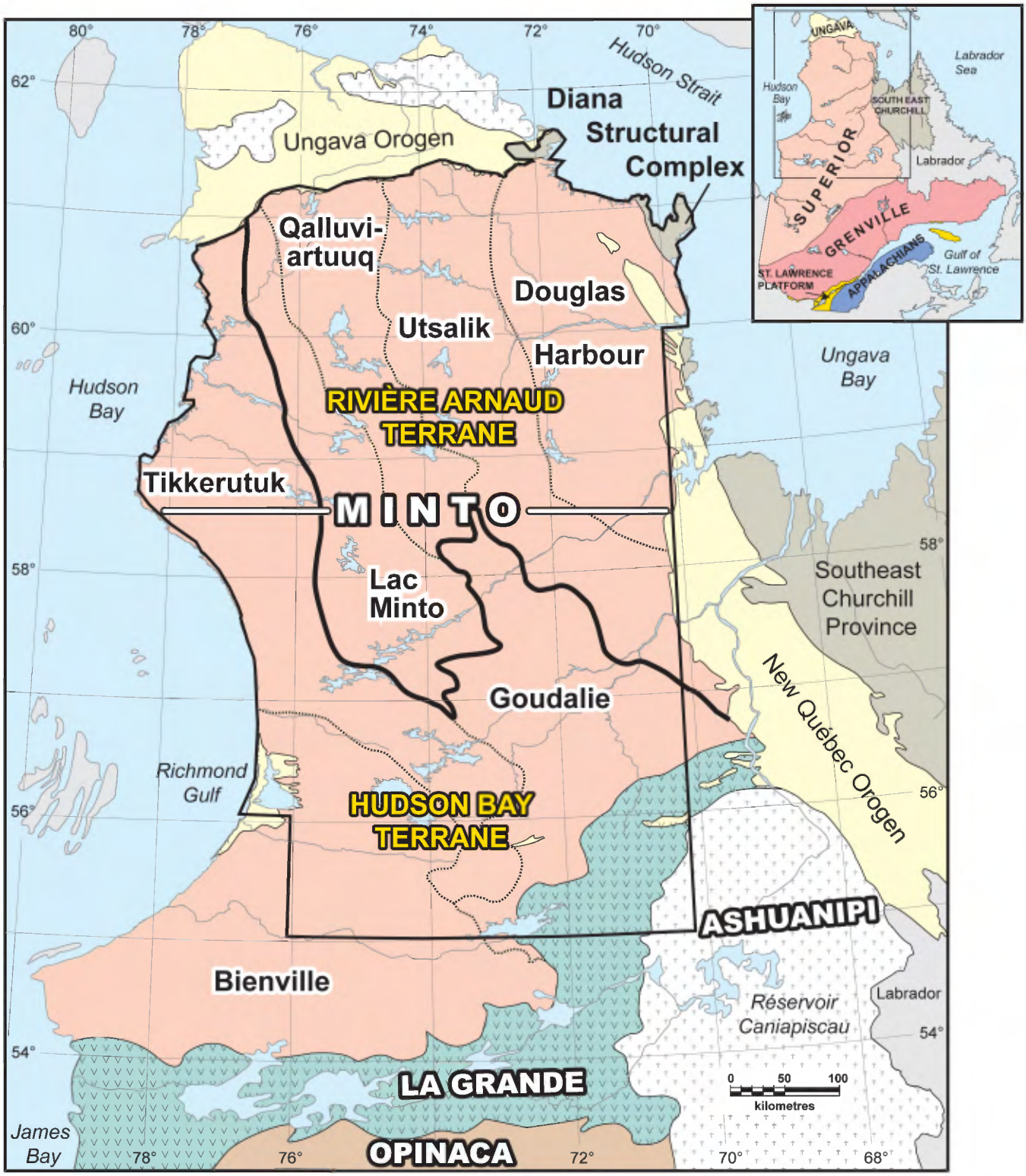

FIGURE 2.2 – Regional geological framework of northern Québec showing domains (black), subprovinces (white), and terranes (yellow) in the northeastern Superior Province (modified after Card and Poulsen, 1998; Percival et al., 1992 and 2001; Leclair, 2005).

Subprovinces

The northeastern Superior Province largely corresponds to the Minto Subprovince (Figure 2.2). Along the southeast edge of the study area, we also find the northeastern extension of the La Grande Subprovince as well as rocks from the northwest corner of the Ashuanipi Subprovince. To the south, the Bienville Subprovince (Card and Ciesielski, 1986) is now considered as a domain included in the Minto Subprovince. Its lithological and structural characteristics led us to propose this modification and thus abandon the term "Bienville Subprovince". In the northeast corner, the Diana Structural Complex corresponds to the transition zone between the Superior and Churchill provinces.

Ashuanipi Subprovince

The Ashuanipi Subprovince (also referred to as the "Ashuanipi Complex"; Percival *et al.*, 1992; Card and Poulsen, 1998) covers a surface area of about 300 km by 300 km in the east part of the Superior Province (Figure 2.1). This area is characterized by irregular magnetic anomalies (Figure 2.3) associated with high-grade metamorphic and plutonic rocks. The Ashuanipi Subprovince is mainly composed of migmatitic paragneisses associated with extensive bodies of orthopyroxene-bearing diatexite (2.68 to 2.66 Ga). An early tonalite-diorite-pyroxenite suite is also present (about 2.72 Ga, Desliens Suite; Percival *et al.*, 2003) along with a few metavolcanic belts (2.71 Ga; Leclair *et al.*, 1998). All of these rocks are deformed and metamorphosed to the granulite facies and are intruded by granitic, granodioritic, tonalitic, and syenitic plutons (2.65 to 2.62 Ga) as well as by anorogenic granite plutons (2.57 Ga) (Percival *et al.*, 1992; Chevé and Brouillette, 1995; David and Parent, 1997; Parent, 1998; Leclair *et al.*, 1998; Lamothe *et al.*, 1998). Paragneisses, intercalated with iron formations, constitute the oldest rocks (Percival *et al.*, 1992). The protoliths of Ashuanipi diatexites are greywackes comparable to those in the Opinaca Subprovince, which is in fact in structural continuity and in transitional contact (Leclair *et al.*, 1998; Lamothe *et al.*, 1998). Diatexite units contain up to 50% enclaves of paragneiss and tonalitic rocks. They are compositionally identical to their country rocks, suggesting the intrusions are derived from crustal sources (Percival, 1991). Peak metamorphic conditions preserved in granulitic rocks reach temperatures on the order of 820 to 900°C and pressures of 6 to 7 kb (Percival, 1991; Guernina and Sawyer, 2003), equivalent to conditions in the middle crust.

Although structural and aeromagnetic features are predominantly E-W-trending in the south part of the Ashuanipi Subprovince (Leclair *et al.*, 1998; Lamothe *et al.*, 1998), the north part is characterized by orientations ranging from NW to NE (Percival, 1993; Chevé and Brouillette, 1995). This shift in structural orientation defines part of the broad curvature corresponding to the Superior orocline. Further west, structures show variable orientations, reflecting a complex polyphase deformational setting (Leclair *et al.*, 1996; Lamothe *et al.*, 2000; Thériault and Chevé, 2001).

The part of the Ashuanipi Subprovince covered under the Far North mapping program is characterized by a significant amount of diatexite (Opiscotéo Suite) and by km-scale units of migmatitic paragneiss (Grosbois Complex). These diatexites are younger (2638 Ma) than other diatexite units in the Ashuanipi Subprovince (2682 to 2650 Ma). The presence of orthopyroxene in paragneisses and diatexites indicates the metamorphic grade reached the granulite facies during partial melting. The paragneisses and diatexites are cut by granodiorite and granite intrusions (Dervieux and Joinville suites) that may be equivalent to other intrusive units mapped elsewhere in the Ashuanipi Subprovince. These diatexites and felsic intrusions are associated with the youngest Archean magmatic events in the region (<2.68 Ga). Tonalitic remnants (2690 Ma; Beausac Suite) are enclaved in diatexites and intrusive units. The boundary between the Ashuanipi Subprovince to the east and the La Grande Subprovince to the west roughly corresponds to the Vaujours Fault, a major structure recognized in the Lac Gayot area (No. 21, Figure 1.1).

La Grande Subprovince

The volcano-plutonic La Grande Subprovince trends E-W in the Baie-James region to an area north of Caniapiscau Reservoir, where it shifts to a NE trend along the contact with diatexites of the Ashuanipi Subprovince (Figure 2.2). Typically associated with a relatively weak aeromagnetic signature (Figure 2.3), the La Grande Subprovince is mainly composed of felsic plutonic rocks in which are engulfed numerous sequences of deformed supracrustal rocks metamorphosed to the upper amphibolite facies. To the south, in the Eastmain area, volcanic rocks were emplaced in four distinct cycles, between 2.75 and 2.70 Ga, essentially in an oceanic setting with no interaction with an earlier crust (Moukhsil *et al.*, 2007; Boily and Moukhsil, 2003). To the north, in the Lac Yasinski area, an early basement of tonalitic gneiss (3.36 to 2.79 Ga) is recognized, unconformably overlain by a platform sequence composed of uraniferous arenite and conglomerate (Apple Formation, >2.75 Ga), itself overlain by a sequence dominated by tholeiitic basalts (2.75 to 2.73 Ga; Goutier and Dion, 2004). Further east, an older volcanic sequence (2.82 Ga) composed of komatiites, basalts, and felic tuffs (Guyer Group; Goutier *et al.*, 2002) was mapped. The interface between volcanic sequences of the Eastmain area to the south and those associated with an earlier crust to the north may correspond to a major tectonic break marking the boundary between two terranes.

The part of the La Grande Subprovince included in the study area (Figure 2.2) is characterized by the presence of remnants of early volcanic rocks (2880 to 2870 Ma; Gayot Complex) and tonalitic gneiss (about 2833 to 2807 Ma; Brésolles Suite), and by the absence of pyroxene-bearing felsic intrusive rocks that occur further north, in the Minto

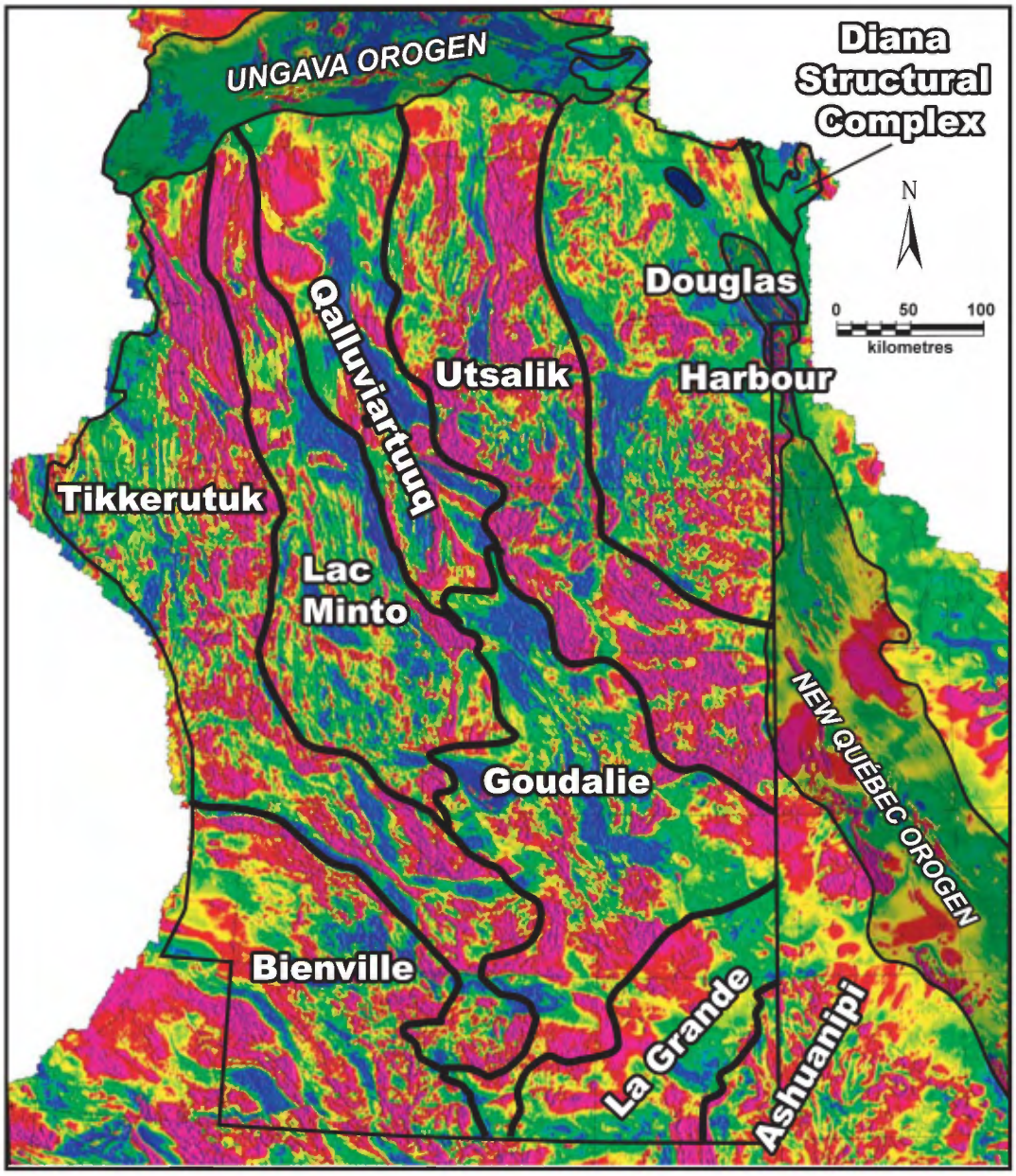

FIGURE 2.3 – Aeromagnetic map of the northeastern Superior Province.

Subprovince. Also, a NW-trending fabric is superimposed upon an earlier NE-trending fabric. Based on these criteria, we changed the location of the boundary between the La Grande and Minto subprovinces in the NESP (Figure 2.2). This boundary still remains inaccurately defined however, as this area is intruded by important tonalitic (Coursolles and Favard suites; 2760 to 2740 Ma) and granitic (Tramont and Maurel suites; 2707 to 2686 Ma) suites common to the two subprovinces. A correlation may be established between volcano-sedimentary rocks of the Gayot Complex and those in the Guyer Group; the two complexes have similar ages and are both composed of basalts, komatiites, and felsic volcanic rocks. Moreover, analyses of zircon xenocrysts and model ages obtained within the study area yielded results similar to those in the Yasinski area, indicating the presence of early crustal sources dating back to 3.3 Ga.

Minto Subprovince

The Minto Subprovince covers most of the study area (Figure 2.2). It was initially described by Card and Ciesielski (1986) as a "high-grade gneiss" terrain namely formed of granulites, due to the presence of pyroxene which was considered as having a metamorphic origin (Eade, 1966; Stevenson, 1968; Herd, 1978). However, recent mapping by the Geological Survey of Canada (Percival and Card, 1994; Percival *et al.*, 1995a, 1996a, and 1997a) and surveys conducted under the Far North Program revealed that

the orthopyroxene associated with charnockitic intrusive suites is largely magmatic in origin. In fact, the presence of pyroxene-bearing felsic intrusive rocks constitutes one of the main distinguishing features of the Minto Subprovince. Consequently, the Minto Subprovince may be described as an essentially plutonic subprovince that also contains remnants of amphibolite- and granulite-grade supracrustal rocks (Percival *et al.*, 1992; Leclair *et al.*, 2006). It comprises numerous stratigraphic units of diverse compositions and ages, broadly trending NNW-SSE, following the regional structural pattern.

Mapping conducted along the Rivière aux Feuilles (Percival and Card, 1994) and in three other areas further north (Percival *et al.*, 1995a, 1996a, and 1997a) enabled Percival *et al.* (1992 and 2001) to recognize close to a dozen different domains within the Minto Subprovince, based on lithological, structural, and aeromagnetic criteria. Work conducted under the Far North Program made it possible to clarify the nature and extent of these major domains. Isotope and geochronology data, as well as the distribution of stratigraphic units can be used to demonstrate that the various magmatic events that affected the entire Minto Subprovince at different times during the Archean transcend domain boundaries. Consequently, domains should be perceived as the products of the superposition of several magmatic events. Domains are characterized by stratigraphic units and geochronology and isotope data that reflect the best-preserved events.

The **Tikkerutuk Domain** (Percival *et al.*, 1992) is located in the west part of the study area (Figure 2.2). It corresponds to a series of contrasting magnetic anomalies trending N-S that shift toward the SE in the south part of the domain (Figure 2.3). The Tikkerutuk Domain is characterized by the presence of an extensive suite of pyroxene-bearing felsic intrusive rocks (Loups Marins Suite) emplaced between 2735 and 2705 Ma. This suite comprises an early orthopyroxene unit (2730 to 2720 Ma) and a clinopyroxene unit (2715 to 2705 Ma) also characterized by the presence of burgundy-coloured plagioclase. The domain also contains a series of small discrete mafic or ultramafic plutons (Qullinaaraaluk Suite; 2720 to 2705 Ma) scattered over a distance of about 450 km, as well as numerous volcano-sedimentary remnants (Innuksuac Complex, Roulier and Melvin belts; 2760 to 2764 Ma) scattered within the vast plutonic bodies. One of these remnants, the Nuvvuagittuq Belt, is the oldest supracrustal sequence (3825 Ma; David *et al.*, 2003; Simard *et al.*, 2004; O'Neil *et al.*, 2007; Cates and Mojzsis, 2007) identified to date in the Superior Province. The Nuvvuagittuq Belt covers a surface area of less than 30 km^2 near the western edge of the Tikkerutuk Domain, in an area characterized by a regional magnetic low previously interpreted as a distinct geological domain, the Inukjuak Domain (Percival *et al.*, 2001; Leclair, 2005). This former domain is now included in the Tikkerutuk Domain given the lithological, geochronological, and isotopic similarities observed between the two domains, and the term "Inukjuak Domain" is abandoned. Model ages obtained in the former Inukjuak Domain and further east in the Tikkerutuk Domain reveal an early history contemporaneous with the Nuvvuagittuq Belt (>3.1 Ga). A tonalite unit (Favard Suite; 2750 to 2740 Ma) and a granite-granodiorite unit (Desbergères Suite; 2720 to 2710 Ma) also occur within the Tikkerutuk Domain. These two units also cover a significant surface area in the south part of the Minto Subprovince, within the Bienville and Goudalie domains, as well as in the north part of the La Grande Subprovince.

The **Bienville Domain** corresponds to the former Bienville Subprovince, introduced by Card and Ciesielski (1986) and later redefined by Ciesielski (1998). The boundary between the Bienville and Minto subprovinces varies from one author to another (Card and Ciesielski, 1986; Ciesielski, 2000; Card and Poulsen, 1998; Percival *et al.*, 2001; Gosselin *et al.*, 2004; Leclair, 2005). However, the extension of stratigraphic units and magnetic anomalies typical of the Minto Subprovince into the Bienville, as well as the similar ages obtained on either side of this boundary led us to reconsider the Bienville as a domain belonging to the Minto Subprovince. The geological and geophysical similarities between the two subprovinces, and the possibility of a common magmatic history had already been evoked (Card and Poulsen, 1998; Percival *et al.*, 2001). Plutonic rocks in the Bienville Domain, as in the Tikkerutuk Domain, are largely Neoarchean in age. Inherited zircon ages and model ages indicate early crustal sources, dating back as early as 3.4 Ga in the Bienville (Chapter 4).

The north half of the Bienville Domain, represented by curvilinear NW-trending aeromagnetic anomalies (Figure 2.3), lies within the study area (Figure 2.2). It is characterized by numerous intrusions of granite and granodiorite (Desbergères Suite; 2720 to 2710 Ma) that invaded pyroxene-bearing felsic intrusive rocks (Loups Marins Suite; 2735 to 2705 Ma), also typical of the Tikkerutuk Domain. The boundary between the Bienville and Tikkerutuk domains corresponds to the Nastapoca deformation zone (Simard *et al.*, 2005b), north of which potassic intrusions of the Desbergères Suite are much less common. This boundary roughly corresponds to that proposed by Ciesielski (1998) between the Bienville and Minto subprovinces. To the south, beyond the study area, the Bienville marks the transition zone between the southern and northern parts of the Superior Province, where the E-W regional structural trend shifts toward the north. This area hosts an extensive granodioritic complex (about 2.71 Ga; Ciesielski, 2000; Goutier *et al.*, 1999) that crosscuts volcano-plutonic sequences in the La Grande Subprovince. This complex also contains a remnant of well-preserved volcano-sedimentary rocks in the Lac Fagnant area (Mercier and Ciesielski, 1983).

The **Lac Minto Domain** (Percival *et al.*, 1992) is characterized by narrow alternating positive and negative aeromagnetic anomalies (Figure 2.3). This domain is composed of extensive volcano-sedimentary units of predominantly sedimentary origin (Kogaluc Complex and Mézard Complex; about 2760 Ma) and an important diatexite unit (Le Roy

Complex; 2697 to 2668 Ma) derived from the partial melting of sedimentary rocks. These units are the remains of a vast sedimentary basin more than 500 km in length. The significant amount of diatexite constitutes the distinguishing feature of the Lac Minto Domain (Percival *et al.*, 1991). This domain also includes a synvolcanic tonalitic suite (Kakiattuq Suite; <2740 Ma) and an enderbitic suite (Lac Minto Suite; 2735 to 2710 Ma). Granitic intrusions (Morrice Suite; 2684 Ma), also occurring as sheet-like intrusions in the south part of the Qalluviartuuq Domain and the north part of the Goudalie Domain, may represent more evolved phases derived from the melting of sedimentary rocks (Figure 3.10). Except for one enclave of early tonalitic gneiss observed near Lac Minto (3.12 Ga; Percival *et al.*, 1992), rocks in the Lac Minto Domain yielded inherited zircon ages and mantle extraction model ages ranging from 2.92 to 2.80 Ga (Chapter 4), suggesting the absence of early (>3.0 Ga) recycled crust, in contrast with domains to the south and west.

The **Goudalie Domain** (Percival *et al.*, 1992) is located in the southeast Minto Subprovince (Figure 2.2), where a major NNW-trending magnetic low is observed (Figure 2.3). It is characterized by the predominance of tonalite-trondhjemite units (Favard, Coursolles, and Sem suites) resulting from a magmatic event that took place from 2760 to 2740 Ma. These units are intruded by granitic and granodioritic plutons (Desbergères, Tramont, Maurel, and Morrice suites; 2.73 to 2.68 Ga) as well as enderbitic plutons (MacMahon Suite; 2735 to 2710 Ma) that are also recognized in adjacent domains. This domain also contains an extensive volcano-sedimentary complex (Duvert Complex; 2724 to 2708 Ma) and diatexites of sedimentary origin (Rivière aux Mélèzes Suite; 2668 Ma). These rocks are concentrated in the north part of the domain, where rare occurrences of early tonalitic gneiss were also identified (3.01 to 2.90 Ga; Percival *et al.*, 1992, 2001). The earliest ages obtained from supracrustal rocks in the volcano-sedimentary complexes of the Goudalie Domain fall between 2.80 and 2.78 Ga (Dupire and Garault complexes).

Kilometre-scale remnants of tonalitic gneiss of the Brésolles Suite (2833 to 2807 Ma) and an equivalent unit (Suluppaugalik Suite; 2808 Ma) occur within the Goudalie Domain. Brésolles gneisses are typical of the La Grande Subprovince. Their presence within the Goudalie Domain suggests these early tonalitic gneisses originally extended further north, prior to younger magmatic events recorded in the Minto Subprovince. Moreover, rocks in the Goudalie Domain have inherited zircon ages and model ages (3.3 to 2.8 Ga; Stern *et al.*, 1994; Boily *et al.*, 2004, 2006a, and 2006b; Chapter 4) comparable to those obtained in the La Grande Subprovince, which suggests the existence of an early basement common to the two. Note that this early crust is absent in domains located to the north of the Goudalie Domain.

The **Qalluviartuuq Domain** (Percival *et al.*, 1997b; Percival and Skulski, 2000) corresponds to the northward extension of the magnetic low that runs along the central axis of the Minto Subprovince down to the Goudalie Domain in the south (Figure 2.3). Although the two domains exhibit a comparable geophysical signature, they are composed of stratigraphic units derived from distinct magmatic events. Moreover, Nd isotope data (Maurice, 2007) indicate that, unlike rocks of the Goudalie Domain, rocks of the Qalluviartuuq Domain are derived from a juvenile source. The Qalluviartuuq Domain is characterized by the presence of extensive early volcano-sedimentary units (Qalluviartuuq-Payne and Duquet complexes; 2.85 to 2.82 Ga) and by an important unit of tonalitic rocks (Rochefort Suite) associated with a magmatic event that took place between 2785 and 2775 Ma. Supracrustal units are dominated by tholeiitic basalts, komatiites, and volcaniclastic rocks with minor amounts of rhyolite, iron formation, and mafic to ultramafic subvolcanic intrusions (Percival *et al.*, 1995b; Madore *et al.*, 2004; Berclaz *et al.*, 2005; Leclerc, 2004). These units are overlain by younger volcanic sequences (2.78 to 2.76 Ga; Percival and Skulski, 2000; Maurice *et al.*, 2009) composed of tholeiitic basalts associated with gabbro, felsic volcanic and volcaniclastic rocks, and iron formation. Metasedimentary rocks unconformably overlie the volcanic sequences. They consist of sandstone and conglomerate with clasts dated at 2768 and 2764 Ma (Percival and Skulski, 2000) indicating the maximum age of sedimentation. Synvolcanic tonalite-trondhjemite intrusions (2.85 to 2.76 Ga) occur within the various volcano-sedimentary units. The Qalluviartuuq Domain also contains a series of relatively late granite and granodiorite plutons (La Chevrotière Suite) and enderbitic intrusions (MacMahon Suite). These plutons, dated between 2735 and 2720 Ma, occur in several domains within the NESP.

The **Utsalik Domain** (Percival *et al.*, 1992) corresponds to a strong N to NW-trending regional aeromagnetic anomaly (Figure 2.3). This domain is namely characterized by intrusive suites of granite, granodiorite, and enderbite, younger than 2735 Ma (La Chevrotière, Rivière aux Feuilles, Dufreboy, Maurel, and MacMahon suites; between 2735 and 2680 Ma) and occurring in more than one domain. Only the Lepelle Suite (2725 to 2720 Ma) is restricted to the north part of the Utsalik Domain. The latter unit is composed of clinopyroxene-bearing granodiorite and corresponds to a very strong magnetic high. The Utsalik Domain also contains a supracrustal unit dominated by sedimentary rocks (Pélican Complex; 2740 to 2733 Ma). The only remains of earlier rocks correspond to the volcano-sedimentary Nantais Complex (2775 Ma) and the tonalitic Kapijuq Suite (2785 to 2775 Ma). These units are centred on narrow magnetic lows less than 20 km wide by about 100 km long, located in the north part of the domain. The western edge of the Utsalik Domain is characterized by sheet-like intrusions of porphyritic monzogranite and granodiorite (2735 to 2720 Ma) of the La Chevrotière Suite. The elongate shape and conformable character of these sheet-like intrusions, parallel to the regional structural trend (see attached stratigraphic map), suggest their emplacement was coeval with deformation.

The eastern limit of the Utsalik Domain roughly corresponds to a major lineament (Lestage-Messin; Labbé, 2001) characterized by shearing and complex folding (Madore *et al.*, 2002; Cadieux *et al.*, 2004). Isotopic data obtained in the Utsalik Domain indicate juvenile sources (T_{DM} < 2.93 Ga); only one sample yielded an earlier model age (T_{DM} = 3.01 Ga; Chapter 4).

The **Douglas Harbour Domain** (Percival *et al.*, 1992) forms the northeast part of the Minto Subprovince (Figure 2.2). This domain is characterized by an extensive unit of tonalitic rocks (Faribault-Thury Suite; 2785 to 2775 Ma) in which are engulfed several volcano-sedimentary remnants (Arnaud Complex) derived from different magmatic events. Some of these remnants have ages comparable to volcano-sedimentary sequences in the La Grande Subprovince (2.88 to 2.87 Ga; Gayot Complex). The Douglas Harbour Domain is also distinguished by the presence of two large ovoid charnockitic massifs (Troie and Qimussinguat complexes; 2740 to 2722 Ma) corresponding to two positive, mottled aeromagnetic anomalies (Figure 2.3). These anomalies contrast with the weak magnetic signature associated with tonalitic and volcano-sedimentary rocks in this domain. Rocks in the north part of the Douglas Harbour Domain are cut by granitic to monzonitic intrusions (Leridon Suite) that were emplaced between 2735 and 2720 Ma. Rocks in the south part of the domain are also cut by porphyroid-textured monzonite and monzodiorite intrusions (Belloy Suite; 2.69 Ga). The western limit of the Douglas Harbour Domain corresponds to ductile deformation zones and hosts small nepheline syenite plutons (Kimber Suite; 2.76 Ga). Rocks in the north part of the Douglas Harbour Domain show model ages indicating they are derived from a juvenile source (T_{DM} < 2.9 Ga). On the other hand, rocks in the Troie Complex show an older isotopic signature (between 3.1 and 3.0 Ga), which reflects interaction with an evolved basement (Chapter 4).

Diana Structural Complex

The Diana Structural Complex covers a small surface area in the northeast corner of the study area (Figure 2.2). It corresponds to the transition zone between the Superior Province to the west and the Churchill Province to the east. This complex is characterized by Archean and Proterozoic units that were intensely affected by ductile deformation and metamorphism during the Paleoproterozoic (Madore and Larbi, 2001). Diabase dykes (about 2.21 to 2.16 Ga; Buchan and Ernst, 2004) were also affected by this deformation.

The complex is largely composed of tonalitic gneiss (2782 Ma) associated with diorite, trondhjemite, and granodiorite. These rocks represent the extensions of Archean units in the Superior Province and are, in part, equivalent to rocks of the Faribault-Thury Suite (2785 to 2775 Ma) recognized further west in the Douglas Harbour Domain (Figure 2.2). The Diana Complex also contains supracrustal remnants occurring as transposed bands within gneiss units. These remnants consist of amphibolite, paragneiss, marble, and metasedimentary calc-silicate rocks. Some amphibolite remnants may be equivalent to Archean volcanic rocks of the Douglas Harbour Domain (Madore and Larbi, 2001). However, several amphibolite bands are the result of the progressive eastward dismemberment of Proterozoic diabase dykes. The sedimentary rocks are most likely Proterozoic in age since similar rocks were not observed to the west in the Douglas Harbour Domain. Archean rocks in the Diana Structural Complex are cut by foliated and mylonitic monzonite intrusions (2756 Ma).

Terranes

The Far North Program resulted in the development of a new geological and geochronological framework for the NESP, in which the remains of an early crust may be recognized in domains of Neoarchean age. Volcanic and plutonic rocks with Eoarchean to Neoarchean crystallization ages (3.82 to 2.66 Ga) occur in the south part of the area, whereas in the north part, crystallization ages only range from the Mesoarchean to the Neoarchean eras (2.88 to 2.64 Ga). Nd isotope analyses (compilation of more than 300 samples of volcanic and plutonic rocks; Maurice, 2007) were used to determine the extent of crustal recycling. Geochronological, isotopic, and stratigraphic data thus revealed the existence of two major terranes that played an important role in the evolution of the Archean crust in the NESP (Figure 2.2). The Hudson Bay Terrane, to the south and west, shows evidence of crust dating back to the Eoarchean (>3600 Ma), whereas the history of the Rivière Arnaud Terrane, to the north, began after 2900 Ma, i.e. in the Mesoarchean era. The two terranes evolved differently until about 2740 Ma. Before this time, the two terranes were affected by different magmatic events, largely marked by mafic volcanism and tonalitic plutonism. After 2740 Ma, potassic and enderbitic magmatism spread across the entire NESP, affecting both terranes in a similar fashion.

The **Hudson Bay Terrane** comprises the southern and western parts of the Minto Subprovince, including the Bienville, Tikkerutuk, and Goudalie domains and extends southward into the La Grande Subprovince (Figure 2.2). This terrane is characterized by the presence of pre-2.9 Ga early crustal remains. In the westernmost part of the Tikkerutuk Domain, volcanic and plutonic rocks in the Nuvvuagittuq Belt (Chapter 3) yielded crystallization ages between 3.8 and 3.6 Ga. Elsewhere in this terrane, a few remnants of tonalitic gneiss yielded ages ranging from 3.0 to 2.9 Ga, and several inherited zircons recovered from younger intrusive rocks yielded ages ranging from 3.2 to 2.9 Ga. Isotopic studies generally reveal enriched signatures suggesting contamination of magmas by a sialic crust, with calculated model ages for the most part ranging between 2.9 and 3.6 Ga. The east part of the Hudson Bay Terrane contains volcanic rocks (Gayot Complex) and tonalitic rocks (Brésolles and Suluppaugalik suites) that formed between 2.9 and 2.8 Ga.

Geological evidence of the time span between 2800 and 2760 Ma is rather rare and well constrained. One of the main characteristics of the Hudson Bay Terrane is the presence of widespread tonalitic units (Favard and Coursolles suites) that extend across its entire breadth, the products of an important tonalitic magmatic event that took place between 2760 and 2740 Ma.

The **Rivière Arnaud Terrane** comprises the northern part of the Minto Subprovince, including the Lac Minto, Qalluviartuuq, Utsalik, and Douglas Harbour domains, as well as the Diana Structural Complex (Figure 2.2). Geochronology data and model ages based on Nd isotope data show that the Rivière Arnaud Terrane is juvenile relative to the Hudson Bay Terrane. This area is formed of crust younger than 2.9 Ga. Only rocks in the south part of the Douglas Harbour Domain yielded earlier model ages, dating back to 3.1 Ga. The earliest units (2850 to 2800 Ma) in the Rivière Arnaud Terrane correspond to volcano-sedimentary complexes (Qalluviartuuq-Payne, Duquet, and Arnaud complexes), as opposed to the Hudson Bay Terrane, where the same period is represented by tonalitic units (Brésolles and Suluppaugalik suites). One of the main characteristics of the Rivière Arnaud Terrane is the presence of widespread tonalitic suites (Faribault-Thury, Rochefort, and Kapijuq suites) that were emplaced between 2790 and 2760 Ma. This also contrasts with the situation in the Hudson Bay Terrane, where remains of this time span are rather scarce. In addition, while a major tonalitic event was taking place in the Hudson Bay Terrane between 2760 and 2740 Ma, evidence of magmatic activity during the same time span was not recorded in the Rivière Arnaud Terrane.

CHAPTER 3
STRATIGRAPHY AND GEOCHRONOLOGY OF THE NORTHEASTERN SUPERIOR PROVINCE

Martin Simard

INTRODUCTION

The formulation of a unified stratigraphy is critical to gain a regional understanding of vast territories. This is why the stratigraphic classification of rocks was a major preoccupation from the onset of fieldwork conducted under the Far North Program. This stratigraphic approach makes it possible to establish relationships between different rock units and to integrate the latter into a global geological evolution model. However, the foundations of stratigraphy were historically developed to classify and name geological entities that follow the Law of superposition, mainly sedimentary rocks and volcanic piles. The North American Stratigraphic Code (MER, 1986) can nevertheless be used to apply the principles of stratigraphy to terrains characterized by the predominance of intrusive and metamorphic rocks. The formulation of a coherent stratigraphy in this type of terrain remains a delicate task however that requires rigorous application of stratigraphic principles.

Goal of stratigraphic synthesis

The stratigraphic synthesis aims to standardize the stratigraphic nomenclature of Archean units developed over the course of 21 different mapping projects carried out under the Far North Program (Figure 1.1). Geochronology data was used to attribute absolute or relative ages to the various stratigraphic units.

Revision of stratigraphic nomenclature

The nomenclature revision is exclusively focused on Archean stratigraphic units, which form the vast majority of units in the northeastern Superior Province (NESP). More than 90 stratigraphic units were initially introduced by various authors to describe the Archean rocks in the study area. Through this revision, many units were grouped together based on lithological assemblages, ages, and spatial distribution. As a result, 68 formal units were maintained (Table 3.1) and 25 units were abandoned (Table 3.2). These units are described in the section entitled "Description of stratigraphic units", which also refers to the stratigraphic map (insert). The main characteristics of formal units are summarized in Table 3.1, where units are listed in alphabetical order, regardless of their rank. A detailed description of these units is also provided in the *Lexique stratigraphique des unités archéennes du nord-est de la Province du Supérieur* (Simard, 2008).

Geochronology data

The geochronology data are derived from two sources (Table 3.3): 1) U/Pb age determinations made by the MRNF on samples collected during mapping surveys under the Far North Program (145 analyses); and 2) U/Pb analytical data compiled from work by the Geological Survey of Canada (79 analyses). Samples collected by the MRNF were analyzed by Jean David in the GÉOTOP laboratories at the Université du Québec à Montréal (UQAM), by isotopic dilution and thermal ionization mass spectrometry (ID-TIMS) or by laser ablation and plasma mass spectrometry (LA-ICP-QMS or LA-MC-ICP-MS). A sub-set of the analytical data with descriptions is presented in a synthesis report (David *et al.*, 2008). The remaining data consist of unpublished results by Jean David.

The MRNF geochronology dataset, combined with that of the Geological Survey of Canada (GSC), constitutes a representative sampling of the majority of Archean units in the NESP. However, sites sampled by the GSC were not revisited during fieldwork carried out under the Far North Program. In many cases, lithologies dated by the GSC are assigned to a specific stratigraphic unit but this assignation remains uncertain. Nevertheless, these data provide important information on the spatial and temporal distribution of the various lithological assemblages in the study area. The entire geochronology dataset was used to develop a stratigraphic model and to position each stratigraphic unit within an evolution model through time (Figures 3.1 and 3.2). The age of units and the regional stratigraphic relationships between Archean units are discussed in the section entitled "Geochronology and regional relationships between Archean units".

DESCRIPTION OF STRATIGRAPHIC UNITS

The following section provides a general description of stratigraphic units in the northeastern Superior Province illustrated on the stratigraphic map (insert) and in Figures 3.3 to 3.11. The stratigraphic order proposed in the map legend and the figures takes into account the many U/Pb ages obtained under the Far North Program as well as field

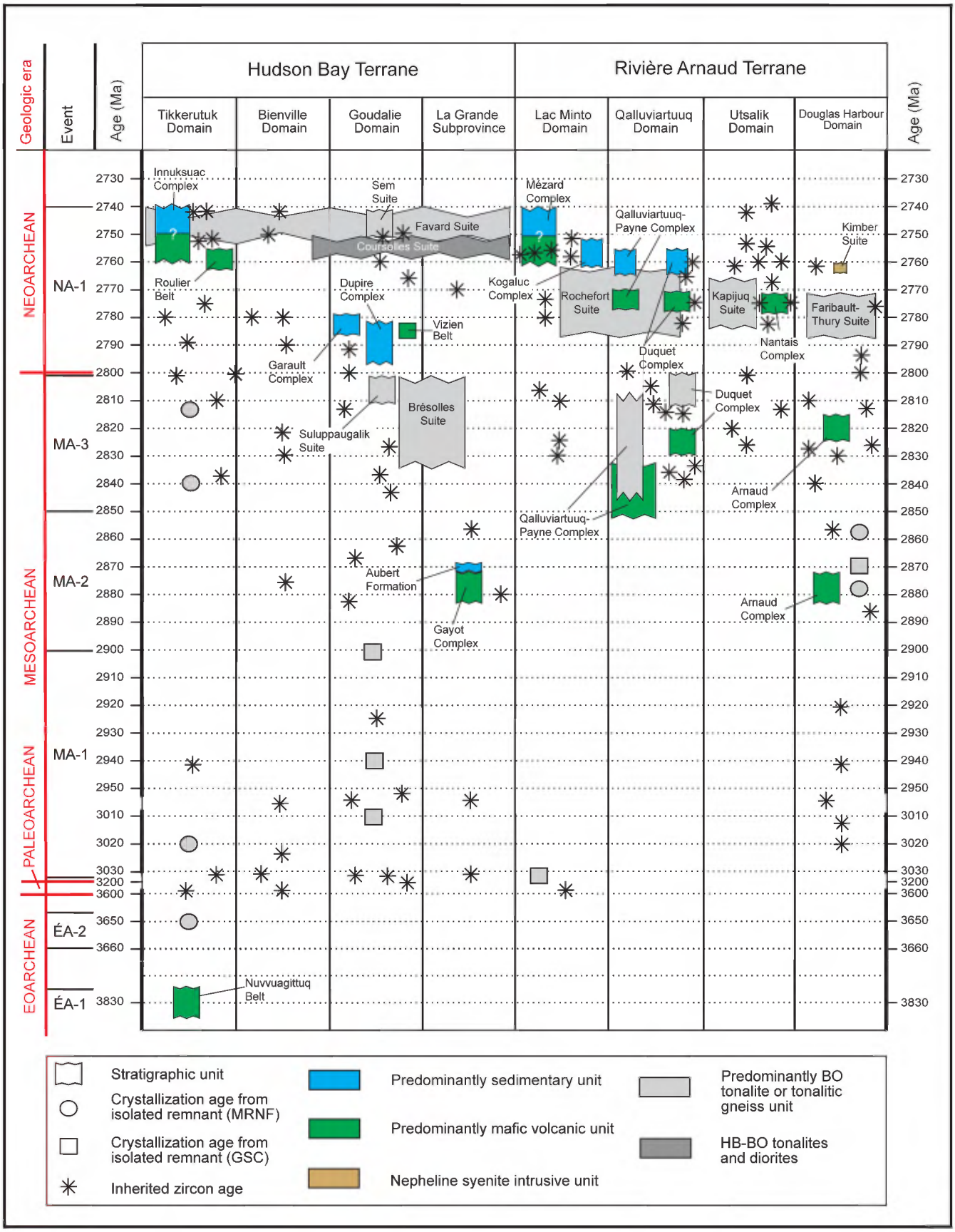

FIGURE 3.1 – Time distribution of stratigraphic units, crystallization ages from isolated remnants, and inherited zircon ages for the Archean eon prior to 2740 Ma.

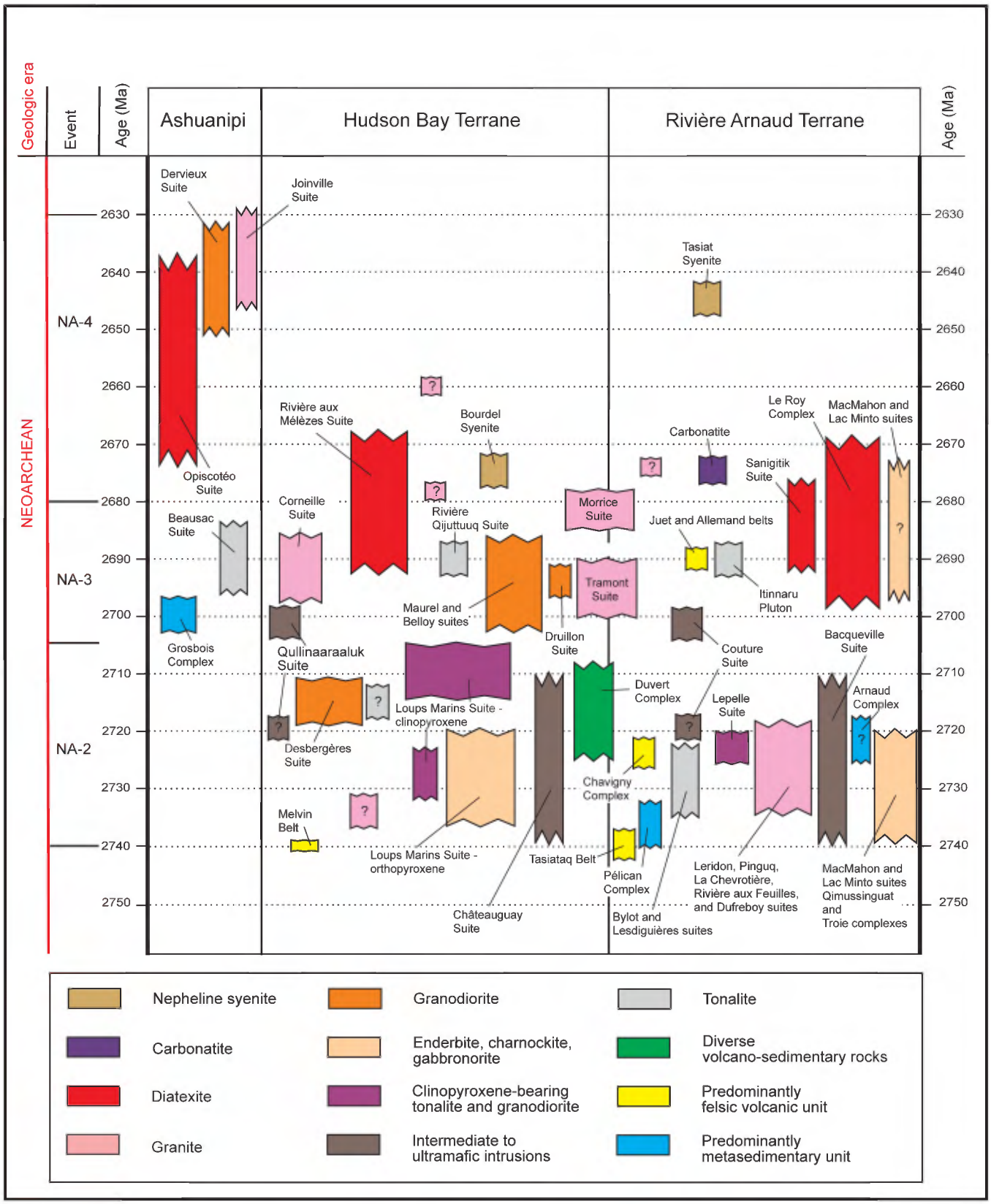

FIGURE 3.2 – Time distribution of stratigraphic units in the Archean eon from 2740 to 2630 Ma.

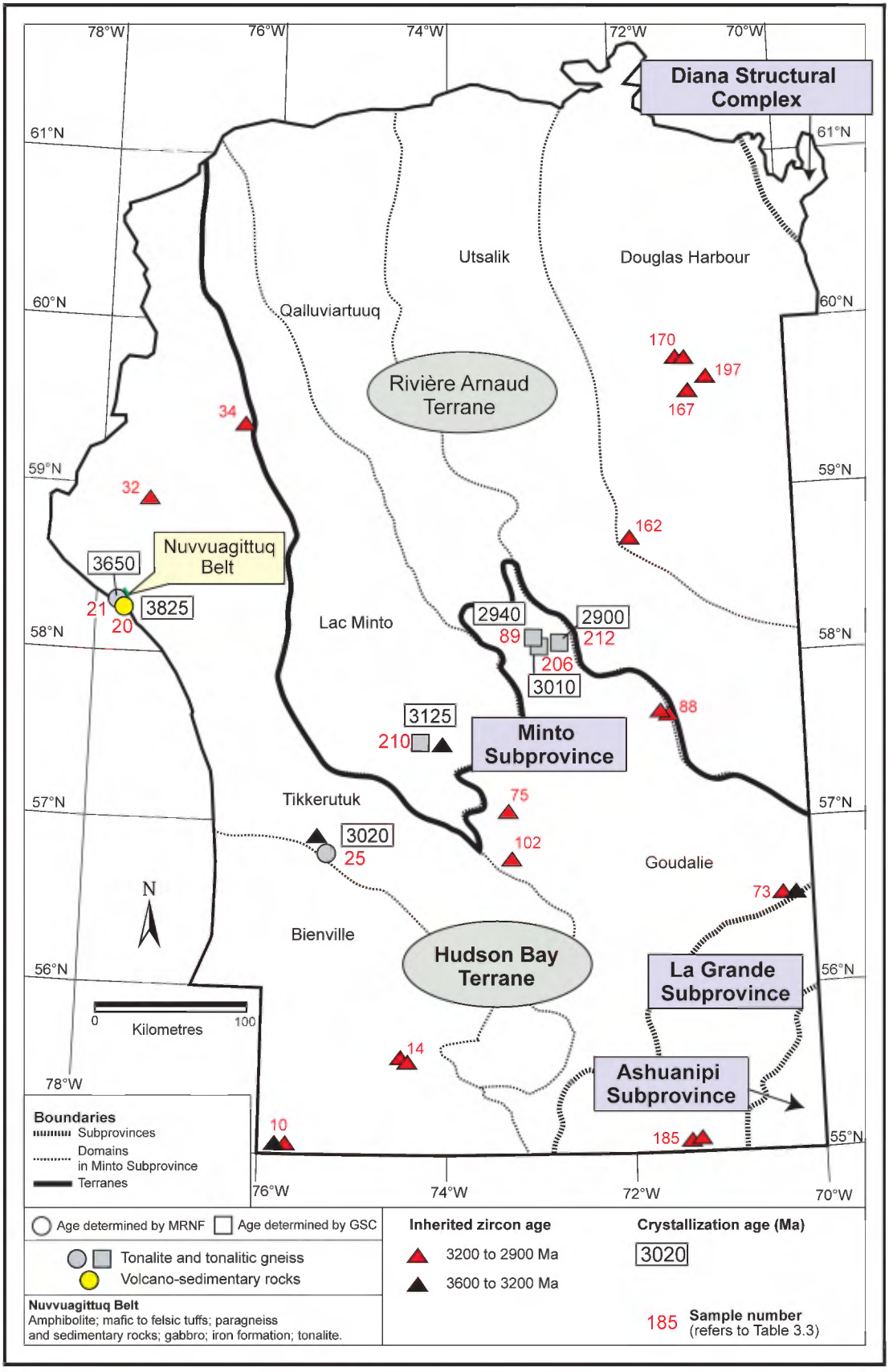

FIGURE 3.3 – Regional distribution of stratigraphic units, crystallization ages, and inherited zircon ages for the time span from 3850 to 2900 Ma.

relationships observed by the various authors of geological reports within the study area (Figure 1.1). The vast majority of units are Archean in age. A few Proterozoic, Paleozoic, and Cenozoic units are also described.

Archean units

Nuvvuagittuq Belt (Anuv)

The *Nuvvuagittuq Belt* (Berclaz *et al.*, 2003; Table 3.1 and Figure 3.3), initially named the Porpoise Cove belt (Simard *et al.*, 2004), is the oldest stratigraphic unit in the NESP. Simard *et al.* (2004) had included this belt in the volcano-sedimentary Innuksuac Complex but given its very early age (3825 Ma; No. 20, Figure 3.3 and Table 3.3), it was excluded from the complex. The Nuvvuagittuq volcano-sedimentary sequence is composed of three lobes corresponding to synforms. The first, covering about 10 km^2, is composed of: 1) amphibolites associated with iron formations and ultramafic sills; 2) mafic to felsic tuffs and paragneisses associated with polygenic conglomerates and quartzites; 3) various schists; 4) gabbros; and 5) gneissic to migmatitic tonalites. The two other lobes, separated from the first by a mylonite zone, are located to the northeast and east of the latter. They are mainly composed of foliated to banded amphibolite. All mafic rocks in the Nuvvuagittuq Belt have a tholeiitic affinity.

Gayot Complex (Agat)

The *Gayot Complex* (Table 3.1 and Figure 3.4) was named by Gosselin and Simard (2001) in the Lac Gayot area (No. 21, Figure 1.1). This complex is composed of volcano-sedimentary rocks occurring in several belts of variable dimensions, isolated from one another. Informal names were given to the largest belts (Gosselin and Simard, 2001; Simard *et al.*, 2002), among which the Pitaval, Coulon, Charras, Vimeux, Vénus, Marylin, Moyer, and Angilbert belts (Figure 7.1). The Gayot Complex comprises ultramafic to felsic volcanic effusive and intrusive rocks as well as a few layers of metasedimentary rocks and iron formation horizons. Tholeiitic basalts are the dominant lithology, and the presence of significant amounts of spinifex-textured komatiites is one of the main characteristics of this unit. Certain belts also contain minor amounts of tonalitic gneiss. Age determinations on felsic rocks yielded ages of 2880 Ma and 2873 Ma (Nos. 184 and 185, Figure 3.4 and Table 3.3). A much younger age of 2719 Ma (No. 186, Figure 3.6 and Table 3.3) was obtained from a felsic injection in the Vénus belt.

Aubert Formation (Aat)

The *Aubert Formation* (Table 3.1 and Figure 3.4) was introduced in the Lac Gayot area (No. 21, Figure 1.1). This unit consists of weakly migmatitic metasedimentary rocks, mainly banded paragneiss with hornblende + biotite, paragneiss with cordierite + sillimanite + andalusite + garnet + biotite, minor schist, and rare iron formation horizons. The unit also contains polygenic conglomerate alternating with quartz sandstone and clayey sandstone. The conglomerate contains clasts of amphibolitic basalt, crystal tuff, tonalitic gneiss, and iron formation derived from the Gayot Complex. The approximate age of sedimentary rocks in the Aubert Formation is estimated between 2.87 and 2.83 Ga.

Qalluviartuuq-Payne Complex (Aqlp)

The *Qalluviartuuq-Payne Complex* (Table 3.1 and Figure 3.4) was introduced by Berclaz *et al.* (2005) to designate the Qalluviartuuq and Lac Payne belts (Percival *et al.*, 1995a; Figure 7.1). In this report, several remnants previously assigned to the Kogaluc Complex (Parent *et al.*, 2003b) and directly located along the southeast extension of the Qalluviartuuq-Payne Complex are also included in the unit. The unit thus redefined extends over about 180 kilometres strike length and is less than 30 kilometres wide. It is composed of supracrustal rocks forming at least two volcano-sedimentary cycles, affected by several phases of deformation. The first volcanic cycle, of tholeiitic affinity, comprises massive amphibolites, mafic gneisses, extrusive ultramafic rocks, layered anorthosites and gabbros as well as intermediate rocks that represent either synvolcanic sills or metamorphosed andesites. Cycle 2, of calc-alkaline affinity, is formed of mafic to felsic lavas and tuffs showing various textures, interlayered with metre-scale beds of sandstone, clayey sandstone, conglomerate, and iron formation. The unit also includes a significant amount of metasedimentary rocks, forming kilometre-scale horizons. Tonalites are locally associated with the volcano-sedimentary rocks. The age of volcano-sedimentary rocks in the Qalluviartuuq-Payne Complex is estimated between 2851 and 2832 Ma (Nos. 83, 84, and 226, Figure 3.4 and Table 3.3), whereas the age of associated tonalites is estimated between 2848 and 2809 Ma (Nos. 95, 100, and 216). A younger age of 2768 Ma was also obtained in one remnant assigned to the complex (No. 215, Figure 3.5 and Table 3.3).

Arnaud Complex (Aarn)

The *Arnaud Complex* (Table 3.1 and Figure 3.4) is a new unit encompassing all volcano-sedimentary remnants that were previously assigned to the Troie, Qimussinguat, and Faribault-Thury complexes (Madore *et al.*, 2000 and 2002; Madore and Larbi, 2001; Cadieux *et al.*, 2004; Leclair *et al.*, 2003). In this complex are included the Faribault, Rivier, Tasiaalujjuaq, Hamelin, Peters-West, Thury, Curotte, Gorribon, Trempe, Buet, Kimber, and Papijjusaq belts (Figure 7.1). This unit is composed of mafic or intermediate volcanic rocks of tholeiitic affinity. Altered, metamorphosed layers of pyroxenite, peridotite, and dunite, as well as komatiitic lava flows are intercalated in the sequence. The unit also includes paragneiss with biotite ± garnet ± sillimanite ± cordierite,

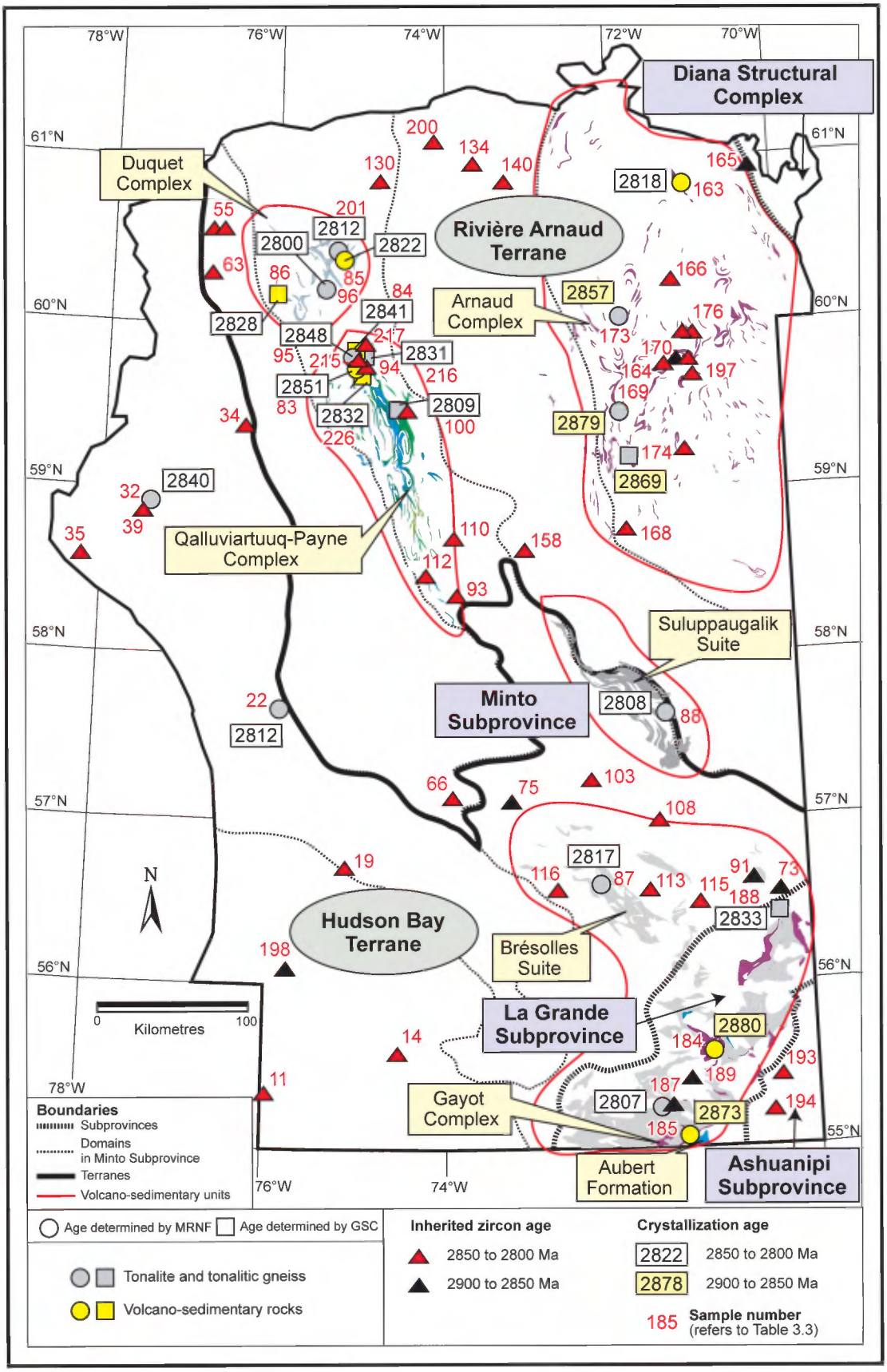

FIGURE 3.4 – Regional distribution of stratigraphic units, crystallization ages, and inherited zircon ages for the time span from 2900 to 2800 Ma.

Stratigraphic legend (Figure 3.4)

Suluppaugalik Suite
Heterogeneous tonalitic gneiss; numerous enclaves and late injections.

Brésolles Suite
Banded, heterogeneous tonalitic and dioritic gneiss; numerous enclaves and late injections.

Duquet Complex
Mafic volcanic rocks of tholeiitic affinity; metasedimentary remnants; minor ultramafic to felsic volcanic rocks.

Arnaud Complex
Mafic to intermediate volcanic rocks of tholeiitic affinity; intrusive and effusive ultramafic rocks; metasedimentary remnants.

Qalluviartuuq-Payne Complex
Mafic to intermediate volcanic rocks of tholeiitic affinity (cycle 1); mafic to felsic rocks of calc-alkaline affinity (cycle 2) (green); metasedimentary rocks (blue).

Aubert Formation
Metasedimentary rocks including paragneiss, minor schist and iron formation, as well as a conglomerate unit with clasts from the Gayot Complex.

Gayot Complex
Tholeiitic basalt, spinifex-textured komatiite, ultramafic to felsic effusive and intrusive rocks; metasedimentary rocks; iron formation; minor gneissic tonalite.

associated with a few layers of marble, calc-silicate rock, and iron formation. Rocks of the Arnaud Complex are typically metamorphosed to the amphibolite facies where they are enclosed in tonalites of the Faribault-Thury Suite, and to the granulite facies where they occur in pyroxene-bearing intrusions of the Qimussinguat and Troie complexes. Ages of 2818 Ma (No. 163, Figure 3.4 and Table 3.3), 2782 Ma (No. 164, Figure 3.5), 2725 and 2718 Ma (Nos. 231 and 197, Figure 3.6) were obtained in various belts of the complex. Consequently, the predominant age of this unit remains uncertain at this time.

Duquet Complex (Aduq)

The *Duquet Complex* (Table 3.1 and Figure 3.4) designates all volcanic and metasedimentary remnants that were previously assigned to the Duquet belt by Madore *et al.* (2004). Volcanic remnants are mainly composed of tholeiitic metabasalts and mafic gneisses locally alternating with layers of ultramafic, intermediate, or felsic rocks as well as thin horizons of paragneiss, conglomerate or rare marble, calc-silicate rock and iron formation. Metasedimentary remnants consist of variably migmatitic paragneiss. The unit also includes tonalitic layers locally associated with the volcano-sedimentary rocks. Samples of volcanic rocks yielded ages of 2822 and 2828 Ma (Nos. 85 and 86, Figure 3.4 and Table 3.3), whereas associated tonalitic rocks yielded ages of 2812 and 2800 Ma (Nos. 201 and 96). A younger age, at 2775 Ma (No. 99, Figure 3.5 and Table 3.3), was obtained in a felsic dyke (Percival *et al.*, 1997b). Finally, clasts in a conglomerate layer were dated at 2764 Ma (Percival and Skulski, 2000).

Brésolles Suite (Abre)

The *Brésolles Suite* (Table 3.1 and Figure 3.4) is located in the La Grande Subprovince and in the Goudalie Domain, within the Hudson Bay Terrane. This unit was introduced in the Lac Gayot area (Figure 1.1) to describe an assemblage of banded gneiss consisting of alternating light-coloured bands composed of biotite tonalite and darker bands composed of diorite, quartz diorite, and melanocratic biotite-hornblende tonalite. The gneisses host abundant amphibolite enclaves of variable dimensions. They are also injected with late tonalitic and granitic material parallel to the foliation, which enhances the heterogeneity of this unit. Numerous folds from 1 to 10 metres in size are commonly observed in rocks of this unit. U/Pb analyses indicate an age ranging between 2833 and 2807 Ma for the Brésolles Suite (Nos. 188, 87, and 187, Figure 3.4 and Table 3.3).

Suluppaugalik Suite (Aspk)

The *Suluppaugalik Suite* (Table 3.1 and Figure 3.4) is located in the Goudalie Domain, within the Hudson Bay Terrane. This unit, named by Parent *et al.* (2001) in the Lac Nedlouc area, is formed of heterogeneous, foliated or gneissic tonalites that exhibit a remarkable lithological and structural complexity at outcrop scale. The gneisses contain numerous enclaves of variable sizes, with compositions ranging from ultramafic to intermediate. The tonalites are invaded by granitic and granodioritic material, which enhances the heterogeneity of the unit. An age of 2808 Ma (No. 88, Figure 3.4 and Table 3.3) was obtained for the Suluppaugalik Suite.

Dupire Complex (Adpr)

The *Dupire Complex* (Table 3.1 and Figure 3.5) was introduced by Parent *et al.* (2001) to describe the volcano-sedimentary rocks in the Lac Dupire area, including five remnants referred to as the Lac Dupire volcano-sedimentary zone (Lamothe, 1997). Gosselin *et al.* (2002) included in this unit the Pastorel and De l'Île belts in the Lacs des Loups Marins area (Figure 1.1). The complex is composed of biotite-hornblende ± garnet paragneiss and biotite ± garnet paragneiss, associated with minor quartzite, tholeiitic metabasalt, metarhyolite and felsic pyroclastic rocks, silicate- and oxide-facies iron formations, and anthophyllite-cordierite-biotite schists. In many locations, mafic and ultramafic sills are intercalated in the volcano-sedimentary sequences. All lithologies in this complex are metamorphosed to the amphibolite facies. The age of this unit is estimated between 2798 and 2787 Ma (Nos. 74 and 75, Figure 3.5 and Table 3.3).

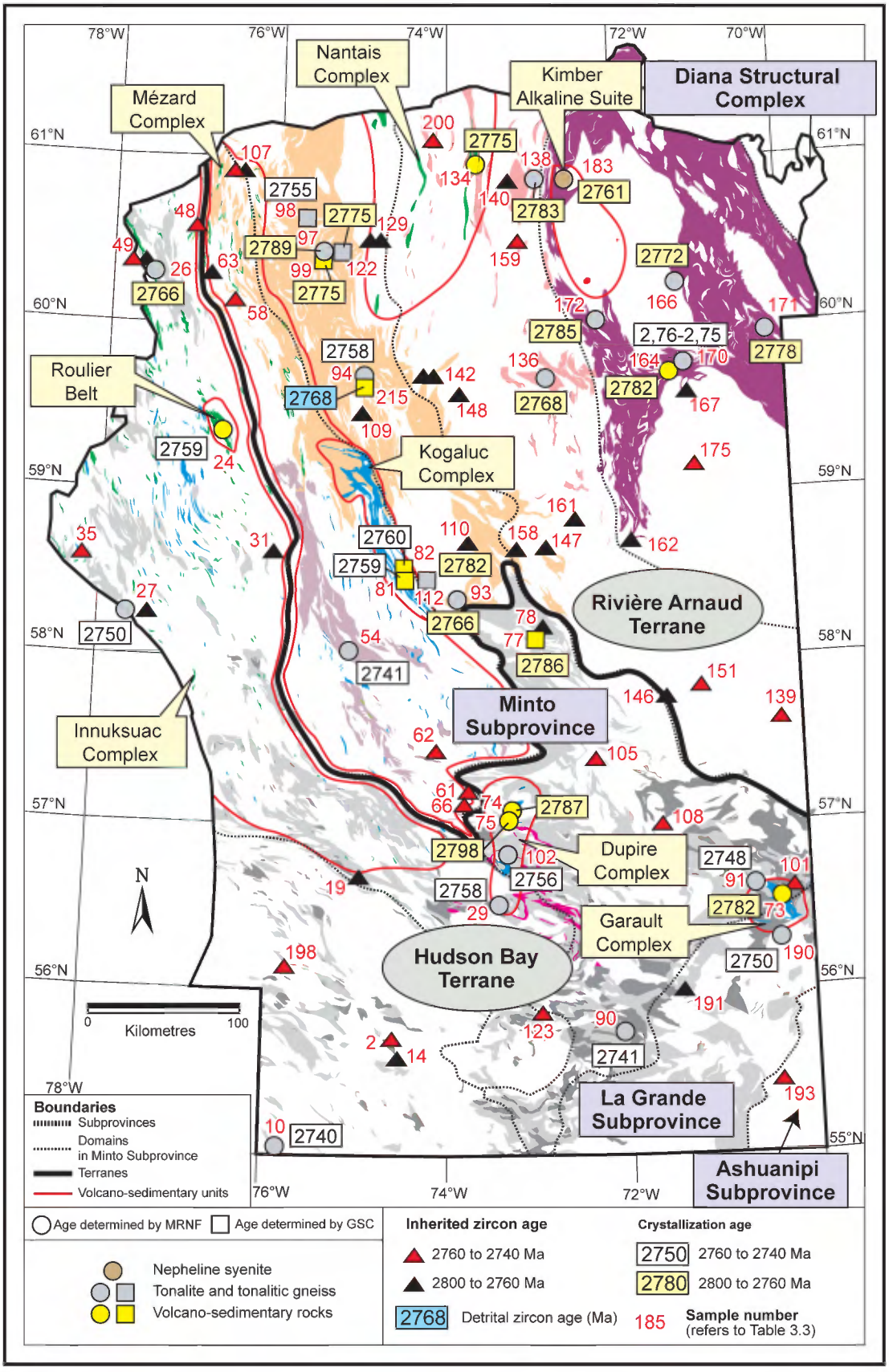

FIGURE 3.5 – Regional distribution of stratigraphic units, crystallization ages, and inherited zircon ages for the time span from 2800 to 2740 Ma.

Stratigraphic legend (Figure 3.5)

Kakiattuq Suite
Granitized biotite tonalite; minor hornblende-biotite tonalite; numerous enclaves of variable composition.

Sem Suite
Biotite-rich tonalite with a diatexitic aspect; numerous enclaves of diorite.

Favard Suite
Granitized biotite trondhjemite and tonalite; minor hornblende-biotite tonalite.

Coursolles Suite
Granitized hornblende-biotite tonalite; early diorite and gabbro.

Innuksuac Complex
Granoblastic amphibolite of tholeiitic affinity (north half in green) and migmatitic paragneiss (south half in blue).

Roulier Belt
Mafic volcanic rocks of tholeiitic affinity; metapelites; felsic tuffs.

Mézard Complex
Granoblastic amphibolite (north half in green) and migmatitic paragneiss (south half in blue).

Kogaluc Complex
Metasedimentary rocks (80%) and calc-alkaline volcanic rocks (20%).

Kimber Alkaline Suite
Massive, homogeneous, undeformed nepheline syenite.

Nantais Complex
Mafic metavolcanic rocks of tholeiitic affinity.

Kapijuq Suite
Foliated to gneissic biotite tonalite and biotite-hornblende tonalite, with a migmatitic aspect.

Rochefort Suite
Foliated to gneissic biotite tonalite and biotite-hornblende tonalite, with a migmatitic aspect.

Faribault-Thury Suite
Foliated to gneissic biotite tonalite and biotite-hornblende tonalite, with a migmatitic aspect.

Garault Complex
Metasedimentary rocks, minor calc-alkaline volcanic rocks.

Dupire Complex
Metasedimentary rocks, mafic to felsic volcanic rocks of tholeiitic affinity.

Garault Complex (Agar)

The *Garault Complex* (Table 3.1 and Figure 3.5) is a unit of volcano-sedimentary rocks primarily located in the Vallerenne belt, in the southeast part of the study area. In this area, Simard *et al.* (2002) recognized two distinct belts separated by a fault, namely the Angilbert-North belt, assigned to the Garault Complex, and the Angilbert-South belt, comprising rocks of the Gayot Complex. In order to eliminate any potential confusion in the nomenclature, the Angilbert-North belt is renamed the Vallerenne belt and the Angilbert-South belt is renamed the Angilbert belt. The Garault Complex is composed of biotite paragneiss, muscovite schist, quartz sandstone, and a few layers of conglomerate. The complex also contains basalts, andesites, felsic volcanic rocks, gabbros, diorites, and minor tonalitic gneiss. All volcanic effusive and intrusive rocks, whether mafic or felsic in composition, have a calc-alkaline affinity. A sample of the Garault Complex yielded an age of 2782 Ma (No. 73, Figure 3.5 and Table 3.3).

Faribault-Thury Suite (Afth)

The *Faribault-Thury Suite* (Table 3.1 and Figure 3.5) encompasses all the tonalitic rocks that were previously assigned to the Faribault-Thury Complex (Madore *et al.*, 2000 and 2001; Madore and Larbi, 2001; Cadieux *et al.*, 2004). The volcano-sedimentary rocks and granitic intrusions that were initially included in this complex are reassigned to the Arnaud Complex and the Leridon Suite respectively, and the term "Faribault-Thury Complex" is abandoned (Table 3.2). The Faribault-Thury Suite is composed of strongly foliated to gneissic tonalites and trondhjemites that commonly exhibit a granoblastic texture. Trondhjemites contain less than 10% biotite, whereas tonalites contain 10 to 40% mafic minerals (hornblende + biotite). Tonalitic to granitic mobilizate (5 to 50%), occurring as centimetre-scale to metre-scale discontinuous veins, gives the tonalites and trondhjemites a migmatitic aspect. Rocks of the Faribault-Thury Suite contain 5 to 25% enclaves of amphibolite, diorite, and gabbro. Tonalite samples yielded ages ranging from 2785 to 2772 Ma (Nos. 172, 171, and 166, Figure 3.5 and Table 3.3) as well as earlier ages ranging from 2879 to 2857 Ma (Nos. 169, 173, and 174, Figure 3.4).

Rochefort Suite (Arot)

The *Rochefort Suite* (Table 3.1 and Figure 3.5) encompasses tonalites that were initially assigned to the suite within the Rivière Arnaud Terrane (Leclair *et al.*, 2002; Berclaz *et al.*, 2005). It also includes some tonalites formerly included in the Rivière aux Feuilles Suite and the Kakiattuq Suite. However, tonalites previously assigned to the Rochefort Suite but located within the Hudson Bay Terrane are reassigned to the Favard Suite. The Rochefort Suite is composed of leucocratic biotite tonalites and trondhjemites and melanocratic biotite-hornblende tonalites, which are foliated to gneissic, medium- to coarse-grained and exhibit an igneous or granoblastic texture. Tonalites of the Rochefort Suite commonly contain a granodioritic or granitic fraction occurring as small pockets, dykes, or veins with sharp or diffuse contacts. Several age determinations made on tonalite samples of the Rochefort Suite yielded ages ranging from 2789 to 2755 Ma (Nos. 93, 94, 97, 98, 112, and 122, Figure 3.5 and Table 3.3).

Kapijuq Suite (Akpj)

Along with the original tonalites of the *Kapijuq Suite* (Table 3.1 and Figure 3.5), this unit also encompasses tonalites formerly assigned to the Bottequin Suite (Cadieux

et al., 2002) and the Nantais volcano-sedimentary belt (Madore *et al.*, 2004). As a result, the term "Bottequin Suite" is abandoned (Table 3.2). The Kapijuq Suite is composed of foliated to gneissic tonalites and trondhjemites that commonly exhibit a granoblastic texture. Tonalites contain 10 to 40% mafic minerals (hornblende + biotite), whereas trondhjemites contain less than 10% (predominantly biotite). The presence of centimetre-scale to metre-scale discontinuous veins of tonalitic to granitic mobilizate (5 to 50%), conformable or cross-cutting the regional foliation, imparts a migmatitic aspect to these rocks. The unit contains 5 to 25% enclaves of amphibolite, diorite, and paragneiss. U/Pb ages of 2783 Ma and 2768 Ma were obtained for tonalites of the Kapijuq Suite (Nos. 138 and 136, Figure 3.5 and Table 3.3).

Nantais Complex (Anan)

The *Nantais Complex* (Table 3.1 and Figure 3.5) is a new volcano-sedimentary unit that includes the Nantais belt as well as the Peltier, Headwind, and Caumartin belts (Figure 7.1; Madore *et al.*, 2004). Initially, the Pélican-Nantais Complex (Percival *et al.*, 1997a; Madore *et al.*, 2002) encompassed metavolcanic rocks of the Nantais belt to the north and metasedimentary rocks of the Pélican belt to the south. Lithological and geochronological differences between the two belts led us to divide the complex into two distinct units, namely the Nantais Complex and the Pélican Complex. The Peltier, Headwind, and Caumartin belts are assigned to the Nantais Complex based on their lithological similarities with rocks of the Nantais belt and their spatial distribution. The term "Pélican-Nantais Complex" is abandoned (Table 3.2).

The Nantais Complex is primarily composed of tholeiitic metabasalts and mafic gneisses with a granoblastic texture, exhibiting centimetre-scale compositional banding. These rock types locally alternate with intermediate to felsic tuffs, conglomerates, and rare ultramafic rocks. Rocks of the Nantais Complex underwent amphibolite-grade to granulite-grade metamorphism. A felsic tuff sample from the Nantais belt yielded an age of 2775 Ma (No. 134, Figure 3.5 and Table 3.3).

Kimber Alkaline Suite (Akmb)

The *Kimber Alkaline Suite* (Table 3.1 and Figure 3.5) designates three small (<30 km^2) discrete intrusions of nepheline syenite located in the northeast part of the Rivière Arnaud Terrane. These homogeneous undeformed rocks exhibit a magmatic granular texture. Pegmatitic and aplitic syenite phases cross-cut the main intrusive body. An age determination made on one of these phases yielded an age of 2761 Ma (No. 183, Figure 3.5 and Table 3.3). This result is remarkable, given the massive and undeformed character of these rocks and the much younger ages (<2680 Ma) obtained for other alkaline intrusions in the NESP.

Kogaluc Complex (Akog)

The *Kogaluc Complex* (Table 3.1 and Figure 3.5) was introduced by Parent *et al.* (2003b) in the Lac Vernon area (Figure 1.1). It consists of discontinuous bands of supracrustal rocks, about 1 to 8 kilometres wide and extending along a NNW-SSE axis for about 15 kilometres strike length. This complex is composed of 80% sedimentary rocks and 20% volcanic rocks, all metamorphosed to the amphibolite facies. A few sedimentary remnants initially included in the Kogaluc Complex were reassigned to the Qalluviartuuq-Payne Complex. Sedimentary rocks include biotite paragneiss, iron formation, sandstone, siltstone, quartzite, argillite, and rare polygenic conglomerate. Volcanic rocks are concentrated in the south part of the complex, where 1- to 10-metre-thick layers of calc-alkaline mafic, intermediate, and felsic volcanic rocks alternate. Primary textures and structures are locally preserved in these rocks. Ages of 2759 Ma and 2760 Ma were obtained for felsic rocks of the Kogaluc Complex (Nos. 81 and 82, Figure 3.5 and Table 3.3).

Mézard Complex (Amez)

The *Mézard Complex* (Table 3.1 and Figure 3.5) was introduced by Berclaz *et al.* (2005) to describe volcano-sedimentary remnants and diatexites mapped in the north part of the Lac Minto Domain (Figure 1.1). This unit is redefined to encompass all sedimentary and volcanic remnants within the Lac Minto Domain, with the exception of volcano-sedimentary rocks of the Kogaluc Complex. The Mézard Complex now includes supracrustal rocks initially assigned to the unit (Berclaz *et al.*, 2005; Maurice *et al.*, 2005a and 2005b) as well as those previously assigned to the Le Roy Complex (Parent *et al.*, 2003b; Berclaz *et al.*, 2005; Simard *et al.*, 2005a) and the Lac Minto Suite (Parent *et al.*, 2001). Diatexites that were included in these three units and that represent the products of melting of sedimentary rocks are reassigned to the Le Roy Complex.

The Mézard Complex is composed of amphibolite-grade and granulite-grade supracrustal rocks occurring in lens-shaped remnants less than 3 kilometres wide by less than 10 kilometres long. Volcanic bands are mainly concentrated in the north part of the complex (Figure 3.5). They contain massive, foliated or banded granoblastic amphibolites and a few intermediate to felsic horizons from 1 to 10 metres in size. Sedimentary bands are composed of foliated to banded, fine- to medium-grained paragneiss that exhibits a characteristic rusty brown to yellowish weathered surface. The paragneisses underwent intense migmatization, which translates into the presence of tonalitic to granitic melt products accounting for up to 50% of the volume of the rock. Iron formations from 1 to 10 metres thick are locally associated with the paragneisses. Paragneiss remnants of the Mézard Complex are concentrated in the south part of the unit. However, paragneisses are probably just as abundant in

the north part of the unit, only in this area, migmatitic paragneisses were not differentiated from diatexites (assigned to the Le Roy Complex). The Mézard Complex has not been dated. The age of many remnants is estimated in the 2760 to 2740 Ma range.

Roulier Belt (Arlr)

The *Roulier Belt* (Table 3.1 and Figure 3.5), introduced by Maurice *et al.* (2005b), corresponds to a volcano-sedimentary sequence about 10 kilometres wide by 30 kilometres long. It is mainly composed of massive to foliated mafic volcanic rocks of tholeiitic affinity. It also includes variably migmatitic metapelite horizons from 1 to 10 metres thick, intercalated in the mafic rock sequence, along with crystal and lapilli tuffs. Primary textures are locally preserved. Gabbro dykes with a well-preserved sub-ophitic texture cross-cut rocks in the belt. A felsic sample yielded an age of 2759 Ma (No. 24, Figure 3.5 and Table 3.3).

Innuksuac Complex (Ainn)

The *Innuksuac Complex* (Table 3.1 and Figure 3.5) encompasses all remnants of volcanic and sedimentary rocks in the Tikkerutuk Domain, with the exception of the Nuvvuagittuq Belt and the Roulier Belt. Certain remnants located in the north part of the domain were initially assigned to the Povungnituk Complex (Maurice *et al.*, 2005b and 2005), whereas small remnants in the south part of the domain had been included in the Melvin Complex (Simard *et al.*, 2005b and 2005a). All these volcano-sedimentary rocks are reassigned to the Innuksuac Complex due to their spatial distribution and their lithological similarities with rocks of the latter unit. As a result, the terms "Povungnituk Complex" and "Melvin Complex" are abandoned (Table 3.2).

Volcanic rocks in the Innuksuac Complex consist of massive, foliated or banded, granoblastic amphibolites of tholeiitic affinity, whose intrusive or effusive origin could not be determined. Ultramafic rocks, paragneiss, and iron formation horizons alternate with the amphibolites. Remnants of migmatitic paragneiss are occasionally associated with layers of intermediate volcanic rocks and silicate-facies iron formations. Volcanic and sedimentary remnants are metamorphosed to the amphibolite and the granulite facies. The Innuksuac Complex has not been dated. The age of most remnants in the complex is estimated between 2760 and 2740 Ma. However, near Hudson Bay, a younger age of <2729 Ma was obtained in a sedimentary rock intercalated in an amphibolite sequence (No. 23, Figure 3.6 and Table 3.3).

Coursolles Suite (Acou)

The *Coursolles Suite* (Table 3.1 and Figure 3.5), named by Simard *et al.* (2002) in the Maricourt area (Figure 1.1), outcrops in the south part of the Minto Subprovince and the northernmost part of the La Grande Subprovince. It mainly consists of hornblende-biotite tonalite, with minor proportions of diorite, quartz diorite, and gabbro. The tonalite contains 10 to 25% centimetre-scale elongated clusters of mafic minerals (hornblende + biotite), whereas diorite-gabbro units contain 25 to 40% mafic minerals that define the foliation. Diorite-gabbro units occur as enclaves in the tonalite or are injected by the latter, indicating their early character. The tonalite contains a granodioritic to granitic phase occurring as bands, lenses or pockets in diffuse contact with the tonalitic phase. Two tonalite samples yielded ages of 2758 Ma and 2756 Ma (Nos. 29 and 102, Figure 3.5 and Table 3.3), interpreted as the main age of emplacement for the unit. Younger ages, at 2716 and 2713 Ma (Nos. 101 and 30, Figure 3.6 and Table 3.3), were also obtained for rocks assigned to the Coursolles Suite, suggesting this suite may also contain rocks related to a much younger magmatic event.

Favard Suite (Afav)

The *Favard Suite* (Table 3.1 and Figure 3.5) covers an extensive surface area in the Hudson Bay Terrane. This unit was defined in the Lac Gayot area (Gosselin and Simard, 2001) and subsequently recognized in many other areas to the north and west (Gosselin *et al.*, 2002 and 2004; Roy *et al.*, 2006; Simard *et al.*, 2002, 2005b, and 2005a). This unit is redefined in this report to encompass tonalites of the Charnière (Parent *et al.*, 2001), Qamanirjuaq and Boizard suites (Simard *et al.*, 2004), as well as a few tonalitic intrusions of the Rivière aux Feuilles Suite (Parent *et al.*, 2001) and the Du Gué Complex (Simard *et al.*, 2002). The new unit also includes tonalites previously assigned to the Rochefort Suite within the Hudson Bay Terrane (Parent *et al.*, 2001; Leclair *et al.*, 2002; Maurice *et al.*, 2005a and 2005b). As a result of these modifications, the terms "Charnière Suite", "Qamanirjuaq Suite", and "Boizard Suite" are abandoned (Table 3.2).

The Favard Suite is composed of biotite trondhjemite and leucotonalite, which contain 2 to 40% enclaves of granoblastic amphibolite and diorite. A few layers of hornblende-biotite tonalite, from 1 to 10 metres thick, locally alternate with the leucotonalites and trondhjemites. Tonalites of the Favard Suite have undergone granitization, which translates into the presence of granitic and granodioritic lenses, bands, or pockets in gradual and diffuse contact with the tonalitic phase. The granitic phase is often significant and may account for up to 50% of exposed outcrops. Several age determinations were made, making it possible to estimate the age of the Favard Suite between 2766 and 2740 Ma (Nos. 10, 26, 27, 90, 91, and 190, Figure 3.5 and Table 3.3). Sample No. 90, a granitized tonalite, yielded an age of 2741 ±4 Ma for the tonalitic phase and an age of 2713 ±2 Ma (Figure 3.7) for the granitic phase. A few samples of tonalite yielded younger ages, at 2719 and 2717 Ma (Nos. 189 and 28, Figure 3.6 and Table 3.3), and one older age of 3020 Ma (No. 25,

Figure 3.3 and Table 3.3), suggesting the Favard Suite may encompass younger and older tonalites that exhibit field characteristics similar to tonalites of this unit.

Sem Suite (Asem)

The *Sem Suite* (Table 3.1 and Figure 3.5) was recognized only in the Lacs des Loups Marins area (No. 17, Figure 1.1). It is composed of heterogeneous tonalite characterized by the presence of 20 to 40% biotite. The heterogeneity of this tonalite is due to its variable grain size and the irregular distribution of biotite that commonly forms wavy, discontinuous bands similar in appearance to schlieren observed in diatexites. The unit also contains abundant enclaves, primarily dioritic in composition. The age of this unit is unknown and its relationship with other units is uncertain.

Kakiattuq Suite (Akkk)

The *Kakiattuq Suite* (Table 3.1 and Figure 3.5), introduced by Parent *et al.* (2003b), is located in the south part of the Lac Minto Domain (Figure 2.2), near the edge of the Hudson Bay Terrane. A few tonalitic intrusions of the Kakiattuq Suite were reassigned to the Rochefort Suite. The Kakiattuq Suite is composed of weakly foliated biotite leucotonalite. Locally, hornblende tonalite horizons from 1 to 10 metres thick alternate with biotite tonalites. In certain locations, these tonalites contain 20 to 50% enclaves of paragneiss, amphibolite, mafic to intermediate gneiss, gabbronorite, and iron formation, which give the rock a heterogeneous aspect. Tonalites of the Kakiattuq Suite contain a granodioritic to granitic phase (10 to 50%) occurring in diffuse contact with the tonalitic phase. An age of 2741 Ma was obtained in a tonalite sample (No. 54, Figure 3.5 and Table 3.3).

Melvin Belt (Amel)

The *Melvin Belt* (Table 3.1 and Figure 3.6) is a small unit of felsic volcanic rocks located along the boundary between the Tikkerutuk and Bienville domains (Figure 2.2). These felsic rocks were initially assigned to the Melvin Complex (Simard *et al.*, 2005b and 2005a) and were informally referred to as the Natwakupaw belt (Simard *et al.*, 2005b), a term now abandoned. The term "Melvin Complex" is also abandoned, and the other lithological assemblages in the Melvin Complex have been assigned to other units (Table 3.2). For instance, sedimentary and mafic volcanic remnants were reassigned to the Innuksuac Complex and small intrusions of granoblastic diorite and gabbro are now included in the Bacqueville Suite. The Melvin Belt is composed of greenish to medium grey, very fine-grained felsic rocks, with or without quartz phenocrysts, with textures ranging from massive to laminated. These calc-alkaline rocks probably represent a mixture of metamorphosed and deformed lavas and tuffs, given the primary textures and structures that are locally preserved. An age of 2741 Ma (No. 19, Figure 3.6 and Table 3.3) was obtained from a rock sample collected in this belt.

Tasiataq Belt (Atsq)

The *Tasiataq Belt* (Table 3.1 and Figure 3.6) was named by Leclair *et al.* (2003) in the Lac Dufreboy area (Figure 1.1). It is largely composed of metamorphosed basalts and andesites, interlayered with felsic volcanic rocks (rhyolite, dacite, and associated tuffs) and silicate-facies iron formations. The belt also includes a few layers of pyroxenite, peridotite, hornblendite, and serpentinite, locally associated with mesocratic gabbro. A felsic sample yielded an age of 2740 Ma (No. 162, Figure 3.6 and Table 3.3).

Pélican Complex (Apel)

The *Pélican Complex* (Table 3.1 and Figure 3.6) is a new unit comprising the Pélican belt and a few other metasedimentary remnants that were previously included in the "Pélican-Nantais Complex", a term now abandoned (Table 3.2; see Nantais Complex). The Pélican Complex is mainly composed of paragneiss with minor amounts of biotite-garnet ± orthopyroxene ± cordierite ± sillimanite schist that exhibits compositional banding. Paragneisses have undergone migmatization, which translates into the presence of centimetre-scale to metre-scale veins of felsic mobilizate (5 to 50%). Oxide-facies, and rarely silicate-facies, iron formations are associated with the paragneisses. The unit also includes amphibolites or mafic gneisses, andesites, dacites, rhyodacites, and felsic schists. A sample of felsic rock yielded an age of 2739 Ma (No. 132, Figure 3.6 and Table 3.3), whereas an age of 2733 Ma (No. 135) was obtained from the mobilizate in a sedimentary rock.

Chavigny Complex (Achy)

The *Chavigny Complex* (Table 3.1 and Figure 3.6) is a volcano-sedimentary unit recognized in the Lac Vernon area (Figure 1.1). It is composed of felsic volcanic rocks (70%), mafic volcanic rocks (20%), and sedimentary rocks (10%). The felsic volcanic rocks mainly consist of rhyolitic to rhyodacitic flows and banded tuffs. Sedimentary rocks, generally associated with the felsic volcanic rocks, consist of greywacke, granoblastic paragneiss, and polygenic conglomerate. Mafic rocks are represented by tholeiitic andesitic basalts and basalts. Oxide-facies and silicate-facies iron formations are intercalated with the various volcanic and sedimentary units. Sericite schists, observed locally, are interpreted as metamorphosed volcanogenic hydrothermal alteration zones. An age of 2722 Ma (No. 53, Figure 3.6 and Table 3.3) was obtained in a felsic volcanic rock.

Duvert Complex (Advt)

The *Duvert Complex* (Figure 3.6 and Table 3.1) is composed of volcano-sedimentary rocks (Parent *et al.*, 2001; Berclaz *et al.*, 2002) occurring in four informal belts: the Duvert, Natuak, Morrice, and Kakiattukallak belts (Figure 7.1). We have added to this unit rocks initially assigned to the Qamaniq (Parent *et al.*, 2001), Vizien (Leclair *et al.*, 2002), and Du Gué (Simard *et al.*, 2002) complexes, based on the spatial distribution and age of these supracrustal rocks. Consequently, the terms "Qamaniq Complex", "Vizien Complex", and "Du Gué Complex" are abandoned (Table 3.2). The Vizien Belt, as defined by Percival and Card (1994), is maintained as a formal unit and is included in the Duvert Complex (Figure 7.1).

The Duvert Complex is composed of kilometre-scale remnants of supracrustal rocks, bounded by shear zones and enclaved in granitoid rocks. These supracrustal rocks are metamorphosed to the amphibolite or the granulite facies and exhibit a fairly well developed granoblastic texture. The various remnants consist of lens-shaped bands dominated either by massive or banded mafic gneisses and amphibolites of tholeiitic affinity, by banded intermediate or felsic volcanic rocks, or by variably migmatitic paragneisses. The complex also contains iron formations and calc-silicate rocks, generally associated with paragneisses, as well as intrusive and effusive ultramafic rocks, associated with amphibolites and mafic gneisses. A felsic sample collected in the Duvert belt yielded an imprecise age of about 2715 Ma (No. 76, Figure 3.6 and Table 3.3).

The *Vizien Belt* (Aviz) is composed of a wide variety of ultramafic to felsic volcanic and plutonic rocks, as well as several sedimentary units. Primary textures are generally well preserved. Ages of 2722 Ma and 2724 Ma were obtained from felsic rocks in the Vizien Belt (Nos. 78 and 79, Figure 3.6 and Table 3.3). Percival *et al.* (1993) attributed a maximum age of 2708 Ma (No. 211) to a granitic clast derived from a conglomerate unit in this belt. An earlier imprecise age, between 2797 and 2786 Ma, was also obtained in a mafic-ultramafic horizon (No. 77, Figure 3.5 and Table 3.3).

Châteauguay Suite (Achg)

The *Châteauguay Suite* (Table 3.1 and Figure 3.6), introduced in the Maricourt area (Figure 1.1), is located in the south part of the Minto Subprovince. It consists of ultramafic to intermediate dykes and tabular intrusions, a few hundred metres thick by a few kilometres long. Mafic rocks are predominant and consist of gabbro and gabbronorite. Intermediate rocks include diorite and rare quartz diorite. Ultramafic rocks include peridotite, pyroxenite, and hornblendite. Rocks of the Châteauguay Suite are foliated to massive and are commonly injected with whitish felsic material, which gives the rock a brecciated aspect. The rocks also generally exhibit a granoblastic texture. The Châteauguay Suite has not been dated. Field observations are used to infer an age of emplacement in the 2740 to 2710 Ma range.

Bacqueville Suite (Abcv)

The *Bacqueville Suite* (Table 3.1 and Figure 3.6), named by Parent *et al.* (2001), is located in the central part of the Minto Subprovince. This unit also includes granoblastic diorite bands previously assigned to the Melvin Complex (Simard *et al.*, 2005b and 2005a; abandoned term, Table 3.2). Former Melvin diorites were reassigned based on lithological and geochemical similiarities between these dioritic rocks and those of the Bacqueville Suite (Chevé, 2005). The Bacqueville Suite consists of metre-scale to kilometre-scale dykes, remnants, sheets, and dismembered bodies of gabbro, gabbronorite, diorite, and rare ultramafic rocks. These rocks are homogeneous, foliated to gneissic, and exhibit a well-developed granoblastic texture. A few intrusions are massive and display well-preserved igneous textures. The unit has not been dated, but field observations are used to infer an age of emplacement between 2740 and 2710 Ma.

Bylot Suite (Abyl)

The *Bylot Suite* (Table 3.1 and Figure 3.6) was named by Maurice *et al.* (2005a) in the Povungnituk area (Figure 1.1). It is mainly composed of tonalite with minor granodiorite and granite. Rocks of this suite are characterized by a migmatitic texture, a wavy to locally gneissic foliation, a variable grain size, and a saccharoidal texture. They contain enclaves of mafic rock, diorite, or paragneiss, as well as biotite schlieren, which give the rocks a heterogeneous aspect similar to diatexites. Ages of 2737 Ma and 2723 Ma (Nos. 55 and 56, Figure 3.6 and Table 3.3) were obtained in these tonalites.

Lesdiguières Suite (Alsd)

The *Lesdiguières Suite* (Table 3.1 and Figure 3.6) was initially introduced by Madore *et al.* (2004) to designate hornblende-biotite tonalites, pyroxene-bearing tonalites, and granites and granodiorites. This suite is redefined as a unit exclusively composed of hornblende-biotite tonalite. Pyroxene-bearing tonalites are reassigned to the MacMahon Suite, and granites and granodiorites to the La Chevrotière Suite. The Lesdiguières Suite is primarily composed of foliated to gneissic biotite-hornblende tonalite, with minor diorite. These rocks commonly display a granoblastic texture and contain a more felsic phase (20%) in the form of *in situ* veining parallel to the gneissosity. An age of 2724 Ma (No. 104, Figure 3.6 and Table 3.3) was obtained from a diorite sample.

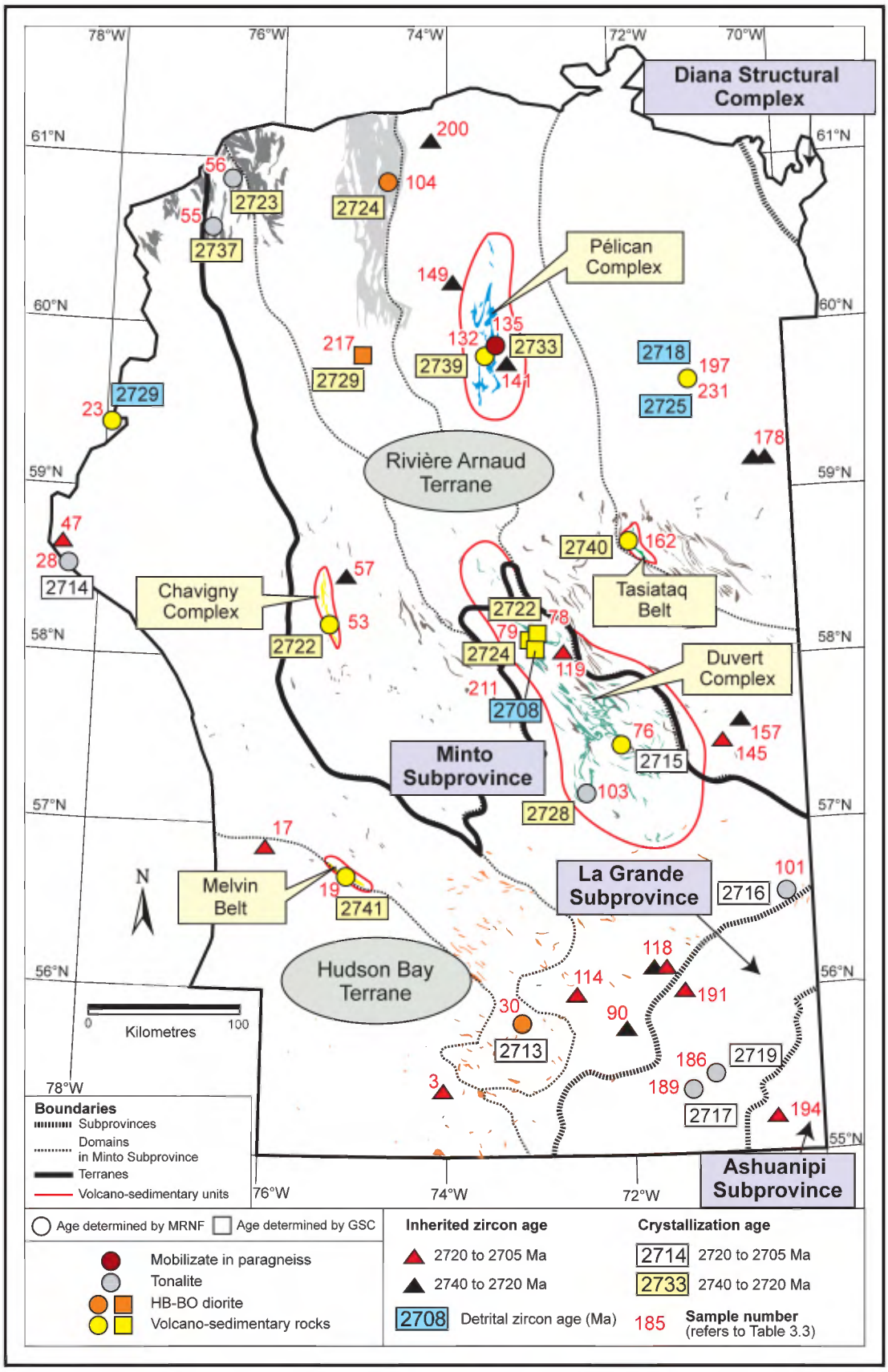

FIGURE 3.6 – Regional distribution of tonalitic units, volcano-sedimentary units, and intermediate to ultramafic intrusions, with corresponding U/Pb ages and inherited zircon ages for the time span from 2740 to 2705 Ma.

Stratigraphic legend (Figure 3.6)

Tonalites

Lesdiguières Suite
Foliated to gneissic biotite-hornblende tonalite, with 20% felsic mobilizate; minor diorite.

Bylot Suite
Tonalite with minor granodiorite and granite; diatexitic aspect.

Intermediate to ultramafic intrusions

Bacqueville Suite
Dykes and lens-shaped intrusions of gabbro, gabbronorite, diorite, and rare ultramafic rocks.

Châteauguay Suite
Dykes and lens-shaped intrusions of gabbro, gabbronorite, diorite, quartz diorite, and rare ultramafic rocks.

Volcano-sedimentary rocks

Duvert Complex
Mafic volcanic rocks of tholeiitic affinity; ultramafic to intermediate volcanic rocks; paragneiss and iron formation.
Vizien Belt: diverse ultramafic to felsic volcanic rocks and sedimentary rocks.

Chavigny Complex
Felsic volcanic rocks (70%); metasedimentary rocks (20%); mafic volcanic rocks (10%).

Pélican Complex
Migmatitic paragneiss; iron formation; mafic to felsic volcanic rocks of diverse origins.

Tasiataq Belt
Foliated basalts and andesites interlayered with felsic volcanic rocks and iron formations.

Melvin Belt
Calc-alkaline felsic volcanic rocks of diverse origins.

Leridon Suite (Alrd)

The *Leridon Suite* (Table 3.1 and Figure 3.7) was introduced by Madore *et al.* (2002) to describe granodioritic and granitic intrusions occurring in the northwest part of the Douglas Harbour Domain. Subsequently, granitic intrusions that were initially assigned to the Qimussinguat and Faribault-Thury complexes within the same domain were reassigned to the Leridon Suite. This suite is composed of homogeneous, massive or foliated granodiorite and granite that contain a minor amount of felsic mobilizate and less than 5% mafic enclaves. These rocks contain 3 to 15% hornblende and biotite. The unit also encompasses several intrusions of granodiorite, granite, and monzonite characterized by a porphyroid texture. It has not been dated, but field observations are used to infer an age of emplacement between 2735 and 2720 Ma.

La Chevrotière Suite (Alcv)

The *La Chevrotière Suite* (Table 3.1 and Figure 3.7), named by Parent *et al.* (2001), designates porphyroid-textured granites, granodiorites, and quartz monzonites that cover a substantial surface area in the north part of the Minto Subprovince. We have assigned to this unit granitic rocks of the La Potherie Batholith (Leclair *et al.*, 2002) and of the Lesdiguières and Rochefort suites (Madore *et al.*, 2004). As a result, the term "La Potherie Batholith" is abandoned (Table 3.2). On the other hand, certain intrusions of the La Chevrotière Suite were reassigned to the Maurel, Desbergères, and Pinguq suites.

Granitoid rocks of the La Chevrotière Suite are pinkish, generally homogeneous, massive to foliated, and exhibit a strong magnetic susceptibility. They contain 10 to 25% mafic minerals (biotite + hornblende) occurring in cm-scale pods stretched along the foliation. The presence of 10 to 40% K-feldspar phenocrysts from 2 to 5 centimetres long, gives these rocks a porphyroid texture. Homogeneous, medium- to coarse-grained granites and granodiorites with an equigranular texture are commonly associated with the porphyroid-textured rocks, but are not as widespread. Also, homogeneous granitoid intrusions are not as voluminous as porphyroid-textured granitoid intrusions. Samples from the La Chevrotière Suite yielded ages ranging from 2734 to 2719 Ma (Nos. 128, 129, 158, 159, 160, and 161, Figure 3.7 and Table 3.3).

Pinguq Suite (Apin)

The *Pinguq Suite* (Table 3.1 and Figure 3.7) is located in the northwest part of the Minto Subprovince. A few intrusions originally assigned to the La Chevrotière Suite were also reassigned to the Pinguq Suite (Table 3.1). This unit, introduced by Maurice *et al.* (2005a), is composed of granite, granodiorite, quartz monzonite, and quartz monzodiorite, all characterized by a porphyroid texture and by the presence of bluish quartz eyes. These rocks contain biotite, are foliated to mylonitic, and form voluminous bodies occurring along N-S-trending shear zones. Small intrusions of homogeneous, equigranular, massive to foliated granite and granodiorite are also associated with these porphyroid-textured rocks. The unit also includes minor quartz syenite and diorite, both biotite-bearing phases. Ages of 2727 Ma and 2725 Ma (Nos. 48 and 49, Figure 3.7 and Table 3.3) were obtained from samples of the Pinguq Suite.

Rivière aux Feuilles Suite (Arfe)

The *Rivière aux Feuilles Suite* (Table 3.1 and Figure 3.7) covers a large surface area in the central part of the region. The Rivière aux Feuilles Suite, as defined by Percival and Card (1994), encompassed pyroxene-hornblende granodiorites, tonalites, granites, diorites, gabbros-pyroxenites, and synplutonic mafic dykes. This suite was redefined by Parent *et al.* (2001) as a unit composed of granodiorites and tonalites, then later by Leclair *et al.* (2002) as a unit exclusively composed of granodiorites. Upon adopting the latter definition, heterogeneous granodiorites previously assigned to the Monchy and Lac Minto suites were reas-

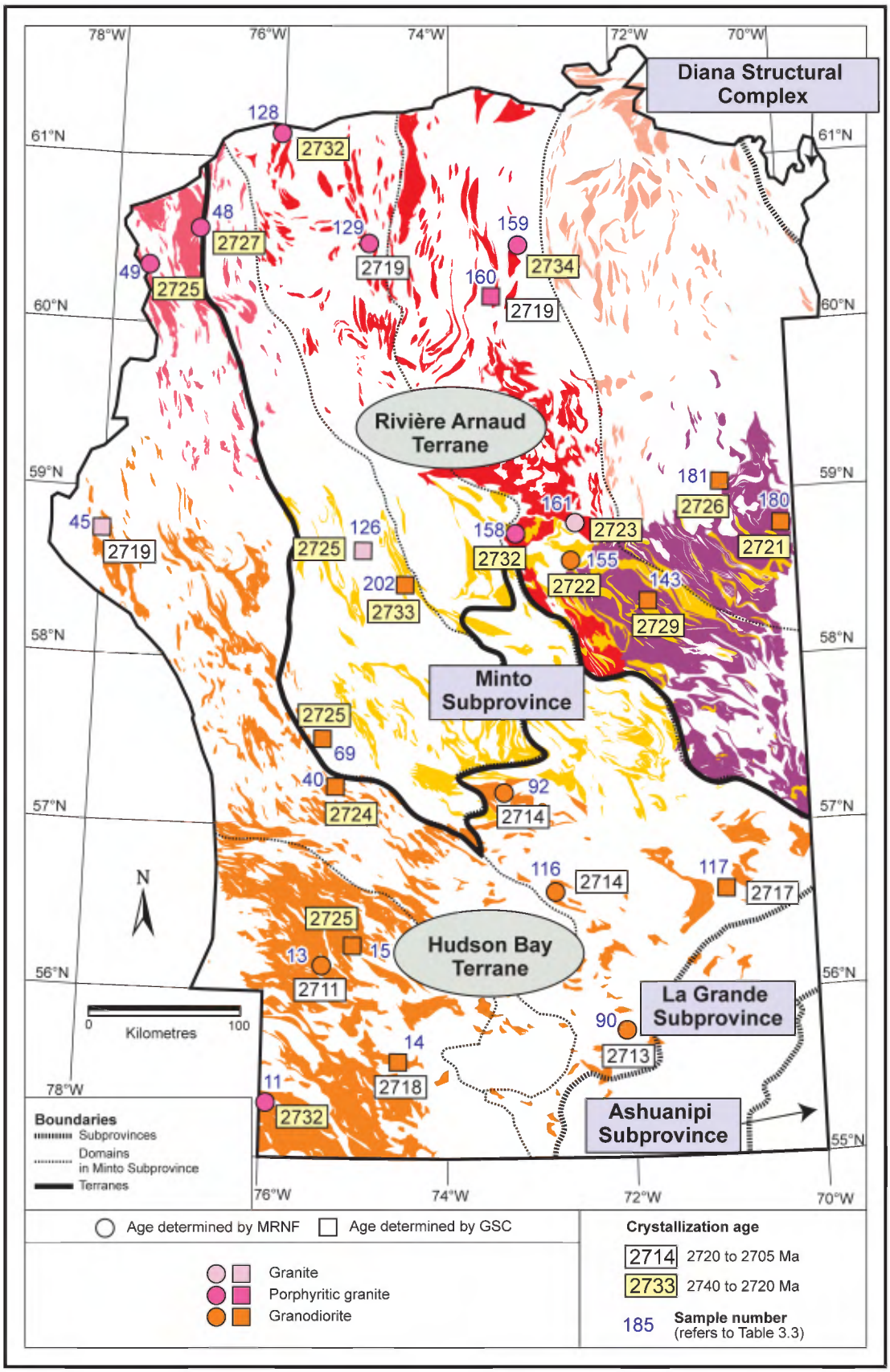

FIGURE 3.7 – Regional distribution of granitic and granodioritic units, with corresponding U/Pb ages for the time span from 2740 to 2705 Ma.

Stratigraphic legend (Figure 3.7)

Desbergères Suite
Homogeneous biotite-hornblende granodiorite and biotite granite; porphyroid-textured granodiorite and granite; numerous tonalitic enclaves.

Dufreboy Suite
Homogeneous biotite-hornblende granite; late injections of aplite and pegmatite. In the Lac Dufreboy area: granodiorite, charnockitic rocks, tonalite, diorite, and gabbro.

Rivière aux Feuilles Suite
Homogeneous biotite-hornblende granodiorite with a granitic phase in diffuse contact; minor pyroxene-bearing granodiorite.

Pinguq Suite
Porphyroid-textured granite, granodiorite, quartz monzodiorite, and quartz monzonite; minor homogeneous granite, granodiorite, and syenite.

La Chevrotière Suite
Porphyroid-textured or equigranular granite and granodiorite; minor porphyroid-textured quartz monzodiorite.

Leridon Suite
Hornblende-biotite granodiorite, granite, and monzonite, occasionally porphyroid-textured.

signed to the Rivière aux Feuilles Suite, whereas tonalites of the Rivière aux Feuilles Suite were reassigned to the Favard and Rochefort suites. As a result, the term "Monchy Suite" is abandoned (Table 3.2).

The Rivière aux Feuilles Suite is composed of massive to foliated biotite-hornblende granodiorite, which commonly contains a granitic phase in diffuse contact with the granodioritic phase (Leclair *et al.*, 2002). In many locations, the presence of abundant enclaves as well as granitic injections give the rock a heterogeneous aspect. In the Lac Nedlouc, Lac Aigneau, and Lac Dufreboy areas (Nos. 14, 15, and 12, Figure 1.1), the Rivière aux Feuilles Suite contains clinopyroxene- and orthopyroxene-bearing granodiorites that were reassigned to other units elsewhere in the Minto Subprovince. Granodiorite samples of the Rivière aux Feuilles Suite yielded ages ranging from 2733 to 2722 Ma (Nos. 69, 126, 202, 155, and 143, Figure 3.7 and Table 3.3).

Dufreboy Suite (Aduy)

The *Dufreboy Suite* (Table 3.1 and Figure 3.7) covers an extensive surface area in the east-central part of the Minto Subprovince. This unit was introduced by Leclair *et al.* (2002) and further defined by Berclaz *et al.* (2002) to describe granites respectively located in the Lac La Potherie and Lac Aigneau areas (Nos. 11 and 15, Figure 1.1). In the Lac Dufreboy area (No. 12, Figure 1.1), Leclair *et al.* (2003) assigned to the Dufreboy Suite an important unit of felsic intrusive rocks mapped by Percival and Card (1994). This undifferentiated unit, which was not examined in the field by MRNF geologists, encompassed granites, granodiorites, porphyritic monzogranites, charnockitic rocks, as well as tonalites, diorites, and gabbros, which are equivalent to rocks assigned to other units in surrounding areas. Outside of this specific area, the Dufreboy Suite is composed of homogeneous, massive to weakly foliated granite that contains less than 15% mafic minerals (biotite + hornblende), predominantly biotite. Aplitic and pegmatitic facies are associated with the granites. Heterogeneous granites and granodiorites located along the northward extension of the Dufreboy Suite, which were initially included in the Troie Complex (Madore *et al.*, 2000), are also assigned to the Dufreboy Suite. Two granodiorite samples, collected in the area initially included in the Troie Complex, yielded ages of 2721 Ma and 2726 Ma (Nos. 180 and 181, Figure 3.7 and Table 3.3).

Desbergères Suite (Adeb)

The *Desbergères Suite* (Table 3.1 and Figure 3.7), named by Simard *et al.* (2002), covers an extensive surface area in the Minto Subprovince. Granodiorites of the Charnière and Voizel suites are reassigned to the Desbergères Suite, as well as some granodiorite intrusions of the La Chevrotière Suite. As a result, the terms "Charnière Suite" and "Voizel Suite" are abandoned (Table 3.2). The Desbergères Suite is composed of generally homogeneous, massive to weakly foliated granodiorite and granite that contain 1 to 8% mafic minerals, represented by biotite in granites and by biotite and minor hornblende in granodiorites. K-feldspar phenocrysts from 1 to 5 centimetres long account for less than 5% of the rock, with the exception of local sub-units from 1 to 10 metres thick that contain more than 25% phenocrysts. The Desbergères Suite also includes a few kilometre-scale porphyroid-textured intrusions (15 to 35% K-feldspar phenocrysts) with transitional contacts with the granites and granodiorites. In many locations, tonalitic restite with diffuse contacts are observed in the potassic facies of this unit. Several age determinations were made on granodiorite samples from this unit, establishing the age of the Desbergères Suite between 2720 and 2710 Ma (Nos. 13, 14, 45, 90, 92, 116, and 117, Figure 3.7 and Table 3.3). Some samples assigned to the Desbergères Suite yielded earlier ages ranging from 2732 to 2724 Ma (Nos. 11, 15, and 40, Figure 3.7 and Table 3.3), which suggests the Desbergères Suite may include intrusions of different ages.

Troie Complex (Atie)

The *Troie Complex* (Table 3.1 and Figure 3.8) was introduced by Madore *et al.* (2000) to describe lithological assemblages corresponding to a strong sub-circular magnetic anomaly observed within the Douglas Harbour Domain (Figure 2.2). Initially, the complex consisted of orthopyroxene-bearing intrusive and metamorphic rocks, porphyroid-textured quartz monzonites and monzodiorites, gneissic granites, migmatitic granites, and supracrustal remnants. We have redefined the Troie Complex as a unit exclusively composed of orthopyroxene-bearing rocks. Supracrustal

rocks are reassigned to the Arnaud Complex, granites to the Dufreboy Suite, and quartz monzonites and monzodiorites to the Belloy Suite. The Troie Complex, under this new definition, comprises orthopyroxene-bearing orthogneisses and foliated to gneissic charnockitic intrusions composed of enderbite, opdalite, with minor amounts of charnockite and hypersthene diorite. These rocks contain 10 to 60% felsic mobilizate with both clino- and orthopyroxene. The Troie Complex also includes hornblende or biotite gabbronorites that form small intrusive bodies less than 20 kilometres in diameter. Gabbronorites also occur as enclaves in granulite-grade rocks. Samples of orthopyroxene-bearing tonalitic gneiss yielded ages of 2741 Ma and 2734 Ma (Nos. 175 and 167, Figure 3.8 and Table 3.3). An age of 2722 Ma (No. 177) was obtained from a gabbronorite.

Qimussinguat Complex (Aqim)

The *Qimussinguat Complex* (Table 3.1 and Figure 3.8) was introduced by Madore *et al.* (2000) to describe lithological assemblages corresponding to a strong ovoid magnetic anomaly located north of the Troie Complex, in the Douglas Harbour Domain (Figure 2.2). The complex initially included orthopyroxene-bearing intrusive and metamorphic rocks, as well as migmatitic granites, granodiorite and granite intrusions, and remnants of granulite-grade supracrustal rocks. The Qimussinguat Complex is redefined as a unit exclusively composed of orthopyroxene-bearing rocks. Supracrustal rocks are reassigned to the Arnaud Complex, and granodiorites and granites to the Leridon Suite. The unit now consists of orthopyroxene-bearing orthogneisses, charnockitic intrusions with a tonalitic composition and more rarely, granodioritic, granitic, and dioritic composition. These rocks are heterogeneous, generally gneissic, and contain 10 to 60% felsic mobilizate with both clino- and orthopyroxene. The unit also includes gabbronorites occurring as small intrusions less than 20 kilometres in diameter or as enclaves in granulite-grade rocks. An age of 2734 Ma (No. 176, Figure 3.8 and Table 3.3) was obtained from a sample of orthopyroxene-bearing tonalitic gneiss.

Lepelle Suite (Alep)

The *Lepelle Suite* (Tableau 3.1 and Figure 3.8) covers practically all of the northern part of the Utsalik Domain (Figure 2.2). It is composed of clinopyroxene-bearing granites and granodiorites initially assigned to the Lepelle and Châtelain suites. These rocks were grouped together into a single unit based on their spatial distribution, their mineralogical similarity, and their age. As a result, the term "Châtelain Suite" is abandoned (Table 3.2). The Lepelle Suite corresponds to a fairly uniform regional positive magnetic anomaly. The homogeneous, strongly foliated granites and granodiorites typically contain burgundy-coloured plagioclase. The rocks are medium-grained and primary igneous textures, commonly porphyroid, are partially obliterated by recrystallization of variable intensity to produce mortar textures. In many locations, these rocks are injected in their enclosing country rocks. They contain enclaves of tonalitic rocks, mafic rocks, and locally, ultramafic rocks. The Lepelle Suite also includes a minor amount of clinopyroxene-bearing tonalite. U/Pb analyses suggest an average age between 2725 and 2720 Ma for the Lepelle Suite (Nos. 140, 142, 141, and 156, Figure 3.8 and Table 3.3).

MacMahon Suite (Acmm)

The *MacMahon Suite* (Table 3.1 and Figure 3.8) designates all orthopyroxene- and clinopyroxene-bearing felsic intrusive rocks in the Utsalik, Qalluviartuuq, and Goudalie domains, with the exception of those assigned to the Lepelle Suite. To the original unit have been added orthopyroxene-bearing rocks previously assigned to the Du Gué Complex in the Maricourt area (No. 18, Figure 1.1), to the Lac Minto Suite in the Lac Vernon area (No. 10, Figure 1.1), and to the Châtelain and Lesdiguières suites in the Lac Couture area (No. 2, Figure 1.1). Clinopyroxene-bearing tonalites of the Nullualuk, Bottequin, and Lesdiguières suites were also reassigned to the MacMahon Suite given their spatial association with orthopyroxene-bearing rocks of the latter suite. As a result of these modifications, the terms "Du Gué Complex", "Nullualuk Suite", and "Bottequin Suite" are abandoned (Table 3.2).

Clinopyroxene-bearing tonalites are homogeneous, foliated, coarse-grained rocks. They are associated with dark grey homogeneous and foliated diorites occurring as enclaves or small intrusions generally less than 1 kilometre in size. The MacMahon Suite is largely dominated by orthopyroxene-bearing rocks, mainly enderbites. These rocks are greenish, homogeneous, medium- to coarse-grained, locally porphyritic, and weakly foliated. Small intrusions of hypersthene diorite, gabbronorite, as well as small ultramafic bodies (<1 km) are associated with the enderbites. The unit also includes large bodies of massive opdalite-charnockite in its northern part. Several U/Pb analyses were conducted, indicating an age between 2729 and 2711 Ma for the MacMahon Suite (Nos. 109, 139, 144, 147, 148, 149, 152, 153, 154, and 168, Figure 3.8 and Table 3.3). Some enderbitic samples assigned to the MacMahon Suite in the easternmost part of the Minto Subprovince yielded much younger ages between 2702 and 2676 Ma (Nos. 145, 146, 150, 151, and 108, Figure 3.10). These results indicate many of the enderbitic intrusions assigned to the MacMahon Suite in this area are in fact related to a much younger magmatic event.

Lac Minto Suite (Amin)

The *Lac Minto Suite* (Table 3.1 and Figure 3.8) was redefined more than once. The term "Lac Minto Suite" was initially introduced by Parent *et al.* (2001) to designate diatexites occurring in the northwest corner of the Lac Nedlouc area (No. 14, Figure 1.1). This unit was traced further north

in the Lac La Potherie area (No. 11), where Leclair *et al.* (2002) also assigned to the suite orthopyroxene-bearing intrusive rocks, then to the west, in the Lac Vernon area (No. 10), where Parent *et al.* (2003b) also included granites and volcano-sedimentary rocks. The Lac Minto Suite was then redefined by Simard *et al.* (2005a) in the Lac Minto area (No. 13, Figure 1.1) as a unit exclusively composed of orthopyroxene-bearing intrusive rocks. This last definition is the one used in this report. The Lac Minto Suite includes all orthopyroxene-bearing rocks in the Lac Minto Domain, previously included in the Lac Minto, Lippens, and Qilalugalik suites and the Le Roy Complex. The terms "Lippens Suite" and "Qilalugalik Suite" are abandoned (Table 3.2).

The Lac Minto Suite is mainly composed of greenish, massive to foliated, and medium- to coarse-grained enderbites. These enderbites contain a charnockitic or opdalitic phase occurring in transitional and diffuse contact. The latter, combined with the presence of abundant partially assimilated enclaves of amphibolite, diorite, or paragneiss, often give the rock a heterogeneous aspect similar to a diatexite. The Lac Minto Suite also includes kilometre-scale lens-shaped intrusions of hypersthene diorite, gabbronorite, and rare ultramafic rocks, as well as charnockite intrusions of variable dimensions. All rock types in this suite exhibit a strong magnetic susceptibility. The results of U/Pb age dating analyses are used to establish an average age between 2735 and 2710 Ma for the Lac Minto Suite (Nos. 60, 61, 63, 65, 66, and 67, Figure 3.8 and Table 3.3). Some enderbites in the Lac Minto Suite yielded ages between 2702 and 2688 Ma (Nos. 34, 62, 68, and 110, Figure 3.10), indicating this suite also contains rocks related to younger magmatic events.

Loups Marins Suite (Alma)

The *Loups Marins Suite* (Table 3.1 and Figure 3.8) encompasses all pyroxene-bearing felsic intrusive rocks located in the Tikkerutuk and Bienville domains (Figure 2.2). This unit was introduced by Gosselin *et al.* (2002) in the Lacs des Loups Marins area (No. 17, Figure 1.1) under the name "Loups Marins Complex". The authors described the unit as a mixture of clinopyroxene- and orthopyroxene-bearing intrusive rocks and orthopyroxene-bearing metamorphic rocks. However, mapping of this complex further south and west demonstrated that the unit is primarily composed of intrusive rocks, with enclaves of metamorphic rocks, and thus the term "Loups Marins Complex" was replaced by the "Loups Marins Suite". This suite includes orthopyroxene- and clinopyroxene-bearing rocks that were initially assigned to the Loups Marins Complex in areas further south (Nos. 17, 20, 19, 16, 13, Figure 1.1), pyroxene-bearing felsic intrusive rocks of the Qilalugalik, Gabillot, and Lussay suites, as well as gabbronorite intrusions of the Cheminade Suite. As a result of these modifications, the latter terms are abandoned (Table 3.2).

The Loups Marins Suite comprises two main units of felsic intrusive rocks, one with orthopyroxene (Alma2) and the other with clinopyroxene (Alma1). Orthopyroxene-bearing rocks are greenish or brownish, medium- to coarse-grained, and show a massive to foliated aspect. They are mainly composed of enderbite and hypersthene quartz diorite, with minor opdalite and charnockite. The orthopyroxene unit also includes kilometre-scale lenses of gabbronorite, hypersthene diorite, and minor ultramafic rocks. The clinopyroxene unit is primarily composed of tonalite, quartz diorite, along with granodiorite and granite that exhibit an equigranular or porphyroid texture. These rocks are medium- to coarse-grained, massive to weakly foliated, and are characterized by the presence of burgundy-coloured plagioclase that gives the rock a purplish tinge. Rocks of the Loups Marins Suite exhibit variable degrees of heterogeneity depending on the amount of partially assimilated enclaves of amphibolite, diorite, and paragneiss, and the proportion of granitic material in the rock. The Loups Marins Suite shows a strongly positive magnetic signature. Age determinations indicate an age ranging between 2735 and 2720 Ma for orthopyroxene-bearing rocks (Nos. 7, 8, 37, 38, and 39, Figure 3.8 and Table 3.3), and between 2715 and 2705 Ma (Nos. 1, 3, 4, 5, 6, 9, and 31) for clinopyroxene-bearing rocks. Some clinopyroxene-bearing rocks yielded ages between 2731 and 2723 Ma however (Nos. 2, 33, and 35). A younger age, at 2693 Ma (No. 36, Figure 3.10), was obtained from a massive hypersthene diorite assigned to the Loups Marins Complex (Gosselin *et al.*, 2002).

Juet Belt (Ajut)

The *Juet Belt* (Table 3.1 and Figure 3.9) is primarily composed of sedimentary rocks and felsic volcaniclastic rocks, with minor amounts of mafic volcanic rocks and gabbros. Initially, these rocks were informally referred to as the Juet Band by Taylor (1982), then as the Juet Formation by Moorhead (1996). The latter interpreted the Juet Formation as a homoclinal, east-facing volcano-sedimentary sequence unconformably overlying the granitic basement. Work by Maurice *et al.* (2005a) made it possible to trace this sequence to the south and west. In an effort to standardize the nomenclature used for volcano-sedimentary sequences in the Minto Subprovince, the latter authors replaced the term "Juet Formation" by "Juet Belt" (Table 3.2).

The sedimentary rocks mainly include laminated sandstone and siltstone, as well as monogenic and polygenic conglomerate. Phyllites and banded iron formations (<10 metres thick) are intercalated with the sandstones and siltstones. Volcaniclastic rocks consist of laminated mafic tuffs, either massive or crystal tuffs, and intermediate to felsic aphanitic or lapilli tuffs. Mafic volcanic rocks of tholeiitic affinity mainly consist of amphibolites where primary textures are rarely preserved. Metamorphosed gabbros cross-cut plutonic country rocks as well as rocks in the Juet Belt. These gabbros are interpreted as the feeder dykes of the volcanic

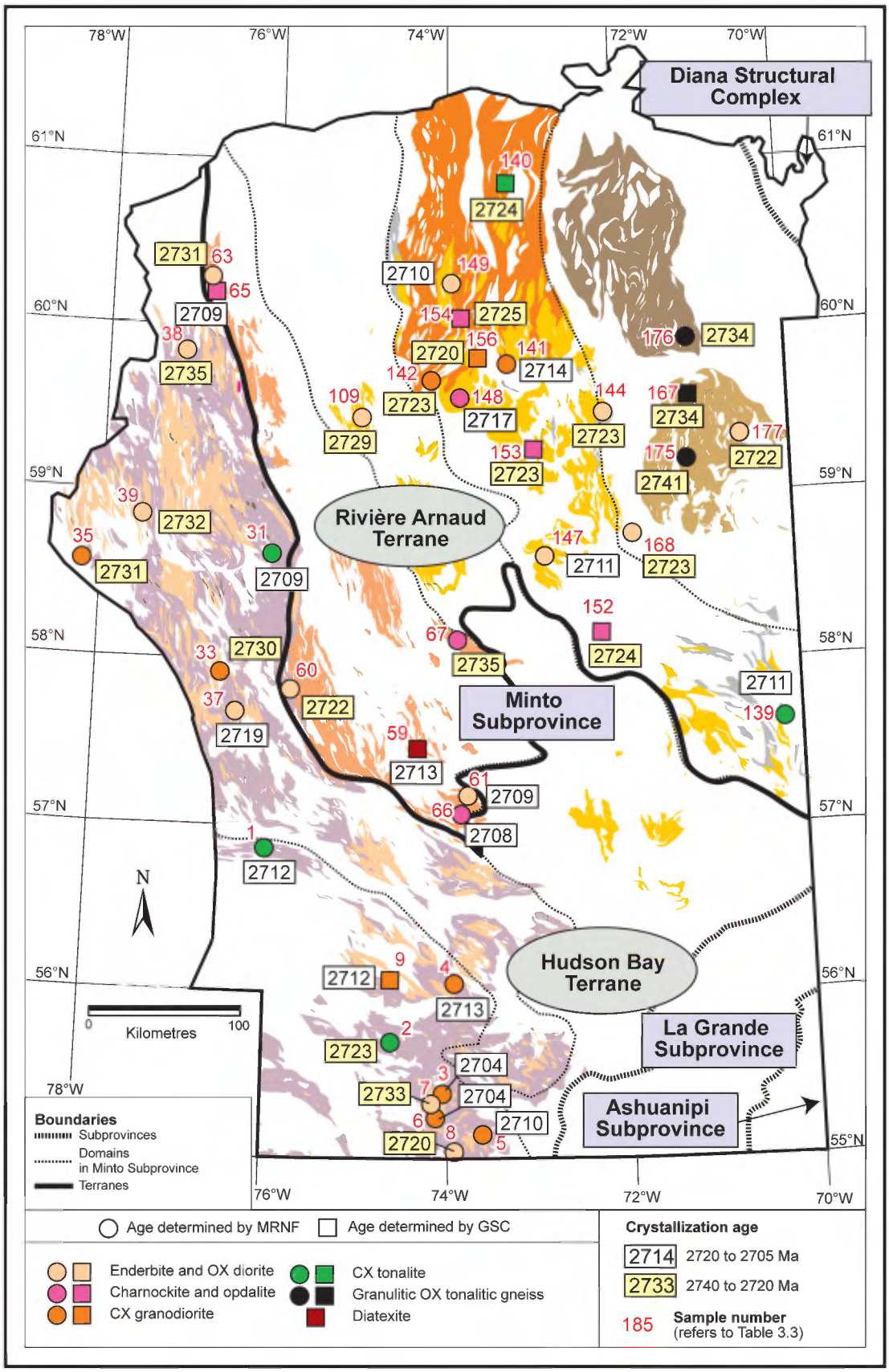

FIGURE 3.8 – Regional distribution of pyroxene-bearing intrusive units, with corresponding U/Pb ages for the time span from 2740 to 2705 Ma.

Stratigraphic legend (Figure 3.8)

Loups Marins Suite
Clinopyroxene unit (purple) composed of tonalite, quartz diorite, granodiorite, and granite, characterized by burgundy-coloured plagioclase.
Orthopyroxene unit (beige) composed of enderbite and hypersthene diorite, with minor charnockite, opdalite, gabbronorite, and ultramafic rocks.

Lac Minto Suite
Homogeneous enderbite; charnockite; small intrusions of hypersthene diorite and gabbronorite.

MacMahon Suite
Enderbite, small intrusions of hypersthene diorite, gabbronorite and ultramafic rocks, and charnockite intrusions (yellow); clinopyroxene-bearing tonalite and diorite (grey).

Lepelle Suite
Homogeneous clinopyroxene-bearing granodiorite and granite, characterized by burgundy-coloured plagioclase; minor clinopyroxene-bearing tonalite.

Qimussinguat Complex
Orthopyroxene orthogneiss; enderbite and minor opdalite, charnockite, and hypersthene diorite; small gabbronorite intrusions.

Troie Complex
Orthopyroxene orthogneiss; enderbite, opdalite, and minor charnockite and hypersthene diorite; small gabbronorite intrusions.

sequence (Maurice *et al.*, 2005a). Metamorphism in the Juet Belt ranges from the greenschist facies to the amphibolite facies southward. The Juet Belt has not been dated. Its age is estimated at about 2700 Ma.

Allemand Belt (Aale)

The *Allemand Belt* (Table 3.1 and Figure 3.9) was initially identified and described by Moorhead (1989), under the term "Lac Allemand Formation". Later on, Madore *et al.* (2004) replaced the term "Lac Allemand Formation" with "Allemand Belt" (Table 3.2) to remain consistent with the preferred lithodemic approach. This belt is composed of amphibolite-grade volcanic and sedimentary rocks. Metavolcanic rocks mainly consist of tholeiitic mafic gneisses and metabasalts that exhibit centimetre-scale compositional banding, and where pillows were locally identified. Mafic to felsic laminated tuffs and a few metre-scale horizons of lapilli tuff are intercalated with the gneisses and metabasalts. Metasedimentary rocks are largely dominated by muscovite schist, which exhibits millimetre-scale compositional banding. A few metre-scale layers of quartzite, conglomerate, and iron formation are interlayered with the schists. The Allemand Belt has not been dated. Its age is estimated at about 2700 Ma.

Grosbois Complex (Agrs)

The *Grosbois Complex* (Table 3.1 and Figure 3.9) was introduced by Gosselin and Simard (2001) under the term "Grosbois Formation" to designate paragneisses mapped in the northeast part of the Ashuanipi Subprovince. Since the unit includes both metamorphic and intrusive rocks, we have replaced the term formation by complex, more appropriate in this case. The Grosbois Complex is composed of migmatitic paragneiss with biotite ± orthopyroxene ± hornblende ± garnet. The rock is dark grey in fresh surface, with a typical rusty brown weathered surface. The presence of whitish bands of tonalitic to granitic mobilizate from 1 millimetre to 10 centimetres in size (5 to 50%) gives the rock a banded aspect. The Grosbois Complex also includes a few decimetre-scale to decametre-scale horizons of oxide-facies iron formation. The Grosbois Complex has not been dated. Paragneisses in this complex are most likely equivalent to other paragneiss units in the Ashuanipi.

Qullinaaraaluk Suite (Aluk)

The *Qullinaaraaluk Suite* (Table 3.1 and Figure 3.9) was introduced in the Lac Vernon area (No. 10, Figure 1.1) to describe small massive mafic and ultramafic intrusions considered to be late. Parent *et al.* (2003b) introduced the Qullinaaraaluk Suite to emphasize the economic significance of these intrusions, following the discovery of Ni-Cu-Co mineralization in a massive ultramafic intrusion (Labbé *et al.*, 2001). Prior to this discovery, similar intrusions further east had been assigned to the Bacqueville Suite (Parent *et al.*, 2001; Leclair *et al.*, 2002). We have reassigned to the Qullinaaraaluk Suite a series of mafic and ultramafic intrusions previously included in the Qilalugalik Suite (abandoned term, Table 3.2) in the Kogaluc Bay area (No. 5, Figure 1.1) and in the Povungnituk and Kovik Bay areas (No. 1, Figure 1.1), based on the similarities between these intrusions and those of the Qullinaaraaluk Suite.

Rocks of the Qullinaaraaluk Suite form small intrusions, generally less than 1 kilometre in diameter. They consist of homogeneous, massive, fine- to medium-grained rocks frequently cut by centimetre-scale to metre-scale felsic injections that give the rocks a brecciated aspect. Poikilitic hornblende phenocrysts (5 to 25%) from 1 to 4 centimetres in size give the rock a spotted aspect. Ultramafic rocks are composed of pyroxenite, hornblendite, and rare peridotite. Mafic rocks consist of gabbro and gabbronorite with variable compositions and textures. Ages of 2707 Ma and 2705 Ma (Nos. 17 and 18, Figure 3.9 and Table 3.3) were obtained from leucogabbro samples. However, a pegmatite cross-cutting the ultramafic intrusion that hosts the Qullinaaraaluk showing (Parent *et al.*, 2003b; Simard *et al.*, 2005a) yielded an earlier age of 2720 Ma (No. 72).

Couture Suite (Acot)

The *Couture Suite* designates all mafic to ultramafic intrusions that were initially assigned to the Couture Suite (Madore *et al*, 2002) and the Lac Calme Suite (Madore *et al.*, 2004; Berclaz *et al.*, 2005). As a result, the term "Lac Calme Suite" is abandoned (Table 3.2). Intrusions of the Couture Suite are generally small (less than 20 km^2). They consist of homogeneous, medium- to coarse-grained rocks that are

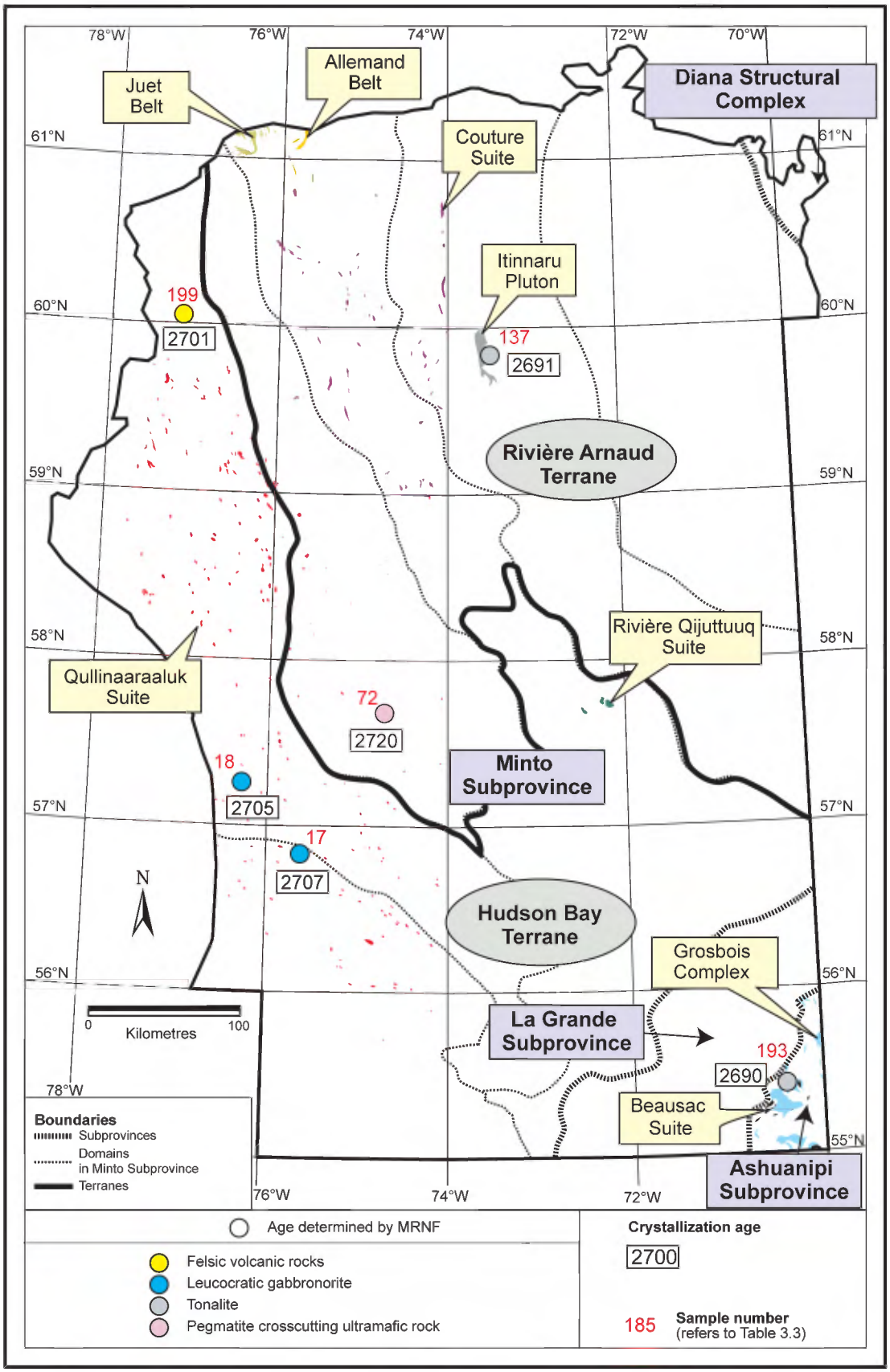

FIGURE 3.9 – Regional distribution of tonalites, volcano-sedimentary rocks, and mafic to ultramafic intrusions, with corresponding U/Pb ages for the time span from 2705 to 2680 Ma.

Stratigraphic legend (Figure 3.9)

Tonalites

Beausac Suite
Foliated to banded biotite-hornblende tonalite; minor quartz monzodiorite and granodiorite.

Rivière Qijuttuuq Suite
Small intrusions of massive, weakly deformed biotite leucotonalite.

Itinnaru Pluton
Biotite±hornblende tonalite and biotite trondhjemite; enclaves of paragneiss and mafic to felsic igneous rocks.

Intermediate to ultramafic intrusions

Couture Suite
Small ultramafic to intermediate intrusions injected with felsic material, producing a brecciated aspect; minor anorthosite.

Qullinaaraaluk Suite
Small ultramafic to mafic intrusions injected with felsic material, producing a brecciated aspect.

Volcano-sedimentary rocks

Grosbois Complex
Migmatitic paragneiss with biotite ± orthopyroxene ± hornblende ± garnet; minor iron formation.

Allemand Belt
Mafic gneiss and amphibolite of tholeiitic affinity; diverse mafic to felsic tuffs; diverse metasedimentary rocks.

Juet Belt
Diverse sedimentary rocks and diverse mafic to felsic tuffs; tholeiitic amphibolite; gabbro.

generally massive in the centre of intrusions and foliated along the margins. Intrusions are injected with granitic to tonalitic material, which gives the rock in some locations a brecciated texture. Ultramafic rocks are composed of pyroxenite and peridotite, whereas intermediate to mafic facies consist of diorite, quartz diorite, gabbro, and minor anorthosite. The mafic to intermediate rocks frequently display a variably developed granoblastic texture superimposed upon the primary igneous texture. Primary igneous textures, particularly cumulate textures, are best preserved in ultramafic rocks. The Couture Suite has not been dated. Its age is estimated at about 2705 Ma.

Itinnaru Pluton (Aiti)

The *Itinnaru Pluton* (Table 3.1 and Figure 3.9) is a new unit introduced to designate a tonalitic intrusion located in the Lac Pélican area (No. 7, Figure 1.1). Cadieux *et al.* (2004) had initially assigned this intrusion to the "Pélican-Nantais Complex" (abandoned term, Table 3.2) due to its proximity to sedimentary rocks of the Pélican belt. However, the age of 2691 Ma (No. 137, Figure 3.9 and Table 3.3) obtained for a tonalitic sample from this pluton suggests there is no genetic link between these tonalites and the volcano-sedimentary rocks of the Pélican belt (2739 Ma). The Itinnaru Pluton is composed of biotite ± hornblende tonalite with minor biotite trondhjemite. These rocks are medium grey, medium-grained, massive to weakly foliated, and contain a few enclaves of paragneiss and mafic to felsic igneous rocks.

Rivière Qijuttuuq Suite (Aqij)

The *Rivière Qijuttuuq Suite* (Table 3.1 and Figure 3.9) is a new unit that designates three small intrusions of tonalite in the Lac Nedlouc area (No. 14, Figure 1.1) previously assigned to the Morrice Suite by Parent *et al.* (2001). However, the association between these tonalites and granites of the Morrice Suite could not be demonstrated, since the Morrice Suite is exclusively composed of granite. Intrusions of the Rivière Qijuttuuq Suite are composed of massive or weakly foliated biotite leucotonalite. This unit has not been dated, but its weakly deformed aspect suggests a relatively young age.

Beausac Suite (Abea)

Located in the Ashuanipi Subprovince, the *Beausac Suite* (Table 3.1 and Figure 3.9) was introduced in the Lac Gayot area (No. 21, Figure 1.1) to describe a unit mainly composed of biotite-hornblende tonalite with minor quartz monzodiorite and granodiorite. Rocks of this unit are greyish, fine- to medium-grained, strongly foliated to banded, and exhibit a relatively well-defined granoblastic texture. Field observations indicate tonalites of the Beausac Suite alternate with paragneisses of the Grosbois Complex. A sample of foliated tonalite in the Lac Gayot area yielded an age of 2690 Ma (No. 193, Figure 3.9 and Table 3.3).

Maurel Suite (Amau)

The *Maurel Suite* (Table 3.1 and Figure 3.10) encompasses granites, granodiorites, monzodiorites, and quartz monzodiorites mapped in the Lac Gayot, Maricourt, Lacs des Loups Marins, and Lac Bienville areas (Nos. 21, 18, 17, 20, Figure 1.1) as well as porphyroid-textured granodiorite intrusions previously assigned to the La Chevrotière Suite in the Lac Aigneau and Lac Dufreboy areas (Nos. 15 and 12, Figure 1.1). The unit also includes granodiorite, monzodiorite, and quartz monzodiorite intrusions of the La Bazinière Suite (Gosselin and Simard, 2001), a unit that was abandoned (Table 3.2) following a reinterpretation of the Lac Gayot area (Gosselin *et al.*, 2004). Intrusive rocks of the Maurel Suite exhibit a porphyroid texture due to the presence of 5 to 40% K-feldspar phenocrysts from 1 to 5 centimetres long. They occur as kilometre-scale plutons or as decimetre-scale to decametre-scale injections in earlier lithologies. The rock is pinkish grey to pink, medium- to coarse-grained, and is weakly foliated. It contains 5 to 25% mafic minerals, comprising variable proportions of biotite and hornblende. Age determinations indicate an age in the

2707 to 2686 Ma range for the Maurel Suite (Nos. 113, 114, 115, 157, 191, and 192, Figure 3.10 and Table 3.3).

Tramont Suite (Atra)

The *Tramont Suite* (Table 3.1 and Figure 3.10) is a granitic unit occurring in the La Grande Subprovince and the southeast part of the Minto Subprovince. Originally, granite intrusions located within the Ashuanipi Subprovince were also included in the Tramont Suite (Gosselin and Simard, 2001). However, field observations suggest a relatively young age for the latter, and so they are reassigned to a new unit, the Joinville Suite. The Tramont Suite is composed of homogeneous biotite-chlorite granite that forms kilometre-scale bodies or occurs as multiple decimetre-scale to decametre-scale injections in earlier lithologies. The rock is pinkish, massive to weakly foliated, and its grain size ranges from fine in smaller intrusions to coarse in more voluminous plutons. Mafic minerals, namely small booklets of biotite or chlorite, make up 1 to 5% of the rock. Granite samples yielded ages of 2701 Ma and 2698 Ma (Nos. 123 and 124, Figure 3.10 and Table 3.3).

Druillon Suite (Adru)

The *Druillon Suite* (Table 3.1 and Figure 3.10) was introduced by Thériault and Chevé (2001) to describe small intrusions of monzonite, monzodiorite, and diorite located in the northeast part of the La Grande Subprovince, south of the Lac Bienville area (No. 20, Figure 1.1). We have reassigned to this unit small intrusions of the Turbar and Ossant suites described in the Lac Bienville area (Gosselin *et al.*, 2004) due to their similar lithological characteristics. As a result of these modifications, the terms "Turbar Suite" and "Ossant Suite" are abandoned (Table 3.2). The Druillon Suite is composed of monzodiorite, quartz monzodiorite, diorite, monzonite, and quartz monzonite. These rocks are homogeneous with a porphyroid texture, and are massive to weakly foliated. They contain 5 to 35% mafic mineral clusters mainly composed of hornblende, biotite, clinopyroxene and locally, orthopyroxene. The unit also includes a few intrusions of homogeneous, massive to weakly foliated porphyroid-textured granite characterized by the presence of sodic amphibole (previously assigned to the Ossant Suite). These granites are most likely related to intermediate rocks of the Druillon Suite. Intrusions of the Druillon Suite have not been dated. They are considered to be late given their massive, weakly deformed nature.

Belloy Suite (Ably)

The *Belloy Suite* (Table 3.1 and Figure 3.10) is a new unit encompassing kilometre-scale intrusions of monzonite and monzodiorite that were initially assigned to the Troie Complex (Madore *et al.*, 2000). A monzonite sample from this suite yielded an age of about 2690 Ma (No. 178, Figure 3.10 and Table 3.3), confirming these rocks are not cogenetic with the older rocks of the Troie Complex. The Belloy Suite is composed of porphyroid-textured monzonite and quartz monzodiorite marked by the presence of 25 to 50% K-feldspar phenocrysts from 1 to 5 centimetres long. These rocks exhibit a massive texture or a foliation defined by aligned phenocrysts. They contain 5 to 25% mafic minerals, namely biotite and green hornblende.

Corneille Suite (Acrn)

The *Corneille Suite* (Table 3.1 and Figure 3.10) is located in the westernmost part of the Minto Subprovince. This unit, named by Simard *et al.* (2004), consists of whitish granite characterized by the presence of bluish grey quartz eyes. This massive to weakly foliated granite shows a heterogeneous grain size ranging from medium to coarse over a distance of a few centimetres. The rock is hololeucocratic; it contains less than 2% chlorite and less than 1% fine-grained garnet. The presence of abundant enclaves (10 to 25%) of paragneiss, amphibolite, diorite, and gabbro, stretched, partially assimilated and injected with granite, gives the rock a heterogeneous aspect. The Corneille Suite also includes minor whitish tonalite exhibiting similar characteristics to those of the granite. Age determinations indicate an age ranging between 2698 and 2688 Ma for this unit (Nos. 46, 47, and 50, Figure 3.10 and Table 3.3).

Morrice Suite (Agdm)

The *Morrice Suite* (Table 3.1 and Figure 3.10) is composed of granitic intrusions located in the central part of the Minto Subprovince. We have added granites previously assigned to the Le Roy Complex (see below) based on their spatial distribution and their relatively late emplacement. In the Lac Nedlouc area, three small late intrusions of tonalite included in the Morrice Suite (Parent *et al.*, 2001) were reassigned to the Rivière Qijuttuuq Suite (see above), given the exclusively potassic character of rocks of the Morrice Suite. The Morrice Suite is composed of homogeneous, massive or foliated, medium- to coarse-grained granite that locally shows a porphyroid texture and that contains 2 to 15% mafic minerals (biotite + hornblende), predominantly biotite. The granite is pinkish to reddish. Pegmatitic phases are commonly associated with the granite. Both granites and pegmatites are injected in the majority of other Archean units and host enclaves of the latter, attesting to the late character of these granitic rocks. A sample of granite yielded an age of 2684 Ma (No. 125, Figure 3.10 and Table 3.3).

Le Roy Complex (Aroy)

The *Le Roy Complex* (Table 3.1 and Figure 3.10) was introduced in the Lac Vernon area (No. 10, Figure 1.1) by Parent *et al.* (2003b) and encompassed diatexites, granites, orthopyroxene-bearing intrusions, and paragneisses located

in the Lac Minto Domain. We have redefined the Le Roy Complex as a unit exclusively composed of diatexites, which form a discontinuous belt trending NW-SE in the Lac Minto Domain. These diatexites had been assigned to the Lac Minto Suite in the Lac Nedlouc area (No. 14, Figure 1.1), to the Le Roy Complex in the Lac Vernon, Lac Minto, and Lac Anuc areas (Nos. 10, 13, and 6, Figure 1.1), and to the Mézard Complex in the Lac Anuc, Kogaluc Bay, Povungnituk, and Kovik Bay areas (Nos. 6, 5, and 1, Figure 1.1). The diatexites contain more than 50% mobilizate (neosome) of granodioritic to granitic, and more rarely tonalitic, composition. They are yellowish grey to rusty brown and typically exhibit an anisometric texture. These rocks contain biotite + garnet ± orthopyroxene ± cordierite ± sillimanite and host enclaves, from 1 to 10 metres in size, of migmatitic paragneiss (paleosome) as well as abundant biotite schlieren defining a wavy foliation that has obliterated primary textures. The anisometric texture, the presence of schlieren and enclaves, and flow textures give this unit a heterogeneous aspect. Two diatexite samples yielded ages of 2697 Ma and 2668 Ma (Nos. 57 and 58, Figure 3.10 and Table 3.3).

Sanigitik Suite (Asan)

The *Sanigitik Suite* (Table 3.1 and Figure 3.10) is a new unit introduced to designate diatexites in the Lac Pélican area (No. 7, Figure 1.1) that were previously assigned to the Faribault-Thury Complex (Table 3.2) and the MacMahon Suite. We have also included in this unit heterogeneous granodiorites with a diatexitic texture previously assigned to the Faribault-Thury Complex in the Lac La Potherie and Lac Dufreboy areas (Nos. 11 and 12, Figure 1.1). These diatexites contain biotite + garnet or biotite ± orthopyroxene assemblages, have a heterogeneous aspect with whitish to greenish tonalitic to granitic mobilizate, biotite schlieren, and abundant enclaves stretched along the foliation. Enclaves consist of paragneiss, amphibolite, diorite, and leucocratic tonalite. This unit has not been dated.

Rivière aux Mélèzes Suite (Aram)

The *Rivière aux Mélèzes Suite* (Table 3.1 and Figure 3.10) is a diatexite unit introduced by Parent *et al.* (2001) in the Lac Nedlouc area (No. 14, Figure 1.1). We have added to this unit diatexites formerly assigned to the Du Gué Complex (abandoned term, Table 3.2) in the Maricourt area (No. 18, Figure 1.2). The Rivière aux Mélèzes Suite is composed of yellowish grey to rusty brown diatexites with biotite + garnet + cordierite + andalusite ± sillimanite, that host 1- to 10-metre-sized enclaves of migmatitic paragneiss and numerous biotite schlieren that define a wavy foliation. The granodioritic to granitic mobilizate (more than 50%) is coarse-grained and heterogranular; it shows a variably porphyritic texture and looks like a poorly crystallized rock. Flow textures obliterate primary textures. One diatexite sample yielded an age of 2668 Ma (No. 105, Figure 3.10 and Table 3.3).

Bourdel Syenite (Abol)

The *Bourdel Syenite* (Table 3.1 and Figure 3.11) forms an isolated intrusion about 6 kilometres in length, located in the south part of the Minto Subprovince. This lithodeme, named by Simard *et al.* (2005b), is composed of homogeneous, medium- to coarse-grained nepheline syenite with a well developed magmatic foliation. This syenite contains 5 to 10% biotite. The rock shows a whitish weathered surface and a speckled aspect due to the presence of greyish nepheline grains from 0.5 to 2 centimetres in diameter. An age of 2675 Ma (No. 51, Figure 3.11 and Table 3.3) was obtained for this syenite.

Tasiat Syenite (Atst)

The *Tasiat Syenite* (Table 3.1 and Figure 3.11) forms an isolated intrusion about 2 kilometres by 3 kilometres in size, located in the north-central part of the Minto Subprovince. This intrusion, named by Berclaz *et al.* (2005), was originally recognized by Percival *et al.* (1995b). It is composed of aegyrine-augite essexite and nepheline-biotite syenite. The rock is medium- to coarse-grained and exhibits a variably developed magmatic foliation. A sample from the Tasiat Syenite yielded an age of 2643 Ma (No. 131, Figure 3.11 and Table 3.3).

Opiscotéo Suite (Aopi)

The *Opiscotéo Suite* (Table 3.1 and Figure 3.11), named by Leclair *et al.* (1998) and recognized in the Lac Gayot area (No. 21, Figure 1.2), is a widespread unit within the Ashuanipi Subprovince (Lamothe *et al.*, 1998 and 2000). It is composed of granodioritic to granitic diatexites with biotite ± orthopyroxene ± clinopyroxene ± garnet. These rocks are heterogranular and show a migmatitic texture, with biotite schlieren and abundant enclaves that give the rock a heterogeneous aspect. Enclaves are largely composed of migmatitic paragneiss with minor amounts of mafic gneiss and tonalitic gneiss. A diatexite sample from the Lac Gayot area yielded an age of 2638 Ma (No. 194, Figure 3.11 and Table 3.3). Elsewhere in the Ashuanipi Subprovince, ages ranging between 2682 and 2650 Ma (Leclair *et al.*, 1998; Chevé and Brouillette, 1995; Percival, 1993) were obtained for these diatexites.

Dervieux Suite (Ader)

The *Dervieux Suite* (Table 3.1 and Figure 3.11) was introduced in the Lac Gayot area (No. 21, Figure 1.1) to describe kilometre-scale bodies of biotite-hornblende granodiorite and granite occurring in the Ashuanipi Subprovince. Gosselin and Simard (2001) mentioned that these intrusions are

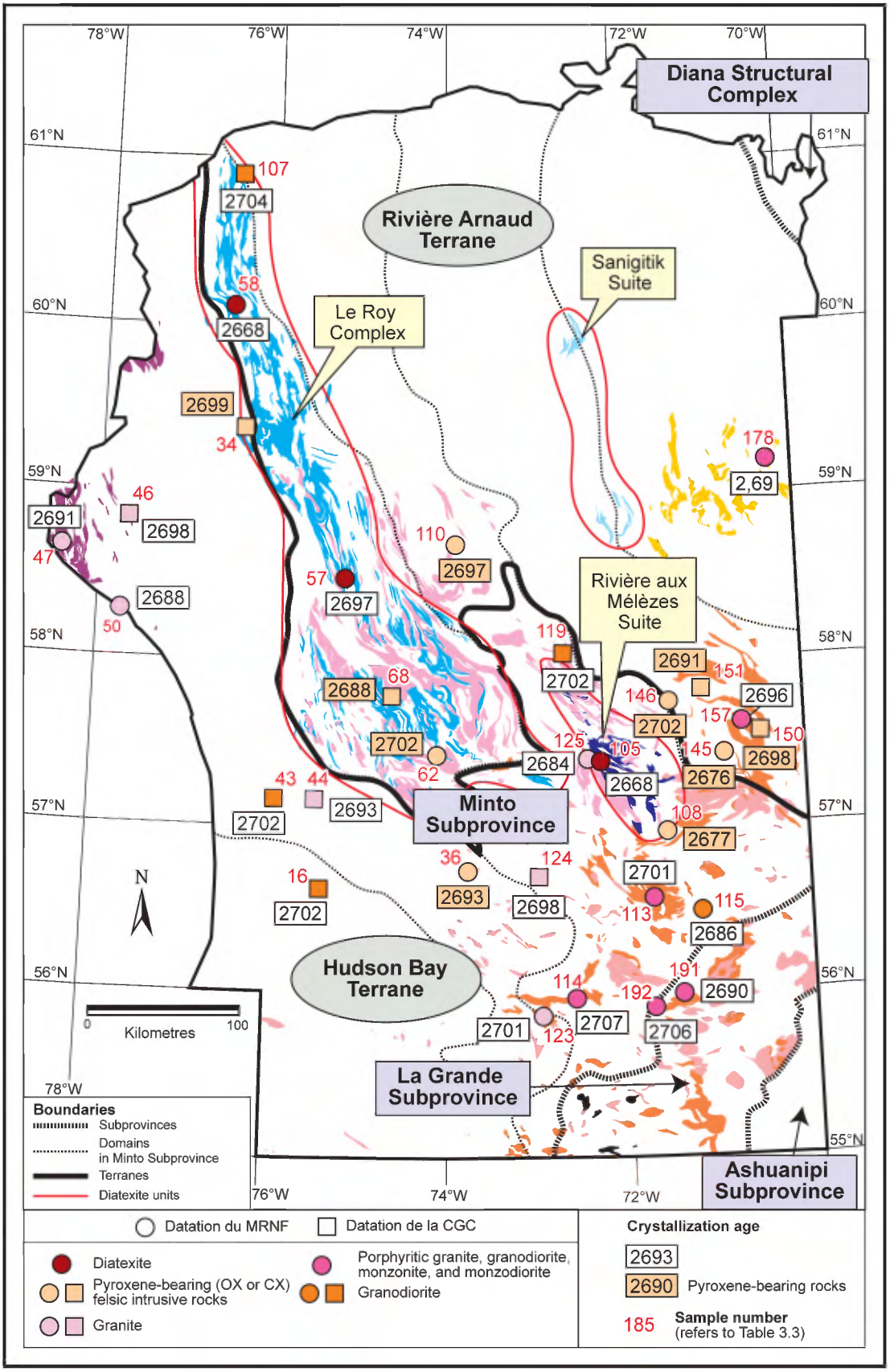

FIGURE 3.10 – Regional distribution of granite, granodiorite, monzodiorite, monzonite, and diatexite units, with corresponding U/Pb ages for the time span from 2705 to 2680 Ma.

Stratigraphic legend (Figure 3.10)

Diatexites

Rivière aux Mélèzes Suite
Granodioritic to granitic diatexite with biotite + garnet + cordierite + andalusite ± sillimanite; numerous enclaves of migmatitic paragneiss.

Sanigitik Suite
Tonalitic to granitic diatexite with biotite + garnet or biotite ± orthopyroxene; numerous enclaves of paragneiss, amphibolite, diorite, and tonalite.

Le Roy Complex
Granodioritic to granitic diatexite with biotite + garnet ± cordierite ± sillimanite ± orthopyroxene; numerous enclaves of migmatitic paragneiss.

Granites, granodiorites, monzodiorites, and monzonites

Morrice Suite
Pinkish to reddish biotite±hornblende granite, homogeneous to locally porphyroid-textured; pegmatite.

Corneille Suite
Whitish chlorite-garnet granite characterized by bluish quartz eyes; numerous enclaves of variable composition; minor whitish tonalite and pegmatite.

Belloy Suite
Porphyroid-textured hornblende-biotite monzonite and quartz monzodiorite.

Maurel Suite
Porphyroid-textured hornblende-biotite granodiorite, granite, monzodiorite, and quartz monzodiorite.

Druillon Suite
Porphyroid-textured monzodiorite, quartz monzodiorite, monzonite, quartz monzonite, and diorite with hornblende + biotite + clinopyroxene ± orthopyroxene; minor granite with sodic amphibole.

Tramont Suite
Homogeneous biotite-chlorite granite.

similar to those in the Maurel Suite. However, intrusions of the Dervieux Suite are inferred to be younger due to the presence of diatexite enclaves of the Opiscotéo Suite. Rocks of the Dervieux Suite are characterized by a porphyroid texture defined by K-feldspar phenocrysts from 1 to 5 centimetres long. The rock is massive to weakly foliated, pinkish grey, and shows a strong magnetic susceptibility. The Dervieux Suite has not been dated.

Joinville Suite (Ajov)

The *Joinville Suite* (Table 3.1 and Figure 3.11) is a new unit we have defined in the Lac Gayot area (No. 21, Figure 1.1). This unit encompasses granitic intrusions located within the Ashuanipi Subprovince that were initially assigned to the Tramont Suite (Gosselin and Simard, 2001). The modification is based on the age difference between granites of the Tramont Suite (2701 to 2698 Ma), occurring in the La Grande and Minto subprovinces, and younger granites of the Ashuanipi Subprovince. The Joinville Suite is composed of homogeneous biotite granite forming kilometre-scale bodies or decimetre-scale to decametre-scale injections in earlier lithologies. The rock is pinkish, massive to weakly foliated, and ranges from fine- to coarse-grained. Mafic minerals, represented by small booklets of biotite or chlorite, generally account for less than 1% of the rock, but may locally reach up to 5%. The Joinville Suite has not been dated. Field relationships indicate that granites of the Joinville Suite cross-cut diatexites of the Opiscotéo Suite (2638 Ma).

Archean and Proterozoic units

Diana Structural Complex

The *Diana Structural Complex* covers a small surface area in the northeasternmost part of the study area (Figure 3.11 and Table 3.1). This complex is part of a wide zone composed of lithological assemblages, most of which are probably Archean in age, that were intensely reworked during the Proterozoic. Evidence of this Proterozoic deformation is namely provided by the presence of dismembered Proterozoic diabase dykes near the margins of the complex. The Diana Structural Complex is located in the transition zone between Archean rocks of the Superior Province and Proterozoic terrains of the Churchill Province. The complex comprises four informal units (Figure 3.11 and attached stratigraphic map). The predominant unit is composed of tonalitic orthogneisses (APdia3), with associated diorites, trondhjemites, and granodiorites. All these rocks are strongly deformed and exhibit a mylonitic foliation and a well-developed stretching lineation. Migmatitic metasedimentary rocks (APdia1) of unknown age, including paragneiss, marble and calc-silicate rocks, form bands transposed parallel to the structural fabric within orthogneisses. Remnants of amphibolite, mafic gneiss, and ultramafic rocks (APdia2) are intercalated with the paragneiss sequences or form bodies covering less than 30 km^2. Finally, foliated or mylonitic porphyroid-textured monzonites and quartz monzonites (PAdia4) form bodies a few kilometres long, elongated parallel to the regional fabric. These intrusive rocks cross-cut the tonalitic gneisses. A sample of tonalitic gneiss yielded an age of 2782 Ma (No. 165, Figure 3.11 and Table 3.3), whereas an age of 2756 Ma was obtained in a monzonite (No. 179, Figure 3.11 and Table 3.3).

Proterozoic units

The Archean rocks of the NESP are surrounded by Proterozoic rock units belonging to the Labrador Trough to the east (New Québec Orogen; Wardle *et al.*, 2002; Clark and Wares, 2006) and the Cape Smith Belt to the north (Ungava Orogen; Taylor, 1982; St-Onge and Lucas, 1990; Lamothe, 1994). To the west, along the coast of Hudson Bay, the Hopewell Islands in the Inukjuak area, and the Nastapoka Islands between Inukjuak and Umiujaq, are also composed of Proterozoic units (Lee, 1965; Chandler, 1988). Proterozoic rocks also outcrop to the south of Umiujaq, in the Lac

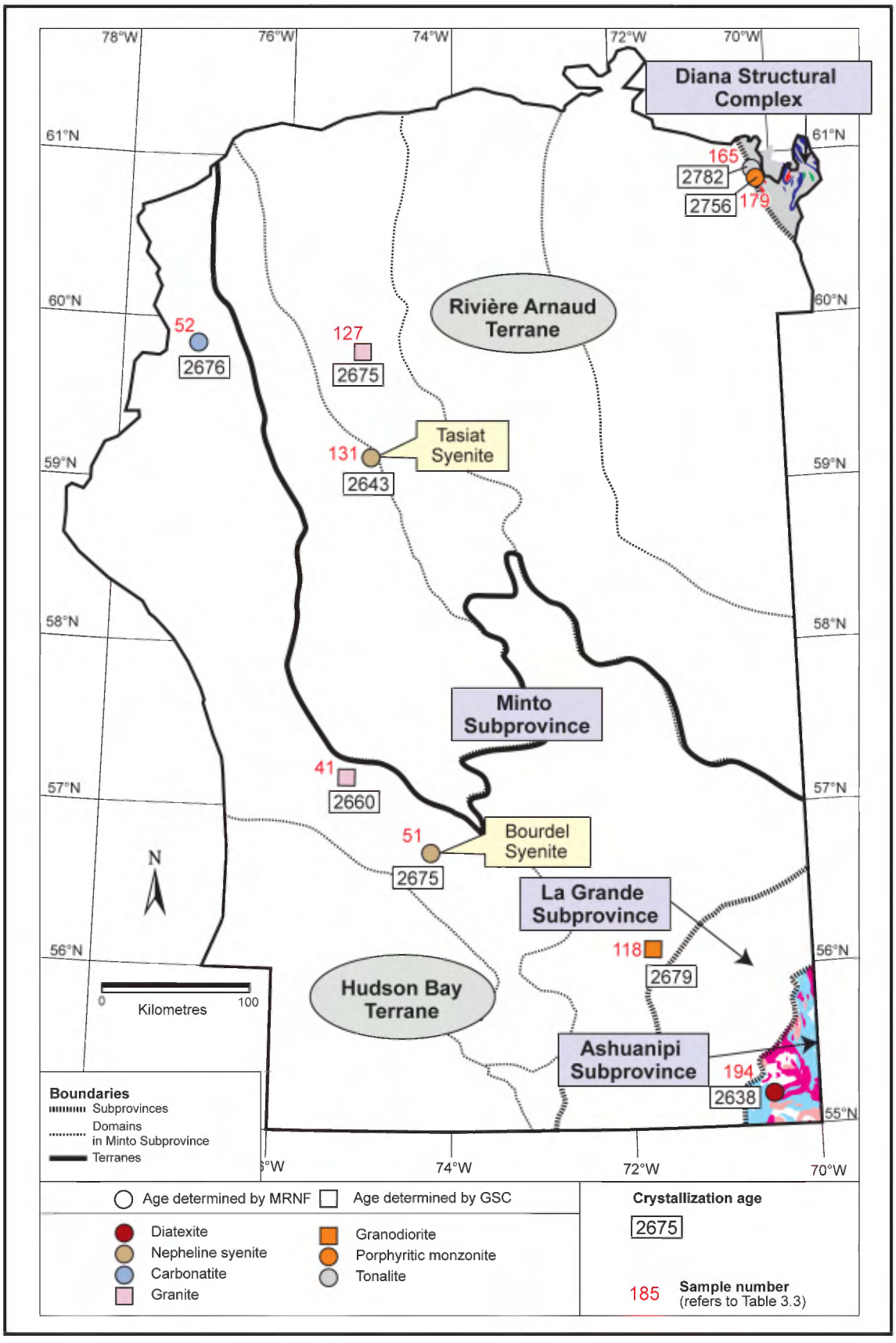

FIGURE 3.11 – Regional distribution of syenites, carbonatites, granites, and diatexites, with corresponding U/Pb ages for the time span from 2680 to 2630 Ma, in addition to units in the Diana Structural Complex.

Stratigraphic legend (Figure 3.11)

ARCHEAN TO PROTEROZOIC

Diana Structural Complex

Foliated to mylonitic monzonite and quartz monzonite, with porphyroid texture.

Tonalitic orthogneiss; trondhjemite, diorite, and granodiorite.

Amphibolite; mafic gneiss; deformed and metamorphosed ultramafic rocks.

Migmatitic paragneiss.

ARCHEAN

Ashuanipi Subprovince

Joinville Suite
Pinkish granite, homogeneous and massive, with less than 1% biotite or chlorite.

Dervieux Suite
Porphyroid-textured biotite-hornblende granodiorite and granite.

Opiscotéo Suite
Granodioritic to granitic diatexite with biotite ± orthopyroxene ± clinopyroxene ± garnet; numerous enclaves of migmatitic paragneiss.

Minto Subprovince

Tasiat Syenite
Nepheline-biotite syenite; aegyrine-augite essexite.

Bourdel Syenite
Nepheline-biotite syenite with well-developed magmatic foliation.

Guillaume-Delisle area (Richmond Gulf Graben; Chandler, 1988). Since work conducted under the Far North Program almost exclusively focused on the Archean rocks of the Superior Province, peripheral Proterozoic units will not be described in this report.

A few Proterozoic units occur within the Archean craton however, namely the Sakami Formation, overlying the Archean basement in the Lac Gayot, Lac Bienville, and Maricourt areas (Nos. 21, 20, and 18, Figure 1.1). Furthermore, numerous diabase dykes cross-cut the Archean bedrock in all map areas, as well as lamprophyre dykes in the Lac Aigneau area (No. 15, Figure 1.1).

Sakami Formation

The *Sakami Formation* (Eade, 1966) occurs in isolated outliers composed of shallowly dipping sedimentary strata unconformably overlying the Archean units. In the La Grande Subprovince, cross-cutting relationships with diabase dykes made it possible to constrain the age of the Sakami Formation between 2500 and 2216 Ma (Goutier *et al.*, 2001). A K-Ar age obtained from micas recovered from a sandstone of the Sakami Formation (Clark, 1984) indicates an age of sedimentation prior to 2230 Ma.

In the NESP, the Sakami Formation forms three main outliers aligned along the Saindon-Cambrien corridor (Moorhead *et al.*, 1999), and a fourth outlier located in the Maricourt area (No. 18, Figure 1.1), covering a few square kilometres and located outside of the corridor.

The Sakami Formation is generally composed of two units: 1) a lower unit of continental deposits mainly consisting of red beds; and 2) an upper unit composed of epicontinental deposits, with whitish to orange-coloured quartz sandstone (Orr, 1979; Clark, 1984). The lower unit, less than 430 metres thick, is composed of conglomerate overlain by arkosic sandstone, mudstone, and siltstone. These assemblages all have a reddish tinge and locally alternate with thin beds of greenish sandstone and argillite. The upper unit, more than 600 metres thick, consists of a homogeneous sequence of massive and cross-bedded orthoquartzite and quartz sandstone.

Diabase dykes

The Archean units of the NESP are cross-cut by numerous Proterozoic diabase dykes, throughout the study area. These diabase dykes, generally less than 100 metres thick, may be traced over several kilometres strike length. They are undeformed and unmetamorphosed, with certain exceptions in areas near Proterozoic orogenies. These rocks are massive and homogeneous, fine- to coarse-grained, and exhibit a dark grey to greenish grey colour with a typical brownish weathered surface. The dykes display aphanitic chilled margins, a few centimetres to a few decimetres in thickness. Ophitic and sub-ophitic textures are most common, although amygdaloidal, porphyritic, or trachytic textures are also observed locally. The rocks are composed of plagioclase and pyroxene, with or without olivine, amphibole, and biotite. Magnetite, occurring in variable proportions, explains the strongly magnetic character of many dykes. The diabase dykes can be assigned to several different swarms with distinct ages and orientations (Chapter 6).

Lamprophyre and carbonatite dykes

A swarm comprising nearly one hundred lamprophyre and carbonatite dykes occurs in the central part of the Lac Aigneau area (No. 15, Figure 1.1). A few dykes were also observed in the northeast part of the Lac Gayot area (No. 21, Figure 1.1). These dykes are 1 centimetre to 1 metre in thickness and trend NW-SE to N-S. The lamprophyre dykes consist of fine-grained or aphanitic ultramafic to mafic rocks and display chilled margins. Ultramafic dykes are distinguished from mafic dykes due to the presence of olivine phenocrysts and the absence of interstitial plagioclase. Lamprophyre dykes occurring in fault zones show a brecciated texture. Carbonatite dykes are spatially associated with carbonatized lamprophyre dykes. The carbonatite is homogeneous, fine- to coarse-grained, and characterized by an orange to rusty brown colour in weathered surface. It

is composed of a carbonate groundmass in which xenoliths of wall rock are commonly enclosed. Age determinations made on two carbonatite dykes yielded ages of 1932 Ma and 1941 Ma (Nos. 195 and 196, Table 3.3).

Diatremes

Two diatremes occur along the margins of the Ungava Trough, in the Lac Couture area (No. 2, Figure 1.1). These rocks were initially recognized by Moorhead (1989), who included the latter in the Povungnituk Group (Ungava Orogen). However, since the relationship between the diatremes and the supracrustal sequence of the Povungnituk Group could not be established, Madore *et al.* (2004) grouped the two intrusions under the term "Kuuvvaluk Diatremes". These consist of two small undeformed circular intrusions about 70 metres in diameter, composed of ultramafic phlogopite-bearing lamprophyre with pyroxene and olivine relics that show well-preserved igneous textures. The lamprophyre is greenish, fine-grained and vesicular, and hosts numerous epidotized xenoliths. The diatremes exhibit fan-shaped columnar jointing that converges toward the centre of the intrusions. These intrusions have not been dated but are most likely Proterozoic in age.

Two diatreme breccias were also observed in the Lac à l'Eau Claire area (No. 16, Figure 1.1), but were not assigned to a specific stratigraphic unit. Field observations suggest these breccias are associated with the emplacement of Proterozoic diabase dykes in this area. They consist of brecciated mafic dykes from 15 to 20 metres thick, that contain clasts of sedimentary rocks and Proterozoic volcanic glass, as well as Archean granitoid clasts. One of these dykes was previously interpreted as a clastic sedimentary dyke by Chandler (1988).

Paleozoic units

Lac Couture Impactite

The Lac Couture Impactite has a nearly perfect circular shape. The presence of impact breccias related to the meteorite crater was first mentioned during an expedition led by Beals (Kitzes, 1964; Beals *et al.*, 1967). Structures and textures typical of meteorite impacts were later identified by Robertson (1965) and Madore *et al.* (2004). An ^{40}Ar-^{39}Ar age of 425 ±25 Ma was obtained from a sample of impact breccia (Bottomley *et al.*, 1990).

Lac à l'Eau Claire Complex

The two rounded depressions that form the Lac à l'Eau Claire are the result of a double meteorite impact (Beals *et al.*, 1956 and 1960). A rock assemblage characterized by impact textures, the Lac à l'Eau Claire Complex, forms a deposit outcropping on a ring of islands located in the centre of the west part of the lake. The pre-erosional thickness of this deposit is estimated at 160 metres (Rondot *et al.*, 1993). The impact rocks were dated using K-Ar (Bostock, 1969), Rb-Sr (Reimold *et al.*, 1981), and Ar-Ar (Bottomley *et al.*, 1990) methods. The ages obtained, at about 280 Ma, indicate that Pennsylvanian cover rocks were present when the impact occurred. Rocks derived from the Lac à l'Eau Claire meteorite impact were not investigated during this field mapping program. These deposits, studied in detail by Rondot *et al.* (1993), were divided into four informal units: 1) a basal breccia, 2) impactite and mylolisthenite dykes; 3) impact-ignimbrite; and 4) impactite. The deposits overlie the variably fractured Archean basement. The presence of maskelynite (vitrified plagioclase) in the Archean rocks indicates high-grade shock metamorphism, with pressure conditions reaching 25 to 30 GPa in the centre of the impact. The presence of a partial cover of Ordovician rocks at the time of impact is suggested by the presence of Ordovician limestone blocks contained in unconsolidated deposits and as enclaves in impactites on the islands of Lac à l'Eau Claire (Rondot *et al.*, 1993).

Cenozoic units

The Pingualuit Crater, formerly referred to as the New Québec Crater, is located just north of the Nantais belt. It is a perfectly circular basin with steep sides, that hosts a lake about 3 kilometres in diameter. Twenty-one fragments of impactite were found near the crater. ^{39}Ar-^{40}Ar ages obtained from the fragments indicate the impact occurred about 1.3 Ma ago (Grieve *et al.*, 1989).

GEOCHRONOLOGY AND REGIONAL RELATIONSHIPS BETWEEN ARCHEAN UNITS

The Archean rocks in the study area underwent a complex evolution spanning a period of about 1.2 Ga. The spatial and temporal distribution of stratigraphic units outlines several events that together describe a process of growth and reworking of the Archean crust in the NESP (Chapter 5). This evolution is marked by an abrupt change at about 2740 Ma, which translates into a change in the composition and spatial distribution of stratigraphic units. Units emplaced prior to 2740 Ma are essentially volcano-sedimentary units and biotite or biotite-hornblende tonalitic units (Figure 3.1), whereas those emplaced after 2740 Ma are mainly composed of granite and granodiorite, clinopyroxene-bearing tonalite and granodiorite, as well as enderbite, charnockite, and diatexite (Figure 3.2).

According to the geologic time scale (Gradstein *et al.*, 2004), Archean units formed during the Eoarchean (pre-3600 Ma), Paleoarchean (3600 to 3200 Ma), Mesoarchean (3200 to 2800 Ma), and Neoarchean (2800 to 2500 Ma) eras. The time span between 3825 and 2890 Ma is represented by a few remnants of volcano-sedimentary and tonalitic rocks, as well as inherited zircons hosted in younger lithologies.

These remains are primarily concentrated in the Hudson Bay Terrane, except for one anomalous area in the east part of the Rivière Arnaud Terrane (Figure 3.3). This confirms the relatively juvenile source for the Rivière Arnaud Terrane, further confirmed by isotopic data (Chapter 4; Figure 4.14). The vast majority of Archean stratigraphic units recognized in the NESP formed during the Neoarchean era, i.e. between 2800 and 2640 Ma.

Eoarchean (pre-3600 Ma)

The only remains of the Eoarchean era (Figure 3.1) were recognized in the westernmost part of the Hudson Bay Terrane. U/Pb analyses conducted on a felsic rock of the Nuvvuagittuq Belt yielded an age of 3825 ±16 Ma (No. 20, Figure 3.3 and Table 3.3; event EA-1, Figure 3.1). Recent studies (Cates and Mojzsis, 2007) have confirmed a minimum age of 3751 ±10 Ma for the rocks in this belt, with results suggesting an age as early as 3800 +55/-52 Ma. A sample of gneissic tonalite from the outer mylonitic edge of one of the synforms in the Nuvvuagittuq Belt yielded a crystallization age of 3650 ±5 Ma (No. 21, Figure 3.3 and Table 3.3; event EA-2, Figure 3.1). This tonalite corresponds to an early remnant, the extent of which has not been determined, hosted in younger tonalites of the Favard Suite (2750 to 2740 Ma).

Paleoarchean (3600 to 3200 Ma)

No Paleoarchean unit was recognized in the NESP (Figure 3.1). However, the existence of magmatic activity during this era is demonstrated by a few Paleoarchean ages obtained for inherited zircons recovered from younger lithologies (Nos. 10, 25, 73, and 210, Figure 3.3 and Table 3.3). These ages are clustered in the Hudson Bay Terrane and the southwesternmost part of the Rivière Arnaud Terrane (No. 210, Figure 3.3).

Mesoarchean (3200 to 2800 Ma)

Stratigraphic and geochronological data can be used to recognize three distinct periods in the Mesoarchean corresponding to successive episodes of growth and reworking of the Archean crust: from 3200 to 2900 Ma, from 2900 to 2850 Ma, and from 2850 to 2800 Ma. These periods respectively correspond to events MA-1, MA-2, and MA-3 (Figure 3.1).

Mesoarchean period from 3200 to 2900 Ma

Ages corresponding to the start of the Mesoarchean era (event MA-1, Figure 3.1) were obtained either as crystallization ages from tonalites (samples Nos. 25, 89, 206, 210, 212) or from inherited zircons hosted in younger lithologies (Figure 3.3 and Table 3.3). The tonalites occur in younger tonalitic units and are interpreted as the remains of early remnants. Their extent has not been determined however, consequently these remnants were not assigned to specific stratigraphic units. The early tonalites show lithological characteristics similar to the younger enclosing tonalites, such that they are difficult to distinguish from one another. Three of the four samples (Nos. 89, 206, 212) are from the Vizien Belt area (Duvert Complex). The majority of inherited zircons with ages corresponding to this period are concentrated in the Hudson Bay Terrane and in the easternmost part of the Rivière Arnaud Terrane (Figure 3.3 and Table 3.3).

Mesoarchean period from 2900 to 2850 Ma

The time span from 2900 to 2850 Ma corresponds to event MA-2 (Figure 3.1). Stratigraphic units from this period are concentrated in the eastern part of the NESP. They mainly correspond to the Gayot Complex and the Aubert Formation, located in the Hudson Bay Terrane (Figure 3.4). Age determinations made on felsic samples from the Gayot Complex yielded ages of 2880 ±2 Ma (Vénus belt; No. 184, Figure 3.4 and Table 3.3) and 2873 ±10 Ma (Coulon belt; No. 185). The Aubert Formation has not been dated, however field observations and the composition of clasts occurring in a conglomerate horizon suggest the sedimentary rocks of this formation are, at least in part, derived from the erosion of the Gayot Complex volcanic edifice (Gosselin and Simard, 2001) and thus are inferred to be younger than 2.87 Ga. Rocks of the Aubert Formation also occur as enclaves in gneissic tonalites of the Brésolles Suite (2833 to 2807 Ma). These observations suggest an approximate age of sedimentation in the 2.87 to 2.83 Ga range for the Aubert Formation.

Further north, crystallization ages of 2879 ±4 Ma and 2869 ±6 Ma (Nos. 169 and 174, Figure 3.4 and Table 3.3) were obtained for tonalites originally assigned to the Faribault-Thury Suite (2785 to 2775 Ma). These tonalites are interpreted as early crustal remains preserved within the main unit. Certain volcano-sedimentary remnants assigned to the Arnaud Complex occur as enclaves within these early tonalites, suggesting part of the Arnaud Complex may be related to a magmatic event coeval with the one responsible for the Gayot Complex (2880 to 2870 Ma). Remains of the time span from 2900 to 2850 Ma are also observed in the east part of the Hudson Bay Terrane, given the presence of inherited zircon ages from this period (Figure 3.4 and Table 3.3).

Mesoarchean period from 2850 to 2800 Ma

The time span from 2850 to 2800 Ma corresponds to event MA-3 (Figure 3.1). This period marks the onset of magmatic activity in the Rivière Arnaud Terrane and is represented by volcano-sedimentary rocks and tonalitic rocks assigned to the Duquet, Qalluviartuuq-Payne, and Arnaud complexes (Figure 3.4). To the south and west, in

the Hudson Bay Terrane, this period is mainly represented by foliated and gneissic tonalites of the Suluppaugalik and Brésolles suites (Figure 3.4).

The age of volcanic rocks in the Qalluviartuuq-Payne Complex ranges, for the most part, between 2851 and 2832 Ma (Nos. 83, 84, and 226, Figure 3.4 and Table 3.3), whereas the age of associated tonalites ranges from 2848 to 2809 Ma (Nos. 95, 100, and 216). Ages of 2822 Ma and 2828 Ma (Nos. 85 and 86, Figure 3.4 and Table 3.3) were obtained from volcanic rocks of the Duquet Complex, whereas tonalitic samples yielded ages of 2812 Ma and 2800 Ma (Nos. 201 and 96). An age of 2818 Ma (No. 163, Figure 3.4 and Table 3.3) was obtained from a volcanic rock in the Buet belt (Arnaud Complex). These geochronology data suggest prolonged, episodic volcanic activity and tonalitic magmatism took place during this time span in the Rivière Arnaud Terrane. Consequently, we consider the main age of these three units to be included in this interval. Several inherited zircons recovered from younger intrusive rocks also yielded ages between 2850 and 2800 Ma, in the Rivière Arnaud Terrane (Figure 3.4). These inherited zircons may be derived from volcano-sedimentary and tonalitic units that were presumably dismembered during the emplacement of younger intrusions.

In the Hudson Bay Terrane, the remains of tonalitic magmatic activity for the time span from 2850 to 2800 Ma are best preserved in the southeast. Ages of 2833 ±5 Ma, 2817 ±7 Ma, and 2807 ±6 Ma (Nos. 188, 87, and 187, Figure 3.4 and Table 3.3) were obtained from tonalitic rocks of the Brésolles Suite, whereas a tonalite of the Suluppaugalik Suite yielded an age of 2808 ±6 Ma (No. 88). The spatial distribution, lithological assemblages, and geochronology data suggest the Brésolles and Suluppaugalik suites are equivalent and related to the same magmatic event. Elsewhere in the Hudson Bay Terrane, other more isolated results indicate the existence of tonalitic activity. In the west, a tonalite was dated at 2812 ±12 Ma (No. 22). This tonalite occurs within a kilometre-scale remnant of volcanic rocks enclosed in tonalites of the Favard Suite (2760 to 2740 Ma). Further north, an age of 2840 ±9 Ma (No. 32) was obtained in a greenish granoblastic metatonalite, which forms an early remnant in a unit of clinopyroxene-bearing tonalite assigned to the Loups Marins Suite (2730 to 2705 Ma). Several inherited zircons recovered from younger lithologies yielded ages between 2850 and 2800 Ma within the Hudson Bay Terrane (Figure 3.4 and Table 3.3). More than half of these are located near rocks of the Brésolles and Suluppaugalik suites, suggesting the two suites were partially assimilated during emplacement of younger intrusions.

Neoarchean (2800 to 2500 Ma)

The spatial distribution of stratigraphic units along with geochronology data indicate the majority of rock units in the study area formed during the Neoarchean era. The Neoarchean era may be divided into two major episodes: the first, from 2800 to 2740 Ma, is characterized by the emplacement of widespread tonalitic units (Figure 3.1), whereas the second, post-2740 Ma, is marked by the emplacement of granites, granodiorites, and pyroxene-bearing felsic intrusive rocks (Figure 3.2).

Neoarchean from 2800 to 2740 Ma

The Hudson Bay and Rivière Arnaud terranes evolved differently in the early Neoarchean, i.e. during the time span from 2800 to 2740 Ma (event NA-1, Figure 3.1) and this is reflected in the spatial and temporal distribution of stratigraphic units. This part of the Neoarchean comprises two periods illustrating the distinct evolution of the two terranes: the period from 2800 to 2760 Ma primarily corresponds to the emplacement of voluminous tonalite intrusions in the Rivière Arnaud Terrane, whereas the period from 2760 to 2740 Ma is associated with tonalitic units in the Hudson Bay Terrane, as well as volcano-sedimentary units occurring on either side of the boundary between the two terranes, in the west part of the study area (Figure 3.5).

Period from 2800 to 2760 Ma

The period between 2800 and 2760 Ma is well represented in the Rivière Arnaud Terrane, with the tonalitic Faribault-Thury, Kapijuq, and Rochefort suites, by the volcano-sedimentary Nantais Complex, and by a few late syenite intrusions assigned to the Kimber Alkaline Suite. In the Hudson Bay Terrane, rocks that formed during this period are concentrated within two small volcano-sedimentary complexes, the Dupire and Garault complexes (figures 3.1 and 3.5).

The Faribault-Thury, Kapijuq, and Rochefort suites (Table 3.1) cover extensive surface areas in the Rivière Arnaud Terrane (Figure 3.5). Several age determinations made on samples from these tonalitic units yielded ages between 2789 and 2755 Ma (Faribault-Thury: Nos. 166, 171, and 172, Kapijuq: Nos. 136 and 138; Rochefort: Nos. 93, 94, 97, 98, 112, and 122; Figure 3.5 and Table 3.3), most of which are in the 2785 to 2775 Ma range. This time span corresponds to the main magmatic event responsible for the emplacement of these rocks. Lithological characteristics and geochronology results suggest the Faribault-Thury, Kapijuq, and Rochefort suites are equivalent. A felsic tuff from the Nantais belt yielded an age of 2775 ±5 Ma (No. 134, Figure 3.5 and Table 3.3). Ages of 2775 Ma (No. 99, Figure 3.5) and 2782 Ma (No. 164, Figure 3.5) were also obtained from quartz-feldspar porphyries in the Duquet and Arnaud complexes respectively, suggesting the occurrence of mafic volcanism contemporaneous with the emplacement of widespread tonalitic suites within the Rivière Arnaud Terrane. Maurice *et al.* (2009) further mentioned the possibility that significant volcanic activity may have occurred at about 2780 Ma in the Rivière Arnaud Terrane. In addition to the age determinations, this hypothesis is based on the regional

distribution of Fe-tholeiites, outlined by a geochemistry study, and which these authors attribute to this particular event. Thus, the Qalluviartuuq-Payne, Duquet, and Arnaud complexes are inferred to be partly equivalent to the Nantais Complex. Note however that most ages obtained in the Qalluviartuuq-Payne, Duquet, and Arnaud complexes link these volcano-sedimentary units to the period from 2850 to 2800 Ma. Finally, age dating analyses on a syenite intrusion of the Kimber Suite yielded an age of 2761 ±1 Ma (No. 183, Figure 3.5 and Table 3.3). These intrusions where thus emplaced at the end of the period between 2800 and 2760 Ma. Several inherited zircons recovered from younger rocks yielded ages in the 2800 Ma to 2760 Ma range in the Rivière Arnaud Terrane (Figure 3.5 and Table 3.3), thereby confirming the existence of an important magmatic event within the latter terrane during this time span.

In the Hudson Bay Terrane, magmatic and volcanic activity appears to have been limited during the time span from 2800 to 2760 Ma. Ages of 2787 ±2 Ma and 2798 ±11 Ma (Nos. 74 and 75, Figure 3.5 and Table 3.3) were obtained from felsic rocks in the Dupire Complex, whereas a sericite schist in the Garault Complex yielded an age of 2782 ±7 Ma (No. 73). An age between 2797 and 2786 Ma (No. 77, Figure 3.5 and Table 3.3) was also obtained from a mafic and ultramafic horizon in the Vizien Belt (Duvert Complex). This result suggests some rocks in this belt are related to a volcanic event coeval with the volcanic activity responsible for rocks of the Dupire and Garault complexes. However, several age determinations made on rocks of the Duvert Complex indicate a younger age for this volcano-sedimentary complex. Several inherited zircons yielded ages in the 2800 to 2760 Ma range, indicating magmatism was probably more important during this time than what can be inferred from the scarce stratigraphic units associated with the latter in the Hudson Bay Terrane (Figure 3.5).

Period from 2760 to 2740 Ma

The time span from 2760 to 2740 Ma corresponds to the formation of volcano-sedimentary rocks assigned to the Kogaluc and Mézard complexes in the Rivière Arnaud Terrane, and to the Roulier Belt and the Innuksuac Complex in the Hudson Bay Terrane (Figure 3.5). The Kogaluc, Mézard, and Innuksuac complexes are characterized by important units of sedimentary origin. Plutonic units related to this period are mostly concentrated in the Hudson Bay Terrane and correspond to the tonalitic Favard, Coursolles, and Sem suites. The Kakiattuq Suite, located near the boundary between the two terranes, is the only tonalitic unit associated with this period in the Rivière Arnaud Terrane.

Ages of 2760 ±5 Ma and 2759 ±3 Ma were obtained from felsic volcanic rocks of the Kogaluc Complex (Nos. 81 and 82, Figure 3.5 and Table 3.3). The age of sedimentary rocks in the Kogaluc Complex remains uncertain however. It is possible that part or all of the sedimentary rocks associated with the second cycle of the Qalluviartuuq-Payne Complex may be equivalent to the Kogaluc Complex. This interpretation is based on an age of 2768 Ma (No. 215, Figure 3.5 and Table 3.3) obtained from a clast in a conglomerate of the Qalluviartuuq-Payne Complex. Several remnants in the Mézard Complex, which occur along the extension of the Kogaluc Complex, are interpreted as the dismembered equivalents of the Kogaluc Complex. The sedimentary rocks of the Mézard and Kogaluc complexes and their migmatitic equivalents (Le Roy Complex, Figure 3.10) constitute an extensive assemblage representing a former sedimentary basin, the age of which remains uncertain. Sedimentary rocks of the Kogaluc Complex are younger than the volcanic rocks (2760 Ma) in the complex and are intruded by post-2740 Ma granitoid rocks. These observations suggest an age between 2760 and 2740 Ma for sedimentary rocks in the Mézard and Kogaluc complexes. However, in the north part of the Mézard Complex, cross-cutting relationships indicate earlier ages for certain volcano-sedimentary rocks. This suggests that certain remnants assigned to the Mézard Complex may in fact be equivalent to the Duquet and Qalluviartuuq-Payne complexes.

To the west, in the Hudson Bay Terrane, a felsic sample from the Roulier Belt yielded an age of 2759 ±1 Ma (No. 24, Figure 3.5 and Table 3.3). In this terrane, the Innuksuac Complex encompasses several remnants of volcano-sedimentary rocks. The age of this complex has not been clearly established. However, the spatial distribution and lithological assemblages of several remnants suggest an age similar to that of the Roulier Belt. It is also quite likely that the supracrustal rocks of the Roulier Belt and the Innuksuac Complex were deposited at the same time as those in the Kogaluc and Mézard complexes (between 2760 and 2740 Ma). An age of <2729 Ma, obtained from a sedimentary rock in a belt assigned to the Innuksuac Complex, suggests this complex may encompass remnants of different ages.

In the Hudson Bay Terrane, the time span from 2760 to 2740 Ma is marked by major tonalitic magmatic activity. Age determinations on samples of the Favard Suite yielded ages between 2766 and 2740 Ma (Nos. 10, 26, 27, 90, 91, and 190, Figure 3.5 and Table 3.3), more commonly in the 2750 to 2740 Ma range. Two tonalitic samples of the Coursolles Suite yielded ages of 2758 ±11 Ma and 2756 ±8 Ma (Nos. 29 and 102, Figure 3.5 and Table 3.3). These results, combined with the spatial distribution of the unit and cross-cutting relationships observed in the field, suggest rocks of the Coursolles Suite represent early phases related to the emplacement of leucotonalites and trondhjemites of the Favard Suite. The Sem Suite has not been dated but we have tentatively assigned it to the time span from 2760 to 2740 Ma, due to its tonalitic composition and its spatial association with the Favard Suite. An age determination made on a tonalite of the Kakiattuq Suite yielded an age of 2741 ±4 Ma (No. 54, Figure 3.5 and Table 3.3), suggesting tonalites in the southwest part of the Rivière Arnaud Terrane are 40 to 30 Ma younger than tonalites observed elsewhere in this terrane.

Several inherited zircon ages correspond to the time span from 2760 to 2740 Ma (Figure 3.5). Most of these ages are clustered in the Hudson Bay Terrane or near its margins, in the Rivière Arnaud Terrane. Similar ages are rare however in the Rivière Arnaud Terrane, indicating magmatic activity in the latter was possibly rather limited during this period. Note however that the analytical error associated with geochronology results is sometimes significant, which may modify the interpretation of inherited ages.

Neoarchean post-2740 Ma

After 2740 Ma, the Neoarchean era is subdivided into three periods corresponding to three successive magmatic events (Figure 3.2):

1. The time span from 2740 to 2705 Ma (NA-2) corresponds to the emplacement of granites, granodiorites, and pyroxene-bearing felsic granitoid rocks that cover extensive portions of the Minto Subprovince;
2. The time span from 2705 to 2680 Ma (NA-3) is characterized by the formation of late granite and granodiorite units and by diatexite units derived from the partial melting of sedimentary rocks;
3. In the Minto Subprovince, the time span from 2680 to 2620 Ma (NA-4) is represented by small late intrusions of nepheline syenite, carbonatite, and granite. In the Ashuanipi Subprovince, this period corresponds to the emplacement of widespread granite and granodiorite units and the partial melting of sedimentary rocks, which produced a significant amount of diatexites.

Period from 2740 to 2705 Ma

The time span from 2740 to 2705 Ma (event NA-2, Figure 3.2) represents a major phase in the construction of the Archean continental crust as it appears today. The diversity of stratigraphic units (figures 3.6, 3.7, and 3.8) and the extensive surface area covered by many of the latter are indicative of the magnitude and diversity of magmatism during this period. The geochronology data compilation shows that U/Pb ages in the 2740 to 2720 Ma range are predominant in the north and west of the study area, whereas ages in the 2720 to 2705 Ma range are largely predominant in the southeast. Ages obtained from inherited zircons recovered in younger lithologies also follow this regional distribution pattern (Figure 3.6).

Stratigraphic units that formed during this period include volcano-sedimentary units, tonalitic units, and ultramafic to intermediate intrusions (Figure 3.6), as well as widespread units of granitic and granodioritic rocks (Figure 3.7) and pyroxene-bearing felsic granitoid rocks (Figure 3.8).

- Volcano-sedimentary units (2740-2705 Ma)

Volcano-sedimentary units that formed between 2740 and 2705 Ma are represented by the Melvin and Tasiataq belts and the Pélican, Chavigny, and Duvert complexes (Figure 3.6). These units contain significant amounts of felsic volcanic rocks, commonly the predominant rock type, which contrasts with the majority of pre-2740 Ma volcano-sedimentary units, where lithological assemblages are dominated by mafic volcanic rocks of tholeiitic affinity. Identical ages were obtained in the Melvin Belt (2741 ±4 Ma), the Tasiataq Belt (2740 ±4 Ma), and the Pélican Complex (2739 ±4 Ma; Nos. 19, 162, 132, Figure 3.6 and Table 3.3). A sample of mobilizate enclosed in a metasedimentary rock of the Pélican Complex also yielded an age of 2733 ±3 Ma (No. 135), which represents the minimum age for the latter. Felsic rocks in the Chavigny (No. 53, Figure 3.6 and Table 3.3) and Duvert (Nos. 78, 79, 76) complexes have comparable ages ranging from 2715 to 2724 Ma. A maximum age of 2708 Ma (No. 211, Figure 3.6 and Table 3.3) was attributed to a conglomerate in the Vizien Belt (Percival *et al.,* 1993). Note that an earlier age, between 2797 and 2786 Ma, had been established for a gabbro horizon in the Vizien Belt (No. 77, Figure 3.5 and Table 3.3). This age is associated with an earlier event, coeval with volcanic activity in the Dupire and Garault complexes. A few ages in the 2740 to 2705 Ma range were obtained in volcano-sedimentary remnants that were assigned to earlier units. In the northwest part of the Minto Subprovince, a maximum age of 2729 ±1 Ma (No. 23, Figure 3.6 and Table 3.3) was established for a sedimentary rock located along the coast of Hudson Bay. These rocks, initially included in the Innuksuac Complex, the age of which is estimated between 2760 and 2740 Ma, were not assigned to a formal unit and their extent is unknown. In the northeast part of the Minto Subprovince, ages of 2725 ±9 Ma and 2718 ±9 Ma (Nos. 231 and 197, Figure 3.6 and Table 3.3) were obtained from detrital zircons respectively hosted in a quartzite and a marble horizon in the Peters-West belt (Figure 7.1). This belt, included in the Arnaud Complex (2818 Ma), thus appears to contain sedimentary rocks related to a much younger event, the extent of which has not been defined. It is possible that certain sedimentary remnants in the Arnaud Complex may be coeval with the Chavigny and Duvert complexes.

- Ultramafic to intermediate intrusive units (2740 to 2705 Ma)

Ultramafic to intermediate intrusions of the Châteauguay and Bacqueville suites are inferred to have formed during the time span from 2740 to 2705 Ma, although the intrusions have not been dated. These intrusions cross-cut tonalites of the Favard and Coursolles suites (2760 to 2740 Ma), but occur as enclaves in younger granitic and granodioritic units (2735 to 2710 Ma). These observations lead us to infer an age of emplacement in the 2740 to 2710 Ma range. Lithological characteristics suggest the Châteauguay and Bacqueville suites are equivalent. In the Lac Minto area (No. 13, Figure 1.1), the discovery of a mineralized showing in a particular facies of ultramafic rocks (Labbé *et al.*, 2001) led Parent *et al.* (2003b) to introduce a new unit, the

Qullinaaraaluk Suite (2705 Ma), encompassing massive and weakly deformed mafic and ultramafic intrusions. In areas further east, prior to the discovery of this showing, intrusions with characteristics similar to those of the Qullinaaraaluk Suite were included in the Bacqueville and Châteauguay suites. Thus, in these areas, the Bacqueville and Châteauguay suites likely contain intrusions that may be equivalent to those of the Qullinaaraaluk Suite.

- Tonalitic units (2740 to 2705 Ma)

Tonalitic rocks from this period are restricted to two minor units located in the north part of the Minto Subprovince, the Bylot and Lesdiguières suites, as well as tonalites or diorites previously assigned to earlier units. Ages of 2737 ±13 Ma and 2723 ±2 Ma (Nos. 55 and 56, Figure 3.6 and Table 3.3) were obtained from tonalites of the Bylot Suite, and a diorite of the Lesdiguières Suite yielded a comparable age of 2724 ±2 Ma (No. 104). Tonalite and diorite samples assigned to the Coursolles (Nos. 30 and 101) and Favard (Nos. 189 and 28) suites, as well as a tonalitic injection in the Vénus volcano-sedimentary belt (No. 186) yielded ages ranging from 2717 to 2713 Ma. These results suggest the Favard and Coursolles suites (Figure 3.5) may contain tonalites resulting from at least two distinct magmatic episodes, a primary episode in the 2760 to 2740 Ma range, and a second episode between 2720 and 2710 Ma, the importance of which is not known at this time.

- Granitic and granodioritic units (2740 to 2705 Ma)

The high proportion of granitic and granodioritic rocks in the Minto Subprovince (~35%; Figure 3.7) attests to the significant potassic magmatism event that took place during this time. The majority of ages in the 2735 to 2720 Ma range are clustered in the northern half of the study area, whereas those ranging from 2725 to 2710 Ma occur mostly in the south, mainly in the southeast (Figure 3.7). Granitic and granodioritic units are represented by the Leridon, La Chevrotière, Pinguq, Rivière aux Feuilles, Dufreboy, and Desbergères suites (Figure 3.7). The Leridon, La Chevrotière, and Pinguq suites cover a significant surface area in the north part of the Minto Subprovince. Samples from the La Chevrotière Suite yielded ages ranging from 2734 to 2719 Ma (Nos. 128, 129, 158, 159, 160, and 161, Figure 3.7 and Table 3.3). Ages of 2727 ±2 Ma (No. 48) and 2725 ±4 Ma (No. 49) were obtained from samples of the Pinguq Suite. The Leridon Suite has not been dated. However, lithological characteristics, spatial distribution, and geochronology results suggest the three suites are equivalent and are derived from the same magmatic event.

The Rivière aux Feuilles and Dufreboy suites are quite extensive in the central part of the Minto Subprovince (Figure 3.7). The Rivière aux Feuilles Suite consists of hornblende-biotite granodiorites with ages ranging between 2733 and 2722 Ma (Nos. 69, 126, 202, 155, and 143, Figure 3.7 and Table 3.3). In the Lac Nedlouc, Lac Aigneau, and Lac Dufreboy areas (Nos. 14, 15, and 12, Figure 1.1), clinopyroxene- and orthopyroxene-bearing granodiorites were not distinguished from hornblende-biotite granodiorites within the Rivières aux Feuilles Suite. The latter pyroxene-bearing granodiorites are probably equivalent to those of the charnockitic MacMahon Suite (2729 to 2720 Ma). In the Lac Dufreboy area (Figure 1.1), the undivided part of the Dufreboy Suite contains porphyritic monzogranites equivalent to porphyritic rocks of the Maurel Suite (2707 to 2686 Ma), charnockitic rocks equivalent to pyroxene-bearing rocks of the MacMahon Suite (2729 to 2720 Ma) and the Troie Complex (2740 to 2725 Ma), tonalites equivalent to those of the Faribault-Thury Suite (2785 to 2775 Ma), as well as gabbros and diorites equivalent to mafic to intermediate intrusions of the Bacqueville Suite (2740 to 2710 Ma). Two granodiorite samples from the undivided part of the Dufreboy Suite in the Lac Dufreboy area, analyzed by the GSC, yielded ages of 2721 Ma and 2726 Ma (Nos. 180 and 181, Figure 3.7 and Table 3.3). However, these rocks may not necessarily belong to the Dufreboy Suite, as these granodiorites may also be equivalent to those of the Rivière aux Feuilles Suite.

The Desbergères Suite covers a large surface area in the south and west of the Minto Subprovince (Figure 3.7). Several age determinations were made on granodiorite samples of this unit. Three samples yielded ages between 2732 and 2724 Ma (Nos. 11, 15, and 40, Figure 3.7 and Table 3.3), comparable to ages obtained for the Pinguq, La Chevrotière, Rivière aux Feuilles, and Dufreboy suites. However, the majority of samples from the Desbergères Suite yielded ages in the 2720 to 2710 Ma range (Nos. 13, 14, 45, 90, 92, 116, and 117, Figure 3.7 and Table 3.3). Sample No. 90 is a granitized tonalite of the Favard Suite. The tonalitic fraction yielded an age of 2741 Ma, whereas the granitic fraction yielded an age of 2713 Ma. This result suggests the late granitic phase observed in tonalites of the Favard, Coursolles, and Sem suites may be related to the emplacement of the Desbergères Suite. Similarly, the granitic phase observed in tonalitic units in the Rivière Arnaud Terrane is inferred to be associated with the emplacement of potassic rocks in this area (La Chevrotière, Leridon, Pinguq, Rivière aux Feuilles, and Dufreboy suites). Some granite and granodiorite samples analyzed by the GSC and collected in an area where the Desbergères Suite is widespread yielded ages ranging from 2702 to 2693 Ma (Nos. 16, 43, and 44, Figure 3.10). These results suggest that in this area, the Desbergères Suite may also contain rocks corresponding to a younger magmatic event.

- Pyroxene-bearing felsic intrusive units (2740 to 2705 Ma)

Extensive units of pyroxene-bearing felsic intrusive rocks provide evidence of widespread "charnockitic"-type magmatism across the Minto Subprovince between 2740 and 2705 Ma (Figure 3.8): the Troie and Qimussinguat

complexes, as well as the Lepelle, MacMahon, Lac Minto, and Loups Marins suites.

The Troie and Qimussinguat complexes form two large ovoid-shaped massifs corresponding to positive magnetic anomalies in the northeast part of the Minto Subprovince. The spatial distribution, age, and lithological assemblages of the two units suggest they are equivalent. Samples of orthopyroxene-bearing tonalitic gneiss yielded ages of 2741 ±8 Ma and 2734 ±5 Ma in the Troie Complex (Nos. 175 and 167, Figure 3.8 and Table 3.3) and an age of 2734 ±3 Ma (No. 176) in the Qimussinguat Complex. An age of 2722 ±3 Ma was obtained from a gabbronorite in the Troie Complex (No. 177). It is possible that tonalitic gneisses may in fact represent recrystallized enderbites corresponding to the early phases of the two complexes. This is supported by the fact that tonalitic rocks with ages in the 2740 to 2730 Ma range are relatively rare in the Minto Subprovince.

The Lepelle, MacMahon, and Lac Minto suites are three contemporaneous units of pyroxene-bearing felsic intrusive rocks that cover a large surface area in the north-central part of the Minto Subprovince (Figure 3.8). U/Pb analyses conducted on samples of the Lepelle Suite indicate an average age between 2725 and 2720 Ma for this unit (Nos. 140, 142, and 156, Figure 3.8 and Table 3.3). A granodiorite sample yielded a slightly younger age, at 2714 ±10 Ma (No. 141). However, considering the error margin, this age may correspond to the average age for the unit. Several U/Pb age determinations made on orthopyroxene-bearing rock samples of the MacMahon Suite yielded ages between 2729 and 2720 Ma (Nos. 109, 144, 152, 153, 154, and 168, Figure 3.8 and Table 3.3). Three samples of enderbite yielded ages of 2711 ±10, 2717 ±10, and 2710 ±10 Ma (Nos. 147, 148, 149), and one sample of clinopyroxene-bearing tonalite was dated at 2711 ±11 Ma (No. 139). If we take into account the error margins associated with these ages, all of these results are comparable. U/Pb age dating analyses on samples of the Lac Minto Suite yielded ages ranging from 2735 to 2710 Ma (Nos. 60, 61, 63, 65, 66, and 67, Figure 3.8 and Table 3.3). A diatexite dated at 2713 Ma (No. 59) is coeval with orthopyroxene-bearing intrusions of the Lac Minto Suite. This diatexite thus predates other diatexites in the Lac Minto Domain assigned to the Le Roy Complex (2697 to 2668 Ma). Several samples of enderbite assigned to the MacMahon and Lac Minto suites yielded much younger ages (2702 to 2676 Ma; Figure 3.10) than other intrusions in these units. These results demonstrate that several enderbitic intrusions assigned to the two suites are in fact related to a younger magmatic event.

Rock samples from the orthopyroxene sub-unit of the Loups Marins Suite yielded ages ranging from 2735 to 2720 Ma (Nos. 7, 8, 37, 38, and 39, Figure 3.8 and Table 3.3). Ages obtained from rocks in the clinopyroxene sub-unit largely fall in the 2715 to 2705 Ma range (Nos. 1, 3, 4, 5, 6, 9, and 31), for an average age of 2712 Ma, with a few ages between 2731 and 2723 Ma (Nos. 2, 33, and 35). These results indicate that clinopyroxene-bearing rocks are generally younger than orthopyroxene-bearing rocks. The two rock types are inferred to be derived from the same magma that presumably evolved over time.

Period from 2705 to 2680 Ma

The Neoarchean period from 2705 to 2680 Ma (event NA-3, Figure 3.2) is mainly characterized by granitic and granodioritic rocks occurring in the central and southern parts of the study area, and by diatexite units in the Minto Subprovince (Figure 3.10). Minor units of tonalite and volcano-sedimentary rocks, as well as ultramafic to mafic intrusions are also associated with this time span (Figure 3.9).

- Volcano-sedimentary units (2705 to 2680 Ma)

Volcano-sedimentary units associated with this period are represented by the Juet and Allemand belts, located in the northernmost part of the Minto Subprovince, and by migmatitic metasedimentary rocks of the Grosbois Complex within the Ashuanipi Subprovince (Figure 3.9).

The Juet and Allemand belts contain similar lithological assemblages and may have equivalent ages, although the Allemand Belt is more strongly metamorphosed. These units have not been dated, but field observations indicate the Juet Belt is clearly younger than enclosing tonalites of the Bylot Suite (2737 to 2723 Ma). The Juet and Allemand belts are well preserved and are interpreted as the last manifestations of late Neoarchean volcanism, at about 2700 Ma. To the southwest of the two belts, an equivalent age of 2701 ±3 Ma was obtained from a felsic rock (No. 199, Figure 3.9 and Table 3.3) collected in a small volcanic remnant that was not assigned to a particular stratigraphic unit.

The Grosbois Complex is a paragneiss unit of limited extent mapped in the northeast part of the Ashuanipi Subprovince (Figure 3.9). It has not been dated, but the paragneisses alternate with tonalitic bands of the Beausac Suite (2690 Ma, Figure 3.9) in the Lac Gayot area (No. 21, Figure 1.1). Paragneisses of the Grosbois Complex are most likely equivalent to paragneisses mapped further south in the Ashuanipi and included in the Hublet Group (Leclair *et al.*, 1998). Migmatitic paragneisses of the Grosbois Complex and elsewhere across the Ashuanipi Subprovince probably represent the partially melted equivalents of metasedimentary rocks in the Opinaca Subprovince assigned to the Mercator Formation (Lamothe *et al.*, 1998 and 2000) and the Laguiche Group (Simard and Gosselin, 1999).

- Ultramafic and mafic intrusive rock units (2705 to 2680 Ma)

Ultramafic and mafic intrusive rocks of the Qullinaaraaluk and Couture suites are associated, in part, with the period from 2705 to 2680 Ma. Two leucogabbros in the Qullinaaraaluk Suite yielded respective ages of 2707 ±1 Ma (No. 17, Figure 3.9 and Table 3.3) at the Flipper showing in the Lac à l'Eau Claire area (Simard *et al.*, 2005b), and 2705 ±1 Ma

(No. 18) at the Tan showing in the Lac Minto area (Simard *et al.*, 2005a). However, an age of 2720 ±2 Ma (No. 72) was obtained from a pegmatite cross-cutting the ultramafic intrusion that hosts the Qullinaaraaluk showing in the Lac Minto area (Parent *et al.*, 2003b; Simard *et al.*, 2005a). The latter result indicates that intrusions of different ages were grouped together in the Qullinaaraaluk Suite. This is also supported by geochemical differences (Chevé, 2005) and by the variety of mineral assemblages and textures observed in intrusions of the Qullinaaraaluk Suite. Note that intrusions equivalent to those of the Qullinaaraaluk Suite were also possibly included in the Bacqueville and Châteauguay suites further east. The Couture Suite has not been dated. Enclaves of intermediate to ultramafic rocks of this suite were observed in granitoid rocks of the Lepelle (about 2720 Ma) and La Chevrotière (2735 to 2720 Ma) suites, whereas in other locations, they appear to intrude the same granitoid rocks. The Couture Suite thus encompasses intrusions of different ages. Lithological similarities between intrusions of the Couture and Qullinaaraaluk suites suggest the two units may be partly equivalent.

- Tonalitic units (2705 to 2680 Ma)

Tonalitic magmatism was not widespread during the Neoarchean period between 2705 and 2680 Ma. This magmatic activity is represented by three minor units, the Itinnaru Pluton and the Rivière Qijuttuuq Suite in the Minto Subprovince, as well as the Beausac Suite in the Ashuanipi Subprovince (Figure 3.9). The age of the Itinnaru Pluton has been established at 2691 ±6 Ma (No. 137, Figure 3.9 and Table 3.3). The Rivière Qijuttuuq Suite has not been dated, but it has tentatively been associated with the latest Neoarchean tonalitic event in the study area, based solely on the weakly deformed aspect of its rocks. Tonalites of the Beausac Suite are located in the northwest part of the Ashuanipi Subprovince, where they occur alternating with paragneisses of the Grosbois Complex. An age of 2690 Ma (No. 193, Figure 3.9 and Table 3.3) was obtained from a foliated tonalite in the Lac Gayot area (No. 21, Figure 1.1).

- Granitic and granodioritic units (2705 to 2680 Ma)

Granitic and granodioritic units associated with the period from 2705 to 2680 Ma are represented by the Tramont, Druillon, Maurel, and Belloy suites, in the east and southeast parts of the study area, and by the Morrice Suite in the central part (Figure 3.10). A less extensive unit, the Corneille Suite, is located further west, along the coast of Hudson Bay.

Samples from the Maurel Suite yielded ages ranging from 2707 to 2686 Ma (Nos. 113, 114, 115, 157, 191, and 192, Figure 3.10 and Table 3.3) and two granite samples of the Tramont Suite yielded ages of 2701 ±4 Ma and 2698 ±6 Ma (Nos. 123 and 124). The two suites have comparable ages and occur within the same general area. Injections of Tramont leucogranite are commonly observed cross-cutting porphyritic intrusions of the Maurel Suite. It is possible that the two units are genetically related, and granites of the Tramont Suite may represent a more evolved phase. In the Lac Dufreboy area (No. 12, Figure 1.1), some leucogranites assigned to the older Dufreboy Suite may have an age equivalent to the Tramont Suite (figures 3.7 and 3.10). Slightly further north, a sample of porphyroid-textured monzonite assigned to the Belloy Suite yielded an approximate age of 2.69 Ga (No. 178, Figure 3.10 and Table 3.3) comparable to the age of porphyroid-textured rocks of the Maurel Suite.

The small intermediate to felsic intrusions assigned to the Druillon Suite in the northwest part of the La Grande Subprovince (Figure 3.10) have not been dated. These intrusions are considered to be late given their massive, weakly deformed aspect. Thériault and Chevé (2001) mentioned a textural and mineralogical similarity between these intrusions and those of the Maurel Suite, as well as with intrusions of the Gamard Suite (Leclair *et al.*, 1998) mapped within the Ashuanipi Subprovince.

In the westernmost part of the Minto Subprovince, two samples of whitish granite of the Corneille Suite yielded ages of 2698 ±1 Ma and 2691 ±1 Ma (Nos. 46 and 47, Figure 3.10 and Table 3.3). An age of 2688 ±2 Ma (No. 50) was obtained from a whitish pegmatite cross-cutting volcano-sedimentary rocks of the Nuvvuagittuq Belt. This pegmatite is interpreted as a late phase associated with the Corneille Suite.

Granites of the Morrice Suite occur in the central part of the Minto Subprovince (Figure 3.10). One granite sample yielded an age of 2684 ±6 Ma (No. 125, Figure 3.10 and Table 3.3). It is possible that granites of the Morrice Suite may represent the more evolved phases associated with the migmatization of sedimentary units in the Minto Subprovince, between 2698 and 2668 Ma. A genetic link between granites of the Morrice Suite and diatexites of the Rivière aux Mélèzes Suite (2668 Ma) and the Le Roy Complex (2698 to 2668 Ma) has been postulated before, by Parent *et al.* (2001 and 2003b).

Four granodiorite samples and one granite sample, analyzed by the GSC, yielded ages ranging from 2704 to 2693 Ma (Nos. 16, 43, 44, 107, and 119, Figure 3.10 and Table 3.3). These sample locations were not revisited, and these rocks have not been assigned to known stratigraphic units. The importance of intrusive rocks related to this time span remains unknown at this time.

- Diatexite units (2705 to 2680 Ma)

Rocks of the Minto Subprovince underwent regional-scale high-temperature metamorphism, which is responsible for the formation of diatexites during the time span from 2705 to 2680 Ma. Geochronology data suggest this metamorphism may have begun at about 2720 Ma and continued locally until about 2670 Ma. Diatexite units in the Minto Subprov-

ince are represented by the Le Roy Complex, the Rivière aux Mélèzes Suite, and the Sanigitik Suite.

The Le Roy Complex covers a large surface area in the Lac Minto Domain (Figure 3.10). Field observations and the geochemical composition of felsic mobilizates suggest diatexites of the Le Roy Complex are derived from the partial melting of sedimentary rocks. The latter most likely formed an extensive sedimentary basin that was dismembered and metamorphosed. The non-melted metasedimentary protolith associated with these diatexites was assigned to the Mézard and Kogaluc complexes. Two diatexite samples from the Le Roy Complex yielded ages of 2697 ±1 Ma and 2668 ±22 Ma (Nos. 57 and 58, Figure 3.10 and Table 3.3).

Diatexites of the Rivière aux Mélèzes Suite are derived from the partial melting of sedimentary rocks possibly associated with the Duvert Complex. An age of 2668 ±11 Ma (No. 105, Figure 3.10 and Table 3.3) was obtained from a diatexite sample of this unit.

Diatexites of the Sanigitik Suite (Figure 3.10) are derived from the partial melting of supracrustal rocks in the west part of the Arnaud Complex. This unit of limited extent has not been dated. Its formation is inferred to be related to an important melting event that affected volcano-sedimentary rocks of the Minto Subprovince between 2705 and 2680 Ma.

- Pyroxene-bearing felsic intrusive rocks (2705 to 2680 Ma)

Several samples of pyroxene-bearing felsic intrusive rocks yielded ages ranging from 2702 to 2676 Ma (Figure 3.10). These granitoid rocks occur in the same general area and are coeval with the granitic Tramont, Maurel, and Morrice suites, as well as diatexites of the Le Roy Complex and the Rivière aux Mélèzes Suite. Initially, these rocks were assigned to the MacMahon Suite (Nos. 108, 110, 145, 146, 150, and 151, Figure 3.10 and Table 3.3), the Lac Minto Suite (Nos. 34, 62, 68), and the Loups Marins Suite (No. 36). Age determinations demonstrate however that these three units also encompass pyroxene-bearing granitoid rocks related to younger magmatic events than those that led to the formation of rocks in the latter units (2735 to 2710 Ma). This more recent charnockitic event appears to be mainly concentrated in the central part of the Minto Subprovince.

Period from 2680 to 2630 Ma

The time span from 2680 to 2630 Ma corresponds to the last Archean magmatic events recorded within the Minto Subprovince. They are represented by isolated intrusions of granodiorite and granite (Nos. 41, 118, and 127, Figure 3.11 and Table 3.3) as well as dykes and small intrusions of carbonatite (No. 52) and syenite, including the Tasiat Syenite (No. 131; 2643 ±8 Ma) and the Bourdel Syenite (No. 51; 2675 ±1 Ma). Magmatic activity was much more extensive in the Ashuanipi Subprovince during this time span.

- Ashuanipi Subprovince

Rocks of the Ashuanipi Subprovince cover a limited surface area in the southeast corner of the study area (Figure 3.11). During the time span from 2680 to 2630 Ma, metasedimentary rocks of the Grosbois Complex underwent significant migmatization, which resulted in the formation of diatexites of the Opiscotéo Suite. The Dervieux and Joinville suites also confirm the occurrence of significant potassic magmatism during this period.

An age of 2638 ±8 Ma (No. 194, Figure 3.11 and Table 3.3) was obtained from a diatexite sample of the Opiscotéo Suite in the Lac Gayot area (Figure 1.1). Several U/Pb analyses of diatexite samples collected in various locations across the Ashuanipi Subprovince yielded ages ranging from 2682 to 2650 Ma (Leclair *et al.*, 1998; Chevé and Brouillette, 1995; Percival, 1993). Ashuanipi diatexites are the products of advanced melting of metasedimentary rocks equivalent to those in the Opinaca Subprovince. Some diatexites are also the result of melting of rocks of the La Grande Subprovince.

The Dervieux Suite has not been dated. However, in the Lac Gayot area, porphyroid-textured granites of the Dervieux Suite contain diatexite enclaves of the Opiscotéo Suite (2638 Ma). In the Lac Hurault area (Thériault and Chevé, 2001), porphyroid-textured rocks equivalent to the Dervieux Suite were assigned to the Gamard Suite, which was dated at 2647 ±2 Ma (Parent, 1998) in the Lac Vallard area (Lamothe *et al.*, 1998). Another possibility is that the Dervieux Suite is equivalent to the Lataignant Suite (Lamothe *et al.*, 2000) composed of porphyroid-textured granites with a strong magnetic susceptibility. Further south in the Ashuanipi Subprovince, ages of 2638 ±2 Ma and 2642 +9/-5 Ma were obtained for these granites (Lamothe *et al.*, 2000).

The Joinville Suite has not been dated. However, granites of this suite cross-cut diatexites of the Opiscotéo Suite (2638 Ma) as well as porphyroid-textured intrusions of the Dervieux Suite.

Diana Structural Complex

Units that make up the Diana Complex appear to be at least partly equivalent to units occurring further west. Tonalitic gneisses are probably equivalent to tonalites of the Faribault-Thury Suite. This correlation is supported by an age of 2782 ±19 Ma (No. 165, Figure 3.11 and Table 3.3) obtained in Diana orthogneisses, an age comparable to that established for the Faribault-Thury Suite. Certain metavolcanic remnants in the Diana Complex may be equivalent to metamorphosed volcanic rocks of the Arnaud Complex. However, several amphibolite bands may also correspond to dismembered and metamorphosed Proterozoic diabase dykes. Metasedimentary rocks in the Diana Complex have no apparent equivalents elsewhere in the Minto Subprovince, and may be associated with Proterozoic units. Finally,

porphyroid-textured monzonite and quartz monzonite intrusions show compositions and textures similar to monzonites of the Leridon Suite. However, the age of 2756 ±8 Ma (No. 179, Figure 3.11 and Table 3.3) obtained from a monzonite in the Diana Complex is earlier than ages obtained in potassic intrusions of the northeastern Superior Province (<2735 Ma).

CONCLUSIONS

As a result of the stratigraphic nomenclature revision of Archean units in the NESP, several names of stratigraphic units were abandoned (Table 3.2). Lithological assemblages in abandoned units were reassigned to other units in order to simplify and standardize the nomenclature (Table 3.1). Subsequently to this revision, Archean rocks in the study area are now grouped into 68 different stratigraphic units (Table 3.1; attached stratigraphic map and legend).

Geochronology analyses conducted by the MRNF (n=140) and the GSC (n=81) on Archean rocks (Table 3.3) contributed in defining the various stratigraphic units. The results reveal that the Archean crust of the NESP is the product of a succession of magmatic events that took place over a time span of about 1.2 Ga. The evolution of this continental crust is marked by two major periods: 1) the time span prior to 2740 Ma, characterized by volcano-sedimentary and tonalitic units; and 2) the time span after 2740 Ma, characterized by granites, granodiorites, and pyroxene-bearing granitoid rocks.

The distribution of stratigraphic units, combined with geochronological and isotopic data (Chapter 4), outline two terranes, one early and the other juvenile, that evolved differently until about 2740 Ma. These terranes correspond to the Rivière Arnaud Terrane to the north and the Hudson Bay Terrane to the south and west. The Nuvvuagittuq Belt (3825 Ma) is the oldest unit recognized in the NESP. However, pre-2900 Ma ages were also obtained in tonalite remnants and from inherited zircons recovered from younger units. These remains demonstrate that prior to 2900 Ma, magmatic activity was essentially concentrated in the Hudson Bay Terrane, as most of the history of the Rivière Arnaud Terrane took place after this time. Stratigraphic units with ages between 2900 and 2850 Ma occur mostly in the east part of the Hudson Bay (the volcanic Gayot Complex and sedimentary Aubert Formation) and Rivière Arnaud (part of the volcanic Arnaud Complex) terranes. During the time span from 2850 to 2800 Ma, volcanic units associated with tonalitic magmatism characterize the Rivière Arnaud Terrane (Qalluviartuuq-Payne and Duquet complexes and part of the Arnaud Complex), whereas tonalitic units (Brésolles and Suluppaugalik suites) provide evidence of an important magmatic episode in the Hudson Bay Terrane. Between 2800 and 2760 Ma, extensive tonalitic units (Rochefort, Kapijuq, and Faribault-Thury suites) were emplaced in the Rivière Arnaud Terrane. This tonalitic magmatism was accompanied by mafic volcanism (Nantais Complex). The emplacement of a few nepheline syenite intrusions (Kimber Alkaline Suite; 2761 Ma) coincides with the end of tonalitic magmatic activity in the east part of the Rivière Arnaud Terrane. The small volcanic Dupire and Garault complexes represent the only stratigraphic units with ages in the 2800 to 2760 Ma range in the Hudson Bay Terrane. However, the presence of inherited zircons in younger intrusions suggests magmatic activity was probably more widespread. Between 2760 and 2740 Ma, magmatic activity was very important in the Hudson Bay Terrane, with the emplacement of the tonalitic Favard, Coursolles, and Sem suites. To this period are also associated extensive sedimentary units with volcanic rocks (Mézard, Kogaluc, Innuksuac complexes and Roulier Belt) and a unit of tonalitic rocks (Kakiattuq Suite) in the west part of the Minto Subprovince, at the boundary between the two terranes.

After 2740 Ma, tonalitic magmatism was replaced by granitic, granodioritic, and enderbitic plutonism, and tholeiitic mafic volcanism was largely replaced by calc-alkaline mafic to felsic volcanism. Several magmatic events successively took place from 2740 to 2630 Ma, simultaneously affecting the Hudson Bay and Rivière Arnaud terranes and creating the current image of the NESP.

The period from 2740 to 2705 Ma corresponds to a succession of major magmatic events responsible for the emplacement of several extensive granitoid units. These events affected both the Rivière Arnaud Terrane and the west part of the Hudson Bay Terrane until 2720 Ma then, from 2720 to 2705 Ma, continued almost exclusively in the Hudson Bay Terrane.

In the Rivière Arnaud Terrane, the period from 2740 to 2720 Ma is represented by magmatism that produced extensive suites of granite and granodiorite (La Chevrotière, Leridon, Pinguq, Dufreboy, and Rivière aux Feuilles suites) and widespread pyroxene-bearing granitoid units (MacMahon, Minto, Lepelle suites, and Troie and Qimussinguat complexes). A few units of tonalite (Bylot and Lesdiguières suites) and a few isolated volcano-sedimentary units (Pélican and Chavigny complexes, and Melvin and Tasiataq belts) are also associated with this time span. In the west part of the Hudson Bay Terrane, enderbitic magmatism responsible for rocks of the Loups Marins Suite (2735 to 2720 Ma) evolved to produce clinopyroxene-bearing granitoid rocks (2720 to 2705 Ma) assigned to the same unit. The granodioritic and granitic Desbergères Suite (2720 to 2710 Ma) covers a large surface area within this terrane, providing evidence for important potassic magmatism between 2720 and 2710 Ma. The formation of the Duvert Complex, including the Vizien Belt, is largely coeval with the Desbergères Suite. Several ultramafic to intermediate intrusions were emplaced in the two terranes between 2740 and 2705 Ma (Châteauguay and Bacqueville suites). However, the absolute age of these intrusions is unknown.

Several late granodiorite and granite intrusions assigned to the Tramont, Maurel, Morrice, and Corneille suites, and monzonite and monzodiorite intrusions assigned to the

Belloy and Druillon suites, are related to the period from 2705 to 2680 Ma. These intrusions are largely concentrated in the central and southeast parts of the study area. Several enderbitic intrusions yielded similar ages but could not be assigned to distinct stratigraphic units. The time span from 2705 to 2680 Ma also corresponds to a melting event that produced a significant amount of diatexites assigned to the Sanigitik and Rivière aux Mélèzes suites and the Le Roy Complex. Diatexites of the Le Roy Complex are derived from the partial melting of sedimentary rocks in the Mézard and Kogaluc complexes; diatexites of the Rivière aux Mélèzes Suite are the result of melting of rocks of the Duvert Complex; and Sanigitik diatexites are derived from the melting of sedimentary rocks assigned to the Arnaud Complex. Late tonalitic intrusions (Rivière Qijuttuuq Suite and Itinnaru Pluton), two small volcano-sedimentary belts (Juet and Allemand belts), as well as several ultramafic to intermediate intrusions (Qullinaaraaluk and Couture suites) also formed during this period.

The last Neoarchean manifestations in the Minto Subprovince correspond to isolated intrusions of granite (2679 to 2660 Ma), carbonatite (2677 Ma), and nepheline syenite (Bourdel Syenite, 2675 Ma; Tasiat Syenite, 2643 Ma). During this time, magmatic activity was concentrated in the Ashuanipi Subprovince, with the emplacement of granodioritic and granitic intrusions of the Dervieux and Joinville suites and the migmatization of sedimentary rocks in the Grosbois Complex (2700 Ma), which led to the formation of diatexites of the Opiscotéo Suite (2680 Ma to 2638 Ma).

The Diana Structural Complex is located in a transition zone between the Minto Subprovince and the Churchill Province. This complex is mainly composed of Archean tonalitic orthogneisses and monzonite intrusions that were reworked during the Proterozoic. It also contains amphibolite bands and boudins, produced by the dismemberment of Archean volcanic units and Paleoproterozoic diabase dykes. Some metasedimentary remnants in the Diana Complex may correspond to Proterozoic deposits.

A few Proterozoic units were also mapped within the Archean craton. They consist of sedimentary rocks of the Sakami Formation, diabase dykes and swarms, lamprophyre and carbonatite dykes occurring in the southeast part of the Utsalik Domain, and a few isolated diatreme breccias and dykes.

The Lac Couture (425 Ma), Lac à l'Eau Claire (280 Ma), and Pingualuit (New Québec, 1.3 Ma) craters represent the remains of meteorite impacts that affected the Archean rocks of the NESP.

TABLE 3.1 - Stratigraphic units in the NESP.

Unit	Stratigraphic code	Dominant lithology	Type area (numbers refer to Figure 1.1)	Author(s)	Other areas (numbers refer to Figure 1.1)	Figure showing location of unit in the text	Average age (based on U/Pb geochronology data)	Modifications
Allemand (Belt)	Aale	Mafic and felsic metavolcanic rocks	Lac Couture (N°2)	Madore *et al.*, 2004	None	Figure 3.9	Not dated (age estimated at about 2700 Ma)	None
Arnaud (Complex)	Aarn	Volcano-sedimentary rocks	Lac Peters (N°8)	New unit	Rivière Arnaud (N°4) Lac Pélican (N°7) Lac Klotz (N°3) Lac La Potherie (N°11) Lac Dufreboy (N°12)	Figure 3.4	2818 Ma, 2782 Ma, 2725 Ma and 2718 Ma (some remnants equivalent to Gayot Complex)	New unit that includes all volcano-sedimentary remnants in the Faribault-Thury, Troie, and Qimussinguat complexes within the Douglas Harbour Domain.
Aubert (Formation)	Aat	Sedimentary rocks	Lac Gayot (N°21)	Gosselin et Simard, 2001	None	Figure 3.4	Not dated (age estimated between 2.87 and 2.83 Ga)	None
Bacqueville (Suite)	Abcv	Ultramafic to intermediate intrusions	Lac Nedlouc (N°14)	Parent *et al.*, 2001	Lac Aigneau (N°15) Lac La Potherie (N°11) Lac Dufreboy (N°12) Lac Vernon (N°10) Lac Minto (N°13) Lac à l'Eau Claire (N°16)	Figure 3.6	Not dated (age estimated between 2740 and 2710 Ma)	Granoblastic diorite rafts previously included in the Melvin Complex (abandoned term) are reassigned to the Bacqueville Suite.
Beausac (Suite)	Abea	Tonalite	Lac Gayot (N°21)	Gosselin and Simard, 2001	None	Figure 3.9	2690 Ma	None
Belloy (Suite)	Ably	Porphyroid-textured monzonite and monzodiorite	Lac Peters (N°8)	New unit	Lac Dufreboy (N°12)	Figure 3.10	2690 Ma	New suite introduced to designate monzonites and monzodiorites previously assigned to the Troie Complex.
Bourdel (Syenite)	Abol	Nepheline syenite	Lac à l'Eau Claire (N°16)	Simard *et al.*, 2005b	None	Figure 3.11	2675 Ma	None
Brésolles (Suite)	Abre	Foliated to gneissic tonalite	Lac Gayot (N°21)	Gosselin and Simard, 2001	Maricourt (N°18) Lacs des Loups Marins (N°17) Lac Bienville (N°20)	Figure 3.4	De 2833 à 2807 Ma	None
Bylot (Suite)	Abyl	Tonalite with diatexitic aspect	Povungnituk (N°1)	Maurice *et al.*, 2005a	None	Figure 3.6	2737 et 2723 Ma	None
Châteauguay (Suite)	Achg	Ultramafic to intermediate intrusions	Maricourt (N°18)	Simard *et al.*, 2002	Lacs des Loups Marins (N°17) Lac Bienville (N°20) Lac Montrochand (N°19)	Figure 3.6	Not dated (age estimated between 2740 and 2710 Ma)	None
Chavigny (Complex)	Achy	Felsic volcanic rocks	Lac Vernon (N°10)	Parent *et al.*,2003b	None	Figure 3.6	2722 Ma	None

TABLE 3.1 - Stratigraphic units in the NESP (continued).

Unit	Stratigraphic code	Dominant lithology	Type area (numbers refer to Figure 1.1)	Author(s)	Other areas (numbers refer to Figure 1.1)	Figure showing location of unit in the text	Average age (based on U/Pb geochronology data)	Modifications
La Chevrotière (Suite)	Alcv	Porphyroid-textured granite and granodiorite	Lac Nedlouc (N°14)	Parent *et al.*, 2001	Lac La Potherie (N°11) Lac Pélican (N°7) Lac Anuc (N°6) Lac Klotz (N°3) Lac Couture (N°2) Povungnituq (N°1)	Figure 3.7	2734 to 2719 Ma	Granites of the Lesdiguières and Rochefort suites as well as rocks of the La Potherie Batholith are reassigned to the La Chevrotière Suite. Porphyritic granites and granodiorites in the Lac Aigneau and Lac Dufreboy areas are reassigned to the Maurel Suite. Granodiorites in the south part of the Kogaluc Bay area are reassigned to the Desbergères Suite. Porphyritic intrusions in the Kogaluc Bay and Povungnituk areas, within the Tikkerutuk and Lac Minto domains, are reassigned to the Pinguq Suite.
Corneille (Suite)	Acrn	White granite	Rivière Innuksuac (N°9)	Simard *et al.*, 2004	Kogaluc Bay (N°5)	Figure 3.10	2698 to 2688 Ma	None
Coursolles (Suite)	Acou	Hornblende-biotite tonalite, diorite and gabbro	Maricourt (N°18)	Simard *et al.*, 2001	Lac Gayot (N°21) Lac Aigneau (N°15) Lacs des Loups marins (N°17) Lac Bienville (N°20) Lac Montrochand (N°19) Lac à l'Eau Claire (N°16) Lac Minto (N°13)	Figure 3.5	2758 and 2756 Ma Younger ages at 2716 and 2713 Ma	None
Couture (Suite)	Acot	Ultramafic to intermediate intrusions	Lac Couture (N°2)	Madore *et al.*, 2004	Lac Anuc (N°6)	Figure 3.9	Not dated (age estimated at about 2705 Ma)	Ultramafic to intermediate intrusions of the Lac Calme Suite (abandoned term) are reassigned to the Couture Suite.
Dervieux (Suite)	Ader	Porphyroid-textured granite	Lac Gayot (N°21)	Gosselin and Simard, 2001	None	Figure 3.11	Not dated; contains enclaves of Opiscotéo Suite diatexite (2638 Ma)	None
Desbergères (Suite)	Adeb	Granodiorite and granite	Maricourt (N°18)	Simard *et al.*, 2002	Lacs des Loups Marins (N°17) Lac Bienville (N°20) Lac Montrochand (N°19) Lac à l'Eau Claire (N°16) Lac Minto (N°13) Rivière Innuksuac (N°9) Kogaluc Bay (N°5)	Figure 3.7	2720 to 2710 Ma Earlier ages between 2732 and 2724 Ma	Granodiorites of the Charnières and Voizel suites (abandoned terms) as well as some intrusions of the La Chevrotière Suite in the Kogaluc Bay area are reassigned to the Desbergères Suite.
Diana (Structural Complex)	Apdia	Tonalitic orthogneiss, amphibolite, paragneiss, porphyroid-textured monzonite	Rivière Arnaud (N°4)	Madore and Larbi, 2001	None	Figure 3.11	2782 Ma for tonalitic orthogneisses 2756 Ma for porphyritic intrusions	None

TABLE 3.1 - Stratigraphic units in the NESP (continued).

Unit	Stratigraphic code	Dominant lithology	Type area (numbers refer to Figure 1.1)	Author(s)	Other areas (numbers refer to Figure 1.1)	Figure showing location of unit in the text	Average age (based on U/Pb geochronology data)	Modifications
Druillon (Suite)	Adru	Porphyroid-textured monzonite, monzodiorite (± quartz monzonite and monzodiorite) and diorite	Lac Hurault (outside of study area)	Thériault and Chevé, 2001	Lac Bienville (N°20) Lac Gayot (N°21)	Figure 3.10	Not dated (age estimated at about 2700 Ma)	The small intrusions of the Turbar Suite as well as two small intrusions of amphibole granite of the Ossant Suite (abandoned terms) are reassigned to the Druillon Suite.
Dufreboy (Suite)	Aduy	Homogeneous biotite-hornblende granite	Lac La Potherie (N°11) Lac Aigneau (N°15)	Leclair *et al.*, 2002 ; Berclaz *et al.*, 2002	Lac Dufreboy (N°12) Lac Peters (N°8)	Figure 3.7	2726 and 2721 Ma	Heterogeneous granites with a diatexitic texture, previously included in the Troie Complex, are reassigned to the Dufreboy Suite.
Dupire (Complex)	Adpr	Volcano-sedimentary rocks	Lac Nedlouc (N°14)	Parent *et al.*, 2001	Lacs des Loups Marins (N°17)	Figure 3.5	2798 and 2787 Ma	None
Duquet (Complex)	Aduq	Volcano-sedimentary rocks	Lac Couture (N°2)	Madore *et al.*, 2004	Povungnituk (N°1)	Figure 3.4	2828 and 2822 Ma for volcano-sedimentary rocks 2812 and 2800 Ma for associated tonalites Younger ages at 2775 and 2764 Ma	The term «Duquet Belt» is replaced by «Duquet Complex».
Duvert (Complex)	Advt	Volcano-sedimentary rocks	Lac Nedlouc (No14)	Parent *et al.*, 2001	Lac Aigneau (N°15) Lac La Potherie (N°12)	Figure 3.6	2724 to 2708 Ma	Volcano-sedimentary rocks of the Qamaniq and Du Gué complexes (abandoned terms) and the Vizien Belt are reassigned to the Duvert Complex. The Vizien Belt is considered as a formal sub-unit of the Duvert Complex.
Faribault-Thury (Suite)	Afth	Foliated to gneissic tonalite and trondhjemite	Lac Peters (N°8)	New unit	Lac Pélican (N°7) Lac Dufreboy (N°12) Lac Klotz (N°3) Rivière Arnaud (N°4)	Figure 3.5	2785 to 2772 Ma Earlier ages between 2879 and 2857 Ma	Tonalites of the Faribault-Thury Complex (abandoned term) are included in the Faribault-Thury Suite. Volcano-sedimentary rocks and granitic rocks in the complex are respectively reassigned to the Arnaud Complex and the Leridon Suite.
Favard (Suite)	Afav	Biotite leucotonalite and trondhjemite	Lac Gayot (N°21)	Gosselin and Simard, 2001	Maricourt (N°18) Lacs des Loups Marins (N°17) Lac Bienville (N°20) Lac Montrochand (N°19) Lac à l'Eau Claire (N°16) Lac Minto (N°13) Rivière Innuksuac (N°9) Kogaluc Bay (N°5) Povungnituk (N°1)	Figure 3.5	2766 to 2740 Ma Younger ages at 2719 and 2717 Ma One earlier age at 3020 Ma	Tonalites of the Charnières, Qamanirjuaq, and Boizard suites (three abandoned terms) as well as tonalites of the Rochefort Suite located within the Hudson Bay Terrane are reassigned to the Favard Suite. A few intrusions of the Rivière aux Feuilles Suite and the Du Gué Complex are also reassigned to the Favard Suite.
Garault (Complex)	Agar	Volcano-sedimentary rocks	Maricourt (N°18)	Simard *et al.*, 2001	None	Figure 3.5	2782 Ma	None

TABLE 3.1 - Stratigraphic units in the NESP (continued).

Unit	Stratigraphic code	Dominant lithology	Type area (numbers refer to Figure 1.1)	Author(s)	Other areas (numbers refer to Figure 1.1)	Figure showing location of unit in the text	Average age (based on U/Pb geochronology data)	Modifications
Gayot (Complex)	Agat	Volcano-sedimentary rocks	Lac Gayot (N°21)	Gosselin and Simard, 2001	Maricourt (N°18)	Figure 3.4	2880 and 2873 Ma 2719 Ma in felsic injection	None
Grosbois (Complex)	Ags	Sedimentary rocks	Lac Gayot (N°21)	Gosselin and Simard, 2001	None	Figure 3.9	Not dated (age estimated at about 2700 Ma)	The term «Grosbois Formation» is replaced by «Grosbois Complex».
Innuksuac (Complex)	Ainn	Volcano-sedimentary rocks	Rivière Innuksuac (N°9)	Simard *et al.*, 2004	Kogaluc Bay (N°5) Lac Minto (N°13) Lac à l'Eau Claire (N°16) Povungnituk (N°1)	Figure 3.5	Unknown (possibly between 2760 and 2740 Ma) One younger age at <2729 Ma in sedimentary rock	Volcano-sedimentary remnants of the Povungnituk and Melvin complexes (abandoned terms), except for the Melvin Belt, are reassigned to the Innuksuac Complex. The Nuvvuagittuq Belt is excluded from the complex.
Itinnaru (Pluton)	Aiti	Tonalite	Lac Pélican (N°7)	New unit	None	Figure 3.9	2691 Ma	New lithodeme introduced to designate a late tonalitic intrusion initially assigned to the Pélican-Nantais Complex (abandoned term).
Joinville (Suite)	Ajov	Granite	Lac Gayot (N°21)	New unit	None	Figure 3.11	Not dated; contains enclaves of Opiscotéo Suite diatexite (2638 Ma)	New suite introduced to designate granites within the Ashuanipi Subprovince previously assigned to the Tramont Suite.
Juet (Belt)	Ajut	Sedimentary and volcaniclastic rocks	Povungnituk (N°1)	Maurice *et al.*, 2005a	None	Figure 3.9	Not dated (age estimated at about 2700 Ma)	None
Kakiattuq (Suite)	Akkk	Biotite leucotonalite and trondhjemite	Lac Vernon (N°10)	Parent *et al.*, 2002a	Lac Anuc (N°6) Lac Minto (N°13) Lac Nedlouc (N°14)	Figure 3.5	2741 Ma	Some tonalites of the Kakiattuq Suite in the Lac Anuc area are reassigned to the Rochefort Suite.
Kapijuq (Suite)	Akpj	Foliated to gneissic tonalite and trondhjemite	Lac Klotz (N°3)	Madore *et al.*, 2002	Lac Couture (N°2) Lac Pélican (N°7)	Figure 3.5	2783 and 2768 Ma	Tonalites of the Bottequin Suite (abandoned term) and tonalites associated with the Nantais Belt are reassigned to the Kapijuq Suite.
Kimber (Alkaline Suite)	Akmb	Nepheline syenite	Lac Klotz (N°3)	Madore *et al.*, 2002	Rivière Arnaud (N°4)	Figure 3.5	2761 Ma	None
Kogaluc (Complex)	Akog	Volcano-sedimentary rocks	Lac Vernon (N°10)	Parent *et al.*, 2002a	Lac Anuc (N°6)	Figure 3.5	2760 and 2759 Ma	Several volcano-sedimentary remnants in the east part of the Kogaluc Complex are reassigned to the Qalluviartuuq-Payne Complex.

TABLE 3.1 - Stratigraphic units in the NESP (continued).

Unit	Stratigraphic code	Dominant lithology	Type area (numbers refer to Figure 1.1)	Author(s)	Other areas (numbers refer to Figure 1.1)	Figure showing location of unit in the text	Average age (based on U/Pb geochronology data)	Modifications
Lac Minto (Suite)	Amin	Enderbite	Lac Minto (N°13)	Simard *et al.*,2005a	Lac Nedlouc (N°14) Lac Vernon (N°10) Kogaluc Bay (N°5) Povungnituk (N°1)	Figure 3.8	2735 to 2710 Ma Younger ages between 2702 and 2688 Ma	All orthopyroxene-bearing rocks in the Lac Minto Domain, previously included in the Lippens and Qilalugalik suites (abandoned terms) and in the Lac Minto Suite and the Le Roy Complex, are reassigned to the Lac Minto Suite. Diatexites initially included in the Lac Minto Suite (Lac Nedlouc area) are reassigned to the Le Roy Complex.
Le Roy (Complex)	Aroy	Diatexite, paragneiss rafts and enclaves	Lac Vernon (N°10)	Parent *et al.*, 2003b	Lac Nedlouc (N°14) Lac La Potherie (N°11) Lac Minto (N°13) Lac Anuc (N°6) Povungnituk (N°1) Kogaluc Bay (N°5)	Figure 3.10	2697 to 2668 Ma	Diatexites of the Mézard Complex and the Lac Minto Suite are reassigned to the Le Roy Complex. Volcano-sedimentary remnants of the Le Roy Complex are reassigned to the Mézard Complex, granites to the Morrice Suite, and orthopyroxene-bearing rocks to the Lac Minto Suite.
Lepelle (Suite)	Alep	Clinopyroxene-bearing granodiorite	Lac Klotz (N°3)	Madore *et al.*, 2002	Lac Couture (N°2) Lac Pélican (N°7) Lac Anuc (N°6)	Figure 3.8	2725 to 2720 Ma	Clinopyroxene-bearing granodiorites initially assigned to the Châtelain Suite (abandoned term) are reassigned to the Lepelle Suite.
Leridon (Suite)	Alrd	Porphyroid-textured granite and granodiorite	Lac Klotz (N°3)	Madore *et al.*, 2002	Rivière Arnaud (N°4) Lac Peters (N°8)	Figure 3.7	Not dated (age estimated between 2735 and 2720 Ma)	A few granitic and monzonitic intrusions in the Lac Peters and Rivière Arnaud areas, initially assigned to the Faribault-Thury and Qimussinguat complexes, are reassigned to the Leridon Suite.
Lesdiguières (Suite)	Alsd	Tonalite	Lac Couture (N°2)	Madore *et al.*, 2004	None	Figure 3.6	2724 Ma	Pyroxene-bearing tonalites are reassigned to the MacMahon Suite, and biotite-hornblende granites and granodiorites to the La Chevrotière Suite.
Loups Marins (Suite)	Alma	Clinopyroxene-bearing tonalite and granodiorite; enderbite, opdalite, and charnockite	Lacs des Loups Marins (N°17)	Gosselin *et al.*, 2002	Lac Bienville (N°20) Lac Montrochand (N°19) Lac à l'Eau Claire (N°16) Lac Minto (N°13) Lac Vernon (N°10) Rivière Innuksuac (N°9) Kogaluc Bay (N°5) Povungnituk (N°1)	Figure 3.8	2735 to 2720 Ma for orthopyroxene-bearing rocks 2715 to 2705 Ma for clinopyroxene-bearing rocks One younger age at 2693 Ma	The term «Loups Marins Complex» is replaced by «Loups Marins Suite». Rocks of the Gabillot, Lussay, and Cheminade suites (abandoned terms) as well as those of the Qilalugalik Suite (abandoned term) located within the Tikkerutuk Domain, are reassigned to the Loups Marins Suite.
MacMahon (Suite)	Acmm	Enderbite, clinopyroxene-bearing tonalite	Lac Nedlouc (N°14)	Parent *et al.*, 2001	Lac Aigneau (N°15) Lac Dufreboy (N°12) Maricourt (N°18) Lac La Potherie (N°11) Lacs des Loups Marins (N°17) Lac Pélican (N°7) Lac Klotz (N°3) Lac Anuc (N°6) Lac Couture (N°2) Lac Vernon (N°10)	Figure 3.8	2729 to 2711 Ma Younger ages between 2702 and 2676 Ma	Orthopyroxene-bearing rocks of the Du Gué Complex and the Châtelain Suite (abandoned terms), of the Lesdiguières Suite, and part of the Lac Minto Suite within the Lac Vernon area are reassigned to the MacMahon Suite. Clinopyroxene-bearing tonalites of the Nullualuk and Bottequin suites (abandoned terms) and the Lesdiguières Suite are also included in the MacMahon Suite.

TABLE 3.1 - Stratigraphic units in the NESP (continued).

Unit	Stratigraphic code	Dominant lithology	Type area (numbers refer to Figure 1.1)	Author(s)	Other areas (numbers refer to Figure 1.1)	Figure showing location of unit in the text	Average age (based on U/Pb geochronology data)	Modifications
Maurel (Suite)	Amau	Porphyroid-textured granodiorite and granite	Lac Gayot (N°21)	Gosselin and Simard, 2001	Maricourt (N°18) Lacs des Loups Marins (N°17) Lac Bienville (N°20)	Figure 3.10	Between 2707 and 2686 Ma	Porphyritic granodiorite intrusions in the Lac Aigneau area and the south part of the Lac Dufreboy area, initially assigned to the La Chevrotière Suite, are reassigned to the Maurel Suite. Porphyritic granodiorites of the La Bazinière Suite (abandoned term) are reassigned to the Maurel Suite (Gosselin et al., 2002).
Melvin (Belt)	Amel	Felsic volcanic rocks	Lac à l'Eau Claire (N°16)	New unit	None	Figure 3.6	2741 Ma	Initially included in the Melvin Complex under the term «Natwakupaw Belt», this volcanic belt is renamed «Melvin Belt». Volcano-sedimentary rocks of the Melvin Complex are reassigned to the Innuksuac Complex, and granoblastic diorites to the Bacqueville Suite.
Mézard (Complex)	Amez	Volcano-sedimentary rocks	Lac Anuc (N°6)	Berclaz *et al.*, 2005	Povungnituk (N°1) Kogaluc Bay (N°5) Lac Vernon (N°10) Lac Minto (N°13) Lac Nedlouc (N°14) Lac à l'Eau Claire (N°16)	Figure 3.5	Unknown (possibly between 2760 and 2740 Ma)	All volcano-sedimentary remnants in the Mézard Complex, the Le Roy Complex, and the Lac Minto Suite, are assigned to the Mézard Complex. Diatexites in these three units are reassigned to the Le Roy Complex.
Morrice (Suite)	Agdm	Granite	Lac Nedlouc (N°14)	Parent *et al.*, 2000	Lac Aigneau (N°15) Lac La Potherie (N°11) Lac Minto (N°13) Lac Vernon (N°10)	Figure 3.10	2684 Ma	Tonalites of the Morrice Suite (Nedlouc) are reassigned to a new unit, the Rivière Qijuttuuq Suite. Granites of the Le Roy Complex are included in the Morrice Suite.
Nantais (Complex)	Anan	Volcano-sedimentary rocks	Lac Klotz (N°3)	New unit	Lac Couture (N°2)	Figure 3.5	2775 Ma	The Pélican-Nantais Complex (abandoned term) is divided into two complexes: the Nantais Complex (dominated by volcanic rocks) and the Pélican Complex (dominated by sedimentary rocks). The Peltier, Headwind, and Caumartin belts are assigned to the Nantais Complex.
Nuvvuagittuq (Belt)	Anuv	Volcano-sedimentary rocks	Rivière Innuksuac (N°9)	Simard *et al.*, 2004; Berclaz *et al.*, 2003	None	Figure 3.3	3825 Ma	The Nuvvuagittuq Belt (formerly the Porpoise Cove Belt; Simard et al., 2003) is excluded from the Innuksuac Complex due to its much earlier age relative to other rocks in the complex.
Opiscotéo (Suite)	Aopi	Diatexites	Lac Bermen (outside of study area)	Leclair *et al.*, 1998	Lac Gayot (N°21)	Figure 3.11	2638 Ma	None
Pélican (Complex)	Appel	Sedimentary rocks	Lac Pélican (N°7)	New unit	Lac Klotz (N°3)	Figure 3.6	2739 Ma 2733 Ma from mobilizate in sedimentary rock	The Pélican-Nantais Complex (abandoned term) is divided into two complexes: the Nantais Complex (dominated by volcanic rocks) and the Pélican Complex (dominated by sedimentary rocks).

TABLE 3.1 - Stratigraphic units in the NESP (continued).

Unit	Stratigraphic code	Dominant lithology	Type area (numbers refer to Figure 1.1)	Author(s)	Other areas (numbers refer to Figure 1.1)	Figure showing location of unit in the text	Average age (based on U/Pb geochronology data)	Modifications
Pinguq (Suite)	Apin	Porphyroid-textured granite, granodiorite, quartz monzonite, and quartz monzodiorite	Povungnituk (N°1)	Maurice *et al.*, 2005a	Kogaluc Bay (N°5)	Figure 3.7	2727 to 2725 Ma	Granite and granodiorite intrusions initially assigned to the La Chevrotière Suite in the Kogaluc Bay and Povungnituk areas are reassigned to the Pinguq Suite.
Qalluvituuq-Payne (Complex)	Aqlp	Volcano-sedimentary rocks	Lac Anuc (N°6)	Berclaz *et al.*, 2005	Lac Vernon (N°10)	Figure 3.4	2851 to 2832 Ma in volcano-sedimentary rocks 2848 to 2809 Ma in associated tonalites One remnant dated at 2768 Ma	Several volcano-sedimentary remnants in the Kogaluc Complex are now included in the Qalluviartuuq-Payne Complex.
Qimussiguat (Complex)	Aqim	Enderbite and orthopyroxene gneiss	Lac Peters (N°8)	Madore *et al.*, 2000	Rivière Arnaud (N°4) Lac Klotz (N°3)	Figure 3.8	2734 Ma	Volcano-sedimentary rocks in the complex are reassigned to the Arnaud Complex and granitic rocks to the Leridon Suite.
Qullinaraaluk (Suite)	Aluk	Mafic-ultramafic intrusions	Lac Vernon (N°10)	Parent *et al.*, 2003b	Lac Minto(N°13) Rivière Innuksuac (N°9) Lac à l'Eau Claire (N°16) Lac Montrochand (N°19) Kogaluc Bay (N°5)	Figure 3.9	2707 and 2705 Ma 2720 Ma in pegmatite crosscutting the ultramafic intrusion at the Qullinaaraaluk showing	Several ultramafic to mafic intrusions previously assigned to the enderbitic Qilalugalik Suite (abandoned term) in the Kogaluc Bay area are reassigned to the Qullinaaraaluk Suite.
rivière aux Feuilles (Suite)	Arfe	Biotite-hornblende granodiorite	Lac Nedlouc (N°14)	Percival and Card, 1994; Parent *et al.*, 2001	Lac Dufreboy (N°12) Lac Aigneau (N°15) Lac La Potherie (N°11) Lac Minto (N°13) Lac Vernon (N°10)	Figure 3.7	Between 2733 and 2722 Ma	Tonalites of the Rivière aux Feuilles Suite are reassigned to the Favard and Rochefort suites, and granodiorites of the Monchy Suite (abandoned term) are reassigned to the Rivière aux Feuilles Suite.
rivière aux Mélèzes (Suite)	Aram	Diatexites	Lac Nedlouc (N°14)	Parent *et al.*, 2000	Lac Aigneau (N°15) Maricourt (N°18)	Figure 3.10	2668 Ma	A diatexite horizon in the Du Gué Complex (abandoned term) is reassigned to the Rivière aux Mélèzes Suite.
rivière Qijuttuuq (Suite)	Aqij	Tonalite	Lac Nedlouc (N°14)	New unit	None	Figure 3.9	Not dated (age estimated between 2705 and 2680 Ma)	New unit introduced to designate three small intrusions of massive, undeformed tonalite initially assigned to the granitic Morrice Suite.
Rochefort (Suite)	Arot	Foliated to gneissic tonalite and trondhjemite	Lac La Potherie (N°11)	Leclair *et al.*, 2002	Lac Pélican (N°7) Lac Anuc (N°6) Lac Vernon (N°10) Lac Couture (N°2) Kogaluc Bay (N°5) Povungnituk (N°1) Lac Nedlouc (N°14)	Figure 3.5	2789 to 2755 Ma	Most tonalites of the Rivière aux Feuilles Suite and some tonalites of the Kakiattuq Suite are reassigned to the Rochefort Suite. Tonalites of the Rochefort Suite located within the Hudson Bay Terrane are reassigned to the Favard Suite.

TABLE 3.1 - Stratigraphic units in the NESP (concluded).

Unit	Stratigraphic code	Dominant lithology	Type area (numbers refer to Figure 1.1)	Author(s)	Other areas (numbers refer to Figure 1.1)	Figure showing location of unit in the text	Average age (based on U/Pb geochronology data)	Modifications
Roulier (Belt)	Arlr	Volcano-sedimentary rocks	Kogaluc Bay (N°5)	Maurice *et al.*, 2005b	None	Figure 3.5	2759 Ma	None
Sanigitik (Suite)	Asan	Diatexite	Lac Pélican (N°7)	New unit	Lac La Potherie (N°11) Lac Dufreboy (N°12)	Figure 3.10	Not dated (age estimated between 2698 and 2680 Ma)	New unit introduced to designate diatexites that were previously included in the Faribault-Thury Complex and the MacMahon Suite.
Sem (Suite)	Asem	Biotite-rich tonalite with a diatexitic aspect	Lacs des Loups Marins (N°17)	Gosselin *et al.*, 2001	None	Figure 3.5	Not dated (age estimated between 2760 and 2740 Ma)	None
Suluppau-galik (Suite)	Aspk	Foliated to gneissic tonalite	Lac Nedlouc (N°14)	Parent *et al.*, 2000	Lac Aigneau (N°15) Lac La Potherie (N°11)	Figure 3.4	2808 Ma	None
Tasiat (Syenite)	Atst	Nepheline syenite	Lac Anuc (N°6)	Percival *et al.*,1995b; Berclaz *et al.*,2005	None	Figure 3.11	2643 Ma	None
Tasiataq (Belt)	Atsq	Volcano-sedimentary rocks	Lac Dufreboy (N°12)	Leclair *et al.*, 2003	None	Figure 3.6	2740 Ma	None
Tramont (Suite)	Atra	Granite	Lac Gayot (N°21)	Gosselin and Simard, 2001	Maricourt (N°18) Lacs des Loups Marins (N°17) Lac Bienville (N°20) Lac Montrochand (N°19)	Figure 3.10	2701 and 2698 Ma	Granites within the Ashuanipi Subprovince that were previously assigned to the Tramont Suite are reassigned to the Joinville Suite.
Troie (Complex)	Atie	Enderbite and orthopyroxene gneiss	Lac Peters (N°8)	Madore *et al.*, 2000	Lac Dufreboy (N°12)	Figure 3.8	Between 2741 and 2722 Ma	Volcano-sedimentary rocks in the complex are reassigned to the Arnaud Complex, granitic rocks to the Dufreboy Suite, and porphyritic monzonites and monzodiorites to the Belloy Suite.

TABLE 3.2 - Abandoned Archean stratigraphic units in the NESP

Unit	Dominant lithology	Type area (Figure 1.1)	Author(s)	Other areas (Figure 1.1)	Modifications
La Bazinière Suite	quartz monzodiorite	Lac Gayot (N°21)	Gosselin and Simard, 2001	None	Potassic rocks of the La Bazinière Suite are reassigned to the Maurel Suite and tonalitic rocks to the Favard and Coursolles suites (Gosselin *et al.*, 2002).
Ossant Suite	Porphyritic amphibole-bearing granite	Lac Bienville (N°20)	Gosselin *et al.*, 2004	Lac Gayot (N°21)	Rock of the Ossant Suite are reassigned to the Druillon Suite.
Turbar Suite	Porphyritic monzonite, monzodiorite, and diorite	Lac Bienville (N°20)	Gosselin *et al.*, 2004	Lac Gayot (N°21)	Rocks of the Turbar Suite are reassigned to the Druillon Suite.
Lac Calme Suite	Ultramafic to intermediate intrusions	Lac Couture (N°2)	Madore *et al.*, 2004	Lac Anuc (N°6)	Rocks of the Lac Calme Suite are reassigned to the Couture Suite.
Grosbois Formation	Migmatitic paragneiss	Lac Gayot (N°21)	Gosselin and Simard, 2001	None	The term «Grosbois Formation» is replaced by «Grosbois Complex».
Lac Allemand Formation	Volcano-sedimentary rocks	Lac Couture (N°2)	Moorhead, 1989	None	The term «Lac Allemand Formation» is replaced by «Allemand Belt»
Juet Formation	Volcano-sedimentary rocks	Povungnituk (N°1)	Moorhead, 1996	None	The term «Juet Formation» is replaced by «Juet Belt»
Cheminade Suite	Gabbronorite and hypersthene diorite	Rivière Innuksuac (N°9)	Simard *et al.*, 2004	None	Rocks of the Cheminade Suite are reassigned to the Loups Marins Suite.
Lussay Suite	Porphyritic clino-pyroxene-bearing granodiorite	Lacs des Loups Marins (N°17)	Gosselin *et al.*, 2002	None	Rocks of the Lussay Suite are reassigned to the Loups Marins Suite.
Gabillot Suite	Porphyritic clino-pyroxene-bearing granodiorite	Rivière Innuksuac (N°9)	Simard *et al.*, 2004	None	Rocks of the Gabillot Suite are reassigned to the Loups Marins Suite.
Qilalugalik Suite	Clinopyroxene-bearing tonalite, granodiorite, and granite; enderbite, charnockite, minor gabbronorite and ultramafic rocks	Lac Vernon (N°10)	Parent *et al.*, 2003b	Rivière Innuksuac (N°9) Kogaluc Bay (N°5) Povungnituk (N°1) Lac Anuc (N°6)	Clinopyroxene-bearing rocks are reassigned to the Loups Marins Suite. Orthopyroxene-bearing rocks within the Tikkerutuk Domain are reassigned to the Loups Marins Suite and those within the Lac Minto Domain to the Lac Minto Suite. Some gabbronorite and ultramafic intrusions are reassigned to the Qullinaaraaluk Suite.
Lippens Suite	Enderbite and charnockite	Lac Nedlouc (N°14)	Parent *et al.*, 2000	Lacs des Loups Marins (N°17)	Rocks of the Lippens Suite are reassigned to the Lac Minto Suite.
Nullualuk Suite	Clinopyroxene-bearing tonalite and diorite	Lac Aigneau (N°15)	Berclaz *et al.*, 2002	Lac Dufreboy (N°12)	Rocks of the Nullualuk Suite are reassigned to the MacMahon Suite.
Châtelain Suite	Clinopyroxene-bearing granodiorite and granite, orthopyroxene-bearing granodiorite	Lac Klotz (N°3)	Madore *et al.*, 2002	Lac Couture (N°2) Lac Pélican (N°7) Lac Anuc (N°6)	Clinopyroxene-bearing rocks are reassigned to the Lepelle Suite and orthopyroxene-bearing rocks to the MacMahon Suite.
Voizel Suite	Homogeneous granite and granodiorite	Rivière Innuksuac (N°9)	Simard *et al.*, 2004	None	Rocks of the Voizel Suite are reassigned to the Desbergères Suite.
Monchy Suite	Heterogeneous granodiorite with abundant tonalitic enclaves	Lac Nedlouc (N°14)	Parent *et al.*, 2001	Lac Aigneau (N°15)	Rocks of the Monchy Suite are reassigned to the Rivière aux Feuilles Suite.
La Potherie Batholith	Granite	Lac La Potherie (N°11)	Leclair *et al.*, 2002	None	Rocks of the La Potherie Batholith are reassigned to the La Chevrotière Suite.
Du Gué Complex	Enderbite and ortho-pyroxene-bearing tonalite, diatexite, paragneiss, biotite tonalite	Maricourt (N°18)	Simard and Gosselin, 2001	None	Orthopyroxene-bearing rocks of the Du Gué Complex are reassigned to the MacMahon Suite, diatexites to the Rivière aux Mélèzes Suite, paragneisses to the Duvert Complex, and tonalites to the Favard Suite.
Vizien Complex	Diverse volcano-sedimentary rocks	Lac La Potherie (N°11)	Leclair *et al.*, 2002	None	The Vizien Complex is reclassified as a lithodeme, under the term «Vizien Belt», which is included in the Duvert Complex.

TABLE 3.2 - Abandoned Archean stratigraphic units in the NESP (concluded).

Unit	Dominant lithology	Type area (Figure 1.1)	Author(s)	Other areas (Figure 1.1)	Modifications
Qamaniq Complex	Remnants of metamorphosed volcano-sedimentary rocks	Lac Nedlouc (N°14)	Parent *et al.*, 2001	Lac Aigneau (N°15) Lac Dufreboy (N°12) Lac La Potherie (N°11)	Volcano-sedimentary remnants of the Qamaniq Complex are reassigned to the Duvert Complex.
Melvin Complex	Felsic volcanic rocks, amphibolite, paragneiss, grano-blastic diorite	Lac à l'Eau Claire (N°16)	Simard *et al.*, 2005b	Lac Minto (N°13)	Felsic volcanic rocks are assigned to a new unit, the Melvin Belt. Amphibolites and paragneisses are reassigned to the Innuksuac Complex, and grano-blastic diorites to the Bacqueville Suite.
Charnière Suite	Biotite granodiorite and leucotonalite	Lac Nedlouc (N°14)	Parent *et al.*, 2001	None	Leucotonalites are reassigned to the Favard Suite and granodiorites to the Desbergères Suite.
Boizard Suite	Heterogeneous tonalite with abundant mafic enclaves	Rivière Innuksuac (N°9)	Simard *et al.*, 2003	None	Rocks of the Boizard Suite are reassigned to the Favard Suite.
Qamanirjuaq Suite	Biotite leucotonalite	Rivière Innuksuac (N°9)	Simard *et al.*, 2004	None	Rocks of the Qamanirjuaq Suite are reassigned to the Favard Suite.
Povungnituk Complex	Volcano-sedimentary rocks	Povungnituk (N°1)	Maurice *et al.*, 2005a	Kogaluc Bay (N°5)	Volcano-sedimentary remnants in the Povungnituk Complex are reassigned to the Innuksuac Complex.
Pélican-Nantais Complex	Volcano-sedimentary rocks	Lac Klotz (N°3)	Madore *et al.*, 2002	Lac Pélican (N°7)	Sedimentary rocks associated with the Pélican Belt are reassigned to the Pélican Complex (new unit) and volcanic rocks of the Nantais Belt are reassigned to the Nantais Complex (new unit).
Bottequin Suite	Tonalite, trondhjemite, and diorite, clinopyroxene-bearing tonalite	Lac Pélican (N°7)	Cadieux *et al.*, 2004	None	Tonalites, trondhjemites, and diorites of the Bottequin Suite are reassigned to the Kapijuq Suite and clinopyroxene-bearing tonalites to the MacMahon Suite.
Faribault-Thury Complex	Tonalite, volcano-sedimentary rocks, granite	Lac Peters (N°8)	Madore *et al.*, 2000	Lac Pélican (N°7) Lac Dufreboy (N°12) Lac Klotz (N°3) Rivière Arnaud (N°4)	Tonalites are reassigned to a new unit, the Faribault-Thury Suite. Volcano-sedimentary rocks are reassigned to the Arnaud Complex (new unit), and granites to the Leridon Suite.

TABLE 3.3 - U/Pb geochronology data in the NESP.

No	Organization	Stratigraphic unit	Lithologic code	Analytical method	Crystallization age (Ma)	Inherited zircon age (Ma)	Secondary age (Ma)	Reference Figure for crystallization age	Zone	Easting	Northing	References
1	MRNF	Loups Marins (Suite)	I1D,CX	ID-TIMS	2712 ±4			Figure 3.8	18	440 006	6 302 915	Simard *et al.*, 2005b (site 3); David, unpublished
2	MRNF	Loups Marins (Suite)	I1D,CX	LA-MC-ICP-MS	2723 ±3	about 2742	2698 ±8	Figure 3.8	18	525 159	6 172 187	Roy *et al.*, 2006 (site 4); David, unpublished
3	MRNF	Loups Marins (Suite)	I1B,CX,PO	LA-MC-ICP-MS	2704 ±5	2710 ±2		Figure 3.8	18	560 705	6 137 416	Roy *et al.*, 2006 (site 2); David, unpublished
4	MRNF	Loups Marins (Suite)	I1B,CX,PO	LA-MC-ICP-MS	2713 ±6			Figure 3.8	18	567 496	6 211 884	Gosselin *et al.*, 2002 (site 5); David *et al.*, 2008
5	MRNF	Loups Marins (Suite)	I1B,CX,PO	LA-MC-ICP-MS	2710 ±4			Figure 3.8	18	588 697	6 111 223	Gosselin *et al.*, 2004 (site 3); David, unpublished
6	MRNF	Loups Marins (Suite)	I2D,CX	LA-MC-ICP-MS	2704 ±5			Figure 3.8	18	556 112	6 122 455	Roy *et al.*, 2006 (site 3); David, unpublished
7	MRNF	Loups Marins (Suite)	I1T	LA-MC-ICP-MS	2733 ±3			Figure 3.8	18	554 037	6 130 648	Roy *et al.*, 2006 (site 5); David, unpublished
8	MRNF	Loups Marins (Suite)	I2Q	LA-MC-ICP-MS	2720 ±2			Figure 3.8	18	568 977	6 098 392	Gosselin *et al.*, 2004 (site 6); David, unpublished
9	GSC	Loups Marins (Suite)	I1S	SHRIMP	2712 ±11			Figure 3.8	18	525 306	6 214 953	Skulski *et al.*, 1998
10	MRNF	Favard (Suite)	I1D,BO	LA-MC-ICP-MS	2740	about 3000 about 3200		Figure 3.5	18	448 691	6 099 946	Roy *et al.*, 2006; David, unpublished
11	MRNF	Desbergères (Suite)	I1B,PO	LA-MC-ICP-MS	2732 ±4	>2820		Figure 3.7	18	438 958	6 132 178	Roy *et al.*, 2006 (site 1); David, unpublished
13	MRNF	Desbergères (Suite)	I1C	ID-TIMS	2711 ±4			Figure 3.7	18	479 642	6 223 971	Simard *et al.*, 2005b (site 4); David, unpublished
14	GSC	Desbergères (Suite)	I1C	SHRIMP	2718 ±7	3064; 3023; 2831; 2780		Figure 3.7	18	529 977	6 159 240	Skulski *et al.*, 1998
15	GSC	Desbergères (Suite)	I1C	SHRIMP	2725 ±6		2690; 2683	Figure 3.7	18	499 257	6 237 732	Percival *et al.*, 2001 (no. B1)
16	GSC	?	I1C	SHRIMP	2702 ±8			Figure 3.10	18	477 306	6 275 824	Percival *et al.*, 2001 (no. B2)
17	MRNF	Qullinaaraaluk (Suite)	I3Q	ID-TIMS/LA-MC-ICP-MS	2707 ±1	2720 ±1		Figure 3.9	18	463 899	6 299 089	Simard *et al.*, 2005b (site 5); David, unpublished
18	MRNF	Qullinaaraaluk (Suite)	I3Q	ID-TIMS/LA-MC-ICP-MS	2705 ±1			Figure 3.9	18	422 950	6 346 560	Simard *et al.*, 2005a (indiceTan); David, unpublished
19	MRNF	Melvin (Belt)	V1	LA-MC-ICP-MS	2741 ±4	2780; 2800		Figure 3.6	18	494 710	6 284 336	Simard *et al.*, 2005b (site 1); David, unpublished
20	MRNF	Nuvvuagittuq (Belt)	V1	ID-TIMS	3825 ±16			Figure 3.3	18	339 799	6 462 996	Simard *et al.*, 2004 (site 1); David, unpublished
21	MRNF	Nuvvuagittuq (Belt)	I1D	ID-TIMS	3650 ±5			Figure 3.3	18	339 479	6 465 022	David, unpublished

TTABLE 3.3 - U/Pb geochronology data in the NESP (continued).

No	Organization	Stratigraphic unit	Lithologic code	Analytical method	Crystallization age (Ma)	Inherited zircon age (Ma)	Secondary age (Ma)	Reference Figure for crystallization age	Zone	Easting	Northing	References
22	MRNF	?	I1D	LA-MC-ICP-MS	2812 ±14			Figure 3.4	18	449 927	6 393 853	Simard *et al.*, 2005a (site 1); David *et al.*, 2008
23	MRNF	Innuksuac (Complex)	S	ID-TIMS	<2729 (détritique)		2688 ±9	Figure 3.6	18	333 610	6 586 759	Maurice *et al.*, 2005b (site 3); David, unpublished
24	MRNF	Roulier (Belt)	V1	ID-TIMS	2759 ±1		2731±3	Figure 3.5	18	407 973	6 579 228	Maurice *et al.*, 2005b (site 1); David, unpublished
25	MRNF	Favard (Suite)	I1D,BO	LA-MC-ICP-MS	about 3020	about 3250		Figure 3.3	18	483 152	6 296 515	Simard *et al.*, 2005b (site 2); David, unpublished
26	MRNF	Favard (Suite)	I1D,BO	LA-MC-ICP-MS	2766 ±3			Figure 3.5	18	360 891	6 688 172	Maurice *et al.*, 2005a (site 2); David, unpublished
27	MRNF	Favard (Suite)	I1D,BO	ID-TIMS/LA-MC-ICP-MS	2750 ±5	2789 ±14	about 2722	Figure 3.5	18	343 858	6 461 555	Simard *et al.*, 2004 (site 3); David, unpublished
28	MRNF	Favard (Suite)	I1D,BO	ID-TIMS	2714 ±2		2685 +11/-6	Figure 3.6	17	654 121	6 490 978	Simard *et al.*, 2004 (site 4); David, unpublished
29	MRNF	Coursolles (Suite)	I1D,HB-BO	ID-TIMS	2758 ±11			Figure 3.5	18	596 244	6 264 785	Gosselin *et al.*, 2002 (site 2); David *et al.*, 2008
30	MRNF	Coursolles (Suite)	I2J,HB	LA-MC-ICP-MS	2713 ±2			Figure 3.6	18	614 839	6 186 540	Gosselin *et al.*, 2004 (site 5); David, unpublished
31	MRNF	Loups Marins (Suite)	I1D,CX	LA-MC-ICP-MS	2709 ±5	2780 ±8		Figure 3.8	18	442 505	6 500 828	Parent *et al.*, 2002 (site 4); David *et al.*, 2008
32	MRNF	?	M1(I1D)	LA-MC-ICP-MS	2840 ±9	2941 ±4	2714 ±4	Figure 3.4	18	360 102	6 534 551	Simard *et al.*, 2004 (site 5); David, unpublished
33	MRNF	Loups Marins (Suite)	I1C,CX	ID-TIMS	2730 ±4		2720	Figure 3.8	18	407 439	6 421 026	Simard *et al.*, 2005a (site 2); David, unpublished
34	GSC	Lac Minto (Suite)	I1C,CX	SHRIMP	2699 ±22	3075; 2810		Figure 3.10	18	396 951	6 582 738	Percival *et al.*, 2001 (no. T3)
35	MRNF	Loups Marins (Suite)	I1C,CX,PO	LA-MC-ICP-MS	2731 ±4	2742 ±4; >2800		Figure 3.8	17	662 720	6 496 472	David, unpublished
36	MRNF	Loups Marins (Suite)	I2Q	LA-MC-ICP-MS	2693 ±6			Figure 3.10	18	575 301	6 287 816	Gosselin *et al.*, 2002 (site 6); David *et al.*, 2008
37	MRNF	Loups Marins (Suite)	I2Q	ID-TIMS	2719 ±1			Figure 3.8	18	417 966	6 394 200	Simard *et al.*, 2005a (site 3); David, unpublished
38	MRNF	Loups Marins (Suite)	I1T	ID-TIMS	2735 +3/-2			Figure 3.8	18	383 310	6 635 559	Maurice *et al.*, 2005b (site 2); David, unpublished
39	MRNF	Loups Marins (Suite)	I1T	LA-MC-ICP-MS	2732 ±1	2837 ±4		Figure 3.8	18	354 476	6 526 940	Simard *et al.*, 2004 (site 6); David, unpublished
40	GSC	Desbergères (Suite)	I1C	TIMS	2724			Figure 3.7	18	486 764	6 343 482	Percival and Card, 1994
41	GSC	Late granite	I1B	TIMS	2660			Figure 3.11	18	490 288	6 338 611	Percival and Card, 1994
43	GSC	?	I1C	TIMS	2702 ±1			Figure 3.10	18	445 404	6 334 874	Percival and Card, 1994

TABLE 3.3 - U/Pb geochronology data in the NESP (continued).

No	Organization	Stratigraphic unit	Lithologic code	Analytical method	Crystallization age (Ma)	Inherited zircon age (Ma)	Secondary age (Ma)	Reference Figure for crystallization age	Zone	Easting	Northing	References
44	GSC	?	I1B	TIMS	2693 + 14/-11			Figure 3.10	18	472 800	6 334 195	Percival *et al.*, 1992 (no. 90-136A); Percival and Card, 1994
45	GSC	Desbergères (Suite)	I1B	SHRIMP	2719 ±14			Figure 3.7	17	673 311	6 516 238	Percival *et al.*, 2001 (no. I1)
46	GSC	Corneille (Suite)	I1B	monazite	2698 ±1			Figure 3.10	18	347 548	6 525 867	Percival *et al.*, 2001 (no. I2)
47	MRNF	Corneille (Suite)	I1B	ID-TIMS/LA-MC-ICP-MS	2691 ±1	>2715		Figure 3.10	17	648 203	6 503 846	Simard *et al.*, 2004 (site 7); David, unpublished
48	MRNF	Pinguk (Suite)	I1B	LA-MC-ICP-MS	2727 ±2	2752 ±3		Figure 3.7	18	390 613	6 717 173	Maurice *et al.*, 2005a (site 7); David, unpublished
49	MRNF	Pinguk (Suite)	I2E	LA-MC-ICP-MS	2725 ±4	2742; 2774		Figure 3.7	18	356 242	6 692 345	Maurice *et al.*, 2005a (site 8); David, unpublished
50	MRNF	Corneille (Suite)	I1G	ID-TIMS	2688 ±2			Figure 3.10	18	339 730	6 463 036	Simard *et al.*, 2004 (site 2); David, unpublished
51	MRNF	Bourdel (Syenite)	I2JF	ID-TIMS	2675 ±1			Figure 3.11	18	547 827	6 286 745	Simard *et al.*, 2005b (site 6); David, unpublished
52	MRNF	Carbonatite	I4Q	ID-TIMS	2676 ±8		2695 ±10	Figure 3.11	18	383 343	6 635 555	Maurice *et al.*, 2005b (site 4); David, unpublished
53	MRNF	Chavigny (Complex)	V1	LA-MC-ICP-MS	2722 ±4			Figure 3.6	18	479 971	6 452 682	Parent *et al.*, 2002 (site 2); David *et al.*, 2008
54	MRNF	Kakiattuq (Suite)	I1D,BO	ID-TIMS	2741 ±4			Figure 3.5	18	492 894	6 434 004	Parent *et al.*, 2002 (site 1); David *et al.*, 2008
55	MRNF	Bylot (Suite)	I1D(M21)	LA-MC-ICP-MS	2737 ±13	2807 ±9 2830 ±5		Figure 3.6	18	398 477	6 717 600	Maurice *et al.*, 2005a (site 1); David, unpublished
56	MRNF	Bylot (Suite)	I1D(M21)	LA-MC-ICP-MS	2723 ±2		about 2710	Figure 3.6	18	412 199	6 750 523	Maurice *et al.*, 2005a (site 9); David, unpublished
57	MRNF	Le Roy (Complex)	M21	ID-TIMS/LA-ICP-QMS	2697 ±2	2731 ±13		Figure 3.10	18	491 006	6 483 933	Parent *et al.*, 2002 (site 3); David *et al.*, 2008
58	MRNF	Le Roy (Complex)	M21	LA-MC-ICP-MS	2668 ±22	2758 ±11		Figure 3.10	18	415 377	6 666 074	Maurice *et al.*, 2005a (site 3); David, unpublished
59	GSC	?	M21	TIMS	2713 ±2		2700 ±1 2699 ±1 2688 ±1	Figure 3.8	18	542 020	6 369 573	Percival *et al.*, 1992 (no. 89-78); Percival and Card, 1994
60	MRNF	Lac Minto (Suite)	I2I,OX	ID-TIMS	2722±5		2692	Figure 3.8	18	456 400	6 409 194	Simard *et al.*, 2005a (site 4); David *et al.*, 2008
61	MRNF	Lac Minto (Suite)	I1T	ID-TIMS/LA-ICP-QMS	2709±2	2756±3		Figure 3.8	18	574 771	6 339 610	Parent *et al.*, 2000 (site 8); David *et al.*, 2008
62	MRNF	Lac Minto (Suite)	I1T	ID-TIMS	2702 ±1	2741 ±3	2695 ±1	Figure 3.10	18	555 107	6 365 541	Simard *et al.*, 2005a (site 5); David, unpublished
63	MRNF	Lac Minto (Suite)	I1T	LA-MC-ICP-MS	2731 ±2	about 2780 about 2810	2711 ±4	Figure 3.8	18	399 553	6 685 034	Maurice *et al.*, 2005a (site 5); David, unpublished

TABLE 3.3 - U/Pb geochronology data in the NESP (continued).

No	Organization	Stratigraphic unit	Lithologic code	Analytical method	Crystallization age (Ma)	Inherited zircon age (Ma)	Secondary age (Ma)	Reference Figure for crystallization age	Zone	Easting	Northing	References
65	GSC	Lac Minto (Suite)	I1S	SHRIMP	2709 ±9	(2736-2720) (2831-2825) (2848-2765)		Figure 3.8	18	400 764	6 676 423	Percival *et al.*, 2001 (no. T1)
66	MRNF	Lac Minto (Suite)	I1P	LA-ICP-QMS	2708 ±18	2824 ±22 2759 ±19	2633 ±12	Figure 3.8	18	572 480	6 333 457	Parent *et al.*, 2001 (site 9); David *et al.*, 2008
67	MRNF	Lac Minto (Suite)	I1P	LA-ICP-QMS	2735 ±8		2681 ±14	Figure 3.8	18	566 512	6 444 296	Leclair *et al.*, 2000 (site 7); David *et al.*, 2008
68	GSC	Lac Minto (Suite)	I1P	TIMS	2688+4/-3		2676 ±2 (monazite)	Figure 3.10	18	524 807	6 404 687	Percival *et al.*, 1992 (no. 89-70); Percival and Card, 1994
69	GSC	Rivière aux Feuilles (Suite)	I1C	TIMS	2725 ±4		2707 ±1 (monazite)	Figure 3.7	18	478 063	6 374 980	Percival *et al.*, 1992 (no. 89-29); Percival and Card, 1994
72	MRNF	Recoupe Qullinaaraaluk (Suite)	I1G	ID-TIMS	2720 ±2			Figure 3.9	18	518 705	6 393 327	Simard *et al.*, 2005a (site 6); David, unpublished
73	MRNF	Garault (Complex)	M8	LA-ICP-QMS	2782 ±7	3203 ±12 3032 ±11 2883 ±12		Figure 3.5	19	418 948	6 266 649	Simard *et al.*, 2002 (site F); David *et al.*, 2008
74	MRNF	Dupire (Complex)	V1	ID-TIMS/LA-ICP-QMS	2787 ±3			Figure 3.5	18	604 475	6 328 112	Parent *et al.*, 2001 (site 6); David *et al.*, 2008
75	MRNF	Dupire (Complex)	V1	LA-ICP-QMS	2798 ±11	2924 ±11 2862 ±16		Figure 3.5	18	602 930	6 325 922	Parent *et al.*, 2001 (site 1); David *et al.*, 2008
76	MRNF	Duvert (Complex)	V1	ID-TIMS/LA-ICP-QMS	about 2715		2672 ±10	Figure 3.6	18	677 547	6 375 597	Parent *et al.*, 2001 (site 5); David *et al.*, 2008
77	GSC	Vizien (Belt)	I4	TIMS	2797 ±2 à 2786 ±1			Figure 3.5	18	617 929	6 440 935	Percival and Card, 1994; Skulski et Percival, 1996 (2797 ±2 de la in compilation by Skulski)
78	GSC	Vizien (Belt)	V1	TIMS	2722+15/-8	2793 ±8		Figure 3.6	18	618 529	6 441 935	Percival and Card, 1994; Skulski and Percival, 1996 (2797 ±2 de la in compilation by Skulski)
79	GSC	Vizien (Ceinture)	V1	TIMS	2724 ±1			Figure 3.6	18	614 912	6 443 383	Percival *et al.*, 1992 (no. 91-03C); Percival and Card, 1994
81	GSC	Kogaluc (Complex)	V1		2759 ±3			Figure 3.5	18	530 650	6 481 739	Skulski *et al.*, 1996 (no. SNB-93-94); Percival *et al.*, 2001
82	GSC	Kogaluc (Complex)	QFP		2760 ±5			Figure 3.5	18	529 621	6 489 154	Skulski *et al.*, 1996 (PBAC-94-158); Percival *et al.*, 2001
83	MRNF	Qalluviartuuq-Payne (Complex)	I3G	LA-MC-ICP-MS	2851 ±4			Figure 3.4	18	499 073	6 621 909	Berclaz *et al.*, 2005 (site 1); David, unpublished
84	GSC	Qalluviartuuq-Payne (Complex)	I2J	TIMS	2841+4/-1			Figure 3.4	18	496 154	6 630 960	Percival *et al.*, 1997b; semble correspondre à l'échantillon PBAW-94-293 de Skulski *et al.*, 1996

TABLE 3.3 - U/Pb geochronology data in the NESP (continued).

No	Organization	Stratigraphic unit	Lithologic code	Analytical method	Crystallization age (Ma)	Inherited zircon age (Ma)	Secondary age (Ma)	Reference Figure for crystallization age	Zone	Easting	Northing	References
85	MRNF	Duquet (Complex)	V1	ID-TIMS	2822 ±2			Figure 3.4	18	480 123	6 685 151	Bourassa, 2002
86	GSC	Duquet (Complex)	V1	TIMS	2828			Figure 3.4	18	444 777	6 671 693	Percival *et al.*, 1996a
87	MRNF	Brésolles (Suite)	M1(I1D)	ID-TIMS	2817 ±7		about 2640	Figure 3.4	18	666 741	6 276 825	Gosselin *et al.*, 2002 (site 1); David *et al.*, 2008
88	MRNF	Sullupaugalik (Suite)	M1(I1D)	ID-TIMS/LA-ICP-QMS	2808 ±6	3096 ±7 2952 ±8	2715 ±24	Figure 3.4	19	350 212	6 391 667	Berclaz *et al.*, 2001 (site 1); David *et al.*, 2008
89	GSC	Vizien area	M1(I1D)	TIMS	2940 ±5			Figure 3.3	18	615 936	6 443 598	Percival and Card, 1994; Percival *et al.*, 1993 (2942±4 dans la in compilation by Skulski)
90	MRNF	Favard (Suite)	I1D	LA-MC-ICP-MS	2741 ±4	2723 ±4		Figure 3.5	18	683 581	6 181 772	Gosselin *et al.*, 2004 (site 4); David, unpublished
90	MRNF	Granitic phase (Favard)	I1C	LA-MC-ICP-MS	2713 ±2	2723 ±4		Figure 3.7	18	683 581	6 181 772	Gosselin *et al.*, 2004 (site 4); David, unpublished
91	MRNF	Favard (Suite)	I1D,BO	ID-TIMS/LA-ICP-QMS	2748 ±2	2868 ±11	2653 ±11	Figure 3.5	19	401 424	6 275 446	Simard *et al.*, 2002 (site B); David *et al.*, 2008
92	MRNF	Desbergères (Suite)	I1C,BO	LA-ICP-QMS	2714 ±8		2630; 2650	Figure 3.7	18	607 007	6 340 301	Parent *et al.*, 2001 (site 7); David *et al.*, 2008
93	MRNF	Rochefort (Suite)	I1D,BO	ID-TIMS/LA-ICP-QMS	2766 ±5	2834 ±8	2691 ±2 2654 ±3	Figure 3.5	18	566 557	6 469 529	Leclair *et al.*, 2002b (site 5); David *et al.*, 2008
94	MRNF	Rochefort (Suite)	I1D,BO	LA-MC-ICP-MS	2758 ±4	2811 ±2		Figure 3.5	18	503 184	6 619 060	Berclaz *et al.*, 2005 (site 3); David, unpublished
95	MRNF	Qalluviartuuq-Payne (Complex)	I1D,BO	LA-MC-ICP-MS	2848 ±11			Figure 3.4	18	498 355	6 630 921	Berclaz *et al.*, 2005 (site 2); David, unpublished
96	MRNF	Duquet (Complex)	I1D,HB-BO	LA-MC-ICP-MS	2800 ±4			Figure 3.4	18	475 650	6 677 337	David, unpublished
97	MRNF	Rochefort (Suite)	I1D,HB-BO	LA-MC-ICP-MS	2789 ±4			Figure 3.5	18	473 989	6 700 420	David, unpublished
98	GSC	Rochefort (Suite)	I1D(M1)	TIMS	2755			Figure 3.5	18	463 312	6 723 379	Percival *et al.*, 1996a (*Open file 3315*)
99	GSC	Duquet (Complex)	QFP	TIMS	2775 ±1			Figure 3.5	18	476 240	6 694 416	Percival *et al.*, 1996a; Percival *et al.*, 1997b
100	GSC	Qalluviartuuq-Payne (complex)	I1D	TIMS	2809 +2/-1	2814		Figure 3.4	18	527 379	6 593 960	Percival and Skulski, 2000 (no. PBAS-96-154)
101	MRNF	Coursolles (Suite)	I1D,HB-BO	ID-TIMS/LA-ICP-QMS	2716 ±16	2760 ±14		Figure 3.6	19	421 085	6 269 338	Simard *et al.*, 2002 (site C); David *et al.*, 2008
102	MRNF	Coursolles (Suite)	I1D,HB-BO	LA-MC-ICP-MS	2756 ±8	2970		Figure 3.5	18	601 770	6 298 160	Gosselin *et al.*, 2002 (site 3); David *et al.*, 2008

TABLE 3.3 - U/Pb geochronology data in the NESP (continued).

No	Organization	Stratigraphic unit	Lithologic code	Analytical method	Crystallization age (Ma)	Inherited zircon age (Ma)	Secondary age (Ma)	Reference Figure for crystallization age	Zone	Easting	Northing	References
103	MRNF	?	I1D,HB-BO	LA-ICP-QMS	2728 ±17	2812 ±13	2551 ±14	Figure 3.6	18	658 525	6 347 037	Parent *et al.*, 2001 (site 3); David *et al.*, 2008
104	MRNF	Lesdiguières (Suite)	I2J,HB-BO	ID-TIMS	2724 ±2			Figure 3.6	18	514 746	6 748 681	David, unpublished
105	MRNF	Riv. aux Mélèzes (Suite)	M21	LA-ICP-QMS	2668 ±11	2750 ±12	2581 ±16	Figure 3.10	18	660 957	6 363 723	Parent *et al.*, 2001 (site 2); David *et al.*, 2008
106	MRNF	Bylot (Suite)	I1C (M21)	ID-TIMS			2686 ±3 (titanite)		18	434 543	6 742 332	Maurice *et al.*, 2005a (site 10); David, unpublished
107	GSC	?	I1C	SHRIMP	2704 ±7	2774; 2757		Figure 3.10	18	420 727	6 752 433	Percival *et al.*, 2001 (no. T2)
108	MRNF	MacMahon (Suite)	I1T	ID-TIMS/LA-ICP-QMS	2677 ±1	2827 ±6; 2749 ±9		Figure 3.10	19	340 985	6 318 990	Simard *et al.*, 2001 (site G); David *et al.*, 2008
109	MRNF	MacMahon (Suite)	I1T	LA-MC-ICP-MS	2729 ±7	2768 ±5		Figure 3.8	18	500 735	6 592 147	Berclaz *et al.*, 2005 (site 5); David, unpublished
110	MRNF	MacMahon (Suite)	I1S	LA-ICP-QMS	2697 ±9	2838 ±14; 2773 ±7	2625 ±26	Figure 3.10	18	564 247	6 507 491	Leclair *et al.*, 2002 (site 6); David *et al.*, 2008
112	GSC	Rochefort (Suite)	I1D, OX	TIMS	2782 ±1	2799 ±2		Figure 3.5	18	545 930	6 482 405	Skulski *et al.*, 1996 (no. PBAC-94-113)
113	MRNF	Maurel (Suite)	I1C,PO	ID-TIMS/LA-ICP-QMS	2701 ±4	2843 ±17	2610	Figure 3.10	19	333 188	6 272 496	Simard *et al.*, 2001 (site E); David *et al.*, 2008
114	MRNF	Maurel (Suite)	I1C,PO	LA-MC-ICP-MS	2707 ±5	2717 ±4	2749 ±5	Figure 3.10	18	650 437	6 204 773	Gosselin *et al.*, 2002 (site 2); David, unpublished
115	MRNF	Maurel (Suite)	I1C	ID-TIMS/LA-ICP-QMS	2686 ±7	2837 ±13	2660	Figure 3.10	19	363 896	6 262 046	Simard *et al.*, 2001 (site D); David *et al.*, 2008
116	MRNF	Desbergères (Suite)	I1C	LA-MC-ICP-MS	2714 ±12	2800		Figure 3.7	18	633 614	6 275 804	Gosselin *et al.*, 2002 (site 4); David *et al.*, 2008
117	GSC	Desbergères (Suite)	I1C	SHRIMP	2717 ±5			Figure 3.7	19	380 716	6 274 777	Percival *et al.*, 2001 (no. G2)
118	GSC	?	I1C	SHRIMP	2679 ±14	2733; 2714		Figure 3.11	19	327 938	6 222 264	Percival *et al.*, 2001 (no. B4)
119	GSC	?	I1C	TIMS	2702 +4/-3	2716 ±5		Figure 3.10	18	636 827	6 434 792	Percival *et al.*, 1992 (no. 90-178A); Percival and Card, 1994
122	GSC	Rochefort (Suite)	I1D (I1C)	TIMS	2775 +5/-2		2765	Figure 3.5	18	485 421	6 700 175	Percival *et al.*, 1996a; Percival *et al.*, 1997b; Percival and Skulski, 2000 (p. 369, no. PBAS-95-1739)
123	MRNF	Tramont (Suite)	I1B	LA-MC-ICP-MS	2701 ±4	2751 ±3	about 2650	Figure 3.10	18	628 285	6 192 165	Gosselin *et al.*, 2004 (site 1); David, unpublished
124	GSC	Tramont (Suite)	I1B	SHRIMP	2698 ±6			Figure 3.10	18	623 659	6 283 913	Percival *et al.*, 2001 (no. B3) (approximate location)
125	MRNF	Morrice (Suite)	I1B	ID-TIMS/LA-ICP-QMS	2684 ±6			Figure 3.10	18	656 165	6 364 710	Parent *et al.*, 2001 (site 4); David *et al.*, 2008

TABLE 3.3 - U/Pb geochronology data in the NESP (continued).

No	Organization	Stratigraphic unit	Lithologic code	Analytical method	Crystallization age (Ma)	Inherited zircon age (Ma)	Secondary age (Ma)	Reference Figure for crystallization age	Zone	Easting	Northing	References
126	GSC	Rivière aux Feuilles (Suite)	I1B	TIMS	2725 ±5			Figure 3.7	18	501 698	6 502 732	Skulski *et al.*, 1996 (no. SNB-93-240)
127	GSC	Late granite	I1B	TIMS	2675 +4/-3		2645	Figure 3.11	18	499 015	6 629 391	Percival et Skulski, 2000 (no. PBA95-1064)
128	MRNF	La Chevretière (Suite)	I1B	ID-TIMS	about 2732		2694 ±6 (titanite)	Figure 3.7	18	445 640	6 780 636	Maurice *et al.*, 2005a (site 4); David, unpublished
129	MRNF	La Chevretière (Suite)	I1B,PO	LA-MC-ICP-MS	2719 ±3	2760 ±2 2783 ±6		Figure 3.7	18	503 257	6 708 074	David, unpublished
130	MRNF	?	I1B,PO	LA-MC-ICP-MS	2753 ±11	2813 ±2			18	512 166	6 746 672	David, unpublished
131	MRNF	Tasiat Syenite	I2JF	LA-MC-ICP-MS	2643 ±8			Figure 3.11	18	503 545	6 558 903	Berclaz *et al.*, 2005 (site 6); David, unpublished
132	MRNF	Pélican (Complex)	V1	LA-MC-ICP-MS	2739 ±4			Figure 3.6	18	582 325	6 632 600	David *et al.*, 2008
133	GSC	Pélican (Complex)	V1	TIMS	2742 ±1				18	582 092	6 632 771	Percival *et al.*, 1997a
134	MRNF	Nantais (Complex)	V1	ID-TIMS	2775 ±5	2820		Figure 3.5	18	574 111	6 760 263	Madore *et al.*, 2001 (site A); David *et al.*, 2008
135	MRNF	Pélican (Complex)	M20	LA-MC-ICP-MS	2733 ±4			Figure 3.6	18	588 846	6 640 201	Cadieux *et al.*, 2004 (site 1); David *et al.*, 2008
136	MRNF	Kapijuq (Suite)	M1(I1D)	ID-TIMS	2768 ±3			Figure 3.5	18	622 985	6 618 594	Cadieux *et al.*, 2004 (site 3); David *et al.*, 2008
137	MRNF	Pluton d'Itin-naru	I1D,BO	LA-MC-ICP-MS	2691 ±6		2659 ±18	Figure 3.9	18	584 205	6 634 333	Cadieux *et al.*, 2004 (site 2); David *et al.*, 2008
138	MRNF	Kapijuq (Suite)	I1D,HB-BO	ID-TIMS	2783 ±7		2755 ±12	Figure 3.5	18	612 711	6 751 462	Madore *et al.*, 2001 (site B); David *et al.*, 2008
139	MRNF	MacMahon (Suite)	I1D,CX	ID-TIMS/LA-ICP-QMS	2711 ±11	2742 ±12	2696 ±2	Figure 3.8	19	427 085	6 390 416	Berclaz *et al.*, 2002 (site 4); David *et al.*, 2008
140	GSC	Lepelle (Suite)	I1D,CX	SHRIMP	2724 ±12	2826; 2761		Figure 3.8	18	594 975	6 748 356	Percival *et al.*, 2001 (no. U2)
141	MRNF	Lepelle (Suite)	I1C,CX	LA-MC-ICP-MS	2714 ±10	2731 ±5		Figure 3.8	18	595 935	6 629 033	Cadieux *et al.*, 2004 (site 6); David *et al.*, 2008
142	MRNF	Lepelle (Suite)	I1C,CX	LA-MC-ICP-MS	2723 ±16	2760 ±4 2775 ±10		Figure 3.8	18	546 890	6 617 286	Berclaz *et al.*, 2005 (site 4); David, unpublished
143	GSC	Riv. aux Feuilles (Suite)	I1C,CX	TIMS	2729 ±3			Figure 3.7	19	341 319	6 471 258	Percival and Card, 1994
144	MRNF	MacMahon (Suite)	I3Q	ID-TIMS	2723 ±2			Figure 3.8	18	661 228	6 598 460	Cadieux *et al.*, 2004 (site 4); David *et al.*, 2008
145	MRNF	MacMahon (Suite)	I1T	ID-TIMS/LA-ICP-QMS	2676 ±1	2717 ±4		Figure 3.10	19	387 800	6 382 400	Berclaz *et al.*, 2002 (site 2); David *et al.*, 2008

TABLE 3.3 - U/Pb geochronology data in the NESP (continued).

No	Organization	Stratigraphic unit	Lithologic code	Analytical method	Crystallization age (Ma)	Inherited zircon age (Ma)	Secondary age (Ma)	Reference Figure for crystallization age	Zone	Easting	Northing	References
146	MRNF	MacMahon (Suite)	I1T	ID-TIMS/LA-ICP-QMS	2702 ±2	2767 ±15	2692; 2675	Figure 3.10	19	350 050	6 404 900	Berclaz *et al.*, 2002 (site 3); David *et al.*, 2008
147	MRNF	MacMahon (Suite)	I1T	LA-ICP-QMS	2711 ±10	2775 ±12		Figure 3.8	18	624 583	6 503 871	Leclair *et al.*, 2002 (site 3); David *et al.*, 2008
148	MRNF	MacMahon (Suite)	I1T-I1S	LA-MC-ICP-MS	2717 ±10	2758 ±9		Figure 3.8	18	565 891	6 605 592	Cadieux *et al.*, 2004 (site 5); David *et al.*, 2008
149	MRNF	MacMahon (Suite)	I1T	ID-TIMS	2710 ±10	2729 ±8	2687 ±9	Figure 3.8	18	559 223	6 681 077	Madore *et al.*, 2001 (site E); David *et al.*, 2008
150	GSC	MacMahon (Suite)	I1S	SHRIMP	2698		2761±5 ?	Figure 3.10	19	411 293	6 378 550	Percival *et al.*, 2001 (no. U1)
151	GSC	MacMahon (Suite)	I1S	SHRIMP	2691 ±5	2753-2700	2687; 2637	Figure 3.10	19	373 133	6 410 162	Percival *et al.*, 2001 (no. U5)
152	GSC	MacMahon (Suite)	I1P	TIMS	2724 ±4		2704 ±2 (monazite)	Figure 3.8	18	663 762	6 450 670	Percival *et al.*, 1992 (no. 90-99); Percival and Card, 1994
153	GSC	MacMahon (Suite)	I1S	SHRIMP	2723 ±7		2700	Figure 3.8	18	615 633	6 572 671	Percival *et al.*, 2001 (no. U3)
154	GSC	MacMahon (Suite)	I1S	SHRIMP	2725 ±5			Figure 3.8	18	565 630	6 657 937	Percival *et al.*, 2001 (no. U3)
155	MRNF	Rivière aux Feuilles (Suite)	I1C	ID-TIMS/LA-ICP-QMS	2722 ±2		2661 ±3 2653 ±2	Figure 3.7	18	641 056	6 498 491	Leclair *et al.*, 2002b (site 2); David *et al.*, 2008
156	GSC	Lepelle (Suite)	I1C	TIMS	2720 ±2			Figure 3.8	18	577 107	6 632 099	Percival *et al.*, 1997a
157	MRNF	Maurel (Suite)	I1B,PO	LA-ICP-QMS	2696 ±7	2729 ±14	2629 ±9	Figure 3.10	19	398 209	6 386 084	Berclaz *et al.*, 2002 (site 5); David *et al.*, 2008
158	MRNF	La Chevrotière (Suite)	I1B,PO	ID-TIMS/LA-ICP-QMS	2732 ±2	2814 ±16 2768 ±13	2690 ±13	Figure 3.7	18	602 701	6 516 404	Leclair *et al.*, 2002 (site 4); David *et al.*, 2008
159	MRNF	La Chevrotière (Suite)	I1B,PO	ID-TIMS	2734 ±2	2754 ±3		Figure 3.7	18	602 013	6 708 778	Madore *et al.*, 2001 (site D); David *et al.*, 2008
160	GSC	La Chevrotière (Suite)	I1B,PO	TIMS	2719 ±1			Figure 3.7	18	584 289	6 674 328	Percival *et al.*, 1997a
161	MRNF	La Chevrotière (Suite)	I1B	ID-TIMS/LA-ICP-QMS	2723 ±2	2782 ±11		Figure 3.7	18	643 393	6 523 553	Leclair *et al.*, 2002 (site 1); David *et al.*, 2008
162	MRNF	Tasiataq (Belt)	V1	ID-TIMS	2740 ±4	2996 ±2 2794 ±3		Figure 3.6	19	331 610	6 511 487	David *et al.*, 2008
163	MRNF	Arnaud (Complex)	V3	ID-TIMS	2818 ±5		1790 ±80	Figure 3.4	19	390 828	6 745 200	Madore et Larbi, 2001 (site D); David *et al.*, 2008
164	MRNF	Arnaud (Complex)	QFP	ID-TIMS/LA-ICP-QMS	2782 ±7	2830 ±16		Figure 3.5	19	367 246	6 620 976	Madore *et al.*, 2000 (site C); David *et al.*, 2008
165	MRNF	Diana (Complex)	M1(I1D)	ID-TIMS/LA-ICP-QMS	2782 ±19	2858 ±11	2670; 1780	Figure 3.11	19	436 445	6 748 776	Madore and Larbi, 2001 (site E); David *et al.*, 2008

TABLE 3.3 - U/Pb geochronology data in the NESP (continued).

No	Organization	Stratigraphic unit	Lithologic code	Analytical method	Crystallization age (Ma)	Inherited zircon age (Ma)	Secondary age (Ma)	Reference Figure for crystallization age	Zone	Easting	Northing	References
166	MRNF	Faribault-Thury (Suite)	M1(I1D)	LA-ICP-QMS	2772 ±15	2827 ±23	2716 ±15	Figure 3.5	19	377 700	6 680 409	Madore and Larbi, 2001 (site B); David *et al.*, 2008
167	GSC	Troie (Complex)	Mi(I1D)	SHRIMP	2734 ±5	3013; 2762		Figure 3.8	19	378 053	6 607 502	Percival *et al.*, 2001 (no. DH2)
168	MRNF	MacMahon (Suite)	I1T	ID-TIMS/LA-ICP-QMS	2723 ±1	2826 ±13		Figure 3.8	19	337 374	6 524 236	David *et al.*, 2008
169	MRNF	Faribault-Thury (Suite)	I1D	ID-TIMS/LA-ICP-QMS	2879 ±4			Figure 3.4	19	334 298	6 596 838	Madore *et al.*, 2000 (site A); David *et al.*, 2008
170	MRNF	Faribault-Thury (Suite)	I1D(M20)	LA-ICP-QMS	2760 à 2750	3020; 2920; 2870; 2840	2710	Figure 3.5	19	377 500	6 628 437	Madore *et al.*, 2000 (site H); David *et al.*, 2008
171	MRNF	Faribault-Thury (Suite)	I1D	LA-ICP-QMS	2778 ±18		1782 ±4	Figure 3.5	19	434 038	6 647 775	Madore *et al.*, 2000 (site B); David *et al.*, 2008
172	MRNF	Faribault-Thury (Suite)	I1D	ID-TIMS	2785 +6/-4			Figure 3.5	18	654 641	6 658 285	Madore *et al.*, 2002 (site F); David *et al.*, 2008
173	MRNF	Faribault-Thury (Suite)	I1D	LA-ICP-QMS	2857 ±7		2750 ±17	Figure 3.4	19	341 173	6 659 535	Madore and Larbi, 2001 (site A); David *et al.*, 2008
174	GSC	Faribault-Thury (Suite)	I1D,HB	SHRIMP	2869 ±6			Figure 3.4	19	338 732	6 565 266	Percival *et al.*, 2001 (no. DH1)
175	MRNF	Troie (Complex)	M1(M7)	ID-TIMS/LA-ICP-QMS	2741 ±8	2778 ±16	2707 (monazite)	Figure 3.8	19	374 675	6 565 340	Madore *et al.*, 2000 (site D); David *et al.*, 2008
176	MRNF	Qimussinguat (Complex)	M1(M7)	ID-TIMS/LA-ICP-QMS	2734 ±3	2810; 2800		Figure 3.8	19	381 005	6 645 671	Madore *et al.*, 2000 (site I); David *et al.*, 2008
177	MRNF	Troie (Complex)	I3Q	ID-TIMS/LA-ICP-QMS	2722 ±3			Figure 3.8	19	411 440	6 579 927	Madore *et al.*, 2000 (site E); David *et al.*, 2008
178	MRNF	Belloy (Suite)	I2F,PO	LA-ICP-QMS	2,69	2730; 2720		Figure 3.10	19	426 769	6 560 157	Madore *et al.*, 2000 (site G); David *et al.*, 2008
179	MRNF	Diana (Complex)	I2F,PO	ID-TIMS/LA-ICP-QMS	2756 ±8		1820 ±100	Figure 3.11	19	438 130	6 748 329	Madore and Larbi, 2001 (site F); David *et al.*, 2008
180	GSC	Dufreboy (Suite)	I1C	TIMS	2721 ±3			Figure 3.7	19	434 522	6 516 502	Machado *et al.*, 1989; Percival and Card, 1994
181	GSC	Dufreboy (Suite)	I1C	SHRIMP	2726 ±8			Figure 3.7	19	394 338	6 547 001	Percival *et al.*, 2001 (no. DH3)
182	GSC	?	I1B	TIMS	2755				19	380 533	6 491 821	Percival and Card, 1994
183	MRNF	Kimber (Suite)	I2D	ID-TIMS	2761 ±1			Figure 3.5	18	632 984	6 752 751	Madore *et al.*, 2002 (site C); David *et al.*, 2008
184	MRNF	Gayot (Complex)	V1	ID-TIMS	2880 ±2			Figure 3.4	19	365 891	6 162 824	Lafrance, 2001; David *et al.*, 2008
185	MRNF	Gayot (Complex)	V1	LA-ICP-QMS	2873 ±10	2980 ±11 3133 ±13		Figure 3.4	19	345 873	6 104 683	Gosselin and Simard, 2001; David *et al.*, 2008
186	MRNF	injection (south of Vénus)?	I1D	ID-TIMS/LA-ICP-QMS	2719 ±3		2643 ±13	Figure 3.6	19	366 320	6 150 521	Gosselin and Simard, 2001; David *et al.*, 2008

TABLE 3.3 - U/Pb geochronology data in the NESP (continued).

No	Organization	Stratigraphic unit	Lithologic code	Analytical method	Crystallization age (Ma)	Inherited zircon age (Ma)	Secondary age (Ma)	Reference Figure for crystallization age	Zone	Easting	Northing	References
187	MRNF	Brésolles (Suite)	M1(I1D)	ID-TIMS/LA-ICP-QMS	2807 ±6	2880 ±13		Figure 3.4	19	328 197	6 126 526	Gosselin and Simard, 2001; David *et al.*, 2008
188	GSC	Brésolles (Suite)	M1(I1D)	SHRIMP	2833 ±5			Figure 3.4	19	418 046	6 253 235	Percival *et al.*, 2001 (no. G1)
189	MRNF	Favard (Suite)	I1D,BO	ID-TIMS/LA-ICP-QMS	2717 ±7	2856 ±12	2684 ±2	Figure 3.6	19	349 315	6 141 571	Gosselin and Simard, 2001; David *et al.*, 2008
190	MRNF	Favard (Suite)	I1D,BO	ID-TIMS/LA-ICP-QMS	2750 ±22		2711 ±15	Figure 3.5	19	415 622	6 238 759	Simard *et al.*, 2002 (site A); David *et al.*, 2008
191	MRNF	Maurel (Suite)	I1C,PO	ID-TIMS/LA-ICP-QMS	2690 ±4	2720; 2770		Figure 3.10	19	348 741	6 206 349	Gosselin and Simard, 2001; David *et al.*, 2008
192	MRNF	Maurel (Suite)	I1C,PO	ID-TIMS/LA-ICP-QMS	2706 ±2		2637 ±29	Figure 3.10	19	329 157	6 198 253	Gosselin and Simard, 2001; David *et al.*, 2008
193	MRNF	Beausac (Suite)	I1D,BO	LA-ICP-QMS	2690 ±7	2747 ±22 2810 ±20	2613 ±24	Figure 3.9	19	411 622	6 142 817	Gosselin and Simard, 2001; David *et al.*, 2008
194	MRNF	Opiscotéo (Suite)	M21	ID-TIMS/LA-ICP-QMS	2638 ±8	2715 ±14 2825 ±18		Figure 3.11	19	404 564	6 118 292	Gosselin and Simard, 2001; David *et al.*, 2008
195	MRNF	Aigneau Dykes	I4Q	LA-ICP-QMS	1932 ±14				19	371 654	6 410 890	David *et al.*, 2008
196	MRNF	Aigneau Dykes	I4O	ID-TIMS	1941 ±3				19	368 710	6 356 954	David *et al.*, 2008
197	MRNF	Arnaud (Complex)	M13	LA-ICP-QMS	2718 ±9 (detrital)	2941 ±11 2812 ±12		Figure 3.6	19	379 247	6 615 309	Madore *et al.*, 2000 (site F); David *et al.*, 2008
198	MRNF			LA-MC-ICP-MS		2700; 2750 about 2875			18	454 654	6 219 813	Simard *et al.*, 2005b (brèche B); David *et al.*, 2009
199	MRNF	?	V1	ID-TIMS	2701 ±3		2696; 2707	Figure 3.9	18	379 524	6 659 329	David, unpublished
200	MRNF	Lepelle (Suite)	I1B, BO	LA-MC-ICP-MS		2729 ±1 2753 ±7 >2800			18	550 560	6 774 617	David, unpublished
201	MRNF	Duquet (Complex)	I1D	ID-TIMS	2812			Figure 3.4	18	486 183	6 700 087	David, unpublished
202	GSC	Riv. Aux Feuilles (Suite)	I1C	TIMS	2733 ±2			Figure 3.7	18	530 328	6 481 423	Skulski *et al.*, 1996 (no. SNB-93-95)
203	GSC	Pélican (Complex)	M21	Monazite			2720; 2702		18	583 780	6 620 334	Percival and Skulski, 2000 (no. PBAS96-149)
204	GSC	?		TIMS			2649		19	336 153	6 512 633	Percival and Card, 1994
205	GSC	?	I3	TIMS	2503				19	356 386	6 462 891	Percival *et al.*, 1992 (no. 90-114); Percival and Card, 1994

TABLE 3.3 - U/Pb geochronology data in the NESP (continued).

No	Organization	Stratigraphic unit	Lithologic code	Analytical method	Crystallization age (Ma)	Inherited zircon age (Ma)	Secondary age (Ma)	Reference Figure for crystallization age	Zone	Easting	Northing	References
206	GSC	Vizien area	M1(I1D)	TIMS	3010 +23/-17			Figure 3.3	18	620 971	6 437 993	Percival *et al.*, 1992 (no. 91-169A) (3100 Ma in Percival and Card, 1994; 3010 Ma in Percival *et al.*, 2001; 3097+73/-47 in compilation by Skulski)
207	GSC	Bacqueville (Suite)?	I2J	TIMS			2693 ±3 2684 ±3		18	541 175	6 451 214	Percival *et al.*, 1992 (no. 89-77B); Percival and Card, 1994 (metamorphic age in Percival and Card and in compilation by Skulski)
208	GSC			TIMS			2696; 2671		18	498 014	6 339 671	Percival *et al.*, 1992 (no. 88-52); Percival and Card, 1994
209	GSC		I3B	TIMS	1998				18	473 512	6 332 173	Percival and Card, 1994
210	GSC	?	M1 (I1D)	TIMS	3125	>3500		Figure 3.3	18	542 980	6 373 294	Percival *et al.*, 1992 (no. 86-56); Percival and Card, 1994 (3543 Ma in compilation by Skulski)
211	GSC	Vizien (Belt)	S4	TIMS	<2708 (detrital)			Figure 3.6	18	617 815	6 441 550	Percival *et al.*, 1993; Percival and Card, 1994 (<2718 Ma)
212	GSC	Vizien area	I1D	TIMS	2900			Figure 3.3	18	635 019	6 442 097	Percival and Card, 1994 (2903+72/-52 Ma in compilation by Skulski)
213	GSC	Duvert (Complex)	S2	monazite			2638; 2635		18	615 229	6 442 234	Percival and Skulski, 2000 (no. PBAS94-274)
214	GSC		I3B	TIMS	2220				18	644 184	6 435 938	Percival and Card, 1994
215	GSC	Qalluviartuuq-Payne (Complex)	S4	TIMS	2768 ±3 (detrital)	2806 ±2		Figure 3.5	18	498 585	6 630 781	Skulski *et al.*, 1996 (no. PBAW-94-292)
216	GSC	Qalluviartuuq-Payne (Complex)	I1C?	TIMS	2831 ±1		2633	Figure 3.4	18	498 585	6 630 781	Skulski *et al.*, 1996 (no. PBAW94-290); Percival and Skulski, 2000 (no. PBAW94-290)
217	GSC	?	I2J	TIMS	2729 ±2	2836 ±2		Figure 3.6	18	496 154	6 630 960	Skulski *et al.*, 1996 (no. PBAW-94-293)
218	GSC	Kogaluc (Complex)	M8	monzite			2643; 2628		18	488 359	6 564 660	Percival and Skulski, 2000 (no.SNB93-495)
219	GSC	Qalluviartuuq-Payne (Complex)	M4	monzite			2648		18	528 029	6 594 235	Percival and Skulski, 2000 (no.PBA95-1477)
220	GSC	Qalluviartuuq-Payne (Complex)	I1D	titanite			2608; 2606		18	521 029	6 598 085	Percival and Skulski, 2000 (no. PBAS96-1418)
221	GSC	Qalluviartuuq-Payne (Complex)	I1D	titanite			2642		18	498 585	6 630 786	Percival and Skulski, 2000 (no. PBAS95-1421)

TABLE 3.3 - U/Pb geochronology data in the NESP (concluded).

No	Organization	Stratigraphic unit	Lithologic code	Analytical method	Crystallization age (Ma)	Inherited zircon age (Ma)	Secondary age (Ma)	Reference Figure for crystallization age	Zone	Easting	Northing	References
222	GSC	Qalluviartuuq-Payne (Complex)	M4	monzite			2688; 2673		18	510 211	6 602 049	Percival and Skulski, 2000 (no. PBA94-618)
223	GSC	Qalluviartuuq-Payne (Complex)	I1D	titanite			2750		18	501 900	6 627 310	Percival and Skulski, 2000 (no. PBAS95-1461)
224	GSC	Kogaluc (Complex)	M21 ou M4	monzite			2701; 2705		18	499 085	6 542 075	Percival and Skulski, 2000 (no. PBA94-516a)
225	GSC	Qalluviartuuq-Payne (Complex)	M21 ou M4	monzite			2702; 2495		18	533 842	6 542 703	Percival and Skulski, 2000 (no. PBA94-255)
226	GSC	Qalluviartuuq-Payne (Complex)	I3G	TIMS	2832 ±2			Figure 3.4	18	498 679	6 621 939	Skulski *et al.*, 1996 (no. QAN-92)
227	GSC		I1D	Titanite			2668; 2625		18	582 587	6 630 211	Percival and Skulski, 2000 (no. PBAS96-63A)
228	GSC	Nantais (Complex)	M8 (M4)	monazite			2703		18	575 400	6 760 736	Percival and Skulski, 2000 (no. PBA95-1538)
229	GSC	Duquet (Complex)	M4	monazite			2679; 2641		18	474 440	6 694 686	Percival and Skulski, 2000 (no. PBAS95-1734)
230	GSC		I1C	Titanite			2686; 2654		18	463 780	6 724 782	Percival and Skulski, 2000 (no. PBAS95-1738)
231	MRNF	Arnaud (Complex)	M12	ID-TIMS/LA-ICP-QMS	2725 ±9 (detrital)		2702 ±2 (titanite)	Figure 3.6	19	379 247	6 615 309	David *et al.*, 2008
232	MRNF	?	M21	ID-TIMS	2691 ±4				19	409 658	6 539 086	David *et al.*, 2008

CHAPTER 4
GEOCHEMISTRY AND NEODYMIUM ISOTOPE DATA IN THE NORTHEASTERN SUPERIOR PROVINCE

Michel Boily and Charles Maurice

INTRODUCTION

This chapter provides an overview of geochemistry studies conducted by Boily *et al.* (2002, 2004, 2006a) on Archean volcanic and plutonic units in the NESP, based on more than 2,400 whole-rock analyses of samples collected under the Far North Program. This report deals with whole-rock major and trace element geochemical compositions and neodymium (Nd) isotope compositions. The latter isotopic data was namely used to delineate the extent of a paleocraton and to establish boundaries between two terranes that evolved distinctly (Figure 2.2).

SOURCES OF DATA

Major and trace element geochemical analyses discussed in this chapter are available in SIGÉOM, where the methods used to determine concentrations for each element are described. More than 330 Nd isotope analyses were conducted on Archean units of the NESP by various authors, and analytical methods are described in the original publications (see compilation by Maurice, 2007).

GEOCHEMISTRY OF ARCHEAN UNITS

Geochemistry studies were carried out on samples collected in the plutonic and volcanic suites of the NESP, with the exception of the Ashuanipi Subprovince (Figure 2.2). The quality of the geochemical synthesis depends on the density of geochemical analyses; consequently, certain units are not discussed due to a lack of data. The results of the geochemistry study are discussed in five themes: 1) volcano-sedimentary rocks; 2) plutonic rocks; 3) ultramafic to intermediate intrusions; 4) migmatites; and 5) nepheline syenite intrusions. By comparing the chemical composition of stratigraphic units within the same category, it is possible to characterize the latter based on their geographic distribution and their age.

Volcano-sedimentary rocks

Volcano-sedimentary sequences were emplaced during magmatic events that took place, for the most part, prior to 2.74 Ga (figures 3.1 and 3.2). Six series of volcanic rocks are defined (Table 4.1):

1. komatiite and basaltic komatiite series (KBK);
2. Mg-tholeiite series (MT);
3. Fe-tholeiite series (FT);
4. contaminated tholeiite series (CT);
5. calc-alkaline basalt, andesite, and dacite series (CABAD);
6. calc-alkaline rhyodacitic to rhyolitic tuff and lava series (CARTL).

Representative analyses for each of these series are listed in Table 4.2. Certain volcano-sedimentary sequences for which only a few analyses are available will not be discussed in this report (Qalluviartuuq-Payne and Kogaluc belts; unpublished data in Skulski *et al.*, 1996). Other sequences for which analyses were not compiled in preparing this chapter have already been the object of detailed work, namely the Vizien Belt (Skulski and Percival, 1996), the Duquet belt (Bourassa, 2002; Maurice *et al.*, 2009), the Buet, Hamelin, and Trempe belts in the Arnaud Complex (Maurice *et al.*, 2003), and the Nuvvuagittuq Belt (O'Neil *et al.*, 2007).

Komatiite and basaltic komatiite series

Rocks in the komatiite and basaltic komatiite series (KBK, Table 4.1) are typical of the Gayot and Arnaud complexes. They also occur in minor proportions in the Tasiataq and Allemand belts, and in the Innuksuac and Duvert complexes (figures 4.1 and 4.2). Boily *et al.* (2002) was able to characterize this series based on samples from the Gayot Complex. Despite the presence of strong alteration (LOI reaching up to 6.2 wt%), komatiites and basaltic komatiites of the Gayot Complex show SiO_2 (43 to 48 wt%), Al_2O_3 (4 to 9 wt%), MgO (18 to 31 wt%), Ni (550 to 1700 ppm), Cr (2100 to 3000 ppm), and TiO_2 (0.2 to 0.5 wt%) contents comparable to those of komatiites exposed in the Abitibi Subprovince (Xie and Kerrich, 1994). They exhibit rare earth element (REE) concentrations ten times below that of chondrites, with profiles where light rare earth elements (LREE) are moderately fractionated relative to heavy rare earth elements (HREE) (Figure 4.3a and e). Certain samples exhibit variable Eu anomalies that cannot be attributed to plagioclase accumulation or fractionation (Figure 4.3a). Coherent variations of elements considered to be immobile (high field strength elements - HFSE, and HREE) suggest Eu anomalies are due to mobility of Eu^{2+} during post-magmatic alteration. Komatiites of the Gayot Complex show low HFSE

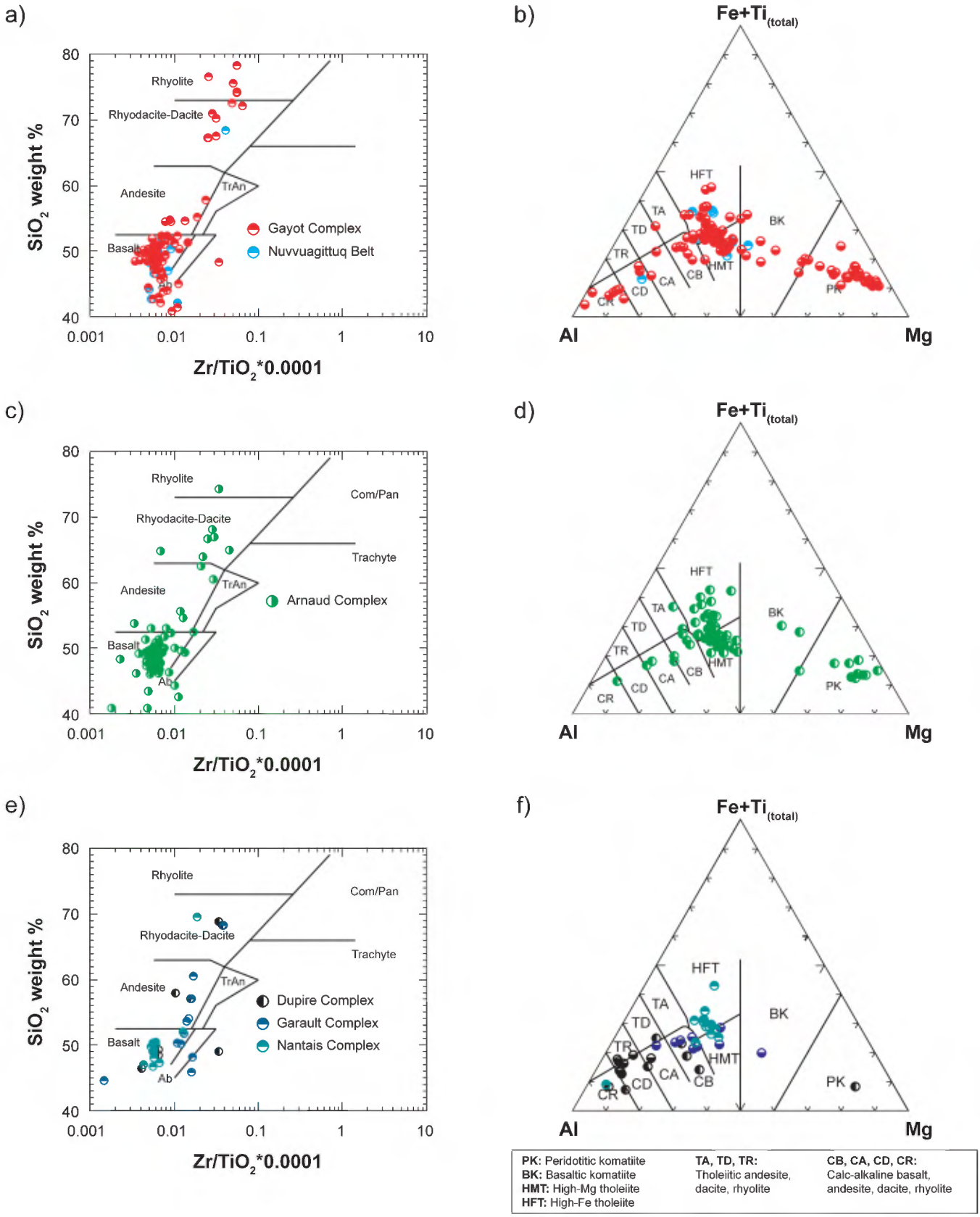

FIGURE 4.1 – Classification diagrams for volcanic rocks in the NESP (Gayot, Arnaud, Dupire, Garault, and Nantais complexes and Nuvvuagittuq Belt): a), c), and e) SiO2 (weight %) vs Zr/TiO2*0.0001; b), d), and f) Jensen cation plot, Mg–Al–Fe+Ti(total).

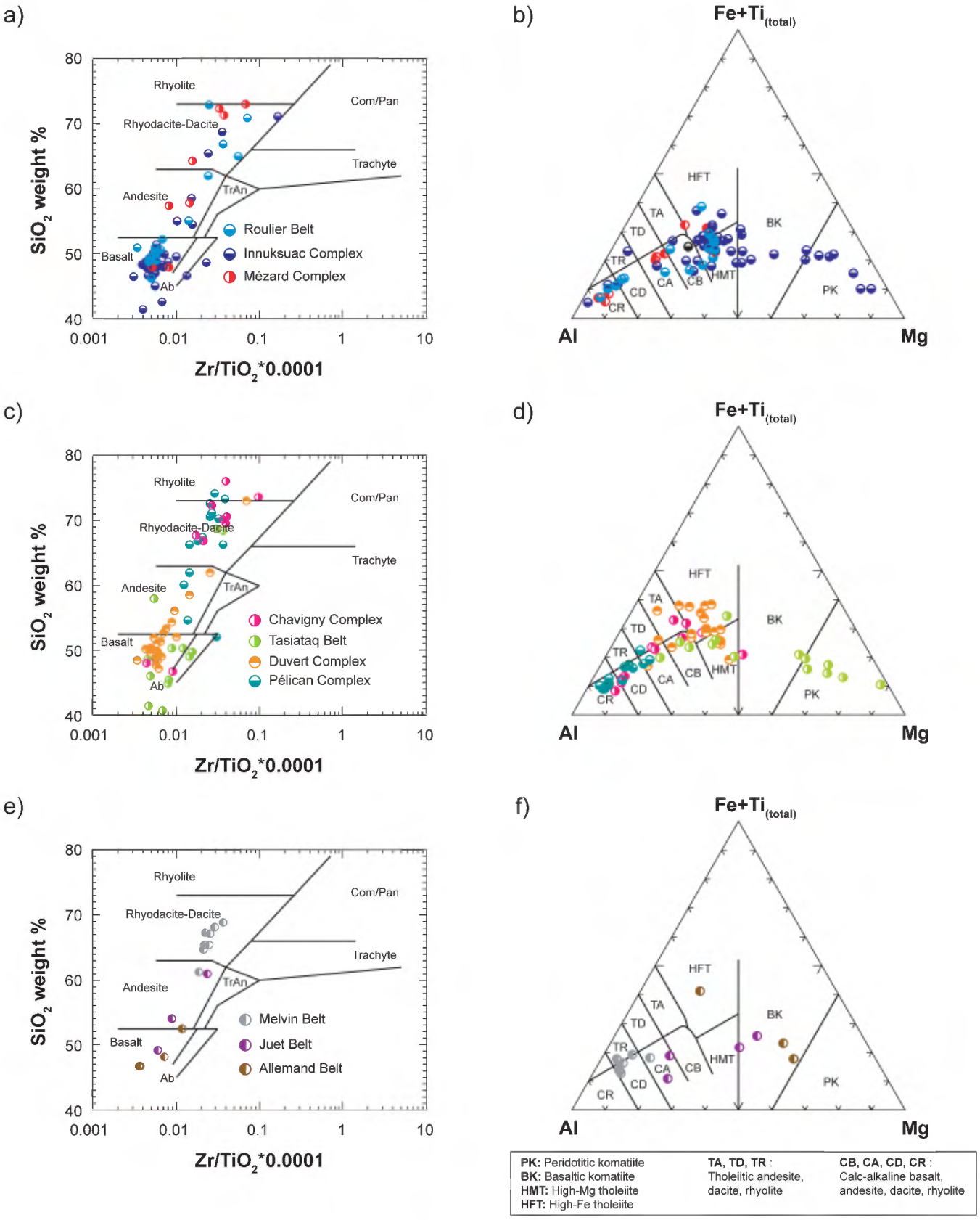

FIGURE 4.2 – Classification diagrams for volcanic rocks in the NESP (Innuksuac, Mézard, Chavigny, Duvert, and Pélican complexes and Roulier, Tasiataq, Melvin, Juet, and Allemand belts): a), c), and e) SiO2 (weight %) vs Zr/TiO2*0.0001; b), d), and f) Jensen cation plot Mg–Al–Fe+Ti(total).

concentrations (Zr = 16 to 34 ppm; Nb = 0.9 to 1.1 ppm) as well as Ti/Zr (74 to 104), Zr/Y (2.2 to 2.7), Al_2O_3/TiO_2 (14 to 34), and $[Gd/Yb]_{CN}$ (1.0 to 1.2) ratios close to chondritic values, typical of Al-undepleted komatiites (Figure 4.4a).

Geochemistry data derived from komatiite samples collected outside of the Gayot Complex cannot be used to establish an accurate classification. It does appear however that most NESP komatiites belong of the Al-undepleted, chondritic variety. It is impossible to discriminate, based on geochemistry data, komatiites and basaltic komatiites as a function of age or geographic distribution.

Mg-tholeiite series

The Mg-tholeiite series (MT, Table 4.1) is present in most volcano-sedimentary units and constitutes the most voluminous volcanic series in the NESP. Our reference series was established using samples collected in the Gayot Complex (Boily *et al.*, 2002). It comprises tholeiitic basalts (SiO_2 = 47 to 55 wt%; MgO = 5 to 12 wt%), with chondrite-normalized REE profiles that are flat to slightly depleted in LREE ($[La/Sm]_{CN}$ = 0.5 to 1.2; $[La/Yb]_{CN}$ = 0.5 to 1.5), at about 10 to 20 times chondritic values (Figure 4.3a and e). All samples show a positive correlation between $FeO_{(total)}$ (9 to 15 wt%) and TiO_2 (0.5 to 1.2 wt%; Figure 4.4b). Mg-tholeiites have Zr/Y (2 to 3), Ti/Zr (70 to 130), and Zr/Nb (15 to 23) ratios similar to chondritic values. $[Nb/Th]_{PM}$ and $[Nb/La]_{PM}$ ratios (Figure 4.4e) indicate a similarity with primitive tholeiites from anomalously thick basaltic piles, such as oceanic plateau basalts (Otong-Java, Caribbean, Kerguelen) and oceanic ridges influenced by mantle plume magmatism (Galapagos; Tomlinson *et al.*, 1997; Fan and Kerrich, 1997; Puchtel *et al.*, 1997). Similarly to Mg-tholeiites of the NESP, oceanic plateau tholeiites are generally enriched in Fe and less depleted in LILE, Th, U, and LREE relative to N-MORBs (Floyd, 1989; Figure 4.4b). Our compilation shows the chemical composition of Mg-tholeiites did not vary significantly over the 180 Ma during which most of these rocks were emplaced in the volcanic belts of the NESP (2.88 to 2.70 Ga).

Fe-tholeiite series

The Fe-tholeiite series (FT, Table 4.1) is widespread and is well represented in the Gayot, Arnaud, Nantais, and Duvert complexes (figures 4.1 and 4.2) and in the Duquet belt (not shown). Boily *et al.* (2002) described a reference series based on samples collected in the Gayot and Duvert complexes. Fe-tholeiites either form stratigraphic assemblages with distinct ages (Maurice *et al.*, 2009) or are intercalated with Mg-tholeiites. Compared to the latter, they are characterized by higher TiO_2 (>1.2 wt%) and $FeO_{(total)}$ (>11 wt%; Figure 4.4b) contents; they form a less magnesian magmatic series (MgO = 4 to 8 wt%) and show more evolved REE profiles (20 to 40 times chondrite; Figure 4.3a and e). They also have higher HFSE concentrations (Zr = 53 to 101 ppm) than Mg-tholeiites, although their Zr/Y (2 to 4), Ti/Zr (84 to 138), and Zr/Nb (16) ratios are comparable. Similarly to volcanic rocks of the Mg-tholeiite series, Fe-tholeiites show a consistent composition throughout the 180 Ma of active volcanism (2.88 to 2.70 Ga). A detailed study of volcanic belts in the north part of the NESP suggests 2.82-Ga Mg-tholeiites form the base of an extensive volcanic pile on which 2.78-Ga Fe-tholeiites are unconformably overlain (Maurice *et al.*, 2009).

Contaminated tholeiite series

Contaminated tholeiites (CT, Figure 4.1) were mostly observed in the Duvert and Innuksuac complexes. The Duvert Complex contains a series of evolved Fe-tholeiites (SiO_2 = 47 to 56 wt%, Mg# = 22 to 39) enriched in TiO_2 (1.5 to 1.9 wt%) and $FeO_{(total)}$ (9 to 17 wt%; Figure 4.4d). These rocks contrast however with Fe-tholeiites described above due to their enrichment in LREE ($[La/Sm]_{CN}$ = 2.3 to 3.1), LILE (Ba and Rb), and their negative Nb-Ta anomalies typical of island arc tholeiites (Figure 4.3h). LREE and LILE enrichment suggests magmatism took place in an oceanic or continental intraplate environment. The Innuksuac Complex also contains tholeiites characterized by major element concentrations typical of Mg-tholeiites (TiO_2 = 1.1 to 1.2 wt%, $Fe_2O_{3(total)}$ = 10 to 17 wt%, and MgO = 5 to 8 wt%), however these rocks are also enriched in LREE ($[La/Yb]_{CN}$ = 1.4 to 10.8), Ba, Th, and U (Figure 4.3d and h). Since they also show negative Nb-Ta anomalies typical of volcanic suites generated in subduction zones, we have classified these basalts in the contaminated tholeiite series. Given the high metamorphic grade and level of recrystallization of these rocks however, another possibility is that they were initially misinterpreted and may in fact represent dioritic intrusions associated with the Bacqueville Suite.

Considering the crystallization ages obtained from samples of the Duvert Complex (<2725 Ma), the contaminated tholeiite series appears to have been emplaced late in the Neoarchean. Although the exact age of contaminated tholeiites of the Innuksuac Complex (2760 to 2740 Ma) is unknown, their age may be estimated at about 2740 Ma, suggesting contaminated tholeiites may represent a rock type that was emplaced once the evolution of the NESP was already well underway.

Calc-alkaline basalt, andesite, and dacite series

This series (CABAD, Table 4.1) is predominant in the Garault, Dupire, and Pélican complexes, but is also present in the Gayot, Arnaud, Innuksuac, Mézard, Duvert, and Chavigny complexes as well as in the Roulier, Tasiataq, and Juet belts (figures 4.1 and 4.2). The reference series was described based on samples collected in the Gayot and Garault complexes (Boily *et al.*, 2002). These aluminous (Al_2O_3 = 12 to 19 wt%) volcanic rocks of calc-alkaline affinity range from basaltic to andesitic in composition (SiO_2 = 46

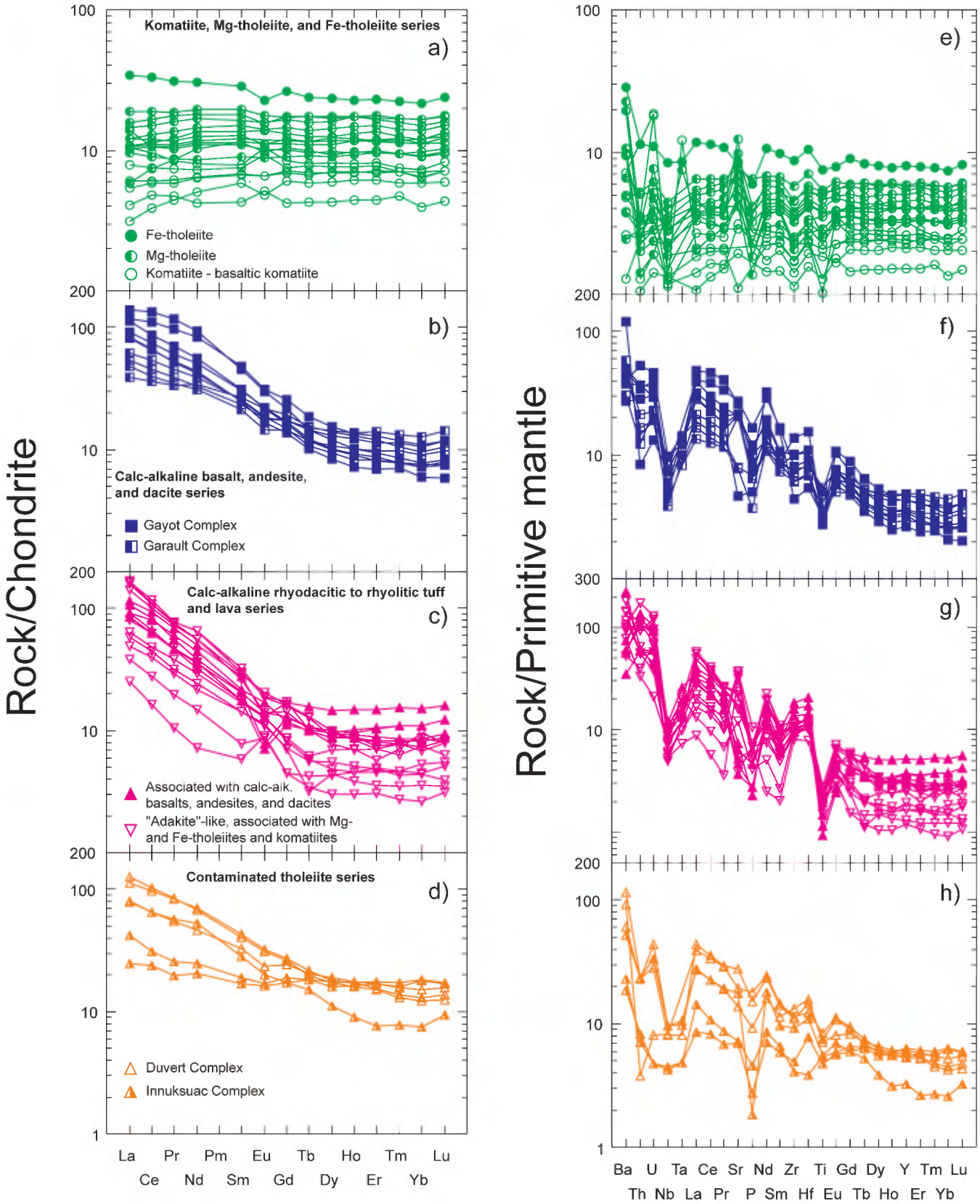

FIGURE 4.3 – Chondrite-normalized REE patterns and primitive mantle-normalized multi-element diagrams for volcanic rocks in the NESP: a) and e) komatiite, Mg-tholeiite, and Fe-tholeiite series; b) and f) calc-alkaline basalt, andesite, and dacite series; c) and g) calc-alkaline rhyodacitic to rhyolitic tuff and lava series; d) and h) contaminated tholeiite series.

to 61 wt%). They are distinguished from Mg-tholeiites and Fe-tholeiites due to their Zr/Y ratios > 3 (Figure 4.4c), their enriched LREE ($[La/Sm]_{CN}$ = 2.4 to 3.6), Th, Sr, and Ba contents, and their negative anomalies in Nb, Ta, P, and Ti typical of subduction zone-related calc-alkaline rocks (Figure 4.3a and f). Some LREE-enriched basalts are also relatively magnesian and primitive (Mg# = 64 to 70).

Although rocks of this series occur in many volcano-sedimentary belts in the NESP, they represent but a small proportion of the volcanic rocks that were emplaced during the Neoarchean. These rocks were abundantly sampled and are probably overrepresented in the geochemistry database. Our compilation work reveals an association between these volcanic rocks and sedimentary sequences, commonly forming a younger volcanic cycle overlying early assemblages composed of komatiites, Mg-tholeiites, and Fe-tholeiites.

Calc-alkaline rhyodacitic to rhyolitic tuff and lava series

This series (CARTL, Table 4.1) is present in most of the volcano-sedimentary units in the NESP. Samples from the Gayot and Dupire complexes were used to describe the reference series for these rocks (Boily *et al.*, 2002). Rhyodacitic to rhyolitic (SiO_2 = 67 to 78 wt%) tuffs and lavas form three distinct groups based on Zr/Y and $[La/Yb]_{CN}$ ratios (Figure 4.4f). Group I shows high Zr/Y (10 to 41) and $[La/Yb]_{CN}$ (16 to 36) ratios, whereas Group II shows moderate Zr/Y (7 to 15) and $[La/Yb]_{CN}$ (6 to 10) ratios (Figure 4.4f). Group III was recognized only in the Dupire Complex and the Duquet belt (Bourassa, 2002). It consists of low-alumina high-silica rhyolites with low Zr/Y and $[La/Yb]_{CN}$ ratios. These rhyolites show signatures comparable to those of so-called "fertile" rhyolites associated with volcanogenic massive sulphide deposits (*e.g.*, Noranda-type deposits). Group I rhyolites are predominant in the Vénus belt (Gayot Complex) and are not as aluminous (Al_2O_3 = 11 to 16 wt%) as Group II rhyolites (Al_2O_3 = 13 to 17 wt%). They are also more strongly differentiated than Group II rocks, with for instance, Sr contents ranging from 72 to 120 ppm. Moreover, Group I rhyolites have negative Eu anomalies, are commonly associated with basalts, andesites, and dacites, and represent the differentiated end-members of a calc-alkaline suite typically associated with subduction settings. Rhyodacitic to rhyolitic volcaniclastic rocks in Group I display certain geochemical characteristics typical of the more evolved members of Cenozoic "adakite" suites, or of tonalitic and trondhjemitic phases in Archean TTG series (Drummond and Defant, 1990; Smithies, 2000).

The felsic volcanic series accounts for only a small volume of volcanic sequences. However, these rocks were almost systematically sampled for geochronology purposes and are thus overrepresented in the geochemistry database. A spatial association between Group II felsic rocks and rocks of the CABAD series was established based on field observations.

Summary of volcanic rock geochemistry

Tholeiitic basalts are the most commonly observed volcanic rocks in the NESP. Detailed studies of volcano-sedimentary belts in the north part of the NESP suggest volcanic assemblages composed of Mg-tholeiites form a lower sequence overlain by an Fe-tholeiite sequence, which originally spread across more than 200 km (Maurice *et al.*, 2009). Contaminated tholeiites and calc-alkaline volcanic rocks occur in volcanic assemblages of various ages. The latter are mainly composed of felsic tuffs and lavas but also include mafic and intermediate lavas. These rock types were abundantly sampled and analyzed, enabling us to document the latter and to conclude that, despite their presence in assemblages of various ages, they account for a significant proportion of younger volcano-sedimentary assemblages.

Felsic and intermediate intrusive rocks

Geological mapping surveys, combined with the results of petrographic, geochemical, and geochronological studies, resulted in the identification of three major series of felsic and intermediate intrusions. These are: 1) tonalites and associated rocks (TTG); 2) granites and monzogranites (GGM); and 3) pyroxene-bearing granitoid rocks. Representative analyses for each series are presented in Table 4.3.

Tonalite – trondhjemite – granodiorite series (TTG)

Rocks of the tonalite-trondhjemite-granodiorite (TTG) series cover a significant surface area within the NESP (figures 3.4, 3.5, 3.6). They were emplaced during various magmatic events that took place mainly between 2830 and 2740 Ma (Figure 3.1). These rocks primarily consist of tonalite, trondhjemite, diorite, and quartz diorite; in fact, rocks with a granodioritic composition were rarely observed. However, the vast majority of these rocks were affected by a granitization process related to the emplacement of younger granodioritic or granitic plutons. This granitization translates into the presence of a granodioritic or granitic phase in gradual and diffuse contact with tonalitic phases. The presence of this late granitic phase may occasionally result in a global granodioritic chemical composition for certain samples of granitized tonalite.

The geochemistry study of tonalitic rocks was conducted using analytical data from samples collected in the Brésolles and Suluppaugalik suites (2833 to 2807 Ma, Figure 3.4), the Faribault-Thury, Rochefort, and Kapijuq suites (2785 to 2775 Ma, Figure 3.5), the Coursolles and Favard suites (2760 to 2740 Ma, Figure 3.5), and the Bylot Suite (2737 to 2723 Ma, Figure 3.6). Data from the Coursolles and Favard suites were used to determine the chemical characteristics typical of the TTG series (Boily *et al.*, 2004). This series includes diorites, quartz diorites, hornblende-biotite tonalites, and biotite trondhjemites. These rocks are metaluminous (A/CNK = 0.5 to 1.0), except the most felsic mem-

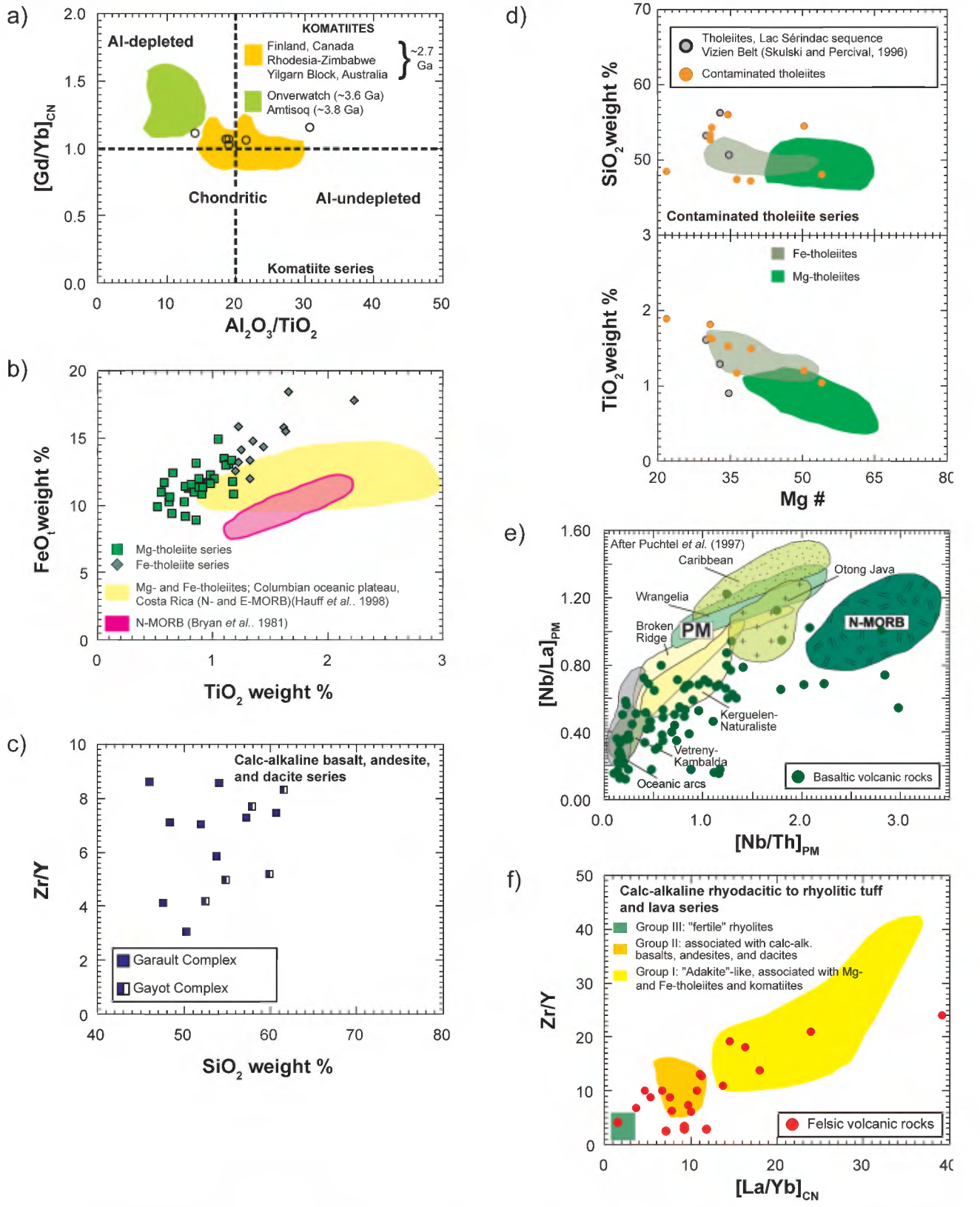

FIGURE 4.4 – Volcanic rocks in the NESP: **a**) [Gd/Yb]CN vs Al_2O3/TiO_2 for the komatiite series. Note the chondritic, Al-undepleted nature of NESP komatiites; **b**) $FeO_{(total)}$ (weight %) vs TiO_2 (weight %) for the Mg- and Fe-tholeiite series; **c**) Zr/Y vs SiO_2 (weight %) for the calc-alkaline basalt, andesite, and dacite series; **d**) TiO_2 (weight %) and SiO_2 (weight %) vs Mg# for the contaminated tholeiite series. Note TiO_2 and SiO_2 enrichment and high degree of differentiation (i.e. low Mg#) of contaminated tholeiites relative to Mg-tholeiites. Tholeiites from the Lac Sérindac sequence (Vizien Belt) are also plotted for comparative purposes; **e**) [Nb/La]PM vs [Nb/Th]PM for basaltic rocks in the NESP. The latter show similarities with plateau basalts (e.g., Kerguelen-Naturaliste and Broken Ridge) and island arc basalts; **f**) Zr/Y vs [La/Yb]CN for the calc-alkaline rhyodacitic to rhyolitic tuff and lava series. The three main groups recognized in calc-alkaline felsic volcanic rocks of the NESP are illustrated.

bers (>70 wt%), which are hyperaluminous (A/CNK = 0.9 to 1.1). Rocks in these suites are magnesian (Figure 4.5a) and overall show calcic to alkali-calcic compositions; only a few samples display calc-alkalic compositions (Figure 4.5b). This distribution is comparable to that obtained by Frost *et al.* (2001) for Archean TTG suites, but contrasts with the chemical characteristics of TTGs in Cordilleran batholiths and volcanic arcs, which show magnesian and calcic compositions.

The tonalitic rocks display low MgO contents that are inversely correlated with SiO_2 and TiO_2 contents (Figure 4.5e and g). Tonalites and trondhjemites of the Coursolles and Favard suites (SiO_2 = 56 to 76 wt%) exhibit high Al_2O_3 (14 to 18 wt%), Na_2O (3.3 to 5.5 wt%), and Sr (164 to 717 ppm) concentrations and low LREE contents (Yb = 0.1 to 2.1 ppm). Consequently, these rocks are characterized by high $[La/Yb]_{CN}$ (6 to 111; $\bar{X}$ = 34), Sr/Y (8 to 232; $\bar{X}$ = 90), and Na_2O/K_2O (0.7 to 7.8; $\bar{X}$ = 2.7) ratios, typical of Archean TTG suites (Martin and Moyen, 2002; Martin, 1999 and 1993; Drummond and Defant, 1990; Arth *et al.*, 1978). Sharper variations in chemical composition are observed in more felsic members (leucocratic tonalites and trondhjemites; SiO_2 = 66 to 76 wt%). Thus, the marked increase in $[La/Yb]_{CN}$, Sr/Y, and Zr/Y ratios in felsic members contrasts with the minor variations outlined in less evolved members (Figure 4.5f). These variations are particularly apparent in rocks of the Favard Suite, where a LREE depletion is observed (Yb_{CN} = 9 to 1; Figure 4.5d). Most tonalites and trondhjemites have normalized rare earth profiles typical of the TTG series, with a moderate enrichment in LREE ($[La/Sm]_{CN}$ = 1 to 23), whereas the most differentiated trondhjemites (SiO_2 > 71 wt%) show low REE contents and strongly positive Eu anomalies, as well as steep negative Nb-Ta, P, and Ti anomalies (Figure 4.5c).

Mafic to intermediate in composition (SiO_2 = 49 to 63 wt%), the diorites and quartz diorites share the same sodic (Na_2O/K_2O = 1.3 to 3.6) and aluminous (Al_2O_3 = 14 to 18 wt%) character as the associated tonalites. These rocks however have higher iron contents ($FeO_{(total)}$ = 3 to 12 wt%) but are low in magnesium (Mg# = 36 to 63; Figure 4.5h). They show elevated Sr (259 to 951 ppm), Ba (247 to 1293 ppm), and LREE (La = 19 to 101 ppm) values typical of TTG *stricto sensu*, while being less depleted in Yb (0.9 to 3.6 ppm) and having more moderate Zr/Y and $[La/Yb]_{CN}$ ratios (Figure 4.5d and f). Analyzed diorite samples show higher REE contents than tonalites and trondhjemites (Figure 4.5d). These diorites are relatively depleted in Cr (20 to 120 ppm; $\bar{X}$ = 66) and in most cases, their SiO_2 contents and Mg# are too low to represent the mafic or intermediate members of an adakitic suite (Figure 4.5h). Moreover, these diorites contrast with intrusive rocks of so-called "sanukitoid" suites, designating syn- to post-tectonic rocks composed of diorites, monzodiorites, and granodiorites that outcrop in the southwest Superior Province (Mg# > 60 and strong enrichment in Ba and Sr - 600 to 1800 ppm; Stern *et al.*, 1989).

The Brésolles, Suluppaugalik, Faribault-Thury, Rochefort, and Kapijuq suites (Figure 4.6), as well as the Bylot Suite (Figure 4.7) exhibit similar geochemical characteristics that indicate an association with Archean TTG as defined above. Consequently, based solely on geochemistry, we were unable to distinguish the different tonalitic units (TTG) of the NESP. These units exhibit similar geochemical characteristics, regardless of their location or their age. The only distinctive trait is the scarcity of mafic to intermediate compositions (diorite to quartz diorite) in early Neoarchean suites of the Rivière Arnaud Terrane (Faribault-Thury, Rochefort, and Kapijuq; 2785 to 2775 Ma) relative to suites located in the Hudson Bay Terrane (Coursolles and Favard; 2760 to 2740 Ma).

Granodiorite – granite – monzogranite (GGM) series

Rocks from the granodiorite-granite-monzogranite (GGM) series cover a very large proportion of the NESP. These rocks were emplaced after 2740 Ma, over the course of two major Neoarchean magmatic events (Figure 3.2). The Leridon, La Chevrotière, Pinguq, Rivière aux Feuilles, Dufreboy, and Desbergères suites (Figure 3.7) were emplaced between 2740 and 2705 Ma, whereas the Maurel, Tramont, Belloy, Corneille, and Morrice suites (Figure 3.10) were emplaced between 2705 and 2680 Ma. A detailed geochemistry study was conducted on the Desbergères Suite and the Tramont and Morrice suites in order to compare the geochemical characteristics of intrusive suites with different ages of emplacement (Boily *et al.*, 2004).

Desbergères Suite

The Desbergères suite is mainly composed of hornblende-biotite granodiorite, with biotite monzogranite and quartz monzodiorite. These rocks are metaluminous to weakly hyperaluminous (A/CNK = 0.9 to 1.2), magnesian, and calc-alkalic to alkali-calcic (Figure 4.8a and b). This composition is typical of dioritic and granodioritic plutons in the inboard portion of Cordilleran batholiths. The Desbergères Suite has an intermediate to felsic composition (SiO_2 = 61 to 75 wt%) and is depleted in $Fe_2O_{3(total)}$ (1.0 to 6.6 wt%), MgO (0.1 to 2.8 wt%), and TiO_2 (0.1 to 0.8 wt%). It also exhibits low Na_2O/K_2O ratios reflecting the potassic character of these rocks. Also, Zr/Y, Rb/Sr, Sr/Y, and $[La/Yb]_{CN}$ ratios appear to increase with increasing silica (Figure 4.8e). This upward trend is moderate from 60 to 70 wt% SiO_2, but becomes quite steep for more felsic compositions (>70 wt% SiO_2).

Chondrite-normalized rare earth element profiles (not shown) illustrate LREE enrichment ($[La/Sm]_{CN}$ = 3 to 11) and moderate to strong HREE depletion ($[La/Yb]_{CN}$ = 10 to 84). These profiles display either no or slightly negative Eu anomalies, whereas multi-element diagrams normalized to the primitive mantle show negative Nb-Ta, Ti, and P anomalies and enriched Ba, Th, and U, which are distinctive traits of intermediate to felsic calc-alkaline Archean plutonic suites.

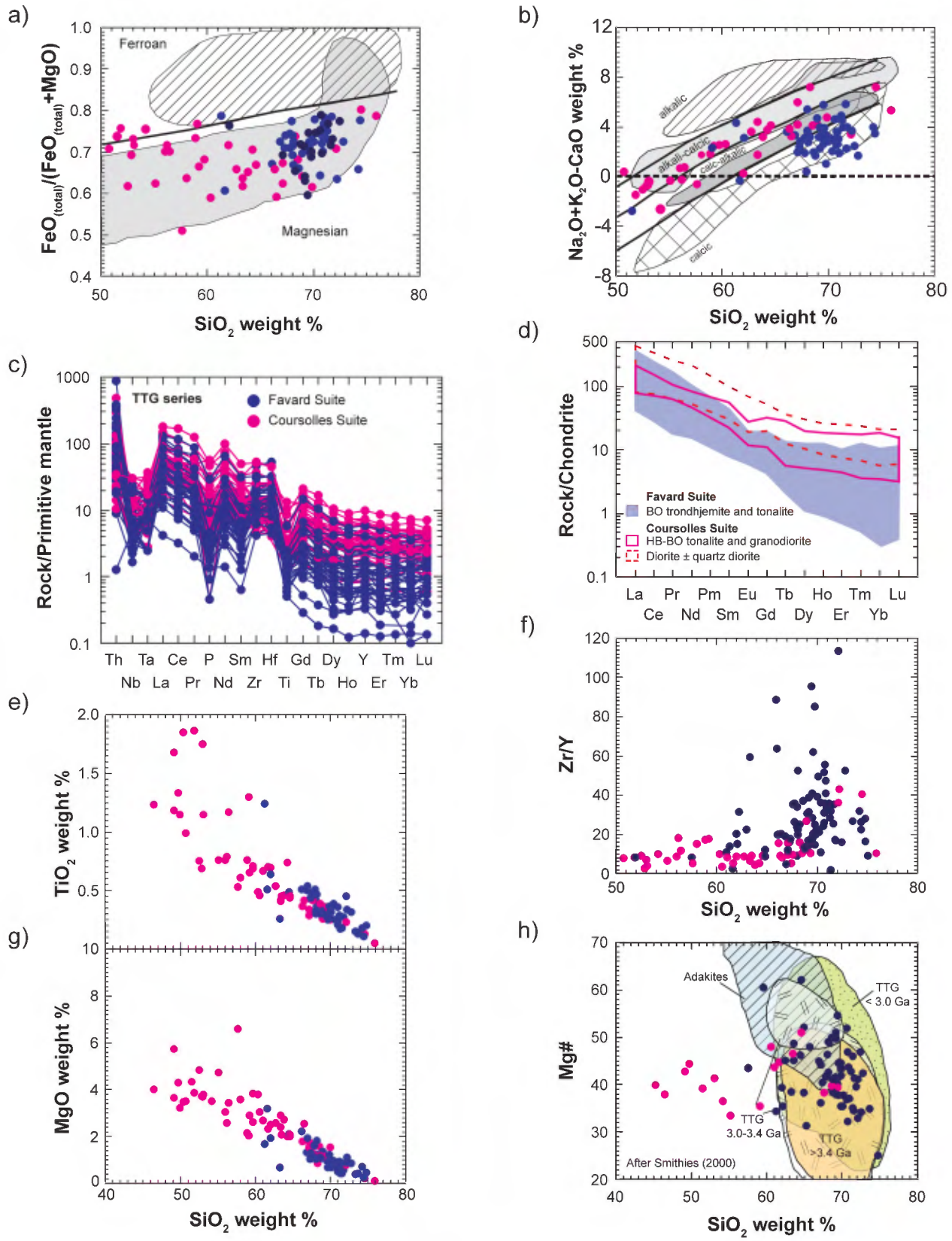

FIGURE 4.5 – TTG series, Coursolles and Favard suites: a) classification diagram by Frost *et al.* (2001), $FeO_{(total)}/(FeO_{(total)}+MgO)$ vs SiO_2 (weight %); **b**) classification diagram by Frost *et al.* (2001), Na_2O+K_2O-CaO (weight %) vs SiO_2 (weight %); **c**) primitive mantle-normalized multi-element diagram; **d**) chondrite-normalized REE patterns, showing gradual decrease in HREE concentrations from dioritic to trondhemitic compositions; **e**) TiO_2 (weight %) vs SiO_2 (weight %); **f**) Zr/Y vs SiO_2 (weight %) showing marked increase in Zr/Y ratio in felsic compositions; **g**) MgO vs SiO_2 (weight %); **h**) Mg# vs SiO_2 (weight %) showing the absence of adakitic compositions in the Favard and Coursolles suites.

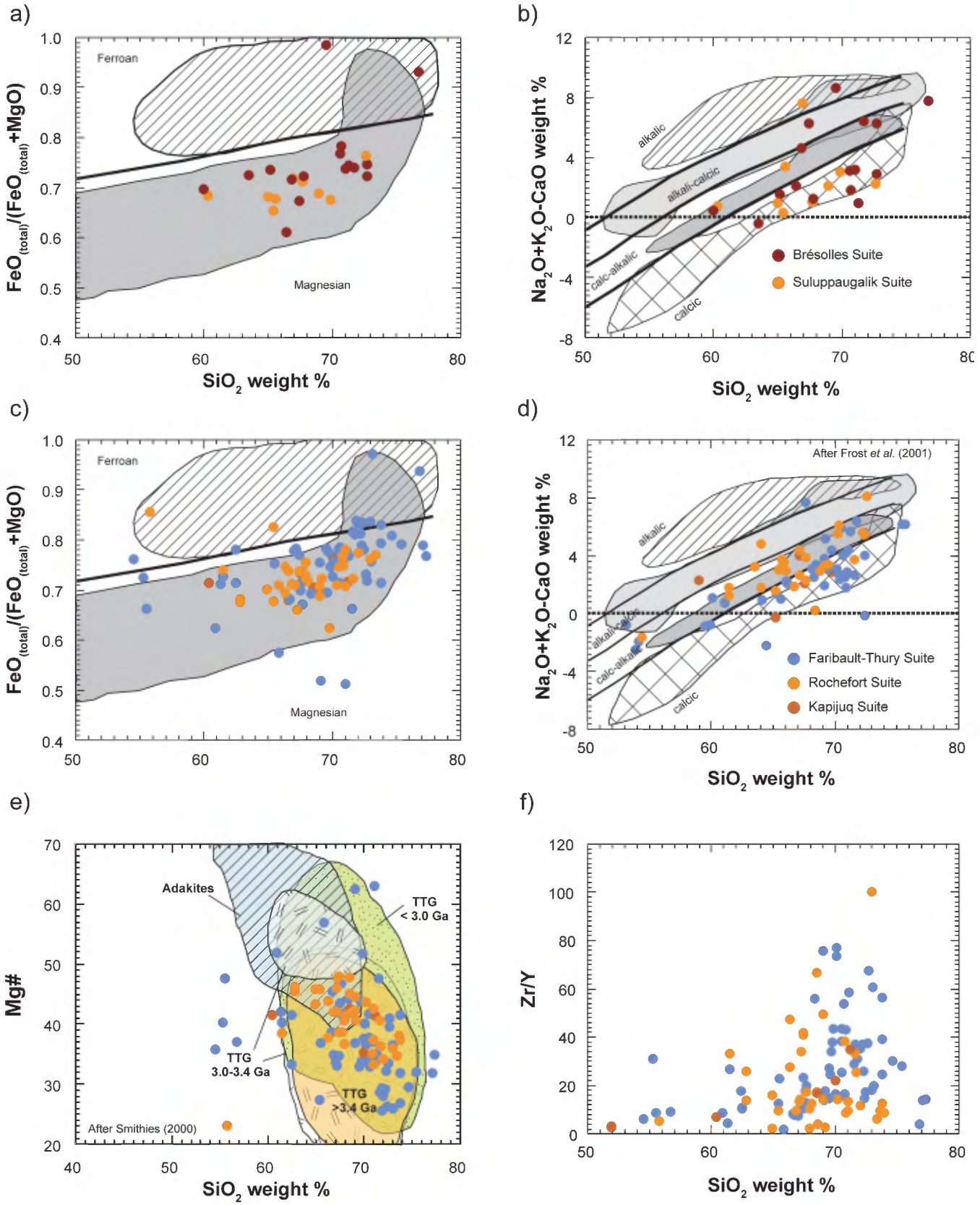

FIGURE 4.6 – TTG series, Brésolles, Suluppaugalik, Faribault-Thury, Rochefort, and Kapijuq suites: **a**) and **c**) classification diagram by Frost *et al*. (2001); $FeO_{(total)}/(FeO_{(total)}+MgO)$ vs SiO_2 (weight %); **b**) and **d**) classification diagram by Frost *et al*. (2001); Na_2O+K_2O-CaO (weight %) vs SiO_2 (weight %); **e**) Mg# vs SiO_2 (weight %) illustrating the absence of adakites in the Faribault-Thury, Rochefort, and Kapijuq plutonic suites (TTG series); **f**) Zr/Y vs SiO_2 (weight %) showing significant variations in Zr/Y ratios for felsic members of the Faribault-Thury, Rochefort, and Kapijuq suites.

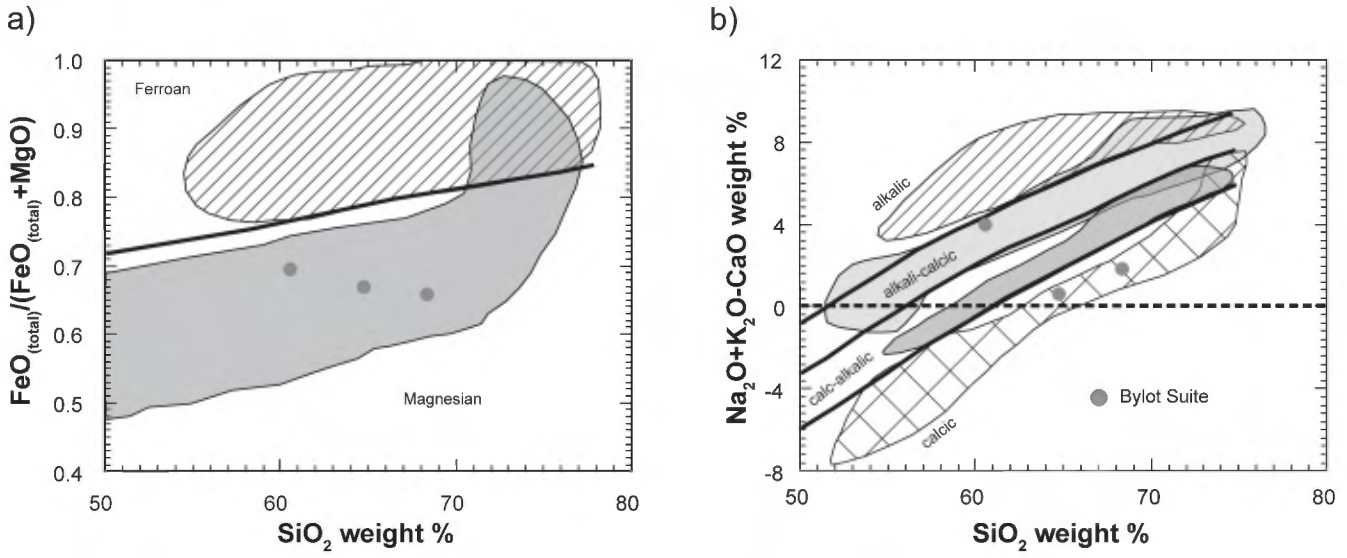

FIGURE 4.7 – TTG series, Bylot Suite: **a**) classification diagram by Frost *et al.* (2001), $FeO_{(total)}/(FeO_{(total)}+MgO)$ vs SiO_2 (weight %); **b**) classification diagram by Frost *et al.* (2001), Na_2O+K_2O-CaO vs SiO_2 (weight %).

Tramont and Morrice suites

The Tramont and Morrice suites are composed of leucocratic, massive and homogeneous biotite-chlorite monzogranites which contain very little mafic minerals (generally about 1%). The monzogranites in these suites are felsic (SiO_2 = 70 to 81 wt%) and weakly hyperaluminous (A/CNK = 0.8 to 1.2). These rocks, much like the plutonic rocks of the Desbergères Suite, plot in the magnesian field and in the calc-alkalic to alkali-calcic fields (Figure 4.8c and d). As silica concentrations increase, $Fe_2O_{3(total)}$, Al_2O_3, CaO, MgO, TiO_2, Zr, Sc, Sr, and Ba decrease (Figure 4.8h), whereas K_2O, Rb, Cs, as well as Rb/Sr ratios increase (Figure 4.8f). However, Zr, Y, LREE, and K/Rb, Zr/Y, and $[La/Yb]_{CN}$ ratios do not vary in accordance with silica concentrations.

Chondrite-normalized rare earth profiles reveal significant REE fractionation ($[La/Yb]_{CN}$ = 20 to 187) and no negative Eu anomalies (not shown). High values for Sr/Y ($\bar{X}$ = 57) and Zr/Y ($\bar{X}$ = 24) ratios are comparable to those observed in Cenozoic adakites and Archean TTG. They also exhibit geochemical signatures midway between strongly fractionated S-type monzogranites and granites derived from the melting of continental crust at great depth (35 to 40 km). By comparing these data with geochemical data from monzogranites of the Preissac-Lacorne Plutonic Complex (Abitibi Subprovince) and granites derived from crustal melting in the Ireteba Pluton (Eldorado Mountains, Nevada), we can conclude that the petrogenetic processes that led to the formation of rocks of the Tramont and Morrice suites are probably the result of a combination of different several geological settings.

Comparison of granodiorite-granite-monzogranite (GGM) units

Given their very similar K_2O, La, Th, Ba, U, Zr, and Nb concentrations, similar Zr/Y and $[La/Yb]_{CN}$ ratios (Figure 4.8e) and their hyperaluminous nature, monzogranites of the Tramont and Morrice suites have geochemical signatures comparable to those of the Desbergères Suite. However, nearly half the samples from the late Tramont and Morrice suites contain between 74 and 80 wt% SiO_2 and are markedly more siliceous than older rocks of the Desbergères Suite (Figure 4.8f).

The geochemical signature of the La Chevrotière, Pinguq, and Dufreboy suites (2740 to 2705 Ma), as well as the Maurel and Belloy suites (2705 to 2680 Ma; Figure 4.9) is comparable to that of the Desbergères, Tramont, and Morrice suites described above. Consequently, it is not possible, given the current level of knowledge, to chemically distinguish granodiorite–granite–monzogranite (GGM) suites that were emplaced between 2740 and 2705 Ma from those emplaced between 2705 and 2680 Ma (Figure 3.2).

Pyroxene-bearing granitoid series

Like the TTG and GGM series, rocks of the pyroxene-bearing granitoid series cover an extensive surface area within the NESP (Figure 3.8). This series, which was mainly emplaced in the time span from 2740 to 2705 Ma (Figure 3.2), is dominated by enderbitic rocks (orthopyroxene-bearing tonalite). It also contains charnockite (orthopyroxene-bearing granite), opdalite (orthopyroxene-bearing granodiorite), orthopyroxene-bearing diorite, and gabbronorite. The Lepelle and Loups Marins suites contrast with other pyroxene-bearing granitoid units due to the presence of

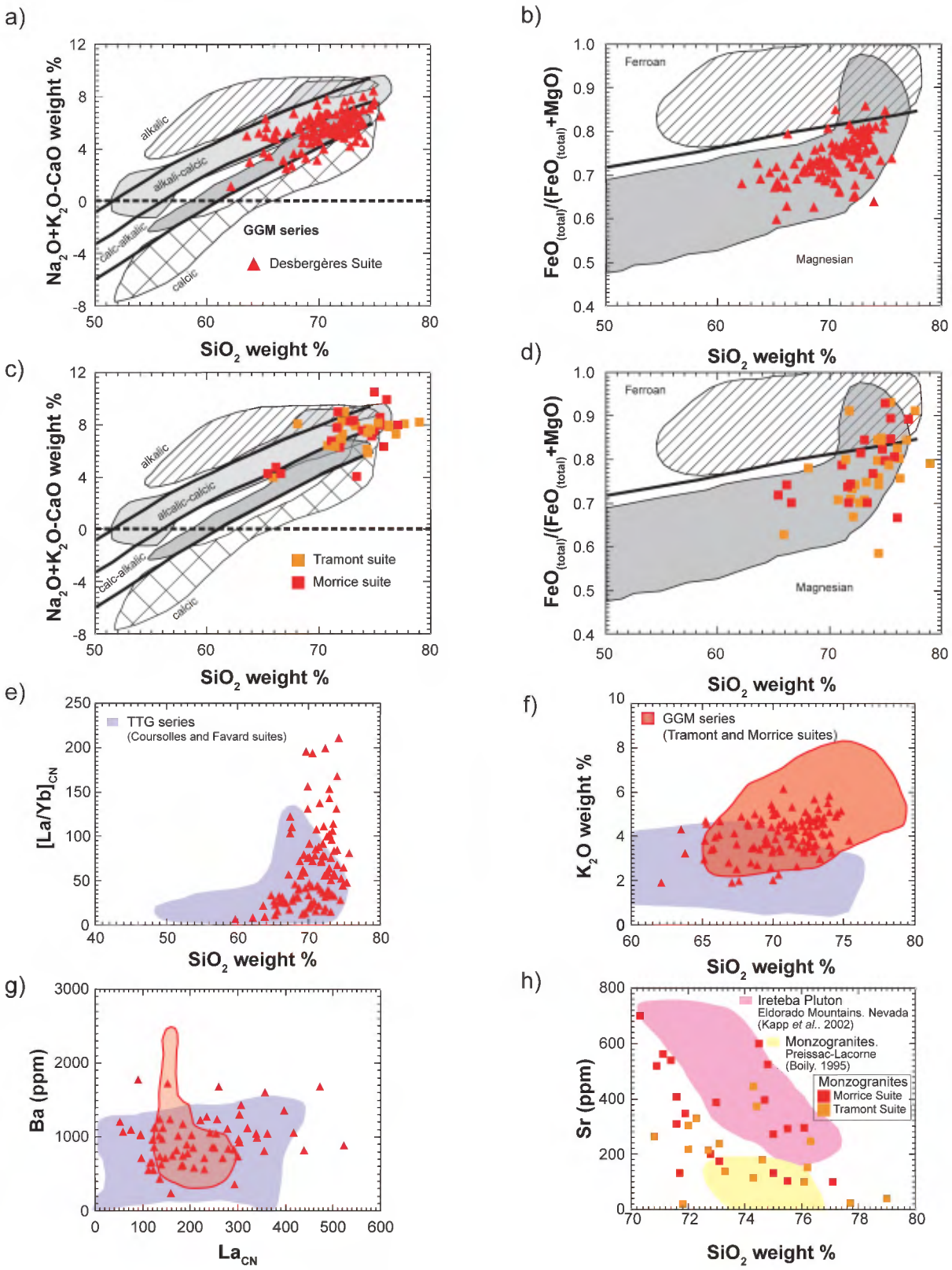

FIGURE 4.8 – GGM series, Desbergères, Morrice, and Tramont suites: **a**) classification diagram by Frost *et al.* (2001), Na_2O+K_2O-CaO (weight %) vs SiO_2 (weight %); **b**) classification diagram by Frost *et al.* (2001), $FeO_{(total)}/(FeO_{(total)}+MgO)$ vs SiO_2 (weight %); **c**) classification diagram by Frost *et al.* (2001), Na_2O+K_2O-CaO (weight %) vs SiO_2 (weight %); **d**) classification diagram by Frost *et al.* (2001), $FeO_{(total)}/(FeO_{(total)}+MgO)$ vs SiO_2 (weight %); **e**) [La/Yb]CN vs SiO_2 (weight %), illustrating significant variations in [La/Yb]CN ratios in felsic members of the Desbergères Suite, similar to the signature of plutons from the TTG series; **f**) K_2O (weight %) vs SiO_2 (weight %) illustrating the potassic nature of the Desbergères Suite and the siliceous composition of the Tramont and Morrice suites; **g**) Ba (ppm) vs LaCN; **h**) Sr (ppm) vs SiO_2 (weight %) showing compositional variations in the Morrice and Tramont suites. Fields for the Ireteba Pluton and Preissac-Lacorne monzogranites are shown for comparative purposes.

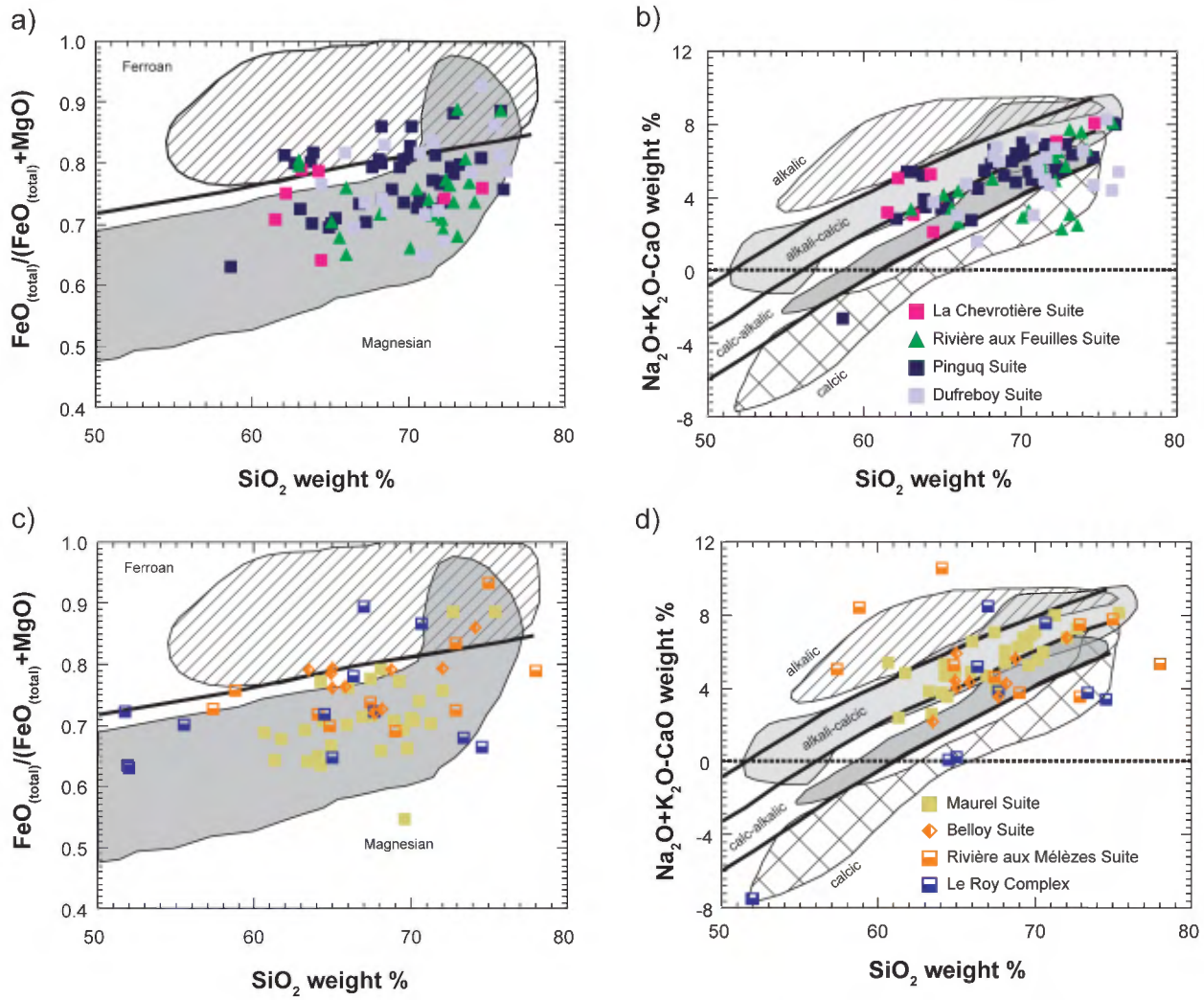

FIGURE 4.9 – GGM series, La Chevrotière, Pinguq, Dufreboy, Maurel, and Belloy suites: **a**) and **c**) classification diagram by Frost *et al.* (2001), $FeO_{(total)}/(FeO_{(total)}+MgO)$ vs SiO_2 (weight %); **b**) and **d**) classification diagram by Frost *et al.* (2001), Na_2O+K_2O-CaO (weight %) vs SiO_2 (weight %).

clinopyroxene-bearing units in which orthopyroxene is absent. The Lepelle Suite mainly consists of clinopyroxene-bearing granodiorite, whereas the Loups Marins Suite comprises two major sub-units: an early (2735 to 2720 Ma) unit of orthopyroxene-bearing rocks, mainly composed of enderbite and hypersthene diorite, and a younger (2715 to 2705 Ma) unit of clinopyroxene-bearing rocks, mainly composed of tonalite and diorite. A detailed geochemistry study was conducted on rocks of the Loups Marins Suite in order to compare its signature with that of other pyroxene-bearing units in the NESP (Boily *et al.*, 2004).

Plutonic rocks of the Loups Marins Suite have a magnesian composition (Figure 4.10a) and a calcic to calc-alkalic affinity (Figure 4.10b). Less evolved members (quartz diorites) have identical SiO_2 (48 to 60 wt%), MgO (2 to 8 wt%), and CaO (4 to 10 wt%) contents, as well as Rb/Sr (0.01 to 0.4) and Zr/Y (1 to 15) ratios, regardless of the type of pyroxene they contain, whether clino- or orthopyroxene. Compared to more felsic members, quartz diorites have higher REE concentrations and show moderate LREE/HREE fractionation ($[La/Yb]_{CN}$ = 12 to 34; Figure 4.10e). These rocks also show progressively increasing Na_2O/K_2O ratios from intermediate to felsic compositions. Enderbites and clinopyroxene-bearing tonalites show comparable decreasing concentrations in CaO, Al_2O_3, $Fe_2O_{3(total)}$, MgO, TiO_2, HREE, and Y, as well as Zr/Y (2 to 46), Sr/Y (8 to 144), and $[La/Yb]_{CN}$ (12 to 49) ratios with increasing silica. Low HREE concentrations in enderbites and clinopyroxene-bearing tonalites result in rapidly increasing $[La/Yb]_{CN}$ ratios for samples with SiO_2 > 70 wt% (Figure 4.10d). The geochemical characteristics described here are similar to those observed for rocks of the TTG series described above. Moreover, intermediate to felsic pyroxene-bearing granitoid rocks of the Loups Marins Suite, as well as diorites and tonalites of the Coursolles and Favard suites, have similar compositions in terms of their normative mineralogy (Figure 4.10c).

Clinopyroxene-bearing monzonites, monzodiorites, granodiorites, and granites commonly display a porphyroid tex-

ture. These rocks contrast with enderbites and clinopyroxene-bearing tonalites due to their potassic character (Na_2O/K_2O = 1.0 to 0.6) and generally higher concentrations in Rb, Sr, and Ba (Figure 4.10f). Clinopyroxene-bearing monzodiorites, quartz monzonites, and syenites have intermediate compositions (SiO_2 = 58 to 65 wt%) and are also enriched in K_2O (3.6 to 8.4 wt%), $Fe_2O_{3(total)}$ (3.4 to 4.6 wt%), and Ba (977 to 3700 ppm). They are however depleted in MgO (1.2 to 1.8 wt%) relative to melanocratic quartz monzodiorites and granodiorites, which exhibit comparable silica concentrations. On a multi-element diagram, the clinopyroxene-bearing monzodiorites, quartz monzonites, and syenites are enriched in LREE, Ba, Th, and U and show negative Nb-Ta anomalies (not shown). HREE and Y concentrations are also depleted, a typical feature in Archean granitoid rocks. Relative to diorites and quartz diorites in TTG suites, these intermediate rocks have higher K_2O and Ba concentrations and higher Rb/Sr and $[La/Yb]_{CN}$ ratios.

The Lepelle Suite is a magnesian, calc-alkalic unit (Figure 4.11a and b) with an intermediate to felsic composition (SiO_2 = 62 to 73 wt%). It is enriched in Ba (200 to 1356 ppm), LREE (La = 29 to 48) and Th (0.5 to 16 ppm) and shows moderate to high Zr/Y (11 to 55) and $[La/Yb]_{CN}$ ratios that increase dramatically in the most felsic members (>70 wt% SiO_2; not shown). Enderbites and intermediate rocks of the Lac Minto Suite exhibit chemical characteristics similar to those of the Loups Marins Suite and typical of TTG series in general, whereas rocks of the MacMahon Suite are more enriched in iron and are alkali-calcic to alkalic (Figure 4.11a and b). The MacMahon Suite also contains gabbroic units, which are generally absent from typical TTG series. Some of these gabbros are magnesian (MgO = 13 to 19 wt%) and have Al_2O_3 < 10 wt%, as well as low concentrations in Ba (50 to 230 ppm), Sr (46 to 259 ppm), La (3.5 to 8.8 ppm) and weakly fractionated REE profiles ($[La/Yb]_{CN}$ = 3 to 7). Other gabbros with Al_2O_3 contents greater than 10 wt% are more enriched in LILE (Ba = 250 to 801 ppm) and exhibit higher $[La/Yb]_{CN}$ ratios (12 to 14).

Pyroxene-bearing rocks of the Troie and Qimussinguat complexes are, like rocks of the Loups Marins Suite, equivalent to rocks of the TTG series, with magnesian, and calcic to calc-alkalic compositions (Figure 4.11c and d). They are generally felsic, rarely intermediate in composition (55 to 65 wt%), in contrast with rocks of the Loups Marins and MacMahon suites. The Troie Complex contains tonalitic (SiO_2 = 59 to 73 wt%) or gabbroic rocks (SiO_2 = 43 to 54 wt%). Some of these gabbroic rocks have compositions similar to Mg-tholeiites (Zr/Y = 1 to 4, $[La/Yb]_{CN}$ = 1 to 2) and occur in the form of enclaves hosted in tonalites and enderbites. They may be genetically related to volcanic rocks of the Arnaud Complex. Other magnesian (MgO = 4 to 15 wt%) gabbros, enriched in LILE (Ba = 265 to 724 ppm) and LREE ($[La/Yb]_{CN}$ = 8 to 24), are similar to rocks assigned to the Qullinaaraaluk or Châteauguay suites, described in the following section. Finally, enderbites in the Troie and Qimussinguat complexes exhibit chemical characteristics similar to those of the Loups Marins Suite and the TTG series.

Summary of felsic to intermediate intrusive rock geochemistry

Felsic intrusive rocks in the tonalite-trondhjemite-granodiorite (TTG) and granodiorite-granite-monzogranite (GGM) series form more than 90% by volume of the Archean crust in the NESP. Apart from the Na-rich character of the TTG series versus the K-rich nature of the GGM series, the two series show very similar compositions and chemical evolutions. For example, increasing $[La/Yb]_{CN}$ ratios with increasing silica content is a phenomenon observed in both series (Figure 4.8e). In fact, the GGM series appears to constitute a potassic equivalent to the TTG series, albeit enriched in lithophile elements (K_2O, Ba, La, Rb, Th, and U) and slightly more siliceous.

Rocks of the pyroxene-bearing granitoid series exhibit chemical characteristics similar to those of TTG rocks. The former are equivalent to TTG rocks but are derived from anhydrous magmas that were emplaced in high-temperature conditions. The age of emplacement of pyroxene-bearing granitoid rocks is generally younger (<2740 Ma) than the age of emplacement of TTG. Mafic or intermediate intrusions (gabbro, diorite, quartz diorite with orthopyroxene and clinopyroxene) are present in most pyroxene-bearing granitoid units. This is a major distinction between pyroxene-bearing granitoid units and tonalitic (TTG) units. Only two lithodemic units, the Coursolles and Favard suites, contain a significant proportion of mafic to intermediate rocks. We suggest that TTGs represent variably hydrated precursors of pyroxene-bearing granitoids assigned to the Loups Marins Suite. In the NESP, the geochemical composition of felsic to intermediate intrusive rocks is not a discriminating element. It cannot be used to characterize units composed of these rock types based on their regional distribution or their age.

Ultramafic to intermediate intrusive rocks

Several small ultramafic to intermediate intrusions were grouped into four lithodemic units: the Châteauguay and Bacqueville suites (Figure 3.6), the age of which is estimated between 2740 and 2705 Ma, and the Couture and Qullinaaraaluk suites (Figure 3.9), where the crystallization age is estimated between 2720 and 2705 Ma. Representative analyses of ultramafic to mafic plutonic rocks are shown in Table 4.3. It is not always an easy task to assign these intrusions to the proper lithodemic unit; certain intrusions probably correspond to early intrusive phases of the TTG series.

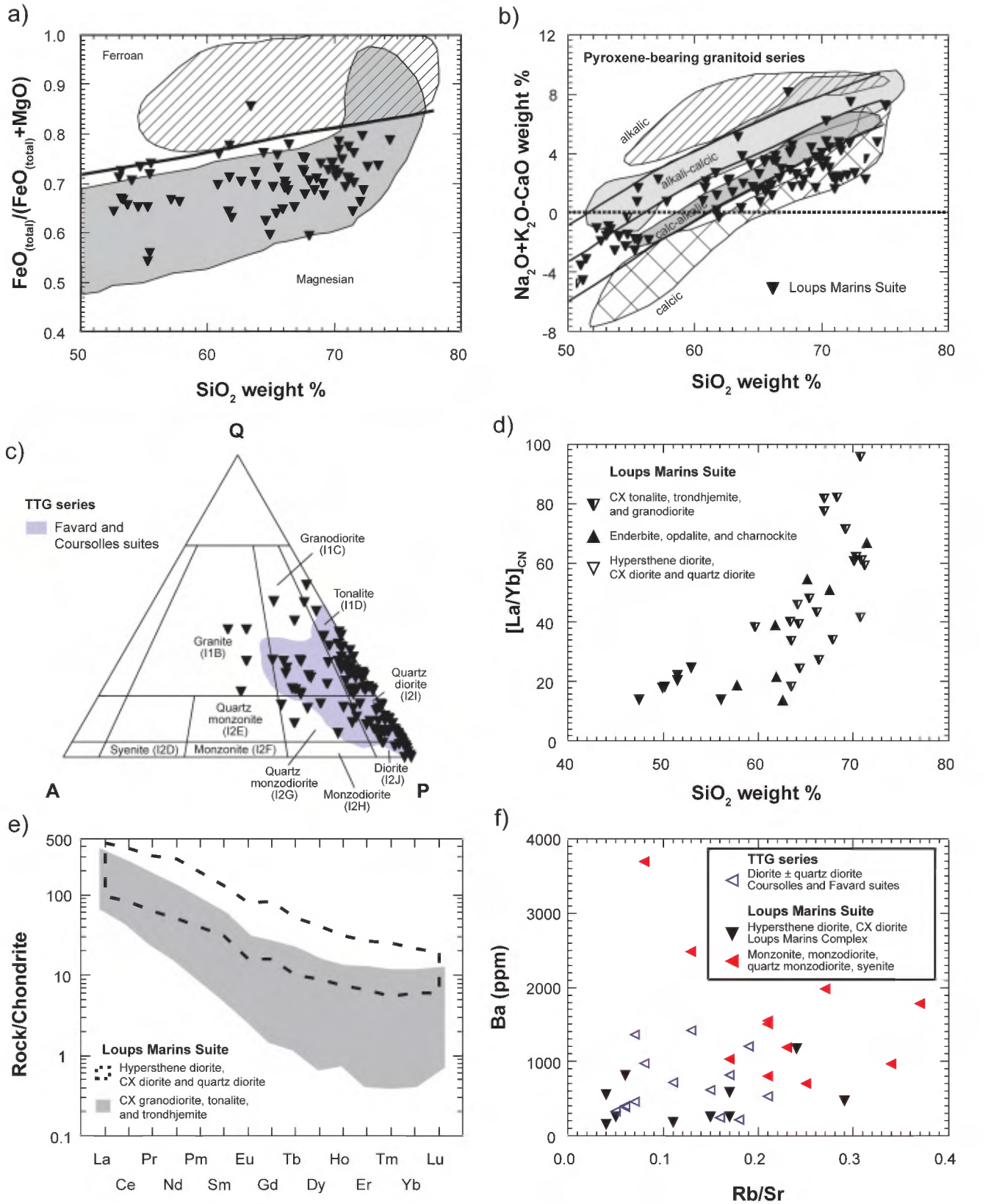

FIGURE 4.10 – Pyroxene-bearing granitoid series, Loups Marins Suite: **a**) classification diagram by Frost *et al.* (2001), $FeO_{(total)}/(FeO_{(total)}+MgO)$ vs SiO_2 (weight %); **b**) classification diagram by Frost *et al.* (2001), Na_2O+K_2O-CaO (weight %) vs SiO_2 (weight %); **c**) QAP diagram by Streckeisen, where rocks of the Loups Marins Suite plot in the field of diorites, quartz diorites, tonalites, and granodiorites, similar to rocks of the Favard and Coursolles suites; **d**) [La/Yb]CN vs SiO_2 (weight %) showing significant variations in [La/Yb]CN ratios for felsic members of the Loups Marins Suite, variations similar to those of plutons in the TTG series; **e**) chondrite-normalized REE patterns, showing REE depletion, particularly HREE, in opdalites, enderbites, charnockites, and CX-bearing tonalites and trondhjemites relative to diorites; **f**) Ba (ppm) vs Rb/Sr, showing the enriched signature of monzonites, quartz monzodiorites, and syenites of the Loups Marins Suite.

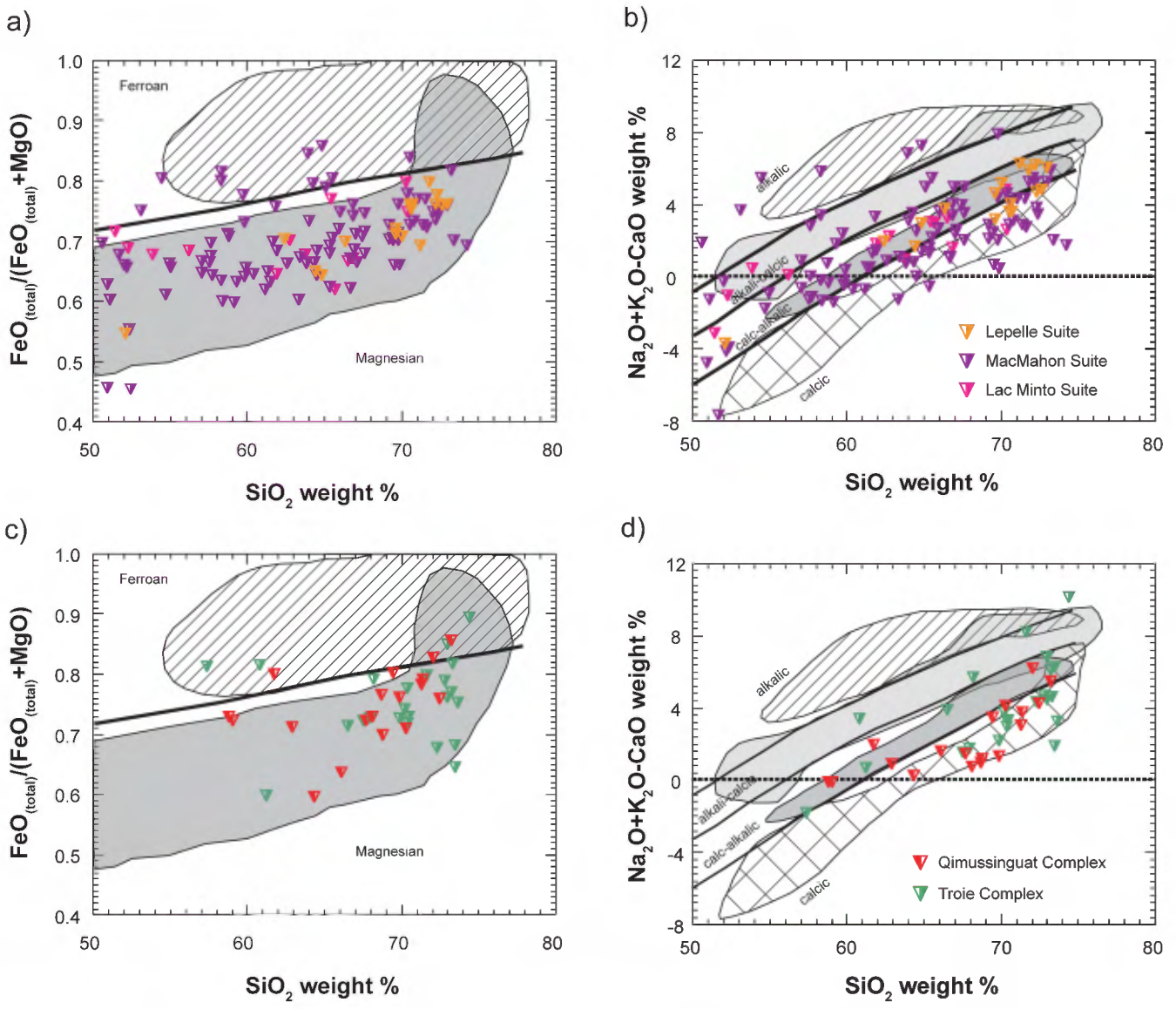

FIGURE 4.11 – Pyroxene-bearing granitoid series, Lepelle, MacMahon, and Lac Minto suites and Troie and Qimussinguat complexes: **a**) and **c**) classification diagram by Frost *et al.* (2001), $FeO_{(total)}/(FeO_{(total)}+MgO)$ vs SiO_2 (weight %); **b**) and **d**) classification diagram by Frost *et al.* (2001), Na_2O+K_2O-CaO (weight %) vs SiO_2 (weight %).

Châteauguay and Bacqueville suites

The Châteauguay and Bacqueville suites comprise diorites, gabbros, and gabbronorites. However, data from diorite samples are insufficient to be discussed in this report. The gabbros and gabbronorites, massive and devoid of cumulate textures, are metaluminous and have a tholeiitic affinity. These rocks display SiO_2 (44 to 53 wt%), MgO (5 to 14 wt%), $Fe_2O_{3(total)}$ (8 to 17 wt%), TiO_2 (0.5 to 1.5 wt%), and CaO (8 to 11 wt%) concentrations comparable to those observed in tholeiitic volcanic rocks occurring in volcano-sedimentary belts in the NESP. However, gabbros and gabbronorites have higher Zr/Y (3 to 8) and $[La/Yb]_{CN}$ (4 to 11) ratios than tholeiites, are also enriched in Ba, Th, U, and LREE, and show negative anomalies in certain HFSE (Nb-Ta and Zr) accompanied by depleted HREE and Y values (Figure 4.12f). These gabbros show a positive correlation between Zr, $Fe_2O_{3(total)}$ and Sr relative to TiO_2 (not shown), and a negative correlation with Mg# (Figure 4.12e). Also, their Mg# (43 to 75) are lower than mantle values (Mg# = 80 to 85), which suggests the parent magmas evolved through crystal fractionation. Several gabbros and gabbronorites with high TiO_2, Sr, and $FeO_{(total)}$ contain green hornblende and biotite, whereas in the remaining samples, clinopyroxene and orthopyroxene are the dominant mafic minerals.

Qullinaaraaluk Suite

The Qullinaaraaluk Suite is metaluminous and tholeiitic. It encompasses a first group of ultramafic rocks (pyroxenites, peridotites, hornblendites) and a second group of mafic rocks (gabbros and gabbronorites). The gabbros and gabbronorites show MgO (5 to 15 wt%), TiO_2 (0.4 to 3.8 wt%), Na_2O+K_2O (2.2 to 5.7 wt%) and $Fe_2O_{3(total)}$ (9 to 17 wt%) contents similar to those observed in Mg-tholeiites in volcano-sedimentary belts (Boily *et al.*, 2006a). They are different however due to their LREE enrichment ($[La/Yb]_{CN}$ = 7 to 17) and high values in Ba (212 to 745 ppm), Th (0.7 to 2.4 ppm), and Sr (224 to 1424 ppm) relative to HFSE (Figure 4.12f). Gabbros and gabbronorites of the Qullinaaraaluk Suite have moderate Zr/Y ratios (2 to 7) comparable to those of rocks in the Châteauguay and Bacqueville suites. Also, they show only a few weakly positive Eu anomalies and exhibit REE profiles comparable to gabbros of the Bacqueville and Châteauguay suites (Figure 4.12d).

Although ultramafic rocks of the Qullinaaraaluk Suite have higher MgO contents and lower Na_2O+K_2O, $Fe_2O_{3(total)}$, REE, Ba, Sr, and TiO_2 concentrations relative to gabbros and gabbronorites, they exhibit certain similarities in terms of their HFSE concentrations (Zr, Hf, Ta, Nb). Based on REE profiles (Figure 4.12b and c), it is possible to distinguish two types of ultramafic rocks. The first type corresponds to ultramafic rocks (MgO = 9 to 21 wt%) with REE profiles similar to those of gabbros and gabbronorites ($[La/Yb]_{CN}$ = 8 to 9), *i.e.* linear profiles with no Eu anomaly (Figure 4.12c). The second type includes Mg-rich hornblendites and pyroxenites (MgO = 6 to 24 wt%) with similar REE fractionation profiles, but with moderate to strongly negative Eu anomalies (Figure 4.12b). This second type of ultramafic rock has a signature similar to that observed in ultramafic intrusions with Ni, Cu, Co, and PGE mineralization (Parent *et al.*, 2003b; Simard *et al.*, 2005a; Chevé, 2005; Figure 4.12a).

Couture Suite

The Couture Suite is a unit composed of anorthosite, gabbro, and leucogabbro; diorite, quartz diorite, and orthopyroxene-bearing diorite; as well as ultramafic rocks, mainly pyroxenite with minor websterite and hornblendite. Anorthosites are rare and are associated with minor gabbro and gabbronorite. They have high Al_2O_3 contents (14 to 30 wt%), with Mg# ranging from 51 to 67. These rocks have low Ni (8 to 85 ppm), Cr (51 to 67 ppm), and TiO_2 (0.1 to 0.9 wt%) contents. Diorites display moderate Mg# (47 to 52) and Zr/Y ratios (2 to 3) close to those of mantle-derived rocks. These diorites also have low Zr (43 to 66 ppm) and Ba (50 to 150 ppm) concentrations.

Data on ultramafic rocks are more abundant. These rocks show Mg# values ranging from 48 to 93, are enriched in Cr (30 to 2500 ppm) but relatively depleted in Ni (15 to 200 ppm). TiO_2 concentrations are relatively low (0.2 to 0.9 wt%) and generally decrease with increasing Mg#, much like Sr, Ba, Zr, Th, La, and Al_2O_3 (Figure 4.12e). These rocks are also enriched in LREE ($[La/Yb]_{CN}$ = 4 to 14) and show REE profiles with no Eu anomalies (Figure 4.12d).

Summary of ultramafic to intermediate intrusive rock geochemistry

REE profiles, multi-element diagrams, and major and trace element variations indicate that all ultramafic to intermediate intrusive suites exhibit similar compositions. These suites mainly consist of gabbroic rocks accompanied by tholeiitic pyroxenite and hornblendite, characterized by LREE and LILE enrichment as well as negative Nb-Ta anomalies.

Migmatitic rocks

Migmatitic rocks in the Minto Subprovince consist of diatexites that formed as a result of the melting of extensive sedimentary basins between 2705 and 2670 Ma. These diatexites were assigned to three units: the Le Roy Complex, the Rivière aux Mélèzes Suite, and the Sanigitik Suite (Figure 3.10).

The Rivière aux Mélèzes Suite is hyperaluminous (A/CNK = 1.0 to 1.6), magnesian, and largely calc-alkalic (Figure 4.9c and d). Important variations in SiO_2 contents (57 to 78 wt%) and Zr/Y ratios (3 to 50) are observed, as well as high concentrations for K_2O (1.3 to 8.4 wt%) and Ba (220 to 3700 ppm). Rocks of the Le Roy Complex are also hyperaluminous (A/CNK = 1.0 to 1.2) and enriched in potassium (0.8 to 7.3 wt% K_2O), with Ba concentrations (50 to 3200 ppm) and major variations in Zr/Y ratios (1 to 119) similar to rocks of the Rivière aux Mélèzes Suite. Overall, diatexites from the two suites show similar geochemical characteristics, which are distinctive however from those of granitoid rocks assigned to the GGM and TTG series, the former being hyperaluminous while the latter are mainly metaluminous.

Nepheline syenites

Nepheline syenites form small intrusions grouped into three lithodemic units. The oldest syenites (2761 Ma) are assigned to the Kimber Suite (Figure 3.5), whereas the Tasiat (2643 Ma) and Bourdel (2675 Ma) syenites are much younger (Figure 3.11).

Rocks of the Kimber Suite are silica-poor (SiO_2 = 52 to 54 wt%), with low MgO (0.2 to 0.9 wt%) and $FeO_{(total)}$ (3.2 to 4.4 wt%) concentrations but high values for alkalis (Na_2O+K_2O = 14 wt%; Figure 4.13a), Ba (400 to 920 ppm), and Sr (767 to 924 ppm), and Zr/Y ratios ranging between 2 and 7. The Tasiat Syenite is also enriched in alkalis (Na_2O+K_2O = 13 wt%; Figure 4.13a), Zr (504 ppm), and Nb (35 ppm), but relatively depleted in La (2 ppm) and Ba (255 ppm). It also shows weakly fractionated REE profiles ($[La/Yb]_{CN}$ = 4; Figure 4.14b), despite its high Zr/Y ratios

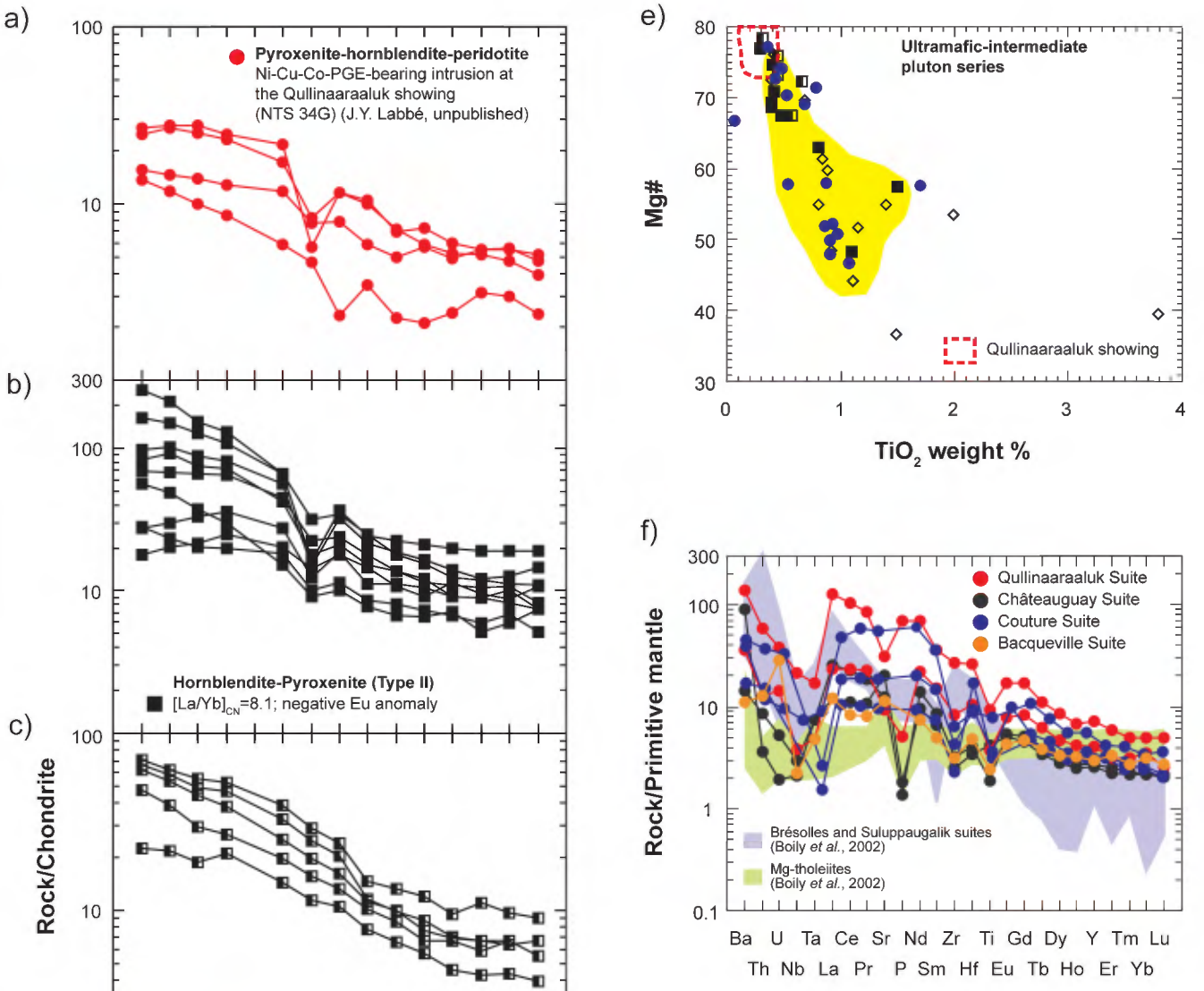

FIGURE 4.12 – Ultramafic to intermediate pluton series, Qullinaaraaluk, Châteauguay, Bacqueville, and Couture suites. Chondrite-normalized REE patterns: **a**) pyroxenite-hornblendite-peridotite, Qullinaaraaluk showing; **b**) Type II hornblendite-pyroxenite; **c**) Type I hornblendite-pyroxenite; **d**) gabbro-gabbronorite; **e**) Mg# vs TiO_2 (weight %) illustrating decreasing TiO_2 content with increasing Mg#, the latter indicating the degree of fractionation in ultramafic to intermediate rocks; **f**) primitive mantle-normalized multi-element diagram, showing enrichment in Ba, Th, U, and LREE, and negative Nb-Ta and P anomalies for certain samples of the Qullinaaraaluk, Châteauguay, and Couture suites. Profiles from the Brésolles and Suluppaugalik suites (TTG series) and Mg-tholeiites are shown for comparative purposes.

(280). The Bourdel nepheline syenite is also enriched in alkalis (Na_2O+K_2O = 14 wt%; Figure 4.13a), but is strongly enriched in Ba (2424 ppm), Sr (2632 ppm), La (38.1 ppm), and depleted in Zr (11 ppm), such that its $[La/Yb]_{CN}$ ratio is high (44; Figure 4.13b) and its Zr/Y ratio is low (2).

NEODYMIUM ISOTOPIC COMPOSITION OF ARCHEAN VOLCANIC AND PLUTONIC UNITS

Neodymium (Nd) isotope studies in Precambrian shields can be used to determine the extent and age of early continental nuclei and their degree of interaction with younger magmatic rocks (Tomlinson *et al.*, 2004). Following the first neodymium isotope studies conducted in the NESP (Stern *et al.*, 1994; Skulski *et al.*, 1996; Skulski and Percival, 1996; Skulski *et al.*, 1998), projects were launched in parallel with MRNF mapping surveys to help unravel the genesis and evolution of the continental crust in this part of the craton (Rabeau, 2003; Boily *et al.*, 2004, 2006a and 2006b; Stevenson *et al.*, 2006). A compilation of more than 330 analytical results (Maurice, 2007) was used to better constrain the evolution of volcanic assemblages and plutonic suites through time. The reader is referred to the work of Boily *et al.* (2004, 2006a, 2006b, 2009) for a detailed discussion of results, based on the various geochemical series and stratigraphic suites in the NESP.

Hudson Bay and Rivière Arnaud terranes

To illustrate the isotopic characteristics of major geological assemblages, we used the geographic distribution of model ages (T_{DM}) and $\varepsilon Nd_{(t)}$ values (Figure 4.14). Since most of the isotopic analyses are from rocks with ages of emplacement between 2.90 and 2.68 Ga, this method is useful to identify and delineate paleocratons.

Based on the data distribution, we were able to identify vast segments of reworked cratonic nuclei in the west and south parts of the NESP (Figure 4.14). These cratonic nuclei constitute a basement that formed during the Eoarchean and Mesoarchean (3.9 to 2.9 Ga) and delineate the extent of the Hudson Bay Terrane. This terrane includes the Bienville (3.2 to 2.9 Ga), Tikkerutuk (3.9 to 2.9 Ga), and Goudalie domains, as well as the northeast part of the La Grande Subprovince (2.8 to 3.3 Ga). It is bordered to the east by a former sedimentary basin now represented by diatexites and paragneiss remnants assigned to the Lac Minto Domain (Figure 4.14). This boundary coincides with a network of faults and deformation zones trending NNW-SSE. The northeast part of the NESP is formed of the Lac Minto, Utsalik, Qalluviartuuq, and Douglas Harbour domains, which make up the Rivière Arnaud Terrane, where only a few samples reveal the involvement of pre-3.0 Ga crust (Figure 4.14). The south part of the Douglas Harbour Domain does however contain several Mesoarchean model ages (2.9 to 3.0 Ga) and this region may in fact belong to the Hudson Bay Terrane.

In addition to Nd isotope data, geological characteristics, crystallization ages and inherited zircon ages (Figure 3.3) can be used to distinguish the Hudson Bay Terrane from the Rivière Arnaud Terrane. All of these put together suggest the two terranes experienced distinct tectonomagmatic evolutions up until 2740 Ma (figures 3.1, 3.4, and 3.5; Chapter 5).

Felsic and intermediate rocks

On the diagram in Figure 4.15a, isotopic compositions for plutonic and volcanic felsic and intermediate rocks (SiO_2 >

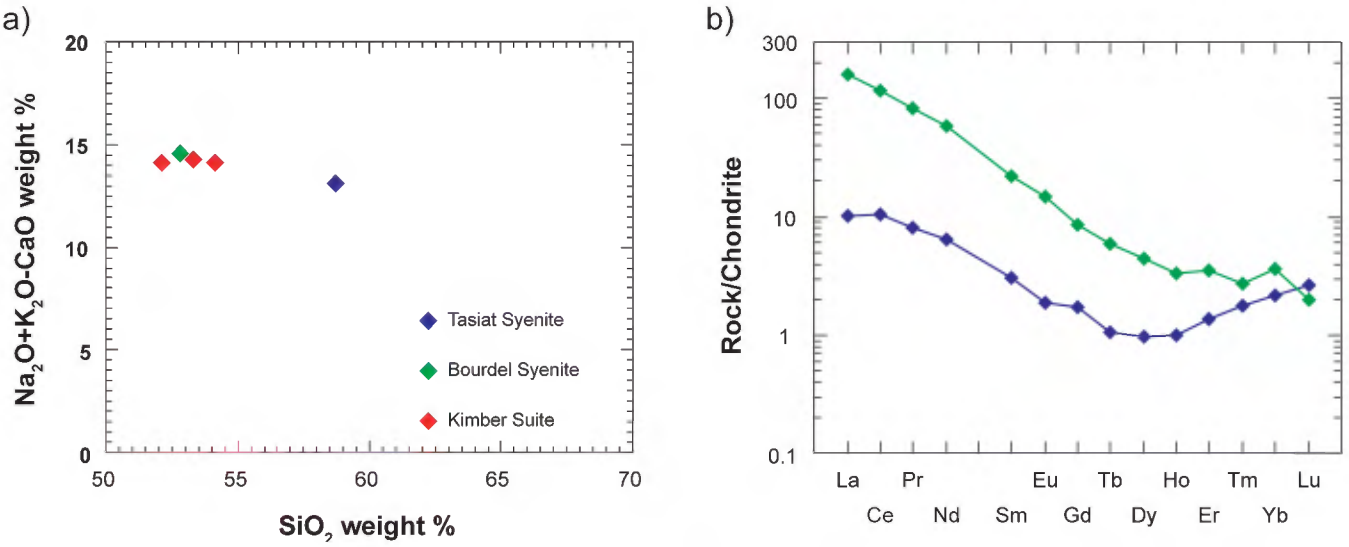

FIGURE 4.13 – **a)** Na_2O+K_2O-CaO (weight %) vs SiO_2 (weight %), illustrating the alkali-rich nature of rocks from the Bourdel and Tasiat syenites and the Kimber Suite; **b)** chondrite-normalized REE patterns.

55 %) outline the importance of recycled early continental crust in the formation of younger magmas. Rocks in the Hudson Bay Terrane (Figure 4.14) are isotopically enriched and show evidence of integration of earlier crust, going as far back as 3.8 Ga. Data acquired in the Rivière Arnaud Terrane on the other hand indicate recycling of crust younger than 3.0 Ga (Figure 4.15a).

Mafic and ultramafic rocks

Figure 4.15b shows that mafic and ultramafic rocks (SiO_2 < 55%) older than 2.74 Ga are distributed along the compositional spectrum calculated for the evolution of a mantle reservoir with a long history of light rare earth element depletion ($X_{\varepsilon Nd}$ = 2.5 ± 0.3, n = 32 for the Rivière Arnaud Terrane and $X_{\varepsilon Nd}$ 1.9 ± 0.8, n = 20 for the Hudson Bay Terrane). In contrast, mafic and ultramafic rocks younger than 2750 Ma show enriched isotopic compositions ($X_{\varepsilon Nd}$ = 0.8 ± 0.3, n = 31 for the Rivière Arnaud Terrane and $X_{\varepsilon Nd}$ = -0.3 ± 0.7, n = 31 for the Hudson Bay Terrane). This compositional shift corresponds to the emergence, from 2.74 Ga onward, of large volumes of potassic (granite and granodiorite) and charnockitic (enderbite, opdalite, charnockite; Chapter 3) magmas. To explain such a major change in the composition of mafic magmas, it is necessary to invoke geological settings that differ through time. Mantle-derived magmas emplaced after 2.74 Ga were injected into a hot, ductile and partially melted continental crust, heated by nearly continuous felsic plutonic magmatism. Crustal assimilation of host rocks by primitive magmas was facilitated by the low temperature contrast and the presence of partial melt products, such that the younger mafic and ultramafic magmas assimilated a greater proportion of the crust into which they were emplaced. From 2.74 Ga onward, the crustal thermal regime was such that the emplacement of mantle-derived magmas with a composition similar to the depleted mantle was no longer possible.

CONCLUSIONS

The NESP comprises less than 10% supracrustal rocks, including volcanic rocks that may be divided into six series based on their chemical composition: 1) komatiites and basaltic komatiites; 2) Mg-tholeiites; 3) Fe-tholeiites; 4) contaminated tholeiites; 5) calc-alkaline basalts, andesites, and dacites; and 6) calc-alkaline rhyodacitic-rhyolitic tuffs and lavas.

The NESP is largely dominated by plutonic rocks which may be divided into four series: 1) TTG (tonalite-trondhjemite-granodiorite); 2) GGM (granodiorite-granite-monzogranite); 3) pyroxene-bearing granitoid rocks; and 4) ultramafic to intermediate plutons.

Volcanic rocks of the komatiite series are mostly chondritic and Al-undepleted. Mg-tholeiites have flat or slightly depleted REE profiles; Zr/Y, Ti/Zr, and Th/Hf ratios close to chondritic values; and moderate or high Mg#. Fe-tholeiites are characterized by enriched TiO_2 and $FeO_{(total)}$, flat or slightly enriched REE profiles and more siliceous compositions. Contaminated tholeiites are evolved, enriched in TiO_2 and are distinguished from the previously described series by their enrichment in LREE and LILE, and their negative Nb-Ta anomalies. The calc-alkaline basalt, andesite, and dacite series is enriched in LREE and LILE and shows negative Nb-Ta anomalies. The calc-alkaline rhyodacitic-rhyolitic tuff and lava series is subdivided into three groups based on Zr/Y andt $[La/Yb]_{CN}$ ratios. Group I has high ratios, Group II moderate ratios, whereas Group III has the lowest ratios. The latter group was recognized only in the Dupire Complex and the Duquet belt (Bourassa, 2002); its chemical signature is comparable to that of so-called "fertile" rhyolites associated with volcanogenic massive sulphide deposits. In the NESP as a whole, it is likely that calc-alkaline volcanic rocks, commonly interlayered with sedimentary sequences, may form a younger cycle of deposition relative to rocks of tholeiitic affinity.

The TTG series actually contains very little granodiorite. Diorites, tonalites, and trondhjemites have high Al_2O_3, Na_2O, and Sr contents, with low to moderate HREE and Y concentrations. Consequently, $[La/Yb]_{CN}$, Sr/Y, and Na_2O/K_2O ratios are high, a typical feature in Archean TTG. However, in the more felsic members of the TTG series, namely leucocratic tonalites and trondhjemites with SiO_2 > 65 wt%, these ratios show significant variations. Rocks of the GGM series are intermediate to felsic in composition (SiO_2 > 60 wt%), with Na_2O/K_2O ratios < 1 that reflect their potassic composition. Also, Zr/Y, Rb/Sr, Sr/Y, and $[La/Yb]_{CN}$ ratios increase with increasing silica, and this trend becomes very steep at higher silica values (>70 wt% SiO_2). The GGM series appears to constitute a potassic, slightly more siliceous equivalent to the TTG series, albeit with slightly higher concentrations in lithophile trace elements (K_2O, Ba, La, Rb, Th, U). The pyroxene-bearing granitoid series is the anhydrous high-temperature equivalent to the TTG and GGM series. Compared with rocks of the TTG series, enderbites and clinopyroxene-bearing tonalites show a similar increase in Na_2O/K_2O ratios from diorites to clinopyroxene-bearing tonalites and enderbites, peaking with leucocratic enderbites and clinopyroxene-bearing trondhjemites. Pyroxene-bearing granitoids also show a comparable increase in Zr/Y, Sr/Y, and $[La/Yb]_{CN}$ ratios. The strongest variations are observed in the most felsic members (>70 wt% SiO_2). Finally, the ultramafic to intermediate intrusive series primarily includes gabbros and gabbronorites as well as tholeiitic pyroxenites and hornblendites. These rocks show enriched LREE and LILE concentrations as well as negative Nb and Ta anomalies which contrast with other tholeiitic series, with the exception of contaminated tholeiites.

The distribution of model ages (T_{DM}) and $\varepsilon Nd_{(t)}$ values compiled for the plutonic and volcanic rocks of the NESP outlines a distinction between the Hudson Bay Terrane and the Rivière Arnaud Terrane. The Hudson Bay Terrane contains fragments of early craton dating back to the Eoarchean

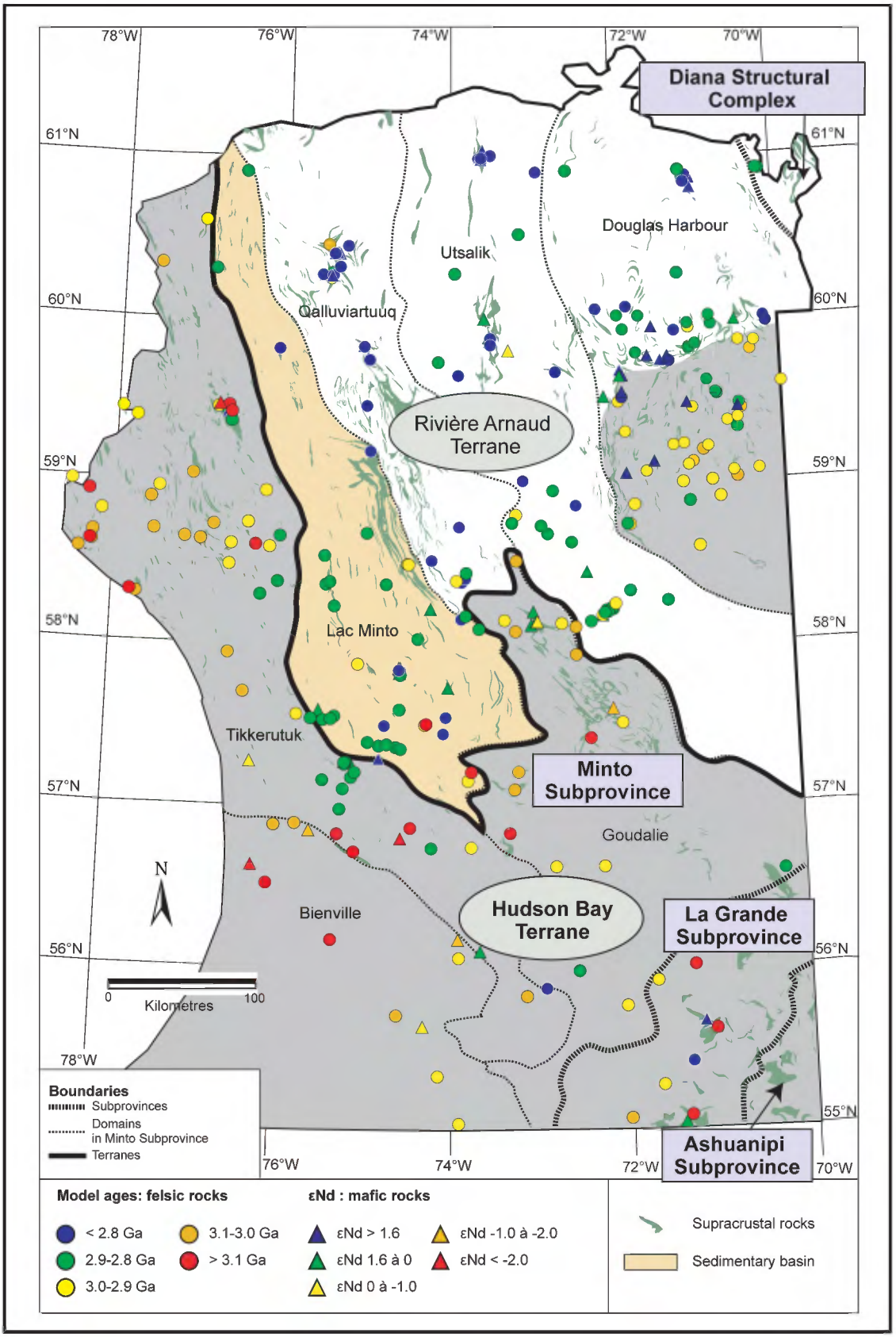

FIGURE 4.14 – Distribution of Nd isotope data in the NESP along with εNd(t) values and mantle extraction model ages (TDM) (after Tomlinson *et al.*, 2004). Different coloured triangles refer to the εNd(t) values (see legend) for mafic to ultramafic rocks or felsic to intermediate rocks with a $^{147}Sm/^{144}Nd$ ratio > 0.14. Different coloured circles refer to model ages (see legend) for felsic to intermediate rocks. Isotopic data come from different laboratories and are compiled in Table 4.4.

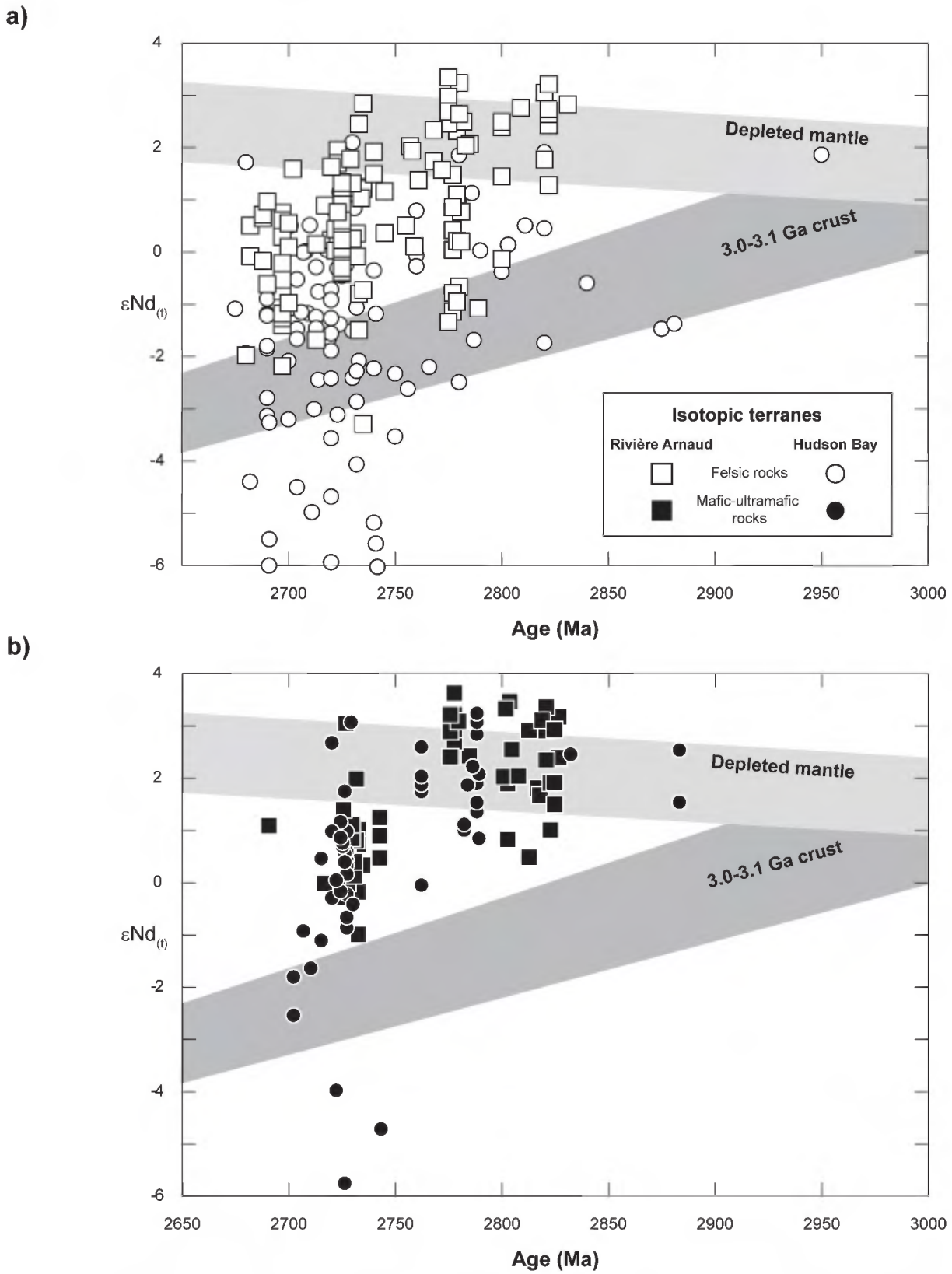

FIGURE 4.15 – εNd(t) vs age of emplacement for: **a**) felsic rocks, and **b**) mafic and ultramafic rocks in the NESP. Samples were subdivided based on their location in the Rivière Arnaud or Hudson Bay terranes. The depleted mantle field was calculated using methods described by DePaolo (1982) and Stern *et al.* (1994). Data derived from compilation by Maurice (2007).

and the Mesoarchean (3.9 to 2.9 Ga). The presence of these fragments in Neoarchean units is indicated by model ages older than 3.0 Ga and by $\varepsilon Nd_{(t)}$ values less than -1. Based on these observations, we can infer that the plutonic and volcanic rocks of the Hudson Bay Terrane are derived from the partial melting of pre-3.0 Ga tonalitic crust, or that they were contaminated by this early crust. The Rivière Arnaud Terrane on the other hand, comprises crust where the earliest tonalitic components are younger than 3.0 Ga. Model ages lower than 3.0 Ga and positive $\varepsilon Nd_{(t)}$ values observed in Neoarchean plutonic and volcanic rocks indicate provenance from a depleted (juvenile) source, or contamination by a tonalitic crust younger than 3.0 Ga with a depleted isotopic composition.

If we exclude the Nd isotope data, it is difficult to characterize the Rivière Arnaud and Hudson Bay terranes solely on the basis of the chemical composition of rocks in the two terranes. Among the most distinctive criteria, one may note that in early Neoarchean suites (2.79 to 2.76 Ga) located within the Rivière Arnaud Terrane, mafic to intermediate rocks are rare. In contrast, the Coursolles and Favard suites, emplaced exclusively in the Hudson Bay Terrane during the Neoarchean (2.76 to 2.74 Ga) contain a significant proportion of mafic to intermediate rocks. Also, the contaminated tholeiite series appears to have been emplaced late in the Neoarchean, after 2.74 Ga. These tholeiites appear to occur exclusively within the Hudson Bay Terrane.

TABLE 4.1 - Synthesis of dominant volcanic series in each stratigraphic unit. KBK: komatiites and basaltic komatiites, MT: Mg-tholeiites, FT: Fe-tholeiites, CT: contaminated tholeiites, CABAD: calc-alkaline basalts, andesites, and dacites, CARTL: calc-alkaline rhyodacitic to rhyolitic tuffs and lavas.

Units	Volcanic series (dominant in bold)	U-Pb ages (Ma)	Location figure	Diagrams
Nuvvuagittuq Belt	**MT**, **FT**	3825	3.3	4.1a) and b)
Gayot Complex	**KBK, MT, FT,** CT, CABAD, CARTL	2880-2873	3.4	4.1a) and b)
Arnaud Complex	**KBK**, **MT**, **FT**, CT, CABAD	2818, 2782, 2725 and 2718	3.4	4.1c) and d)
Garault Complex	**CABAD**, MT, CARTL	2782	3.5	4.1e) and f)
Dupire Complex	**BADCA**, **TM,** TLRCA	2798-2787	3.5	4.1e) and f)
Nantais Complex	**FT,** MT	2775	3.5	4.1e) and f)
Innuksuac Complex	**MT, KBK, CARTL**, CT, CABAD	2760-2740 (estimated)	3.5	4.2 a) and b)
Mézard Complex	**TM**, **TLRCA,** BADCA	2760-2740 (estimated)	3.5	4.2 a) and b)
Roulier Belt	**MT, CARTL**, CABAD	2759	3.5	4.2 a) and b)
Melvin Belt	**CARTL**	2741	3.6	4.2 e) and f)
Pélican Complex	**CABAD, CARTL**	2739	3.6	4.2 c) and d)
Tasiataq Belt	**MT, KBK**, CABAD	2740	3.6	4.2 c) and d)
Duvert Complex	**MT, FT, KBK, CT**, CABAD, CARTL	2724-2708	3.6	4.2 c) and d)
Chavigny Complex	**CARTL, MT**, CABAD	2722	3.6	4.2 c) and d)
Allemand Belt	**KBK,** FT	2700 (estimated)	3.9	4.2 e) and f)
Juet Belt	**CABAD**, TM	-	3.9	4.2 e) and f)

TABLE 4.2 - Representative geochemical analyses of volcanic rocks from each series identified in the NESP.

Series	Fe-tholeiites	Mg-tholeiites					Contaminated tholeiites					Calc-alkaline dacites, rhyodacites, rhyolites	
Unique sample number (SIGÉOM)	1999029388	1994004177	1998018423	1998018452	1998020758	1998020764	2002037227	2002037368	2002037364	1998020747	1998020752	1998018468	1999029417
NTS	24D	34H	23M	23M	34H	34H	34B15	34C09	34B11	34H	34H	23M	23M
UTM zone	19	18	19	19	18	18	18	18	18	18	18	19	19
Easting	429287	597696	359588	341471	655718	668012	526425	435009	494710	659317	670950	345873	365891
Northing	6239974	6331083	6168902	6100308	6357784	6397651	6293531	6262944	6284336	6393475	6385310	6104683	6162824
Lithology	V3	V3	V3	V3	V3	V3	V3	V2	V1 TU	V3	V3	V1 TU	V1 TX
SiO_2 (weight %)	49.70	49.92	48.80	50.10	48.50	50.40	47.40	61.17	68.15	52.70	53.30	72.50	75.50
TiO_2	1.63	0.68	0.82	1.01	0.76	0.81	1.17	0.61	0.38	1.82	1.64	0.42	0.25
Al_2O_3	13.40	14.74	14.60	15.00	15.00	14.30	16.35	16.73	15.70	14.00	14.10	14.30	13.00
$Fe_2O_{3(total)}$	17.20	12.72	12.80	13.30	12.70	12.70	17.37	6.31	3.87	15.80	15.00	2.06	1.93
MnO	0.25	0.19	0.20	0.18	0.21	0.19	0.37	0.07	0.04	0.19	0.18	0.03	0.06
MgO	5.14	8.56	7.67	6.91	8.92	7.98	5.01	2.85	1.15	3.55	3.39	0.49	0.60
CaO	7.85	11.47	10.00	11.30	12.30	11.10	8.56	3.43	2.61	7.95	7.71	1.54	1.77
Na_2O	2.21	1.29	2.08	1.76	1.66	1.68	2.72	3.79	3.88	3.35	3.57	4.03	2.73
K_2O	1.32	0.30	1.00	0.18	0.19	0.26	0.45	1.94	3.55	1.38	1.62	3.51	3.77
P_2O_5	0.13	0.02	0.07	0.08	0.04	0.05	0.10	0.16	0.11	0.39	0.33	0.14	0.06
LOI	1.09	1.21	1.37	0.75	0.52	0.89	0.40	2.80	0.40	0.25	-0.03	0.43	0.59
Ba (ppm)	198	25	135	26	17	68	131.00	678.00	993.00	647	803	1560	520
Rb	80	7	61	1	5	3	12.50	136.20	85.20	37	38	52	135
Sr	174	94	130	164	101	115	152.20	370.10	719.10	410	588	110	78
Cs	1.23	2.45	0.90	0.22	0.46	0.16	0.70	7.80	3.60	0.58	0.54	5.00	3.50
Ta	0.35	n.a.	0.31	n.a.	n.a.	n.a.	0.20	0.50	0.40	n.a.	0.33	0.55	1.07
Nb	6.00	1.56	2.12	2.40	1.33	1.98	3.20	5.10	4.30	5.89	5.73	8.63	8.19
Hf	3.24	1.03	1.31	1.69	1.04	1.35	1.20	3.60	3.20	3.80	4.50	5.24	4.15
Zr	96.8	29.5	37.3	51.1	25.7	39.7	45.90	115.20	109.00	126.9	123.2	178.3	122.0
Y	36.6	15.6	18.2	23.0	18.9	18.0	28.70	14.10	6.00	25.9	24.4	14.1	16.6
Th	0.96	0.16	0.21	0.23	0.00	0.29	0.70	8.00	4.70	0.32	2.00	5.11	11.36
U	0.23	0.18	0.10	0.06	0.07	0.08	0.10	2.50	0.80	0.17	0.59	0.94	2.17
Cr	76	n.a.	310	n.a.	390	330	n.a.	n.a.	n.a.	20	20	n.a.	20
Ni	130	n.a.	120	n.a.	110	86	109.50	25.40	23.90	27	18	n.a.	100
La	8.10	1.95	2.50	2.89	1.39	2.89	9.90	33.70	13.90	27.01	30.26	21.91	25.12
Ce	20.22	5.19	6.72	7.91	4.49	7.34	19.20	62.30	27.40	59.10	63.17	48.78	50.96
Pr	2.96	2.54	1.04	1.30	0.81	1.12	2.43	6.96	2.99	7.92	8.11	5.77	5.33

TABLE 4.2 - Representative geochemical analyses of volcanic rocks from each series identified in the NESP (continued).

Series	Fe-tholeiites	Mg-tholeiites					Contaminated tholeiites					Calc-alkaline dacites, rhyodacites, rhyolites	
Unique sample number (SIGÉOM)	1999029388	1994004177	1998018423	1998018452	1998020758	1998020764	2002037227	2002037368	2002037364	1998020747	1998020752	1998018468	1999029417
Nd	14.34	4.57	5.51	6.81	4.80	5.85	11.60	26.20	11.30	32.85	31.62	20.69	17.98
Sm	4.34	1.55	1.86	2.30	1.75	1.94	2.90	4.40	2.20	6.52	6.23	3.33	3.20
Eu	1.32	0.61	n.a.	0.82	0.65	0.64	0.99	1.19	0.66	1.87	1.80	0.98	0.45
Gd	5.39	0.87	2.40	3.00	2.29	2.48	3.91	3.37	1.46	5.58	5.37	2.42	2.60
Tb	0.89	0.38	0.43	0.52	0.41	0.43	0.69	0.49	0.12	0.81	0.74	0.37	0.40
Dy	5.94	2.07	2.95	3.64	2.78	3.13	4.46	2.53	1.12	4.58	4.39	2.21	2.54
Ho	1.28	0.60	0.66	0.83	0.66	0.68	0.97	0.48	0.22	0.97	0.91	0.49	0.54
Er	3.80	1.73	1.92	2.50	1.97	1.94	2.91	1.35	0.59	2.54	2.49	1.36	1.70
Tm	0.57	0.26	0.29	0.36	0.31	0.30	0.44	0.20	0.09	0.35	0.33	0.21	0.28
Yb	3.64	1.66	1.88	2.34	1.88	2.04	3.11	1.47	0.61	2.23	2.10	1.39	1.86
Lu	0.60	0.26	0.31	0.38	0.29	0.32	0.44	0.20	0.09	0.35	0.32	0.22	0.31

TABLE 4.2 - Representative geochemical analyses of volcanic rocks from each series identified in the NESP (continued).

Series	Calc-alkaline dacites, rhyodacites, rhyolites			Calc-alkaline basalts, andesites					Komatiites, basaltic komatiites					
Unique sample number (SIGÉOM)	1999029423	1999029557	1998028963	1998020755	1999029554	1999029390	1999029392	1999029542	1998018511	1999029408	1999029424	1999029429	1999023665	1999029320
NTS	23M	23M	34H	34H	23M	24D	24D	24D	23M	23M	23M	23M	24D	24D
UTM zone	19	19	18	18	19	19	19	19	19	19	19	19	19	19
Easting	367455	365445	604475	665371	368130	426369	419628	418385	351223	367370	366320	364405	388050	388253
Northing	6163629	6162404	6328112	6404932	6166774	6255383	6264500	6264350	6097894	6162079	6162529	6161429	6216350	6216416
Lithology	V1 TU	V1 TU	V1 TU	V2	V3	V3	V2	V2	V4	V4	V4	V4	V4	V4
SiO_2 (weight %)	78.30	67.50	68.30	58.50	54.10	50.20	60.50	57.10	46.90	46.60	48.30	47.30	45.30	44.00
TiO_2	0.20	0.50	0.39	0.88	0.90	0.69	0.72	0.70	0.49	0.40	0.28	0.45	0.41	0.22
Al_2O_3	11.40	16.20	14.50	15.80	16.30	13.90	16.80	17.70	9.29	7.58	6.03	8.35	8.15	6.77
$Fe_2O_{3(total)}$	1.76	5.03	3.18	9.28	9.99	13.50	8.66	7.89	11.60	11.90	10.10	12.00	11.70	13.40
MnO	0.05	0.10	0.02	0.13	0.15	0.22	0.07	0.15	0.17	0.21	0.19	0.20	0.20	0.14
MgO	0.55	1.95	3.11	4.36	5.60	7.86	2.36	3.16	18.90	19.30	21.60	18.30	19.80	25.00
CaO	1.76	4.18	0.14	6.54	6.68	8.85	3.39	4.38	10.60	9.47	8.83	9.58	8.40	3.12
Na_2O	3.72	1.78	1.79	2.64	2.86	3.33	3.63	3.40	1.11	0.52	0.39	1.06	0.59	0.25
K_2O	1.55	2.03	8.18	1.89	1.84	0.56	2.01	2.70	0.21	0.05	0.02	0.07	0.12	1.44
P_2O_5	0.06	0.10	0.09	0.13	0.15	0.19	0.24	0.26	0.06	0.01	0.01	0.01	0.02	0.01
LOI	0.79	0.65	0.86	0.70	1.29	1.30	1.92	1.95	1.80	3.81	4.40	3.02	4.28	5.25
Ba (ppm)	394	243	803	350	329	192	350	336	18	0	9	0	n.a.	33
Rb	56	68	136	104	73	22	147	145	1	3	1	2	7	21
Sr	98	136	43	242	168	540	429	451	100	66	41	23	8	61
Cs	5.00	2.10	5.00	5.00	1.51	0.39	5.00	5.00	0.22	5.00	0.92	0.53	1.38	0.50
Ta	0.76	0.58	0.87	0.40	0.59	0.41	0.53	n.a.	n.a.	n.a.	n.a.	n.a.	n.a.	n.a.
Nb	7.52	6.41	7.53	5.58	6.85	4.22	5.27	4.12	0.82	0.94	0.85	0.94	0.90	1.07
Hf	3.64	4.40	4.78	3.94	3.19	1.69	3.39	3.38	0.90	0.60	0.48	0.72	0.74	0.71
Zr	106.9	153.1	146.5	128.6	113.0	49.6	111.2	114.1	26.8	15.8	12.8	19.1	19.5	25.2
Y	17.1	15.3	13.5	21.7	22.2	16.1	14.8	15.6	11.9	9.5	6.9	11.0	10.4	14.8
Th	10.13	4.96	11.37	5.98	1.42	2.41	3.14	2.91	0.21	0.09	0.01	0.11	0.08	0.30
U	1.93	1.26	3.22	1.54	0.40	0.64	0.74	0.84	0.06	0.03	0.09	0.04	0.39	0.38
Cr	20	20	20	220	97	730	150	240	n.a.	2500	2200	2100	2500	2400
Ni	100	100	n.a.	75	100	240	100	100	630	560	570	550	540	660
La	20.00	21.70	25.54	19.73	12.90	32.89	26.74	21.78	1.86	0.74	0.97	1.27	1.44	2.47
Ce	38.26	40.50	47.71	41.00	27.79	82.70	53.19	45.56	4.62	2.36	2.94	3.56	3.73	5.84
Pr	4.44	4.44	2.24	5.08	3.69	11.21	6.72	5.78	0.70	0.42	0.45	0.56	0.58	0.80

TABLE 4.2 - Representative geochemical analyses of volcanic rocks from each series identified in the NESP (concluded).

Series	Calc-alkaline dacites, rhyodacites, rhyolites			Calc-alkaline basalts, andesites					Komatiites, basaltic komatiites					
Unique sample number (SIGÉOM)	1999029423	1999029557	1998028963	1998020755	1999029554	1999029390	1999029392	1999029542	1998018511	1999029408	1999029424	1999029429	1999023665	1999029320
Nd	15.14	16.47	17.08	19.57	15.26	43.75	26.21	23.80	3.39	2.36	1.96	2.99	3.00	3.75
Sm	2.70	3.13	3.07	4.43	3.58	6.92	4.73	4.68	1.14	0.90	0.65	1.02	1.04	1.20
Eu	0.41	0.81	0.58	1.07	1.05	1.74	1.25	1.29	0.54	0.28	0.30	0.38	0.38	0.60
Gd	2.30	2.65	1.26	3.71	3.53	4.42	3.35	3.46	1.55	1.24	0.86	1.42	1.46	1.72
Tb	0.38	0.40	0.37	0.59	0.57	0.54	0.44	0.46	0.29	0.22	0.16	0.25	0.26	0.30
Dy	2.46	2.39	5.08	3.67	3.60	3.08	2.51	2.60	1.94	1.50	1.09	1.77	1.76	2.08
Ho	0.57	0.52	0.44	0.78	0.78	0.58	0.51	0.52	0.43	0.35	0.25	0.40	0.39	0.45
Er	1.73	1.48	2.45	2.26	2.34	1.55	1.35	1.44	1.28	1.02	0.73	1.14	1.18	1.35
Tm	0.28	0.22	0.20	0.31	0.34	0.22	0.20	0.20	0.18	0.15	0.12	0.18	0.18	0.19
Yb	1.85	1.45	1.33	2.10	2.17	1.32	1.26	1.23	1.20	1.00	0.67	1.10	1.09	1.23
Lu	0.31	0.24	0.21	0.33	0.36	0.21	0.20	0.19	0.18	0.15	0.11	0.18	0.18	0.21

TABLE 4.3 - Representative geochemical analyses of plutonic rocks from each series identified in the NESP.

Series	TTG							
Unique sample number (SIGÉOM)	2002037362	2002037363	2001037099	2001038415	1998018405	1998018406	1998028964	2000024115
NTS	34B14	34B13	33P09	33P14	23M05	23M06	34H03	34A09
UTM zone	18	18	18	18	18	18	18	18
Easting	483152	440006	683581	614839	328197	349315	607007	666741
Northing	6296515	6302915	6181772	6186540	6126526	6141571	6340301	6276825
Lithology	I1E, BO	I1D, HB, BO, CX	I1C, HB±BO	I2J, HB	I1D, M3	I1D	I1C	I2J
SiO_2 (weight %)	73.59	68.57	68.00	52.80	65.20	74.40	70.40	60.00
TiO_2	0.13	0.39	0.30	0.69	0.70	0.11	0.41	0.78
Al_2O_3	15.01	15.63	15.80	17.40	15.80	15.00	15.70	17.10
$Fe_2O_{3(total)}$	1.59	3.54	2.90	9.32	4.96	0.97	3.62	6.47
MnO	0.02	0.04	0.02	0.14	0.10	0.01	0.04	0.11
MgO	0.43	1.18	1.05	3.74	1.60	0.25	0.95	2.54
CaO	1.83	3.61	2.54	6.96	4.20	2.74	3.37	5.50
Na_2O	4.99	4.62	4.26	4.48	4.39	5.48	4.48	4.42
K_2O	1.93	1.43	3.68	1.76	1.35	0.70	1.39	1.56
P_2O_5	0.01	0.11	0.12	0.10	0.23	0.03	0.12	0.15
LOI	0.40	0.80	0.49	2.41	0.65	0.29	0.44	0.98
Total	99.93	99.92	99.16	99.80	99.18	99.98	100.92	99.61
Ba (ppm)	475	299	992	248	249	93	566	200
Rb	48	50	123	90	72	25	54	74
Sr	411	440	402	563	359	601	577	210
Cs	0.40	0.20	1.59	0.54	5.00	0.82	3.00	1.09
Ta	0.40	0.20	0.36	0.36	0.36	0.30	0.30	0.44
Nb	3.20	5.70	5.23	6.42	7.85	1.17	2.90	9.33
Hf	1.70	3.60	n.a.	n.a.	4.56	1.68	3.70	5.18
Zr	69.1	116.7	153.4	72.6	170.6	48.3	134.5	205.1
Y	2.6	8.5	6.5	27.0	12.4	0.6	4.3	16.6
Th	4.00	8.60	5.84	6.39	1.91	0.77	9.00	1.09
U	0.50	0.40	1.08	1.90	0.68	0.23	0.60	0.44
Cr	n.a.	n.a.	20	20	n.a.	n.a.	20	n.a.
Ni	4	13	100	100	n.a.	n.a.	3	n.a.
La	10.00	40.10	18.42	37.80	25.79	2.88	43.80	13.96
Ce	17.20	69.20	34.65	83.33	51.17	5.70	74.60	32.40
Pr	1.68	7.15	4.08	10.05	6.10	0.56	8.39	4.54
Nd	7.10	26.00	15.06	40.11	22.61	1.93	28.90	18.56
Sm	1.20	3.40	2.46	7.81	3.75	0.28	4.40	4.08
Eu	0.35	0.95	0.68	1.25	0.92	0.32	0.74	0.88
Gd	0.87	2.26	2.09	6.59	3.11	0.17	2.28	3.66
Tb	0.08	0.21	0.23	0.85	0.41	0.02	0.15	0.53
Dy	0.49	1.31	1.30	4.98	2.18	0.12	1.10	2.90
Ho	0.10	0.27	0.25	0.93	0.42	0.02	0.14	0.60
Er	0.27	0.73	0.72	2.63	1.14	0.06	0.37	1.55
Tm	0.05	0.09	0.10	0.37	0.16	0.01	0.00	0.22
Yb	0.27	0.58	0.68	2.26	0.97	0.07	0.39	1.36
Lu	0.03	0.08	0.10	0.34	0.16	0.01	0.02	0.21

TABLE 4.3 - Representative geochemical analyses of plutonic rocks from each series identified in the NESP (continued).

Series	Intermediate-ultramafic plutonic rocks				
Unique sample number (SIGÉOM)	2000024120	2000024121	2002037335	2002037370	2003039899
NTS	34A04	34A04	34B13	34C09	34F08
UTM zone	18	18	18	18	18
Easting	582194	566738	463899	424475	524975
Northing	6216626	6224531	6299089	6275624	6329926
Lithology	I3A	I3A, BO	I3A	I3Q	I4B
SiO_2 (weight %)	46.20	50.80	49.26	52.47	47.03
TiO_2	0.90	0.41	0.80	2.03	0.19
Al_2O_3	13.40	9.10	5.14	14.66	2.90
$Fe_2O_{3(total)}$	13.70	9.49	16.41	11.83	15.09
MnO	0.18	0.18	0.25	0.13	0.28
MgO	9.28	14.20	14.13	4.52	15.97
CaO	9.05	11.20	9.80	5.63	12.09
Na_2O	2.24	1.84	0.90	2.93	0.58
K_2O	0.41	0.84	0.81	2.50	0.32
P_2O_5	0.04	0.03	0.11	1.50	0.04
LOI	4.10	1.72	1.80	1.50	2.10
Total	99.50	99.81	99.41	99.70	96.59
Ba (ppm)	624	101	250	962	57
Rb	7	28	26	80	16
Sr	423	261	198	651	32
Cs	0.05	0.20	0.10	0.80	0.00
Ta	0.30	0.30	0.20	0.70	0.10
Nb	1.49	2.10	2.70	15.20	2.90
Hf	1.05	1.25	3.20	8.00	0.50
Zr	27.9	36.1	93.2	300.6	14.2
Y	11.5	12.4	18.6	32.8	22.6
Th	0.31	0.72	1.10	5.00	0.40
U	0.04	0.11	0.30	0.80	0.10
Cr	n.a.	n.a.	n.a.	n.a.	n.a.
Ni	n.a.	n.a.	1347	50	4389
La	8.31	17.22	16.20	86.10	16.50
Ce	19.71	39.67	41.00	182.60	57.60
Pr	3.00	5.12	6.23	23.22	7.47
Nd	13.51	20.23	30.10	93.10	31.70
Sm	3.12	3.98	6.80	15.90	6.10
Eu	0.85	0.91	1.30	2.82	0.80
Gd	2.68	3.08	3.50	6.24	4.64
Tb	0.37	0.40	0.67	1.21	0.69
Dy	2.06	2.25	3.50	6.24	4.17
Ho	0.41	0.45	0.69	1.12	0.87
Er	1.07	1.20	1.52	2.81	2.24
Tm	0.16	0.17	0.23	0.37	0.30
Yb	1.06	1.08	1.72	2.46	2.29
Lu	0.15	0.16	0.19	0.37	0.29

TABLE 4.3 - Representative geochemical analyses of plutonic rocks from each series identified in the NESP (continued).

Series	GGM								
Unique sample number (SIGÉOM)	1998018403	2000024104	2001037069	1998018404	2000024106	2001037083	1998028977	2002037371	2002037373
NTS	23M13	34A10	33P15	23M14	34A04	33P15	34H08	33B16	34B03
UTM zone	18	18	18	18	18	18	18	18	18
Easting	329157	633614	628285	364128	567496	650437	656165	533260	479642
Northing	6198253	6275804	6192165	6203788	6211884	6204773	6364710	6300787	6223971
Lithology	I1C, HB	I1C, BO	I1M, ±HB±BO	I1M, BO	I1C	I1C, HB+BO	I1M	I1M, BO	I1C, BO+HB
SiO_2 (weight %)	64.20	72.00	72.00	73.10	61.90	64.10	75.50	72.87	66.87
TiO_2	0.48	0.28	0.20	0.21	0.82	0.42	0.08	0.16	0.41
Al_2O_3	16.70	14.00	14.40	14.30	16.00	15.60	14.20	13.97	15.35
$Fe_2O_{3(total)}$	4.28	2.34	1.71	1.72	5.55	4.71	0.85	1.87	4.12
MnO	0.05	0.03	0.02	0.01	0.07	0.08	0.01	0.02	0.05
MgO	1.13	0.68	0.55	0.64	2.30	2.28	0.09	0.45	1.41
CaO	2.94	1.53	1.54	0.70	3.87	3.70	0.67	1.68	3.63
Na_2O	4.71	3.36	3.38	4.24	3.93	4.00	3.45	3.43	3.94
K_2O	3.54	4.97	4.90	4.60	3.81	3.45	5.17	4.65	2.80
P_2O_5	0.15	0.07	0.02	0.10	0.34	0.10	0.13	0.05	0.14
LOI	0.75	0.39	0.44	0.62	0.70	0.61	0.38	0.70	1.10
Total	98.93	99.65	99.16	100.24	99.29	99.05	100.53	99.85	99.82
Ba (ppm)	1633	580	815	1032	1105	645	353	817	842
Rb	142	189	118	191	160	158	250	167	86
Sr	467	269	305	239	450	367	100	422	475
Cs	4.94	3.29	3.27	5.00	1.17	2.08	11.90	0.90	0.30
Ta	0.51	0.78	0.56	0.70	0.31	0.31	0.60	0.10	0.30
Nb	6.90	7.89	3.16	4.50	9.47	7.76	4.70	2.90	5.90
Hf	7.20	4.70	n.a.	4.50	8.72	n.a.	1.60	2.70	4.20
Zr	267.9	140.2	88.2	136.5	314.4	183.1	44.0	82.6	140.9
Y	13.7	11.3	3.8	4.4	16.8	19.2	2.2	5.0	11.8
Th	10.45	24.50	39.40	17.70	22.78	12.66	11.40	20.30	9.00
U	3.99	1.51	3.89	2.30	0.80	0.90	3.30	0.60	0.40
Cr	n.a.	n.a.	20	n.a.	n.a.	79	20	n.a.	n.a.
Ni	n.a.	n.a.	100	3	n.a.	100	1	4	6
La	25.99	49.23	63.08	42.30	128.80	40.79	14.10	27.70	35.00
Ce	54.68	88.24	106.90	71.10	207.61	86.16	26.60	48.60	63.70
Pr	6.67	9.75	10.68	7.19	24.73	9.63	2.81	5.24	6.84
Nd	24.97	31.78	31.53	23.50	82.24	34.46	10.10	16.90	25.30
Sm	4.74	4.65	2.94	3.00	10.71	6.01	2.00	3.00	4.20
Eu	1.22	0.76	0.63	0.70	2.08	0.89	0.34	0.63	0.94
Gd	3.41	2.97	1.72	1.54	5.91	4.83	1.28	1.80	3.09
Tb	0.48	0.39	0.15	0.19	0.67	0.58	0.12	0.26	0.40
Dy	2.70	2.01	0.73	0.80	3.18	3.27	0.67	1.20	2.15
Ho	0.54	0.38	0.14	0.15	0.59	0.63	n.a.	0.18	0.43
Er	1.39	1.05	0.36	0.40	1.46	1.73	0.13	0.40	1.13
Tm	0.20	0.15	0.06	0.05	0.20	0.24	n.a.	0.05	0.15
Yb	1.28	0.98	0.38	0.41	1.20	1.47	0.14	0.31	1.05
Lu	0.20	0.15	0.06	0.08	0.19	0.23	n.a.	0.05	0.15

TABLE 4.3 - Representative geochemical analyses of plutonic rocks from each series identified in the NESP (concluded).

Series	Pyroxene-bearing granitoid rocks									
Unique sample number (SIGÉOM)	2002036338	2002036251	2002036318	2002036346	1998020798	1998028956	2000024114	2001038420	2003039962	2003039974
NTS	33O08	33O08	33O01	33O10	34H04	34H04	34A12	33P04	34F15	34F09
UTM zone	18	18	18	18	18	18	18	18	18	18
Easting	560705	554037	556112	525159	572480	574771	575301	568977	407439	417966
Northing	6137416	6130648	6122455	6172187	6333457	6339610	6287816	6098392	6421026	6394200
Lithology	I2F, BO, CX	I1T, BO	I2F, CX, BO	I1D, CX. BO, HB	I1T	I1T	I1T	I2J, CX	I1C, CX	I1T
SiO_2 (weight %)	59.32	65.15	60.22	64.24	71.90	68.80	57.10	61.60	68.67	55.52
TiO_2	0.72	0.38	0.41	0.65	0.30	0.46	0.60	0.69	0.69	0.77
Al_2O_3	18.32	16.06	18.91	16.00	14.30	15.20	17.90	15.40	13.84	18.69
$Fe_2O_{3(total)}$	5.27	4.40	3.76	5.50	2.94	4.08	7.59	6.48	4.76	7.71
MnO	0.06	0.04	0.05	0.05	0.04	0.08	0.14	0.10	0.06	0.11
MgO	1.49	1.75	0.99	1.76	1.28	2.35	3.41	3.24	1.04	2.95
CaO	3.20	4.61	2.16	4.39	2.43	3.79	4.90	4.31	2.72	7.25
Na_2O	4.30	4.18	4.28	4.37	3.85	4.26	4.42	4.32	3.43	4.36
K_2O	6.10	1.19	7.50	1.60	3.89	1.31	2.77	2.64	2.68	1.01
P_2O_5	0.28	0.12	0.20	0.22	0.09	0.13	0.51	0.21	0.32	0.36
LOI	0.50	1.90	1.10	1.10	0.29	0.47	0.74	0.87	0.80	0.50
Total	99.56	99.78	99.58	99.88	101.31	100.93	100.08	99.86	99.01	99.23
Ba (ppm)	1980	377	1545	459	671	387	811	751	1484	599
Rb	163	28	119	76	109	32	76	43	81	42
Sr	601	551	566	488	328	367	450	461	383	848
Cs	1.90	0.30	0.50	0.60	0.30	0.00	0.34	0.24	0.10	1.00
Ta	0.30	0.20	0.20	0.30	0.10	0.50	0.30	0.34	0.40	0.30
Nb	5.00	2.80	1.80	6.40	2.50	9.10	5.85	7.04	11.90	5.60
Hf	16.50	4.10	12.00	4.00	2.30	3.90	1.40	n.a.	7.90	2.00
Zr	744.6	144.1	581.8	140.2	85.1	126.7	46.9	188.9	292.3	74.3
Y	16.9	4.2	9.5	11.0	5.0	36.6	21.7	11.8	36.8	19.9
Th	19.30	4.30	2.50	9.50	2.60	1.10	3.23	1.81	6.50	2.20
U	1.50	0.30	0.20	0.20	0.10	0.50	0.38	0.57	0.50	0.90
Cr	n.a.	n.a.	n.a.	n.a.	49	81	n.a.	140	n.a.	n.a.
Ni	5	7	3	9	n.a.	35	n.a.	100	5	14
La	190.70	34.20	58.90	47.20	25.80	17.30	67.62	36.80	68.70	36.10
Ce	339.80	58.30	103.40	84.70	43.60	34.60	141.40	74.63	164.20	71.30
Pr	34.63	5.29	11.59	8.92	4.40	4.33	18.24	8.44	17.63	8.28
Nd	128.10	17.90	46.00	34.30	16.20	19.80	69.54	32.97	74.60	35.00
Sm	15.20	2.40	6.80	4.80	2.50	5.10	11.38	5.47	13.20	5.80
Eu	3.24	1.02	3.44	1.06	0.76	0.89	1.50	1.14	2.37	1.83
Gd	9.65	1.36	4.60	3.14	1.58	5.68	7.68	3.91	9.89	4.65
Tb	0.88	0.18	0.43	0.40	0.20	0.95	0.92	0.46	1.42	0.77
Dy	3.75	0.96	2.01	1.95	1.02	6.95	4.34	2.77	6.97	3.35
Ho	0.60	0.19	0.33	0.33	0.15	1.24	0.81	0.49	1.19	0.68
Er	1.42	0.38	0.84	0.93	0.50	3.71	1.94	1.35	3.10	1.73
Tm	0.22	0.06	0.12	0.12	0.05	0.50	0.24	0.19	0.43	0.28
Yb	1.48	0.45	0.77	0.86	0.55	3.01	1.42	1.14	2.81	1.63
Lu	0.24	0.07	0.10	0.11	0.04	0.36	0.22	0.18	0.41	0.26

TABLE 4.4 - Nd isotopic composition of volcanic and plutonic rocks in the NESP.

No.	Sample	NTS	Zone	UTM NAD83		Rock type	Age (Ga)		$^{143}Nd/^{144}Nd$	$^{147}Sm/^{144}Nd$	εNd(t)	Tdm	Nd	Sm	Reference	Laboratory
				Easting	Northing							(Ga)	(ppm)	(ppm)		
1	1999022705	25D	19	384986	6742596	Tonalite	2.775	interpreted	0.51097	0.0985	2.46	2.76	30.36	4.95	Maurice, 2007	GEOTOP-UQAM-McGill
2	1999022802	25D	19	382138	6750707	Felsic tuff	2.820	interpreted	0.51138	0.1242	1.77	2.85	4.20	0.86	Maurice, 2007	GEOTOP-UQAM-McGill
3	2002034706	25D	19	385921	6746926	Basalt	2.820	interpreted	0.51208	0.1638	0.99	-	9.15	2.48	Maurice, 2007	GEOTOP-UQAM-McGill
4	2002034707	25D	19	389130	6737980	Basalt	2.820	interpreted	0.51289	0.2053	1.89	-	6.89	2.34	Maurice, 2007	GEOTOP-UQAM-McGill
5	2002034708	25D	19	384827	6744658	Basalt	2.820	interpreted	0.51281	0.1994	2.33	-	4.19	1.38	Maurice, 2007	GEOTOP-UQAM-McGill
6	99-CM-021	25D	19	386247	6747125	Tonalite	2.775	interpreted	0.51083	0.0896	2.97	2.73	22.76	3.38	Maurice, 2007	GEOTOP-UQAM-McGill
7	2001038727	35B	18	480286	6685177	Rhyolite	2.820	U-Pb age	0.51224	0.1671	3.05	2.68	24.03	6.64	Maurice, 2007	GEOTOP-UQAM-McGill
8	2001038770	35B	18	485960	6699182	Tonalite	2.780	U-Pb age	0.51077	0.0877	2.64	2.76	14.78	2.15	Maurice, 2007	GEOTOP-UQAM-McGill
9	2002034705	35B	18	476681	6693734	Rhyolite	2.820	interpreted	0.51086	0.0891	4.50	2.68	29.58	4.36	Maurice, 2007	GEOTOP-UQAM-McGill
10	2002034740	35B	18	474896	6677813	Basalt	2.820	interpreted	0.51125	0.1144	2.89	2.77	26.07	4.93	Maurice, 2007	GEOTOP-UQAM-McGill
11	2002034742	35B	18	475218	6677867	Basalt	2.820	interpreted	0.51127	0.1147	3.09	2.75	38.78	7.36	Maurice, 2007	GEOTOP-UQAM-McGill
12	2002034757	35B	18	479015	6693697	Basalt	2.820	interpreted	0.51128	0.1159	2.91	2.76	17.50	3.36	Maurice, 2007	GEOTOP-UQAM-McGill
13	2002034759	35B	18	479814	6693545	Basalt	2.820	interpreted	0.51158	0.1347	1.86	2.85	11.21	2.50	Maurice, 2007	GEOTOP-UQAM-McGill
14	2002034835	35B	18	476503	6693409	Basalt	2.775	interpreted	0.51215	0.1617	3.07	-	21.61	5.78	Maurice, 2007	GEOTOP-UQAM-McGill
15	2002034836	35B	18	478396	6693872	Basalt	2.775	interpreted	0.51228	0.1683	3.20	-	12.85	3.58	Maurice, 2007	GEOTOP-UQAM-McGill
16	2000024407	35A	18	580389	6762274	Tonalite	2.775	interpreted	0.51055	0.0732	3.34	2.72	3.36	0.41	Maurice, 2007	GEOTOP-UQAM-McGill
17	2000025301	35A	18	574652	6760056	Felsic tuff	2.775	interpreted	0.51077	0.0873	2.69	2.75	31.28	4.52	Maurice, 2007	GEOTOP-UQAM-McGill
18	2002034722	35A	18	573525	6760162	Basalt	2.775	interpreted	0.51238	0.1754	2.68	-	15.92	4.62	Maurice, 2007	GEOTOP-UQAM-McGill
19	2002034727	35A	18	573860	6760132	Basalt	2.775	interpreted	0.51257	0.1861	2.39	-	17.63	5.43	Maurice, 2007	GEOTOP-UQAM-McGill
20	2002034729	35A	18	574071	6760139	Gabbro	2.775	interpreted	0.51289	0.2021	2.92	-	4.38	1.47	Maurice, 2007	GEOTOP-UQAM-McGill
21	2002034732	35A	18	575496	6764750	Basalt	2.775	interpreted	0.51271	0.1905	3.61	-	8.88	2.80	Maurice, 2007	GEOTOP-UQAM-McGill
22	2002034733	35A	18	574279	6758304	Basalt	2.775	interpreted	0.51258	0.1850	3.14	-	10.24	3.13	Maurice, 2007	GEOTOP-UQAM-McGill
23	2002034735	35A	18	574565	6758271	Basalt	2.775	interpreted	0.51279	0.1958	3.20	-	8.85	2.87	Maurice, 2007	GEOTOP-UQAM-McGill
24	2002034736	35A	18	574676	6758205	Basalt	2.775	interpreted	0.51281	0.1982	2.87	-	10.46	3.43	Maurice, 2007	GEOTOP-UQAM-McGill
25	2000030239	34P	18	577550	6649640	Andesite	2.740	interpreted	0.51120	0.1139	1.23	2.83	30.37	5.72	Maurice, 2007	GEOTOP-UQAM-McGill
26	2001032360	34P	18	662226	6623896	Felsic tuff	2.740	U-Pb age	0.51079	0.0892	1.92	2.77	34.79	5.14	Maurice, 2007	GEOTOP-UQAM-McGill
27	00-JY-9014A1	34P	18	581804	6636234	Basalt	2.740	interpreted	0.51129	0.1207	0.46	2.90	9.52	1.90	Maurice, 2007	GEOTOP-UQAM-McGill
28	00-JY-9031A1	34P	18	582289	6634062	Andesite	2.740	interpreted	0.51112	0.1101	0.88	2.85	19.61	3.57	Maurice, 2007	GEOTOP-UQAM-McGill
29	00-JY-9019C2	34P	18	582105	6636755	Felsic tuff	2.740	interpreted	0.51080	0.0910	1.49	2.79	21.50	3.24	Maurice, 2007	GEOTOP-UQAM-McGill
30	2000030236	34P	18	595935	6629033	Granodiorite	2.714	U-Pb age	0.51137	0.1260	-0.03	2.93	108.97	22.73	Maurice, 2007	GEOTOP-UQAM-McGill
31	2000030267	34P	18	622985	6618594	Tonalitic gneiss	2.768	U-Pb age	0.51151	0.1285	2.34	2.77	14.26	3.03	Maurice, 2007	GEOTOP-UQAM-McGill
32	2000030268	34P	18	565891	6605592	Opdalite	2.717	U-Pb age	0.51025	0.0609	0.89	2.79	11.07	1.12	Maurice, 2007	GEOTOP-UQAM-McGill
33	2000030269	34P	18	661228	6598460	Gabbronorite	2.723	U-Pb age	0.51205	0.1600	1.38	2.87	11.89	3.15	Maurice, 2007	GEOTOP-UQAM-McGill
34	2001032305	34O	18	548491	6618284	Granodiorite	2.723	U-Pb age	0.51022	0.0599	0.77	2.80	34.63	3.43	Maurice, 2007	GEOTOP-UQAM-McGill

TABLE 4.4 - Nd isotopic composition of volcanic and plutonic rocks in the NESP (continued).

No.	Sample	NTS	Zone	UTM NAD83		Rock type	Age (Ga)		$^{143}Nd/^{144}Nd$	$^{147}Sm/^{144}Nd$	εNd(t)	Tdm	Nd	Sm	Reference	Laboratory
				Easting	Northing							(Ga)	(ppm)	(ppm)		
35	2001032362	34O	18	503184	6619060	Tonalite	2.758	U-Pb age	0.51070	0.0849	1.94	2.78	17.67	2.48	Maurice, 2007	GEOTOP-UQAM-McGill
36	2001032366	34O	18	500735	6592147	Enderbite	2.729	U-Pb age	0.51106	0.1041	1.78	2.77	23.53	4.05	Maurice, 2007	GEOTOP-UQAM-McGill
37	2002034818	35C	18	399553	6685034	Enderbite	2.731	U-Pb age	0.51099	0.1029	0.82	2.84	12.43	2.12	Maurice, 2007	GEOTOP-UQAM-McGill
38	2002034823	35C	18	390613	6717173	Monzogranite	2.727	U-Pb age	0.51087	0.0993	-0.27	2.90	54.82	9.01	Maurice, 2007	GEOTOP-UQAM-McGill
39	2002034831	35C	18	360911	6688164	Tonalite	2.766	U-Pb age	0.51059	0.0907	-2.22	3.04	34.07	5.12	Maurice, 2007	GEOTOP-UQAM-McGill
40	2002034878	35C	18	412148	6750505	Tonalitic diatexite	2.722	U-Pb age	0.51112	0.1102	0.75	2.84	13.25	2.42	Maurice, 2007	GEOTOP-UQAM-McGill
41	2003031401	34N	18	381226	6543354	Enderbite	2.730	interpreted	0.51058	0.0891	-2.43	3.02	28.24	4.16	Maurice, 2007	GEOTOP-UQAM-McGill
42	2003031412	34N	18	340859	6583459	Tonalite	2.760	interpreted	0.51045	0.0776	-0.29	2.91	24.28	3.12	Maurice, 2007	GEOTOP-UQAM-McGill
43	2003031452	34N	18	383329	6635664	Carbonatite	2.680	U-Pb age	0.51143	0.1234	1.70	2.75	62.86	12.83	Maurice, 2007	GEOTOP-UQAM-McGill
44	2003031457	34N	18	333610	6586759	Sedimentary rock	2.729	U-Pb age	0.51154	0.1355	0.11	2.95	75.75	16.98	Maurice, 2007	GEOTOP-UQAM-McGill
45	2003031558	34N	18	443097	6632133	Monzogranite	2.720	interpreted	0.51047	0.0715	1.63	2.76	19.65	2.33	Maurice, 2007	GEOTOP-UQAM-McGill
46	2003031406	34N	18	398642	6589523	Tonalite	2.720	interpreted	0.51077	0.0942	-0.63	2.91	17.21	2.68	Maurice, 2007	GEOTOP-UQAM-McGill
47	2003031416	34N	18	399398	6589871	Basalt	2.760	interpreted	0.51263	0.1913	1.71	-	6.67	2.11	Maurice, 2007	GEOTOP-UQAM-McGill
48	2003031417	34N	18	399398	6589871	Gabbro	2.720	interpreted	0.51115	0.1261	-4.38	3.30	34.17	7.13	Maurice, 2007	GEOTOP-UQAM-McGill
49	2003031418	34N	18	404910	6587376	Gabbro	2.720	interpreted	0.51222	0.1739	-0.11	3.19	6.45	1.86	Maurice, 2007	GEOTOP-UQAM-McGill
50	2003031432	34N	18	407973	6579228	Felsic tuff	2.760	U-Pb age	0.51049	0.0777	0.45	2.86	53.21	6.84	Maurice, 2007	GEOTOP-UQAM-McGill
51	2003031435	34N	18	405516	6590197	Tonalite	2.720	interpreted	0.51038	0.0865	-5.48	3.19	24.06	3.45	Maurice, 2007	GEOTOP-UQAM-McGill
52	2003031441	34N	18	405516	6590197	Basalt	2.760	interpreted	0.51280	0.2007	1.84	-	7.97	2.65	Maurice, 2007	GEOTOP-UQAM-McGill
53	2003031489	34N	18	404958	6584275	Basalt	2.760	interpreted	0.51293	0.2057	2.56	-	5.16	1.75	Maurice, 2007	GEOTOP-UQAM-McGill
54	2003031498	34N	18	407561	6585298	Basalt	2.760	interpreted	0.51268	0.1932	2.00	-	4.97	1.59	Maurice, 2007	GEOTOP-UQAM-McGill
55	2003031499	34N	18	407561	6585298	Tonalite	2.720	interpreted	0.51031	0.1046	-13.29	3.80	6.02	1.04	Maurice, 2007	GEOTOP-UQAM-McGill
56	1998018108	24M	19	386868	6558777	Granodiorite	2.740	interpreted	0.51050	0.0845	-2.25	3.01	24.00	3.10	Boily *et al.*, 2009	Pacific Center, UBC
57	1998018233	24M	19	434038	6647775	Tonalite	2.690	U-Pb age	0.51089	0.0955	0.96	2.79	14.00	1.80	Boily *et al.*, 2009	Pacific Center, UBC
58	1998018235	24M	19	372632	6641292	Tonalite	2.733	interpreted	0.51134	0.1177	2.45	2.73	9.00	2.30	Boily *et al.*, 2009	Pacific Center, UBC
59	1998018403	23M	19	329157	6198253	Granodiorite	2.701	U-Pb age	0.51127	0.1233	-1.10	3.00	31.00	5.50	Boily *et al.*, 2004	Pacific Center, UBC
60	1998018404	23M	19	364128	6203788	Granite	2.682	interpreted	0.51026	0.0831	-0.10	3.24	23.04	3.17	Boily *et al.*, 2006a	Pacific Center, UBC
61	1998018405	23M	19	328197	6126526	Tonalite	2.803	U-Pb age	0.51093	0.1041	0.12	2.95	21.66	3.73	Boily *et al.*, 2004	Pacific Center, UBC
62	1998018406	23M	19	349315	6141571	Tonalite	2.730	U-Pb age	0.51082	0.0898	2.08	2.75	1.48	0.22	Boily *et al.*, 2004	Pacific Center, UBC
63	1998018423	23M	19	359588	6168902	Mafic volcanic	2.881	interpreted	0.51279	0.1981	2.50	-	4.95	1.62	Boily *et al.*, 2004	Pacific Center, UBC
64	1998018452	23M	19	341471	6100308	Mafic volcanic	2.881	interpreted	0.51288	0.2053	1.50	-	6.36	2.16	Boily *et al.*, 2004	Pacific Center, UBC
65	1998018468	23M	19	345873	6104683	Felsic volcanic	2.875	U-Pb age	0.51076	0.1018	-1.49	3.11	19.17	3.23	Boily *et al.*, 2004	Pacific Center, UBC
66	1998020752	34H	18	670950	6385310	Mafic volcanic	2.708	interpreted	0.51122	0.1223	-1.67	3.05	31.62	6.23	Boily *et al.*, 2009	Pacific Center, UBC
67	1998020798	34H	18	572480	6333457	Enderbite	2.725	U-Pb age	0.51081	0.0957	-0.33	2.90	13.52	2.14	Boily *et al.*, 2004	Pacific Center, UBC
68	1998028811	24M	19	426769	6560157	Granite	2.697	U-Pb age	0.51095	0.1029	-0.41	2.89	12.00	1.50	Boily *et al.*, 2009	Pacific Center, UBC

TABLE 4.4 - Nd isotopic composition of volcanic and plutonic rocks in the NESP (continued).

No.	Sample	NTS	Zone	UTM NAD83		Rock type	Age (Ga)		$^{143}Nd/^{144}Nd$	$^{147}Sm/^{144}Nd$	εNd(t)	Tdm	Nd	Sm	Reference	Laboratory
				Easting	Northing							(Ga)	(ppm)	(ppm)		
69	1998028847	24M	19	361765	6621869	Mafic volcanic	2.782	interpreted	0.51304	0.2117	2.41	-	6.00	3.90	Boily *et al.*, 2009	Pacific Center, UBC
70	1998028956	34H	18	574771	6339610	Enderbite	2.709	U-Pb age	0.51195	0.1616	-1.19	-	18.70	5.00	Boily *et al.*, 2004	Pacific Center, UBC
71	1998028959	34H	18	677547	6375597	Felsic volcanic	2.708	U-Pb age	0.51122	0.1173	-0.01	2.90	26.01	5.05	Boily *et al.*, 2004	Pacific Center, UBC
72	1998028963	34H	18	604475	6328112	Felsic volcanic	2.787	U-Pb age	0.51102	0.1135	0.10	2.94	13.49	2.42	Boily *et al.*, 2004	Pacific Center, UBC
73	1998028964	34H	18	607007	6340301	Granodiorite	2.750	U-Pb age	0.51063	0.0928	-2.35	3.04	24.74	3.80	Boily *et al.*, 2004	Pacific Center, UBC
74	1998028977	34H	18	656165	6364710	Granite	2.682	U-Pb age	0.51122	0.1291	-4.46	3.30	8.57	1.83	Boily *et al.*, 2004	Pacific Center, UBC
75	1999022905	25D	19	438130	6748329	Granite	2.755	U-Pb age	0.51057	0.0817	0.51	2.86	44.00	4.60	Boily *et al.*, 2009	Pacific Center, UBC
76	1999022906	25D	19	436445	6748776	Tonalite	2.777	U-Pb age	0.51138	0.1239	1.48	2.85	12.00	2.20	Boily *et al.*, 2009	Pacific Center, UBC
77	1999022908	25D	19	341173	6659535	Tonalite	2.809	U-Pb age	0.51156	0.1311	2.76	2.76	6.00	1.40	Boily *et al.*, 2009	Pacific Center, UBC
78	1999022909	25D	19	377700	6680409	Tonalite	2.772	U-Pb age	0.51053	0.0771	1.57	2.81	12.00	1.00	Boily *et al.*, 2009	Pacific Center, UBC
79	1999022910	25D	19	390828	6745200	Mafic volcanic	2.820	U-Pb age	0.51289	0.2012	3.34	-	6.00	2.50	Boily *et al.*, 2009	Pacific Center, UBC
80	1999029390	24D	18	426369	6255383	Mafic volcanic	2.787	interpreted	0.51092	0.1011	0.81	2.88	41.29	6.91	Boily *et al.*, 2006a	Pacific Center, UBC
81	1999029417	23M	19	366936	6163053	Felsic volcanic	2.881	interpreted	0.51096	0.1121	-1.39	3.14	14.99	2.78	Boily *et al.*, 2004	Pacific Center, UBC
82	2000024029	34A	18	601770	6298160	Tonalite	2.756	U-Pb age	0.51165	0.1497	-2.64	-	12.11	3.00	Boily *et al.*, 2004	Pacific Center, UBC
83	2000024104	34A	18	633614	6275804	Granodiorite	2.714	U-Pb age	0.51073	0.0926	-0.78	2.92	30.87	4.73	Boily *et al.*, 2004	Pacific Center, UBC
84	2000024106	34A	18	567496	6211884	Enderbite	2.713	U-Pb age	0.51052	0.0818	-1.26	2.93	79.99	10.83	Boily *et al.*, 2004	Pacific Center, UBC
85	2000024114	34A	18	575301	6287816	Enderbite	2.690	U-Pb age	0.51085	0.1012	-1.87	2.98	64.92	10.87	Boily *et al.*, 2004	Pacific Center, UBC
86	2000024115	34A	18	666741	6276825	Tonalite	2.811	U-Pb age	0.51148	0.1041	-1.07	3.14	15.56	3.56	Boily *et al.*, 2004	Pacific Center, UBC
87	2000024120	34A	18	582194	6216626	Mafic-UM rock	2.713	interpreted	0.51158	0.1365	0.43	2.91	13.02	2.94	Boily *et al.*, 2004	Pacific Center, UBC
88	2000024121	34A	18	566738	6224531	Mafic-UM rock	2.713	interpreted	0.51125	0.1223	-1.14	3.01	18.83	3.81	Boily *et al.*, 2004	Pacific Center, UBC
89	2000024492	35A	18	654641	6658285	Tonalite	2.785	U-Pb age	0.51028	0.0628	2.07	2.80	8.75	0.88	Boily *et al.*, 2009	Pacific Center, UBC
90	2000024494	35A	18	559223	6681077	Enderbite	2.728	U-Pb age	0.51101	0.1029	1.23	2.81	51.50	8.77	Boily *et al.*, 2009	Pacific Center, UBC
91	2000024495	35A	18	602013	6708778	Granite	2.734	U-Pb age	0.51031	0.0647	1.03	2.80	16.84	1.86	Boily *et al.*, 2009	Pacific Center, UBC
92	2000024497	35A	18	612711	6751462	Tonalite	2.783	U-Pb age	0.51059	0.0795	2.04	2.80	14.14	1.83	Boily *et al.*, 2009	Pacific Center, UBC
93	2000024498	35A	18	574111	6760263	Felsic volcanic	2.775	U-Pb age	0.51079	0.0993	-1.34	3.01	9.46	1.52	Boily *et al.*, 2009	Pacific Center, UBC
94	2000024504	35A	18	632984	6752751	Syenite	2.761	U-Pb age	0.51068	0.0853	1.37	2.82	59.65	8.43	Boily *et al.*, 2009	Pacific Center, UBC
95	2001037069	33P	18	628285	6192165	Granite	2.701	U-Pb age	0.51017	0.0567	0.49	2.80	34.31	3.22	Boily *et al.*, 2004	Pacific Center, UBC
96	2001037083	33P	18	650437	6204773	Granodiorite	2.707	U-Pb age	0.51104	0.1104	-1.17	2.97	25.94	4.73	Boily *et al.*, 2004	Pacific Center, UBC
97	2001037099	33P	18	683581	6181772	Tonalite	2.741	U-Pb age	0.51097	0.1077	-1.20	3.00	15.26	2.72	Boily *et al.*, 2004	Pacific Center, UBC
98	2001038415	33P	18	614839	6186540	Tonalite	2.713	U-Pb age	0.51125	0.1233	-1.47	3.04	37.40	7.63	Boily *et al.*, 2004	Pacific Center, UBC
99	2001038420	33P	18	568977	6098392	Enderbite	2.713	U-Pb age	0.51096	0.1040	-0.31	2.90	32.97	5.47	Boily *et al.*, 2004	Pacific Center, UBC
100	2001038748	35B	18	475673	6677573	Tonalite	2.800	U-Pb age	0.51111	0.1145	-0.14	2.98	7.74	1.46	Boily *et al.*, 2009	Pacific Center, UBC
101	2001038752	35B	18	473946	6700461	Tonalite	2.789	U-Pb age	0.51115	0.1188	-1.08	3.05	5.23	1.03	Boily *et al.*, 2009	Pacific Center, UBC
102	2002036251	33O	18	554051	6130661	Enderbite	2.733	U-Pb age	0.51052	0.0853	-2.10	3.00	17.90	2.40	Boily *et al.*, 2006a	Pacific Center, UBC

TABLE 4.4 - Nd isotopic composition of volcanic and plutonic rocks in the NESP (continued).

No.	Sample	NTS	Zone	UTM NAD83		Rock type	Age (Ga)		$^{143}Nd/^{144}Nd$	$^{147}Sm/^{144}Nd$	εNd(t)	Tdm	Nd	Sm	Reference	Laboratory
				Easting	Northing							(Ga)	(ppm)	(ppm)		
103	2002036318	33O	18	556113	6122455	Monzonite	2.704	U-Pb age	0.51079	0.1060	-4.52	3.19	42.65	7.48	Boily *et al.*, 2006a	Pacific Center, UBC
104	2002036338	33O	18	560705	6137416	Monzonite	2.704	U-Pb age	0.51053	0.0825	-1.49	2.93	110.98	15.15	Boily *et al.*, 2006a	Pacific Center, UBC
105	2002036346	33O	18	525149	6172148	Tonalite	2.723	U-Pb age	0.51065	0.0947	-3.13	3.08	34.30	4.80	Boily *et al.*, 2006a	Pacific Center, UBC
106	2002037218	34B	18	547810	6286995	Granite	2.675	U-Pb age	0.51055	0.0813	-1.11	2.88	27.30	3.40	Boily *et al.*, 2006a	Pacific Center, UBC
107	2002037227	34B	18	526425	6293531	Mafic volcanic	2.741	interpreted	0.51223	0.1734	-1.50	-	10.23	3.02	Boily *et al.*, 2006a	Pacific Center, UBC
108	2002037335	34B	18	463899	6299089	Mafic-UM rock	2.700	U-Pb age	0.51158	0.1424	-1.84	-	30.10	6.80	Boily *et al.*, 2006a	Pacific Center, UBC
109	2002037362	34B	18	483152	6296515	Tonalite	3.020	U-Pb age	0.51084	0.1065	-0.07	3.15	7.10	1.20	Boily *et al.*, 2009	Pacific Center, UBC
110	2002037363	34B	18	440006	6302915	Tonalite	2.712	U-Pb age	0.51061	0.0917	-3.03	3.05	26.00	3.40	Boily *et al.*, 2006a	Pacific Center, UBC
111	2002037364	34B	18	494710	6284336	Felsic volcanic	2.741	U-Pb age	0.51087	0.1183	-6.87	3.47	11.30	2.20	Boily *et al.*, 2006a	Pacific Center, UBC
112	2002037368	34C	18	435009	6262944	Felsic volcanic	2.741	interpreted	0.51093	0.1178	-5.60	3.37	26.20	4.40	Boily *et al.*, 2006a	Pacific Center, UBC
113	2002037370	34C	18	424475	6275624	Mafic-UM rock	2.700	interpreted	0.51086	0.1042	-2.58	3.05	93.10	15.90	Boily *et al.*, 2006a	Pacific Center, UBC
114	2002037371	34B	18	533260	6300787	Granite	2.732	interpreted	0.51080	0.1065	-4.08	3.19	16.90	3.00	Boily *et al.*, 2006a	Pacific Center, UBC
115	2002037373	34B	18	479602	6223971	Granodiorite	2.711	U-Pb age	0.51082	0.1094	-5.00	3.25	25.30	4.20	Boily *et al.*, 2006a	Pacific Center, UBC
116	2003039899	34F	18	422950	6346560	Mafic-UM rock	2.705	interpreted	0.51115	0.1160	-0.96	2.97	31.70	6.10	Boily *et al.*, 2009	Pacific Center, UBC
117	2003039962	34F	18	407439	6421026	Granodiorite	2.730	U-Pb age	0.51093	0.1061	-1.53	3.01	74.60	13.20	Boily *et al.*, 2009	Pacific Center, UBC
118	2003039974	34F	18	417966	6394200	Enderbite	2.719	U-Pb age	0.51094	0.1065	-1.66	3.01	35.00	5.80	Boily *et al.*, 2009	Pacific Center, UBC
119	2003039977	34G	18	555107	6365541	Enderbite	2.702	U-Pb age	0.51128	0.1161	1.59	2.77	16.40	3.30	Boily *et al.*, 2009	Pacific Center, UBC
120	99-EN-3100	24D	19	421085	6269338	Tonalite	2.718	U-Pb age	0.51107	0.1092	0.03	2.89	20.25	3.66	Boily *et al.*, 2009	Pacific Center, UBC
121	YB9920	35B	18	476762	6680728,88	Mafic volcanic	2.822	interpreted	0.51346	0.2341	2.38	-	13.50	4.10	Bourassa, 2002	GEOTOP-UQAM-McGill
122	YB9921	35B	18	476771	6680709,75	Felsic volcanic	2.822	interpreted	0.51126	0.1190	1.28	2.89	11.40	2.00	Bourassa, 2002	GEOTOP-UQAM-McGill
123	YB9929	35B	18	476874	6680992,86	Felsic volcanic	2.822	interpreted	0.51264	0.1904	2.42	-	28.60	7.90	Bourassa, 2002	GEOTOP-UQAM-McGill
124	YB9935	35B	18	476955	6681002,88	Mafic volcanic	2.822	interpreted	0.51298	0.2063	3.16	-	8.10	2.40	Bourassa, 2002	GEOTOP-UQAM-McGill
125	YB9936	35B	18	477891	6679417,05	Tonalite	2.822	interpreted	0.51134	0.1195	2.64	2.79	9.00	1.70	Bourassa, 2002	GEOTOP-UQAM-McGill
126	YB9952	35B	18	476606	6682254,83	Felsic volcanic	2.822	interpreted	0.51192	0.1492	3.21	-	16.50	3.80	Bourassa, 2002	GEOTOP-UQAM-McGill
127	YB9960	35B	18	476810	6682054,05	Alteration	2.822	interpreted	0.51256	0.1886	1.48	-	6.30	1.90	Bourassa, 2002	GEOTOP-UQAM-McGill
128	YBTON99	35B	18	476846	6682246,66	Tonalite	2.822	U-Pb age	0.51134	0.1197	2.73	2.78	15.91	3.15	Bourassa, 2002	GEOTOP-UQAM-McGill
129	1999027402	34I	18	569463	6475994	Diatexite	2.700	interpreted	0.51118	0.1145	0.10	2.88	5.87	1.11	Rabeau, 2003	GEOTOP-UQAM-McGill
130	1999027405	34I	18	603372	6484773	Paragneiss	2.800	interpreted	0.51117	0.1182	-0.40	3.01	17.41	3.40	Rabeau, 2003	GEOTOP-UQAM-McGill
131	1999027406	34I	18	578653	6437734	Enderbite	2.682	interpreted	0.51092	0.0999	-0.08	2.85	11.90	1.97	Rabeau, 2003	GEOTOP-UQAM-McGill
132	1999027407	34I	18	562957	6470490	Granite	2.680	interpreted	0.51091	0.1047	-1.98	2.99	13.82	2.39	Rabeau, 2003	GEOTOP-UQAM-McGill
133	1999027409	34I	18	569395	6446468	Enderbite	2.730	interpreted	0.51116	0.1138	0.25	2.89	15.92	3.00	Rabeau, 2003	GEOTOP-UQAM-McGill
134	1999027410	34I	18	596018	6443989	Granite	2.680	interpreted	0.51065	0.0897	-1.95	2.95	21.73	3.23	Rabeau, 2003	GEOTOP-UQAM-McGill
135	1999027411	34I	18	568941	6472163	Tonalite	2.780	interpreted	0.51039	0.0654	3.23	2.73	44.35	4.80	Rabeau, 2003	GEOTOP-UQAM-McGill
136	1999027413	34I	18	607110	6539695	Granite	2.723	interpreted	0.51067	0.0818	1.95	2.75	48.99	6.63	Rabeau, 2003	GEOTOP-UQAM-McGill

TABLE 4.4 - Nd isotopic composition of volcanic and plutonic rocks in the NESP (continued).

No.	Sample	NTS	Zone	UTM NAD83		Rock type	Age (Ga)		$^{143}Nd/^{144}Nd$	$^{147}Sm/^{144}Nd$	εNd(t)	Tdm	Nd	Sm	Reference	Laboratory
				Easting	Northing							(Ga)	(ppm)	(ppm)		
137	1999027414	34I	18	603584	6436532	Tonalite	2.780	interpreted	0.51053	0.0886	-2.51	3.07	32.64	4.78	Rabeau, 2003	GEOTOP-UQAM-McGill
138	1999027416	34I	18	620062	6509293	Enderbite	2.697	interpreted	0.51062	0.0817	0.61	2.80	9.39	1.27	Rabeau, 2003	GEOTOP-UQAM-McGill
139	1999027417	34I	18	627654	6533428	Granite	2.723	interpreted	0.51112	0.1112	0.32	2.88	58.04	10.68	Rabeau, 2003	GEOTOP-UQAM-McGill
140	1999027419	34I	18	566512	6444296	Enderbite	2.730	U-Pb age	0.51087	0.0946	1.31	2.80	10.29	1.61	Rabeau, 2003	GEOTOP-UQAM-McGill
141	1999027421	34I	18	564247	6507491	Enderbite	2.682	U-Pb age	0.51061	0.0809	0.50	2.80	4.82	0.64	Rabeau, 2003	GEOTOP-UQAM-McGill
142	1999027422	34I	18	641056	6498491	Granodiorite	2.723	U-Pb age	0.51105	0.1067	0.47	2.86	55.93	9.80	Rabeau, 2003	GEOTOP-UQAM-McGill
143	1999027423	34I	18	643393	6523553	Granite	2.723	U-Pb age	0.51089	0.0945	1.70	2.77	36.59	5.72	Rabeau, 2003	GEOTOP-UQAM-McGill
144	1999027424	34I	18	566557	6469529	Tonalite	2.768	U-Pb age	0.51053	0.0762	1.74	2.80	12.98	1.64	Rabeau, 2003	GEOTOP-UQAM-McGill
145	1999027426	34I	18	624583	6503871	Enderbite	2.697	U-Pb age	0.51113	0.1126	-0.21	2.90	52.98	9.87	Rabeau, 2003	GEOTOP-UQAM-McGill
146	1999027427	34I	18	600148	6510723	Granite	2.732	interpreted	0.51091	0.1000	0.35	2.87	51.08	8.45	Rabeau, 2003	GEOTOP-UQAM-McGill
147	1999027428	34I	18	602701	6516403	Granite	2.732	U-Pb age	0.51113	0.1132	-0.08	2.92	56.89	10.65	Rabeau, 2003	GEOTOP-UQAM-McGill
148	1999027433	24L	19	331610	6511487	Felsic volcanic	2.786	U-Pb age	0.51077	0.0918	1.11	2.86	8.57	1.30	Rabeau, 2003	GEOTOP-UQAM-McGill
149	1999027434	24L	19	333285	6510918	Granite	2.723	U-Pb age	0.51118	0.1166	-0.33	2.94	37.60	7.25	Rabeau, 2003	GEOTOP-UQAM-McGill
150	1999027436	24L	19	391630	6537745	Enderbite	2.704	U-Pb age	0.51050	0.0815	-1.68	2.94	16.96	2.29	Rabeau, 2003	GEOTOP-UQAM-McGill
151	1999027438	24L	19	371607	6537508	Granite	2.690	interpreted	0.51099	0.1070	-1.20	2.95	61.76	10.94	Rabeau, 2003	GEOTOP-UQAM-McGill
152	1999027439	24L	19	337374	6524236	Tonalite	2.706	interpreted	0.51082	0.0982	-1.17	2.94	29.58	4.81	Rabeau, 2003	GEOTOP-UQAM-McGill
153	1999027440	24L	19	375313	6524405	Enderbite	2.704	interpreted	0.51083	0.0969	-0.54	2.90	27.47	4.41	Rabeau, 2003	GEOTOP-UQAM-McGill
154	1999027441	24L	19	396382	6526171	Granite	2.690	U-Pb age	0.51065	0.0883	-1.23	2.92	63.26	9.25	Rabeau, 2003	GEOTOP-UQAM-McGill
155	1999027442	24L	19	408795	6539125	Granite	2.700	U-Pb age	0.51079	0.0992	-2.10	3.00	64.78	10.63	Rabeau, 2003	GEOTOP-UQAM-McGill
156	2000025701	34J	18	479971	6452682	Felsic volcanic	2.722	U-Pb age	0.51069	0.0881	0.02	2.87	41.31	6.02	Rabeau, 2003	GEOTOP-UQAM-McGill
157	2000025708	34J	18	537138	6430347	Paragneiss	2.800	interpreted	0.51087	0.0968	1.45	2.85	63.10	10.11	Rabeau, 2003	GEOTOP-UQAM-McGill
158	2000025730	34J	18	442505	6500828	Tonalite	2.710	U-Pb age	0.51074	0.0891	0.50	2.83	14.01	2.07	Rabeau, 2003	GEOTOP-UQAM-McGill
159	2000025740	34J	18	473122	6487216	Granodiorite	2.722	interpreted	0.51056	0.0799	0.44	2.83	41.92	5.55	Rabeau, 2003	GEOTOP-UQAM-McGill
160	2000025754	34J	18	476824	6469403	Tonalite	2.745	interpreted	0.51114	0.1128	0.36	2.89	25.62	4.78	Rabeau, 2003	GEOTOP-UQAM-McGill
161	2000025755	34J	18	474109	6467617	Tonalite	2.745	interpreted	0.51145	0.1281	1.16	2.85	34.85	7.39	Rabeau, 2003	GEOTOP-UQAM-McGill
162	2000025759	34J	18	515223	6467700	Enderbite	2.700	interpreted	0.51093	0.0994	0.55	2.83	23.14	3.81	Rabeau, 2003	GEOTOP-UQAM-McGill
163	MLB91-001	34I	18	n.a.	n.a.	Rhyolite	2.724	U-Pb age	0.51083	0.0966	-0.10	2.89	18.51	2.95	Skulski and Percival, 1996	GSC
164	MLB91-003B	34I	18	n.a.	n.a.	Dacite	2.724	interpreted	0.51094	0.1016	0.11	2.88	18.44	3.10	Skulski and Percival, 1996	GSC
165	MLB91-004A	34I	18	n.a.	n.a.	Mafic volcanic	2.724	interpreted	0.51230	0.1745	1.13	-	9.91	2.86	Skulski and Percival, 1996	GSC
166	PBA91-069A	34I	18	n.a.	n.a.	Dacite	2.724	interpreted	0.51099	0.1061	-0.35	2.92	39.36	6.91	Skulski and Percival, 1996	GSC
167	PBA91-100	34I	18	n.a.	n.a.	Gabbro	2.940	interpreted	0.51254	0.1937	-0.73	-	10.00	3.20	Skulski and Percival, 1996	GSC
168	PBA92-2008C	34I	18	n.a.	n.a.	Andesitic basalt	2.718	interpreted	0.51253	0.1916	-0.33	-	7.62	2.41	Skulski and Percival, 1996	GSC
169	PBA92-2008G	34I	18	n.a.	n.a.	Andesitic basalt	2.718	interpreted	0.51278	0.1973	2.64	-	1.34	4.13	Skulski and Percival, 1996	GSC
170	PBA92-2010	34I	18	n.a.	n.a.	Ultramafic schist	2.786	interpreted	0.51270	0.1924	2.80	-	3.63	1.55	Skulski and Percival, 1996	GSC

TABLE 4.4 - Nd isotopic composition of volcanic and plutonic rocks in the NESP (continued).

No.	Sample	NTS	Zone	UTM NAD83		Rock type	Age (Ga)		$^{143}Nd/^{144}Nd$	$^{147}Sm/^{144}Nd$	εNd(t)	Tdm	Nd	Sm	Reference	Laboratory
				Easting	Northing							(Ga)	(ppm)	(ppm)		
171	PBA92-2011	34I	18	n.a.	n.a.	Komatiite	2.786	interpreted	0.51265	0.1891	3.03	-	1.42	1.42	Skulski and Percival, 1996	GSC
172	PBA-94-275	34I	18	n.a.	n.a.	Gabbro	2.718	interpreted	0.51231	0.1755	0.95	-	8.67	2.52	Skulski and Percival, 1996	GSC
173	SNB93-003	34I	18	n.a.	n.a.	Pyroxenite	2.786	interpreted	0.51324	0.2208	3.21	-	1.18	0.43	Skulski and Percival, 1996	GSC
174	SNB93-004	34I	18	n.a.	n.a.	Gabbro	2.786	U-Pb age	0.51352	0.2385	2.19	-	0.64	1.62	Skulski and Percival, 1996	GSC
175	SNB93-007	34I	18	n.a.	n.a.	Andesitic basalt	2.786	interpreted	0.51294	0.2091	1.50	-	7.38	2.55	Skulski and Percival, 1996	GSC
176	SNB93-009	34I	18	n.a.	n.a.	Basalt	2.724	interpreted	0.51173	0.1440	0.83	-	3.04	12.75	Skulski and Percival, 1996	GSC
177	SNB93-010	34I	18	n.a.	n.a.	Gabbro	2.724	interpreted	0.51204	0.1642	-0.20	-	2.09	7.70	Skulski and Percival, 1996	GSC
178	SNB93-013	34I	18	n.a.	n.a.	Peridotite	2.724	interpreted	0.51098	0.1206	-5.79	3.39	0.58	2.90	Skulski and Percival, 1996	GSC
179	SNB93-016	34I	18	n.a.	n.a.	Andesitic basalt	2.786	interpreted	0.51290	0.2053	2.04	-	8.41	2.85	Skulski and Percival, 1996	GSC
180	SNB93-12	34I	18	n.a.	n.a.	Rhyolite	2.724	U-Pb age	0.51097	0.1079	-1.40	3.00	93.32	16.67	Skulski and Percival, 1996	GSC
181	SNB-93-14	34I	18	n.a.	n.a.	Andesite	2.724	interpreted	0.51136	0.1207	1.71	2.78	14.45	2.89	Skulski and Percival, 1996	GSC
182	SNB-93-14	34I	18	n.a.	n.a.	Andesite	2.724	interpreted	0.51136	0.1207	1.71	2.78	14.45	2.89	Skulski and Percival, 1996	GSC
183	PBAC94-113	34J	18	545878	6484235	Tonalite	2.782	U-Pb age	0.51085	0.0924	2.50	2.77	9.80	1.50	Skulski *et al.*, 1996	GSC
184	PBAC94-158	34J	18	529646	6481707	Felsic volcanic	2.757	U-Pb age	0.51068	0.0832	2.02	2.78	24.00	3.30	Skulski *et al.*, 1996	GSC
185	PBAS94-150A	n.a.	18	n.a.	n.a.	Orthopyroxenite	2.780	interpreted	0.51134	0.1207	1.84	2.82	9.80	1.90	Skulski *et al.*, 1996	GSC
186	PBAS94-150B	n.a.	18	n.a.	n.a.	Hornblendite	2.780	interpreted	0.51138	0.1256	0.97	2.89	33.00	6.60	Skulski *et al.*, 1996	GSC
187	PBAS94-150C	n.a.	18	n.a.	n.a.	Pyroxenite	2.780	interpreted	0.51152	0.1325	1.08	2.89	15.00	3.30	Skulski *et al.*, 1996	GSC
188	PBAS94-502	34O	18	503545	6558903	Syenite	2.643	U-Pb age	0.51084	0.0913	0.86	2.75	1.30	0.23	Skulski *et al.*, 1996	GSC
189	PBAS94-763	n.a.	18	n.a.	n.a.	Basalt	2.830	interpreted	0.51308	0.2135	2.42	-	6.30	2.10	Skulski *et al.*, 1996	GSC
190	PBAW94-290	34O	18	498555	6630551	Granodiorite	2.831	U-Pb age	0.51113	0.1082	2.83	2.78	40.00	7.00	Skulski *et al.*, 1996	GSC
191	PBAW94-293	34O	18	498124	6630932	Mafic-UM rock	2.729	U-Pb age	0.51117	0.1094	1.97	2.76	14.00	2.70	Skulski *et al.*, 1996	GSC
192	SNB93-131	n.a.	18	n.a.	n.a.	Andesite	2.760	interpreted	0.51137	0.1271	-0.08	2.97	16.00	3.40	Skulski *et al.*, 1996	GSC
193	SNB93-240	34J	18	501670	6502706	Granite	2.725	U-Pb age	0.51045	0.0750	0.08	2.85	3.80	0.53	Skulski *et al.*, 1996	GSC
194	SNB93-94	34J	18	529646	6481707	Felsic volcanic	2.759	U-Pb age	0.51097	0.1050	0.11	2.91	13.00	2.10	Skulski *et al.*, 1996	GSC
195	SNB93-95	34J	18	530296	6481401	Granodiorite	2.733	U-Pb age	0.51081	0.0995	-1.49	2.99	14.00	2.30	Skulski *et al.*, 1996	GSC
196	GS3-12	34I	18	669998	6453208	Granodiorite	2.725	interpreted	0.51026	0.0634	0.42	2.83	32.90	3.45	Stern *et al.*, 1994	GSC
197	GSI-15	34I	18	663058	6448900	Mafic dyke	2.725	interpreted	0.51099	0.1040	0.40	2.86	46.89	8.06	Stern *et al.*, 1994	GSC
198	GSI-16	34I	18	663058	6448900	Mafic dyke	2.725	interpreted	0.51095	0.1013	0.56	2.85	31.50	6.28	Stern *et al.*, 1994	GSC
199	GSI-17	34I	18	663058	6448900	Mafic dyke	2.725	interpreted	0.51119	0.1152	0.29	2.89	37.63	1.12	Stern *et al.*, 1994	GSC
200	GSI-3	34I	18	663058	6448900	Enderbite	2.725	interpreted	0.51091	0.1011	-0.26	2.90	23.88	4.00	Stern *et al.*, 1994	GSC
201	GSI-5	34I	18	663058	6448900	Mafic dyke	2.725	interpreted	0.51115	0.1110	0.94	2.83	31.82	5.85	Stern *et al.*, 1994	GSC
202	GSI-6	34I	18	663058	6448900	Mafic dyke	2.725	interpreted	0.51103	0.1070	0.13	2.89	51.01	9.05	Stern *et al.*, 1994	GSC
203	PBA-89-28B	34G	18	492439	6335269	Diatexite	2.713	interpreted	0.51099	0.1044	0.11	2.87	28.01	4.84	Stern *et al.*, 1994	GSC
204	PBA-89-50	34G	18	525000	6381875	Diatexite	2.713	interpreted	0.51077	0.0917	0.15	2.86	9.57	1.45	Stern *et al.*, 1994	GSC

TABLE 4.4 - Nd isotopic composition of volcanic and plutonic rocks in the NESP (continued).

No.	Sample	NTS	Zone	UTM NAD83		Rock type	Age (Ga)		$^{143}Nd/^{144}Nd$	$^{147}Sm/^{144}Nd$	εNd(t)	Tdm	Nd	Sm	Reference	Laboratory
				Easting	Northing							(Ga)	(ppm)	(ppm)		
205	PBA-89-56A	34G	18	543461	6372138	Tonalite	3.125	interpreted	0.51004	0.0776	-2.64	3.35	31.68	4.07	Stern *et al.*, 1994	GSC
206	PBA-89-56B	34G	18	543461	6372138	Tonalite	3.125	interpreted	0.51006	0.0778	-2.49	3.34	28.26	3.64	Stern *et al.*, 1994	GSC
207	PBA-89-77C	34G	18	545555	6451028	Mafic-UM rock	2.725	interpreted	0.51083	0.0940	0.76	2.83	33.69	5.23	Stern *et al.*, 1994	GSC
208	PBA-90-136A	34G	18	472900	6333450	Granite	2.690	interpreted	0.51071	0.0908	-0.91	2.90	34.27	5.15	Stern *et al.*, 1994	GSC
209	PBA-90-137A	34G	18	487850	6344300	Granodiorite	2.725	interpreted	0.51158	0.1361	0.63	2.90	23.13	5.21	Stern *et al.*, 1994	GSC
210	PBA-91-125	34I	18	615588	6450226	Peridotite	2.786	interpreted	0.51259	0.1887	1.86	-	1.25	0.39	Stern *et al.*, 1994	GSC
211	PBA-91-170	34I	18	615492	6450256	Peridotite	2.786	interpreted	0.51285	0.2045	1.32	-	1.50	0.51	Stern *et al.*, 1994	GSC
212	PBA-91-185	34I	18	614208	6440963	Andesite	2.724	interpreted	0.51131	0.1215	0.52	2.88	15.41	3.10	Stern *et al.*, 1994	GSC
213	PBA-91-187	34I	18	617419	6443223	Andesitic basalt	2.724	interpreted	0.51122	0.1169	0.36	2.88	30.80	5.96	Stern *et al.*, 1994	GSC
214	PBA-91-188	34I	18	618473	6443564	Andesite	2.724	interpreted	0.51131	0.1241	-0.45	2.96	25.07	5.15	Stern *et al.*, 1994	GSC
215	PBAB-89-65	34G	18	558000	6397200	Mafic-UM rock	2.725	interpreted	0.51170	0.1427	0.64	-	13.13	3.24	Stern *et al.*, 1994	GSC
216	PBAC-89-76	34B	18	454250	6303950	Granite	2.690	interpreted	0.51071	0.0970	-3.15	3.06	54.47	8.14	Stern *et al.*, 1994	GSC
217	PBAS-89.74	34G	18	487700	6345500	Granodiorite	2.725	interpreted	0.51065	0.0854	0.32	2.85	50.26	7.10	Stern *et al.*, 1994	GSC
218	PBAS-89-11	34G	18	486884	6327366	Granodiorite	2.725	interpreted	0.51125	0.1180	0.45	2.88	43.65	8.52	Stern *et al.*, 1994	GSC
219	PBAS-89-14	34G	18	464450	6375900	Enderbite	2.725	interpreted	0.51089	0.0965	0.98	2.82	10.20	1.63	Stern *et al.*, 1994	GSC
220	PBAS-89-19	34G	18	454688	6378671	Granite	2.690	interpreted	0.51085	0.1013	-1.82	2.98	25.34	4.24	Stern *et al.*, 1994	GSC
221	PBAS-89-21D	34G	18	472838	6374797	Enderbite	2.725	interpreted	0.51074	0.0888	0.78	2.82	9.42	1.38	Stern *et al.*, 1994	GSC
222	PBAS-89-23	34G	18	470718	6377609	Enclave mafique	2.725	interpreted	0.51129	0.1190	0.98	2.84	21.83	4.30	Stern *et al.*, 1994	GSC
223	PBAS-89-24	34G	18	469733	6381589	Enclave mafique	2.725	interpreted	0.51223	0.1713	0.88	-	11.10	3.14	Stern *et al.*, 1994	GSC
224	PBAS-89-28	34G	18	480612	6377255	Enderbite	2.725	interpreted	0.51056	0.0801	0.40	2.84	6.02	0.80	Stern *et al.*, 1994	GSC
225	PBAS-89-29B	34G	18	478146	6375399	Enderbite	2.725	interpreted	0.51063	0.0833	0.63	2.83	21.16	2.92	Stern *et al.*, 1994	GSC
226	PBAS-89-34	34G	18	496327	6412924	Paragneiss	2.700	interpreted	0.51116	0.1166	-0.98	2.97	17.45	3.37	Stern *et al.*, 1994	GSC
227	PBAS-89-42	34G	18	503499	6359404	Granite	2.690	interpreted	0.51080	0.0949	-0.62	2.89	39.50	6.20	Stern *et al.*, 1994	GSC
228	PBAS-89-46	34G	18	511159	6357034	Enderbite	2.725	interpreted	0.51096	0.0999	1.18	2.81	4.94	0.82	Stern *et al.*, 1994	GSC
229	PBAS-89-47	34G	18	522738	6356086	Enderbite	2.725	interpreted	0.51126	0.1171	1.01	2.83	25.21	4.89	Stern *et al.*, 1994	GSC
230	PBAS-89-51	34G	18	526116	6354825	Enderbite	2.725	interpreted	0.51102	0.1032	1.13	2.81	25.67	4.39	Stern *et al.*, 1994	GSC
231	PBAS-89-53	34G	18	514788	6370795	Enderbite	2.725	interpreted	0.51097	0.1002	1.34	2.80	11.03	1.83	Stern *et al.*, 1994	GSC
232	PBAS-89-55	34G	18	516581	6357859	Enderbite	2.725	interpreted	0.51128	0.1184	0.91	2.84	27.77	5.44	Stern *et al.*, 1994	GSC
233	PBAS-89-57	34G	18	511074	6348199	Enclave mafique	2.725	interpreted	0.51296	0.2062	3.03	-	4.50	1.54	Stern *et al.*, 1994	GSC
234	PBAS-89-59	34G	18	525485	6409712	Mafic-UM rock	2.725	interpreted	0.51094	0.1018	0.18	2.88	1.98	1.34	Stern *et al.*, 1994	GSC
235	PBAS-89-60	34G	18	525304	6410329	Mafic-UM rock	2.725	interpreted	0.51106	0.1093	-0.03	2.90	16.16	3.03	Stern *et al.*, 1994	GSC
236	PBAS-89-61	34G	18	524699	6409743	Mafic-UM rock	2.725	interpreted	0.51097	0.1038	-0.04	2.89	9.00	1.55	Stern *et al.*, 1994	GSC
237	PBAS-89-62	34G	18	525158	6410020	Mafic-UM rock	2.725	interpreted	0.51185	0.1509	0.76	-	6.44	1.61	Stern *et al.*, 1994	GSC
238	PBAS-89-63	34G	18	524360	6410347	Mafic-UM rock	2.725	interpreted	0.51110	0.1099	0.38	2.87	18.98	3.45	Stern *et al.*, 1994	GSC

TABLE 4.4 - Nd isotopic composition of volcanic and plutonic rocks in the NESP (continued).

No.	Sample	NTS	Zone	UTM NAD83		Rock type	Age (Ga)		$^{143}Nd/^{144}Nd$	$^{147}Sm/^{144}Nd$	εNd(t)	Tdm	Nd	Sm	Reference	Laboratory
				Easting	Northing							(Ga)	(ppm)	(ppm)		
239	PBAS-89-64	34G	18	524360	6410347	Mafic-UM rock	2.725	interpreted	0.51081	0.0925	0.83	2.82	19.95	3.05	Stern *et al.*, 1994	GSC
240	PBAS-89-65	34G	18	525212	6408684	Enderbite	2.688	interpreted	0.51047	0.0724	0.65	2.79	13.77	1.65	Stern *et al.*, 1994	GSC
241	PBAS-89-7	34G	18	494850	6338750	Granodiorite	2.725	interpreted	0.51088	0.0973	0.53	2.85	30.68	4.94	Stern *et al.*, 1994	GSC
242	PBAS-89-70	34G	18	525466	6405640	Enderbite	2.688	U-Pb age	0.51052	0.0778	-0.17	2.84	10.29	1.33	Stern *et al.*, 1994	GSC
243	PBAS-89-71	34G	18	524480	6408945	Enderbite	2.688	interpreted	0.51040	0.0687	0.71	2.78	8.00	0.91	Stern *et al.*, 1994	GSC
244	PBAS-89-75	34G	18	487800	6345850	Mafic-UM rock	2.725	interpreted	0.51152	0.1329	0.66	2.89	11.14	3.17	Stern *et al.*, 1994	GSC
245	PBAS-89-76	34G	18	488900	6345800	Granodiorite	2.725	interpreted	0.51142	0.1274	0.46	2.90	35.82	7.55	Stern *et al.*, 1994	GSC
246	PBAS-89-77	34G	18	491850	6345400	Mafic-UM rock	2.725	interpreted	0.51133	0.1220	0.73	2.86	20.22	4.02	Stern *et al.*, 1994	GSC
247	PBAS-89-78	34G	18	542500	6371500	Diatexite	2.713	interpreted	0.51035	0.0735	-1.68	2.94	15.43	1.82	Stern *et al.*, 1994	GSC
248	PBAS-89-81	34G	18	556676	6376769	Enderbite	2.725	interpreted	0.51041	0.0692	1.32	2.78	14.29	1.64	Stern *et al.*, 1994	GSC
249	PBAS-89-9	34B	18	484800	6313500	Granodiorite	2.725	interpreted	0.51059	0.0831	-0.18	2.88	22.37	3.08	Stern *et al.*, 1994	GSC
250	PBAS-90-100	34I	18	665775	6452573	Granodiorite	2.725	interpreted	0.51078	0.0930	0.04	2.87	29.87	4.60	Stern *et al.*, 1994	GSC
251	PBAS-90-101	34I	18	669735	6454498	Granodiorite	2.725	interpreted	0.51081	0.0942	0.23	2.86	31.35	4.89	Stern *et al.*, 1994	GSC
252	PBAS-90-107	34I	18	651697	6478412	Mafic-UM rock	2.725	interpreted	0.51156	0.1334	1.09	2.85	32.52	1.19	Stern *et al.*, 1994	GSC
253	PBAS-90-111	24L	19	379722	6493171	Granodiorite	2.725	interpreted	0.51102	0.1082	-0.48	2.93	44.48	7.96	Stern *et al.*, 1994	GSC
254	PBAS-90-112	34I	18	666643	6451296	Granodiorite	2.725	interpreted	0.51081	0.0958	-0.25	2.90	33.27	5.27	Stern *et al.*, 1994	GSC
255	PBAS-90-113	24L	19	355148	6457298	Granodiorite	2.725	interpreted	0.51061	0.0824	0.60	2.83	52.79	7.20	Stern *et al.*, 1994	GSC
256	PBAS-90-116	34I	18	634970	6442589	Tonalite	2.950	interpreted	0.51057	0.0859	1.84	2.95	11.55	1.64	Stern *et al.*, 1994	GSC
257	PBAS-90-117	34I	18	634213	6444375	n.a.	2.790	interpreted	0.51134	0.1264	0.01	2.98	27.25	5.70	Stern *et al.*, 1994	GSC
258	PBAS-90-118	34H	18	645332	6421425	Paragneiss	2.700	interpreted	0.51058	0.0903	-3.22	3.05	6.51	0.97	Stern et al., 1994	GSC
259	PBAS-90-82	34I	18	671688	6456996	Granodiorite	2.725	interpreted	0.51089	0.1003	-0.25	2.90	34.63	5.75	Stern *et al.*, 1994	GSC
260	PBAS-90-89	24L	19	329991	6465680	Granodiorite	2.725	interpreted	0.51050	0.0788	-0.31	2.88	30.20	3.94	Stern *et al.*, 1994	GSC
261	PBAS-90-93	34I	18	655129	6444516	Enderbite	2.725	interpreted	0.51067	0.0882	-0.41	2.90	24.07	3.51	Stern *et al.*, 1994	GSC
262	PBAS-90-95	34I	18	644715	6440405	Granite	2.690	interpreted	0.51084	0.1036	-2.81	3.05	18.72	3.21	Stern *et al.*, 1994	GSC
263	PBAS-90-99	34I	18	664430	6450667	Enderbite	2.725	interpreted	0.51056	0.0820	-0.39	2.89	18.11	2.46	Stern *et al.*, 1994	GSC
264	S-89-68	34G	18	525010	6407000	Mafic dyke	2.688	interpreted	0.51106	0.1044	1.07	2.79	33.77	5.83	Stern *et al.*, 1994	GSC
265	2001025901	34K	18	354476	6526940	Enderbite	2.732	U-Pb age	0.51079	0.1004	-2.30	3.04	13.10	2.18	Stevenson *et al.*, 2006	GEOTOP-UQAM-McGill
266	2001025902	34K	18	343858	6461555	Tonalite	2.750	U-Pb age	0.51035	0.0808	-3.55	3.09	7.29	0.98	Stevenson *et al.*, 2006	GEOTOP-UQAM-McGill
267	2001025905	34K	18	377512	6499620	Granodiorite	2.720	interpreted	0.51109	0.1172	-2.44	3.10	10.70	2.08	Stevenson *et al.*, 2006	GEOTOP-UQAM-McGill
268	2001025906	34K	18	356381	6505078	Tonalite	2.820	interpreted	0.51026	0.0737	-1.76	3.03	8.46	1.03	Stevenson *et al.*, 2006	GEOTOP-UQAM-McGill
269	2001025907	34K	18	360102	6534551	Tonalite	2.840	U-Pb age	0.51024	0.0704	-0.61	2.99	9.45	1.10	Stevenson *et al.*, 2006	GEOTOP-UQAM-McGill
270	2001025908	34K	18	407893	6480635	Granodiorite	2.720	interpreted	0.51063	0.0904	-1.91	2.99	16.10	2.41	Stevenson *et al.*, 2006	GEOTOP-UQAM-McGill
271	2001025911	34K	18	435462	6492525	Granite	2.720	interpreted	0.51047	0.0785	-0.93	2.91	54.70	7.11	Stevenson *et al.*, 2006	GEOTOP-UQAM-McGill
272	2001025912	34L	17	654121	6490978	Tonalite	2.714	U-Pb age	0.51077	0.0995	-2.46	3.04	17.60	2.90	Stevenson *et al.*, 2006	GEOTOP-UQAM-McGill

TABLE 4.4 - Nd isotopic composition of volcanic and plutonic rocks in the NESP (continued).

No.	Sample	NTS	Zone	UTM NAD83		Rock type	Age (Ga)		$^{143}Nd/^{144}Nd$	$^{147}Sm/^{144}Nd$	εNd(t)	Tdm	Nd	Sm	Reference	Laboratory
				Easting	Northing							(Ga)	(ppm)	(ppm)		
273	2001025913	34L	17	662720	6496472	Granite	2.720	interpreted	0.50994	0.0596	-4.70	3.07	72.00	7.10	Stevenson *et al.*, 2006	GEOTOP-UQAM-McGill
274	2001025914	34L	17	645719	6536724	Tonalite	2.691	interpreted	0.51017	0.0671	-3.28	2.99	22.20	2.47	Stevenson *et al.*, 2006	GEOTOP-UQAM-McGill
275	2001032793	34K	18	388253	6498083	Granodiorite	2.720	interpreted	0.51027	0.0747	-3.58	3.05	19.60	2.42	Stevenson *et al.*, 2006	GEOTOP-UQAM-McGill
276	2001032884	34K	18	441033	6468509	Tonalite	2.820	interpreted	0.51064	0.0843	1.89	2.84	44.70	6.24	Stevenson *et al.*, 2006	GEOTOP-UQAM-McGill
277	2001032899	34K	18	425895	6494097	Granodiorite	2.720	interpreted	0.51044	0.0909	-5.95	3.24	14.50	2.18	Stevenson *et al.*, 2006	GEOTOP-UQAM-McGill
278	2001032903	34K	18	429150	6459703	Granodiorite	2.720	interpreted	0.51038	0.0727	-0.74	2.89	7.23	0.87	Stevenson *et al.*, 2006	GEOTOP-UQAM-McGill
279	2001032906	34K	18	432938	6531053	Tonalite	2.820	interpreted	0.51072	0.0922	0.44	2.93	17.30	2.64	Stevenson *et al.*, 2006	GEOTOP-UQAM-McGill
280	2001032908	34K	18	420746	6509377	Granodiorite	2.720	interpreted	0.51036	0.0732	-1.29	2.92	17.30	2.10	Stevenson *et al.*, 2006	GEOTOP-UQAM-McGill
281	2001032911	34K	18	409153	6494847	Granodiorite	2.720	interpreted	0.51040	0.0762	-1.58	2.94	28.00	3.53	Stevenson *et al.*, 2006	GEOTOP-UQAM-McGill
282	2001032938	34K	18	397289	6508144	Enderbite	2.732	interpreted	0.51039	0.0803	-2.88	3.03	11.10	1.47	Stevenson *et al.*, 2006	GEOTOP-UQAM-McGill
283	01-MP-1102A	34L	17	661623	6496799	Tonalite	2.691	interpreted	0.51010	0.0847	-10.85	3.47	11.70	1.64	Stevenson *et al.*, 2006	GEOTOP-UQAM-McGill
284	01-MP-1102B	34L	17	661623	6496799	Granite	2.691	interpreted	0.50998	0.0641	-6.04	3.12	6.49	0.69	Stevenson *et al.*, 2006	GEOTOP-UQAM-McGill
285	01-MP-1115A	34L	17	658133	6530829	Tonalite	2.691	interpreted	0.51042	0.0876	-5.52	3.17	14.40	2.09	Stevenson *et al.*, 2006	GEOTOP-UQAM-McGill
286	01-XH-6060A	34K	18	320806	6518621	Enderbite	2.732	interpreted	0.51049	0.0805	-1.08	2.93	22.60	3.01	Stevenson *et al.*, 2006	GEOTOP-UQAM-McGill
287	01-XH-6188A	34L	17	662944	6502871	Granodiorite	2.720	interpreted	0.51004	0.0626	-3.79	3.03	52.80	5.47	Stevenson *et al.*, 2006	GEOTOP-UQAM-McGill
288	1046B	24M	19	354134	6551120	Charnockite	2.735	interpreted	0.51317	0.2184	2.83	-	1.90	5.26	Boily *et al.*, 2009	GEOTOP-UQAM-McGill
289	1058F	24M	19	376216	6552339	Diorite	2.697	interpreted	0.51111	0.1124	-0.53	2.92	5.92	31.83	Boily *et al.*, 2009	GEOTOP-UQAM-McGill
290	1064D	24M	19	381922	6551773	Enderbite	2.735	interpreted	0.51085	0.1069	-3.30	3.14	6.04	34.13	Boily *et al.*, 2009	GEOTOP-UQAM-McGill
291	1074A2	24M	19	333747	6597151	Tonalite	2.779	interpreted	0.51091	0.1042	-0.67	2.98	3.2	18.55	Boily *et al.*, 2009	GEOTOP-UQAM-McGill
292	1077A	24M	19	331118	6597585	Tonalite	2.779	interpreted	0.51127	0.1209	0.41	2.93	4.8	23.99	Boily *et al.*, 2009	GEOTOP-UQAM-McGill
293	1102A	24M	19	347838	6652435	Diorite	2.697	interpreted	0.51073	0.0886	0.29	2.83	11.84	80.75	Boily *et al.*, 2009	GEOTOP-UQAM-McGill
294	2146C	24M	19	357297	6642370	Basalt	2.800	interpreted	0.51276	0.1980	1.98	-	2.04	6.23	Boily *et al.*, 2009	GEOTOP-UQAM-McGill
295	2250F	24M	19	435723	6645611	Felsic tuff	2.800	interpreted	0.51102	0.1025	2.39	2.79	3.9	22.99	Boily *et al.*, 2009	GEOTOP-UQAM-McGill
296	3002A	24M	19	397135	6595620	Gabbronorite	2.730	interpreted	0.51123	0.1177	0.30	2.86	3.47	17.81	Boily *et al.*, 2009	GEOTOP-UQAM-McGill
297	3003B	24M	19	398712	6595510	Diorite	2.697	interpreted	0.51103	0.1039	0.67	2.82	8.05	46.83	Boily *et al.*, 2009	GEOTOP-UQAM-McGill
298	3026A	24M	19	413450	6587172	Gabbronorite	2.730	interpreted	0.51090	0.0981	0.71	2.84	7.54	46.45	Boily *et al.*, 2009	GEOTOP-UQAM-McGill
299	3029A	24M	19	415996	6587634	Enderbite	2.735	interpreted	0.51072	0.0996	-3.29	3.11	3.60	21.84	Boily *et al.*, 2009	GEOTOP-UQAM-McGill
300	3044B	24M	19	378995	6588875	Gabbronorite	2.730	interpreted	0.51126	0.1205	-0.20	2.94	3.87	19.41	Boily *et al.*, 2009	GEOTOP-UQAM-McGill
301	3046B	24M	19	378253	6588364	Basalt	2.805	interpreted	0.51265	0.1919	2.00	-	2.54	8.00	Boily *et al.*, 2009	GEOTOP-UQAM-McGill
302	3058A	24M	19	346264	6547919	Tonalite	2.779	interpreted	0.51021	0.0668	-0.97	2.95	3.77	34.08	Boily *et al.*, 2009	GEOTOP-UQAM-McGill
303	3065A	24M	19	332852	6642167	Granodiorite	2.779	interpreted	0.51056	0.0812	0.88	2.86	8.13	60.52	Boily *et al.*, 2009	GEOTOP-UQAM-McGill
304	3070A	24M	19	337966	6641377	Tonalite	2.779	interpreted	0.51113	0.1112	1.09	2.87	9.33	50.69	Boily *et al.*, 2009	GEOTOP-UQAM-McGill
305	3076A	24M	19	342925	6643501	Tonalite	2.779	interpreted	0.51014	0.0539	2.32	2.78	0.33	3.7	Boily *et al.*, 2009	GEOTOP-UQAM-McGill
306	3079A2	24M	19	377500	6628437	Trondjhemite	2.779	interpreted	0.51048	0.0769	0.76	2.86	0.83	6.52	Boily *et al.*, 2009	GEOTOP-UQAM-McGill

TABLE 4.4 - Nd isotopic composition of volcanic and plutonic rocks in the NESP (concluded).

No.	Sample	NTS	Zone	UTM NAD83		Rock type	Age (Ga)		$^{143}Nd/^{144}Nd$	$^{147}Sm/^{144}Nd$	εNd(t)	Tdm	Nd	Sm	Reference	Laboratory
				Easting	Northing							(Ga)	(ppm)	(ppm)		
307	3079D1	24M	19	377500	6628437	Trondhjemite	2.779	interpreted	0.51024	0.0633	0.07	2.85	1.01	9.64	Boily *et al.*, 2009	GEOTOP-UQAM-McGill
308	3079D2	24M	19	377500	6628437	Trondhjemite	2.779	interpreted	0.51057	0.0832	0.19	2.9	1.78	12.92	Boily *et al.*, 2009	GEOTOP-UQAM-McGill
309	3087A	24M	19	425235	6631816	Tonalite	2.779	interpreted	0.51025	0.0686	-0.76	2.94	2.56	22.56	Boily *et al.*, 2009	GEOTOP-UQAM-McGill
310	3094A	24M	19	389870	6651231	Trondhjemite	2.779	interpreted	0.51047	0.0077	0.54	2.88	0.169	13.29	Boily *et al.*, 2009	GEOTOP-UQAM-McGill
311	3102A	24M	19	396704	6651676	Monzogranite	2.735	interpreted	0.51141	0.1253	1.20	2.84	1.86	8.97	Boily *et al.*, 2009	GEOTOP-UQAM-McGill
312	3117A	24M	19	347155	6624901	Paragneiss	2.720	interpreted	0.51080	0.0937	0.21	2.86	4.46	28.75	Boily *et al.*, 2009	GEOTOP-UQAM-McGill
313	3155A	24M	19	426508	6559769	Monzonite	2.697	interpreted	0.51086	0.0982	-0.50	2.89	9.06	55.78	Boily *et al.*, 2009	GEOTOP-UQAM-McGill
314	3202C	24M	19	406665	6544640	Monzonite	2.697	interpreted	0.51108	0.1132	-1.39	2.99	4.98	26.59	Boily *et al.*, 2009	GEOTOP-UQAM-McGill
315	3206B3	24M	19	394583	6604457	Dunite	2.815	interpreted	0.51158	0.1351	1.66	-	0.19	0.85	Boily *et al.*, 2009	GEOTOP-UQAM-McGill
316	3216D	24M	19	332242	6611252	Komatiite	2.810	interpreted	0.51231	0.1779	0.46	-	0.93	3.16	Boily *et al.*, 2009	GEOTOP-UQAM-McGill
317	3217A	24M	19	331976	6612866	Basalt	2.800	interpreted	0.51288	0.2026	2.53	-	1.9	5.67	Boily *et al.*, 2009	GEOTOP-UQAM-McGill
318	3226B	24M	19	352148	6623987	Peridotite	2.815	interpreted	0.51311	0.2173	1.74	-	0.55	1.53	Boily *et al.*, 2009	GEOTOP-UQAM-McGill
319	3230A2	24M	19	381005	6645671	Tonalite	2.779	interpreted	0.51126	0.0698	0.30	2.88	1.04	9.00	Boily *et al.*, 2009	GEOTOP-UQAM-McGill
320	3242B	24M	19	411440	6579927	Gabbronorite	2.730	interpreted	0.51091	0.1038	-1.01	2.97	13.52	78.71	Boily *et al.*, 2009	GEOTOP-UQAM-McGill
321	3249A	24M	19	405105	6579389	Monzonite	2.697	interpreted	0.51094	0.1036	-0.74	2.91	10.00	58.35	Boily *et al.*, 2009	GEOTOP-UQAM-McGill
322	3256D	24M	19	388926	6543232	Basalt	2.730	interpreted	0.51114	0.1106	1.01	2.83	4.68	25.58	Boily *et al.*, 2009	GEOTOP-UQAM-McGill
323	3258A	24M	19	367134	6563300	Monzonite	2.697	interpreted	0.51105	0.1108	-1.27	2.97	7.05	38.45	Boily *et al.*, 2009	GEOTOP-UQAM-McGill
324	3266A	24M	19	374675	6565340	Enderbite	2.735	interpreted	0.51077	0.0956	-0.77	2.94	1.99	12.58	Boily *et al.*, 2009	GEOTOP-UQAM-McGill
325	3288B	24M	19	438618	6602060	Trondhjemite	2.779	interpreted	0.51047	0.0817	0.19	2.98	0.97	7.17	Boily *et al.*, 2009	GEOTOP-UQAM-McGill
326	3327A	24M	19	412733	6643361	Basalt	2.800	interpreted	0.51234	0.1784	0.80	-	4.07	13.79	Boily *et al.*, 2009	GEOTOP-UQAM-McGill
327	3350C	24M	19	412993	6586208	Basalt	2.800	interpreted	0.51264	0.1915	2.01	-	2.23	7.04	Boily *et al.*, 2009	GEOTOP-UQAM-McGill
328	4072A	24M	19	382346	6642315	Enderbite	2.733	interpreted	0.51100	0.1082	-0.78	2.96	3.47	19.38	Boily *et al.*, 2009	GEOTOP-UQAM-McGill
329	4113B	24M	19	386431	6630551	Monzogranite	2.735	interpreted	0.51105	0.1051	1.24	2.82	3.00	17.25	Boily *et al.*, 2009	GEOTOP-UQAM-McGill
330	5058B4	24M	19	331625	6601959	Basalt	2.800	interpreted	0.51272	0.1918	3.46	-	2.23	7.03	Boily *et al.*, 2009	GEOTOP-UQAM-McGill
331	6075A	24M	19	416484	6633292	Tonalite	2.779	interpreted	0.51135	0.1258	0.20	2.96	2.86	13.74	Boily *et al.*, 2009	GEOTOP-UQAM-McGill
332	6127A	24M	19	420246	6542277	Monzonite	2.697	interpreted	0.51089	0.1047	-2.19	3.02	7.59	43.79	Boily *et al.*, 2009	GEOTOP-UQAM-McGill
333	6130B	24M	19	422928	6543682	Diorite	2.697	interpreted	0.51095	0.1054	-1.20	2.95	9.20	52.73	Boily *et al.*, 2009	GEOTOP-UQAM-McGill
334	6193C2	24M	19	337951	6624567	Komatiite	2.810	interpreted	0.51319	0.2186	2.89	-	0.64	1.77	Boily *et al.*, 2009	GEOTOP-UQAM-McGill
335	6264B	24M	19	331704	6547557	Pyroxenite	2.720	interpreted	0.51183	0.1397	4.11	-	3.37	14.58	Boily *et al.*, 2009	GEOTOP-UQAM-McGill
336	7033C	24M	19	333403	6573349	Trondhjemite	2.779	interpreted	0.51085	0.0990	1.18	2.93	0.99	6.04	Boily *et al.*, 2009	GEOTOP-UQAM-McGill
337	7176A	24M	19	367246	6620976	Felsic tuff	2.800	interpreted	0.51072	0.0858	2.49	2.79	8.07	56.84	Boily *et al.*, 2009	GEOTOP-UQAM-McGill
338	7177B	24M	19	367409	6620560	Basalt	2.800	interpreted	0.51259	0.1852	3.31	-	2.08	6.79	Boily *et al.*. 2009	GEOTOP-UQAM-McGill

CHAPTER 5
GEOLOGICAL EVOLUTION OF THE NORTHEASTERN SUPERIOR PROVINCE

Alain Leclair

The geological evolution of the northeastern Superior Province spans more than 1.2 billion years in the Archean eon. It is characterized by a complex history of volcanism, sedimentation, plutonism, and polyphase deformation and metamorphism; manifestations of episodic growth and repeated reworking of the continental crust from 3.82 to 2.62 Ga. The most important geological evidence preserved in the rocks of this region are: 1) the predominance of Neoarchean suites (about 90% of the bedrock); 2) the presence of Mesoarchean relicts; 3) the preservation of Eoarchean crustal remnants, including the oldest volcano-plutonic complex (3.8 to 3.6 Ga, Nuvvuagittuq Belt) recognized in the Superior Province.

One of the most significant features revealed by the Neoarchean rocks is the widespread recycling of extensive nuclei of Eoarchean and Mesoarchean basement. A review of model ages (T_{DM}) and inherited zircon ages obtained in these rocks confirms an interaction between early crustal components and younger magmatic suites, suggesting an efficient recycling process of crustal material throughout its evolution. Among the most distinctive characteristics of this part of the Superior, one may note:

- the presence of a significant proportion of variably recycled early crust (>2.80 Ga);
- the presence of numerous small greenstone belts scattered within voluminous tonalite-trondhjemite suites (2.88 to 2.72 Ga);
- the presence of numerous late plutons of granite, granodiorite, and pyroxene-bearing granitoid rocks, spread across the entire area (<2.74 Ga);
- a structural style dominated by steep fabrics enhanced by plutonic sheets generally trending NW-SE to N-S;
- the prevalence of high-temperature, low-pressure regional metamorphism.

The proposed evolution model for the study area involves the formation of early cratonic nuclei (3.9 to 2.9 Ga; Hudson Bay Terrane) and domains composed of volcanic and intrusive rocks derived from a younger juvenile crustal source (<3.0 Ga; Rivière Arnaud Terrane). Integration of geochronology (U/Pb) and isotope (Nd) data with the results of geological surveys enable us to interpret the extent of reworked paleocratons and to ascertain the geographic distribution of stratigraphic units related to each phase in the region's geological evolution (see chapters 3 and 4). A side-by-side comparison of the chronostratigraphy of the Hudson Bay and Rivière Arnaud terranes shows the two regions underwent distinct geological evolutions up until about 2.74 Ga (figures 3.1 and 5.1). The Hudson Bay Terrane formed on the remains of Eoarchean to Mesoarchean-age evolved sialic crust, whereas the Rivière Arnaud Terrane formed from a Mesoarchean primitive crust in an oceanic setting. Early volcanic and tonalitic gneiss complexes in the latter terrane were affected by the successive emplacement of tonalite-trondhjemite intrusions (TTG) until the early Neoarchean (about 2.74 Ga). Subsequently, the two terranes underwent a similar geological evolution, namely characterized by potassic (granite and granodiorite) and charnockitic (pyroxene-bearing granitoid) plutonism that spread across the entire NESP (Figure 3.2). This post-2.74 Ga plutonism coincides with the main phase of deformation responsible for the dominant NW-SE to N-S-trending structural fabric.

The interpretation of stratigraphic, geochronological, and isotopic data derived from supracrustal and igneous rocks leads us to recognize four major phases of crustal growth and reworking, each comprising up to three distinct geologic events (Figure 5.1). The **first phase** of evolution, from 3.9 to 2.9 Ga, is characterized by the formation of paleocratons and encompasses two Eoarchean magmatic events (EA-1 and EA-2) and one Mesoarchean event (MA-1) that remains cryptic. The **second phase,** constrained between 2.9 and 2.74 Ga, essentially corresponds to the deposition of tholeiitic basalt, komatiite, and sedimentary sequences, as well as the emplacement of voluminous tonalitic suites. This phase of evolution essentially comprises two Mesoarchean magmatic events (MA-2 and MA-3) and one Neoarchean event characterized by tonalitic magmatism that took place in a diachronous fashion on a regional scale (NA-1). The **third phase**, from 2.74 to 2.68 Ga, marks a major change in the type of magmatism, as evidenced by the emplacement of syn- to post-tectonic intrusions of granodiorite, granite, and pyroxene-bearing granitoid rocks. The two main Neoarchean plutonic events (NA-2 and NA-3) spread across most of the region. The **fourth phase** of evolution, between 2.68 and 2.62 Ga, counts only one event (NA-4) characterized by the emplacement of small, localized intrusions of granite, syenite, and carbonatite, as well as hydrothermal activity primarily channelled along ductile and brittle permeable zones. This phase also corresponds to a period of intense magmatic activity in the Ashuanipi Subprovince.

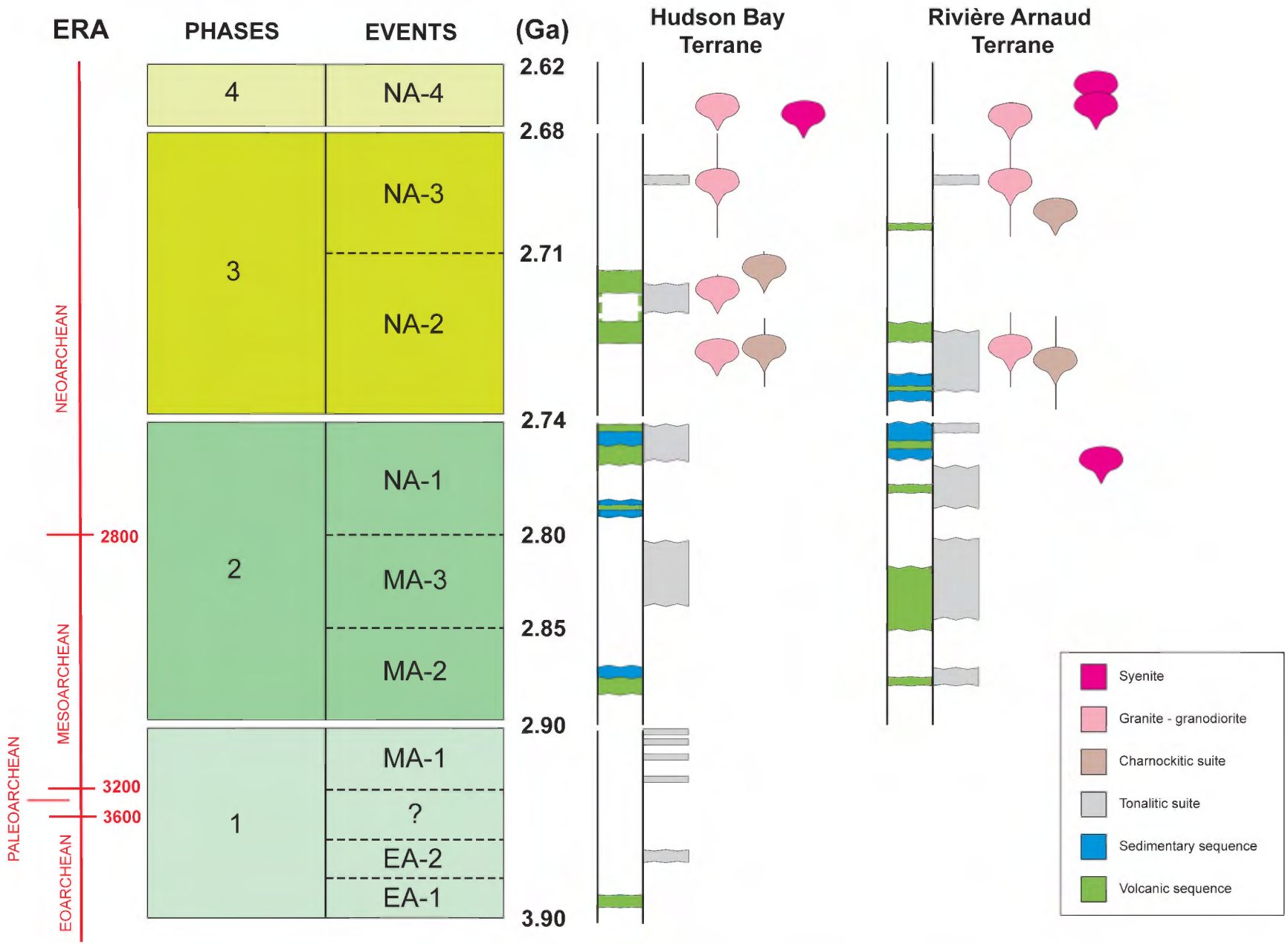

FIGURE 5.1 – Diagram illustrating the various events that occurred in the Hudson Bay and Rivière Arnaud terranes.

In this chapter, the main events associated with each of the four phases of crustal growth and reworking that occurred during the Archean eon in the NESP are described. Periodic pulses of magmatism and superposition of several phases of deformation have made it difficult to characterize the earliest events. No Paleoarchean rocks (from 3.60 to 3.20 Ga) have been recognized in the region. However, Nd isotope data and inherited zircon ages obtained in younger rocks reveal the presence of rocks from this time span, suggesting a Paleoarchean basement did indeed exist and was deeply recycled.

PHASE 1: FROM 3.9 TO 2.9 GA

The first phase in the Archean geological evolution of the northeastern Superior Province is mainly revealed by inherited zircon ages and Nd isotopic compositions suggesting the presence of reworked sialic crust as old as 3.9 Ga. The distribution of Nd model ages delineates the extent of paleocratons (3.9 to 2.9 Ga) in the Hudson Bay Terrane, as well as an early cratonic fragment (3.1 to 2.9 Ga) isolated within the Rivière Arnaud Terrane (Chapter 4). The gap between these ages suggests the presence of at least three extensive reworked segments derived from an Eoarchean to Mesoarchean basement (Figure 4.14). In the field, early crustal remnants composed of rocks dated between 3.9 and 2.9 Ga were recognized in a few locations but are restricted to the Hudson Bay Terrane (Chapter 3). These rocks document at least three major events (EA-1, EA-2, and MA-1; figures 3.1 and 5.1).

Event EA-1 (about 3.82 Ga)

The earliest magmatic event recorded in the NESP is represented by the volcanic rocks of the Nuvvuagittuq Belt. These rocks form a volcano-sedimentary sequence preserved in three isoclinal synforms located at the western edge of the Tikkerutuk Domain (Chapter 3). Volcanism was accompanied by deposition of volcaniclastic rocks, quartzite, conglomerate, and iron formation. Studies on the age and structure of this sequence indicate a complex history of magmatism and deformation that began in the Eoarchean, with the formation of volcanic rocks. A felsic horizon interpreted as a tuff was dated at 3825 ±16 Ma (David *et al.*, 2003; Nadeau, 2003). Subsequent geochronology studies have confirmed a minimum age of about 3.75 Ga for the same horizon (Cates and Mojzsis, 2007). The supracrustal rocks are cut by gabbroic and ultramafic sills. Geochemistry studies indicate the latter are derived from a mantle source that was already depleted at the time (O'Neil *et al.*, 2006a, 2007). Moreover, isotopic compositions suggest the iron formations are indeed chemically derived sediments, indicating the possibility that biogenetic processes were already at work in the Eoarchean (O'Neil *et al.*, 2006b, 2007). There is very little information available on the depositional and tectonic setting in which the volcano-sedimentary rocks of the Nuvvuagittuq Belt formed. Nevertheless, certain parallels may be drawn in terms of age and history of deposition and deformation between this belt and the Isua volcanic sequence in Greenland (about 3.8 to 3.7 Ga; Appel *et al.*, 2003). Recent isotopic studies (Böhm *et al.*, 2003; Skulski *et al.*, 2000; Stevenson *et al.*, 2006) indicate a possible regional correlation between the Nuvvuagittuq Belt and recycled Eoarchean crust recognized along the northwest margin of the Superior Province, in northern Ontario and Manitoba.

Event EA-2 (about 3.65 Ga)

The second Eoarchean magmatic event is recognized only in the westernmost part of the Tikkerutuk Domain, where gneissic tonalites dated at 3650 ±5 Ma (David *et al.*, 2004) form the external mylonitic border of one of the synforms in the Nuvvuagittuq Belt (Chapter 3). The tonalites are characterized by high-strain zones associated with L/S tectonites that exhibit a shallowly-plunging mineral lineation. These zones possibly correspond to thrust faults that developed either during the emplacement of tonalites, or prior to the emplacement of enclosing plutonic units (>2.75 Ga). Sm-Nd and Lu-Hf isotopic compositions suggest these gneissic tonalites are derived from the melting of earlier volcano-sedimentary rocks, most likely those of the Nuvvuagittuq Belt (Stevenson and Bizzarro, 2007).

Event MA-1 (3.20 to 2.90 Ga)

Event MA-1 (3.20 to 2.90 Ga) is recorded after a hiatus of more than 400 Ma, *i.e.* from 3.6 to 3.2 Ga, corresponding to the Paleoarchean era. This magmatic event is represented by tonalitic rocks occurring as small units or enclaves scattered within the Hudson Bay Terrane (Chapter 3). The majority of tonalitic gneisses dated between 3.12 and 2.90 Ga are exposed near the northern edge of the Goudalie Domain (Figure 3.3). In this area, a sequence in the Vizien Belt includes a tonalitic basement dated at 2940 ±5 Ma, which is unconformably overlain by much younger clastic sediments (<2718 Ma; Percival *et al.*, 1993). Another tonalitic remnant (3.02 Ga) is located within the Nastapoca deformation zone (Simard *et al.*, 2005b). The Nastapoca zone not only coincides with a major lithological change between the Bienville and Tikkerutuk domains, but it also corresponds to a major dichotomy in the structural trend to the north and south of the zone. It is possible that this deformation zone, which was probably reactivated on many occasions during the Neoarchean, may correspond to a paleosuture between Eoarchean to Mesoarchean cratonic nuclei, in which tectonic slivers of >3.0 Ga tonalitic crust have been preserved.

Isotopic data reveal the presence of an extensive reworked Mesoarchean basement, although the limited occurrence of >2.90 Ga Mesoarchean rocks is an indication of the intensity of this reworking. Nd isotopic compositions and inherited zircon ages suggest that between 3.20 and 2.90 Ga,

the continental crust was much more extensive than indicated by the few preserved remnants of tonalitic rock. Evidence of contamination by crust from this time span is concentrated within the Hudson Bay Terrane (figures 3.3 and 4.14). However, isotopic data provide evidence of interaction with a basement of equivalent age in the south part of the Douglas Harbour Domain, within the Rivière Arnaud Terrane (Figure 4.14). Considering that the history of the Rivière Arnaud Terrane began after 2.9 Ga (chapters 3 and 4), the paleocraton identified in the south part of the Douglas Harbour Domain either corresponds to a detached segment of the Hudson Bay Terrane, or to a cratonic nucleus around which the juvenile rocks of the Rivière Arnaud Terrane formed.

PHASE 2: FROM 2.90 TO 2.74 GA

The second phase in the geological evolution of the NESP, which comprises three major events (MA-2, MA-3, and NA-1; figures 3.1 and 5.1), is primarily represented by the emplacement of numerous volcano-sedimentary sequences and tonalite-trondhjemite-diorite suites (low-K TTG series; Chapter 4), the latter becoming progressively voluminous over time. Many supracrustal belts contain at least two distinct volcanic assemblages separated by unconformities that generally correspond to a time span of about 20 or 40 Ma. Phase 2 is namely characterized by the formation of continental crust derived from a juvenile <2.9 Ga source associated with the Rivière Arnaud Terrane. Volcano-sedimentary sequences occurring in this terrane are dominated by tholeiitic basalts intercalated with komatiites and mafic and ultramafic intrusions, and associated with felsic tuffs, rhyolites, clastic sediments, and iron formations (Chapter 3). This volcanism was followed by significant tonalitic magmatism (2790 to 2760 Ma) that affected the entire terrane and that contributed to the construction of the continental crust. The geological history of the Hudson Bay Terrane during this phase is marked primarily by the occurrence of widespread Neoarchean tonalitic magmatism (2.76 to 2.74 Ga).

Event MA-2 (2.90 to 2.85 Ga)

Mesoarchean event MA-2 is namely characterized by the formation of volcano-sedimentary sequences in the Gayot Complex and part of the Arnaud Complex, along the eastern margin of the Hudson Bay and Rivière Arnaud terranes (Chapter 3). Similar lithological assemblages and ages in the two sequences suggest a likely regional correlation. In addition, the geochemical signature of tholeiitic and komatiitic lavas in the two sequences are comparable to Al-undepleted komatiites in the Abitibi Subprovince (Chapter 4). These lavas exhibit juvenile isotopic signatures ($\varepsilon Nd_{(t)} >$ +0.80). In most cases, the komatiites and tholeiites may be interpreted as components of plateau-type oceanic crust (Boily *et al.*, 2009) that did not assimilate a significant volume of earlier rocks. On the other hand, inherited zircon ages (>2.90 Ga) and relatively enriched isotopic signatures ($\varepsilon Nd_{(t)}$ = -1.42 and -1.53) recorded in certain felsic tuffs (2.88 and 2.87 Ga) interlayered with komatiitic and tholeiitic lavas in the Gayot Complex suggest interaction with more evolved crust. Observed isotopic variations may possibly be related to the formation of a mantle plume that would have erupted through thinned continental crust represented by the eastern margin of the Hudson Bay Terrane, proximal to an oceanic basin. This oceanic crust may have extended several hundred kilometres further north, as suggested by correlations between the Gayot and Arnaud complexes.

Volcanism during event MA-2 is accompanied by the emplacement of tonalite-trondhjemite intrusions in the east part of the Rivière Arnaud Terrane (Chapter 3). This Mesoarchean tonalitic magmatism appears to be fairly limited, since all of the tonalite samples and inherited zircons with ages between 2.88 and 2.85 Ga occur in the vicinity of the Gayot and Arnaud complexes (with the exception of No. 198, Figure 3.4).

Event MA-3 (2.85 to 2.80 Ga)

Event MA-3 marks the end of the Mesoarchean era and is characterized by significant volcanic activity related to the formation of oceanic crust in the Rivière Arnaud Terrane. This activity resulted in the emplacement of some of the volcano-sedimentary sequences in the Qalluviartuuq-Payne, Duquet, and Arnaud complexes, and was accompanied by synvolcanic tonalitic magmatism (Chapter 3). Rocks in the Qalluviartuuq-Payne Complex comprise at least two volcanic cycles with juvenile isotopic compositions (Skulski *et al.*, 1996; Berclaz *et al.*, 2005; Leclerc, 2004; Chapter 4); a tholeiitic volcanic cycle (2.85 to 2.81 Ga) overlain by a calc-alkaline volcanic cycle of uncertain age. Tholeiitic basalts, rhyolites and felsic tuffs, as well as synvolcanic tonalites, which form volcano-plutonic assemblages (2.82 to 2.80 Ga) in the Duquet and Arnaud complexes, also show juvenile isotopic compositions ($\varepsilon Nd_{(t)}$ = +1.0 to +3.1; Bourassa, 2002; Maurice *et al.*, 2009). This suggests the emplacement of mafic and felsic lavas, accompanied by tonalitic plutonism, took place in an oceanic regime with no interaction with evolved continental crust.

In the Hudson Bay Terrane, event MA-3 corresponds to the emplacement of the tonalitic Brésolles and Suluppaugalik suites in the southeast part of the area, and the emplacement of a few tonalitic intrusions further west (Chapter 3). The tonalites show evidence of contamination by 3.1 to 2.9-Ga evolved continental crust, and contain numerous enclaves of amphibolitic rocks probably volcanic in origin. However, no supracrustal sequences with ages equivalent to these tonalites have been recognized in the Hudson Bay Terrane. Although the Brésolles Suite occurs within the same area as the earlier volcanic sequences of the Gayot Complex (about 2.88 Ga), there is no evidence to suggest a particular petrogenetic link between the two units. Consequently, the

origin of these tonalitic suites, *i.e.* whether they are derived from the partial melting of pre-existing or contemporaneous basaltic rocks, cannot be ascertained with confidence.

Nd model ages and inherited zircon ages from Neoarchean rocks represent the remains of a regionally extensive crust aged between 2.85 and 2.80 Ga (figures 3.4 and 4.14). The limited extent of this crust on surface today most likely reflects intense reworking of the bedrock during the Neoarchean. This is particularly evident in the Bienville, Tikkerutuk, Lac Minto, and Utsalik domains, where no rocks dating back to event MA-3 were identified (except for those at sites No. 22 and 32, Figure 3.4).

Event NA-1 (2.80 to 2.74 Ga)

Event NA-1 is characterized by volcanism and sedimentation in nearly all the domains in the NESP, and by tonalitic plutonism that occurred in a diachronous fashion from northeast to southwest. The oldest supracrustal sequences (2.79 to 2.78 Ga) associated with this event occur within the Hudson Bay Terrane and correspond to the Dupire and Garault complexes, as well as an early sequence of the Vizien Belt (Duvert Complex; Chapter 3). These supracrustal sequences are composed of clastic sedimentary rocks and ultramafic to felsic rocks of tholeiitic or calc-alkaline affinity, with variable $\varepsilon Nd_{(t)}$ values (+0.10 to +3.20; Chapter 4). The juvenile (2786 Ma; $\varepsilon Nd_{(t)} > +1.3$) tholeiitic mafic-ultramafic sequence in the Vizien Belt has been interpreted as a tectonic sliver of plateau-type oceanic crust (Skulski and Percival, 1996).

Early Neoarchean tonalitic magmatism is one of the key elements of event NA-1. These tonalitic units (TTG series from 2.79 to 2.74 Ga) cover an extensive part of the region (Figure 3.5 and stratigraphic map, insert) and their distribution in time and space outlines differences in the magmatic evolution of the two terranes, up until 2.74 Ga. The emplacement of tonalite intrusions in the Rivière Arnaud Terrane predates the emplacement of such intrusions in the Hudson Bay Terrane. Tonalitic units are represented by the older Faribault-Thury, Kapijuq, and Rochefort suites (2.79 to 2.76 Ga) in the Rivière Arnaud Terrane, and by the younger Favard, Coursolles, and Sem suites (2.76 to 2.74 Ga) in the Hudson Bay Terrane. On average, tonalites of the first group display relatively depleted isotopic values ($\varepsilon Nd_{(t)} = +1.41 \pm 1.04$), whereas the second group shows relatively enriched values ($\varepsilon Nd_{(t)} = -0.71 \pm 1.29$).

Mafic to felsic lavas that erupted between 2.78 and 2.76 Ga formed some of the greenstone belts assigned to the Arnaud, Nantais, Duquet, Qalluviartuuq-Payne, and Kogaluc complexes in the Rivière Arnaud Terrane, as well as some in the Innuksuac Complex and in the Roulier Belt in the Hudson Bay Terrane (Chapter 3). Tholeiitic basalts, which are predominant in the Rivière Arnaud Terrane, as well as associated felsic volcanic and volcaniclastic rocks, display positive isotopic values ($\varepsilon Nd_{(t)} = +1$ to +4; Chapter 4; Boily *et al.*, 2009; Maurice *et al.*, 2009) indicative of juvenile crust. On the other hand, a felsic tuff in the Nantais Complex yielded a negative value ($\varepsilon Nd_{(t)} = -1.4$; $T_{DM} = 3.01$ Ga) and contains inherited zircons dated at 2.82 Ga (No. 134, Table 3.3) supporting interaction with more evolved material. It is possible that significant volcanic activity did indeed take place at about 2780 Ma in the Hudson Bay Terrane, as suggested by the abundance of Fe-tholeiites assigned exclusively to this event within the terrane (Maurice *et al.*, 2009). Basaltic to rhyodacitic rocks in the Innuksuac Complex have $\varepsilon Nd_{(t)}$ values ranging from -1.5 to -6.9, corresponding to Nd model ages of 3.36 to 3.46 Ga (Chapter 4) and indicating the influence of an early sialic crust, typical of the Hudson Bay Terrane. Certain volcanic rocks in this complex belong to the contaminated tholeiite series, which is restricted to the Hudson Bay Terrane (Chapter 4). Tholeiitic basalts and felsic tuffs in the Roulier Belt (about 2.76 Ga) have relatively depleted $\varepsilon Nd_{(t)}$ values (+0.5 to +2.5) and are intruded by gabbros and tonalites with isotopic signatures among the most enriched in the region ($\varepsilon Nd_{(t)} = -0.1$ to -13; Maurice *et al.*, 2009).

Event NA-1 is also represented by the deposition of a substantial amount of clastic sedimentary rocks including some iron formations as well as minor volcanic rocks in the Mézard and Kogaluc complexes, within the Lac Minto Domain. These rocks and their metamorphic equivalents (diatexites of the Le Roy Complex; Chapter 3) represent a former sedimentary basin with a strike length of at least 500 kilometres, extending along the boundary between the Hudson Bay and Rivière Arnaud terranes. Sedimentation in the marginal basin took place in the time span from 2.76 to 2.74 Ga (Chapter 3). Ages of 2935 to 2748 Ma obtained from detrital zircons recovered in a sandstone of the Qalluviartuuq-Payne Complex (Percival and Skulski, 2000) indicate provenance from local sources, namely volcano-plutonic complexes, mixed with an older crustal source possibly located further west in the Hudson Bay Terrane. A regional study of detrital zircons would be required to determine with more accuracy the age and source of sedimentary rocks in the Lac Minto Domain. The metasedimentary rocks in this domain extend toward the southeast and form a discontinuous belt with rocks of the Rivière aux Mélèzes Suite located in the Goudalie Domain (Figure 3.10). It may be possible that at one point, all these sedimentary rocks formed the northeast margin of the Hudson Bay Terrane. However, based on currently available data, no clear correlations can be established between the two units.

PHASE 3: FROM 2.74 TO 2.68 GA

The third phase in the geological evolution of the NESP marks an important change in the nature of magmatism, shifting from dominantly tonalitic (TTG series) to largely granitic (GGM series) and charnockitic (Figure 5.1; chapters 3 and 4). This period is also characterized by calc-alkaline felsic volcanism and sedimentation. Magmatic and volcanic activity are related to two major events (NA-2 and NA-3)

that coincide with the peak of regional metamorphism. Granitic and charnockitic intrusions associated with this event transcend domain boundaries.

Event NA-2 (2.74 to 2.71 Ga)

Event NA-2 is namely characterized by the emplacement of widespread granite-granodiorite and enderbite-charnockite plutons in the Minto Subprovince (Figure 3.2). However, plutonic rocks related to this event are much more widespread in the Tikkerutuk and Utsalik domains (figures 3.7 and 3.8). These large plutons, several kilometres in size each, account for more than 50% of the region's plutonic rocks.

Plutonism during event NA-2 was accompanied by felsic volcanism, possibly in a continental setting, which was preserved in several volcanic units (Figure 3.6; Chapter 3).

Event NA-2 is also characterized by the onset of regional metamorphism, at high temperature and low pressure conditions.

Event NA-3 (2.71 to 2.68 Ga)

Neoarchean event NA-3 is characterized by the emplacement of granite and granodiorite plutons (Chapter 3) in the southeast part of the region, while magmatic activity progressively shifted to the Ashuanipi Subprovince. This event also corresponds to the peak of metamorphism responsible for the transformation of volcanic rocks into amphibolites and sedimentary rocks into diatexites. It is essentially the result of a heat transfer in the upper crust, due to the emplacement of voluminous intrusions of granitic and charnockitic magmas after 2740 Ma. Several scenarios have been proposed to explain the high-temperature low-pressure regional metamorphism in the region (Bégin and Pattison, 1994; Percival and Skuski, 2000; Bédard, 2003; Thompson, 2006). The end of this event corresponds to the final phases of cratonization in the Minto and La Grande subprovinces, to the end of high-temperature metamorphism, and the onset of cooling in the continental crust.

PHASE 4: FROM 2.68 TO 2.62 GA

Event NA-4 (2.68 to 2.62 Ga)

The final phase in the Archean geological evolution of the northeastern Superior Province includes only one event (NA-4). In the Minto Subprovince, this last Neoarchean event is associated with the formation of oblique shear zones in which a few late units of granite and granodiorite, syenite, and carbonatite were emplaced, evidence of late- to post-kinematic hydrothermal activity. This activity also led to the production of late- to post-metamorphic fluids, mainly along permeable ductile and brittle zones. It was accompanied by localized retrograde metamorphism to the greenschist facies along permeable zones.

In the Ashuanipi Subprovince, the time span from 2.68 to 2.62 Ga is marked by a major episode of magmatism, deformation, and granulite-grade metamorphism. It is characterized by the presence of orthopyroxene-bearing diatexites (2.68 to 2.66 Ga), granite, granodiorite, tonalite, and syenite plutons (2.65 to 2.62 Ga) as well as anorogenic granitic intrusions (2.57 Ga) (Percival *et al.*, 1992; Chevé and Brouillette, 1995; David and Parent, 1997; Parent, 1998; Leclair *et al.*, 1998; Lamothe *et al.*, 1998). The latter are associated with the youngest Archean magmatic event recorded in the Superior Province.

CHAPTER 6
MAFIC DYKE SWARMS IN THE NORTHEASTERN SUPERIOR PROVINCE

Charles Maurice

INTRODUCTION

Mafic dyke swarms are the products of major magmatic events that have taken place in all Archean shields over the past 2.5 billion years (Ernst *et al.*, 1995). These swarms may be very impressive in terms of number, width, and length of the dykes. The most important swarms can reach 1000 kilometres in length (Fahrig and West, 1986), and the volume of magma needed to fill a single dyke can be compared to about 100 years of basaltic magma production along modern mid-ocean ridges (McHone *et al.*, 2005). Although they constitute sizable geological units, the scientific community showed very little interest for these rocks prior to the first International Conference on Mafic Dyke Swarms that took place in Toronto in 1986 (Halls and Fahrig, 1987).

The study of mafic dyke swarms contributes to the understanding of a region's geological history. Their emplacement may mark the final phases in the stabilization of continental crust, or signal the initiation of tectonic activity during the development of contemporaneous volcano-sedimentary belts (Weaver and Tarney, 1981). Because they were rapidly emplaced over large areas, they represent ideal temporal markers with which to constrain regional stress fields, uncover evidence relating to tectonic processes, and provide information on the geochemical nature of mantle sources at the time of their emplacement. The compilation presented in this section (Figure 6.1) and the map accompanying this report improves our understanding of the distribution of mafic dyke swarms in the NESP, not only by providing a geographic correlation tool for fragmented Archean cratons (Bleeker and Ernst, 2006) but also by recognizing deep fracture networks that may have served as favourable zones for the emplacement of diamondiferous kimberlites.

MAFIC DYKE SWARMS

General characteristics

Dyke swarms that intruded Archean cratons may comprise dykes of variable sizes (several centimetres to 200 metres wide), with the smallest most likely representing apophyses of larger dykes. The Mackenzie swarm, the largest in the world (Northwest Territories, Nunavut, and Ontario; Fahrig and West, 1986), covers an area of approximately 2.7 million square kilometres with a maximum length of 2,500 kilometres. This type of giant swarm commonly displays radiating patterns (up to 150° from a focal point) and only appeared at about 2.5 Ga (Halls, 1987). Dyke compositions vary from pyroxenitic (Molson dykes, Manitoba; Scoates and Mecek, 1978) to monzodioritic (parts of the Great Abitibi Dyke; Ernst and Bell, 1992), but basaltic compositions with normative quartz are the most abundant.

Geochronology studies on dykes from the same swarm indicate the dykes were emplaced very rapidly over a large area (1267 to 1272 Ma for the Mackenzie dykes; Heaman and LeCheminant, 1993). However, dykes of different ages but similar appearance may be oriented in the same direction, and in such cases, a major dating program is required to tell them apart (French *et al.*, 2004; Jourdan *et al.* 2006). Swarms of different ages may display cross-cutting relationships, although this is not observed between major swarms. For example, the Mackenzie dykes (about 1.27 Ga) do not cut across the Matachewan dykes (about 2.47 Ma), the older swarm having likely affected the crust by compressing the host rock (Ernst *et al.*, 1995).

Emplacement and tectonic setting

The geometry and emplacement of a dyke swarm are governed by the tectonic stress field at the time of the intrusion. The magnitude of the intrusion varies considerably depending on whether the tectonic model invokes mantle plumes, in order to explain the radial pattern of some swarms (LeCheminant and Heaman, 1989; Ernst *et al.*, 1995; Ernst and Buchan, 2001), or aulacogens (aborted rifts; Fahrig *et al.*, 1986; Fahrig, 1987).

Two models are proposed to explain the feeder mechanism for dyke swarms (Halls, 1987). They are fed either horizontally from a magmatic chamber at depth in the crust or mantle, or vertically from a subcrustal magmatic chamber as large as the swarm itself, or that migrates during the intrusion. Dyke propagation in the crust has long been assumed to be vertical, but a seismic study of dykes related to a volcanic centre in Iceland indicated lateral flow over more than 100 kilometres (Sigurdsson, 1987). Studies on the magnetic fabric of major swarms have also concluded that dykes propagate horizontally (Ernst, 1989; Ernst and Baragar, 1992), although certain factors may have obscured such fabrics (McHone *et al.*, 2005). Whatever the chosen model, it remains that geochemical studies of mafic dyke swarms indicate parent magmas underwent a significant degree of fractional crystallization in magmatic chambers at pressures lower than or equal to those found at the base of the continental crust (Baragar *et al.*, 1996).

NEW COMPILATION MAP

Methodology

The most recent compilation of mafic dyke swarms in the northeastern Superior Province was by Buchan and Ernst (2004). Due to its scale (1:5,000,000) and the fact that it was published before the Far North Program was completed, the compilation map provides an incomplete portrait of the region. Moreover, the strongly magnetic character of late Archean granitoid rocks made it difficult to distinguish and trace mafic dykes in the NESP based on magnetic maps, and aerial photographs were only useful to follow the biggest dykes in the northeast part of the region, where dyke swarms are already well known (Fahrig and West, 1986).

The SIGÉOM database was used to compile more than 1,782 sites where Proterozoic dykes have been identified. In ambiguous cases, the authors consulted the geologists' handwritten notes and any available thin sections or samples. The SIGÉOM database was then standardized by assigning the lithological code "I3B" (diabase) to all sites where Proterozoic dykes were observed. Even though, in principle, this term refers to a texture more than a type of lithology, its usage makes it easier to discriminate between Archean gabbroic dykes and the Proterozoic dykes.

The compilation was used to produce a thematic map (insert). The map shows the location of all observations sites compiled in the database, which also includes the orientation and thickness of each dyke. If this information was missing, the corresponding field was left blank. However, if the thickness was missing but other information suggested the dyke is of significant size (written notes from the geologist, the size of the dyke relative to the rest of the outcrop, the medium- to coarse-grained nature of the hand sample or thin section), the station was assigned a value of 99 to indicate that the dyke constitutes an appreciable volume of the outcrop. On the thematic map, dykes with no observation sites attached were digitized based on existing compilation studies (Fahrig and West, 1986; Buchan and Ernst, 2004) or regional maps published by the GSC (Figure 1.1). Dykes ≥10 metres thick and traced from a single observation site were arbitrarily assigned a length of 20 kilometres, whereas dykes ≥5 metres but <10 metres thick were assigned a length of 10 kilometres. In keeping with the objective of providing a regional portrait, dykes less than 5 metres thick were not traced on the compilation map, although they were retained in the database.

PROTEROZOIC UNITS

Supracrustal rocks (2.17 to 1.80 Ga)

Archean rocks in the NESP are surrounded by Proterozoic rocks (Figure 2.2; Figure 6.1) that were emplaced during the Trans-Hudsonian orogeny (Lewry and Collerson, 1990; Circum-Ungava geosyncline; Dimroth *et al.*, 1970). These rocks belong to the Labrador Trough (New Québec Orogen) in the east (Wardle *et al.*, 2002; Clark and Wares, 2006) and the Cape Smith Belt (Ungava Orogen) in the north (Taylor, 1982; St-Onge and Lucas, 1990; Lamothe, 1994). In the west, the Belcher, Hopewell, and Nastapoka islands are also made up of Proterozoic rocks (Lee, 1965; Chandler, 1988). Proterozoic rocks of the Richmond Gulf Graben are also well exposed south of Umiujaq in the Lac Guillaume-Delisle area (Chandler, 1988). Finally, Proterozoic sedimentary rocks of the Sakami Formation overlie the Archean craton in the Lac Gayot, Lac Bienville, and Lac Maricourt areas (Figure 1.1, Nos. 21, 20, and 18).

The supracrustal rocks of the Labrador Trough, oriented NNW-SSE, were emplaced during three volcano-sedimentary cycles from about 2.17 to 1.80 Ga (Clark and Wares, 2006 and references therein). The oldest rocks from Cycle 1 have an age of about 2.17 Ga (Rohon *et al.*, 1993), and this cycle may have ended around 2.06 Ga (see discussion in Clark and Wares, 2006). Cycle 2 includes a platform sequence for which deposition has been constrained between 1.88 and 1.87 Ga based on U/Pb ages from gabbroic sills, a carbonatite dyke, and felsic volcanic rocks (Chevé and Machado, 1988; Findlay *et al.*, 1995; Machado *et al.*, 1997; Wodicka *et al.*, 2002). Finally, Cycle 3 produced synorogenic molasses that were deposited at about 1.80 Ga (Hoffman, 1987; Clark and Wares, 2006).

The supracrustal rocks of the Cape Smith Belt, oriented E-W, include volcano-sedimentary rocks that were emplaced following the opening of a basin in the northern part of the Superior Province (Hynes and Francis, 1982; St-Onge and Lucas, 1993). The oldest rocks were mapped in the south part of the belt, in the Povungnituk Group. The age of a gabbroic sill intercalated in the sedimentary rocks at the base of the sequence places the start of deposition before 2.04 Ga (Machado *et al.*, 1993). The age of a rhyolite in the upper part of the Povungnituk Group indicates that volcanism and sedimentation continued until about 1.96 Ga (Parrish, 1989). The second magmatic episode was dominated by tholeiitic to picritic basalts of the Chukotat Group, thrust over rocks of the Povungnituk Group. The age of these rocks is less well known, but they are probably coeval with Cycle 2 rocks of the Labrador Trough, as suggested by a gabbroic sill, intruded in the upper part of the sequence and dated at about 1.88 Ga (St-Onge *et al.*, 1990). The siliciclastic rocks of the Spartan Group and the intermediate to felsic volcanic rocks of the Parent Group (about 1.86 to 1.87 Ga; Machado *et al.*, 1993) were thrust over rocks of the Chukotat Group. Further north is the Watts Group (2.00 Ga; Parrish, 1989), interpreted as a dismembered oceanic suite (the Purtuniq ophiolite; Scott *et al.*, 1992) obducted onto the volcano-sedimentary units to the south.

Other Proterozoic volcano-sedimentary rocks occur in the western part of the NESP, but absolute age relationships are less well defined. The Belcher Islands in Hudson Bay (Figure 1.1) consist of deformed sedimentary rocks intercalated with two continental basalt units (Eskimo and Flaherty formations;

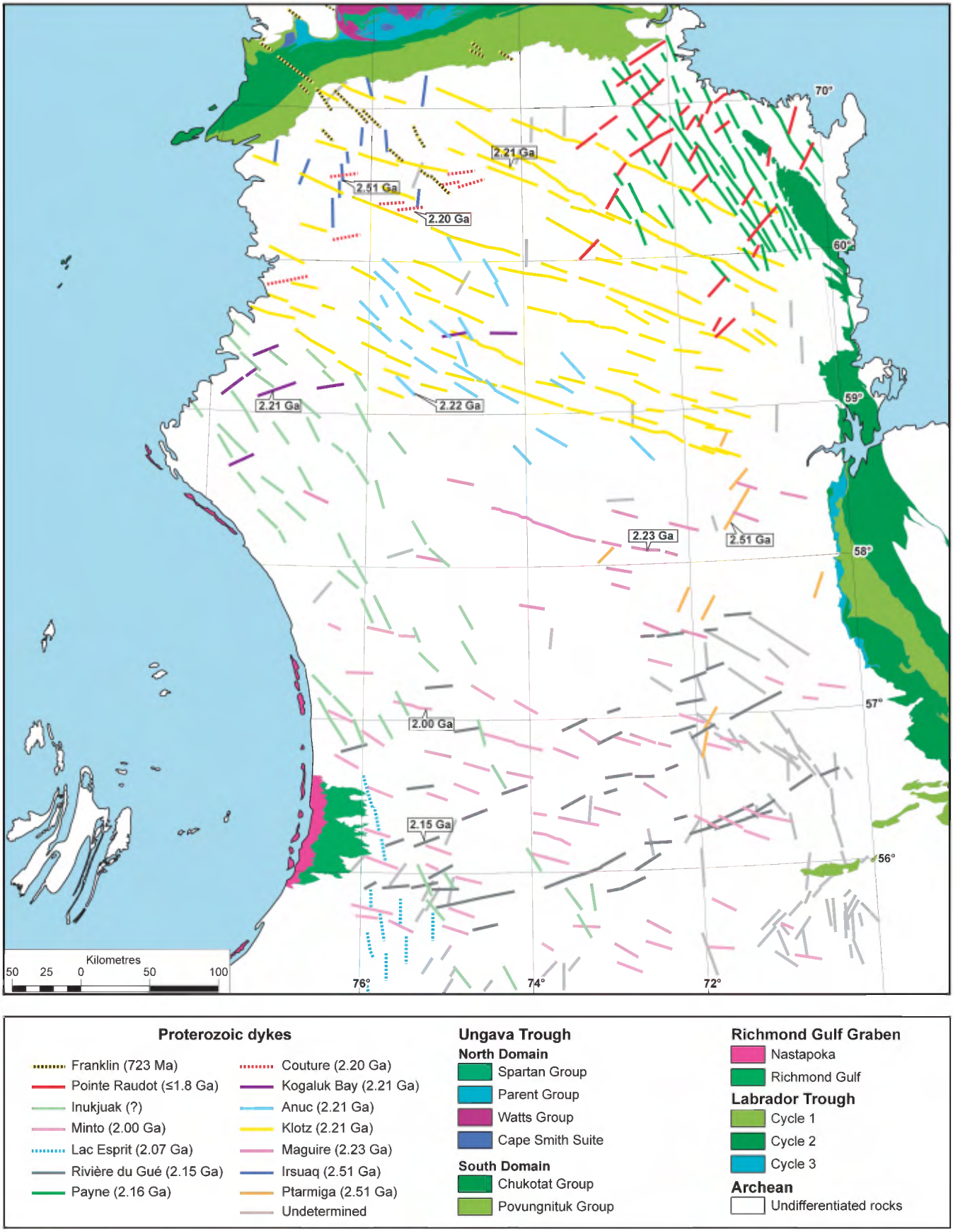

FIGURE 6.1 – Distribution of Proterozoic mafic dyke swarms in the northeastern Superior Province.

Ricketts and Donaldson, 1981; Legault *et al.*, 1994). A Pb-Pb isochron diagram for a basalt sample belonging to the youngest formation yielded an imprecise age of 1.96 ±0.08 Ga (Todt *et al.*, 1984). On the eastern shore of Hudson Bay, in the Lac à l'Eau Claire area (Figure 1.1, No.16), similar Proterozoic volcano-sedimentary rocks (the Richmond Gulf and Nastapoka groups; Chandler, 1988) are less deformed and unconformably overlie the Archean basement. Analyses of diagenetic apatite grains from a sandstone unit at the base of the Richmond Gulf Group yielded an age of 2.03 ±0.03 Ga (Chandler and Parrish, 1989).

Mafic dyke swarms (2.51 to 2.00 Ga)

The many dyke swarms cross-cutting Archean rocks in the NESP offer a unique complement to the geological history of Proterozoic volcano-sedimentary units. Dykes illustrated on map C006 (insert) are grouped into different-coloured swarms based on their orientation and, whenever possible, their age if geochronology data exist. It is important to realize, however, that in the absence of a major dating program, dykes of different ages but similar compositions may well show the same orientation (French *et al.*, 2004; Jourdan *et al.* 2006). The ten U/Pb ages discussed in this section are taken from Buchan *et al.* (1998) or from work done by David and Maurice at the GÉOTOP-UQÀM-McGill centre. The results of the latter will likely be published in 2009.

All ten dated dykes are Paleoproterozoic in age. The two earliest swarms in the study area were emplaced at the Archean-Proterozoic transition. In the eastern part of the area, the Ptarmigan swarm (2.51 Ga; Figure 6.1; Buchan *et al.*, 1998) consists of NE-trending dykes reaching up to 45 metres thick. In the northwest part of the area, the Irsuaq swarm (Figure 6.1) is composed of scattered dykes trending N to NNW, reaching up to 200 metres thick. Their age is identical to that of the Ptarmigan dykes.

Nearly 300 Ma separate these two swarms from many others that were emplaced between 2.2 and 2.0 Ga. The radiometric age of the W- to NW-trending Maguire dykes (Figure 6.1) is poorly defined (2.23 ±0.03 Ga; Buchan *et al.*, 1998). These dykes occur in the central part of the study area where they intruded a 28,000-km^2 zone that was injected by only a few mafic dykes. Given the uncertainty regarding their age, these dykes may be contemporaneous with numerous dykes generated at about 2.21 Ga during the magmatic event responsible for the emplacement of the widespread Klotz swarm (WNW; Buchan *et al.*, 1998) and the Anuc and Kogaluc Bay swarms (NW and ENE; Figure 6.1).

The Couture swarm (Figure 6.1) consists of a few WSW- to W-trending dykes in the northern part of the region, parallel to the Cape Smith Belt. Their emplacement at 2.20 Ga may have been related to the opening of the extensional basin that preceded deposition of the Povungnituk Group sedimentary rocks. As for the Payne swarm (Figure 6.1), it consists of a dense population of NNW-trending dykes parallel to the rocks of the Labrador Trough. The age of these dykes has been bracketed between 2.16 and 2.17 Ga (personal communication with S. Pehrsson, as cited in Ernst and Buchan, 2004) and likely marks the rifting of Archean rocks and coeval emplacement of Cycle 1 basalts in this region (Clark and Wares, 2006). Petrographic data collected east of the Labrador Trough reveal these dykes experienced amphibolite facies recrystallization and were thus emplaced prior to the Trans-Hudsonian orogeny (>1.8 Ga; Madore and Larbi, 2001). Also in the northeast part of the region, the Pointe Raudot swarm (Figure 6.1) consists of NE-trending dykes. Although radiometric ages are not available, the mineral assemblage of a folded dyke demonstrates, in contrast to the Payne dykes, that the Pointe Raudot swarm did not reach the amphibolite facies. This implies a synchronous or late emplacement with respect to the Trans-Hudsonian orogeny (≤1.8 Ga).

The Rivière du Gué dykes (Figure 6.1) are oriented ENE, parallel to outliers of the Sakami Formation preserved in half-grabens in the Archean craton. They are interpreted as vestiges of the "Cambrian Lake aulacogen" (Hoffman, 1988), even though the hypothesis of an aborted rift is not supported by paleocurrent directions measured in Sakami rocks (Clark, 1984; Clark and Wares, 2006). Within the context of Hoffman's model (1988), however, the Rivière du Gué swarm would delimit the extent and minimum age (2.15 Ga) of such a rift. The swarm's age is similar to that obtained for a felsic volcanic rock from Cycle 1 in the Labrador Trough (2.14 Ga; personal communication with T. Krogh, as cited in Machado *et al.*, 1997). Further south, the age of the Minto swarm (Figure 6.1), oriented WNW to NW, is identical to that of the Watts Group in the northern part of the Cape Smith Belt (2.00 Ga; Buchan *et al.*, 1998).

In the Lac Montrochand region (No. 19, Figure 1.1), Roy *et al.* (2006) mentioned the possibility that N- to NNW-trending dykes (Figure 6.1) may belong to the Lac Esprit swarm (2.07 Ga; Hamilton *et al.*, 2001), for which the type locality is in the Baie-James region (Goutier *et al.*, 1999). The Inukjuak swarm (Figure 6.1) along Hudson Bay comprises several NW-trending dykes (Budkewitsch *et al.*, 1991; Legault *et al.*, 1994), but their radiometric age has not yet been determined. Our compilation work also recognized a number of dykes with no radiometric ages or that do not belong to any major swarms. These dykes, shown on the compilation map, display preferential orientations similar to those of the swarms described above but are present in too few numbers to define new swarms, or are deemed too far from type localities to be grouped with existing swarms.

The youngest dykes in the region trend NW and cut rocks of the Cape Smith Belt (Figure 6.1). These dykes are thus younger than 1.8 Ga and were assigned to the Neoproterozoic Franklin swarm (about 723 Ma) by Buchan and Ernst (2004). Since none of these dykes have been isotopically dated, they may in fact belong to the Mesoproterozoic Mackenzie swarm (about 1.27 Ga).

Petrography

The mafic dykes are massive and homogenous, dark grey to greenish grey with a characteristic brownish colour on weathered surfaces. Grain size varies from fine to coarse, depending on the size of the dyke. They display a few centimetres of aphanitic chilled margins. Ophitic and subophitic textures are the most common, although amygdaloidal, porphyritic or trachytic textures are observed locally. The rock, generally gabbroic in composition, consists of clinopyroxene and plagioclase. Orthopyroxene and olivine are rarely observed. Magnetite is always present in variable amounts, which explains the variable magnetic susceptibility of these rocks. Interstitial quartz is common, either as grains or as intergrowths (symplectic texture). Igneous textures are always preserved, even when pyroxene is replaced by actinolite or hornblende, plagioclase by sericite, and olivine by talc or serpentine. Traces of zircon and baddeleyite complete the mineral assemblage. With the exception of the Ptarmigan and Irsuaq swarms, which are known to be gabbronoritic (olivine + clinopyroxene + orthopyroxene), the work to date does not allow swarms to be distinguished based on petrographic composition.

Geochemistry

The geochemistry of the NESP dykes is the subject of detailed work (Maurice *et al.*, 2005b, 2007). This work is based on geochemical analyses in the database included with the digital ArcGIS version of compilation map C006 that accompanies this report. This database contains the major and trace element analyses for 199 samples, in addition to Nd analyses for 30 samples that were analyzed at the GÉOTOP-UQÀM-McGill centre. The "code" field contains the descriptor "a" or "f" to indicate whether the sample was interpreted as altered or fresh. Most of the altered samples came from dykes intruding Archean rocks in the Lac à l'Eau Claire area (No. 16, Figure 1.1).

CONCLUSIONS

The appearance of mafic dyke swarms relatively late in the Earth's history suggests major changes in crust and mantle dynamics took place at the Archean-Proterozoic transition at about 2.5 Ga. Mafic dykes found throughout the NESP are markers of such changes.

Recent studies demonstrate that several generations of mafic dykes can be found within the same swarm, suggesting that magmas were emplaced along pre-existing lithospheric weaknesses (Mège and Korme, 2004; Jourdan *et al.*, 2004; French *et al.*, 2004; Jourdan *et al.* 2006). Similarly, several kimberlite fields display aligned pipes, suggesting that deep structures played a role in their distribution (Wilkinson *et al.*, 2001). Given that mafic dyke swarms in the Slave Province are much older (2.23 to 1.27 Ga) than the Eocene diamondiferous kimberlites at Lac de Gras, such ancient fracture networks very likely provided favourable zones along which kimberlites were emplaced (Wilkinson *et al.*, 2001). In addition to providing a clearer portrait of the geometry and extent of known mafic dyke swarms and documenting new swarms, the present compilation may contribute to the future development of a regional exploration model for diamondiferous kimberlites in the NESP.

CHAPTER 7
MINERAL OCCURRENCES AND METALLOGENY OF THE NORTHEASTERN SUPERIOR PROVINCE

Jean-Yves Labbé and Pierre Lacoste

INTRODUCTION

The prime objective of the Far North Program was to open a vast yet little-known territory to exploration through an ambitious regional mapping campaign. Since promoting the mineral potential of the region was key in the fundamental goals of the program, mineral occurrences and metallogeny studies were the object of considerable thought and effort. The main objectives of this part of the program were to inventory, characterize, and classify mineral occurrences and their geological setting, and if applicable, to develop a regional metallogenic model. This chapter provides a descriptive overview of mineral occurrences discovered either by MRNF field crews during the Far North Program, or by prospectors and exploration crews from the private sector. This chapter also discusses prospective geological environments for the discovery of deposit types observed in the northeastern Superior Province (NESP). A map of mineral occurrences (insert) accompanies this chapter, showing the location of the 170 mineral occurrences inventoried in the SIGÉOM database and listed in Table 7.1.

Methodology

From the onset of the Far North Program, ore deposit and metallogenic studies were conducted in parallel with mapping surveys. The results discussed here are largely derived from the work of the two authors, parts of which were published in geological reports, in distinct study reports (Labbé, 2005; Labbé and Lacoste, 2001 and 2004; Labbé *et al.*, 2003), in promotional documents (Labbé *et al.*, 1998, 1999, and 2001; Labbé, 2001) and finally, in a mineral potential assessment report (Labbé, 2002).

Most of the mineral occurrences of interest were visited during the Far North Program. This fieldwork took place largely within volcano-sedimentary belts, since many of the showings occur in this type of setting. When required, mapping traverses were also conducted in the vicinity in order to decipher the regional geological setting. However, given the complex logistics involved in these mapping surveys, only a few showings were studied in detail. Data provided in exploration work reports from mining companies were used to complement data collected in the field.

More than 6,000 rock samples collected under the Far North Program, within the scope of mapping projects and the metallogenic study, were analyzed for elements of economic interest. Assay results were integrated into SIGÉOM. About 600 thin sections including 150 polished sections were studied to characterize mineralized zones, associated alteration zones, and surrounding geological settings (host rocks).

Previous exploration work

The first signs of interest for metals in the region go as far back as the end of the 17th century. At the time, the Hudson's Bay Company sent ships back to England using galena-rich dolomite as ballast. The dolomite had been collected from Proterozoic units near Lac Guillaume-Delisle (Almond, 1947). The lead (and probably zinc) ore in these rocks was sold on the London market. In the late 1940s and early 1950s, Gulf Lead Mines carried out significant exploration work on these Pb-Zn showings.

From the late 1950s to the 1970s, several mining companies, including Great Whale Iron Mines, explored the southwest part of the region in search of iron ore. These activities revealed the presence of iron ore deposits in the Lac Fagnant area, although these deposits were never mined.

From the mid-1970s until the early 1980s, the Proterozoic basins in the southern part of the region attracted the attention of several mining companies exploring for uranium. The company Uranerz, in particular, performed a lot of work in the Lac Gayot area. Eldorado Nuclear, Seru Nucléaire and Société de Développement de la Baie James (SDBJ) were also active in the same area.

It was only in the 1990s that gold and base metal exploration began in the NESP. The discovery of Archean greenstone belts in the Rivière aux Feuilles area and near lakes Qalluviartuuq, Duquet, and Dupire (Percival and Card, 1994; Percival *et al.*, 1995a and 1996a; Lamothe, 1997) brought Cominco and SOQUEM to the region to explore for volcanogenic sulphides and gold, soon followed by Virginia Gold Mines.

The Far North Program had a positive impact on mineral exploration in this vast and poorly known territory. In 1997, a lake-bottom sediment survey revealed several geochemical targets that were the subject of reconnaissance work by a consortium involving SOQUEM, Virginia Gold Mines and Cambior, and by Noranda and Falconbridge. The discovery of several new volcano-sedimentary belts, as soon as mapping began, also generated considerable interest. Overall, the results of the Far North Program have opened up new areas for mineral exploration throughout the Minto Subprovince.

In the Lac Gayot area, in the southeast part of the region, Virginia Gold Mines undertook a major exploration program that led to the discovery of several Ni-Cu-PGE showings and gave rise to a partnership with BHP-Billiton. A little farther west, in the same area, Makamikex (Ressources Vaujour) discovered a copper showing in ultramafic rocks. In the southwest part of the region, Virginia Gold Mines explored for gold in the Lac Fagnant area. To the northeast, in the Lac Tasiaalujjuaq area, the SOQUEM–Virginia Gold Mines–Cambior consortium discovered a few polymetallic volcanogenic showings. These partners also conducted exploration work in the Pélican-Nantais area while pursuing projects in the Qalluviartuuq-Payne and Duquet areas. The presence of a major uranium anomaly in lake-bottom sediments in the Lac Nedlouc area attracted SOQUEM and Cambior to explore this part of the region.

In 2000, an MRNF mapping team discovered a Ni-Cu showing in an ultramafic intrusion, giving rise to exploration projects southwest of Lac Minto. Falconbridge and SOQUEM found several Ni-Cu-PGE showings in 2001 and 2002, and during this same period, a team of prospectors from the Nunavik Mineral Exploration Fund (NMEF) discovered several Cu-Ag showings along the shores of Lac Guillaume-Delisle.

The diamond exploration craze that hit the Monts Otish in the Baie-James region during the early years of the new millennium gradually extended northward after the discovery of alkaline intrusions in the Lac Aigneau area (Berclaz *et al.*, 2002) and kimberlite indicator minerals in the Lac Bienville area (Parent *et al.*, 2002). Several companies carried out exploration work in the Lac Gayot area (Ashton-SOQUEM, Majescor-Diamondex), west of Lac Minto (Canadian Royalties), in the Lac Aigneau area (Western Hemisphere Mining), and in the Lac Faribault area (Antoro).

Volcano-sedimentary belts

Most of the mineral occurrences discussed in this report are located within volcano-sedimentary belts or are intimately associated with the latter. These belts generally correspond to informal lithodemic units assigned to formal volcano-sedimentary complexes (Simard, 2008). Only the Nuvvuagittuq, Melvin, Roulier, and Tasiataq belts are formal units (Chapter 3). Informal unit names are mentioned in this chapter, essentially serving as geographic markers. Figure 7.1 shows the location and extent of the main volcano-sedimentary belts identified in the NESP.

SECONDARY ENVIRONMENT GEOCHEMISTRY

Far North Program lake-bottom sediment geochemistry survey

The Far North Program started in 1997 with a major lake-bottom sediment geochemistry survey financed by the MRNF and five partners from the mining industry. The survey encompassed all of the territory covered by the Far North Program, with the exception of lands north of the 61st parallel and an area in the southeast corner that had been covered in the past (Beaumier, 1986). The surveyed region, measuring 350,000 km^2, represents approximately one quarter of the province of Québec. In all, 26,220 samples were collected using a 12-km^2 grid, for an average spacing of 3.4 kilometres between samples. The samples were analyzed at the Centre de recherche minérale du Québec laboratory (now COREM). The elements Al, Ag, Ba, Be, Bi, B, Cd, Ca, Ce, Cr, Co, Cu, Eu, Fe, Ga, Ge, K, La, Li, Mg, Mn, Mo, Na, Ni, P, Pb, Sm, Sc, Sr, Th, Ti, V, Y, Zn, and Zr were analyzed by plasma atomic emission spectrometry following partial digestion by nitric acid. The elements As, Au, Br, Cs, Sb, Se, Tm, U, and W were analyzed by neutron activation. All the geochemical data have been entered into SIGÉOM and are available in digital format on CD-ROM (MRN, 1998).

Geochemistry maps

Figures 7.2 to 7.7 display the regional distribution of copper, zinc, nickel, cobalt, uranium, and arsenic, respectively. Even though these elements were selected for their economic interest, their distribution patterns do not provide exploration targets *per se*; instead, they provide a regional representation of the dispersal of these elements in the secondary environment. The figures showing the regional distribution of gold and silver are not included herein; they revealed only a few isolated anomalies due to the relatively high detection levels.

The geochemical data were interpreted by the inverse distance weighting method using ArcGIS Spatial Analyst software. The legend for the figures comprises seven grade intervals (blue to red) defined by the 50th, 80th, 90th, 95th, 98th, and 99th percentiles, except for arsenic where the 50th percentile was omitted due to the abundance of values below detection limit. The geochemistry layers on figures 7.2 to 7.7 were overlain on a shaded image of the total magnetic field to emphasize the structural grain.

Copper distribution (Figure 7.2) reveals a large zone of enrichment corresponding to the northern part of the Goudalie Domain (Figure 2.2) where several volcano-sedimentary belts are found. The correlation between copper anomalies and supracrustal rocks has been used to identify the most promising sites for the discovery of new volcano-sedimentary belts in the NESP (Labbé *et al.*, 1999). Figure 7.2 also reveals that weak copper values in the west part of the region correspond to the Tikkerutuk and Bienville domains (Figure 2.2). These domains also have low zinc (Figure 7.3) and nickel values (Figure 7.4), except in the central part of the Tikkerutuk Domain where a few zones with higher levels of nickel are visible. Areas with higher nickel values generally reflect greenstone belts containing ultramafic rocks. A good example of this is the Vénus belt

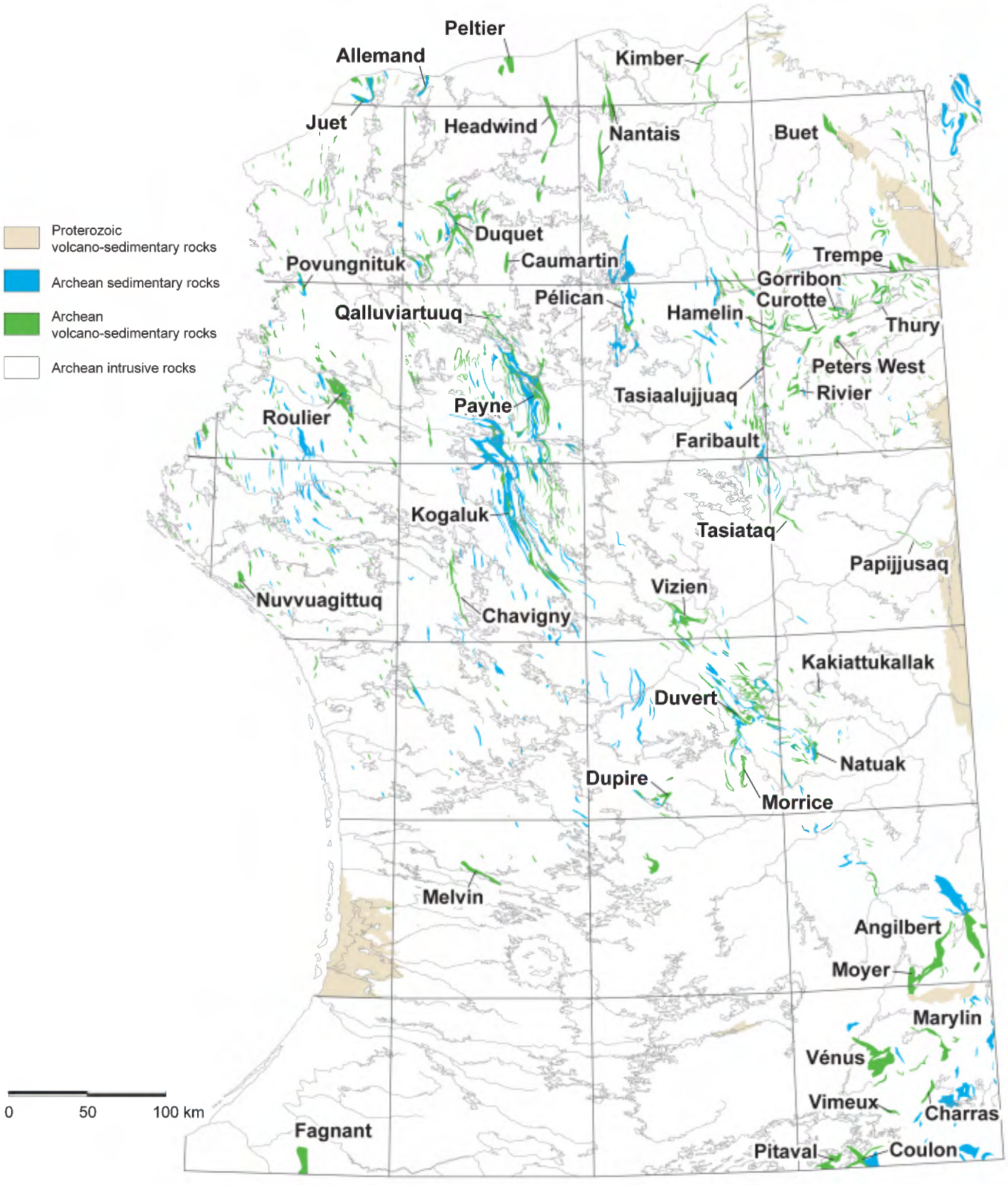

FIGURE 7.1 – Location of the main volcano-sedimentary belts in the northeastern Superior Province.

(Figure 7.1) in the southeast part of the region (Figure 7.4). In the case of cobalt, no correlation was observed between anomalous values and the presence of volcano-sedimentary rocks (Figure 7.5).

Uranium distribution (Figure 7.6) reveals two areas with high values in the east-central part of the region. These areas contain several uranium showings associated with Archean granitic rocks. As is the case for copper, there is a correlation between uranium anomalies and volcano-sedimentary belts. Thus, uranium distribution, like copper, was used to determine the most promising areas to discover new volcano-sedimentary belts (Labbé *et al.*, 1999).

Finally, arsenic distribution (Figure 7.7) shows several relatively isolated anomalies, notably in the east where Proterozoic rocks of the Labrador Trough are exposed. Anomalous zones of variable intensity are superimposed on the Fagnant, Nantais, Payne, Kogaluc, Chavigny, Vizien, and Duvert belts. A large anomalous zone in the northwest part of the region, west of Qalluviartuuq, coincides with several gold-rich (0.5 to 1.6 g/t Au) zones in volcano-sedimentary rocks, within diatexites (Berclaz *et al*, 2003b).

MINERAL OCCURRENCES

In this section, the main mineral occurrences are described, classified into 21 different types, which were then grouped into 5 broad categories based on their age and their syngenetic or epigenetic character:

1. Archean syngenetic occurrences (types 1 to 6);
2. Proterozoic syngenetic occurrences (types 7 and 8);
3. Archean epigenetic occurrences (types 9 to 17);
4. Archean or Proterozoic (?) epigenetic occurrences (types 18 and 19); and
5. Proterozoic epigenetic occurrences (types 20 and 21).

Mineral occurrences are considered syngenetic when mineral deposition is coeval with the formation of host rocks, and epigenetic when mineralization is associated with deformation, metamorphism, or both. The classification scheme used to categorize mineral occurrences takes into account genetic aspects, based on the nomenclature of Eckstrand *et al.* (1995), and descriptive aspects, based on the textural and structural features of mineralized zones. For showings where very little information is available or very little work has been conducted, the classification is more descriptive. For example, most occurrences in the "Polymetallic disseminations (Ag ± Cu ± Zn)" category correspond to disseminated sulphide zones, the importance of which was revealed upon reception of assay results, *i.e.* after fieldwork. Consequently, no subsequent work was carried out on these occurrences for purely logistical reasons.

For each of the five broad categories, each type of mineral occurrence is described in detail, including: 1) a description of the deposit type and its geological setting; 2) examples of this type of mineralization within the study area; and 3) a discussion of its economic significance and an assessment of its discovery potential within the NESP.

Archean syngenetic occurrences

Six types of syngenetic mineral occurrences associated with Archean rocks were recognized in the study area (Figure 7.8). These are: Algoma-type iron formations (type 1), volcanogenic sulphides (type 2), magmatic Ni-Cu occurrences (type 3), Fe-Ti-V occurrences in mafic intrusions (type 4), U-Th occurrences in porphyry granites (type 5), and porphyry-type Mo-W occurrences (type 6). Volcanogenic sulphide occurrences are subdivided into three categories: predominantly copper-rich (2a), zinc-rich (2b), and gold-rich (2c) occurrences. Moreover, magmatic Ni-Cu occurrences associated with komatiites (3a) are distinguished from those hosted in mafic and ultramafic intrusions.

Most of these mineral occurrences are located in volcano-sedimentary environments, except magmatic Ni-Cu deposits associated with late mafic and ultramafic intrusions (type 3b). U-Th occurrences in porphyry granites (type 5) and porphyry-type Mo-W showings (type 6) are spatially correlated with the Duvert and Morrice volcano-sedimentary belts (Parent *et al.*, 2001), although a genetic link with these rocks has not been clearly established.

Algoma-type iron formations (type 1)

Algoma-type iron formations (Gross, 1995a) represent the second largest source of iron in the world, after Lake Superior-type iron formations. They commonly exhibit regular banding produced by the presence of thin siliceous layers alternating with thin bands composed of iron-rich minerals occurring as oxides, silicates, sulphides, or carbonates. These rocks form in volcanic settings and are generally accompanied by mafic to felsic lavas and fine-grained to sandy sedimentary rocks.

Overall, oxide-facies iron formations (magnetite, hematite) are the most interesting from an economic standpoint. They have generally undergone either deformation (folding or faulting) leading to thickening, or recrystallization and increased grain size due to metamorphism, or both. Their thickness ranges from 30 to 100 metres, over a strike length of more than one kilometre.

Algoma-type iron formation occurrences were described in two locations: in the Nuvvuagittuq Belt and the Fagnant belt (Figure 7.8). Occurrences in the Fagnant area, by far the most important, are briefly described below.

Fagnant belt

The main Algoma-type iron ore occurrences were discovered in the 1950s in the Lac Fagnant area, in the southwest part of the NESP. Note that since this map area (NTS 33N) was not included in the Far North Program, these mineral occurrences were not visited during our fieldwork. Two

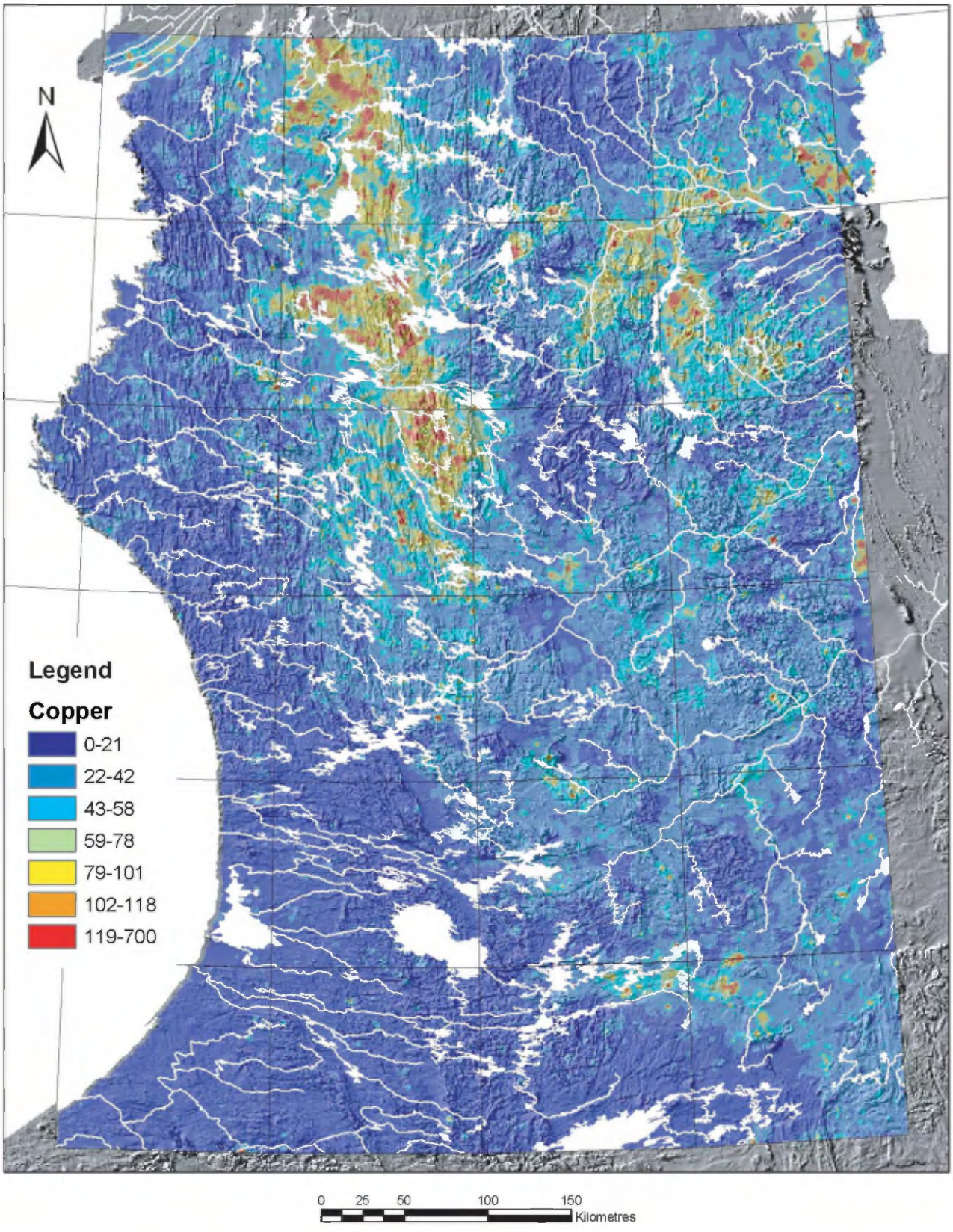

FIGURE 7.2 – Copper distribution in lake-bottom sediments, overlain on shaded image of total magnetic field. Copper values are in ppm.

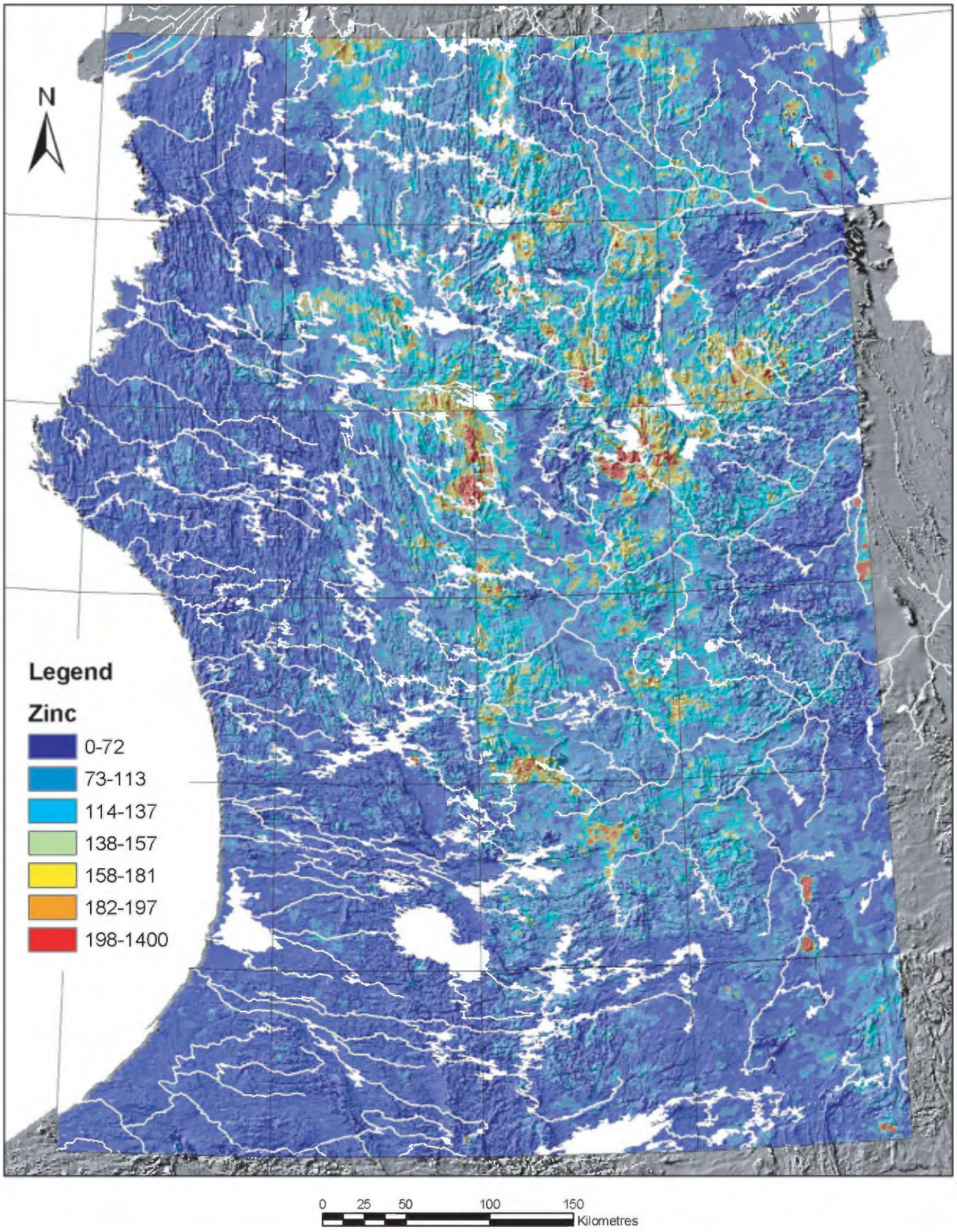

FIGURE 7.3 – Zinc distribution in lake-bottom sediments, overlain on shaded image of total magnetic field. Zinc values are in ppm.

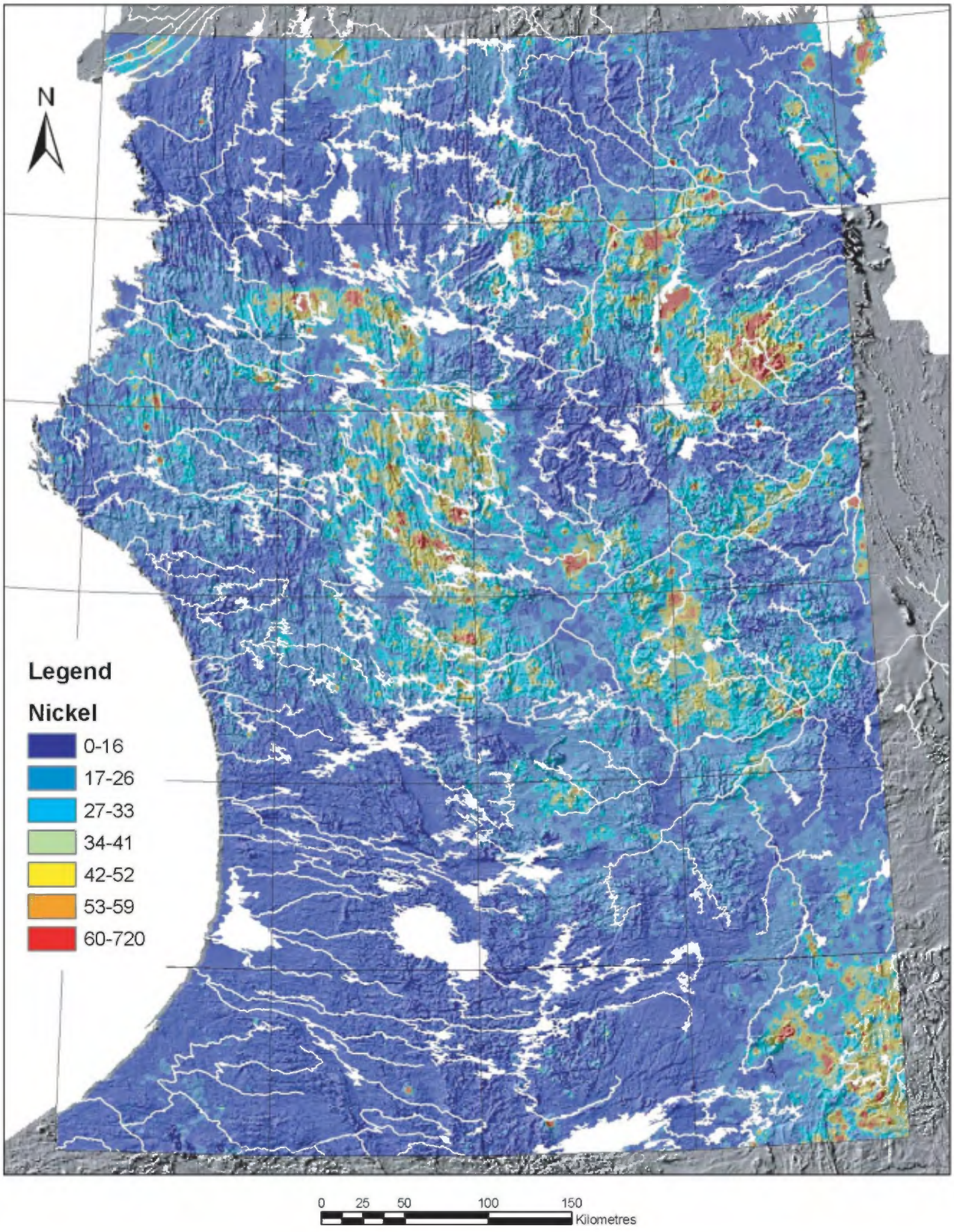

FIGURE 7.4 – Nickel distribution in lake-bottom sediments, overlain on shaded image of total magnetic field. Nickel values are in ppm.

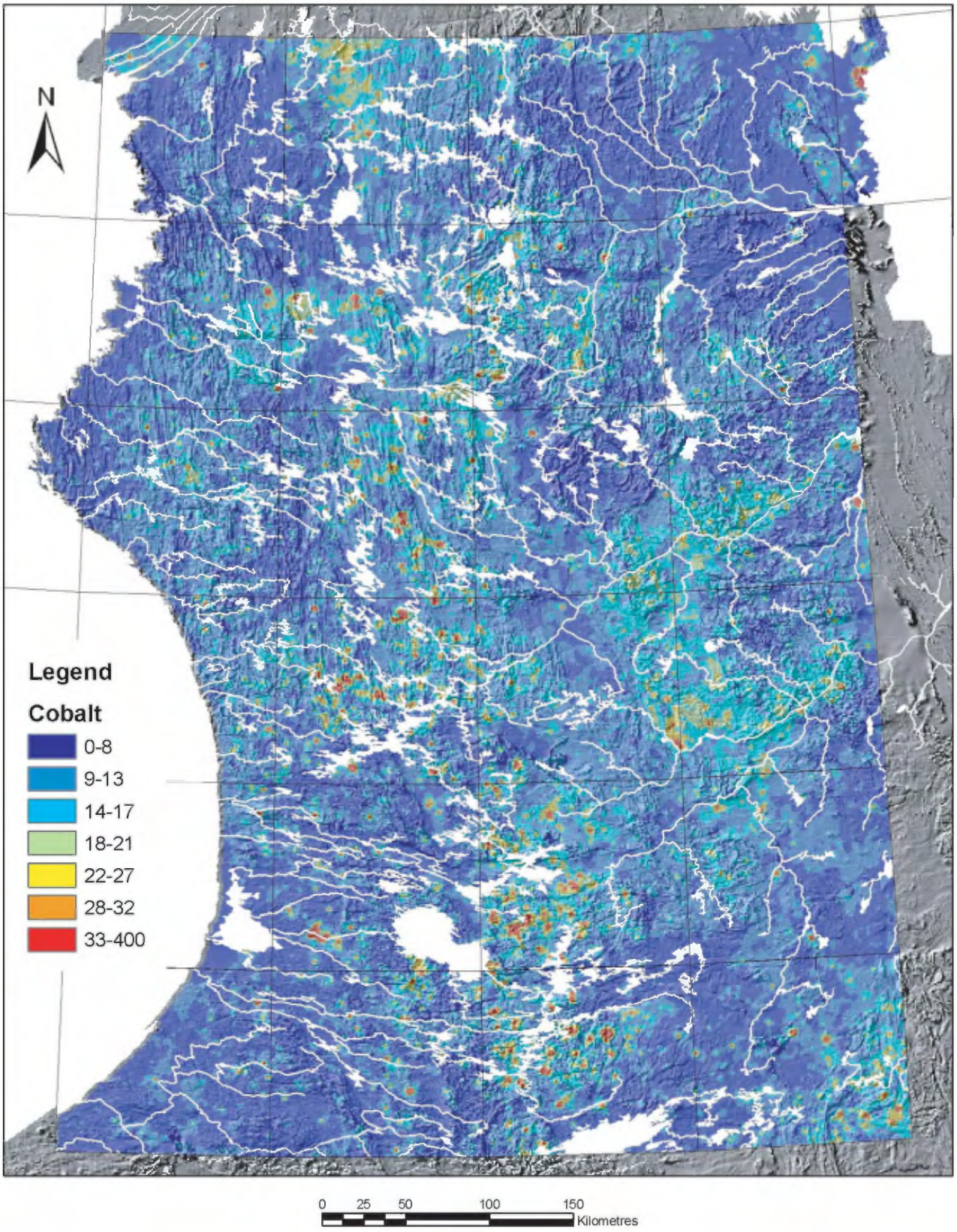

FIGURE 7.5 – Cobalt distribution in lake-bottom sediments, overlain on shaded image of total magnetic field. Cobalt values are in ppm.

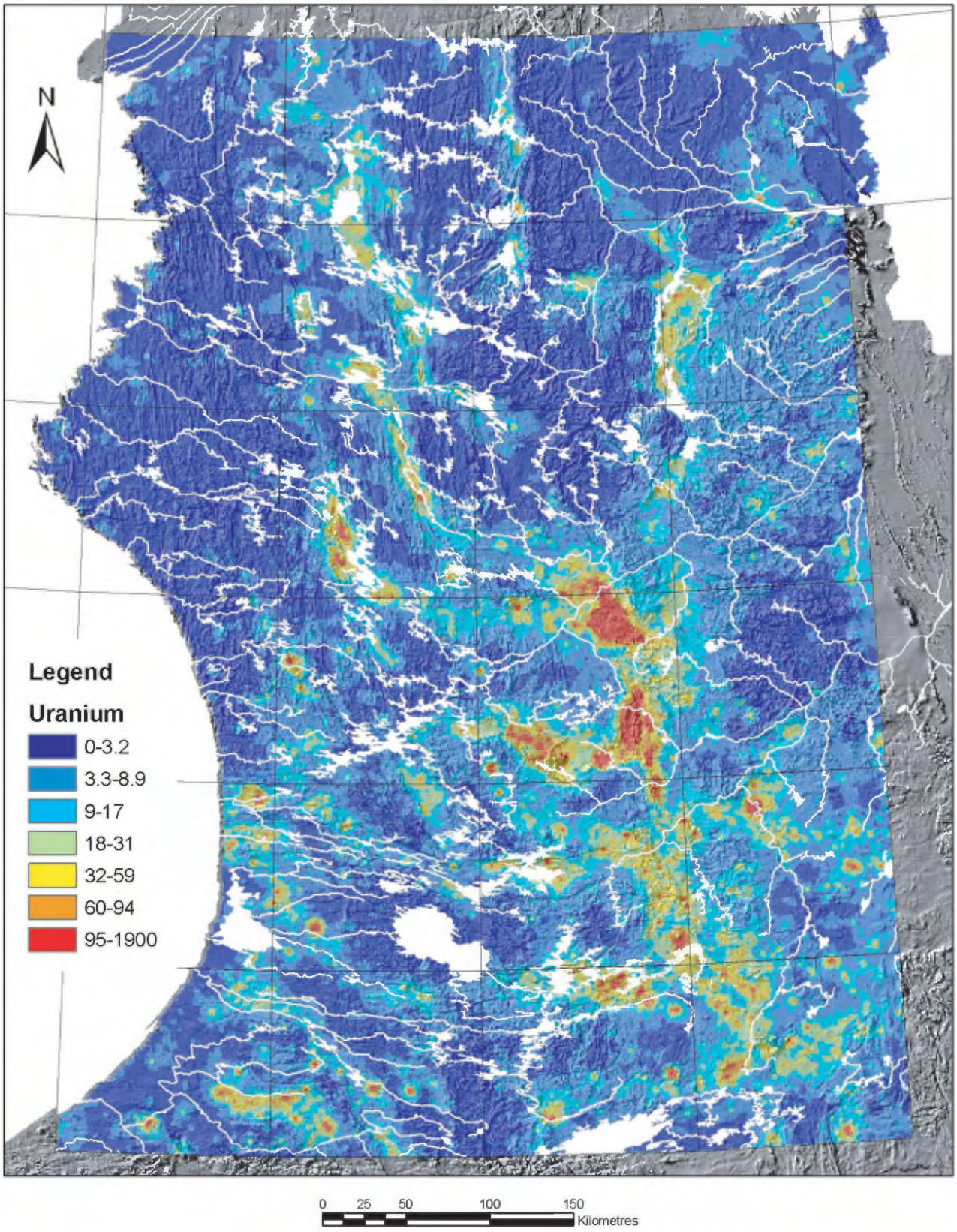

FIGURE 7.6 – Uranium distribution in lake-bottom sediments, overlain on shaded image of total magnetic field. Uranium values are in ppm.

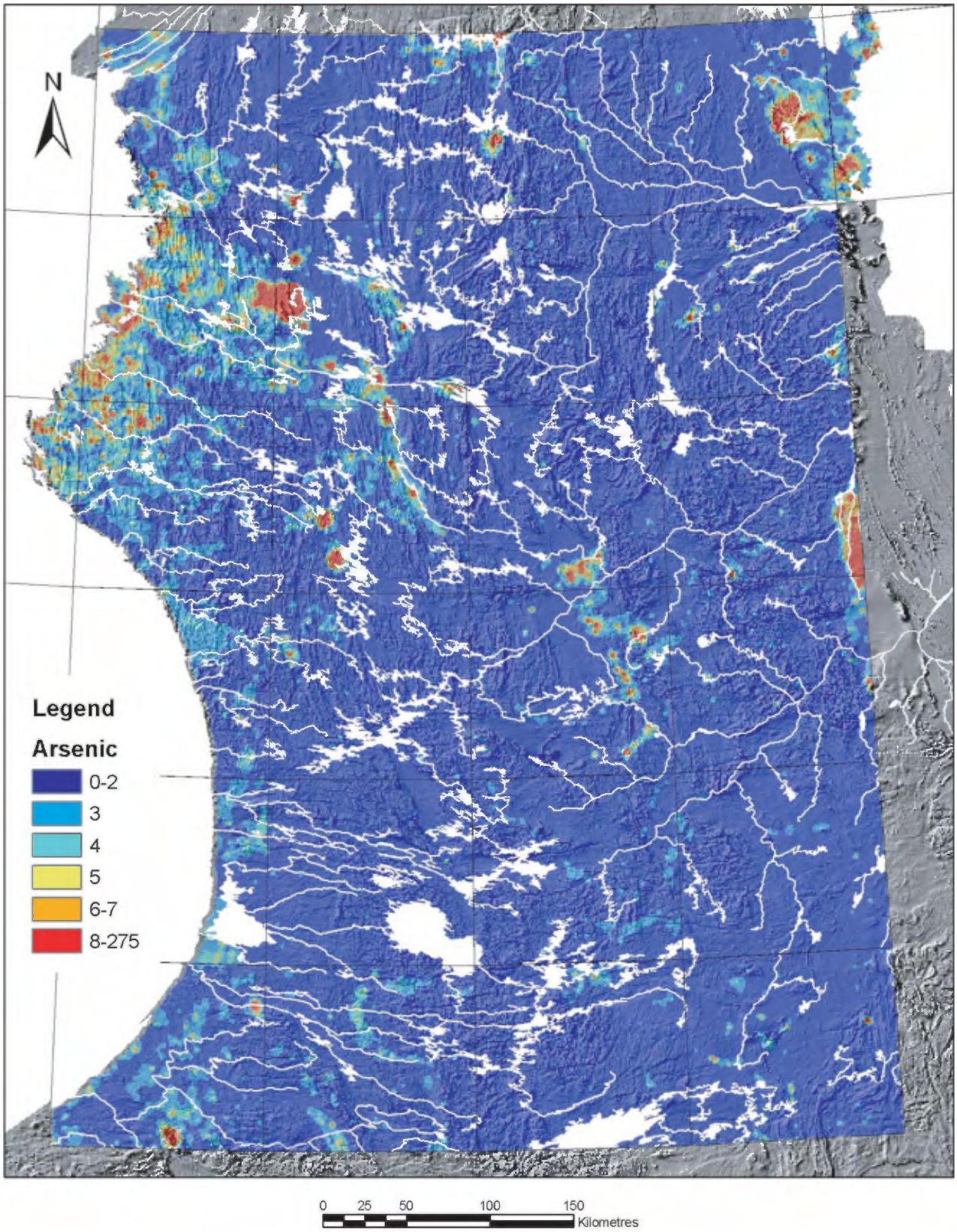

FIGURE 7.7 – Arsenic distribution in lake-bottom sediments, overlain on shaded image of total magnetic field. Arsenic values are in ppm.

important deposits are known within the study area: *Great Whale A* and *Great Whale D*. The *Great Whale E* deposit is located further south, beyond the study area. The three deposits are associated with mafic metavolcanic rocks and paragneisses, within volcano-sedimentary sequences.

The *Great Whale A* deposit has a strike length of nearly 5 kilometres, extending along a NNW-SSE axis. Several layers of iron formation alternate with paragneiss horizons over an average thickness of about 500 metres (see Figure 4 in Eade, 1966). In certain areas, the iron formation may reach up to 300 metres wide. The iron ore is generally fine-grained, except near granitic intrusions, where it is locally recrystallized. Ore reserves at this deposit were estimated in the late 1970s at 538 Mt at an average grade of 36.7% Fe (Dufour, 1978).

The *Great Whale D* deposit is located 25 kilometres east of *Great Whale A*. Following the trace of an east-plunging E-W-trending synform, the banded iron formation, in the form of a horseshoe about 1.2 kilometres by 1.5 kilometres in size, is cored by paragneisses and surrounded by granites. The iron formation may reach up to 300 metres thick. Magnetite is coarser-grained here than at the *Great Whale A* deposit. Reserves at the *Great Whale D* deposit are estimated at 148.5 Mt at an average grade of 36.8% Fe (Dufour, 1978).

Economic interest and mineral potential

Work on the *Great Whale A*, *D,* and *E* iron ore deposits reached a very advanced stage of development in the late 1970s and early 1980s. The project even involved plans for the construction of a deep-sea port along the coast of Hudson Bay, with a railway line to connect the port and the deposits, ore mills and a pellet plant (Juteau, 1975a and 1975b; Dufour, 1978). However, the project was put on hold when iron ore prices plummeted in the early 1980s and the Great Whale hydroelectric project was abandoned by Hydro-Québec. A significant increase in iron ore prices could rekindle interest for iron formations in this area.

Numerous iron formation horizons were identified within greenstone belts during the Far North Program, and there is genuine potential to discover other Algoma-type iron ore deposits in this vast territory. However, since no detailed work was conducted on these iron formations, assessing their potential is a difficult task. The Dupire, Kogaluc, Payne, Vénus, and Thury belts appear to offer the greatest potential (Figure 7.1). The Dupire belt (Lamothe, 1997; Parent *et al.*, 2001) contains thick sequences of magnetite iron formation, outlined by a strongly positive anomaly on the regional aeromagnetic map. Given its geographically remote location (in the centre of the region), the viability of a potential deposit is unlikely however. On the other hand, in the northeast part of the area, iron formations in the Thury belt (Madore *et al.*, 2000) may represent an interesting target. Located about 50 kilometres from the mouth of the Rivière Arnaud on Ungava Bay, these iron formations are composed of metamorphosed and recrystallized magnetite, with grains locally reaching a few millimetres in size.

Volcanogenic sulphides (type 2)

Volcanogenic massive sulphide deposits (Franklin *et al.*, 1981; Franklin, 1993 and 1995) have played a major role in the mining history of Québec. They have namely contributed to the world renown of the Archean Abitibi Greenstone Belt.

Volcanogenic sulphide occurrences in the NESP are found within volcanic units that were metamorphosed to the amphibolite and granulite facies. Mineralized zones are characterized by the presence of metamorphic minerals such as anthophyllite, cordierite, garnet, and biotite, resulting from the impact of regional metamorphism on sericite and chlorite alteration zones associated with volcanogenic systems. The presence of gahnite, sillimanite, staurolite, gedrite, and kyanite was also noted in certain locations.

Several volcano-sedimentary belts host mineralized showings or alteration parageneses that may be related to volcanogenic systems. A total of 16 showings or mineralized zones of this type were inventoried (see accompanying map of mineral occurrences). Five areas in particular stand out, namely the Duquet, Nantais, Tasiaalujjuaq, Qalluviartuuq, and Coulon belts (Figure 7.8).

A description of the main volcanogenic sulphide showings in the NESP and prospective environments for this type of mineralization has already been published in a previous report (Labbé and Lacoste, 2001), consequently we will only briefly review the main showings here.

Duquet belt

The Duquet belt is one of the areas in the NESP with the strongest potential for volcanogenic mineralization. Six volcanogenic occurrences (Figure 7.9) were discovered in this belt, in two areas with distinct geological settings (Chapdelaine and Villeneuve, 2000; Villeneuve, 2000). Many of these showings have particularly high gold grades, making them that much more interesting.

The FB zone (Figure 7.9) is mainly characterized by mafic units overlying a tonalitic intrusion interpreted as synvolcanic. An extensive hydrothermal alteration zone, outlined by the presence of anthophyllite-cordierite-chlorite-garnet schists, borders and delineates the intrusion. A few layers of ultramafic rocks and iron formations are also observed. Three volcanogenic sulphide showings are associated with this zone. The *Francoeur* showing corresponds to a folded massive sulphide horizon (pyrite, sphalerite, chalcopyrite, pyrrhotite) about one metre thick on average (Chapdelaine and Villeneuve, 2000), hosted in an anthophyllite-garnet schist probably derived from a mafic protolith and in contact with an iron formation. Best results are: 6.4% Cu, 3.4% Zn, 0.18 g/t Au, and 64 g/t Ag over 1.5 m (channel sample). The *Havre Sigouin* showing

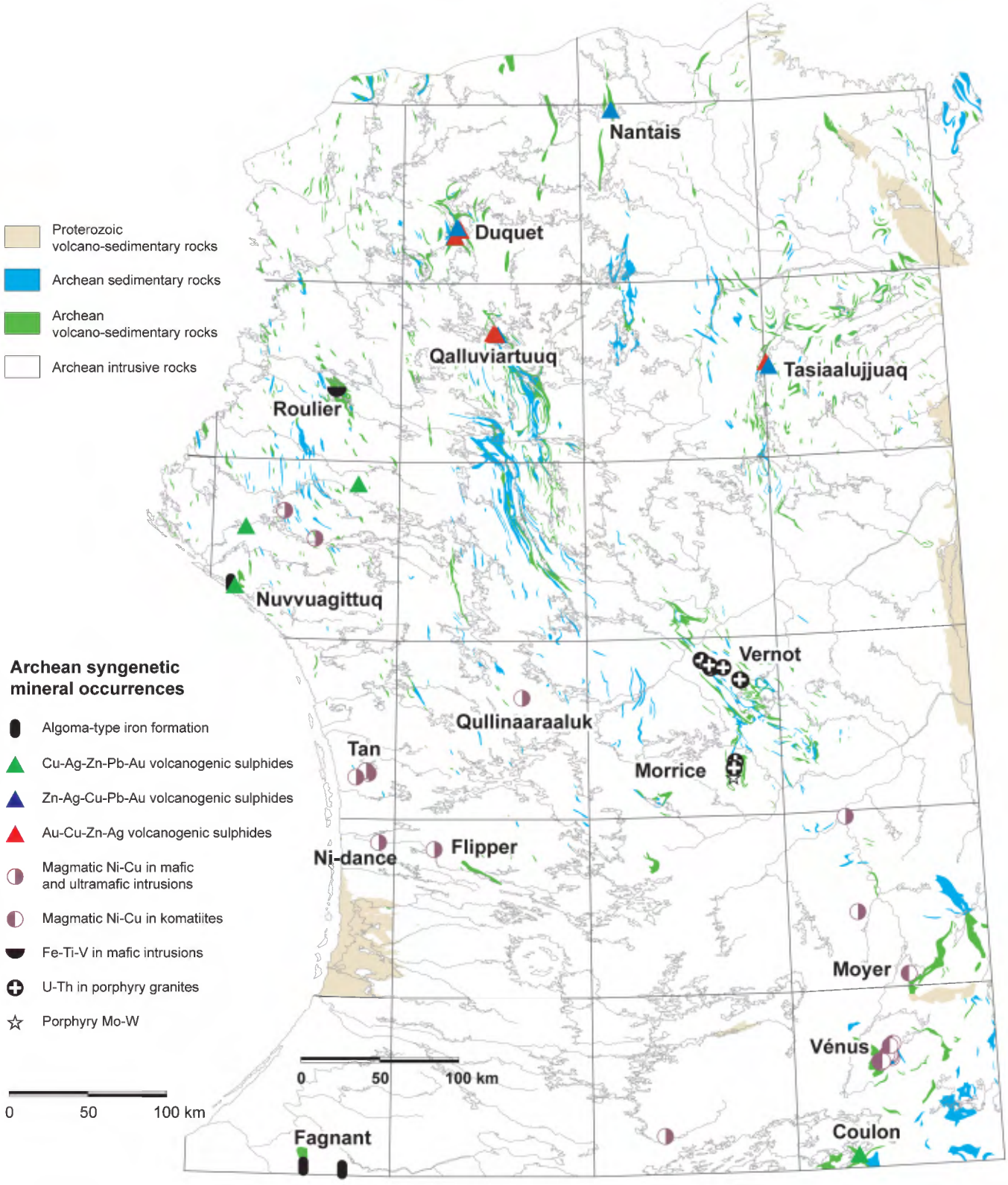

FIGURE 7.8 – Location of Archean syngenetic mineral occurrences.

is located about 400 metres northeast of the *Francoeur* showing. The mineralized zone contains disseminated chalcopyrite and centimetre-scale veining in a metabasalt with garnet porphyroblasts (up to 3 cm) and anthophyllite. Grab samples yielded grades reaching 12.58 g/t Au, 10.4% Cu, and 46 g/t Ag. The *Scrap Yard* showing consists of centimetre- to decimetre-scale veins of massive to semi-massive sphalerite locally accompanied by magnetite, pyrrhotite and chalcopyrite, hosted in an altered mafic rock with anthophyllite, chlorite, garnet, and cordierite. A metre-scale layer of ultramafic rock altered to serpentine, talc, steatite, and fuchsite occurs near the mineralized zone. A channel sample graded 4.6% Zn over 2.3 m (Chapdelaine and Villeneuve, 2000).

About 5 kilometres northeast of the FB zone, the Petite zone (Figure 7.9) encompasses three volcanogenic showings consisting of several scattered mineralized zones. The Petite zone is characterized by the presence of rhyolitic units and greenschist-facies metamorphism, *i.e.* lower metamorphic grade than the FB zone (amphibolite facies). Hydrothermal alteration in the volcanic rocks also appears to be less intense than in the FB zone. Sericite is observed in the Petite zone, but mineral assemblages with anthophyllite, cordierite, and garnet are absent. Rhyolitic units in this zone appear to have undergone local silicification. They occur as massive flows, lobes and breccias, as well as fine- to coarse-grained tuffs. The *COM* showing consists of decimetre- to metre-scale massive sulphide lenses with a few sulphide veins. Mineralization is mainly composed of pyrite, with sphalerite, galena, chalcopyrite, and local arsenopyrite. Grades of 34.29 g/t Au, 533 g/t Ag, 1.46% Pb, and 7.4% Zn were obtained in a channel sample (Cuerrier, 1997). At the *Plozin* showing, grab samples yielded grades of 4.26 g/t Au, 370 g/t Ag, 4.55% Pb, and 10.3% Zn. Finally, the *Secteur 3 - North* showing, located northwest of the two former showings, corresponds to a disseminated sulphide zone (pyrite, sphalerite, arsenopyrite) hosted in chloritized and silicified mafic rocks. A channel sample yielded grades of 7.2% Zn, 0.68% Cu, and 9.3 g/t Ag over 0.5 m (Virginia Gold Mines; press release dated February 10, 2000).

Nantais belt

The Nantais belt, in the north part of the study area (Figure 7.8), offers an interesting setting for volcanogenic occurrences. It consists of a metabasalt sequence with a few gabbroic layers or sills, occurring in contact with an assemblage of felsic volcaniclastic rocks. A discontinuous horizon of magnetite iron formation occurs in the felsic rocks, near the contact with the mafic sequence. The mafic/felsic contact is folded and characterized by the presence of anthophyllite, andalusite, sillimanite, staurolite, biotite, and gahnite, indicative of a hydrothermal alteration zone metamorphosed to the amphibolite facies. The chemical characteristics of these altered rocks are described in Labbé and Lacoste (2001).

The *Cabane* showing corresponds to a vein some 2 to 3 metres long by about 15 centimetres thick, composed of massive to semi-massive sphalerite and galena. The vein was followed along a rhyolite lens a few tens of metres wide, enclosed within the mafic sequence. It corresponds either to a stringer zone or to a remobilized volcanogenic mineralization. A study of polished thin sections revealed the presence of pyrrhotite, argentite, and tetrahedrite. A grab sample collected in the vein yielded grades of 2.48% Zn, 7.00% Pb, 0.12% Cu, 1600 g/t Ag, and 0.47 g/t Au. Two gold showings associated with disseminated sulphides in mafic rocks were also identified about 2 kilometres southeast of the *Cabane* showing.

Qalluviartuuq belt

In the Qalluviartuuq belt (Figure 7.8), volcanogenic occurrences were identified in mafic volcanic rocks located near an anorthositic intrusion. No felsic volcanic horizons were observed near the showings. Hydrothermal alteration is indicated by the presence of anthophyllite, biotite, and local gahnite (Labbé and Lacoste, 2001), or by cordierite, anthophyllite, sillimanite, and biotite (Cattalani and Heidema, 1993). The rocks are metamorphosed to the amphibolite facies. Three volcanogenic sulphide showings were recognized. The *Île-aux-Mulots 1* showing corresponds to disseminations and veinlets of sphalerite, pyrite, chalcopyrite, and pyrrhotite. Channel samples yielded grades of 3.3% Zn and 0.3% Cu over 4.8 m, and 14.2% Zn over 0.8 m (Poirier, 1994). At the *Île-aux-Mulots 2* showing, a grab sample collected in a mineralized zone with pyrite, chalcopyrite and local native copper graded 1.8% Cu, 2.5 g/t Au, and 25 g/t Ag. The mineralized zone at the *Qalluviartuuq SW* showing is similar to that observed at the *Île-aux-Mulots 2* showing. Grades of 1.10% Cu, 1.21 g/t Au, and 14 g/t Ag (Cattalani and Heidema, 1993) were obtained in a grab sample.

Tasiaalujjuaq belt

Two mineral occurrences, the *Airo* and *Tasi* showings, are associated with mafic to felsic metavolcanic rocks in the Tasiaalujjuaq belt, northeast of the study area (Figure 7.8). Within the metavolcanic sequence, a hydrothermal alteration zone some 5 to 20 metres thick was traced over nearly 2 kilometres strike length along a north-south axis (Labbé and Lacoste, 2001). This alteration zone is characterized by the presence of a cordierite-anthophyllite-garnet-biotite-staurolite-sillimanite schist. It appears to correspond to the extension of an electromagnetic anomaly a few kilometres in length, located immediately to the south (St-Hilaire, 1998). The rocks in this area are metamorphosed to the amphibolite facies. The *Tasi* showing (Jourdain, 1998) was discovered during follow-up work on a multi-element anomaly in lake-bottom sediments whose signature suggested the possibility of Olympic Dam-type mineralization. The mineralized zone consists of chalcopyrite veinlets associated with a biotite-

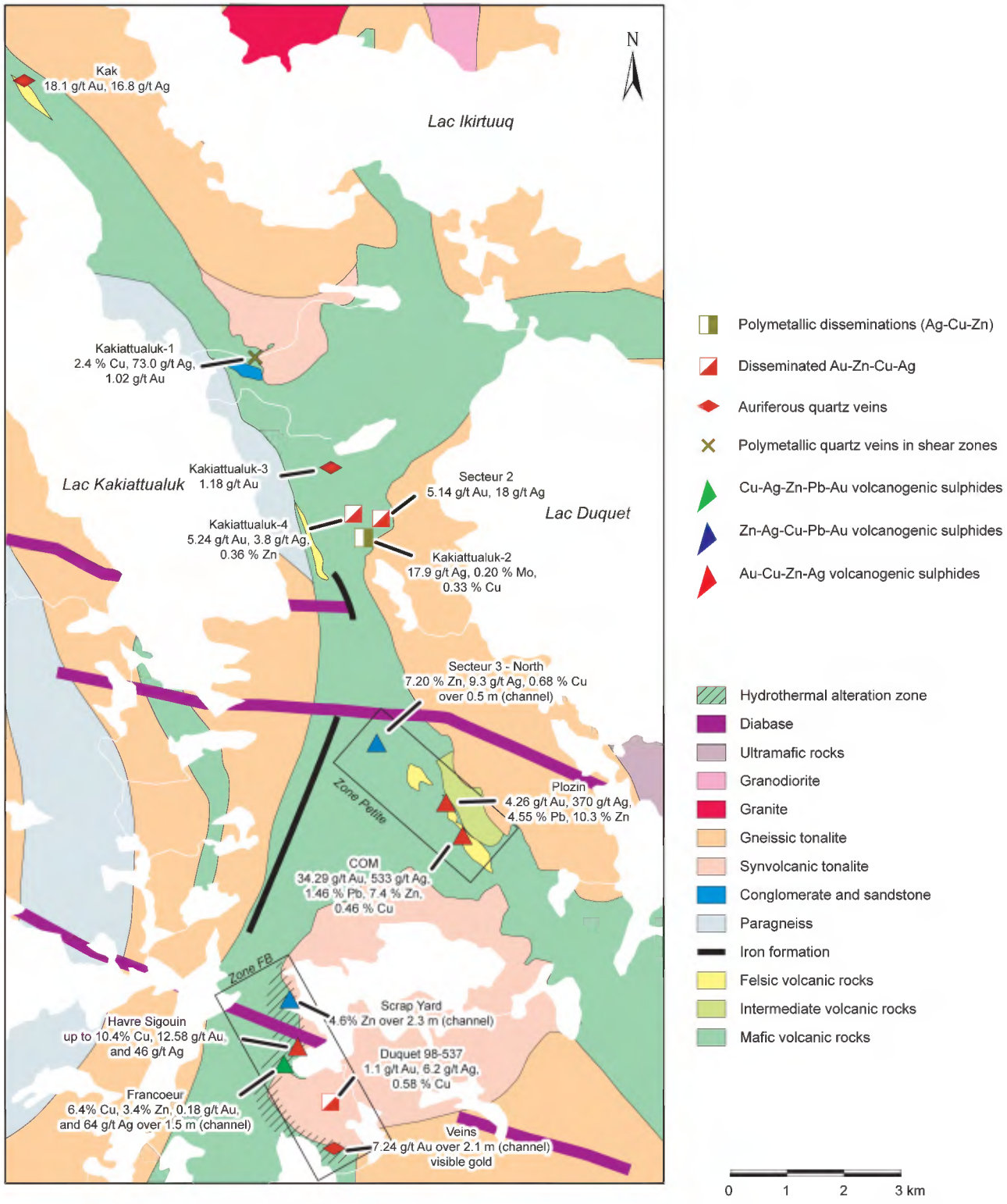

FIGURE 7.9 – Main mineral occurrences in the Lac Duquet area, geology modified after Chapdelaine and Villeneuve (2000).

rich shear zone in a tonalitic intrusion. One grab sample yielded grades of 6.95 g/t Au, 524 g/t Ag, 5.8% Cu, and 0.68% Zn. The close relationship between the mineralized zone and an alteration zone located in a mafic to felsic volcanic environment strongly suggests a volcanogenic context. Another possibility is that the veins may be the result of remobilization of a volcanogenic massive sulphide zone. The *Airo* showing (Madore *et al.*, 2000), located a bit more than one kilometre further south near the same alteration zone, occurs in a similar environment. In this location, the mineralized zone consists of disseminated pyrite in a silicified host rock. A grab sample graded 10 g/t Ag, but did not contain significant amounts of copper, zinc, or gold.

Coulon belt

The Coulon belt (Gosselin and Simard, 2001) is located along the southern edge of the region, near the southeast corner of the map area (Figure 7.8). It is mainly composed of mafic volcanic units associated with metasedimentary layers of variable grain size. This belt extends along a north-south direction for nearly 50 kilometres, beyond the study area (Thériault and Chevé, 2001). In this area, an important mineralized zone associated with a volcanogenic setting is present. The *DOM* zone (outside the map area) contains massive, semi-massive, or disseminated sulphide layers from 1 to 10 metres thick, hosted in a bimodal volcanic sequence. One grab sample graded up to 22.37% Zn, 3.07% Cu, 7.3% Pb, 482 g/t Ag, and 0.5 g/t Au, whereas the best drill intercept is 9.94% Zn, 2.12% Pb, 96 g/t Ag, and 0.73% Cu over 19.5 m (Virginia Gold Mines; press release dated April 29, 2004).

The *Julie-Sig* showing was discovered in 2003 in the north part of the belt, by a team of prospectors from Virginia Gold Mines (Huot *et al.*, 2004a). The host rock is a quartzofeldspathic mylonite with biotite, chlorite, actinolite, sericite, and epidote that cuts across a predominantly mafic metavolcanic sequence. The mineralized zone, mainly composed of up to 30% disseminated chalcopyrite, with pyrrhotite, pyrite, and minor sphalerite and galena, most likely corresponds to a remobilized volcanogenic occurrence. This mineralized zone extends in a discontinuous fashion over a little more than one kilometre, ranging from about 20 centimetres to nearly 4 metres wide (Huot *et al.*, 2004a). Several samples were collected along the zone; best results are 8.71% Cu, 0.2% Zn, 0.5% Pb, 0.28% Ni, and 425 g/t Ag.

Economic interest and mineral potential

Volcanogenic massive sulphide deposits constitute very interesting exploration targets, particularly in Archean bimodal volcanic assemblages where these types of deposits are well documented. Chalcopyrite- or sphalerite-rich massive sulphide lenses often contain high-grade mineralized zones that can be mined at a profit despite their relatively small volume.

Volcanic rocks in the NESP offer interesting potential for the discovery of volcanogenic sulphides. To date, work carried out in the search for this type of mineralization has been fairly limited. Other than recent work conducted in the Coulon belt, to the south of the study area, drill holes were completed in the Duquet volcano-sedimentary sequence, but the depth extension of mineralized zones has not been investigated.

The remoteness and isolated character of the NESP make it more difficult to carry out exploration and development work, which can diminish the profitability of a project. The high level of deformation and metamorphism in volcano-sedimentary belts contributes in reducing the volume (small belts) and grade of ore deposits (remobilization of mineralization). However, the presence of high gold grades at many showings adds a particularly interesting dimension. It is possible that the deformation, sometimes intense, responsible for the dismemberment of volcanic sequences and sulphides lenses, may also be responsible for the associated gold content.

Magmatic Ni-Cu (type 3)

Magmatic Ni-Cu deposits (Naldrett, 1981 and 1999) constitute the type of mineralization that has attracted the most exploration spending in recent years in the Far North. Four types of magmatic Ni-Cu deposits are documented in the literature (Eckstrand, 1995): 1) deposits associated with an astrobleme (Sudbury); 2) deposits associated with a rift or with continental plateau basalts (Noril'sk-Talnakh, Duluth); 3) deposits associated with komatiites (Kambalda, Raglan); and 4) deposits associated with mafic and ultramafic intrusions (Voisey's Bay). Two of these deposit types were recognized in the NESP, namely those associated with komatiites and with mafic and ultramafic intrusions.

Occurrences associated with komatiites - Lac Gayot area

Ni-Cu deposits associated with komatiites represent a major source of nickel; just think of the very well documented ore deposits in the Yilgarn Block of Western Australia (Barnes *et al.*, 1999). Exploration for this type of mineral deposit is based on a deep knowledge of the volcanology of ultramafic sequences. These generally very extensive sequences may reach up to several tens of kilometres in length (up to 400 km; Hill, 2001) and up to a few hundred metres in thickness. However, mineralized zones associated with these rocks have limited thicknesses (a few tens of metres) and occur in very specific volcanic environments. It is very important to recognize the various volcanic facies that can host this type of mineralization.

Two sub-types of komatiite-associated Ni-Cu deposits are documented (Barnes *et al.*, 1999; Naldrett, 1999; Hill, 2001). The first sub-type consists of massive sulphide bodies overlain by net-textured and disseminated sulphide facies

(Kambalda-type), whereas the second corresponds to large volumes of disseminated sulphides (Mount Keith-type).

In the southeast part of the region, the Lac Gayot area is very prospective for komatiite-associated Ni-Cu mineralization (Figure 7.8). Several Ni-Cu showings were discovered in the Vénus volcano-sedimentary belt (Figure 7.1), more specifically in the south part of the belt. The arcuate Vénus belt extends over nearly 30 kilometres along strike and reaches up to 10 kilometres wide in its central part (Gosselin and Simard, 2001). This area was mapped in detail by exploration crews from Virginia Gold Mines (Savard and Chapdelaine, 1999; Chapdelaine, 2002 and 2003; Huot *et al.*, 2004b) and by Lafrance (2001).

The south part of the Vénus belt corresponds to a south- and southeast-facing homoclinal volcanic sequence. Deformation is much less intense here than in most of the volcano-sedimentary belts in the NESP. Metamorphic grade ranges from the upper greenschist facies to the middle amphibolite facies. Overall, volcanic textures and structures are relatively well preserved.

The base of the homoclinal sequence mainly consists of granitoid rocks overlain by a felsic volcanic pile largely composed of rhyolitic tuffs with a few layers of rhyolite, andesite, and local basalt, iron formation, and polygenic conglomerate (Figure 7.10). The felsic volcanic pile hosts four important layers of ultramafic rock, from 100 to 400 metres thick, originally described as thick fractionated flows (TFF; Chapdelaine, 2002) and later reinterpreted as sills (M. Chapdelaine, personal communication, February 2005). The felsic rocks are overlain by an extensive exhalative horizon, composed of silicate- to sulphide-facies iron formation, extending for about 10 kilometres along strike and locally reaching 25 metres thick. This horizon is overlain by a unit composed of thin spinifex-textured komatiitic flows (SXF; Chapdelaine, 2002). This unit is overlain by komatiitic basalts, then basalts in which a magnetite iron formation horizon was traced for several kilometres along strike. The main Ni-Cu showings in the area are hosted in the ultramafic sills within the felsic sequence, specifically in horizons TFF-1, TFF-2, TFF-3, and NGH (Figure 7.10).

The TFF-1 horizon (Figure 7.10) is the most important in terms of volume of rock. It consists of olivine ortho- and mesocumulates and hosts the *Zone 03* deposit. The TFF-2 horizon, less continuous than TFF-1, also consists of olivine orthocumulates with a few layers of less differentiated komatiitic material. This horizon hosts the *Zone 03-SE* and *Gayot* occurrences *(Loup showing*; Gosselin and Simard, 2001*)*. The TFF-3 horizon is sporadically exposed in the eastern part of the sequence. It mainly consists of gabbroic augite-plagioclase cumulates with basal komatiitic layers localized in structures that most likely correspond to channels. Komatiites at the base of the TFF-3 horizon host the *De Champlain, L,* and *Baseline* occurrences. Finally, the Nancy-Gagnon Horizon (NGH) appears to be unconformable relative to the volcanic sequence. This horizon, composed of olivine orthocumulates and aphanitic komatiites, was recognized on both sides of the TFF-1 horizon (Figure 7.10). No cross-cutting relationships between the two horizons, NGH and TFF-1, was observed in the field however. The NGH (Figure 7.10) is interpreted as a feeder dyke (M. Chapdelaine, personal communication, February 2005) that may have played a role in the development of horizons TFF-1 and TFF-2. Rocks of the NGH host the *Nancy*, *Pyrox,* and *Gagnon* showings.

Ni-Cu mineral occurrences observed in the Vénus belt are very similar to deposits described in Kambalda, in Western Australia.

Occurrences associated with mafic and ultramafic intrusions - Lac Minto area

The second type of Ni-Cu mineralization observed in the region is associated with late pyroxenite intrusions of the Qullinaaraaluk Suite (Chapter 3). Although this suite also includes gabbros and gabbronorites, mineral occurrences appear to be associated exclusively with ultramafic facies. Intrusions of the Qullinaaraaluk Suite are weakly deformed, often display a brecciated aspect, and are generally less than one kilometre in diameter.

The *Qullinaaraaluk* showing (Labbé *et al.*, 2001; Simard *et al.*, 2005a; Baker, 2005) was discovered in the summer of 2000 (Parent *et al.*, 2003b) during a mapping survey conducted by the MRNF. This discovery triggered a prospecting rush in the Lac Minto area, which led to the discovery of a few other occurrences with similar characteristics. The *Qullinaaraaluk* showing consists of a massive sulphide lens exposed over a strike length of about 15 metres by a few metres wide, as well as an adjacent disseminated sulphide zone extending over several tens of metres. Ground-based geophysical surveys conducted by Falconbridge and SOQUEM (Hughes *et al.*, 2002) have shown that the mineralized zone exposed at the *Qullinaaraaluk* showing does not appear to extend at depth. In the massive sulphide zone, nickel grades reach 2.60%, whereas the highest copper and cobalt grades are 1.80% and 0.27% respectively (Labbé *et al.*, 2001). The intrusion that hosts the *Qullinaaraaluk* showing extends for about 700 metres strike length in an ENE direction, *i.e.* at right angles to the regional foliation recorded in enclosing diatexites (Figure 7.11). At first glance, this relationship suggests the intrusion is late relative to enclosing diatexites of the Le Roy Complex (Chapter 3). However, a pegmatite that cross-cuts the mineralized intrusion was dated at 2720 Ma (No. 72, Figure 3.9), which is much older than ages obtained for diatexites of the Le Roy Complex (2697 to 2668 Ma; Nos. 57 and 58, Figure 3.10). It is possible that the migmatitic foliation in diatexites may have simply followed the original gneissosity of melted paragneisses, the age of which is estimated at about 2760 Ma (Chapter 3).

A second showing of the same type, the *Tan* showing (Larocque and Laferrière, 2003), was discovered west of Lac Minto in 2001, during follow-up work on a lake-bottom

sediment geochemistry anomaly. The intrusion that hosts the *Tan* showing is mainly composed of plagioclase-hornblende pyroxenite, with a few layers of gabbronorite and gabbro, forming three lobes enclosed in a tonalite (Figure 7.11). The age of this intrusion was determined at 2705 Ma (No. 18, Figure 3.9), indicating the Qullinaaraaluk Suite may encompass intrusions of different ages (Chapter 3). The main mineralized zone, with its conspicuous 50-metre-wide gossan, consists of massive to semi-massive sulphides accompanied by net-textured and disseminated sulphides. Hydrothermal remobilization of chalcopyrite was locally observed along the margins of pegmatite injections. A few isolated disseminated sulphide zones were also observed in a few locations within the intrusion, outside of the main zone. A grab sample collected in the massive sulphide zone yielded grades of 1.82% Ni, 3.46% Cu, and 5.77 g/t PGE, whereas the best drill intercept graded 1.01% Ni, 1.16% Cu, and 0.8 g/t PGE+Au over 8.08 m (Larocque and Laferrière, 2003).

Several other showings of lesser importance were recognized in ultramafic intrusions of the Qullinaaraaluk Suite, in the west-central part of the study area (Figure 7.8). The *Tan W* and *Tan NW* showings (Larocque and Laferrière, 2003), located in the vicinity of the Tan showing, correspond to disseminated sulphide zones. Further south, the *Ni-dance* showing (Simard *et al.*, 2005b) consists of very rusty and highly weathered gabbronorite and pyroxenite that form an extensive gossan. About 30 kilometres east of *Ni-dance*, the *Flipper* showing (Simard *et al.*, 2005b) shows a thin layer of massive to semi-massive sulphides, along with disseminated sulphides, outlined by a large rusty zone along an escarpment on the side of a hill. The country rock consists of gabbronorite dated at 2707 Ma (No. 17, Figure 3.9).

Economic interest and mineral potential

Magmatic Ni-Cu deposits represent particularly interesting exploration targets given their potential association with platinum group elements (PGE). Since the early 2000s, significant mining and exploration activities are ongoing in the eastern part of the Ungava Trough, near the Raglan mine. Komatiite-associated magmatic Ni-Cu occurrences in the Lac Gayot area show many similarities with mineralized zones in the Raglan area, despite the fact that host rocks in the latter are Proterozoic in age.

A geochemistry study on the PGE potential of mafic and ultramafic rocks in the NESP demonstrated that the parent

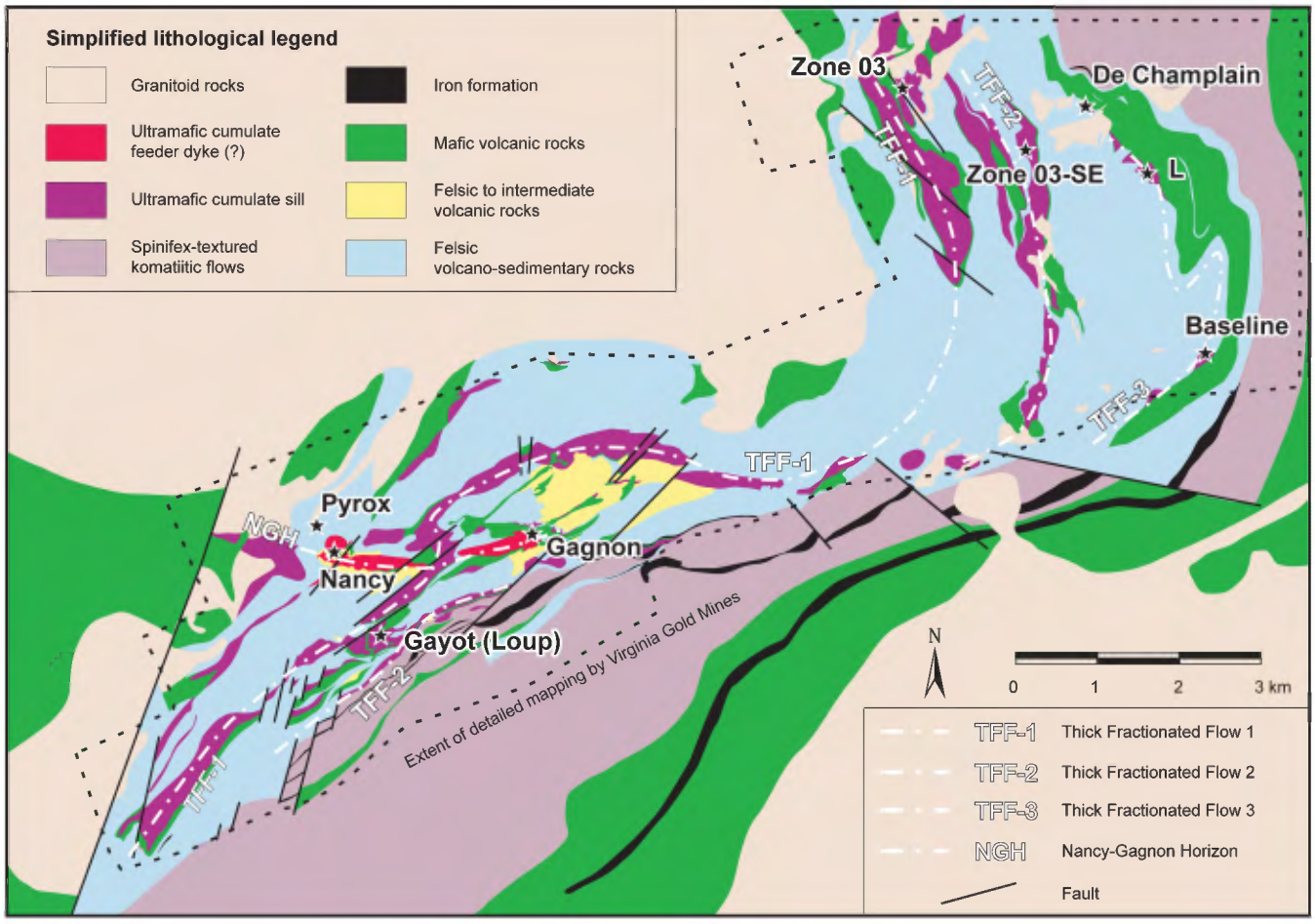

FIGURE 7.10 – Ni-Cu showings associated with komatiites in a segment of the Vénus Belt, geology modified after Chapdelaine (2002) and Lafrance (2001).

magmas from which komatiitic rocks of the Lac Gayot area originated, as well as those from which ultramafic intrusions of the Qullinaaraaluk Suite are derived in the Lac Minto area, are favourable for PGE mineralization (Labbé, 2005).

The economic potential of volcano-sedimentary belts in the Gayot Complex was revealed by the discovery of several Ni-Cu occurrences associated with komatiites. Supracrustal rocks of the Gayot Complex remain a prime target for this type of deposit. Further north, volcano-sedimentary belts in the Arnaud Complex (Figure 3.4) also offer interesting potential for this type of mineral deposit. Many of these belts have lithological assemblages similar to those of the Gayot Complex and may have equivalent ages (Chapter 3). Moreover, anomalous Ni-Cr values were obtained in ultramafic rocks from two belts in the Arnaud Complex (Madore *et al.*, 2000). The geochemistry study also suggested ultramafic rocks in certain belts of the Arnaud Complex are favourable for PGE mineralization (Labbé, 2005).

The Qullinaaraaluk Suite constitutes another interesting target, as it encompasses several intrusions distributed over a few hundred kilometres in the west part of the study area (Figure 3.9). Further east, the Couture Suite may also represent a target for Ni-Cu exploration. This unit encompasses several intermediate to ultramafic intrusions interpreted as coeval with intrusions of the Qullinaaraaluk Suite (Chapter 3). Finally, to the south, ultramafic intrusions similar to those of the Qullinaaraaluk Suite but assigned to the Châteauguay and Bacqueville suites may host new Ni-Cu showings similar to those discovered in intrusions of the Qullinaaraaluk Suite.

Fe-Ti-V in mafic intrusions (type 4)

There are two types of iron-titanium deposits in mafic intrusions (Gross, 1995b): 1) titanium-iron deposits in anorthositic intrusions; and 2) iron-titanium deposits in gabbro-anorthosite intrusions. The first type mainly consists of ilmenite and is found in Proterozoic anorthosites. The Lac Tio ore deposit, north of Havre-Saint-Pierre, is a well-known example. The second type encompasses titaniferous magnetite concentrations associated with layered or massive gabbroic intrusions, which do not appear to be restricted to a specific geological period. An example of this type of deposit is found in the Archean rocks of the Lac Doré Complex, in the Chibougamau area.

In the volcano-sedimentary Roulier Belt (Figure 7.8), a magnetite showing may be considered as a titaniferous magnetite occurrence associated with gabbroic intrusions (Gross, 1995b). The *Roulier* showing consists of a magnetitite horizon several metres thick, within a strongly deformed volcanic sequence metamorphosed to the amphibolite facies (Maurice *et al.*, 2005b). These rocks were mapped as magnetite iron formations within a mafic volcanic sequence, with anorthositic gabbros in close proximity. However, their titanium and vanadium content and their mineral assemblage observed in polished thin sections suggest instead that they consist of titaniferous magnetite-rich layers within a gabbroic intrusion. One sample yielded grades of 67.75% $Fe_2O_{3(total)}$, 14% TiO_2, and 5321 ppm V. This sample is composed of 85% opaque minerals, mainly titanomagnetite with ilmenite lamellae, along with traces of pyrrhotite and chalcopyrite. Silicate phases include hornblende, garnet, chlorite, and biotite.

The extent of the gabbroic intrusion that hosts the *Roulier* showing and the relative importance of its iron-titanium-vanadium-rich horizons have not been investigated. The folded mineralized horizon was observed over a width of 2 to 3 metres by about twenty metres length. A more detailed study is warranted to better assess the homogeneity of the mineralization and the significance of this mineral occurrence. However, the remoteness of this zone, far from major urban centres, diminishes its appeal as a potential source of Fe-Ti-V.

U-Th in porphyry granites (type 5)

This type of mineralization is hosted in granitic rocks in the Rivière Vernot and Lac Morrice areas (Figure 7.8). A significant uranium anomaly in lake-bottom sediments prompted SOQUEM and Cambior to prospect this region in 1998 and 1999. Their work led to the discovery of several minor showings of uranium, thorium, and locally, rare earth elements (Figure 7.8). These showings were not visited during our field program. The information provided below is taken from Quirion (1999).

A radiometric survey conducted in 1998 (Ryder-Turner, 1998) attracted attention on a hematized, pinkish to reddish granite. Uranium and thorium mineralization is primarily disseminated in the coarse-grained (pegmatitic) phases of the granite. Average uranium and thorium concentrations in the granite are on the order of 25 to 30 ppm and 50 to 100 ppm respectively. These grades, particularly high relative to "normal" granites, explain the regional uranium anomaly in lake-bottom sediments. The highest grades obtained from granite samples are on the order of 600 ppm U and 0.2% Th (Quirion, 1999).

This type of setting shows similarities with the Rössing ore deposit in Namibia (Berning *et al.*, 1976). The latter, in operation since 1976, currently accounts for about 6% of worldwide uranium production. It consists of a disseminated, low-grade bulk-tonnage deposit hosted in a pegmatitic granite intruded in a sequence mainly composed of paragneiss. The ore grade at Rössing is 350 ppm U (Quirion, 1999).

Porphyry Mo-W (type 6)

Only one Mo-W showing was discovered, in the Lac Morrice area (Figure 7.8), during a prospecting campaign led by SOQUEM and Cambior in the search for uranium (Quirion, 1998). Information on this showing is fairly limited (Quirion, 1998 and 1999). The molybdenum mineralization appears to be disseminated in a granite similar to that hosting

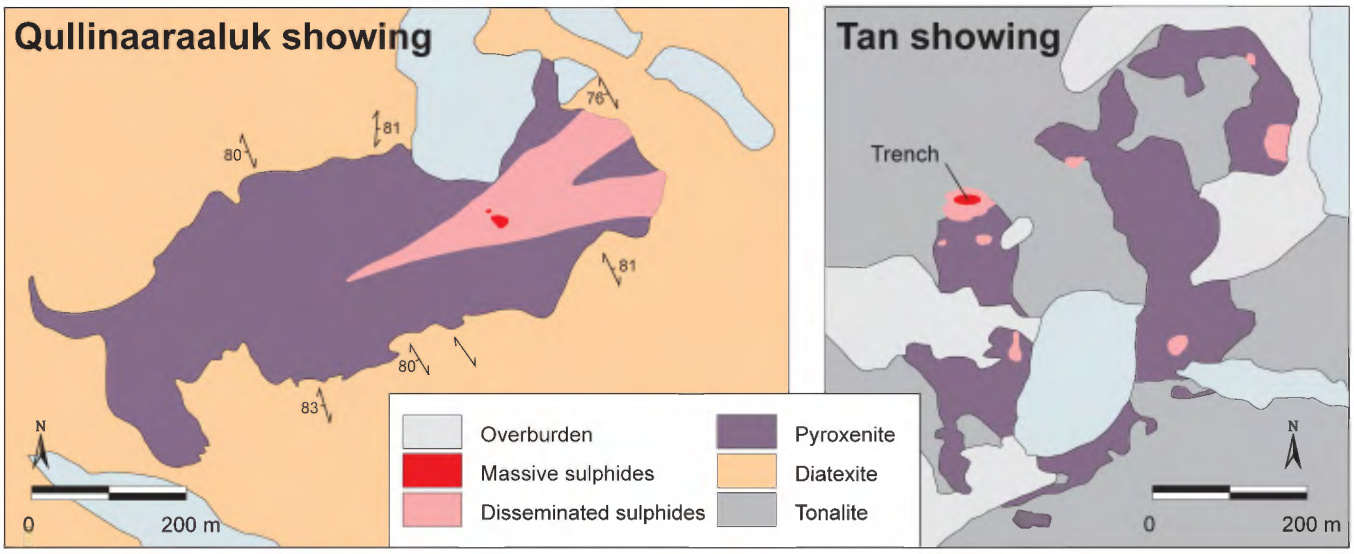

FIGURE 7.11 – Schematic representations of mineralized intrusions assigned to the Qullinaaraaluk Suite: Qullinaaraaluk showing (Labbé *et al.*, 2001) and Tan showing (Larocque and Laferrière, 2003).

uranium mineralization. One granite sample yielded a grade of 1.5% Mo (Quirion, 1998). This showing can probably be classified as a porphyry Mo-W occurrence.

Proterozoic syngenetic occurrences

Two types of Proterozoic syngenetic occurrences are known within the study area: 1) redbed Cu-Ag occurrences (type 7); and 2) sedimentary uranium occurrences (type 8). Redbed Cu-Ag occurrences are associated with either mafic volcanic units (type 7a) or sedimentary units (type 7b) of the Richmond Gulf Group in the Lac Guillaume-Delisle area (Figure 7.12). Sedimentary uranium occurrences are reported in the Lac Gayot area, at the base of sedimentary sequences of the Sakami Formation. This unit encompasses a series of small sedimentary basins bordered by normal faults and unconformably overlying the Archean basement.

Redbed Cu-Ag (type 7)

Redbed copper deposits mainly occur in continental volcano-sedimentary sequences. Two varieties of deposits associated with redbeds are documented: sedimentary redbeds (Kirkham, 1995a) and volcanic redbeds (Kirkham, 1995b). These diagenetic deposits develop late in the construction of the volcano-sedimentary sequence. Nevertheless, they are not considered here as epigenetic occurrences related to tectonic or metamorphic processes.

Cu-Ag occurrences in the Lac Guillaume-Delisle area

Cu-Ag showings associated with redbeds in the Lac Guillaume-Delisle area (Figure 7.12) are volcanic in origin (type 7a), except two showings, which are associated with sedimentary rocks (type 7b). Most of these showings were discovered in 2000 and 2001 by a field crew from the Nunavik Mineral Exploration Fund (NMEF) (Gauthier, 2001). The mineralization, mainly composed of chalcocite and local bornite, is not affected by surface weathering like other iron sulphides. The absence of rust explains in a sense why these showings have remained unnoticed until recently. The mineral occurrences were examined and described in detail by Labbé and Lacoste (2004).

The geology of Proterozoic units in the Lac Guillaume-Delisle area was described in detail by Chandler (1988). The Archean basement, consisting of granites and granodiorites of the Desbergères Suite and tonalites of the Favard Suite (Chapter 3), is unconformably overlain by Aphebian rocks of the Richmond Gulf Group. The Richmond Gulf Group encompasses three formations, which are from the base upward: the Pachi Formation, consisting of a basal conglomerate overlain by pinkish arkosic arenites; the Persillon Formation, composed of amygdaloidal and hematized subaerial basalt flows interlayered with beds of red argillite; overlain by the Qingaaluk Formation, a sequence of monogenic conglomerate, red argillites and mudstones, with cross-laminated coarse-grained sandstone. The Pachi Formation is intruded by a large sill of fine-grained gabbro (Wiachuan Intrusion). The Nastapoka Group unconformably overlies units of the Richmond Gulf Group. The base of the Nastapoka Group corresponds to a sedimentary sequence composed of arkose and quartz arenite, conglomerate, mudstone, and laminated and stromatolitic carbonate rocks. These rocks are overlain by subaerial basalt flows that form the top of the pile in this area. All of these Proterozoic units occur in undeformed, weakly metamorphosed, subhorizontal strata.

Cu-Ag occurrences in volcanic redbeds (type 7a) are found exclusively in basalts of the Persillon Formation (Figure 7.13). The maximum thickness of this basaltic unit is estimated at 70 metres (Chandler, 1988). The basalts

exhibit textures and structures typical of subaerial flows and are locally very strongly hematized. They are commonly amydgaloidal and very rarely porphyritic.

All the showings examined in the field contain chalcocite, locally accompanied by bornite and rare covellite. Chalcopyrite is practically absent. Malachite and azurite were observed in fracture planes or in cracks exposed to weathering. Fresh-cut surfaces do not show this blue-green colour typical of copper carbonate alteration. Chalcocite is either disseminated or in amygdules. A petrographic study suggests chalcocite is not an infill product, but rather a replacement of carbonate phases (Labbé and Lacoste, 2004).

Most of the mineralized zones have a limited extent and are isolated from one another. Some of the showings appear to be related to fractures, whose role in the ore deposition process remains obscure. The *Bornite* showing (Figure 7.13) is characterized by an important network of subvertical NW-SE-trending fractures coated with malachite and azurite. A few veinlets of chalcocite and bornite were also observed. A sample collected by the NMEF on this showing reportedly yielded 40% Cu and 400 g/t Ag (R. Gauthier, personal communication, 2001).

The *Graben* showing is an example of Cu-Ag mineralization associated with sedimentary rocks (type 7b). In fact, the mineralization, mainly chalcocite, is finely disseminated in sandstones of the Pachi Formation and in the Wiachuan gabbroic intrusion. The mineralized zone at the *Graben* showing is more extensive and continuous than at other Cu-Ag showings, but its average grade, on the order of 0.75% Cu and 15 g/t Ag, is somewhat lower.

Economic interest and mineral potential

Copper deposits in volcanic redbeds represent a marginal source of copper and silver on a global scale. Except for ore deposits in the Northern Michigan district, where nearly 5.4 million tonnes of copper were produced from 1845 to 1968 (White, 1968), there are very few examples of ore deposits mined at a profit. The Sustut deposit in British Columbia hosts an estimated resource of 43.5 million tonnes of ore grading 0.81% Cu (Kirkham, 1995b). In the Northern Michigan district, several ore deposits were mined, namely the Calumet-Hecla and Kearsarge deposits, where production and reserves total 114 million tonnes of ore grading 2.4% Cu and 161 million tonnes of ore at 1.0% Cu respectively (Kirkham, 1995b).

Areas where copper is mined from volcanic redbed deposits are characterized by very thick basaltic flows. For example, in the Northern Michigan district, the Portage Lake lava sequence, which hosts the copper deposits, has a minimum thickness of nearly 5 kilometres, locally reaching nearly 10 kilometres (White, 1968). At the Sustut deposit in British Columbia, the volcanic pile corresponding to the base and middle part of the Takla Group is about 3 kilometres thick (Harper, 1977), whereas the Karmutsen volcanic rocks on Vancouver Island are more than 5 kilometres thick (Lincoln, 1981).

In the Lac Guillaume-Delisle area, the maximum thickness of the Persillon Formation is estimated at 70 metres (Chandler, 1988), which is significantly less than at most known deposits of this type. This difference in volume does not diminish the importance of copper and silver grades obtained from known occurrences in basalts of the Persillon Formation, but it is obvious that any potential mineralized zone could not compare in scope with deposits in Michigan.

It is important to note that, to our knowledge, basalts forming the top of the Nastapoka Group have not been explored for Cu-Ag occurrences in volcanic redbeds. Their characteristics, fairly similar to rocks of the Persillon Formation, suggest they may also host this type of mineralization. However, the thickness of this basalt unit is not much greater than the basaltic sequence in the Persillon Formation.

Basalts in the Lac Guillaume-Delisle area may host high-grade, low-tonnage mineralized zones. In the case of the *Bornite* showing, the presence of fracturing appears to have played a role in the mineralization process by enabling the formation of chalcocite and bornite veinlets. Several brittle faults affect the rocks of the Persillon Formation, particularly to the south of Lac Guillaume-Delisle. These faults may have facilitated the formation of high-grade mineralized veins in this area.

Proterozoic units in the Lac Guillaume-Delisle area show interesting potential for the discovery of new redbed-type Cu-Ag showings. However, these rocks are located within the Lacs Guillaume-Delisle et à l'Eau-Claire Park Project, or on Category I lands of the Umiujaq Inuit community, in areas withdrawn from staking. Interest for this area is thus greatly diminished.

Sedimentary U (type 8)

Two uranium deposits were identified in Proterozoic sedimentary rocks of the Sakami Formation, in the Lac Gayot area, southeast of the region (Figure 7.12). The *Lac Gayot* and *Lac Bert* deposits (Gehrish *et al.*, 1982; Gehrish, 1987; Clark and Wares, 2006) were discovered and investigated in the 1970s by the SDBJ and Uranerz Exploration and Mining Ltd. These two deposits were not visited; descriptions provided below are taken mainly from Gehrish *et al.* (1982).

Uranium occurrences in the Lac Gayot area are considered syngenetic and synsedimentary, with some evidence locally of early diagenetic remobilization. They occur along the interface between a greenish laminated argillite unit and an arkosic wacke unit representing a low-energy lake-bottom environment. Mineralization is more important in areas where the base of the arkosic wacke unit is slightly oxidized. It consists of very finely disseminated pitchblende associated with traces of sulphides (chalcopyrite, bornite, pyrite, chalcocite, molybdenite) and organic matter. A few millimetre-scale bands of massive pitchblende were observed locally. The mineralized horizon ranges from 20 centimetres to about 2 metres in thickness.

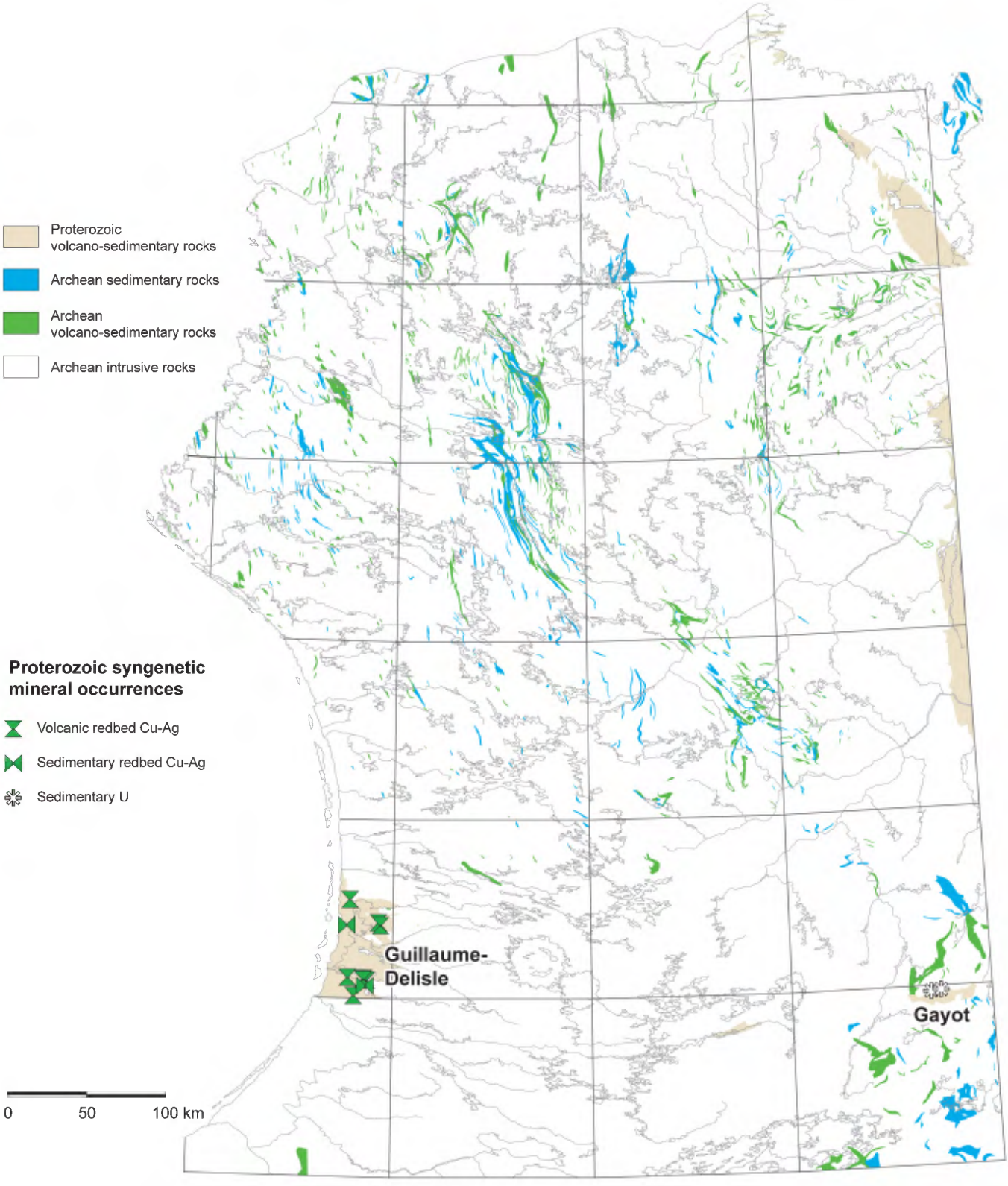

FIGURE 7.12 – Location of Proterozoic syngenetic mineral occurrences.

Reserves at the *Lac Gayot* deposit were estimated, in 1979, at 50 Mt grading 0.1% U_3O_8 or between 10 Mt and 15 Mt at 0.25% U_3O_8 (Schumacher and Fouques, 1979).

The potential for discovering new showings of this type is fairly limited in the NESP given the limited extent of Proterozoic sedimentary rocks of the Sakami Formation. In addition to the Lac Gayot basin, three other sedimentary basins were identified in the study area. The Lac Pons basin is located just east of the Lac Gayot basin, at the edge of the study area. In the Lac Bienville area (Gosselin *et al.*, 2004), about 100 kilometres west of the Lac Gayot basin, occurs the Petite rivière de la Baleine basin also known as the Mildred basin. The latter, somewhat smaller than the Lac Gayot basin, was also explored during the 1970s. Another small outlier (a few square kilometres) was recognized in the summer of 1999 in the Lac Maricourt area (Simard *et al.*, 2002), about 50 kilometres north of the Lac Gayot basin. To our knowledge, no uranium exploration has been carried out to date in these rocks.

Archean epigenetic occurrences

Nine types of Archean epigenetic occurrences, either syntectonic or synmetamorphic in origin, were observed in rocks of the NESP:

1. Ag ± Cu ± Zn polymetallic disseminations (type 9);
2. disseminated Au ± Zn ± Cu ± Ag (type 10);
3. iron formation-hosted gold (type 11);
4. auriferous quartz veins (type 12);
5. polymetallic quartz veins in shear zones (type 13);
6. polymetallic sulphide veins in ultramafic rocks (type 14);
7. rare earth elements in carbonate rocks (type 15);
8. vein uranium (type 16);
9. remobilized Mo in fault zones (type 17).

Most of these mineral occurrences are associated with volcano-sedimentary rocks. Only uranium and molybdenum occurrences are hosted in granitoid rocks.

Polymetallic disseminations (Ag ± Cu ± Zn) (type 9)

Mineral occurrences classified as Ag ± Cu ± Zn polymetallic disseminations are based on descriptive rather than genetic considerations. This type of mineral occurrence encompasses small showings of minor importance, poorly known and where very little work has been carried out. In many cases, these showings may contain a few grams per tonne of silver with minor amounts of copper or zinc. The host rock may be quite variable in composition, and most of the mineral occurrences are likely the result of a local remobilization of metals during deformation or metamorphism.

Only two showings were visited out of twenty-eight known occurrences (Figure 7.14). In most cases, information available on these mineral occurrences is very limited and may be consulted in mineral deposit files included in the SIGÉOM database.

Disseminated Au ± Zn ± Cu ± Ag (type 10)

Mineral occurrences classified as disseminated Au ± Zn ± Cu ± Ag also correspond to a deposit type based on descriptive rather than genetic characteristics. In most cases, they consist of concentrations of disseminated sulphides in shear zones or ductile faults. Host rocks either consist of mafic volcanic rocks, or more rarely so, paragneisses or tonalites. These mineral occurrences have high gold contents and may be related to orogenic gold deposits (auriferous veins) or gold-rich volcanogenic deposits. A few showings of this type were visited, in the Nantais and Qalluviartuuq volcano-sedimentary belts (Figure 7.14).

In the Nantais belt, two disseminated gold showings, about 700 metres apart, are associated with a sheared metabasalt. The *Nantais 1* showing was discovered in 1998 by a field crew from SOQUEM, Virginia Gold Mines and Cambior, during follow-up work on lake-bottom sediment geochemistry anomalies (Francoeur and Chapdelaine, 1999). The mineralized zone, with disseminated pyrite, pyrrhotite, arsenopyrite, and native copper, yielded a grade of 4.7 g/t Au. The *Nantais 2* showing (Madore *et al.*, 2002; Labbé and Lacoste, 2001) is located northwest of *Nantais 1*. The mineralized zone, 2 to 3 metres wide by 10 to 20 metres long, is mainly composed of disseminated sulphides with a 10 to 15-centimetre-thick semi-massive sulphide band, composed of pyrrhotite with minor chalcopyrite and sphalerite. Grades of 7.9 g/t Au and 7.2 g/t Ag were obtained from grab samples. These two gold showings may be derived from a volcanogenic mineralization that was remobilized along a shear zone. Rhyolitic units favourable for volcanogenic mineralization outcrop about one kilometre north of the *Nantais 2* showing.

In the Qalluviartuuq belt, gold-rich disseminated sulphide zones were observed in three locations near Pointe-aux-Gossans, along the shores of Lac Qalluviartuuq (Poirier, 1994; Berclaz *et al.*, 2005). Two of the showings, *Pointe-aux-Gossans 1* and *Pointe-aux-Gossans 2*, are located within the same rusty and highly siliceous unit, most likely felsic in composition, intercalated in a sequence of foliated metabasalts. The rusty unit was traced discontinuously over more than one kilometre. Its thickness ranges from a few decimetres to a few tens of metres, averaging 1 to 2 metres thick. The mineralization consists of disseminated pyrrhotite, chalcopyrite, and pyrite with local millimetre- to centimetre-scale concentrations of massive sulphides subparallel to the schistosity. The *Pointe-aux-Gossans 1* showing graded up to 47 g/t Au, 50 g/t Ag and 0.5% Cu, whereas a sample from the *Pointe-aux-Gossans 2* showing graded 27.4 g/t Au, 31.5 g/t Ag and 0.5% Cu (Poirier, 1994). About 4 kilometres northwest of *Pointe-aux-Gossans 2*, along the extension of the metabasalt unit, the *Qalluviartuuq-NW* showing (Berclaz *et al.*, 2005) consists of disseminated to semi-massive pyrite with traces of chalcopyrite. The mineralized zone, less than 1 metre thick, marks the contact between the metabasalt horizon and a paragneiss unit. Best grades reach up to 8 g/t Au, 18 g/t Ag, and 0.14% Cu.

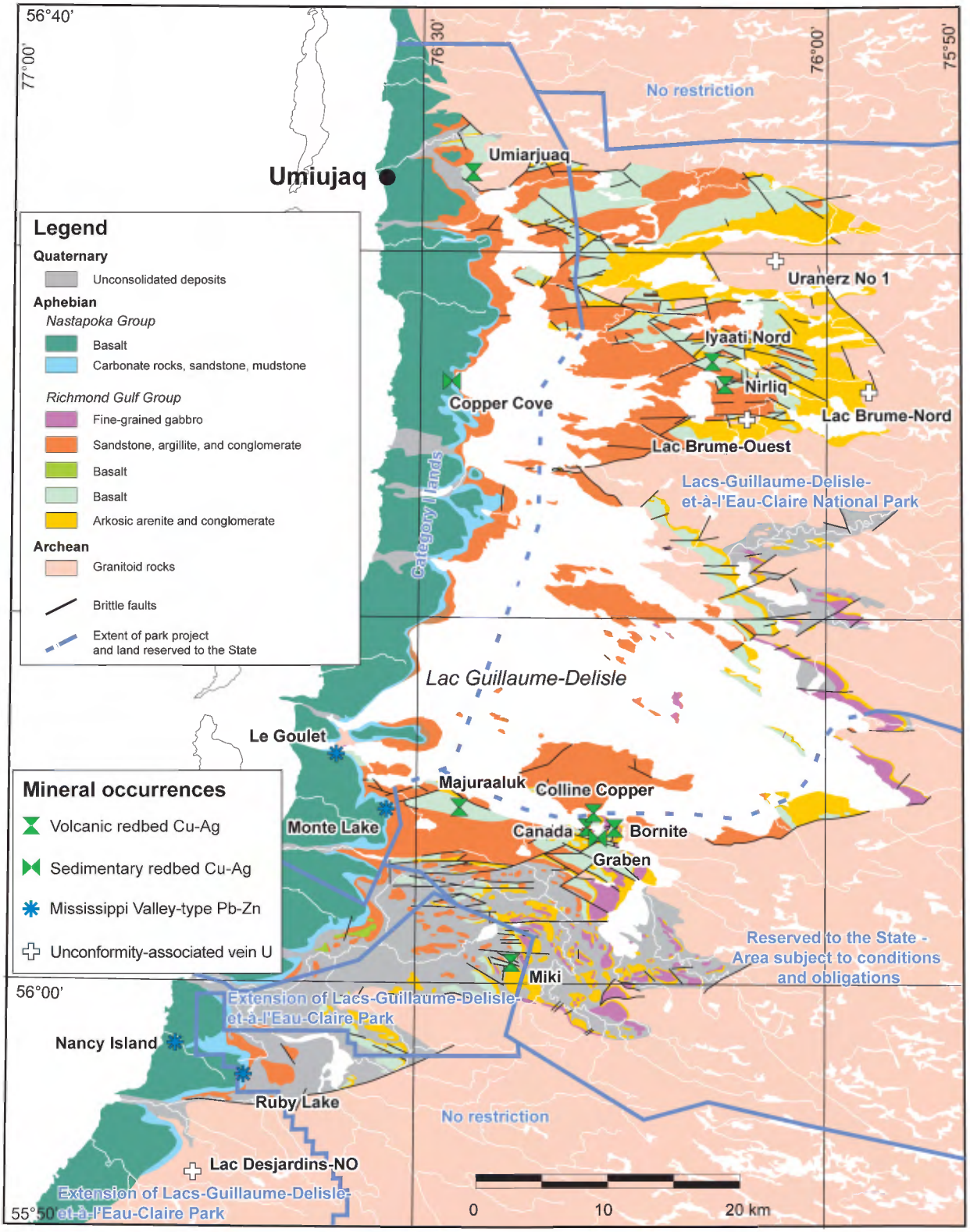

FIGURE 7.13 – Mineral occurrences in the Lac Guillaume-Delisle area, geology after Chandler (1988).

A few showings of disseminated Au ± Zn ± Cu ± Ag are also present in the Duquet belt (*Kakiattualuk-4*, *Secteur 2,* and *810091* occurrences; Madore *et al.*, 2004). These occurrences were not examined during our field work. Mineralization consists of disseminated pyrite in metabasalts, except for one showing where the host rock is tonalitic. These mineralized zones are associated with shear zones.

These disseminated Au ± Zn ± Cu ± Ag showings do not represent first-order exploration targets. They generally correspond to discontinuous mineralized zones of limited extent, where the economic potential hardly appears viable. These showings do however indicate that auriferous hydrothermal processes were active during deformation of volcano-sedimentary units, which may have concentrated significant volumes of sulphides in specific lithological or geochemical traps. These mineralized zones may be of some interest as metallogenic tracers in the search for other epigenetic gold occurrences.

Iron formation-hosted gold (type 11)

On an empirical basis, gold deposits in iron formations may be subdivided into two groups: stratiform and non-stratiform deposits (Kerswill, 1993 and 1995). Epigenetic non-stratiform deposits are associated with faults or shear zones, but maintain a very intimate link with iron formations (stratabound). Certain stratiform deposits, namely the Lupin ore deposit in Nunavut (Bullis *et al.*, 1994), may be considered as syngenetic deposits. In the Southern Cross Province of Western Australia, iron formation-hosted gold deposits in the Yilgarn Block are incontestably epigenetic (Groves *et al.*, 1988) and are interpreted, largely on the basis of their mineralogy, as auriferous skarns (Mueller and Groves, 1991; Mueller, 1997). The few gold deposits that were mined in the Yilgarn are not very large.

Gold occurrences associated with iron formations in the NESP are found in an environment comparable to that of deposits in the Yilgarn Block. They are epigenetic in origin, and the structural control is quite obvious. The most important showings are located in the Payne and Kogaluc belts, although showings of this type are also reported in the Duquet, Narsaaluk, Duvert, Dupire, Hamelin, Juet, Fagnant, and Gayot belts (Figure 7.14).

Payne belt

The Payne belt hosts four gold showings associated with iron formations, considered among the most important occurrences of this type in the NESP: the *Amaruk*, *Avingaluk*, *Tulugak,* and *Zone 1998* showings (Figure 7.15). Consequently, this area was the focus of detailed exploration work. The first two showings were briefly visited during our fieldwork. Descriptions provided herein are taken from a report by Chapdelaine (1999a), who mapped some of these zones in detail.

At the *Amaruk* zone, the oxide-facies iron formation extends along strike for about 1.5 kilometres and ranges in thickness from one to nearly five metres in fold hinges. It is in contact with paragneisses and amphibolites (metabasalts). The mineralization, namely disseminated pyrrhotite, arsenopyrite, and pyrite, is concentrated in the iron formation, primarily near the contacts with enclosing sedimentary rocks and in fold hinges. Alteration is present in the form of actinolite, hornblende, diopside, hedenbergite, and garnet, typical of skarn facies described in ore deposits of the Yilgarn Block, Western Australia (Mueller and Groves, 1991; Mueller, 1997). These skarns are interpreted as metasomatic replacements of oxide-facies iron formations during prograde metamorphism (Chapdelaine, 1999a). Deformation controls mineralization. First, the mineralization is mainly concentrated along sheared lithological contacts and in early fold hinges, forming decimetre- to metre-scale gold zones of variable grade. The subsequent development of shear bands, locally superimposed upon mineralized skarn zones, leads to the remobilization of gold in centimetre- to decimetre-scale layers along the shear bands and in late fold hinges. Gold grades obtained in the latter may reach several grams per tonne. Best results from channel samples collected on the *Amaruk* zone are: 8.86 g/t Au over 3.16 m and 16.14 g/t Au over 3.30 m. The best drill intercepts graded 4.61 g/t Au over 8.40 m; 5.28 g/t Au over 1.30 m; and 24.36 g/t Au over 0.75 m.

At *Avingaluk*, lithologies and mineralized zones are comparable to those at *Amaruk*, although the iron formation here is much more voluminous. It extends for about 4 kilometres along strike, averaging two to three metres in thickness, going up to ten metres in fold hinges. Skarn zones are also more voluminous than at *Amaruk* and spread out beyond the iron formations into the amphibolites. Late shear bands, where part of the mineralization at the *Amaruk* zone was remobilized, were not observed at *Avingaluk*, nevertheless gold grades are very interesting. A grab sample graded 36.86 g/t Au and a channel sample yielded 1.8 g/t Au over 7.9 m (Chapdelaine, 1999a).

The *Tulugak* zone is a much smaller-scale version of the two previous occurrences. Lithologies are comparable but occur in discontinuous layers. Mineralization is the same as at *Avingaluk*, but in smaller quantities, and gold grades do not exceed 3.24 g/t Au (Cuerrier, 1998).

Zone 1998 was the site of very little work. Mineralization is fairly similar to the other zones, except that the highest gold grades were obtained in diopside-garnet-rich paragneisses. One sample graded 16 g/t Au (Chapdelaine, 1999a).

Kogaluc belt

The Rivière Kogaluc area was one of the first locations in the NESP where gold-bearing iron formations were recognized. Six mineralized zones are exposed (*Kogaluc 1 to 6*; Figure 7.15). These occurrences are very similar to

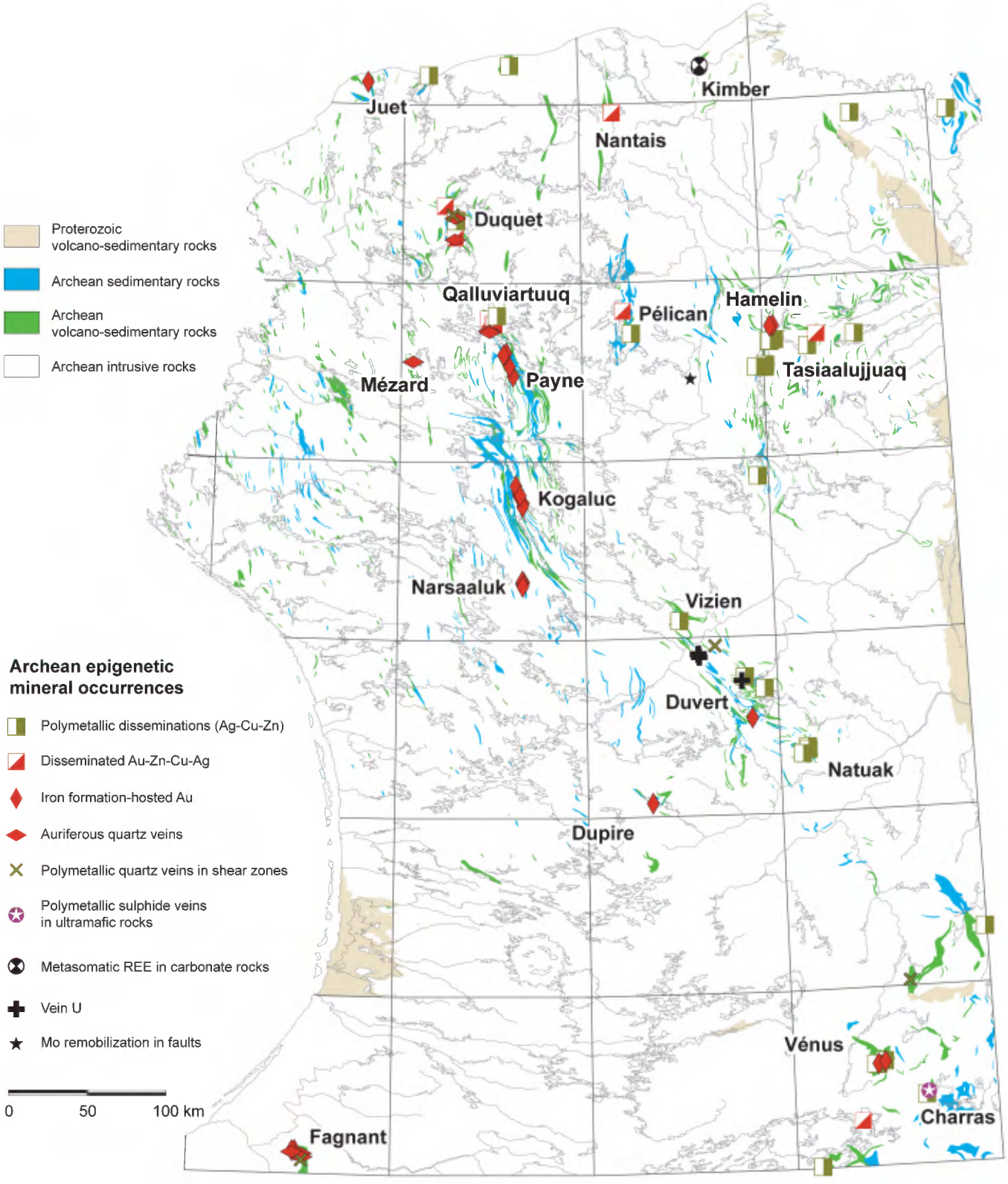

FIGURE 7.14 – Location of Archean epigenetic mineral occurrences.

those observed in the Payne belt. They occur in silicate- and sulphide-facies iron formations, and their emplacement was controlled by two phases of deformation (Francoeur, 1996; Chapdelaine, 1998). The iron formation horizons are not as voluminous as those found at *Amaruk* or *Avingaluk*. Pyrrhotite, pyrite, and arsenopyrite mineralization is associated with rocks enriched in grunerite, hornblende, garnet, and local chlorite. Mineralized zones in the Kogaluc belt commonly contain epidote, in veinlets or as pervasive alteration, which does not appear to be related to the gold mineralization. In fact, epidote-rich rocks contain very little to no gold. Epidote and chlorite are probably the products of retrograde metamorphism. Overall, the metamorphic grade in the Kogaluc belt appears to be lower than in the Payne belt. The best gold grades obtained in each of the six mineralized zones in the Kogaluc belt are listed in Figure 7.15.

Narsaaluk area

The Narsaaluk area (Figure 7.14) is located about 50 kilometres south of the Kogaluc belt, along the extension of the Payne and Kogaluc belts. Volcano-sedimentary bands in the Narsaaluk area were assigned to the Mézard Complex. Mineral occurrences in these rocks are similar to those observed in the Kogaluc and Payne belts, although iron formation horizons are more discontinuous and less extensive. Five gold showings were discovered in these iron formations (Villeneuve and Chapdelaine, 1999). Very little exploration has been conducted here, thus very little information is available on these showings. Reported gold grades from grab samples range from 1 to 7.9 g/t Au.

Dupire belt

Gold showings in iron formations exposed south of Lac Dupire were among the first to be discovered in the Far North (Chapdelaine, 1995; Lamothe, 1997). The *Dupire* showing (3.4 g/t Au) occurs in an iron formation with magnetite and grunerite, hosting finely disseminated pyrrhotite and chalcopyrite as well as disseminated arsenopyrite bands in quartz-chlorite veins cross-cutting the regional foliation. This mineralized zone is attributed to an episode of late deformation (Lamothe, 1997).

Economic interest and mineral potential

Gold occurrences in iron formations represent an interesting exploration target in volcano-sedimentary belts. This deposit type includes a few world-class ore deposits: the Lupin deposit in Nunavut (Bullis *et al.*, 1994), Homestake in South Dakota, and Morro Velho in Brazil (Kerswill, 1995). In Australia, ore deposits in the Yilgarn Block occur in environments that are very similar to those of occurrences observed in the NESP. However, they constitute more modest mines. For example, the Nevoria mine, one of the larger ore deposits of its type in the Southern Cross Province, produced, from 1907 to 1994, 389,500 tonnes of ore grading 6.3 g/t Au from underground operations and 3.15 million tonnes of ore grading 2.7 g/t Au from open pit operations (Mueller, 1997).

All the volcano-sedimentary belts in the NESP offer an interesting potential for the discovery of new gold showings in iron formations, even belts where this type of mineralization has not yet been observed. In addition to the few belts discussed above, gold occurrences associated with iron formations are also inventoried in the Vénus, Fagnant, Duvert, Hamelin, Duquet, and Juet belts (Figure 7.14). Iron formation horizons were also observed elsewhere, namely in the Charras, Moyer, Papijjusaq, Tasiaalujjuaq, Rivier, Gorribon, Thury, and Nuvvuagittuq belts.

Auriferous quartz veins (type 12)

Auriferous quartz vein deposits (Robert, 1995), also known as mesothermal gold deposits or orogenic lode gold deposits, are common and very well documented in the Abitibi Subprovince. Gold is disseminated within quartz and carbonate veins or their wall rocks, associated with shear zones or faults formed during brittle-ductile deformation. This type of mineralization, which is typical of greenstone belts, occurs in both volcano-sedimentary rocks and associated intrusive rocks.

Auriferous quartz veins are much less common in the more metamorphosed volcano-sedimentary belts of the NESP, where orogenic gold is typically associated with disseminated sulphides in rocks sheared by dominantly ductile deformation. A few auriferous quartz veins have been observed in the Fagnant, Qalluviartuuq, and Duquet belts (Figure 7.14) where the metamorphic grade is generally lower than most of the other volcano-sedimentary belts in the NESP. A small gold showing in an irregular quartz pocket was also found in a belt assigned to the Mézard Complex, to the west of the Qalluviartuuq and Payne belts (Figure 7.14).

Fagnant belt

The schistose rocks that constitute the Fagnant belt are very different from the gneissic rocks generally observed in other greenstone belts of the NESP. Three auriferous quartz veins have been identified in the Fagnant belt and are described in reports by Girard (1999) and Milord and Girard (2000).

In general, the quartz veins cut through schistose host rocks, which are mostly metabasalts. Gold is restricted to the veins and is associated with sulphide phases that vary from one showing to another. The sulphide assemblage may include arsenopyrite, pyrrhotite, pyrite, galena, chalcopyrite or sphalerite. According to Milord and Girard (2000), the gold-bearing veins are probably the products of remobilized disseminated mesothermal mineralization. The host rocks display little alteration.

Qalluviartuuq belt

Along the shores in the west part of Lac Qalluviartuuq, at the *Anorthosite 1* and *Anorthosite 2* showings, gold is associated with pyrite and chalcopyrite in millimetre- to centimetre-scale quartz veins of limited lateral extent. The veins display an anastomosing pattern in coarse-grained, sheared and locally mylonitic anorthositic rocks (Poirier, 1994; Berclaz *et al.*, 2005). One sample yielded 2.8 g/t Au and 2.14% Cu.

Duquet belt

In the southern part of the Duquet belt, mineralization at the *Veines* showing (Madore *et al.*, 2004) is associated with several centimetre- to decimetre-scale quartz veins that cross-cut the fabric of a muscovite-chlorite schist. The schist marks the contact zone between mafic volcanic units and a tonalitic intrusion thought to be synvolcanic. Mineralization consists mainly of pyrite and trace amounts of chalcopyrite and sphalerite, disseminated along the quartz vein margins. A few rare gold grains were observed within the veins (M. Chapdelaine, personal communication, 2000). A channel sample yielded 7.24 g/t Au over 2.1 m.

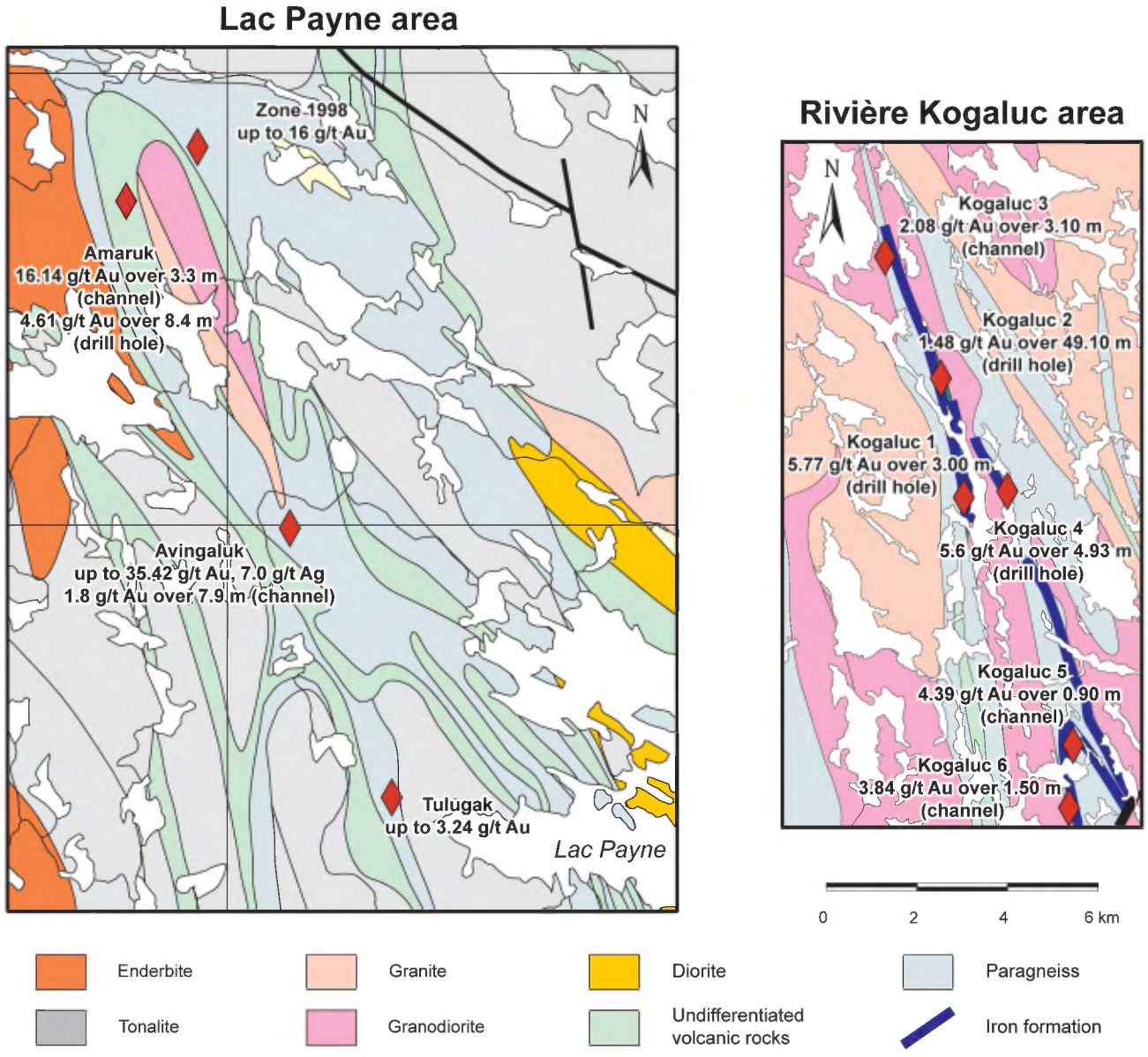

FIGURE 7.15 – Iron formation-hosted gold occurrences in the Lac Payne area (geology modified after Berclaz *et al.*, 2005) and the Rivière Kogaluc area (geology modified after Parent *et al.*, 2003b).

A little more than ten kilometres north of the *Veines* showing, the *Kakiattualuk-3* showing (Chapdelaine, 1999b) consists of a quartz vein with disseminated pyrite and arsenopyrite, cross-cutting metabasalts and metatuffs of intermediate composition. A grab sample from the vein yielded 1.18 g/t Au (Chapdelaine, 1999b).

Economic interest and mineral potential

At the present time, auriferous quartz veins in the NESP are of little economic interest due to their narrow widths and limited extent. This type of deposit is associated with brittle-ductile deformation zones that affect weakly to moderately metamorphosed sequences. The Fagnant belt and the central parts of larger volcano-sedimentary belts, where the metamorphic grade is less intense, represent the most favourable areas for discovering new gold showings associated with quartz veins.

Polymetallic quartz veins in shear zones (type 13)

This type of mineral occurrence, based on the descriptive character of the mineralization, encompasses a few mineralized zones of uncertain origin. They may consist of disseminated sulphides hosted in veins or irregular quartz injections associated with intense shear zones. These showings were not investigated in the field and available information is limited. Among the four showings included in this category, only the *Kakiattualuk-1* showing, located in the Duquet belt, yielded grades worthy of interest. Grades of 2.4% Cu, 73 g/t Ag, and 1 g/t Au (Chapdelaine, 1999b) were obtained in decimetre-scale quartz veins with chalcopyrite. These veins are associated with a shear zone that marks the contact between a basalt and a porphyritic tonalite.

Polymetallic sulphide veins in ultramafic rocks (type 14)

Only one showing, located in the Charras belt in the southeast part of the study area, corresponds to this deposit type (Figure 7.14). The *Isabel* showing (De Corta *et al.*, 1999) consists of several centimetre-scale veins of massive chalcopyrite cross-cutting an ultramafic rock at right angles to the regional foliation. The ultramafic rocks are part of a volcano-sedimentary sequence that also includes layers of mafic volcanic rocks, iron formations, sandstone, conglomerate, and calcitic marble horizons. The intrusive or extrusive nature of the ultramafic unit was not clearly established. They probably represent flows and sills. The chalcopyrite veins are not affected by the regional fabric that overprints ultramafic rocks and more intensely, surrounding sedimentary units. Between veins, the ultramafic rocks host millimetre- to centimetre-scale pockets of massive to semi-massive chalcopyrite, occurring as late infilling of porosity or local breaks. The lack of deformation in the veins and the relatively low nickel grades relative to copper indicate the mineralization is clearly late- to syn-tectonic. Three trenches were excavated on the showing. Best results are: 2.98% Cu and 3.27 g/t Au over 2.45 m in channel sample.

The presence of Ni-Cu mineralization associated with ultramafic rocks in the Lac Gayot area suggests the possibility that chalcopyrite veins at the *Isabel* showing may be the products of local remobilization of magmatic Ni-Cu mineralization hosted in ultramafic rocks of the Charras belt. Although no nickel occurrences were discovered in the immediate vicinity of the *Isabel* showing, the setting is certainly favourable for this type of mineralization. The Vaujours Fault (Gosselin and Simard, 2001), which runs a few tens of metres south of the Ni-Cu showings and which borders the volcano-sedimentary rocks of the Charras belt to the northwest, separating them from tonalites to the southeast, may have been involved in the remobilization of copper and gold.

The chalcopyrite veins at the *Isabel* showing, although very rich in copper, do not appear to have significant economic potential given their limited extent. However, the origin of this mineralized zone remains poorly understood, such that the potential for this type of mineralization is difficult to ascertain.

Rare earth elements in carbonate rocks (type 15)

Light rare earth element occurrences were discovered in 2000, in carbonate rocks of the Kimber belt (Madore *et al.*, 2002) in the northwest part of the study area (Figure 7.14). These carbonate rocks are interpreted as marbles of sedimentary origin and not as carbonatites (Labbé *et al.*, 2003). Mineral occurrences associated with these carbonate rocks are different from rare metal deposits associated with carbonatite intrusions (Richardson and Birkett, 1995). The rare earth element occurrences are most likely epigenetic; they may result from a metasomatic event related to the emplacement of syenite intrusions further south.

The south part of the Kimber belt is composed of an assemblage of carbonatized mafic to intermediate volcanic rocks, marbles, calc-silicate rocks, iron formations, and paragneisses, separated from a non-carbonated mafic volcanic sequence by a metre-scale layer of semi-massive sulphides (Figure 7.16). A tonalite, likely synvolcanic, cross-cuts the non-carbonated mafic unit. A horizon of schistose calcitic marble, about 10 metres thick, extends for about 2 kilometres strike length along a north-south axis, within the carbonatized volcanic sequence. The north and south extremities of this schistose marble horizon are composed of coarse-grained recrystallized calcitic marble in layers from one to ten centimetres thick (Figure 7.16).

Light rare earth element occurrences with grades on the order of 1.59% REE_2O_3 (rare earth oxides) are hosted in recrystallized marbles in the south part of the horizon (*Lataille South* showing; Figure 7.16), whereas average grades in the central part of the same horizon, where it is thickest (and not recrystallized), range from 0.14% REE_2O_3 to 0.38% REE_2O_3 (Labbé *et al.*, 2003). The rare earth

element-bearing mineral was identified using a scanning electron microscope as allanite. It occurs as fine disseminations in the schistose marble, and coarser-grained disseminations in recrystallized marble.

The source of these mineral occurrences remains an enigma. The presence of enriched rare earth element concentrations in carbonate rocks is consistent with a syngenetic mineralization in carbonatite intrusions or in volcanic carbonatite layers. However, field observations and the chemical composition of the marble suggest instead a sedimentary origin (see discussion in Labbé *et al.*, 2003). These marbles may have acted as a chemical trap and become enriched in rare earth elements during a metasomatic event contemporaneous with the emplacement of syenite intrusions. No intrusions of this type are reported near the mineralized zones, however two nepheline syenite intrusions were mapped a few tens of kilometres further south, along the same structural lineament (Kimber Alkaline Suite, Chapter 3). It is possible that a similar intrusion, that is not exposed or simply hasn't been mapped, may have affected the rocks of the Kimber belt.

The very particular nature of these rare earth element occurrences is such that the chances of discovering other showings of this type are slim in the NESP. Within the Kimber belt, the north and south extensions of the mineralized zone were not investigated. However, the grades obtained, the remoteness of these rocks, and the presence of allanite (not a rare earth-rich mineral) rather than bastnaesite or monazite, are three elements that lead us to consider the economic potential of these rocks as marginal.

Vein uranium (type 16)

Vein uranium occurrences (Ruzicka, 1995a) are the result of remobilization of uranium in fractures, shear zones, or stockworks. In the NESP, syngenetic U-Th occurrences in the granitic rocks of the Rivière Vernot and Lac Morrice areas are accompanied by a few showings derived from the hydrothermal remobilization of uranium and thorium (Figure 7.14), along fault planes or in shear zones. According to Quirion (1998), uranium mineralization occurs in veins or pockets of black quartz, biotite and magnetite, locally forming breccias. Observed mineralized zones are commonly limited in extent but may show very interesting grades, reaching up to 0.13% U and 0.43% Th. The potential to discover high-grade uranium veins remains fairly interesting in this area.

Mo remobilization in faults (type 17)

This deposit type is represented by only one showing, located southeast of Lac Pélican (Figure 7.14). The *Tikimurtuk* showing (Cadieux *et al.*, 2004) consists of pyrite and molybdenite veinlets hosted in granitic rocks, near a brittle-ductile fault zone outlined by strong hematite alteration. Molybdenum grades in this mineralized zone reach 0.3% Mo. No information is available on the size and extent of this showing, which appears to be of little economic interest.

Archean or Proterozoic (?) epigenetic occurrences

Archean or Proterozoic epigenetic occurrences encompass two types of occurrences hosted in Archean granitoid rocks: Cu-Co quartz-magnetite veins (type 18) and polymetallic quartz veins (type 19). These mineral occurrences are obviously epigenetic, occurring as veins cross-cutting granitic rocks, but their age has not been determined. The brittle nature of host structures, ubiquitous hematization in the immediate vicinity of showings, and the proximity of Proterozoic volcano-sedimentary rocks suggest these mineral occurrences may be post-Archean in age.

Cu-Co quartz-magnetite veins (type 18)

In the Lac Veillon area (Figure 7.17), a regional brittle fault trending NW-SE, *i.e.* cross-cutting the regional foliation, shows intense hematization and silicification over a strike length of about 2 kilometres. Two copper-cobalt showings, *Cipmyluk 1* and *Cipmyluk 2* (Madore *et al.*, 2004) are found along this fault segment. At *Cipmyluk 1*, pockets of chalcopyrite and pyrite are found inside quartz veins and locally in wall rocks. The country rock is a foliated and fractured granodiorite, injected with magnetite veins and quartz veins that cross-cut the foliation. Magnetite injections are locally very intense. At *Cipmyluk 2*, the mineralized zone practically forms a breccia with a magnetite matrix and pockets of chalcopyrite and pyrite. Just like at *Cipmyluk 1*, quartz and magnetite injections cross-cut the regional foliation in the granodiorite. Grades at *Cipmyluk 1* and *Cipmyluk 2* (Madore *et al.*, 2004) are respectively: 2.20% Cu and 125 ppm Co, and 3.40% Cu and 731 ppm Co.

Discovered during a reconnaissance campaign by Virginia Gold Mines (M. Chapdelaine, personal communication, 2001), these isolated mineral occurrences of limited economic interest were the object of very little subsequent work. However, the setting may be an interesting one. There are many similar brittle faults in this area that may be prospective for this type of mineralization. Moreover, breccias with a magnetite matrix observed at *Cipmyluk 2* resemble those of Olympic Dam-type IOCG deposits (Oreskes and Hitzman, 1993; Gandhi and Bell, 1995). These deposits are associated with fracture zones that affect continental supracrustal rocks in generally Proterozoic, late- to post-orogenic settings. Assuming the Archean granodiorites that host the *Cipmyluk* showings were at one point unconformably overlain by Proterozoic supracrustal units, it is possible that the mineral occurrences in this area may represent the roots of an IOCG-type system.

Polymetallic quartz veins (type 19)

A few quartz and carbonate veins containing sulphide pockets were observed near the Nuvvuagittuq Belt (Lee,

1965; Gauthier, 2001; Simard *et al.*, 2004), along the coast of Hudson Bay (Figure 7.17). In contrast with the quartz veins described in previous sections, these polymetallic quartz veins do not appear to be associated with regional faults. Here, the veins cross-cut strongly deformed and generally hematized Archean lithologies. They consist of undeformed quartz-carbonate veins from one to ten centimetres wide, generally straight and regular over several tens of metres. Locally, these veins contain centimetre-scale pockets of chalcopyrite, sphalerite, or galena. Despite the very high Cu-Pb-Zn grades obtained locally, these veins have little economic interest given their small size.

In the northeast part of the study area, north of the Kimber belt (Figure 7.17), the *Lac Grunérite* showing (Madore *et al.*, 2002) is composed of several metre-scale quartz veins with up to 5% sulphides (pyrite, pyrrhotite, chalcopyrite), cross-cutting foliated tonalites and granodiorites. A grab sample graded 0.56% Cu. The surface extent of the mineralized zone is unknown, but this showing is likely fairly similar to those in the Nuvvuagittuq area.

Proterozoic epigenetic occurrences

Two types of Proterozoic epigenetic occurrences were identified in the Lac Guillaume-Delisle area (Figure 7.17): Mississippi Valley-type Pb-Zn occurrences (type 20) and vein uranium occurrences associated with the unconformity between Archean and Proterozoic rocks (type 21). The first type is hosted in sedimentary rocks of the Nastapoka Group, whereas the second is hosted in granitic rocks of the Archean basement.

Mississippi Valley-type Pb-Zn (type 20)

Mississippi Valley-type Pb-Zn deposits (Leach and Sangster, 1993; Sangster, 1995) are composed of galena and sphalerite infilling cavities in typically dolomitic units included in platform sequences deposited along the margins of cratonic sedimentary basins, in stable tectonic conditions. Karstic dissolution of carbonate units causes layers to collapse and the subsequent infilling of cavities by ore-bearing fluids leads to the formation of breccias with galena- and sphalerite-rich matrix. Mineralized zones are unconformable at the scale of the deposit, but stratabound at the scale of the district. A single horizon of carbonate rocks may host several small deposits. Mississippi Valley-type deposits may represent significant sources of lead and zinc.

In the Lac Guillaume-Delisle area (Figure 7.13), the Nastapoka Group (Chandler, 1988) contains a stromatolitic dolomite horizon that hosts lead and zinc occurrences. These mineralized showings are known since the end of the 17th century. In the 1940s, following exploration programs, resource estimates were published for three of these deposits (Moffat, 1946; Almond, 1947; Almond *et al.*, 1947; Harwood, 1949). At the *Ruby Lake* deposit, located southwest of Lac Guillaume-Delisle (Figure 7.13), the stromatolitic dolomite horizon contains centimetre- to decimetre-scale injections of coarse-grained galena and finer-grained honey-coloured sphalerite. Mineral resources were estimated at 525,000 tonnes at an average grade of 1.26% Zn and 1.02% Pb (Chandler, 1988). About 25 kilometres further north, the mineralized zone at *Monte Lake* (Figure 7.13) is fairly similar to the one at *Ruby Lake*, except that sphalerite is not as widespread. Estimated resources at *Monte Lake* are 120,000 tonnes of ore grading 1.75% Pb. The *Nancy Island* deposit (Figure 7.13) was discovered in drill hole a few kilometres west of *Ruby Lake.* In this location, carbonate sedimentary units are overlain by basalt flows that mark the top of the Nastapoka Group. Mineral resources at *Nancy Island* are estimated at 267,000 tonnes at a grade of 2.15% Zn and 0.72% Pb. A fourth occurrence, *Le Goulet,* is located a few kilometres northwest of *Monte Lake* (Figure 7.13). No resource estimate was calculated, but grades in grab samples reach up to 15% Pb and 340 g/t Ag (Germain, 1964).

The discovery potential for additional Mississippi Valley-type Pb-Zn occurrences in dolomitic layers of the Nastapoka Group seems excellent. This carbonate unit is undeformed, dips shallowly to the west (about 15°), and extends across several tens of kilometres. Carbonate layers appear as whitish horizons in the cliffs that border the western shore of Lac Guillaume-Delisle and are visible over a strike length of about 75 kilometres along a north-south axis. Based on existing literature, exploration work was largely focused to the southwest of Lac Guillaume-Delisle, and it is quite likely that little prospecting was done outside of this area. The northward extension of the mineralized horizon offers interesting mineral potential for Pb-Zn deposits, despite the fact that the carbonate rocks in this area are overlain by basalts over a few tens of metres or may be difficult to access where they are exposed along cliff faces. Nevertheless, it is important to mention that these rocks are located in an area where claim acquisition and exploration work are restricted. The prospective units are for the most part located either in Category I lands of the Umiujaq Inuit community, or within the Lacs Guillaume-Delisle et à l'Eau-Claire National Park Project (Figure 7.13).

Unconformity-associated vein U (type 21)

Unconformity-associated uranium deposits (Ruzicka, 1995b) represent an important source of uranium, namely in the Athabasca Basin in Saskatchewan. These deposits generally occur at the base of Proterozoic sandstone sequences unconformably overlying metamorphic rocks that predate the Middle Proterozoic. Two styles of mineralization are commonly observed: polymetallic mineralization (U-Ni-Co-As) primarily located at the unconformity itself, and monometallic mineralization (U) in rocks underlying the unconformity. Monometallic mineralized zones are generally associated with fault zones in the basement.

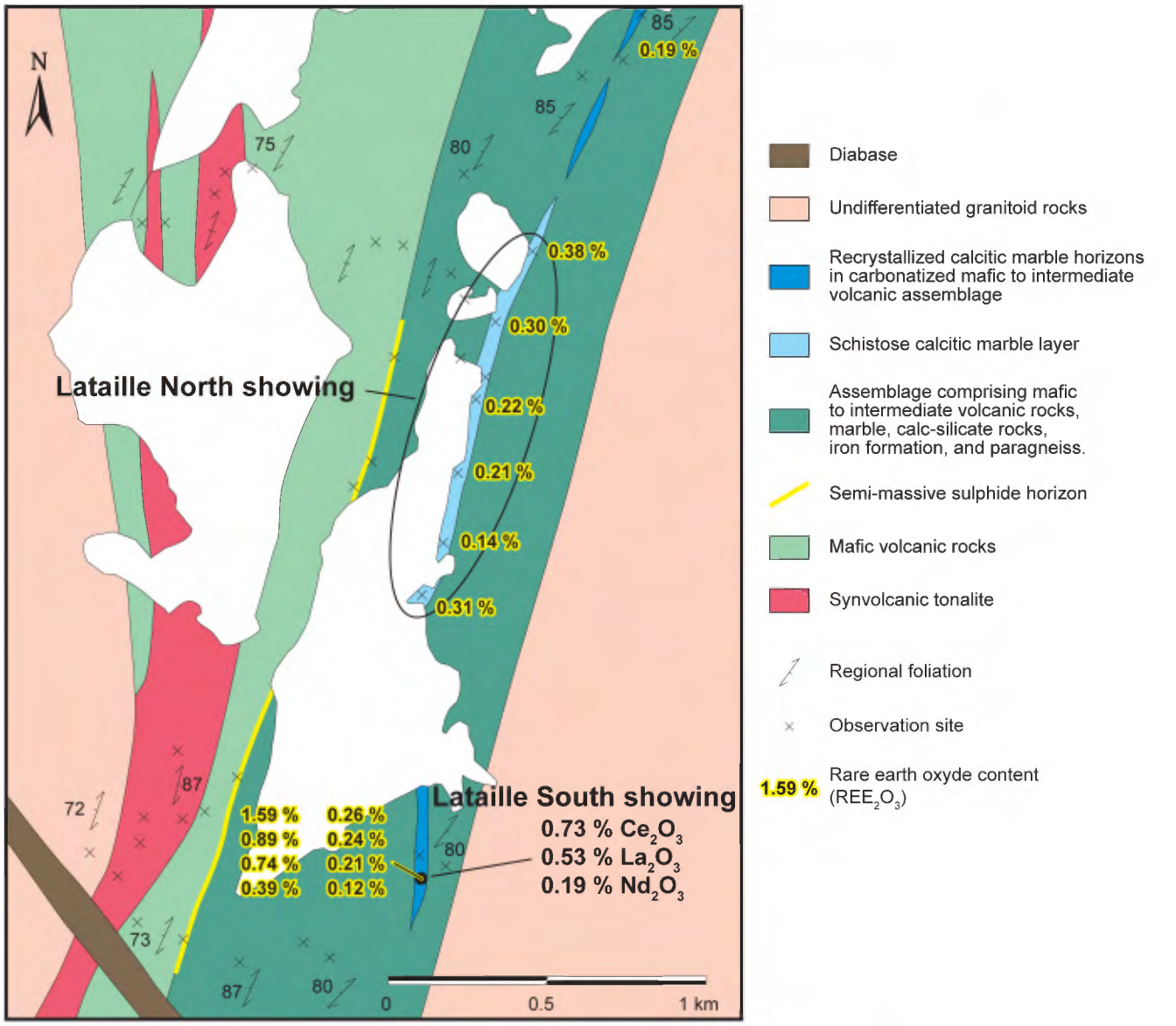

FIGURE 7.16 – Location of REE-mineralized samples in the south part of the Kimber Belt (geology modified after Labbé *et al.*, 2003).

In the Lac Guillaume-Delisle area, the angular unconformity between Proterozoic rocks of the Richmond Gulf Group (Chandler, 1988) and the Archean granitic basement may represent a favourable setting for this type of mineralization. Four uranium showings are in fact attributed to this type of deposit (figures 7.13 and 7.17). Madon (1977 and 1979), and Madon and Winter (1980) provided brief descriptions of these mineralized zones. Uranium is primarily found in fractures or faults that affect the Archean basement, near the unconformity with Proterozoic sandstones. At the *Uranerz No 1* showing, a grab sample with pyrite and uraninite veins yielded a grade of 1.31% U_3O_8.

Showings in the Lac Guillaume-Delisle area may represent an interesting potential for uranium deposits. However, similarly to Mississippi Valley-type occurrences, known showings and the most prospective rocks are located within the Lacs Guillaume-Delisle et à l'Eau Claire Park Project, where claim designation is prohibited (Figure 7.13).

POTENTIAL FOR OTHER TYPES OF MINERAL OCCURRENCES

In addition to the showings and deposits described above, there is also a potential to discover other types of mineralized zones in the NESP. Many volcano-sedimentary belts in the NESP exhibit distinctive features relative to Abitibi rocks. In addition to the higher metamorphic grade and the limited size of the belts, there are also differences in terms of lithological assemblages. For example, calcitic marble units mapped in many belts of the NESP are absent

in the Abitibi Belt. These rocks attest to a shallow marine environment that may correspond to an emerging island arc or an active continental margin setting. Geochemical and isotopic (εNd) characteristics of some belts in the NESP outline the contribution of an early sialic crust during volcanism (Chapter 4). Given this "continental" character, volcano-sedimentary belts in the NESP are akin to belts in the Baie-James region, which were also emplaced upon a granitic basement (Goutier *et al.*, 2001).

These "continental" characteristics have some impact on the type of mineralization one may find in these volcano-sedimentary belts. For example, epithermal gold deposits or porphyry-type Cu-Au deposits may be good targets to search for in supracrustal rocks of the NESP. Also, Witwatersrand-type uranium- and gold-rich paleoplacers are another potential model, and some examples are in fact known within sediments of the Apple Formation in the Baie-James region (Gauthier, 2000).

Rocks in the NESP also offer interesting potential for primary diamond deposits in kimberlites (Mitchell, 1991; Kjarsgaard, 1996), even though no kimberlites have been identified to date. The discovery of diamond-bearing kimberlites in the Monts Otish area triggered a rush across the entire Baie-James region. This interest for diamond exploration is starting to spread further north, into the NESP where some exploration work in the search for diamonds was carried out. In fact, many parts of the NESP are cited in MRNF publications for their potential to host kimberlites. A study of kimberlites and lineaments in Québec outlined the Allemand-Tasiat zone in the northwest part of the study area, and the Saindon-Cambrien zone in the southeast, as prospective areas for kimberlite discoveries (Moorhead *et al.*, 1999). The lamprophyre and carbonatite dykes identified in the Lac Aigneau area (Berclaz *et al.*, 2002) are considered as a potential indicator of the presence of kimberlites (Moorhead *et al.*, 2000). The latter authors also identified a few geochemical targets based on Ba, Ce, and Cr anomalies in lake-bottom sediments. A preliminary potential assessment study for kimberlite discoveries, based primarily on a study of lineaments, proposed a few targets to guide reconnaissance work (Labbé, 2001; 2002). Studies of kimberlite indicator minerals in till or in eskers (Beaumier *et al.*, 2002a; Parent *et al.*, 2004) also led to recommendations for potential exploration targets, namely in the Lac Bienville area.

CONCLUSIONS

A total of 170 mineral occurrences were inventoried within the area targeted by the Far North Program. These showings were classified into 21 ore deposit types based on mineralization, composition of host rocks, and structural setting. The presence of these mineral occurrences and their diversity attest to the broad potential that exists within the NESP. At first glance, the number of occurrences may seem low for such a vast region. Note however that mapping is still in the reconnaissance stage (1/250,000) and that very little prospecting and exploration work has been carried out, most of it very localized. The NESP does have potential for the discovery of new mineral occurrences, and certain types of mineralization are clearly more promising than others. Based on our current state of knowledge, deposit types with the most potential are volcanogenic sulphides, magmatic Ni-Cu deposits associated with komatiites or ultramafic intrusions, iron formation-hosted gold deposits, and auriferous quartz veins. The potential for sedimentary uranium deposits may also be of interest, notwithstanding the limited extent of sedimentary basins likely to host such mineral occurrences.

Previous exploration work carried out in volcano-sedimentary belts of the NESP was often inspired by methods developed in supracrustal rocks of the Abitibi Belt, where lode gold deposits in shear zones and Noranda-type volcanogenic massive sulphide deposits are largely predominant. In the NESP, the high metamorphic grade adds a new dimension that commands a certain adaptation. Thus, alteration minerals observed in metamorphosed belts of the NESP are not the same as those observed in the Abitibi Belt. Also, exploration models must be adapted to take into account the "continental" character of supracrustal rocks in the NESP. In certain volcano-sedimentary belts, settings appear more favourable for the discovery of porphyry copper deposits than for volcanogenic sulphide lenses.

Finally, the presence of a swarm of lamprophyre and carbonatite dykes, the discovery of kimberlite indicator minerals in tills, and the recognition of extensive regional corridors that host alkaline intrusions are all features pointing to a promising potential for the discovery of kimberlites and diamonds in the NESP.

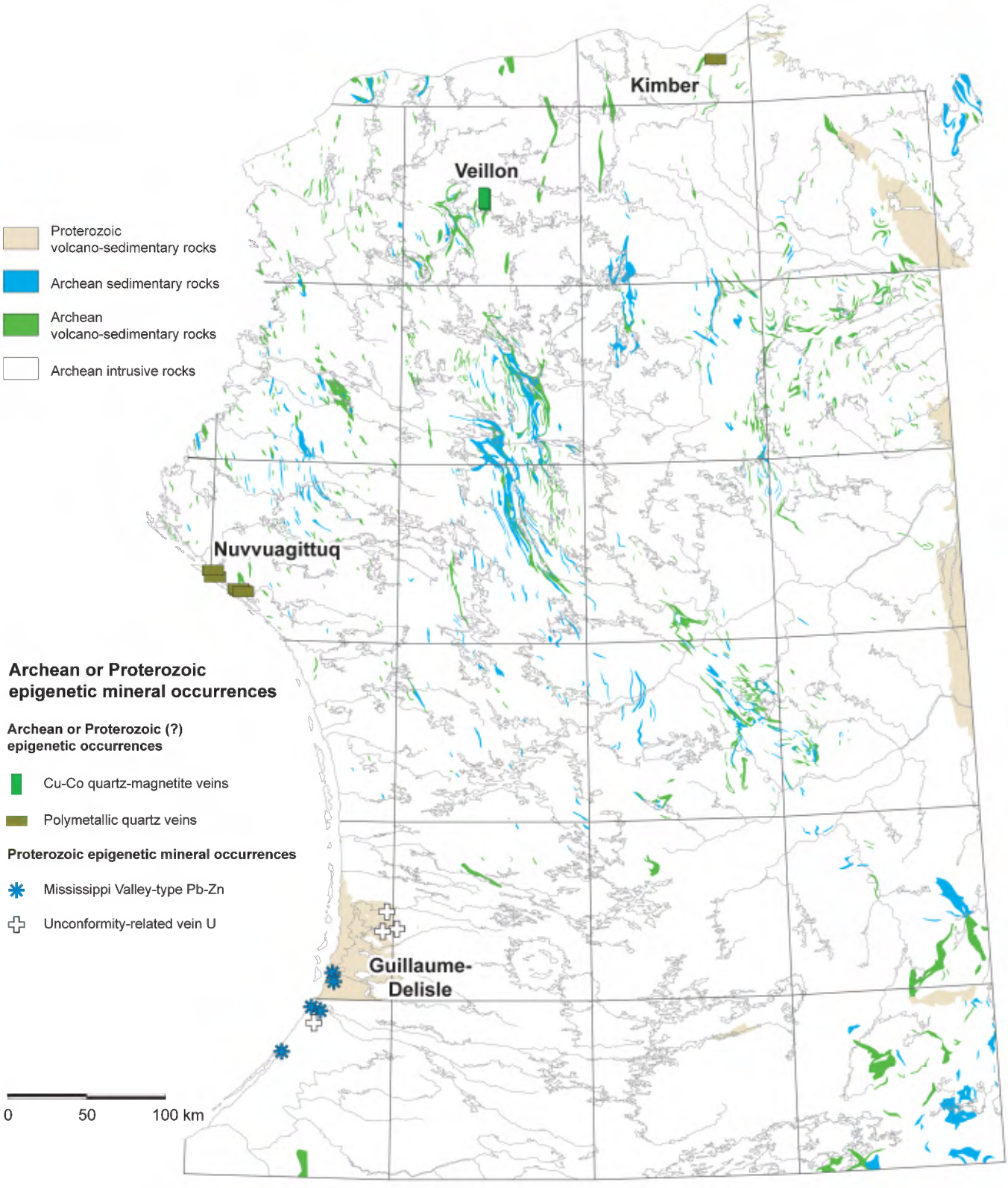

FIGURE 7.17 – Location of Archean and/or Proterozoic epigenetic mineral occurrences.

TABLE 7.1 - Inventory of mineral occurrences in the NESP.

No.	Name	Visited	Type	Typology	Description of mineralization	Grades
1	Sample 809092	n	9b	Poly diss. volc.	Disseminated CP in metabasalt	0.71% Cu
2	Sample 809269	n	9d	Poly diss. intr..	Disseminated CP in gabbro and GL-PY vein	1.08% Cu, 45.5% Pb, 45.7 g/t Ag
3	Julie-Sig	n	2a	Cu volc. sulph.	Disseminated sulphides (CP-PO-PY±SP±GL) in quartzo-feldspathic mylonite	8.71% Cu, 0.2% Zn, 0.5% Pb, 0.3% Ni, 425 g/t Ag
4	Sample 113716	n	9b	Poly diss. volc.	Disseminated PY-GL-SP in metabasalt	8.5 g/t Ag
5	Pitaval	n	9b	Poly diss. volc.	Disseminated CP-PY in felsic tuff	9.18 g/t Ag, 0.13% Cu
6	Gabi	n	10b	Diss. Au volc.	Disseminated sulphides (SP-GL?) in shear zone	1.5 g/t Au, 1.48% Pb, 1.64% Zn
7	Gino-Laurent	n	9c	Poly diss. IF	Disseminated PY-PO in iron formation	25.2 g/t Ag, 0.14 g/t Au, 0.58% Cu, 0.14% Ni
8	Isabel	y	14	Sulph. vein UM	Massive CP veins in ultramafic rock	up to 6.70% Cu, 17 g/t Au, 5 g/t Ag
9	Gay-820203	n	9c	Poly diss. IF	Disseminated PO-CP in iron formation	0.67% Cu, 2.6 g/t Ag, 0.08% Zn
10	Exhalite	n	11	IF-hosted Au	Massive to semi-massive PO-PY-CP bands	2.18 g/t Au, 6 g/t Ag
11	Gay-820202	n	9c	Poly diss. IF	Disseminated PO-CP-PY in iron formation	40.5 g/t Ag, 0.34 g/t Au, 0.32% Pb
12	Gayot (Loup)	y	3b	Mag. Ni-Cu kom.	Disseminated, net-textured, and massive sulphides (PO-PD±PY±CP) at the base of an ultramafic flow	2.01% Ni, 0.34% Cu, 0.57 g/t PGE over 3.15 m (channel)
13	BIF	y	11	IF-hosted Au	PO veinlets	5.6 g/t Au, 3.8 g/t Ag, 0.10% Cu
14	Nancy	y	3b	Mag. Ni-Cu kom.	Disseminated, net-textured, and massive sulphides (PO-PD±PY±CP) at the base of an ultramafic flow	9.0% Ni, 0.6% Cu, 9.0 g/t PGE over 2.55 m (drill hole)
15	MS-99-28	n	9c	Poly diss. IF	Disseminated PO-CP-PY in iron formation	12 g/t Ag
16	Gagnon	y	3b	Mag. Ni-Cu kom.	Disseminated, net-textured, and massive sulphides (PO-PD±PY±CP) at the base of an ultramafic flow	2.17% Ni, 0.42% Cu, 2.46 g/t PGE over 0.45 m (channel)
17	Pyrox	n	3b	Mag. Ni-Cu kom.	Disseminated sulphides in pyroxenite	0.95% Ni, 0.25% Cu, 1.13 g/t Pd, 0.5 g/t Pt, 4.0 g/t Ag
18	Baseline	y	3b	Mag. Ni-Cu kom.	Massive sulphides (PO-PD±PY±CP) at the base of an ultramafic flow	1.98% Ni, 0.11% Cu, 1.2 g/t PGE
19	L	y	3b	Mag. Ni-Cu kom.	Disseminated, net-textured, and massive sulphides (PO-PD±PY±CP) at the base of an ultramafic flow	2.20% Ni, 1.41% Cu, 2.29 g/t PGE over 11.4 m (drill hole)
20	Zone 03-SE	y	3b	Mag. Ni-Cu kom.	Disseminated sulphides (PO-PD±PY±CP) in thick ultramafic flow	1.05% Ni, 0.12% Cu, 0.39 g/t PGE over 8.7 m (channel)
21	Pb-Zn	y	2b	Zn volc. sulph.	Disseminated sulphides (PO-SP-GL-CP) in chloritized felsic tuff	35.2 g/t Ag, 3.82% Pb, 2.7% Zn
22	De Champlain	y	3b	Mag. Ni-Cu kom.	Disseminated sulphides (PO-PD±PY±CP) at the base of an ultramafic flow	9.97% Ni, 0.32% Cu, 0.22% Co, 4.46 g/t PGE over 30 cm (channel)
23	Zone 03	y	3b	Mag. Ni-Cu kom.	Disseminated sulphides (PO-PD-PY-CP) in thick ultramafic flow	1.28% Ni, 0.15% Cu over 1.2 m (drill hole)
24	Malorie	n	3b	Mag. Ni-Cu kom.	Disseminated, net-textured, and massive sulphides (PO-PD±PY±CP) at the base of an ultramafic flow	7.46% Ni, 0.06% Cu, 0.3% Co, 1.82 g/t PGE
25	Pistolaté	n	3b	Mag. Ni-Cu kom.	Disseminated, net-textured, and massive sulphides (PO-PD±PY±CP) at the base of an ultramafic flow	2.96% Ni, 1.5% Cu, 1.08 g/t PGE
26	Lac Gayot	n	8	Sedimentary U	Finely disseminated PB ± CP ± PY ± GL	50 Mt at 0.10 % U_3O_8
27	Lac Bert	n	8	Sedimentary U	Finely disseminated PB in thin bands parallel to bedding in siltstone	894 ppm U_3O_8 over 15 cm (drill hole)
28	Lac Moyer	n	13	Poly qz vn shear	PY-CP-PO in cm-scale boudinaged QZ veins	0.71% Cu, 4.9 g/t Ag
29	Moyer West	y	3b	Mag. Ni-Cu kom.	Semi-massive sulphides (PY-PO) in pyroxenite	0.32% Ni, 0.37% Cu
30	Chalifour	n	3a	Mag. Ni-Cu intr.	PY (PO?) in sheared ultramafic intrusion	0.30% Ni, 0.31% Cu
31	Angilbert South	y	9a	Poly diss. sed.	PY, disseminated and in massive veins in paragneiss	29 g/t Ag, 0.16 g/t Au, 0.2% Co, 0.08% Cu
32	Chateauguay		3a	Mag. Ni-Cu intr.	Disseminated PY-PO in massive pyroxenite	0.32% Ni, 0.37% Cu
33	Natuak-90	n	9b	Poly diss. volc.	Disseminated PY in siliceous horizon	8 g/t Ag, 0.22 g/t Au, 0.31% Zn, 0.14% Pb
34	Natuak-4539	n	9c	Poly diss. IF	PY-PO-AS, disseminated or in mm-scale laminae in iron formation	0.78% Zn, 6 g/t Ag, 0.20% Pb

TABLE 7.1 - Inventory of mineral occurrences in the NESP (continued).

No.	Name	Visited	Type	Typology	Description of mineralization	Grades
35	Natuak-1210	n	9b	Poly diss. volc.	Disseminated PY-PO in felsic horizon associated with ultramafic rocks	0.25% Ni, 0.39% Cr
36	Tuk-Tuk showing	n	9c	Poly diss. IF	Disseminated PY ± CP in iron formation	0.63% Cu, 2 g/t Ag
37	Panache showing	n	10a	Diss. Au sed.	PY-SP±CP±AS, disseminated and in veinlets in sheared paragneiss	1.3 g/t Au, 7.2 g/t Ag, 3.08% Zn, 0.77% Pb
38	Birthday	n	9a	Poly diss. sed.	Disseminated CP-PO in paragneiss	6.9 g/t Ag, 0.25% Cu
39	CB-188 showing	n	9d	Poly diss. intr.	Disseminated PY in tonalite	11.9 g/t Ag
40	Airo showing	y	2b	Zn volc. sulph.	Disseminated PY ± SP in metarhyolite	10 g/t Ag
41	Tasi	y	2c	Au volc. sulph.	Disseminated sulphides (PY-CP) in AT-CD rocks	6.95 g/t Au, 5.80% Cu, 524 g/t Ag
42	RG-12 showing	n	9d	Poly diss. intr.	Finely disseminated CP in tonalite	0.71% Cu, 4.3 g/t Ag
43	SL-56 showing	n	9a	Poly diss. sed.	Disseminated PY-PO±CP in paragneiss	11.8 g/t Ag, 0.14 g/t Au, 0.07% Cu
44	SL-54 showing	n	9b	Poly diss. volc.	Disseminated PO in metabasalt	9.6 g/t Ag, 0.19% Cu
45	SL-41 showing	n	9b	Poly diss. volc.	Disseminated PO-PY±CP in amphibolite	7.8 g/t Ag
46	CB-136 showing	n	11	IF-hosted Au	PO ± PY bands and veinlets	3.02 g/t Au
47	PB-98 showing	n	11	IF-hosted Au	Semi-massive to disseminated PO ± PY in shear zone	1.26 g/t Au, 0.80% Zn
48	Cap Jagged	n	9a	Poly diss. sed.	Disseminated PY-CP in paragneiss	7 g/t Ag, 0.10% Cu
49	Rivière Renouvé	n	9d	Poly diss. intr.	Disseminated PY-PO-CP in gabbro	1.38% Cu, 5 g/t Ag
50	Great Whale (D deposit)	n	1	Algoma-type IF	Massive magnetite layers, locally recrystallized	148.5 Mt at 36.8% Fe
51	Great Whale (A deposit)	n	1	Algoma-type IF	Banded iron formation with fine-grained magnetite	538 Mt at 36.7% Fe
52	Lac Fagnant-South	n	13	Poly qz vn shear	PO-GL in QZ-HM veins along conglomerate-metapelite contact	35.8 g/t Ag, 0.83% Pb
53	Lac Fagnant-Centre	n	12	Au qz vein	AS ± PO ± PY ± CP in quartz veins	up to 20.34 g/t Au, 2.5% Cu, 8.6 g/t Ag
54	Lac Fagnant-North	n	12	Au qz vein	PO-PY-CP bands and veins	2.7 g/t Au
55	Cuesta	n	12	Au qz vein	Polymetallic quartz veins in sheared metabasalts	up to 13.39 g/t Au, 19.7 g/t Ag
56	Esker	n	12	Au qz vein	Several zones of quartz veining hosting various sulphides, mainly AS	up to 39.5 g/t Au, 7.7% Pb, 8.9% Zn, 220 g/t Ag, 0.6% Cu
57	Peridotite	n	11	IF-hosted Au	Disseminated CP and PY in iron formation enclave	2.64 g/t Au, 2.1 g/t Ag, 0.18% Cu
58	Mac's Lead	n	20	MVT	Massive to disseminated GL-SP-PY	6.21% Pb, 1.28% Zn, 1700 g/t Ag
59	Lac Desjardins-NO	n	21	Unconf. vein U.	Very little information on mineralization	0.32% U_3O_8
60	Ruby Lake	y	20	MVT	Massive to disseminated GL-SP-PY	525 000 t at 1.26% Zn, 1.02% Pb
61	Nancy Island	n	20	MVT	Massive to disseminated GL-SP-PY	267 000 t at 2.15% Zn, 0.72% Pb
62	Sophie	n	3a	Mag. Ni-Cu intr.	Disseminated sulphides (PO-PY-CP) in foliated gabbro	0.36% Ni, 0.30% Cu, 0.33 g/t Pt, 0.20 g/t Pd, 0.18 g/t Au
63	Lac Brume-North	n	21	Unconf. vein U	Very little information on mineralization	0.20% U_3O_8
64	Flipper	y	3a	Mag. Ni-Cu intr.	Disseminated sulphides (PO-PY-CP) in pyroxenite	1.28% Ni, 1.01% Cu, 0.15% Co
65	Miki	y	7a	Volc. redbed	CT and BO, disseminated and infilling amygdules in basalts	0.59% Cu, 4.9 g/t Ag
66	Bornite	y	7a	Volc. redbed	CT and BO, disseminated and in veinlets in basalts	4.46% Cu, 48.2 g/t Ag
67	Graben	y	7b	Sed. redbed	Disseminated CT and BO in gabbro and sandstone	1.15% Cu, 29.2 g/t Ag
68	Canada	y	7a	Volc. redbed	CT and BO, disseminated and filling fractures in basalts	3.21% Cu, 16,9 g/t Ag
69	Colline Copper	y	7a	Volc. redbed	CT and BO, disseminated and infilling amygdules in basalts	2.84% Cu, 12.9 g/t Ag
70	Majuraaluk	y	7a	Volc. redbed	CT, disseminated and infilling amygdules in basalts	1.49% Cu, 17.3 g/t Ag
71	Monte Lake	y	20	MVT	Massive to disseminated GL-SP-PY	120 000 t at 1.75% Pb, traces Ag

TABLE 7.1 - Inventory of mineral occurrences in the NESP (continued).

No.	Name	Visited	Type	Typology	Description of mineralization	Grades
72	Le Goulet	n	20	MVT	Massive to disseminated GL	340 g/t Ag, 15% Pb
73	Lac Brume-West	n	21	Unconf. vein U	Very little information on mineralization	0.10 % U_3O_8
74	Nirliq	y	7a	Volc. redbed	CT and BO, disseminated and infilling amygdules in basalts	11.43% Cu, 81.9 g/t Ag
75	Copper Cove	n	7b	Sed. redbed	Disseminated CP-PO-PY in arkose	1.10% Cu
76	Iyaati North	y	7a	Volc. redbed	CT and BO, disseminated and infilling amygdules in basalts	4.29% Cu, 26,4 g/t Ag
77	Uranerz No 1	n	21	Unconf. vein U	PY-UR veinlets	1.31% U_3O_8
78	Umiarjuaq	y	7a	Volc. redbed	Disseminated CT in basalt	0.72% Cu, 5.7 g/t Ag
79	Ni-dance	y	3a	Mag. Ni-Cu intr.	Disseminated sulphides (PO-PY-CP) in pyroxenite	0.83 g/t Pt, 10.6 g/t Pd, 0.34% Cu, 0.11% Ni
80	Tan W	n	3a	Mag. Ni-Cu intr.	Disseminated sulphides (PO-PY-CP) in pyroxenite	0.56 g/t Pt, 0.98 g/t Pd, 0.25% Ni, 0.27% Cu
81	Tan	y	3a	Mag. Ni-Cu intr.	Disseminated, semi-massive, and massive sulphides (PO-PY-CP) in pyroxenite	1.82% Ni, 3.46% Cu, 5.77 g/t PGE
82	Tan NW	n	3a	Mag. Ni-Cu intr.	Disseminated sulphides (PO-PY-CP) in pyroxenite	0.34% Ni, 0.40% Cu
83	Qullinaaraaluk	y	3a	Mag. Ni-Cu intr.	Disseminated, semi-massive, and massive sulphides (PO-PY-CP) in pyroxenite	2.60% Ni, 0.15% Cu, 0.24% Co
84	Morrice: AC-98-18	n	6	Porphyry Mo-W	Disseminated MO in granite	1.50% Mo
85	Dupire	y	11	IF-hosted Au	AS in quartz-chlorite veins	3.42 g/t Au
86	Morrice-Dubé	n	5	U-Th porph. gran.	No information on mineralization	490 ppm Th
87	Morrice-Carrier	n	5	U-Th porph. gran.	No information on mineralization	830 ppm Th, 0.27% REE
88	Duvert-Site-9	n	11	IF-hosted Au	Disseminated PO-PY±AS (?)	1.30 g/t Au
89	Duvert-Site-1	n	9b	Poly diss. volc.	Disseminated PY-PO-CP±AS in silicified felsic horizon	0.85% Cu, 0.22 g/t Au
90	17243 showing	n	5	U-Th porph. gran.	No information on mineralization	0.19% Th, 0.75% REE
91	Vernot-Quirion-17	n	5	U-Th porph. gran.	No information on mineralization	638 ppm U
92	Vernot-Quirion-29	n	5	U-Th porph. gran.	No information on mineralization	0.2% Th
93	Vernot-Dubé-1	n	5	U-Th porph. gran.	No information on mineralization	650 ppm Th, 0.17% REE
94	Vernot-St-Georges	n	5	U-Th porph. gran.	No information on mineralization	590 ppm Th
95	Vernot-Larocque-18	n	16	Vein U	No information on mineralization	0.13% U, 330 ppm Th
96	Vernot-Larocque-4	n	16	Vein U	No information on mineralization	0.44% Th, 2.8% REE
97	Vernot-Quirion-4	n	16	Vein U	No information on mineralization	560 ppm Th, 0.19% REE
98	Patou showing	n	13	Poly qz vn shear	PY-CP ± BN in brecciated QZ veins	0.5% Cu
99	Vernot-Quirion-21	n	16	Vein U	No information on mineralization	512 ppm U, 400 ppm Th
100	Vernot-Dubé-5	n	5	U-Th porph. gran.	No information on mineralization	480 ppm Th
101	Vernot-Dubé-6	n	5	U-Th porph. gran.	No information on mineralization	990 ppm Th
102	Duvert-Site-3	n	9b	Poly diss. volc.	Disseminated PY-AS in siliceous horizon associated with ultramafic rocks	0.25% Ni, 0.12% Co, 0.13% Cu, 0.27 g/t Au
103	Vizien	n	9b	Poly diss. volc.	Disseminated to semi-massive PY-PO±CP±SP in meta-volcanic rocks	6 g/t Ag, 0.17% Cu, 0.12% Ni, 0.38% Zn
104	Bonenfant	y	9c	Poly diss. IF	CP, disseminated and in veinlets in iron formation	0.54% Cu
105	PNAR-99-02	n	11	IF-hosted Au	Disseminated PY in QZ-BO-GR mobilizate	1 g/t Au
106	PNAR-99-01	n	11	IF-hosted Au	Disseminated PY	7.0 g/t Au
107	PNAR-99-03	n	11	IF-hosted Au	Disseminated PY-CP-AS in QZ-GR-HB mobilizate	1 g/t Au
108	Narsaaluk-98	n	11	IF-hosted Au	Disseminated PY in QZ-GR-GN mobilizate	1.56 g/t Au

TABLE 7.1 - Inventory of mineral occurrences in the NESP (continued).

No.	Name	Visited	Type	Typology	Description of mineralization	Grades
109	PNAR-99-04	n	11	IF-hosted Au	Disseminated PO	7.9 g/t Au
110	Kogaluc 6	y	11	IF-hosted Au	PO-PY±CP, disseminated or in veinlets	3.84 g/t Au over 1.50 m (channel)
111	Kogaluc 5	y	11	IF-hosted Au	PO-PY±CP, disseminated or in veinlets	4.39 g/t Au over 0.9 m (channel)
112	Kogaluc 4	y	11	IF-hosted Au	PO-PY±CP, disseminated or in veinlets	4.92 g/t Au over 5.57 m (channel)
113	Kogaluc 1	y	11	IF-hosted Au	PO-PY±CP, disseminated or in veinlets	5.77 g/t Au over 3.00 m (channel)
114	Kogaluc 2	y	11	IF-hosted Au	PO-PY±CP, disseminated or in veinlets	1.48 g/t Au over 49.1 m (channel)
115	Kogaluc 3	y	11	IF-hosted Au	PO-PY±CP, disseminated or in veinlets	2.08 g/t Au over 3.10 m (channel)
116	Tupirviapik SE	y	19	Poly qz vein	CP-SP-GL pods in quartz-carbonate veins	2.80% Pb, 26.3 g/t Ag, 0.55% Cu
117	Tupirviapik	y	19	Poly qz vein	CP pods in quartz-carbonate veins	10.7% Cu, 8.8 g/t Ag
118	Tupirviapik NW	y	19	Poly qz vein	CP-SP±GL pods in quartz-carbonate veins	2.31% Zn, 15.2 g/t Ag
119	MP-1078	n	2a	Cu volc. sulph.	Sulphide (CP?) veinlets in AT-CD-GR schist	0.58% Cu, 6.4 g/t Ag, 0.33 g/t Au
120	Anse au Marsoin-East	n	1	Algoma-type IF	Magnetite iron formation in contact with amphibolite	32.16% Fe
121	Unnusiutilik	y	19	Poly qz vein	CP-SP-GL pods in quartz-carbonate veins	3.15% Cu, 3.62% Zn, 0.59% Pb, 62.9 g/t Ag
122	Unnusiutilik-North	y	19	Poly qz vein	CP-GL±SP pods in quartz-carbonate veins	2.82% Pb, 0.53% Cu, 0.32% Zn, 4 g/t Ag
123	MP-1008	n	3a	Mag. Ni-Cu intr.	Disseminated sulphides (PO-PY-CP) in pyroxenite	0.52% Ni, 0.33% Cu
124	Last Chance	n	3a	Mag. Ni-Cu intr.	Disseminated sulphides (PO-CP) in pyroxenite	0.40% Ni, 0.19% Cu, 0.15 g/t Pt, 0.20 g/t Pd
125	JD-8045	n	2a	Cu volc. sulph.	No information on mineralization	0.73% Cu, 3.6 g/t Ag
126	PN-2055		2a	Cu volc. sulph.	Disseminated sulphides with a few layers (veins?) of massive PY	1.14% Cu, 1.6 g/t Ag
127	Roulier	y	4	Fe-Ti-V intr.	Layer of magnetitite several metres thick	5321 ppm V, 14% TiO_2
128	Tulugak	n	11	IF-hosted Au	Disseminated PO-PY-AS	3.24 g/t Au
129	Avingaluk	y	11	IF-hosted Au	Disseminated to semi-massive PO-PY-AS	1.8 g/t Au over 7.9 m (channel), 35.4 g/t Au
130	Amaruk	y	11	IF-hosted Au	Disseminated to semi-massive PO-PY-AS	4.61 g/t Au over 8.4 m (drill hole)
131	Zone 1998	n	11	IF-hosted Au	Disseminated PY-AS	up to 16 g/t Au
132	Ile-aux-Mulots 1	y	2b	Zn volc. sulph.	Disseminated to semi-massive sulphides (PY-PO-SP-CP-GL) associated with AT-BO alteration in metabasalts	3.3% Zn sur 4.8 m; 2.34% Cu, 26 g/t Ag sur 0.3m (channel)
133	Ile-aux-Mulots 2	n	2c	Zn volc. sulph.	Disseminated PY-CP in mafic rocks with AT-CD-BO-GR	1.80% Cu, 2.5 g/t Au, 25 Ag
134	Qalluviartuuq SW	n	2c	Zn volc. sulph.	Disseminated PY-CP in mafic gneisses altered to AT-SM-BO-GR	1.10 % Cu, 1.2 g/t Au, 14 g/t Ag
135	Anorthosite 1	y	12	Au qz vein	Disseminated PY and CP in quartz veins associated with shear zones	2.14% Cu, 2.8 g/t Au, 12 g/t Ag
136	Anorthosite 2	y	12	Au qz vein	Disseminated PY and CP in quartz veins associated with shear zones	1.4 g/t Au, 6 g/t Ag, 0.5% Cu
137	Mézard	n	12	Au qz vein	Disseminated PY in 10-cm QZ-GR pocket	1.61 g/t Au, 1.6 g/t Ag
138	Qalluviartuuq-NW	n	10b	Diss. Au volc.	Disseminated to semi-massive PY ± CP	8 g/t Au, 18 g/t Ag, 0.14% Cu
139	Pointe-Aux-Gossans-1	y	10b	Diss. Au volc.	Disseminated PO-PY-AS-CP in sheared felsic to intermediate volcanic rocks	47.2 g/t Au, >50 g/t Ag, 0.5% Cu
140	Pointe-Aux-Gossans-2	y	10b	Diss. Au volc.	Disseminated PO-PY-AS-CP in sheared felsic to intermediate volcanic rocks	27.4 g/t Au, 31.5 g/t Ag, 0.5% Cu
141	Lac Qalluviartuuq-North	n	9b	Poly diss. volc.	Disseminated PY-CP in mafic gneiss	2.40% Cu, 18 g/t Ag
142	Tukimurtuk	n	17	Mo in faults	PY-MB veinlets associated with fault zone	0.30% Mo
143	Tasiaalujjuaq	n	9d	Poly diss. intr.	Disseminated CP-PY in foliated diorite	0.75% Cu, 3.9 g/t Ag, 0.14 g/t Au

TABLE 7.1 - Inventory of mineral occurrences in the NESP (concluded).

No.	Name	Visited	Type	Typology	Description of mineralization	Grades
144	Lac du Pelican	n	9b	Poly diss. volc.	Disseminated PY in felsic tuff enclave within felsic intrusion	4.72 % Zn, 29.2 g/t Ag, 0.24 g/t Au
145	Pelican	y	10b	Au volc. sulph.	Disseminated to massive PY in metabasalts associated with paragneiss and iron formation	1.2 g/t Au, 5.6 g/t Ag, 0.26 % Cu
146	Nantais 1	y	10b	Diss. Au volc.	Disseminated PY-PO-AS in shear zone within metabasalts	4.7 g/t Au, 5.2 g/t Ag
147	Nantais 2	0	10b	Diss. Au volc.	PY-CP-SP, disseminated and in thin semi-massive bands in sheared metabasalts	7.9 g/t Au, 7.2 g/t Ag
148	Cabane	y	2b	Zn volc. sulph.	Massive SP-GL vein, 15-20 cm thick, in felsic volcanic rocks with AT-AD-BO-GR	2.48 % Zn, 7 % Pb, 1600 g/t Ag, 0.12 % Cu, 0.47 g/t Au
149	Veines	y	12	Au qz vein	Fine-grained PY along QZ vein selvages with visible gold locally	7.24 g/t Au over 2.1 m (channel)
150	Kak	n	10a	Au qz vein	Disseminated PY in shear zone	18.1 g/t Au, 16.8 g/t Ag
151	810091	n	10c	Diss. Au intr.	Disseminated PY in sheared tonalite	1.1 g/t Au, 6.2 g/t Ag, 0.58 % Cu
152	Francoeur	y	2a	Cu volc. sulph.	Massive sulphide (PY-CP-SP) pockets, 10 cm to 1 m in size, and disseminated sulphides in AT-bearing mafic rock	6.4% Cu, 3.4% Zn, 0.18 g/t Au, 64 g/t Ag over 1.5 m (channel)
153	Havre Sigouin	y	2c	Au volc. sulph.	Disseminated CP and PY in AT schist, a few CP veins	10.4 % Cu, 12.6 g/t Au, 46 g/t Ag
154	Scrap Yard	y	2b	Zn volc. sulph.	10-cm veins with massive SP and disseminated CP in anthophyllite schist	4.6 % Zn sur 2.3 m (channel)
155	COM	y	2c	Au volc. sulph.	Massive sulphide (PY-SP-GN-CP-AS) lenses, 10 cm to 1 m in size, in metarhyolite	up to 34.3 g/t Au, 533 g/t Ag, 1.46% Pb, 7.4% Zn
156	Plozin	y	2c	Au volc. sulph.	Three mineralized zones (quartz-sulphide veining or disseminated sulphides) in metarhyolite	up to 10.3% Zn, 4.55% Pb, 4.26 g/t Au
157	Secteur 3 - Nord	n	2b	Zn volc. sulph.	Disseminated PY-SP-AS in tuffaceous rock	7.2% Zn, 9.3 g/t Ag, 0.68% Cu over 0.5 m (channel)
158	Kaliattualuk-2	n	9b	Poly diss. volc.	Disseminated PY±AS±CP in shear zone	17.9 g/t Ag, 0.20 % Mo
159	Secteur 2	n	10b	Diss. Au volc.	Disseminated PY in sheared intermediate metavolcanic rocks	5.14 g/t Au, 18 g/t Ag
160	Kakiattualuk-4	n	10b	Diss. Au volc.	Disseminated PY in metabasalt	5.24 g/t Au
161	Kakiattualuk-3	n	12	Au qz vein	Disseminated PY and AS in quartz vein	1.18 g/t Au
162	Kakiattualuk-1	n	13	Poly qz vn shear	CP in QZ veins associated with shear zone	2.4 % Cu, 73.4 g/t Ag, 1.0 g/t Au
163	Cipmyluk 1	y	18	Cu-Co vein	CP-PY pods in quartz veins	2.2 % Cu, 0.01 % Co
164	Cipmyluk 2	y	18	Cu-Co vein	CP-PY in magnetite veins	3.4 % Cu, 0.07 % Co
165	Juet	n	11	IF-hosted Au	Disseminated PY-AS	6.4 g/t Au
166	Peltier	n	9b	Poly diss. volc.	No information on mineralization	8 g/t Ag
167	Allemand	n	9b	Poly diss. volc.	No information on mineralization	0.8 % Cu, 2.9 g/t Ag
168	Lac Grunérite	n	19	Poly qz vein	Disseminated CP-PY-PO in quartz veins	0.56 % Cu, 2 g/t Ag
169	Lataille Sud	y	15	REE carb.	Disseminated AL in recrystallized marble	1.36% REE
170	Lataille Nord	y	15	REE carb.	Disseminated AL in schistose marble	0.31% REE

Mineral codes

AD - Andalusite
AL - Allanite
AS - Arsenopyrite
AT - Anthophyllite
BN - Bornite
BO - Biotite
CD - Cordierite
CP - Chalcopyrite
CT - Chalcocite
GL - Galena
GN - Grunerite
GR - Garnet
HB - Hornblende
HM - Hematite
MO - Molybdenite
QZ - Quartz
PB - Pitchblende
PD - Pentlandite
PO - Pyrrhotite
PY - Pyrite
SM - Sillimanite
SP - Sphalerite
UR - Uraninite

REFERENCES

ALMOND, L.B., 1947 – Geological report on Richmond Gulf area. Ministère des Ressources naturelles et de la Faune, Québec; GM 9731, 17 pages.

ALMOND, L.B. – MOFFAT, W.W. – HARWOOD, T.A., 1947 – Report on the property. Ministère des Ressources naturelles et de la Faune, Québec; GM 9733, 60 pages.

APPEL, P.W.U. – MOORBATH, S. – TOURET, J.L.R., 2003 – Early Archaean processes and the Isua Greenstone Belt, West Greenland. Precambrian Research; volume 126, pages 173-179.

ARTH, J.G. – BARKER, F. – PETERMAN, Z.E. – FRIEDMAN, I., 1978 – Geochemistry of the gabbro-diorite-tonalite-trondhjemite suite of southwest Finland and its implication for the origin of tonalite and trondjhemite magmas. Journal of Petrology; volume 19, pages 289-316.

AUBERT DE LA RUE, E., 1948 – Geological survey through the Ungava Peninsula. Arctic; volume 1, pages 135-136.

AVRAMTCHEV, V., 1985 – Carte géologique du Québec. Ministère de l'Énergie et des Ressources, Québec; DV 84-02, carte n° 2000, scale 1/500,000.

BAKER, M., 2005 – Pétrologie et métallogénie de l'indice de Ni-Cu-Co de Qullinaaraaluk et d'intrusions mafiques-ultramafiques du Domaine du lac Minto, Sous-province de Minto, Québec. M.Sc. thesis, Université Laval, Québec, 256 pages.

BARAGAR, W.R.A. – ERNST, R.E. – HULBERT, L. – PETERSON, T., 1996 – Longitudinal petrochemical variations in the Mackenzie dyke swarm, northwestern Canadian Shield. Journal of Petrology; volume 37, pages 317-359.

BARNES, S.J. – HILL, R.E.T. – PERRING, C.S. – DOWLING, S.E., 1999 – Komatiite flow fields and associated Ni-sulphide mineralization with examples from the Yilgarn Block, Western Australia. *In*: Dynamic processes in magmatic ore deposits and their applications in mineral exploration, R.R. Keays, C.M. Lesher and P.C. Lightfoot (ed.). Geological Association of Canada; Short Course Volume 13, pages 159-194.

BEALS, C.S. – FERGUSON, G.M. – LANDAU, A., 1956 – A search for analogies between lunar and terrestrial topography on photographs of the Canadian Shields. Journal of the Royal Astronomical Society, Canada; volume 50, pages 203-211 and 250-261.

BEALS, C.S. – INNES, M.J.S. – ROTTENBERG, J.A., 1960 – The search for fossil meteorite craters. Current Science, Bangalore (India); volume 29, pages 205-218 and 249-262.

BEALS, C.S. – DENCE, M.R. – COHEN, A.J., 1967 – Evidence for impact origin of Lac Couture. Publication of the Dominion Observatory, Ottawa; volume 31.

BEAUMIER, M., 1986 – Géochimie des sédiments de lac – Région de la rivière Caniapiscau. Ministère des Ressources naturelles, Québec; DP 86-23, 40 maps.

BEAUMIER, M., 2001 – Kimberlites et le potentiel diamantifère dans le Grand-Nord : comparaison avec la région du lac de Gras. *In:* Projet de cartographie du Grand-Nord – Rapport d'atelier. Ministère des Ressources naturelles, Québec; MB 2001-03, pages 5-11.

BEAUMIER, M. – PARENT, M. – PARADIS, S., 2002a – Exploration du diamant dans les sédiments d'eskers de la région du lac Bienville (33P) et dans les tills des régions des lacs Anuc (34O) et Vernon (34J). Ministère des Ressources naturelles, Québec; DP 2002-01.

BEAUMIER, M. – PARENT, M. – PARADIS, S., 2002b – Minéraux lourds dans le till et exploration pour le diamant dans la région du lac Vernon (34J). Ministère des Ressources naturelles, Québec; ET 2002-02, 39 pages.

BÉDARD, J.H., 2003 – Evidence for regional-scale, pluton-driven, high-grade metamorphism in the Archaean Minto Block, northern Superior Province, Canada. Journal of Geology; volume 111, pages 183-205.

BÉDARD, J.H. – BROUILLETTE, P. – MADORE, L. – BERCLAZ, A., 2003 – Archaean cratonization and deformation in the northern Superior Province, Canada; an evaluation of plate tectonic versus vertical tectonic models. Precambrian Research; volume 127, pages 61-87.

BÉDARD, J.H., 2006 – A catalytic delamination-driven model for coupled genesis of Archaean crust and sub-continental lithospheric mantle. Geochimica et Cosmochimica Acta; volume 70, pages 1188-1214.

BÉGIN, N.J. – PATTISON, D.R.M., 1994 – Metamorphic evolution of granulites in the Minto Block, northern Québec: extraction of peak P-T conditions taking account of late Fe-Mg exchange. Journal of Metamorphic Geology; volume 12, pages 411-428.

BELL, R., 1877 – Report on an exploration of the east coast of Hudson Bay. Geological Survey of Canada; Report of Progress, 1877-78.

BELL, R., 1885 – Observations on the geology, mineralogy, zoology and botany of the Labrador Coast, Hudson Strait and Bay. Geological Survey of Canada; Report of Progress, 1882-84.

BERCLAZ, A. – CADIEUX, A.-M. – SHARMA, K.N.M. – DAVID, J. – PARENT, M. – LECLAIR, A., 2002 – Geology of the Lac Aigneau area (23E and 24F/04). Ministère des Ressources naturelles, Québec; RG 2001-05, 44 pages.

BERCLAZ, A. – GODIN, L. – DAVID, J. – MAURICE, C. – PARENT, M. – FRANCIS, D. – STEVENSON, R. – LECLAIR, A., 2003 - Geology of the Nuvvuagittuq Belt (ca. 3.8 Ga), northeastern Superior Province: Towards a multidisciplinary approach. *In*: Abstracts of oral presentations and posters, Québec Exploration 2003. Ministère des Ressources naturelles, de la Faune et des Parcs, Québec; DV 2003-10, page 50.

BERCLAZ, A. – MAURICE, C. – LACOSTE, P. – DAVID, J. – LECLERC, F. – SHARMA, K.N.M. – LABBÉ, J.-Y. – GOULET, N. – BÉDARD, J. – VALLIÈRES, J., 2005 - Geology of the Lac Anuc area (34O). Ministère des Ressources naturelles et de la Faune, Québec; RG 2003-05, 55 pages.

BERNING, J. – COOKE, R. – HIEMSTRA, S.A. – HOFFMAN, U., 1976 – The Rössing uranium deposit, South West Africa. Economic Geology; volume 71, pages 351-368.

BLEEKER, W. – ERNST, R., 2006 – Short-lived mantle generated magmatic events and their dyke swarms: The key unlocking Earth's paleogeographic record back to 2.6 Ga, *In:* Dyke Swarms – Time Markers of Crustal Evolution, E. Hanski, S. Mertanen, T. Rämö and J. Vuollo (ed.). A.A. Balkema Publishers, Rotterdam.

BÖHM, C.O. – HEAMAN, L.M. – STERN, R.A. – CORKERY, M.T. – CREASER, R.A., 2003 – Nature of Assean Lake ancient crust, Manitoba: a combined SHRIMP–ID-TIMS U-Pb geochronology and Sm–Nd isotope study. Precambrian Research; volume 126, pages 55-94.

BOILY, M., 1995 – La pétrogénèse du batholite de Preissac-Lacorne : Implications pour la métallogénèse des gisements de MHT. Ministère des Ressources naturelles; ET 95-05, 49 pages.

BOILY, M. – LACOSTE, P. – LABBÉ, J.Y., 2002 – Géochimie des ceintures et lambeaux volcano-sédimentaires du domaine de Goudalie, bloc de Minto, Province du Supérieur, Québec. Ministère des Ressources naturelles, Québec; MB 2002-03, 50 pages.

BOILY, M. – MOUKHSIL, A., 2003 – Géochimie des assemblages volcaniques de la ceinture de roches vertes de la Moyenne et de la Basse-Eastmain, Province du Supérieur, Québec. Ministère des Ressources naturelles, Québec; ET 2002-05, 31 pages.

BOILY, M. – LECLAIR, A. – MAURICE, C. – BERCLAZ, A. – DAVID, J., 2004 – Étude lithogéochimique et isotopique du Nd des assemblages volcaniques et plutoniques de la région sud du Grand-Nord québécois. Ministère des Ressources naturelles, de la Faune et des Parcs, Québec; RP 2004-01, 28 pages.

BOILY, M. – LECLAIR, A. – MAURICE, C. – BERCLAZ, A. – DAVID, J., 2006a – Étude géochimique et isotopique du Nd des assemblages volcaniques et plutoniques du nord-est de la Province du Supérieur (NEPS). Ministère des Ressources naturelles et de la Faune, Québec; GM 62031, 50 pages.

BOILY, M. – LECLAIR, A. – BERCLAZ, A. – LABBÉ, J.-Y. – LACOSTE, P. – SIMARD, M. – MAURICE, C., 2006b – Terrane definition in the northeastern Superior Province. Geological Association of Canada; Abstracts Volume 31, page 16.

BOILY, M. – LECLAIR, A. – MAURICE, C. – BÉDARD, J.H. – BERCLAZ, A. – DAVID, J., 2009 – Paleo- to Mesoarchean basement recycling and terrane definition in the Northeastern Superior Province, Québec, Canada. *In*: Superior Province: the nature and evolution of the Archean continental lithosphere, G. Stott and W. Mueller (ed.). Precambrian Research; volume 168, pages 23-44

BOSTOCK, H. H., 1969 – The Clearwater Complex, New Quebec. Geological Survey of Canada; bulletin 178, 63 pages.

BOTTOMLEY, R.J. – YORK, D. – GRIEVE, R.A.F., 1990 – ^{40}Ar -^{39}Ar dating of impact craters. Proceedings of the 20th Lunar and Planetary Sciences Conference; pages 421-431.

BOURASSA, Y., 2002 – Géologie, géochimie, géochronologie et métallogénie des indices volcanogènes à Cu-Zn-Au-Ag de la Ceinture Archéenne de Duquet, Bouclier Supérieur, Nord du Québec. M.Sc. thesis, Université du Québec à Montréal, Montréal (Québec), 78 pages.

BRYAN, W.B. – THOMPSON, G. – LUDDEN, J.N., 1981. Compositional Variation in Normal MORB from 22-25 (degree) N: Mid-Atlantic and Kane Fracture Zone. Journal of Geophysical Research; 86, pages 11815-11836.

BUCHAN, K.L. – ERNST, R.E., 2004 – Diabase dyke swarms and related units in Canada and adjacent regions. Geological Survey of Canada; Map 2022A, scale 1/5,000,000

BUCHAN, K.L. – MORTENSEN, J.K. – CARD, K.D. – PERCIVAL, J.A., 1998 – Paleomagnetism and U-Pb geochronology of diabase dyke swarms of Minto block, Superior Province, Quebec, Canada. Canadian Journal of Earth Sciences; volume 35, pages 1054-1069.

BUDKEWITSH, P. – HYNES, A.J. – FRANCIS, D.M., 1991 – Coast-parallel dykes in the northern Nastapoka arc, Hudson Bay: feeder dykes to Proterozoic sills of the Nastapoka Group? Geological Association of Canada; Program with Abstracts, volume 16, page 16.

BULLIS, H.R. – HUREAU, R.A. – PENNER, B.D., 1994 – Distribution of gold and sulfides at Lupin, Northwest Territories. Economic Geology; volume 89, pages 1217-1227.

CADIEUX, A.-M. – BERCLAZ, A. – LABBÉ, J.-Y. – LACOSTE, P. – DAVID, J. – SHARMA, K.N.M., 2004 - Geology of the Lac du Pélican area (34P). Ministère des Ressources naturelles, Québec; RG 2002-08, 48 pages.

CARD, K.D., 1990 – A review of the Superior Province of the Canadian Shield, a product of Archean accretion. Precambrian Research; volume 48, pages 99-156.

CARD, K.D. – CIESIELSKI, A., 1986 – Subdivisions of the Superior Province of the Canadian Shield. Geoscience Canada; volume 13, pages 5-13.

CARD, K.D. – POULSEN, K.H., 1998 – Geology and mineral deposits of the Superior Province of the Canadian Shield. *In*: Geology of the Precambrian Superior and Grenville Provinces and Precambrian Fossils in North America, S. Lucas and M.R. St-Onge (co-ordinators). Geological Survey of Canada; Geology of Canada, number 7, pages 13-194.

CATES, N.L. – MOJZSIS, S.J., 2007 – Pre-3750 Ma supracrustal rocks from the Nuvvuagittuq supracrustal belt, northern Quebec. Earth and Planetary Science Letters; volume 255, pages 9-21.

CATTALANI, S. – HEIDEMA, J.H., 1993 – Qalluviartuuq permit, Cominco Ltd.-Soquem joint venture, report of work, 1993. Ministère des Ressources naturelles et de la Faune, Québec; GM 52254, 56 pages.

CHANDLER, F.W., 1988 – The early proterozoic Richmond Gulf Graben, East Coast of Hudson Bay, Quebec. Geological Survey of Canada; bulletin 362, 76 pages.

CHANDLER, F.W. – PARRISH, R.R., 1989 – Age of the Richmond Gulf Group and implications for rifting in the Trans-Hudson orogen, Canada. Precambrian Research; volume 44, pages 277-288.

CHAPDELAINE, M., 1995 – Rapport des travaux 1995, Projet Minto (1121), Permis Dupire. Ministère des Ressources naturelles et de la Faune, Québec; GM 53833, 25 pages.

CHAPDELAINE, M., 1998 – Rapport technique des travaux, été 1997, Projet Minto, Permis Kogaluc. Ministère des Ressources naturelles et de la Faune, Québec; GM 55935, 277 pages.

CHAPDELAINE, M., 1999a – Rapport des travaux de cartographie et de prospection, été 1998, Projet Minto, Propriété Payne. Ministère des Ressources naturelles et de la Faune, Québec; GM 56553, 166 pages.

CHAPDELAINE, M., 1999b – Rapport des travaux de cartographie et de prospection, été 1998, Projet Minto, Propriété Duquet. Ministère des Ressources naturelles et de la Faune, Québec; GM 56484, 142 pages.

CHAPDELAINE, M., 2002 – Report on summer 2001 trenching and geological mapping program, Gayot project. Ministère des Ressources naturelles et de la Faune, Québec; GM 59126, 148 pages.

CHAPDELAINE, M., 2003 – Report on summer 2002 geological reconnaissance program, Gayot project. Ministère des Ressources naturelles et de la Faune, Québec; GM 59876, 62 pages.

CHAPDELAINE, M. – VILLENEUVE, P.-A., 2000 – Projet Duquet, rapport des travaux de cartographie et de prospection : été 1999. Ministère des Ressources naturelles et de la Faune, Québec; GM 57834, 113 pages.

CHEVÉ, S., 2005 – Lithogéochimie de la région du lac Minto (34F et 34G). Ministère des Ressources naturelles, de la Faune et des Parcs, Québec; MB 2005-01.

CHEVÉ, S. – BROUILLETTE, P., 1995 – Géologie et métallogénie de la partie nord-est de la Sous-province d'Ashuanipi (Nouveau-Québec). Ministère des Ressources naturelles, Québec; MM 95-01, 6 pages.

CHEVÉ, S.R. – MACHADO, N., 1988 – Reinvestigation of the Castignon Lake carbonatite complex, Labrador Trough, New Quebec. Geological Association of Canada-Mineralogical Association of Canada; Program with Abstracts, volume 13, page 20.

CIESIELSKI, A., 1998 – Compilation géologique de la partie orientale de la province du Supérieur, Québec. Geological Survey of Canada; Open File 3580, scale 1/1,000,000.

CIESIELSKI, A., 2000 – Géologie et lithogéochimie de la partie occidentale de la sous-province de Bienville et des zones adjacentes dans l'est de la province de Supérieur, Québec. Geological Survey of Canada; Open File 3550,, 90 pages.

CLARK, T., 1984 – Géologie de la région du lac Cambrien, Territoire du Nouveau-Québec. Ministère de l'Énergie et des Ressources, Québec; ET 83-02, 71 pages.

CLARK, T. – WARES, R., 2006 - Lithotectonic and Metallogenic Synthesis of the New Québec Orogen (Labrador Trough). Ministère des Ressources naturelles et de la Faune, Québec; MM 2005-01, 175 pages.

CUERRIER, G., 1998 – Propriété Payne (1121-2), rapport des travaux, été 1997. Ministère des Ressources naturelles et de la Faune, Québec; GM 55885, 187 pages.

DAVID, J. – PARENT, M., 1997 – Géochronologie U-Pb du Projet Moyen-Nord. Ministère des Ressources naturelles et de la Faune, Québec; GM 59903, 88 pages.

DAVID, J. – MAURICE, C. – SIMARD, M., 2008 – Datations isotopiques effectuées dans le nord-est de la Province du Supérieur - Travaux de 1998,1999 et 2000. Ministère des Ressources naturelles et de la Faune, Québec; DV 2008-05.

DAVID, J. – PARENT, M. – STEVENSON, R. – NADEAU, P. – GODIN, L., 2002 – La séquence supracrustale de Porpoise Cove, région d'Inukjuak : un exemple unique de croûte paléoarchéenne (ca. 3.8 Ga) dans la Province du Supérieur. *In:* L'exploration minérale au Québec – Notre savoir, vos découvertes, Séminaire d'information sur la recherche géologique, Programme et résumés. Ministère des Ressources naturelles, Québec; DV 2002-10, page 33.

DAVID, J. – PARENT, M. – STEVENSON, R. – NADEAU, P. – GODIN, L., 2003 – The Porpoise Cove supracrustal sequence, Inukjuak area: a unique example of Paleoarchean crust (ca. 3.8 Ga) in the Superior Province. Geological Association of Canada; Program with Abstracts, volume 28, CD-ROM.

DAVID, J. – GODIN, L. - BERCLAZ, A. - MAURICE, C. - PARENT, M. – FRANCIS, D. - STEVENSON, R., 2004 - Geology and geochronology of the Nuvvuagittuq Supracrustal Sequence: An example of Paleoarchean crust (ca. 3.8 Ga) in the Northeastern Superior Province [abstract]: *in* Eos Transactions, CGU/AGU/SEG/EEGS Joint Assembly, Abstract no. V23D-03.

DE CORTA, H. - SAULNIER, I. - PETIT, N., 1999 - Rapport d'une campagne de cartographie, prospection et décapage, propriété Vaujours. Ministère des Ressources naturelles et de la Faune, Québec; GM 57411, 94 pages.

DePAOLO, D.J., 1982 - Neodymium isotopes in the Colorado Front Range and the crust-mantle evolution in the Proterozoic. Nature; volume 291, pages 193-196.

DIMROTH, E., 1978 - Région de la Fosse du Labrador (54°30 -56°30): Ministère des Ressources naturelles, Québec, RG-193, 396 p.

DIMROTH, E. – BARAGAR, W.R.A. – BERGERON, R. – JACKSON, G.D., 1970 – The filling of the Circum-Ungava geosyncline. *In*: Symposium on Basins and Geosynclines of the Canadian Shield (A.J. Baer, editor). Geological Survey of Canada; paper 70-40, pages 45-142.

DRESSLER, B., 1979 – Région de la Fosse du Labrador (56°30 -57°15). Ministère des Ressources naturelles, Québec; RG-195, 117 pages

DRUMMOND, M.S. – DEFANT, M.J., 1990 – A model for trondhjemite-tonalite-dacite genesis and crustal growth via slab melting: Archaean to modern comparisons. Journal of Geophysical Research; volume 95, pages 21503-21521.

DUFOUR, R., 1978 – Réévaluation des gisements et description d'un projet d'exploitation. Ministère des Ressources naturelles et de la Faune, Québec; GM 33616, 156 pages.

EADE, K.E., 1966 – Fort George River and Kaniapiskau River (west half) map-areas, New-Quebec. Geological Survey of Canada; Memoir 339, 84 pages.

ECKSTRAND, O.R., 1995 – Nickel-copper sulphide. *In*: Geology of Canadian Mineral Deposit Types, O.R. Eckstrand, W.D. Sinclair, and R.I. Thorpe (ed.). Geological Survey of Canada; Geology of Canada, volume 8, pages 584-605.

ECKSTRAND, O.R. – SINCLAIR, W.D. – THORPE, R.I. (editors), 1995 - Geology of Canadian Mineral Deposit Types. Geological Survey of Canada; Geology of Canada, volume 8, 640 pages.

ERNST, R.E., 1989 –The Great Abitibi dyke, Southeastern Superior Province, Canada. Ph.D. thesis, Carleton University, Ottawa, Ontario, Canada, 579 pages.

ERNST, R.E. – BELL, K., 1992 – Petrology of the Great Abitibi dyke, Superior Province. Journal of Petrology; volume 33, pages 423-469.

ERNST, R.E. – BARAGAR, W.R.A., 1992 – Evidence from magnetic fabric for the flow pattern of magma in the Mackenzie giant radiating swarm. Nature; volume 356, pages 511-513.

ERNST, R.E. – HEAD, J.W. – PARFITT, E. – GROSFILS, E. – Wilson, L., 1995 – Giant radiating dyke swarms on Earth and Venus. Earth Science Review; volume 39, pages 1-58.

ERNST, R.E. – BUCHAN, K.L., 2001 – Large mafic magmatic events through time and links to mantle-plume heads. *In:* Mantle Plumes: Their Identification Through Time, R.E. Ernst and K.L. Buchan (ed.). Geological Society of America; Special Paper 352, pages 483-575.

FAHRIG, W. F., 1987 – The tectonic settings of continental mafic dyke swarms: failed arms and early passive margin. *In*: Mafic dyke swarms, W.F. Fahrig and H.C. Halls (ed.). Geological Association of Canada; Special Paper 34, pages 331-348.

FAHRIG, W.F. – WEST, T. D., 1986 – Diabase dyke swarms of the Canadian Shield. Geological Survey of Canada; map 1672A, scale 1/4,873,900.

FAHRIG, W.F. – CHRISTIE, K.W. – CHOWN, E.H. – JANES, J. – MACHADO, N., 1986 – The tectonic significance of some basic dyke swarms in the Canadian Superior Province with special reference to the geochemistry and paleomagnetism of the Mistassini swarm, Quebec, Canada. Canadian Journal of Earth Sciences; volume 23, pages 238-253.

FAN, J. – KERRICH, R., 1997 – Geochemical characteristics of aluminium depleted komatiites and HREE-enriched low-Ti tholeiites, western Abitibi greenstone belt: A heterogenous mantle-plume convergent margin environment. Geochimica et Cosmochimica Acta; volume 61, pages 4723-4744.

FINDLAY, J.M. – PARRISH, R.R. – BIRKETT, T. – WATANABE, D.H., 1995 – U-Pb ages from the Nimish Formation and Montagnais glomeroporphyritic gabbro of the central New Quebec Orogen, Canada. Canadian Journal of Earth Sciences; volume 32, pages 1208-1220.

FLAHERTY, R.J., 1918 – Two traverses across Ungava Peninsula. Geographic Review; volume 6, pages 116-132.

FLOYD, P.A., 1989 – Geochemical features of intraplate oceanic plateau basalts. *In*: Magmatism in the Ocean Basins, A.D. Saunders and M.J. Norry (ed.). Geological Society Special Publications number 42, pages 215-230.

FRANCOEUR, G., 1996 – Projet Minto (1121), Permis de Kogaluc, Rapport des travaux 1996. Ministère des Ressources naturelles et de la Faune, Québec; GM 54360, 202 pages.

FRANCOEUR, G. – CHAPDELAINE, M., 1999 – Projet Grand-Nord, rapport des travaux 1998. Ministère des Ressources naturelles et de la Faune, Québec; GM 56437, 148 pages.

FRANKLIN, J.M., 1993 – Volcanic-associated massive sulphide deposits. *In*: Mineral deposit modeling, R.V. Kirkham, W.D. Sinclair, R.I. Thorpe and J.M. Duke (ed.). Geological Association of Canada; Special Paper 40, pages 315-334.

FRANKLIN, J.M., 1995 - Volcanic-associated massive sulphide base metals. In: Geology of Canadian Mineral Deposit Types, O.R. Eckstrand, W.D. Sinclair, and R.I. Thorpe (ed.). Geological Survey of Canada; Geology of Canada, volume 8, pages 158-183.

FRANKLIN, J.M. – LYDON, J.W. – SANGSTER, D.F., 1981 – Volcanic-associated massive sulfide deposits. *In*: Economic Geology, Seventy-fifth Anniversary Volume, 1905-1980, B.J. Skinner (ed.). Economic Geology; pages 485-627.

FRENCH, J.E. – ATKINSON, B. – HEAMAN, L.M. – CHACKO, T. – ARMSTRONG, J. – CAIRNS, S. – HARTLAUB, R., 2004 – Application of electron microprobe chemical baddeleyite dating to reconnaissance geochronological investigations of mafic dyke swarms from the Slave Province, N.W.T. Geological Association of Canada-Mineralogical Association of Canada, Program with Abstracts; volume 29, page 442.

FROST, R.B. – BARNES, C. G. – COLLINS, W. J. – ARCULUS, R. J. – ELLIS, D. J. – FROST, C. D., 2001 – A Geochemical Classification for Granitic Rocks. Journal of Petrology; volume 42, pages 2033-2048.

GANDHI, S.S. – BELL, R.T., 1995 – Kiruna/Olympic Dam-type iron, copper, uranium, gold, silver. *In*: Geology of Canadian Mineral Deposit Types, O.R. Eckstrand, W.D. Sinclair, and R.I. Thorpe (ed.). Geological Survey of Canada; Geology of Canada, volume 8, pages 513-522

GAUTHIER, M., 2000 – Styles et répartition des gîtes métallifères du territoire de la Baie James (Québec). Chronique de la Recherche minière; numéro 539, pages 17-61.

GAUTHIER, R., 2001 – Nunavik mineral exploration Fund, Activity report 1998-2001. Ministère des Ressources naturelles et de la Faune, Québec; GM 60307, 160 pages.

GEHRISH, W., 1987 – Late Aphebian syngenetic uranium mineralization at Gayot Lake, Northern Quebec, Canada. Monograph Series on Mineral Deposits; volume 27, pages 49-57.

GEHRISH, W. – GATZWEILER, R. – LAMBERT, R., 1982 – The syngenetic U-deposit at Gayot Lake, New Quebec. Ministère des Ressources naturelles et de la Faune, Québec; GM 57799, 48 pages.

GERMAIN, L., 1964 – Geological Report. Ministère des Ressources naturelles et de la faune, Québec; GM 15679, 22 pages.

GEOLOGICAL SURVEY OF CANADA, 2004 – Gravity databases. Department of Natural Resources, Canada, Ottawa, Ontario.

GIRARD, R., 1999 – Travaux d'exploration 1999, rapport intérimaire, projet Lac Fagnant. Ministère des Ressources naturelles et de la Faune, Québec; GM 57500, 348 pages.

GOSSELIN, C. – SIMARD, M., 2001 - Geology of the Lac Gayot area (NTS 23M). Ministère des Ressources naturelles, Québec; RG 2000-03, 28 pages.

GOSSELIN, C. – SIMARD, M. – DAVID, J., 2002 - Geology of the Lacs des Loups Marins area (34A). Ministère des Ressources naturelles, Québec; RG 2002-06, 37 pages.

GOSSELIN, C. – ROY, P. – DAVID, J., 2004 - Geology of the Lac Bienville area (33P). Ministère des Ressources naturelles, Québec; RG 2003-04, 36 pages.

GOUTIER, J. – DION, C., 2004 – Geology and Mineralization of the La Grande Subprovince, James Bay. *In*: Abstracts of oral presentations and posters, Québec Exploration 2004. Ministère des Ressources naturelles, Québec; DV 2004-07, page 21.

GOUTIER, J. – DION, C. – OUELLET, M.-C. – DAVIS, D.W. – DAVID, J. – PARENT, M., 2002 – Géologie de la région du lac Guyer (33G/05, 33G/06, 33G/11). Ministère des Ressources naturelles, Québec; RG 2001-15, 53 pages.

GOUTIER, J. – DION, C. – DAVID, J. – DION, D.-J., 1999 – Géologie de la région de la passe Shimusuminu et du lac Vion (33F/11 ET 33F/12). Ministère des Ressources naturelles, Québec; RG 98-17, 41 pages.

GOUTIER, J. – BOUCHAN, K.L. – HAMILTON, M.K. – ERNST, R.E., 2001 – Les essaims de dykes de gabbro protérozoïques de la Baie-James et leur implication stratigraphique. *In*: L'exploration minérale au Québec, de brillantes perspectives, Séminaire d'information sur la recherche géologique, programme et résumés. Ministère des Ressources naturelles, Québec; DV 2001-08, page 38.

GOUTIER, J. – DION, C. – OUELLET, M.-C., 2001 – Géologie de la région de la colline Bezier (32G/12) et du lac de la Montagne de Pin (32G/13). Ministère des Ressources naturelles, Québec; RG 2001-13, 53 pages.

GOUTIER, J. – OUELLET, M.-C. – DION, C., 2001 – Synthèse géologique de la région des lacs Sakami (33F) et Guyer (33G), Baie-James. *In*: L'exploration minérale au Québec, de brillantes perspectives, Séminaire d'information sur la recherche géologique, Programmes et résumés. Ministère des ressources naturelles, Québec; DV 2001-08, page 17.

GRADSTEIN, F.M. – OGG, J.G. – SMITH, A.G. (ed.), 2004 – A Geologic Time Scale. Cambridge University Press.

GRIEVE, R.A.F. – ROBERTSON, P.B. – BOUCHARD, M.A. – ALEXOPOULOS, J.S., 1989 – Origin and age of the cratere du Nouveau-Québec. *In*: L'Histoire naturelle du cratère du Nouveau-Québec. Collection Environnement et Géologie, volume 7, Université de Montréal, 420 pages.

GROSS, G.A., 1995a - Algoma-type iron-formation. *In*: Geology of Canadian Mineral Deposit Types, O.R. Eckstrand, W.D. Sinclair, and R.I. Thorpe (ed.). Geological Survey of Canada; Geology of Canada, volume 8, pages 66-73.

GROSS, G.A., 1995b - Mafic intrusion-hosted titanium-iron. *In*: Geology of Canadian Mineral Deposit types, O.R. Eckstrand, W.D. Sinclair, and R.I. Thorpe (ed..). Geological Survey of Canada; Geology of Canada, volume 8, pages 573-582.

GROVES, D.I. – PHILLIPS, G.N. – FALCONER, L.J. – HOUSTOUN, S.M. – HO, S.E. – BROWNING, P. – DAHL, N. – MCNAUGHTON, N.J., 1988 – Evidence for an epigenetic origin for BIF-hosted gold deposits in greenstone belts of the Yilgarn Block, Western Australia. *In*: Recent advances in understanding Precambrian gold deposits, S.E. Ho and D.I. Groves (ed.). Geology Department and University Extension, University of Western Australia; Publication number 11, pages 167-179.

GUERNINA, S. – SAWYER, E.W., 2003 – Large-scale melt-depletion in granulite terranes; an example from the Archean Ashuanipi Subprovince of Quebec. Journal of Metamorphic Geology; volume 21, pages 181-201.

HALLS, H.C., 1987 – Dyke swarms and continental rifting: Some concluding remarks. *In*: Mafic Dyke Swarms, H.C. Halls and W.F. Fahrig (ed.). Geological Association of Canada; Special Paper 34, pages 483-492.

HALLS, H.C. – FAHRIG, W.F. (ed.), 1987 – Mafic Dyke Swarms. Geological Association of Canada; Special Paper 34, 503 pages.

HAMILTON, M.A. – GOUTIER, J. – MATTHEWS, W., 2001 – U-Pb baddeleyite age for the Paleoproterozoic Lac Esprit dyke swarm, James Bay region, Quebec. Radiogenic Age and Isotopic Studies; Report 14. Geological Survey of Canada; Current Research 2001-F5, pages 1-6.

HARWOOD, T.A., 1949 – The lead zinc deposits of Richmond Gulf. Ministère des Ressources naturelles et de la Faune, Québec; GM 00678, 59 pages.

HARPER, G., 1977 – Geology of the Sustut copper deposit in B.C. The Canadian Institute of Mining and Metallurgy Bulletin; volume 70, pages 97-104.

HAUFF, F. – HOERNLE, K. – SCHMINCKE, H.U. – WERNER, R., 1998. A mid-Cretaceous origin for the Galapagos hotspot: volcanological, petrological and geochemical evidence from Costa Rican oceanic crustal segments. Geology Rundschau; volume 86, pages 141-145.

HEAMAN, L.M. – LECHEMINANT, A.N., 1993 – Paragenesis and U-Pb systematics of baddeleyite (ZrO_2). Chemical Geology; volume 110, pages 95-126.

HERD, R. K., 1978 – Notes on metamorphism in New Quebec. *In:* Metamorphism in the Canadian Shield, J.A. Fraser and W.W. Heywood (ed.). Geological Survey of Canada; Paper 78-10, pages 79-83.

HILL, R.E.T., 2001 – Komatiite volcanology, volcanological setting and primary geochemical properties of komatiite-associated nickel deposits. Geochemistry: Exploration, Environment, Analysis; volume 1, pages 365-381.

HOCQ, M., 1994 – La Province du Supérieur. *In*: Géologie du Québec. Ministère des Ressources naturelles, Québec; MM 94-01, pages 7-20.

HOFFMAN, P.F., 1987 – Early Proterozoic fore-deeps, foredeep magmatism and Superior-type iron-formations of the Canadian shield. *In*: Proterozoic Lithospheric Evolution, A. Kröner (ed.). American Geophysical Union; Geodynamics Series, volume 17, pages 85-98.

HOFFMAN, P.F., 1988 – United plates of America, the birth of a craton: Early Proterozoic assembly and growth of Laurentia. Annual Review of Earth and Planetary Science; volume 16, pages 543-603.

HOFFMAN, P.F., 1989 – Precambrian geology and tectonic history of North America. *In:* The Geology of North America – An overview, A.W. Bally and A.R. Palmer (ed.). Geological Society of America; The Geology of North America, volume A, pages 447-512.

HUGHES, W. – TRUDEAU, Y. – GIROUX, N. – CHAMPAGNE, C. – LAFERRIÈRE, A. – FOURNIER, J.-D., 2002 – Travaux d'exploration 2001, Géologie et Géophysique, Projet Ninuk, région du lac Minto, Nord du Québec. Ministère des Ressources naturelles et de la Faune, Québec; GM 60327, 106 pages.

HUOT, F. – CHAPDELAINE, M. – ARCHER, P., 2004a – Technical report and recommandations, reconnaissance program, Coulon project, Quebec. Ministère des Ressources naturelles et de la Faune, Québec; GM 60761, 70 pages.

HUOT, F. – CHAPDELAINE, M. – ARCHER, P., 2004b – Technical report and recommandations, reconnaissance program, Gayot project, Quebec. Ministère des Ressources naturelles et de la Faune, Québec; GM 60727, 122 pages.

HYNES, A. – FRANCIS, D.M., 1982 – A transect of the Early Proterozoic Cape Smith foldbelt, New Quebec. Tectonophysics; volume 88, pages 23-59.

JOURDAN, F. – FÉRAUD, G. – BERTRAND, H. – KAMPUNZU, A.B. – TSHOSO, H. – LE GALL, B. – TIERCELIN, J.J. – CAPIEZ, P., 2004 – The Karoo triple junction questioned: evidence from $^{40}Ar/^{39}Ar$ Jurassic and Proterozoic ages and geochemistry of the Okavango dyke swarm (Botswana). Earth and Planetary Science Letters; volume 222, pages 989-1006.

JOURDAN, F. – FÉRAUD, G. – BERTRAND, H. – WATKEYS, M.K. – KAMPUNZU, A.B. – LE GALL, B., 2006 – Basement control on dyke distribution in Large Igneous Provinces: Case study of the Karoo triple junction. Earth and Planetary Science Letters; volume 241, pages 307-322.

JOURDAIN, V., 1998 – Projet Olympic (1241) – Rapport sur les travaux d'exploration de la saison 1998. Ministère des Ressources naturelles et de la Faune, Québec; GM 56814.

JUTEAU, L., 1975a – Rapport des possibilités de transport du minerai de fer. Ministère des Ressources naturelles et de la Faune, Québec; GM 31131, 118 pages.

JUTEAU, L., 1975b – Rapport de mise en production des gisements de fer. Ministère des Ressources naturelles et de la Faune, Québec; GM 31132, 24 pages.

KAPP, J.D. – MILLER, C.F. – MILLER, J.F., 2002 – Ireteba Pluton, Eldorado Mountains, Nevada: Late, Deep-Source Peraluminous Magmatism in the Cordillera Interior. Journal of Geology; volume 110, pages 649-669.

KERSWILL, J.A., 1993 – Models for iron-formation-hosted gold deposits. *In*: Mineral deposit modeling, R.V. Kirkham, W.D., Sinclair, R.I. Thorpe and J.M. Duke (ed.). Geological Association of Canada; Special Paper 40, pages 171-199.

KERSWILL, J.A., 1995 - Iron-formation-hosted stratabound gold. In: Geology of Canadian Mineral Deposit Types, O.R. Eckstrand, W.D. Sinclair, and R.I. Thorpe (ed.). Geological Survey of Canada; Geology of Canada, volume 8, pages 367-382.

KIRKHAM, R.V., 1995a - Sediment-hosted stratiform copper. *In*: Geology of Canadian Mineral Deposit Types, O.R. Eckstrand, W.D. Sinclair, and R.I. Thorpe (ed.). Geological Survey of Canada; Geology of Canada, volume 8, pages 223-240.

KIRKHAM, R.V., 1995b - Volcanic redbed copper. In: Geology of Canadian Mineral Deposit Types, O.R. Eckstrand, W.D. Sinclair, and R.I. Thorpe (ed.). Geological Survey of Canada; Geology of Canada, volume 8, pages 241-252.

KITZES, R., 1964 – Exploring craters in the Earth. Nature and Sciences; volume 1, pages 10-12.

KJARSGAARD, B.A., 1995 - Kimberlite-hosted diamond. *In*: Geology of Canadian Mineral Deposit Types, O.R. Eckstrand, W.D. Sinclair, and R.I. Thorpe (ed.). Geological Survey of Canada; Geology of Canada, volume 8, pages 561-568.

KRANCK, E.H., 1951 – On the geology of the east coast of Hudson Bay and James Bay. Acta Geographica; volume 11.

KRANCK, E.H. – SINCLAIR, G.W., 1963 – Clearwater Lake, New Quebec. Geological Survey of Canada; Bulletin 100, 25 pages.

KRETZ, R., 1960 – Geological observations in northern New Quebec. Geological Survey of Canada; Paper 60-12, 17 pages.

LABBÉ, J.-Y., 2001 – Crustal lineaments and kimberlite discovery potential in western Nouveau-Québec. Ministère des Ressources naturelles, Québec; PRO 2001-02, 8 pages.

LABBÉ, J.-Y., 2002 – Évaluation du potentiel de découverte de kimberlites dans la région du Grand-Nord du Québec – Intégration de géodonnées par la technologie d'analyse spatiale. Ministère des Ressources naturelles, Québec; EP 2002-05, 1 CD-ROM.

LABBÉ, J.-Y., 2005 – Les éléments du groupe du platine dans la partie nord-est de la Province du Supérieur. Ministère des Ressources naturelles et de la Faune, Québec; ET 2004-03, 33 pages.

LABBÉ, J.-Y. – LACOSTE, P., 2001 – Environnements propices aux minéralisations polymétalliques de type volcanogène dans le Grand Nord québécois. Ministère des Ressources naturelles, Québec; MB 2001-07, 29 pages.

LABBÉ, J.-Y. – LACOSTE, P., 2004 – Minéralisations en Cu-Ag dans les basaltes protérozoïques de la région du lac Guillaume-Delisle, Nouveau-Québec. Ministère des Ressources naturelles, de la Faune et des Parcs, Québec; ET 2004-02, 32 pages.

LABBÉ, J.-Y. – BANDYAYERA, D. – GOSSELIN, C. – LECLAIR, A. – MADORE, L. – PARENT, M. – SIMARD, M., 1998 – Potentiel minéral du nord du Québec : Nouvelles ceintures volcano-sédimentaires dans la Sous-province de Minto. Ministère des Ressources naturelles, Québec; PRO 98-04, 10 pages.

LABBÉ, J.-Y. – CHOINIÈRE, J. – BEAUMIER, M., 1999 –Areas favourable to the discovery of new volcano-sedimentary rock belts in the Minto Subprovince. Ministère des Ressources naturelles, Québec; PRO 99-07, 8 pages.

LABBÉ, J.-Y. – LACOSTE, P. – LECLAIR, A. – PARENT, M., 2001 – The Qullinaaraaluk Ni-Cu-Co showing: a new type of mineralization in the Archean rocks of the Far North. Ministère des Ressources naturelles, Québec; PRO 2001-05, 12 pages.

LABBÉ, J.-Y. – LACOSTE, P. – MADORE, L. – LARBI, Y. – SHARMA, K.N.M., 2003 – Minéralisations en terres rares dans les roches carbonatées de la ceinture de Kimber, projet Grand-Nord. Ministère des Ressources naturelles, de la Faune et des Parcs, Québec; ET 2002-08, 21 pages.

LACOSTE, P. – MADORE, L. – LARBI, Y. – SHARMA, K.N.M., 2001 – Texture et assemblage minéralogique : une ébauche de la carte régionale du métamorphisme dans le NE de la Province du Supérieur (Péninsule de l'Ungava). *In*: Projet de cartographie du Grand-Nord – Rapport d'atelier. Ministère des Ressources naturelles, Québec; MB 2002-01, pages 45-49.

LAFRANCE, I., 2001 – Caractérisation des minéralisations nickélifères associées aux komatiites de la Ceinture Archéenne de Vénus, Nouveau-Québec. M.Sc. thesis, Université du Québec à Montréal, Montréal (Québec), 185 pages.

LAMOTHE, D., 1994 – Géologie de la Fosse de l'Ungava, Nouveau-Québec. *In:* Géologie du Québec. Ministère des Ressources naturelles, Québec; MM 94-01, pages 67-74.

LAMOTHE, D., 1997 – Géologie de la région du lac Dupire (SNRC 34H/03). Ministère des Ressources naturelles, Québec; RG 96-01, 17 pages.

LAMOTHE, D. – PICARD, C. – MOORHEAD, J., 1984 – Bande de Cap Smith-Maricourt, région du lac Beauparlant : Ministère des Ressources naturelles, Québec; DP 84-39.

LAMOTHE, D. – LECLAIR, A. – CHOINIÈRE, J., 1998 – Géologie de la région du lac Vallard (SNRC 23C). Ministère des Ressources naturelles, Québec; RG 98-13, 29 pages.

LAMOTHE, D. – THÉRIAULT, R. – LECLAIR, A., 2000 – Géologie de la région du lac Nitchequon (SNRC 23 E). Ministère des Ressources naturelles, Québec; RG 99-14, 43 pages.

LAROCQUE, M. – LAFERRIÈRE, A., 2003 – Tan Property J/V Project, Northern Quebec, 2001-2002 assessment report. Ministère des Ressources naturelles et de la Faune, Québec; GM 60458, 297 pages.

LEACH, D.L. – SANGSTER, D.F., 1993 – Mississippi Valley-type lead-zinc deposits. *In:* Mineral deposit modeling, R.V. Kirkham, W.D. Sinclair, R.I. Thorpe and J.M. Duke (ed.). Geological Association of Canada; Special Paper 40, pages 289-314.

LECHEMINANT, A.N. – HEAMAN, L.M., 1989 – Mackenzie igneous events, Canada: Middle Proterozoic hotspot magmatism associated with ocean opening. Earth and Planetary Science Letters; volume 96, pages 38-48.

LECLAIR, A., 2005 – Géologie du nord-est de la Province du Supérieur, Québec. Ministère des Ressources naturelles et de la Faune, Québec; DV 2004-04, 19 pages.

LECLAIR, A. – LAMOTHE, D. – CHOINIÈRE, J. – DION, D.J., 1996 – Perspectives sur la structure et le potentiel minéral des roches archéennes du sud-est de la province du Supérieur; Ministère des Ressources naturelles du Québec, Québec; PRO 96-05, 10 pages.

LECLAIR, A. – LAMOTHE, D. – CHOINIÈRE, J. – PARENT, M., 1998 – Géologie de la région du lac Bermen (SNRC 23F). Ministère des Ressources naturelles, Québec; RG 97-11, 40 pages.

LECLAIR, A. – BERCLAZ, A. – DAVID, J. – PERCIVAL, J. A., 2001a – Regional geological setting of Archean rocks in the northeastern Superior Province. Geological Association of Canada-Mineralogical Association of Canada; Abstracts, volume 26, page 84.

LECLAIR, A. – BERCLAZ, A. – DAVID, J. – GOSSELIN, C. – LABBÉ, J.-Y. – LACOSTE, P. – LARBI, Y. – MADORE, L. – MAURICE, C. – PARENT, M. – ROY, P. – SHARMA, K. N. M. – SIMARD, M., 2001b – Le nord-est de la Province du Supérieur et son évolution géologique entre 3,0 et 2,6 Ga. *In*: L'exploration minérale au Québec, de brillantes perspectives, Séminaire d'information sur la recherche géologique, programme et résumés. Ministère des Ressources naturelles, Québec; DV 2001-08, page 11.

LECLAIR, A.D. – PARENT, M. – DAVID, J. – DION, D.-J. – SHARMA, K.N.M., 2002 - Geology of the Lac La Potherie area (34I). Ministère des Ressources naturelles, Québec; RG 2001-04, 40 pages.

LECLAIR, A. – BERCLAZ, A. – PARENT, M. – CADIEUX, A.-M. – SHARMA, K.N.M., 2003 – Géologie – Lac Dufreboy (24L). Ministère des Ressources naturelles, Québec; carte SI-24L-C2G-03C, scale 1/250,000.

LECLAIR, A. – BERCLAZ, A. – DAVID, J. – FAR NORTH WORKING GROUP, 2004 – The Northeastern Superior Province in Quebec's Far North: A regional synthesis. *In*: Lithoprobe Report 86, Lithoprobe Secretariat, University of British Columbia.

LECLAIR, A. – LABBÉ, J.-Y. – BERCLAZ, A. – DAVID, J. – GOSSELIN, C. – LACOSTE, P. – MADORE, L. – MAURICE, C. – ROY, P. – SHARMA, K.N.M. – SIMARD, M., 2006 – Government geoscience stimulates mineral exploration in the Superior Province, northern Quebec. Geoscience Canada; volume 33, no. 2, pages 60-75.

LECLERC, F., 2004 – Évolution tectonostratigraphique et métamorphique de la ceinture volcano-sédimentaire de Qalluviartuuq-Payne, nord-est de la Province du Supérieur. M.Sc. thesis, Université du Québec à Montréal, Montréal, 101 pages.

LEE, S.M., 1965 – Inussuaq - Pointe Normand area, New Quebec. Ministère des Richesses naturelles du Québec; RG 119(A), 138 pages.

LEGAULT, F. – FRANCIS, D. – HYNES, A. – BUDKEWITSH, P., 1994 – Proterozoic continental volcanism in the Belcher Island: implications for the evolution of the Circum Ungava fold Belt. Canadian Journal of Earth Sciences; volume 31, pages 1536-1549.

LEWRY, J.F. – COLLERSON, K.D., 1990 – The Trans-Husdon Orogen: extent, subdivision, and problems. *In*: The Early Proterozoic Trans-Hudson Orogen of North America, J.F. Lewry and M.R. Stauffer (ed.). Geological Association of Canada; Special Paper 37, pages 1-4.

LIN, S. – PERCIVAL, J.A. – WINSKY, P.A. – SKULSKI, T. – CARD, K.D., 1995 – Structural evolution of the Vizien and Kogaluc greenstone belts in Minto block, northeastern Superior Province, northern Quebec. *In*: Current Research 1995-C, Geological Survey of Canada; pages 121-130.

LIN, S. – PERCIVAL, J.A. – SKULSKI, T., 1996 – Structural constraints on the tectonic evolution of a late Archean greenstone belt in the northeastern Superior Province, northern Quebec (Canada). Tectonophysics; volume 265, pages 151-167.

LINCOLN, T.N., 1981 – The redistribution of copper during low-grade metamorphism of the Karmutsen volcanics, Vancouver Island, British Columbia. Economic Geology; volume 76, pages 2147-2161.

LOW, A.P., 1889 – Report on an exploration in James Bay and country east of Hudson Bay drained by the Big Great Whale and Clearwater Rivers. Geological Survey of Canada; Annual Report, volume III, part J, 1887-88.

LOW, A.P., 1898 – Report on a traverse of the northern part of the Labrador Peninsula from Richmond Gulf to Ungava Bay. Geological Survey of Canada; Annual Report, volume IX, part L.

LOW, A.P., 1902 – Report on an exploration of the east coast of Hudson Bay from Cape Wolstenholme to the south end of James Bay. Geological Survey of Canada; Annual Report, volume XIII, part D, 84 pages.

MACHADO, N. – GOULET, N. – GARIÉPY, C., 1989 – U-Pb geochronology of reactivated Archean basement and of Hudsonian metamorphism in the northern Labrador Trough. Canadian Journal of Earth Sciences; volume 26, pages 1-15.

MACHADO, N. – CLARK, T. – DAVID, J. – GOULET, N., 1997 – U-Pb ages for magmatism and deformation in the New Quebec Orogen. Canadian Journal of Earth Sciences; volume 34, pages 716-723.

MACHADO, N. – DAVID, J. – SCOTT, D.J. – LAMOTHE, D. – PHILIPPE, S. – GARIÉPY, C., 1993 – U-Pb geochronology of the western Cape Smith belt, Canada: New insights on the age of initial rifting and arc magmatism. Precambrian Research; volume 63, pages 211-224.

MADON, Z., 1977 – Report on exploration work, project 71-87. Ministère des Ressources naturelles et de la Faune, Québec; GM 33656, 79 pages.

MADON, Z., 1979 – Report on 1978 exploration works. Ministère des Ressources naturelles et de la Faune, Québec; GM 34314, 17 pages.

MADON, Z. – WINTER, L.D.S., 1980 – Report on exploration works. Ministère des Ressources naturelles et de la Faune, Québec; GM 36330, 117 pages.

MADORE, L. – BANDYAYERA, D. – BÉDARD, J.H. – BROUILLETTE, P. – SHARMA, K.N.M. – BEAUMIER, M. – DAVID, J., 2000 - Geology of the Lac Peters area (24M). Ministère des Ressources naturelles, Québec; RG 99-16, 43 pages.

MADORE, L. – LARBI, Y., 2001 - Geology of the Rivière Arnaud area (25D) and adjacent coastal areas (25C, 25E, and 25F). Ministère des Ressources naturelles, Québec; RG 2001-06, 35 pages.

MADORE, L. – LARBI, Y. – SHARMA, K.N.M – LABBÉ, J-Y. – LACOSTE, P. –DAVID, J. – BROUSSEAU, K. – HOCQ, M., 2002 - Geology of the Lac Klotz (35A) and the Cratère du Nouveau-Québec (southern half of 35H) areas. Ministère des Ressources naturelles, Québec; RG 2002-05, 41 pages.

MADORE, L. – LARBI, Y. – LABBÉ, J-Y. – SHARMA, K.N.M – LACOSTE, P. –DAVID, J., 2004 - Geology of the Lac Couture (35B) and Lacs Nuvilik (35G, southern half) areas. Ministère des Ressources naturelles, Québec; RG 2003-02, 42 pages.

MARTIN, H., 1993. The mechanism of petrogenesis of the Archean continental crust-Comparison with modern processes. Lithos; volume 30, pages 373-388.

MARTIN, H., 1999 – Adakitic magmas: modern analogues of Archean granitoids. Lithos; volume 46, pages 411-429.

MARTIN, H. – MOYEN, J.F., 2002 – Secular changes in tonalite-trondhjemite-granodiorite composition as markers of the progressive cooling of Earth. Geology; volume 30, pages 329-322.

MAURICE, C., 2007 – Nouvelles données isotopiques du néodyme dans le NE de la Province du Supérieur, Nunavik, Québec. Ministère des Ressources naturelles et de la Faune, Québec; RP 2006-06, 13 pages.

MAURICE, C. – FRANCIS, D. – MADORE, L., 2003 – Constraints on early Archean crustal extraction and tholeiitic-komatiitic volcanism in greenstone belts of the Northern Superior Province. Canadian Journal of Earth Sciences; Volume 40, pages 431-445.

MAURICE, C. – BERCLAZ, A. – DAVID, J. – SHARMA, K.N.M. – LACOSTE, P., 2005a - Geology of the Povungnituk (35C) and Kovik Bay (35F) areas. Ministère des Ressources naturelles, de la Faune et des Parcs, Québec; RG 2004-05, 41 pages.

MAURICE, C. – LACOSTE, P. – BERCLAZ, A. – DAVID, J. – SHARMA, K.N.M., 2005b – Géologie de la région de Kogaluc Bay (34N et 34M). Ministère des Ressources naturelles, de la Faune et des Parcs, Québec; RG 2004-01, 35 pages.

MAURICE, C. – DAVID, J. – O'NEIL, J. – FRANCIS, D., 2007 – Insights on the enriched isotopic nature of Proterozoic dyke swarms in the Northeastern Superior Province. Goldschmidt Conference Abstracts, Geochimica et Cosmochimica Acta; 71 (15), Supplement 1, page A640.

MAURICE, C – DAVID, J – BÉDARD, J.H. – FRANCIS, D., 2009 – Evidence for a widespread mafic cover sequence and its implications for continental growth in the Northeastern Superior Province. *In*: Superior Province: the nature and evolution of the Archean continental lithosphere, G. Stott and W. Mueller (ed.). Precambrian Research.

MCHONE, J.G. – ANDERSON, D.L. – BEITEL, E.K. – FIALKO, Y.A., 2005 – Giant Dikes: Patterns and Plate Tectonics. *In*: Plates, plumes, and paradigms, G.R. Foulger, J.H. Natland, D.C. Presnall and D.L. Anderson (ed.). Geological Society of America; Special Paper 388, pages 401-420.

MÈGE, D. – KORME, T., 2004 – Dyke swarm emplacement in the Ethiopian Large Igneous Province: not only a matter of stress. Journal of Volcanology and Geothermal Research; volume 132, pages 283-310.

MER, 1986 – Code stratigraphique nord-américain. Ministère de l'Énergie et des Ressources, Québec; DV 86-02, 58 pages.

MERCIER, E. – CIESIELSKI, A., 1983 – Un reliquat de zone volcano-sédimentaire dans la sous-province archéenne d'Ungava, Québec. *In:* Current Research, Part B. Geological Survey of Canada; Paper 83-01B, 1983, pages 165-175.

MILORD, I. – GIRARD, R., 2000 – Travaux d'exploration 2000, rapport final, projet Lac Fagnant. Ministère des Ressources naturelles et de la Faune, Québec; GM 58687, 348 pages.

MITCHELL, R.H., 1991 – Kimberlites and lamproites: primary source of diamonds. Geoscience Canada; volume 18, pages 1-16.

MOFFAT, W.W., 1946 – A report on the Gulf lead Mines property – Hudson Bay (summer 1946). Ministère des Ressources naturelles et de la Faune, Québec; GM 9734, 15 pages.

MOORHEAD, J., 1988 – Géologie de la région du lac Vigneau, Fosse de l'Ungava: Ministère des Ressources naturelles, Québec : DP 88-05.

MOORHEAD, J., 1989 – Géologie de la région du lac Chukotat (Fosse de l'Ungava). Ministère des Ressources naturelles, Québec; ET 87-10, 56 pages.

MOORHEAD, J., 1996 – Géologie de la région du lac Hubert (Fosse de l'Ungava). Ministère des Ressources naturelles, Québec; ET 91-06, 111 pages.

MOORHEAD, J. – BEAUMIER, M. – LEVEBVRE, D.L. – BERNIER, L. – MARTEL, D., 1999. Kimberlites, linéaments et rifts crustaux au Québec. Ministère des Ressources naturelles, Québec; MB 99-35, 50 pages.

MOORHEAD, J. – PERREAULT, S. – BERCLAZ, A. – SHARMA, K.N.M. – BEAUMIER, M. – CADIEUX, A.-M., 2000 – Kimberlites and Diamonds in Northern Québec. Ministère des Ressources naturelles, Québec; PRO 99-09, 10 pages.

MOUKHSIL, A. – LEGAULT, M. – BOILY, M. – DOYON, J. – SAWYER, E. – DAVIS, D.W., 2007 - Geological and metallogenic synthesis of the Middle and Lower Eastmain greenstone belt (Baie-James). Ministère des Ressources naturelles et de la Faune, Québec; ET 2007-01, 58 pages.

MRN, 1998 – Résultats d'analyses de sédiments de fond de lacs, Grand Nord du Québec. Ministère des Ressources naturelles, Québec; DP-98-01, digital data.

MUELLER, A.G., 1997 – The Nevoria gold skarn deposit in Archean iron-formation, Southern Cross greenstone Belt, Western Australia: I. Tectonic setting, petrography, and classification. Economic Geology; volume 92, pages 181-209.

MUELLER, A.G. – GROVES, D.I., 1991 – The classification of Western Australian greenstone-hosted gold deposits according to wallrock-alteration mineral assemblages. Ore Geology Reviews; volume 6, pages 291-331.

NADEAU, P., 2003 – Structural evolution of the Porpoise Cove area, Northeastern Superior Province, Northern Quebec. M.Sc. Thesis, Simon Fraser University, 95 pages.

NALDRETT, A.J., 1981 – Nickel sulfide deposits: classification, composition, and genesis. *In*: Economic Geology, Seventy-fifth Anniversary Volume, 1905-1980, Skinner, B.J. (ed.). Economic Geology; pages 628-685.

NALDRETT, A.J., 1999 – World-class Ni-Cu-PGE deposits: key factors in their genesis. Mineralium Deposita, volume 34, pages 227-240.

O'NEIL, J. – MAURICE, C. – STEVENSON, R.K. – FRANCIS, D., 2006a – The geology of the 3.8 Ga Porpoise Cove (Nuvvuagittuq) greenstone belt, Northeasten Superior Province, Northern Quebec. GAC-MAC; Program with Abstracts, volume 31, page 112.

O'NEIL, J. – CLOQUET, C. – STEVENSON, R.K. – FRANCIS, D., 2006b – Fe isotope systematics of banded iron formation from the 3.8 Ga Nuvvuagittuq greenstone belt, Northeastern Superior Province, Canada. GAC-MAC; Program with Abstracts, volume 31, page 111.

O'NEIL, J. – MAURICE, C. – STEVENSON, R.K. – LAROCQUE, J. – CLOQUET, C. – DAVID, J. – FRANCIS, D., 2007 – The geology of the 3.8 Ga Nuvvuagittuq (Porpoise Cove) greenstone belt, Northeasten Superior Province, Canada. *In*: Earth's Oldest Rocks, Developments in Precambrian Geology, Vol. 15,

M. J. van Kranendonk, R. Hugh Smithies and V. Bennett (ed.), pages 219-250.

ORESKES, N. – HITZMAN, M.W., 1993 – A model for the origin of Olympic Dam-type deposits. *In:* Mineral Deposit Modeling, R.V. Kirkham, W.D Sinclair, R.I. Thorpe and J.M. Duke (ed.). Geological Association of Canadal; Special Paper 40, pages 615-633.

ORR, R., 1979 – Gayot lake area project no. 71-86, Assessment report 1979. Ministère de l'Énergie et des Ressources, Québec; GM-36171.

PARADIS, S.J. – PARENT, M., 2005 – Géologie des formations en surface, Lac Vernon, Québec. Geological Survey of Canada; «A» Series maps Nos. 2071A and 2072A.

PARENT, M., 1998 – Géochronologie U-Pb du Projet Moyen-Nord, Phase II. Ministère des Ressources naturelles et de la Faune du Québec; GM 59904, 61 pages.

PARENT, M. – LECLAIR, A. – DAVID, J. – SHARMA, K.N.M., 2001 - Geology of the Lac Nedlouc area (NTS 34H and 24E). Ministère des Ressources naturelles, Québec; RG 2000-09, 40 pages.

PARENT, M. – BEAUMIER, M. – PARADIS, S.J., 2002 – A new high-potential target for diamond exploration in northern Québec - Chromium picroilmenites in esker sediments of the Lac Bienville (33P) region.. Ministère des Ressources naturelles, Québec; PRO 2002-03, 7 pages.

PARENT, M. – PARADIS, S.J. – BEAUMIER, M., 2003a – Dynamique glaciaire polyphasée et dispersion glacio-sédimentaire dans la région du lac Anuc (34O), nord du Québec. *In:* Projet de cartographie du Grand-Nord – Rapport d'atelier, Ministère des Ressources naturelles, Québec; MB 2003-01, pages 55-61.

PARENT, M. – LECLAIR, A. – DAVID, J. – SHARMA, K.N.M. – LACOSTE, P., 2003b - Geology of the Lac Vernon area (34J). Ministère des Ressources naturelles, Québec; RG 2002-07, 37 pages.

PARENT, M. – BEAUMIER, M. – GIRARD, R. – PARADIS, S.J., 2004 – Diamond exploration in the Archean craton of northern Québec : Kimberlite indicator minerals in eskers of the Saindon-Cambrien corridor. Ministère des Ressources naturelles, Québec; MB 2004-02, 17 pages.

PARRISH, R. R., 1989 – U-Pb geochronology of the Cape Smith belt and Sugluk block, northern Quebec. Geoscience Canada; volume 16, pages 126-130.

PERCIVAL, J.A., 1991 – Granulite-facies metamorphism and crustal magmatism in the Ashuanipi complex, Quebec – Labrador, Canada. Journal of Petrology; volume 32, pages 1261-1297.

PERCIVAL, J.A., 1993 – Geology, Ashuanipi complex, Schefferville Area, Newfoundland-Québec. Geological Survey of Canada; «A» Series Map 1785A, scale 1/125,000.

PERCIVAL, J.A. – CARD, K.D., 1992 – Geology of the Vizien greenstone belt. Geological Survey of Canada; Open file 2495, scale 1/50,000.

PERCIVAL, J.A. – CARD, K.D., 1994 – Geology, Lac Minto – Rivière aux Feuilles. Geological Survey of Canada; Map 1854A, scale 1/500,000.

PERCIVAL, J.A. – SKULSKI, T., 2000 – Tectonothermal evolution of the northern Minto Block, Superior Province, Quebec, Canada. The Canadian Mineralogist; volume 38, p. 345-378.

PERCIVAL, J.A. – CARD, K.D. – STERN, R.A. – BÉGIN, N.J., 1990 – A geologic transect of northeastern Superior Province, Ungava Peninsula, Quebec: the Lake Minto area. *In*: Current Research, Part C, Geological Survey of Canada; Paper 90-1C, pages 133-141.

PERCIVAL, J.A. – CARD, K.D. – STERN, R.A. – BÉGIN, N.J., 1991 – A geologic transect of the Leaf River area, northeastern Superior Province, Ungava Peninsula, Quebec. *In*: Current Research, Part C, Geological Survey of Canada; Paper 91-1C, pages 55-63.

PERCIVAL, J.A. – MORTENSEN, J.K. – STERN, R.A. – CARD, K.D. – BEGIN, N.J., 1992 – Giant granulite terranes of northeastern Superior Province; the Ashuanipi Complex and Minto Block. Canadian Journal of Earth Sciences; volume 29, pages 2287-2308.

PERCIVAL, J.A. – CARD, K.D. – MORTENSEN, J.K., 1993 – Archean unconformity in the Vizien greenstone, Ungava Peninsula, Quebec. *In*: Current Research, Part C, Geological Survey of Canada; Paper 93-1C, pages 319-328.

PERCIVAL, J.A. – SKULSKI, T. – CARD, K.D., 1995a – Geology, Rivière Kogaluc – Lac Qalluviartuuq region (parts of 34J and 34O). Geological Survey of Canada; Open File 3112, scale 1: 250 000.

PERCIVAL, J.A. – SKULSKI, T. – LIN, S. – CARD, K.D., 1995b – Granite-greenstone terranes of the northern Goudalie domain, northeastern Superior Province, Quebec. *In*: Current Research 1995-C, Geological Survey of Canada; pages 141-150.

PERCIVAL, J.A. – SKULSKI, T. – NADEAU, L., 1996a – Geology, Lac Couture, Quebec. Geological Survey of Canada; Open File 3315, scale 1: 250 000.

PERCIVAL, J.A. – SKULSKI, T. – NADEAU, L., 1996b – Granite-greenstone terranes of the northern Minto block, northeastern Superior Province, Quebec. *In*: Current Research 1996-C, Geological Survey of Canada; pages 157-167.

PERCIVAL, J.A. – SKULSKI, T. – NADEAU, L., 1997a – Reconnaissance geology of the Pelican-Nantais belt, northeastern Superior Province, Quebec. Geological Survey of Canada; Open File 3525, scale 1: 250 000.

PERCIVAL, J.A. – SKULSKI, T. – NADEAU, L., 1997b – Granite-greenstone terranes of the northern Minto Block, northeastern Quebec: Pélican-Nantais, Faribault-Leridon and Duquet belts. *In*: Current Research, 1997-C, Geological Survey of Canada; pages 211-221.

PERCIVAL, J.A. – STERN, R.A. – SKULSKI, T., 2001 – Crustal growth through successive arc magmatism: reconnaissance U-Pb SHRIMP data from the northeastern Superior Province, Canada. Precambrian Research; volume 109, pages 203-238.

PERCIVAL, J.A. – STERN, R.A. – RAYER, N., 2003 – Archeen adakites from the Ashuanipi Complex, eastern Superior Province, Canada; geochemistry, geochronology and tectonic significance. Contributions to Mineralogy and Petrology; volume 145, pages 265-280.

PERCIVAL, J.A. – SANBORN-BARRIE, M. – SKULSKI, T. – WHALEN, J. – WHITE, D. – STOTT, G. – LECLAIR, A. – CORKERY, T., 2006 – New insights from Earth's largest craton stimulate Superior research opportunities. GAC-MAC; Program with Abstracts, volume 31, pages 118.

PERCIVAL, J.A. – LECLAIR, A. – SANBORN-BARRIE, M. – SKULSKI, T. – STOTT, G. – CORKERY, T. – BERCLAZ, A. – BOILY, M., submitted – Geology and tectonic evolution of the Superior Province, Canada. Geological Association of Canada, Special Volume.

POIRIER, G., 1994 – Projet Minto-Vizien, Permis Qalluviartuuq. Ministère des Ressources naturelles, Québec; GM 52818, 59 pages.

PUCHTEL, I.S. – HOFFMAN, M.W. – MEZGER, K. – JOCHUM, K.P. – SHCHIPANSKY, A.A. – SAMSONOV, A.V., 1997 – Oceanic plateau model for continental crustal growth in the Archaean: A case study from the Kostomuksha greenstone belt, NW Baltic Shield. Earth and Planetary Sciences Letters; volume 155, pages 57-74.

QUIRION, D., 1998 – Rapport sur les travaux d'exploration 1998, Vernot (1250) et Morrice (1251). Ministère des Ressources naturelles et de la Faune, Québec; GM 56517, 111 pages.

QUIRION, D., 1999 – Rapport sur les travaux d'exploration, projet Vernot (1250), Ungava, 1999. Ministère des Ressources naturelles et de la Faune, Québec; GM 57402, 125 pages.

RABEAU, O., 2003 – Étude de l'évolution du néodyme dans la croûte continentale du nord-est de la province du Supérieur, Nunavik, Québec. M.Sc. thesis, Université du Québec à Montréal, Montréal (Québec), 80 pages.

REIMOLD, W.C. – GRIEVE, R.A.F. – PALME, H., 1981 – Rb-Sr dating of the impact melt from East Clearwater, Quebec. Contributions to Mineralogy and PÉTRology; volume 76, pages 73-76.

RICHARDSON, D.G. – BIRKETT, T.C., 1995 - Carbonatite-associated deposits. *In*: Geology of Canadian Mineral Deposit Types, O.R. Eckstrand, W.D. Sinclair, and R.I. Thorpe (ed.). Geological Survey of Canada; Geology of Canada, volume 8, pages 541-558.

RICKETTS, B.D. – DONALDSON, J.A., 1981 – Sedimentary history of the Belcher Group of Hudson Bay. *In*: Proterozoic Basins of Canada, F.H.A. Campbell (ed.). Geological Survey of Canada; Paper 81-10, pages 235-254.

ROBERTSON, P.B., 1965 – Petrography of the bedrock and breccia erratics in the region of Lac Couture, Quebec. M.Sc. Thesis, The Pennsylvania State University.

ROBERT, F., 1995 - Quartz-carbonate vein gold. *In*: Geology of Canadian Mineral Deposit types, O.R. Eckstrand, W.D. Sinclair, and R.I. Thorpe (ed.). Geological Survey of Canada; Geology of Canada, volume 8, pages 350-366.

ROHON, M.-L. – VIALETTE, Y. – CLARK, T. – ROGER, G. – OHNENSTETTER, D. – VIDAL, P., 1993 – Aphebian mafic-ultramafic magmatism in the Labrador Trough (New Quebec): its age and the nature of its mantle source. Canadian Journal of Earth Sciences; volume 30, pages 1582-1593.

RONDOT, J. – PLANTE, L. – SÉGUIN, M.K., 1993 – Géologie postarchéenne de la partie centrale du lac à l'Eau Claire ouest (Nouveau-Québec). Ministère de l'Énergie et des Ressources, Québec; ET 92-06, 21 pages.

ROY, C., 1989 – Géologie de la région du lac Bélanger, Fosse de l'Ungava. Ministère des Ressources naturelles, Québec; MB 89-13, 117 pages.

ROY, P. – TURCOTTE, S. – SHARMA, K.N.M. – DAVID, J., 2006 - Geology of the Lac Montrochand area (33O). Ministère des Ressources naturelles et de la Faune, Québec; RG 2005-04, 42 pages.

RUZICKA, V., 1995a - Vein uranium. *In*: Geology of Canadian Mineral Deposit Types, O.R. Eckstrand, W.D. Sinclair, and R.I. Thorpe (ed.). Geological Survey of Canada; Geology of Canada, volume 8, pages 278-283.

RUZICKA, V., 1995b - Unconformity-associated uranium. *In*: Geology of Canadian Mineral Deposit Types, O.R. Eckstrand, W.D. Sinclair, and R.I. Thorpe (ed.). Geological Survey of Canada; Geology of Canada, volume 8, pages 197-210.

RYDER-TURNER, A., 1998 – Final report on data acquisition and processing, fixed wing magnetic and radiometric geophysical survey, Morrice and Vernot grids. Ministère des Ressources naturelles et de la Faune, Québec; GM 56516, 26 pages.

SANGSTER, D.F., 1995 - Mississippi Valley-type lead-zinc. *In*: Geology of Canadian Mineral Deposit Types, O.R. Eckstrand, W.D. Sinclair, and R.I. Thorpe (ed.). Geological Survey of Canada; Geology of Canada, volume 8, pages 253-261.

SAVARD, M. – CHAPDELAINE, M., 1999 – Projet Gayot : rapport technique des travaux, été 1999. Ministère des Ressources naturelles et de la faune, Québec; GM 57115, 39 pages.

SCOATES, R.F.J. – MACEK, J.J., 1978 – Molson Dyke swarm. Manitoba Mineral Resources Division; Geological Paper 78-1.

SCHUMACHER, F. – FOUQUES, J.P., 1979 – Rapport de synthèses des travaux réalisés depuis 1974 jusqu'au 31 décembre 1978 sur les permis SES. Ministère des Ressources naturelles et de la Faune, Québec; GM 37017, 157 pages.

SCOTT, D.J. – HELMSTAEDT, H. – BICKLE, M.J., 1992 – Purtuniq ophiolite, Cape Smith Belt, northern Quebec, Canada: a reconstructed section of Early Proterozoic oceanic crust. Geology; volume 20, pages 173-176.

SHARMA, K. N. M., 1996 - Légende générale de la carte géologique - édition revue et augmentée. Ministère des Ressources naturelles, Québec; MB 96-28, 89 pages.

SIGURDSSON, H., 1987 – Dyke injection in Iceland: A review. *In*: Mafic dyke swarms, W.F. Fahrig and H.C. Halls (ed.). Geological Association of Canada; Special Paper 34, pages 55–65.

SIMARD, M., 2008 – Lexique stratigraphique des unités archéennes du nord-est de la Province du Supérieur. Ministère des Ressources naturelles et de la Faune, Québec; DV 2008-03, 107 pages.

SIMARD, M. – GOSSELIN, C., 1999 – Géologie de la région du lac Lichteneger (SNRC 33B). Ministère des Ressources naturelles, Québec; RG 98-15, 25 pages.

SIMARD, M. – GOSSELIN, C. – DAVID, J., 2002 - Geology of the Maricourt area (24D). Ministère des Ressources naturelles, Québec; RRG 2001-07, 41 pages.

SIMARD, M. – PARENT, M. – DAVID, J. – SHARMA, K.N.M., 2004 - Geology of the Rivière Innuksuac area (34K and 34L). Ministère des Ressources naturelles, Québec; RG 2003-03, 42 pages.

SIMARD, M. – CHEVÉ, S – DAVID, J. – LABBÉ, J.-Y. – SHARMA, K. N.M., 2005a – Géologie de la région du lac Minto (34F et 34G). Ministère des Ressources naturelles, de la Faune et des Parcs, Québec; RG 2004-04, 25 pages.

SIMARD, M. – PARENT, M. – THÉRIAULT, R. – DAVID, J. – LACOSTE, P. – SHARMA, K. N.M., 2005b - Geology of the Lac à l'Eau Claire area (34B and 34C). Ministère des Ressources naturelles et de la Faune, Québec; RG 2004-06, 48 pages.

SKULSKI, T. – PERCIVAL, J.A., 1996 – Allochtonous 2.78 Ga oceanic plateau slivers in a 2.72 Ga continental arc sequence; Vizien greenstone belt, northeastern Superior Province, Canada. Lithos; volume 37, pages 163-179.

SKULSKI, T. – PERCIVAL, J.A. – STERN, R.A., 1996 – Archean crustal evolution in the central Minto block, northern Quebec. *In*: Radiogenic Age and Isotope Studies; report 9. Geological Survey of Canada; Current Research 1995-F, pages 17-31.

SKULSKI, T. – STERN, R.A. – CIESIELSKI, A., 1998 – Timing and sources of granitic magmatism, Bienville subprovince, northern Quebec. Geological Association of Canada-Mineralogical Association of Canada, Program with Abstracts; volume 23, page A-175.

SKULSKI, T. – CORKERY, T. – STONE, D. – WHALEN, J.B. – STERN, R.A., 2000 – Geological and geochronological investigations in the Stull Lake-Edmund Lake greenstone belt and granitoid rocks of the northwestern Superior Province. *In:* Report of Activities 2000, Manitoba Industry, Trade and Mines, Manitoba Geological Survey, p. 117-128.

SMITHIES, R.H., 2000 – The Archaean tonalite-trondhjemite-granodiorite (TTG) series is not an analogue of Cenozoic adakite. Earth and Planetary Sciences Letter; volume 182, pages 115-125.

STERN, R.A. – HANSON, G.N. – SHIREY, S.B., 1989 – PÉTRogenesis of mantle-derived, LILE-enriched Archean monzodiorites and trachyandesites (sanukitoids) in southwestern Superior Province. Canadian Journal of Earth Sciences; volume 26, pages 1688-1712.

STERN, R.A. – PERCIVAL, J.A. – MORTENSEN, J.K., 1994 – Geochemical evolution of the Minto block: a 2.7 Ga continental magmatic arc built on the Superior proto-craton. Precambrian Research; volume 65, pages 115-153.

STEVENSON, I.M., 1968 – A geological reconnaissance of Leaf River Map-Area, New Quebec and Northwest Territories. Geological Survey of Canada; Memoir 356, 112 pages.

STEVENSON, R.K – BIZZARRO, M., 2007 – Crustal anatexis in the early Archean: Geochemical and isotopic evidence from the ca. 3.66 Ga Nuvvuagittuq Tonalite Suite. Goldschmidt Conference Abstracts, Geochimica et Cosmochimica Acta; 71 (15), Supplement 1, page A974.

STEVENSON, R.K. – DAVID, J. – PARENT, M., 2006 – Crustal evolution of the western Minto Block, northern Superior Province, Canada. Precambrian Research; volume 145, pages 229-242.

ST-HILAIRE, C., 1998 – Levé électromagnétique, magnétique et spectrométrique héliporté, région du Grand-Nord. Ministère des Ressources naturelles et de la Faune, Québec; GM 56815, 35 pages.

ST-ONGE, M.R. – LUCAS, S.B., 1990 – Evolution of the Cape Smith Belt: Early Proterozoic continental underthrusting, ophiolite obduction, and thick-skinned folding. *In:* The Early Proterozoic Trans-Husdon Orogen of North America, J.F. Lewry and M.R. Stauffer (ed.). Geological Association of Canada; Special Paper 37, pages 313-351.

ST-ONGE, M.R. – LUCAS, S.B., 1993 – Geology of the eastern Cape Smith Belt: parts of the Kangiqsujuaq, Cratère du Nouveau Québec, and lacs Nuvilik map areas, Quebec. Geological Survey of Canada; Memoir 438, 110 pages.

ST-ONGE, M.R. – LUCAS, S.B., 1997 – Geological maps and descriptive notes and legend, parts of northern Quebec and Northwest Territories. Geological Survey of Canada; Maps 1911A to 1916A.

STOCKWELL, C.H., 1982 – Proposals for time classification and correlation of Precambrian rocks and events in Canada and adjacent areas of the Canadian Shield, Part 1: A time classification of Precambrian rocks and events. Geological Survey of Canada; Paper 80-19, 135 pages.

STOTT, G.M., 1997 – The Superior Province, Canada. *In:* Greenstone Belts, M.J. de Wit, and L.D. Ashwcoll (ed.). Monographs on Geology and Geophysics 35, Oxford Clarendon; pages 480-507.

TAYLOR, F.C., 1982 – Reconnaissance geology of a part of the Canadian Shield, northern Quebec and Northwest Territories. Geological Survey of Canada; Memoir 399, 32 pages.

THÉRIAULT, R. – CHEVÉ, S., 2001 – Géologie de la région du lac Hurault (SNRC 23L). Ministère des Ressources naturelles, Québec; RG 2000-11, 49 pages.

THOMPSON, P.H., 2006 – Grand Nord metamorphic project, 2005 reports 1 and 3. Ministère des Ressources naturelles et de la Faune, Québec; GM 62017, 69 pages.

TODT, W. – CHAUVEL, C. – ARNDT, N. – HOFMANN, A.W., 1984 – Pb isotopic composition and age of Proterozoic komatiites and related rocks from Canada. EOS; volume 65, page 1169.

TOGOLA, N., 1992 – Géologie de la baie de Korac, Fosse de l'Ungava. Ministère des Ressources naturelles, Québec; ET 91-07, 39 pages.

TOMLINSON, K.Y. – STOTT, G.M. – PERCIVAL, J.A. – SONE, D., 2004 – Basement terrane correlations and crustal recycling in the western Superior province; Nd isotopic character of granitoid and felsic volcanic rocks in the Wabigoon subprovince, N. Ontario, Canada. Precambrian Research; volume 132, pages 245-274.

VILLENEUVE, P.-A., 2000 – Rapport des travaux de forage et de reconnaissance 2000, propriété Duquet. Ministère des Ressources naturelles et de la Faune, Québec; GM 58641, 171 pages.

VILLENEUVE, P.-A. – CHAPDELAINE, M., 1999 – Projet Minto, Permis Narsaaluk, Rapport des travaux 1999. Ministère des Ressources naturelles et de la Faune, Québec; GM 57239, 23 pages.

WARDLE, R.J. – JAMES, D.T. – SCOTT, D.J. – HALL, J., 2002 – The southeastern Churchill Province: synthesis of a Paleoproterozoic transpressional orogen. Canadian Journal of Earth Sciences; volume 39, pages 639-663.

WEAVER, B.L. – TARNEY, J., 1981 – The Scourie dyke suite: petrogenesis and geochemical nature of the Proterozoic subcontinental mantle. Contributions to Mineralogy and PÉTRology; volume 78, pages 175-188.

WHITE, W.S., 1968 – The native-copper deposits of Northern Michigan. *In*: Ore deposits of the United States, 1933-1967: The Graton-Sales volume, Ridge, J.D. (ed.). American Institute of Mining, Metallurgical and Petroleum Engineers Inc., New York; pages 303-325.

WILKINSON, L. – KJARSGAARD, B.A. – LECHEMINANT, A.N. – HARRIS, J., 2001 – Diabase dyke swarms in the Lac de Gras area, Northwest Territories and their significance to kimberlite exploration: initial results. *In*: Current Research, Part C; Geological Survey of Canada; Paper 2001-C8, 17 pages.

WODICKA, N. – MADORE, L. – LARBI, Y. – VICKER, P., 2002 – Géochronologie U-Pb de filons-couches mafiques de la Ceinture de Cape Smith et de la Fosse du Labrador. *In:* L'exploration minérale au Québec, Notre savoir, vos découvertes, Séminaire d'information sur la recherche géologique, Programme et résumés, 2002. Ministère des Ressources naturelles, Québec; DV 2002-10, page 48.

XIE, Q. – KERRICH, R., 1994 – Silicate-perovskite and majorite signature komatiites from the Archean Abitibi Greenstone Belt: Implications for early mantle differentiation and stratification. Journal of Geophysical Research; volume 99, pages 15799-15812.

Ressources naturelles
et Faune
Québec